昭和33年12月25日　昭和36年6月8日　印刷［毎月1回］
第3種郵便物認可　昭和36年6月15日　発行［15日発行］

CHEMISTRY HALL LIBRARY

BULLETIN

OF THE

CHEMICAL SOCIETY OF JAPAN

STATE
UNIVERSITY
AUG 19 1961
LIBRARY

Vol. 34 No. 6 June 1961

CONTENTS

General and Physical

Nuclear Magnetic Resonance Study of the Steric Effect in Dimethylphenols . . . I. YAMAGUCHI 744

A UAO Treatment of the van der Waals Force . . . . . T. YONEZAWA, H. KATO, K. MOROKUMA and K. FUKUI 747

On the Electrical Conductivity of the Organic Thin Films: Perylene, Coronene and Violanthrene . . . . . H. INOKUCHI, H. KURODA and H. AKAMATU 749

Proton Magnetic Resonance Studies on the Thermally Dehydrated Products of Alumina Trihydrate . . . . . T. SAITO 757

Infrared Spectra of Water of Crystallization in Some Inorganic Chlorides and Sulfates. . I. GAMO 760

Infrared Absorption Spectra of Water of Crystallization in Copper Sulfate Penta- and Monohydrate Crystals . . . . . I. GAMO 764

Polymerization of Propylene with Tin Tetraalkyl-Titanium Tetrachloride Catalyst . . . . . N. ASHIKARI and M. HONDA 767

On the pd Hybridization of the Sulfur Atom in Thiothiophten. I. The Calculations of the Overlap Integrals Involving d Orbitals . . . . . K. MAEDA 785

The Effects of pH on the Flocculation of Quartz Aqueous Suspensions . . . . . T. OHYAMA, J. SHIMOHZAKA and S. USUI 790

Differential Thermal Analysis of Aluminum Soaps . . . . . S. SHIBA 804

Differential Thermal Analysis of the Systems Aluminum Soap-Hydrocarbon. . . . . S. SHIBA 809

Diffusion in Glassy Polymers. II. Effects of Polymer-penetrant Interaction; Diffusion of Ethyl Methyl Ketone in Atactic Polystyrene . . . . . H. ODANI, J. HAYASHI and M. TAMURA 817

Infrared Spectra of Acyclic Imides. III. Infrared Dichroism of Dipropionamide and *N*-Acetylpropionamide Crystals . . . . . T. UNO and K. MACHIDA 821

Theory on the Light Scattering of High Polymer Solutions Considering the Anisotropy of Segments . . . . . M. NAKAGAKI 834

Iodine-catalyzed Thermal cis-trans Isomerization of Azobenzene . . . . . S. YAMASHITA 842

n-π Absorption Spectra of Some Aliphatic Aldehydes. . . . . H. OSHIMA 846

A Molecular Orbital Treatment of Triallyl Isocyanurates and Related Allyl Esters . . . . . K. FUKUI, H. KATO, T. YONEZAWA, F. TANIMOTO and H. KITANO 851

Studies on the Chemical Equilibrium Lag during the Rapid Expansion through the Rocket Nozzle. . . . . S. TSUCHIYA 854

Infrared Spectra and the Structure of Some Metal-oxamide Complexes . . . . . Y. KURODA, M. KATO and K. SONE 877

Analytical and Inorganic

Spectrophotometric Determination of Nitrite in Nitrate and Sulfate. . . . . Y. KATSUBE, K. UESUGI and J. H. YOE 743

Spectrophotometric Determination of Uranium with Sodium 2′′,6′′-dichloro-4′-hydroxy-3,3′-dimethylfuchsone-5,5′-dicarboxylate . . . . . Y. KATSUBE, K. UESUGI and J. H. YOE 826

Studies on Metal Complex Species Using an Anion Exchange Resin. I. Derivation of Equations and Application to Mercury(II)-Nitrate Complex. . . . . H. WAKI 829

Solvent Extraction of Inorganic Nitrates with Diphosphonate Ester. I. Zirconium, Yttrium and Lanthanide Nitrates . . . . . H. SAISHO 859

(Continued on inside cover)

Published by the Chemical Society of Japan

THE CHEMICAL SOCIETY OF JAPAN
(NIPPON KAGAKUKAI)

Founded in 1948

Successor to the former Chemical Society of Japan founded in 1878 and to the Society of Chemical Industry, Japan founded in 1898.

BULLETIN OF THE CHEMICAL SOCIETY OF JAPAN

Editor: Tadao SHIBA, Tokyo Institute of Technology, Tokyo
Assistant Editor: Tadashi SUEHIRO, Gakushuin University, Tokyo
Editorial Board:

Yoshié BANSHO	Hidehiro GOTÔ	Keniti HIGASI
Yoshimasa HIRATA	Hiroo INOKUCHI	Tatsujiro ISHIMORI
Tadashi KAMIKUBO	Michio KOBAYASHI	Ichiro MIYAGAWA
Masazumi NAKAGAWA	Shigeru OAE	Shigeru OHASHI
Kazuo SATAKE	Syûzô SEKI	Osamu SIMAMURA
Yoshitada TOMODA	Iwao YASUMORI	Koshiro YOSHIOKA

(Continued from outside cover)

Organic and Biological

Studies on the Chemical Decomposition of Simple Sugars. X. Acetol Formation from ^{14}C-Labeled Hexoses . . . . . R. GOTO, J. HAYAMI, K. KUDO and S. OTANI 753
Neutron and γ-Irradiation of Propionamide . . . . . E. TACHIKAWA and G. TSUCHIHASHI 770
Stereochemistry and Mechanisms of Catalytic Hydrogenolysis and Hydrogenation. I. Catalytic Hydrogenolysis of Optically Active Compounds with Raney Nickel . . . . . S. MITSUI and S. IMAIZUMI 774
Dehydrogenation of Secondary Alcohols with Reduced Copper. IV. Catalytic Dehydrogenation of Isopropyl Alcohol (Part 2) . . . . . K. KAWAMOTO 795
Dehydrogenation of Secondary Alcohols with Reduced Copper. V. Catalytic Dehydrogenation of *sec*-Butyl Alcohol . . . . . K. KAWAMOTO 799
The Preparation of Diethyl Phosphate . . . . . T. MUKAIYAMA and T. FUJISAWA 812
Non-benzenoid Aromatic Heterocycles. V. An Attempted Synthesis of 4,7-Dihydro-4,7-phenanthroline Derivatives. . . . . H. KATO and M. OHTA 814
The Mannich Base of Troponoid and its Application. V. On the Mannich Base of 3-Isopropyltropolone (α-Thujaplicin). . . . . K. OGURA 839
Cyclic Acetylenes. V. Syntheses and Properties of Strained Cyclic Ethers of *o,o'*-Dihydroxydiphenyldiacetylene . . . . . F. TODA and M. NAKAGAWA 862
Cyclic Acetylenes. VI. Transannular and Proximity Effects in the Cyclic Derivatives of *o,o'*-Dihydroxydiphenyldiacetylene. . . . . F. TODA and M. NAKAGAWA 874

Applied

Fischer-Tropsch Synthesis with Tubular Reactor of 18.11. Catalyst Bed. I. Reactor with Constant Temperature Wall . . . . . M. KURAISHI, M. KURITA, T. HOSOYA, H. ICHINOKAWA, K. OGAWA and H. UCHIDA 780

Short Communications

Nuclear Magnetic Resonance of Tar Products. II . . . . . S. FUJIWARA and T. WAINAI 881
The Crystallinity of Polyaldehydes . . . . . H. SOBUE and H. KUBOTA 883
Syntheses of Two Kinds of Metal-free Tetra-azaporphines by the Urea-melt Method. N. FUKADA 884
Constituents of the Antibiotic, Glumamycin . . . . . M. INOUE 885
Anionoid Substitution of Bromo-3,4-benzotropolones . . . . . S. EBINE 887
The Synthesis of 3-α-Carboxyethylcyclopentanol Lactone . . . . . T. TANAKA 888
4,5-Dimethoxycanthin-6-one and 2,6-Dimethoxy-*p*-benzoquinone from *Picrasma ailanthoides* Planchon . . . . . N. INAMOTO, S. MASUDA, O. SIMAMURA and T. TSUYUKI 888
The Crystal Structure of Phenazine-5,10-dioxides . . . . Y. NAMBA, T. ODA and T. WATANABÉ 889
Synthesis of Isoxazolecarboxylic Acids from Schiff Bases and Nitroacetate. . . . . S. ZEN and S. UMEZAWA 890
Polarographic Studies of Metallic Complexes. VI. Tetracyanocobaltate(III) Complex. . . . . N. MAKI and R. TSUCHIDA 891
Catalytic Dimerization of Monoalkyl Acetylenes . . . . . N. HAGIHARA, M. TAMURA, H. YAMAZAKI and M. FUJIWARA 892
Electron Spin Resonance of Tetracene-Antimony Pentachloride . . . . . Y. MATSUNAGA 893

n is 1 or 2 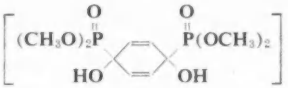

The infrared absorption spectrum of this product (III) did not show the absorption bands of the carbonyl group of *p*-benzoquinone, but strong absorption bands of phenyl group (1450, 1510 cm^{-1})[9], P=O (1265 cm^{-1})[9] and P–O–C (Arom) linkages (1205 cm^{-1})[9] were observed. (see Fig. 1).

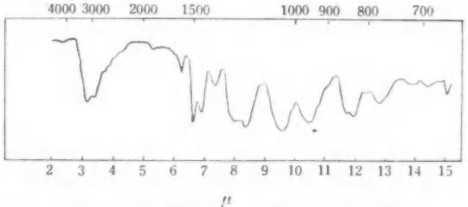

Fig. 1 The infrared spectrum of *O*, *O*-dimethyl-*O*-(*p*-hydroxy-phenyl)phosphorate (III) (liquid).

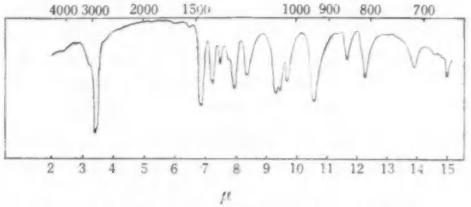

Fig. 2 The infrared spectrum of *O*, *O*-dimethyl-*O*-(4-hydroxy-2, 3, 5, 6-tetrachloro-phenyl)phosphorate (IV) (in Nujol).

Moreover, the product showed the color reaction of phenol by ferric chloride and a hydrolysis of the product produced hydroquinone.

From the above results, it was presumed that the reaction of *O*, *O*-dimethyl phosphonate with the carbonyl group of *p*-benzoquinone did not produce the usual α-hydroxy phosphonate but 4-hydroxy-phenyl phosphorate (III).

In the above experiments, there remained uncertainty whether the product is the pure material or not, because the product is an undistillable oil. However, the above presumption against the above experimental results was confirmed by the reaction of *O*, *O*-dimethyl phosphonate with chloranil. The reaction of one or two moles ratio of *O*, *O*-dimethyl phosphonate with one mole ratio of chloranil produced the same crystals which melt at 237~239°C.

9) L. J. Bellamy, "The Infrared Spectra of Complex Molecules"; Jhon Wiley & Sons. (1958).

The melting point of these crystals coincided with that of *O*, *O*-dimethyl-*O*-(4-hydroxy-2, 3, 5, 6-tetrachlorophenyl)phosphorate (IV) which was prepared by Ramirez's method[10] and the mixed melting point did not decrease.

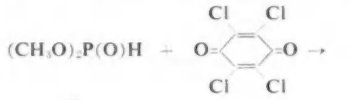

(I)

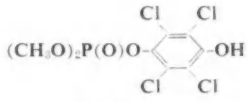

(IV)

It seems that the above reactions have different mechanism from the usual reactions of phosphonate with carbonyl groups of aldehydes and ketones.

It is considered that *O*, *O*-dialkyl phosphonate have polymerized form of two or three molecules by hydrogen bonding at the free state[11-13], but in aldol type reactions, the hydrogen atom is released easily as proton and the phosphonate becomes the phosphite-form[14]:

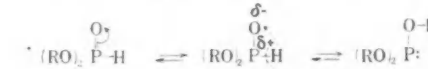

Therefore, when the phosphonate reacts with the aldehydes or ketones, this hydrogen atom cuts itself off as proton from phosphite molecule and the phosphite group reacts with the electrophilic carbon atom of carbonyl group just as the aldehyde group in aldol condensation does.

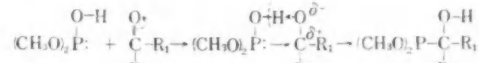

When the phosphonate reacts with the carbonyl group which has an ethylenic double bond in conjugated system, the phosphorus atom links the β-carbon atom of carbonyl group[15]. This reaction might be explained by the same mechanism as above.

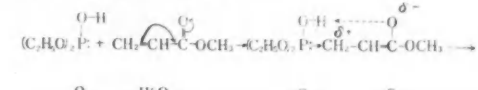

10) F. Ramirez, *J. Am. Chem. Soc.*, **81**, 587 (1959).
11) B. A. Arbuzov, *Doklady Akad. Nauk S. S. S. R.*, **54**, 599 (1946).
12) B. A. Arbuzov, ibid., **54**, 787 (1946).
13) B. A. Arbuzov, ibid., **55**, 31 (1947).
14) M. Murakami, "Hanno-Yuukikagaku", Asakura-Syoten (1949), p. 316.
15) E. C. Ladd, Can. Pat. 509034.

If the reaction of the phosphonate with the quinone has the same ionic mechanism, it may be considered that the quinone have the formula IIIA as excited resonance form[16]. According to this mechanism, it is normal that the phosphorus atom attacks the carbon atom of the quinone nucleus.

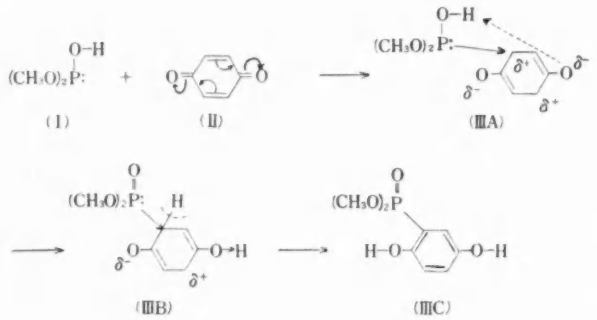

(I) (II) (IIIA) (IIIB) (IIIC)

In fact, hydrogen halides, benzene sulfonic acids or xanthic acids react with quinone and link the carbon atom of quinone nucleus according to the above mechanism[16]. But the reaction of phosphonate can not be explained by the above mechanism, since the experimental facts show the production of the phosphorate.

On the other hand, it is well known that the reaction of trialkyl phosphites with α-halocarbonyl compounds does not produce the phosphonates as in Arbuzov's reaction but phosphorates as in Perkow's reaction[17].

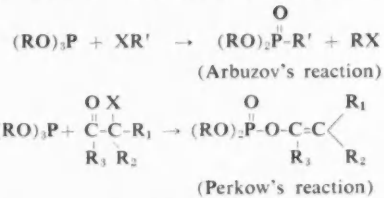

(Arbuzov's reaction)

(Perkow's reaction)

On the above reaction mechanism, Allen[18] and Pudovik[19] have reported that the trialkyl phosphites attack the electrophilic carbon atom of carbonyl group and then the phosphorus atom forms the oxide ring as the intermediate:

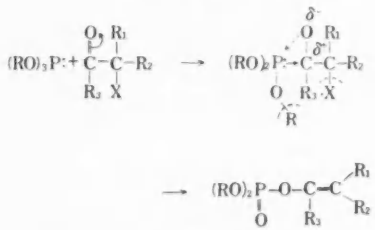

In the reaction of *O*, *O*-dimethyl phosphonate with *p*-benzoquinone, it is considered that the reaction mechanism is the same as above, namely, phosphite group attacks the nucleophilic carbon atom of quinone nucleus and then the phosphorus atom forms the oxide ring as intermediate because there is a carbonyl group at α-position.

Accordingly, the phosphorus atom cuts itself off from the quinone nucleus instead of eliminating the hydrogen atom and then the phosphorate is produced.

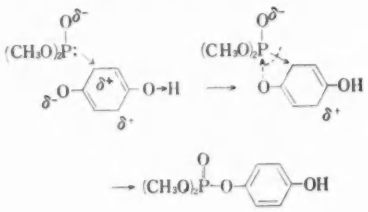

(III)

It is well explained by this mechanism that the phosphonate reacts with *p*-benzoquinone by 1 : 1 mole ratio and does not produce the α-hydroxy phosphonate but produces phosphorate and, moreover, when the water is presented in this reaction, hydroquinone is produced.

Namely, in the presence of water, the phosphorus atom forms the oxide ring between the oxygen atom of water instead of the oxygen atom of quinone. So, Perkow's rearrangement occurs between the phosphonate and the water.

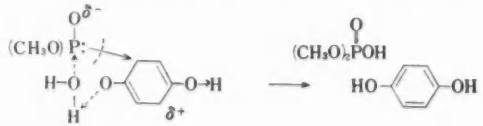

16) M. Murakami, "Hanno-Yuukikagaku", Asakura-Syoten. (1949), p. 351.
17) W. Perkow, *Chem. Ber.*, **88**, 662 (1955).
18) J. Allen, *J. Am. Chem. Soc.*, **77**, 2871 (1955).
19) A. N. Pudovik, *J. Gen. Chem., USSR*, **26**, 2503 (1956).

Experimental

Reaction of *O*, *O*-Dimethyl Phosphonate with *p*-Benzoquinone.—To a solution of 15 g. of *p*-benzoquinone and 0.5 g. of triethylamine in 45 ml. of dioxane was gradually added under cooling by water 32.0 g. of *O*, *O*-dimethyl phosphonate. After the addition, the reaction mixture was stirred for 7 hr. at 70°C and then allowed to stand over night at room temperature. The reaction mixture was condensed in vacuo (0.3 mmHg) at 60°C, 30.0 g. of the pale yellow oil was obtained.

This oil was dissolved in acetone and then ligroin was added gradually. The upper layer was separated by decantation, and the lower layer was concentrated in vacuo. The viscous oil was obtained and yielded 25.0 g. (83%) n_D^{26} 1.5205.

Found: P, 14.3. Calcd. for $C_8H_{11}O_5P$: P, 14.2%.

The same reaction using 16.5 g. of *O*, *O*-dimethyl phosphonate instead of 32.0 g. of *O*, *O*-dimethyl phosphonate, produced 23.8 g. of same oil.

Hydrolysis of *O*, *O*-Dimethyl-*O*-(4-hydroxy-phenyl)phosphorate (III).—The mixture of 10.0 g. of *O*, *O*-dimethyl-*O*-(4-hydroxy-phenyl)phosphorate (III) and 30 ml. of 8% hydrochloric acid was heated at 80°C for 50 hr. The water layer was extracted continuously with ether and then the ether layer was dried over anhydrous sodium sulfate. After removal of the ether, the residue was recrystallized from benzene.

Four grams of *p*-hydroquinone was obtained and melted at 170~171°C. The melting point of a mixture of the hydroquinone and the authentic specimen did not decrease.

Reaction of *O*, *O*-Dimethyl Phosphonate with Chloranil.—To a solution of 24.6 g. of chloranil in 250 ml. of dioxane was added by drop-wise 11.0 g. of *O*, *O*-dimethyl phosphonate under cooling with ice water. After the addition, the reaction mixture was stirred for 5 hr. at 80°C and then cooled. The reaction mixture was concentrated under a reduced pressure and the crude crystals were precipitated. The crystals were recrystallized from methanol, melted at 237~239°C. and yielded 22.0 g. (61%). A mixture of these crystals and the authentic *O*, *O*-dimethyl-*O*-(4-hydroxy-2, 3, 5, 6-tetrachloro-phenyl)-phosphorate which was prepared by Ramirez's method[10] melted at 238~239°C.

Found: P, 9.2; Cl, 39.73. Calcd. for $C_8H_7Cl_4O_5P$: P, 8.7; Cl, 39.88%.

Reaction of *O*, *O*-Dimethyl Phosphonate with *p*-Benzoquinone under the Presence of Water.—The solution of 15 g. of *p*-benzoquinone in 100 ml. of methanol which contained 5% water was added to the solution of 16.5 g. of *O*, *O*-dimethyl phosphonate in 50 ml. of benzene. After the reaction mixture was stirred, benzene, water and alcohol were removed and then the residue was extracted continuously with ether. The ether layer was dried over anhydrous sodium sulfate. After removal of the ether, the residue was recrystallized from benzene and 10.8 g. of the hydroquinone was obtained and melted at 171~172°C.

The author wishes to express his thanks to Professor Shinichirou Fujise and Professor Tarou Yamazaki of Tohoku University for helpful suggestions in the preparation of this manuscript. He also wishes to thank to the Sumitomo Chem. Co. Ltd., for permission to publish this work. He is indebted to his co-workers in the microanalytical section in this laboratory. He also wishes to express his thanks to Mr. M. Nakagawa for his earnest assistance.

Sumitomo Chemical Co., Ltd.
Osaka Works
Konohana-ku, Osaka

Internal Rotation and Low Frequency Spectra of Esters, Monosubstituted Amides and Polyglycine

By Tatsuo MIYAZAWA*

(Received September 20, 1960)

Monosubstituted amides, polypeptides and proteins have been known to exhibit several prominent bands characteristic to the –CONH– group. The bands at about 3300 cm^{-1} and 3100 cm^{-1} are now considered to be due to the Fermi resonance between the fundamental N–H stretching vibration and the first overtone of the amide II vibration[1]. The amide I (1650 cm^{-1}), the amide II (1550 cm^{-1}), and the amide III (1250 cm^{-1}) vibrations involve the C=O stretching, the C–N stretching and the N–H in-plane bending modes. These vibrations have long been subjects of controversy; however, their nature has finally been elucidated

* Present address: Institute for Protein Research, Osaka University, Kita-ku, Osaka.

1) R. M. Badger and A. D. E. Pullin, *J. Chem. Phys.*, 22, 1142 (1954); T. Miyazawa, *J. Mol. Spectroscopy*, 4, 168 (1960).

by a normal coordinate treatment of *N*-methylacetamide[2]. The amide IV (650 cm^{-1}), the amide V (750 cm^{-1}), and the amide VI (600 cm^{-1}) bands have been found to be due primarily to the O=C–N bending[2], the N–H out-of-plane bending[4], and the C=O out-of-plane bending modes[3], respectively. The torsional vibration (the amide VII) around the C–N bond is directly related to the potential barrier hindering internal rotation about the C–N bond. For the molecule of *N*-methylformamide the band at 356 cm^{-1} has been assigned to this torsional mode[5].

Internal rotation around the C–N bond of the peptide group is one of the most important factors in determining the conformation or the secondary structure of polypeptides and proteins. Since biological activities of proteins are closely related to their secondary structures an extended spectroscopic study of the hindering potential was undertaken. The torsional vibrations in the low frequency region were assigned and normal coordinate treatments were made of the out-of-plane vibrations for the purpose of determining the potential barrier.

Monosubstituted amides exhibit infrared spectra analogous to those of esters and the analyses of the spectra of esters provide useful information in studying amide spectra. It may be remarked that esters and monosubstituted amides are isoelectronic with each other and, in addition, the mass of NH is not very different from the mass of the oxygen atom. Therefore spectroscopic studies were made of esters as well as of the monosubstituted amides in question.

Internal Rotation around the C–O Bond of Esters

Electron diffration studies of the molecular structures of methyl formate and methyl acetate were made by O'Gorman et al.[6] and the molecule was found to be in the cis form

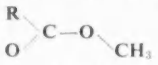

(R=H or CH_3)

The observed diffraction haloes were in accord with a structure slightly twisted from the planar structure by an internal rotation angle of about 25°. More recently the structure of methyl formate, however, was precisely determined by a microwave absorption measurement and the molecule was established to be in the planar cis form[7]. In the present study, therefore, the infrared spectra of esters will be discussed in terms of the planar cis structure.

Infrared spectra of methyl formate and methyl acetate in the gaseous state and in nonpolar solutions have been measured by Wilmshurst[8] in the region above 300 cm^{-1}. In the present work the measurements were extended out to 190 cm^{-1} so that the torsional frequencies might be observed.

Infrared Absorption Measurements.—For the measurements in the region 400～190 cm^{-1} a Perkin Elmer Model 12C spectrometer equipped with a cesium iodide prism[9] was used. Infrared spectra of methyl formate were measured in the gaseous state, in the solid nitrogen matrix, and in the crystalline state. The vapor spectra were obtained at room temperature with a 10 cm. gas cell and the gas pressure was 30 or 156 mmHg. The observed spectra are shown in Figs. 1 and 2A. A strong band was observed at 325 cm^{-1} with shoulders at about 305 cm^{-1} and at 340 cm^{-1}, in agreement with a previous result[8]. No other strong band, however, was observed below 300 cm^{-1}. The matrix spectra were recorded at 20°K for the molar ratio (N_2 : ester) of 32 or 100, where 140 micromoles of the ester sample was dispersed in the matrix over an area of about 2 cm^2. The nitrogen gas used as the matrix material was purified by passing over copper at 600°C and then through a liquid nitrogen bath. The experimental technique of the matrix isolation method was described before[10]. The observed matrix spectra are shown in Fig. 2B. Two prominent bands were observed at

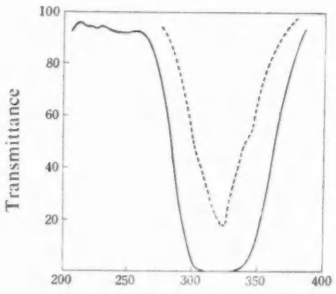

Fig. 1. Infrared spectra of methyl formate vapor, solid line : p=156 mmHg, broken line : p=30 mmHg.

2) T. Miyazawa, T. Shimanouchi and S. Mizushima, *J. Chem. Phys.*, **29**, 611 (1958).
3) T. Miyazawa, T. Shimanouchi and S. Mizushima, ibid., **24**, 408 (1956); T. Miyazawa, *J. Chem. Soc. Japan, Pure Chem. Sec.* (*Nippon Kagaku Zasshi*), **77**, 171, 321, 526 (1956).
4) H. K. Kessler and G. B. B. M. Sutherland, *J. Chem. Phys.*, **21**, 570 (1953).
5) D. E. DeGraaf and G. B. B. M. Sutherland, ibid., **26**, 716 (1957).
6) J. M. O'Gorman, Wm. Shand and V. Schomaker, *J. Am. Chem. Soc.*, **72**, 4222 (1950).
7) R. F. Curl, *J. Chem. Phys.*, **30**, 1529 (1959).
8) J. K. Wilmshurst, *J. Mol. Spectroscopy*, **1**, 201 (1957).
9) T. Miyazawa, *J. Chem. Phys.*, **29**, 421 (1958).
10) E. D. Becker and G. C. Pimentel, ibid., **25**, 224 (1956).

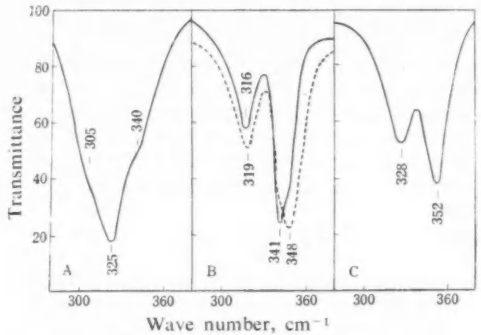

Fig. 2. Infrared spectra of methyl formate. A: vapor, B: matrix (solid line: molar ratio=100, broken line: ratio=32), C: crystal.

316 and 341 cm^{-1} for the molar ratio of 100 and these peaks shifted to 319 and 348 cm^{-1} for a lower ratio of 32. In preparing the crystalline specimen the ester gas was sprayed on a cesium bromide window kept at 140°K and the frozen sample was once slowly warmed up to a temperature slightly below the sublimation point allowing enough time for annealing and then cooled to 150°K for the absorption measurement. The observed crystalline spectrum is shown in Fig. 2C. Two bands were observed at 328 and 352 cm^{-1}, corresponding to the matrix bands at 319 and 348 cm^{-1}, respectively.

Infrared measurements in the vapor phase at room temperature were also made in the region 250~170 cm^{-1} by the use of the grating spectrometer described by Bohn et al.[11] The path length of the vapor cell was 70 cm.; however, no band of methyl formate vapor was observed at a gas pressure of 50~100mmHg. On the other hand a fairly strong band of methyl acetate was observed at 213 cm^{-1} with a gas pressure of 53 mmHg as shown in Fig. 3.

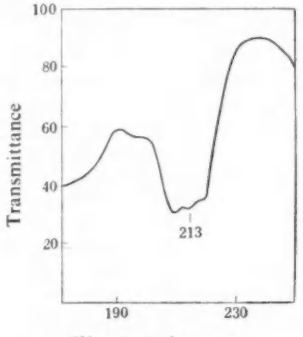

Fig. 3. Infrared spectrum of methyl acetate vapor.

Vibrational Assignment of Methyl Formate. —The vibrational modes of methyl formate expected in the region below 400 cm^{-1} are the C–O–methyl bending mode and the twisting modes around the ester C–O bond and around the O–methyl bond. The strong vapor band at 325 cm^{-1} corresponds to the fairly strong polarized Raman line at 332 cm^{-1} in the liquid state and may be assigned to the C–O–methyl bending mode. The twisting frequencies depend of course upon the potential barrier hindering internal rotation. The three-fold potential barrier of the O–methyl bond has been determined to be 1150±100 cal./mol.[7] and the corresponding twisting frequency will be of the order of 150 cm^{-1}. On the other hand the potential barrier of the ester C–O bond may be of the same order of height as the barrier, 10 kcal./mol., of formic acid monomer[12] and the corresponding twisting frequency may well be in the region 400~200 cm^{-1}. Excepting the 325 cm^{-1} band assigned to the C–O–methyl bending mode, however, no other band with more than 5% absorption was observed with the cell length of 10 cm. and with the gas pressure of 150 mmHg. It may be noted that the 325 cm^{-1} band has a rather peculiar contour, suggesting the possibility of the overlapping of the bands due to the C–O–methyl bending mode and due to the C–O torsional mode.

In the solid matrix the complications arising from rotational fine structures are absent. In the case of formic acid[12] the O=C–O bending mode and the C–O twisting mode exhibit a vibration-rotation band with complicated contour in the vapor phase, whereas in the matrix the two frequencies were resolved. Therefore the matrix isolation technique was used in the present case of methyl formate and the vapor band at 325 cm^{-1} was resolved into two distinct peaks in the nitrogen matrix. In order to establish the fact that these peaks are due to the two vibrational modes, C–O–methyl bending and C–O twisting of a single species, the effect of the molar ratio was observed (see Fig. 2B). On decreasing the molar ratio from 100 to 32, however, the relative intensities of the two peaks did not change appreciably, and these two peaks may now be assigned to the two modes mentioned above. It was not possible to decide which of the two peaks in the matrix was due to the twisting mode. Nevertheless the frequency of 325 cm^{-1} may be taken to be the twisting frequency in the vapor phase.

11) C. R. Bohn, N. K. Freeman, W. D. Gwinn, J. L. Hollenberg and K. S. Pitzer, ibid., **21**, 719 (1953).

12) T. Miyazawa and K. S. Pitzer, ibid., **30**, 1076 (1959).

Vibrational Assignment of Methyl Acetate.—The molecule of methyl acetate has three skeletal in-plane bending modes and one skeletal out-of-plane bending mode. The Raman lines or the infrared bands at 640, 433, 303 and 610 cm^{-1} have been assigned to these skeletal modes[8,13]. In the region below 400 cm^{-1} three torsional frequencies are expected, one around the ester C–O bond, one around the O–methyl bond, and the last one around the C–methyl bond. As in the case of methyl formate the torsional frequency around the O–methyl bond will be of the order of 150 cm^{-1}. The potential barrier around the C–methyl bond of methyl acetate has not been determined as yet; however, it will not be too different from the value of 483±25 cal./mol. as found for acetic acid monomer[14]. The corresponding torsional frequency will be of the order of 100 cm^{-1}. The observed infrared band of methyl acetate at 213 cm^{-1} is most reasonably assigned to the torsional mode around the ester C–O bond. The reduced moment of inertia for the internal rotation is greater for methyl acetate than for methyl formate and thus a torsional frequency somewhat lower than 325 cm^{-1} of methyl formate may be expected for methyl acetate.

Normal Coordinate Treatment of Out-of-plane Vibrations.—In order to estimate the twofold potential barrier of the ester C–O bond the normal coordinate treatments were made of the out-of-plane vibrations of methyl formate and methyl acetate. The methyl groups of these esters were treated as single dynamic units. The symmetry coordinates and the inverse kinetic energy matrix were derived previously[12]. The bond lengths used in the calculation were $r(C{=}O) = 1.22$ Å, $r(C{-}O) = 1.36$ Å, r(O–methyl) $= 1.46$ Å, $r(C{-}H) = 1.07$ Å and r(C–methyl) $= 1.52$ Å, and all the valence angles were taken to be 120° for simplicity.

The out-of-plane potential function was expressed in terms of the out-of-plane bending constant for the three bonds of the carbonyl carbon atom, H_Ω, the torsional potential constant for the ester C–O bond, H_θ, and the interaction constant, $H_{\Omega\theta}'$. In the case of formic acid monomer[12] the interaction constant $H_{\Omega\theta}' = -0.00_5$ has been found to be negligible as compared to the potential constants, $H_\Omega = 0.58_3$ and $H_\theta = 0.13_1$. In the present treatments of esters the interaction constant was neglected. In calculating the torsional potential constant the correction for the anharmonicity of the two-fold torsional potential function, $V = V_2 \cdot (1-\cos 2\theta)/2$ was made to the observed torsional frequency. The correction $\nu_0 - \nu$ is equal to $h/8\pi^2 cI_r$ where h is Planck's constant, c the light velocity, and I_r the reduced moment of inertia for intramolecular rotation[12]. The values of the correction were calculated to be 6 and 3 cm^{-1} for the cis form and the trans form of methyl formate and 2 cm^{-1} for both the cis form and trans form of methyl acetate. The CH out-of-plane bending frequency of 1019 cm^{-1} and the corrected torsional frequency of 331 cm^{-1} were used for the calculation of the potential constants of $H_\Omega = 0.55_8$ and $H_\theta = 0.18_2$ (in unit of 10^{-11} erg). Then the two-fold potential barrier of methyl formate was found to be 13.$_1$ kcal./mol. The potential constants of methyl acetate were calculated to be $H_\Omega = 0.533$ and $H_\theta = 0.221$ from the skeletal out-of-plane bending frequency of 607 cm^{-1} and the corrected torsional frequency of 215 cm^{-1}. The two-fold potential barrier of methyl acetate was found to be 15.$_9$ kcal./mol. It may be noted that the potential barriers of esters are higher than those of formic acid (10 kcal./mol.) and of acetic acid (10 kcal./mol.)[15].

Trans Form of Esters.—The trans isomer of formic acid monomer has been found by the infrared spectra in the vapor phase, and the energy of the trans isomer has been found to be 2 kcal./mol. higher than the more abundant cis isomer[12]. The normal coordinate treatment of the out-of-plane vibrations was also made of the trans form of methyl formate as an aid in assigning the bands due to the trans form. Since the torsional potential constant of the trans isomer has been found to be the same as that of the cis isomer in the case of formic acid, the potential function of the cis form of methyl formate was also used for the treatment of the trans form. The C–H out-of-plane bending frequency and the torsional frequency were calculated to be 1053 and 233 cm^{-1}, respectively. As shown in Fig. 1, however, no band with more than 5% absorption has been observed in the vicinity of 233 cm^{-1}. From the intensity of the 325 cm^{-1} band, the abundance ratio trans/cis was estimated to be less than 1% and the energy difference between the two forms is considered to be greater than 2.7 kcal./mol.

The relaxation absorption of sound in liquid ethyl formate has been ascribed to the rotational isomerism around the ester C–O bond[16]. Actually, however, there is also the rotational isomerism around the O–CH_2 bond of ethyl formate, and the hindering potential previously estimated from the ultrasonic studies may not be compared with the present results.

13) T. Miyazawa, *J. Chem. Soc. Japan, Pure Chem. Sec.* (*Nippon Kagaku Zasshi*), **77**, 619 (1956).
14) W. J. Tabor, *J. Chem. Phys.*, **27**, 974 (1957).
15) T. Miyazawa, unpublished.
16) J. Karpovich, *J. Chem. Phys.*, **22**, 1767 (1954); D. Tabuchi, ibid., **28**, 1014 (1958).

Internal Rotation around the C–N Bond of the Peptide Group

The stable conformation of the peptide group has been established to be the planar trans form by Mizushima et al.[17] The vibrational analysis of *N*-methyl acetamide and *N*-methyl formamide will therefore be made with the planar trans structure,

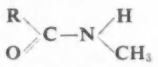

***N*-Methylacetamide.**—The vibrational assignment as well as the normal coordinate treatment of the in-plane vibrations have been made[2,3,13] and the nature of the skeletal bending vibrations at 436 and 289 cm^{-1} have already been elucidated. The Raman spectrum of liquid *N*-methylacetamide has been carefully measured by Sugita[18] and a new weak line has been observed at 206 cm^{-1}. Since the methyl torsional frequencies around the C–methyl bond and around the N–methyl bond will be lower than 150 cm^{-1} as in the case of methyl acetate, the Raman line at 206 cm^{-1} is most reasonably assigned to the torsional frequency around the C–N bond of the peptide group. It may be noted that this frequency is not very different from the corresponding frequency 213 cm^{-1} of methyl acetate.

In the present study an approximate normal coordinate treatment of the out-of-plane vibrations was made, treating the methyl groups and the NH group as single dynamic units. The bond lengths used were the same as those used in the treatment of the in-plane vibrations[2]. Because of the approximate nature of the present treatment, the correction for the anharmonicity of the torsional frequency was not made. From the observed skeletal out-of-plane bending frequency of 600 cm^{-1} (the amide VI band) and the torsional frequency of 206 cm^{-1} the potential constants were calculated to be $H_D=0.50_8$ and $H_\theta=0.19_5$, and then the two-fold potential barrier was estimated to be 14 kcal./mol. The bond order of the C–N bond of the peptide group may be estimated to be 0.3∼0.4 from the torsional potential constant as in the case of formic acid. This value agrees with the bond order 0.3∼0.4 derived from the bond distances.

***N*-Methylformamide.** — Infrared and Raman spectra of liquid *N*-methylformamide have been measured by DeGraaf and Sutherland[5]. The polarized Raman line at 302 cm^{-1} has been assigned to the C–N–methyl skeletal bending vibration and the depolarized line at 356 cm^{-1} to the torsional vibration around the peptide C–N bond. These frequencies correspond to the frequency of 325 cm^{-1} observed for methyl formate.

The normal coordinate treatment of the out-of-plane vibrations of *N*-methylformamide was made as in the case of *N*-methylacetamide. The C–H bond length was taken as 1.07 Å and the other lengths were the same as those of *N*-methylacetamide. From the C–H out-of-plane bending frequency[3] of 1015 cm^{-1} and the torsional frequency of 356 cm^{-1} the potential constants were calculated to be $H_D=0.53_2$ and $H_\theta=0.20_2$. This torsional potential constant corresponds to the potential barrier of 14 kcal./mol.

The two-fold potential barrier of the C–N bond of the peptide group has been estimated by Pauling and Corey[19] to be about 30 kcal./mol. As the results of the present spectroscopic studies, however, the values of the potential barrier of *N*-methylacetamide and *N*-methylformamide were both found to be about 14 kcal./mol., and this lower value is to be used in discussing the relative stabilities of the various conformations of a polypeptide chain.

Low Frequency Infrared Spectra of Polyglycine I and II

Infrared absorption spectra have been widely used in studying the conformations of polymer chains. In the case of polypeptide chains the correlations between the chain conformations and the amide I and II frequencies were first noticed by Elliott and Ambrose[20]; that is to say the folded conformation exhibits the amide I and II bands at about 1650 and 1540 cm^{-1} whereas the extended conformation exhibits the bands at 1630 and 1520 cm^{-1}. Recently these correlations were given theoretical interpretations and were refined and extended to cover the random coil conformation, the α helix, the antiparallel-chain extended conformation, and the parallel-chain extended conformation as well as Nylon 66[21]. These refined correlations, although useful for synthetic polypeptides and certain fibrous proteins, may not be too dependable in proteins exhibiting ill-defined amide I and II bands[22]. Therefore it should be worthwhile to find out other characteristic bands whose frequencies change more sensitively than do the amide I and II bands.

17) S. Mizushima, T. Shimanouchi, S. Nagakura, K. Kuratani, T. Tsuboi, H. Baba and O. Fujioka, *J. Am. Chem. Soc.*, 72, 3490 (1950).
18) T. Sugita, unpublished.
19) L. Pauling and R. B. Corey, *Proc. Nat. Acad. Sci.*, 37, 251 (1951).
20) A. Elliott and E. J. Ambrose, *Nature*, 165, 921 (1950).
21) T. Miyazawa, *J. Chem. Phys.* 32, 1647 (1960); T. Miyazawa and E. R. Blout, *J. Am. Chem. Soc.*, 83, 712 (1961).
22) M. Beer, G. B. B. M. Sutherland, K. N. Tanner and D. L. Wood, *Proc. Royal Soc.*, A249, 147 (1959).

The N–H stretching vibration is localized in the N–H bond and involves only the nitrogen in the main chain of polypeptides. Its frequency, then, will not change appreciably with the chain conformation. On the other hand the torsional mode around the peptide C–N bond involves the C_α–C–N–C_α atoms in the main chain and its frequency is expected to be most sensitive to the conformational change of the chain. In this connection normal coordinate treatments of the skeletal vibrations of the polymers of the type, $(-CH_2-)_n$ and $(-CH_2-O-)_n$, have been made, and in fact the low frequencies primarily due to the torsional modes have been found to change most sensitively with the chain conformation[23].

Polyglycine has been known to exist in two forms[24]; polyglycine I is in the antiparallel-chain extended conformation and polyglycine II is in the helical conformation with three-fold screw axis[21,24,25]. In the present study the infrared spectra of these two forms of polyglycine were measured as Nujol paste in the region 400~190 cm^{-1}. The samples used were kindly given by Mr. Tsuchiya of the University of Tokyo. As shown in Fig. 4 polyglycine I exhibits a band at 217 cm^{-1}. This frequency appears to correspond to the frequency of 206 cm^{-1} observed for *N*-methylacetamide and is most reasonably assigned to the torsional mode around the C–N bond of the antiparallel-chain extended conformation. On the other hand polyglycine II* exhibits the corresponding band at 365 cm^{-1}. It is remarkable to note that the torsional frequency of polyglycine I is almost doubled by the transformation to polyglycine II. The amide VII band is thus found to be most sensitive to the conformation of polypeptide chains. It would be worth while to find out more extensive correlations between the various conformations and the infrared spectra in the low frequency region.

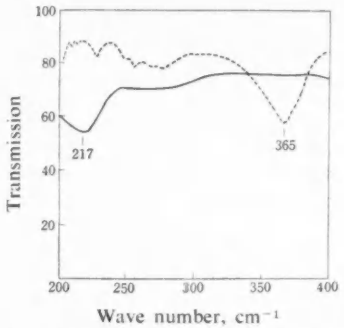

Fig. 4. Infrared spectra of polyglycine I (solid line) and polyglycine II (broken line).

The author wishes to thank Professor K. S. Pitzer of the University of California for his interest and encouragement and to Mr. Shoji Tsuchiya of the University of Tokyo for generously supplying the samples of polyglycine. The present work was partly supported by the American Petroleum Institute Research Project 50.

Department of Chemistry
University of California
Berkeley, California, U. S. A.

Institute for Protein Research
Osaka University
Kita-ku, Osaka

23) T. Miyazawa, *Spectrochim. Acta*, **16**, 1231, 1233 (1960); *J. Chem. Phys.*, in press.
24) C. H. Bamford, L. Brown, E. M. Cant, A. Elliott, W. E. Hanby and B. R. Malcolm, *Nature*, **176**, 396 (1955).
25) F. H. C. Crick and A. Rich, ibid., **176**, 780 (1955).
* The weak peaks observed in the region 200~280 cm^{-1} are presumably due to water vapor.

The Behavior of Fission Products Captured in Graphite Powder by Nuclear Recoil. IV. Further Studies on the Diffusion of Xenon-133 in Graphite

By Seishi YAJIMA, Sumio ICHIBA, Yuichiro KAMEMOTO, Koreyuki SHIBA and Masaharu KORI

(Received September 3, 1960)

Several papers have been published on the diffusion of fission products in graphite[1-7]. Only artificial graphite in a form similar to a fuel element, a disk or a pellet, was used in those experiments. On the other hand, the authors have studied the diffusion of fission products in many kinds of graphite such as amorphous carbon, artificial graphite, and natural graphite. The diffusion of xenon[6], iodine[7], and tellurium[7] in graphite was previously reported. However, more recent study by the authors suggests that in the determination of activation energy of diffusion in such a complicated material as graphite the use of Fick's law is not entirely satisfactory and that fission products in graphite have many energy states. Consequently, this experiment has been undertaken to determine the diffusion rate of fission product xenon-133 in graphite and the distribution of xenon-133 among such energy states as mentioned above.

Theoretical Consideration

In general, the escape rate v of fission products captured in imperfections with energy E is given by

$$v=-\frac{dn}{dt}=-\int\frac{n(x,y,t)}{a(x,y)}dxdy\,\nu \times\exp[-(E_D+E)/kT] \qquad (1)$$

where

$n(x,y,t)$: number of fission products captured in a small region between x and $x+dx$, and y and $y+dy$.

$a(x,y)$: number of jumps of fission products required to escape from the graphite.

E_D : activation energy of diffusion of fission products.

T : temperature in °K.

ν : frequency of vibration of a fission product in the graphite.

k : Boltzmann constant.

If an isothermal escape rate of a fission product in a sample is determined at T_1,

$$v_1=-\int\frac{n_1(x,y,t)}{a(x,y)}dxdy\,\nu \times\exp[-(E_D+E)/kT_1] \qquad (2)$$

After time t, if T_1 is instantly increased to T_2 and an isothermal escape rate is determined at the temperature,

$$v_2=-\int\frac{n_2(x,y,t)}{a(x,y)}dxdy\,\nu \times\exp[-(E_D+E)/kT_2] \qquad (3)$$

When being extrapolated to t, n_1 is equal to n_2. Then,

$$\ln(v_2/v_1)=\frac{E_D+E}{k}\,\frac{T_2-T_1}{T_1T_2} \qquad (4)$$

or

$$E_D+E=\frac{2.303\,kT_1T_2}{T_2-T_1}\log(v_2/v_1) \qquad (4')$$

When the fission products are caught in imperfection distributed over various energy states of graphite, Eq. 4 must be carefully applied to the calculation of activation energies. As Mugnuson et al.[8] discussed, however, if the difference of temperature T_1 and T_2 is taken as small as possible, the most important activation energy of the diffusion of fission products within the range of T_1 and T_2 is calculated according to Eq. 4.

Experimental

Preparation of Samples.—A mixture of 1 g. of graphite powder and 60 mg. of uranium dioxide was irradiated with thermal neutrons (thermal

1) D. Schulz, "Summary Report for January, February, and March, 1947", ANL-4006, Sec. I. 6, 62 (Oct. 3, 1947).

2) C. A. Smith and C. T. Young, "Diffusion of Fission Fragments from Uranium-Impregnated Graphite", NAA-SR-72 (May 4, 1951).

3) D. Cubicciotti, "The Diffusion of Xenon from Uranium Carbide-Impregnated Graphite", NAA-SR-194 (Oct. 13, 1952).

4) C. T. Young and C. A. Smith, "Preliminary Experiments on Fission Product Diffusion from Uranium-Impregnated Graphite in the Range 1800~2200°C", NAA-SR-232 (March 25, 1953).

5) L. B. Doyle, "High-Temperature Diffusion of Individual Fission Element from Uranium Carbide-Impregnated Graphite", NAA-SR-255 (Sept. 11, 1953).

6) T. Nakai, S. Yajima, K. Shiba, J. Osugi and D. Shinoda, This Bulletin 33, 497 (1960).

7) S. Yajima, S. Ichiba, Y. Kamemoto and K. Shiba, ibid., 34, 493 (1961).

8) G. D. Mugnuson, W. Palmer and J. S. Koehler, *Phys. Rev.*, **109**, 1990 (1958).

neutron flux, about 5×10^{11} neutrons/cm^2/sec.) for five hours in an experimental hole of JRR-1 reactor. After irradiation the mixture was treated with a hot 4 N nitric acid solution to dissolve uranium dioxide and neptunium-239 produced. In order to measure the activity of xenon-133 without any influence of other fission xenon nuclides and iodine-133, the irradiated graphite samples were cooled for four days before use.

Particle sizes of graphite samples used in this experiment and the analytical data on impurities are shown in Table I.

TABLE I. PARTICLE SIZES OF GRAPHITE SAMPLES AND ANALYTICAL DATA OF IMPURITIES

	Sample		
	AG (Artificial graphite)	NG-1 (Natural graphie-1)	NG-2 (Natural graphite-2)
Particle size (micron)	30	1	50
Impurity			
Ash (total)	0.07%	0.3%	0.8%
SiO_2	250 p.p.m.	220 p.p.m.	3700 p.p.m.
Al_2O_3	210	60	3500
Fe_2O_3	130	24	300
MgO	15	24	100
CaO	70	36	300
V_2O_5	—	0.12	0.5
MnO	—	—	—
Na_2O	20	12	25
K_2O	15	12	20
NiO	—	0.06	—
ThO_2	—	2.4	—
CuO	—	—	—
B_2O_5	0.1	0.02	0.5

Determination of Activation Energy.—A flow system is illustrated in Fig. 1. Furnace-C_1 and Furnace-C_2 consisted of an alundum tube with a nichrome winding. The temperature of the furnaces could be increased to 1150°C and kept constant at a temperature with a transformer. The temperature was measured with a platinum-platinum rhodium thermocouple. The temperature of Furnace-C_2 was always kept about 50°C higher than that of Furnace-C_1.

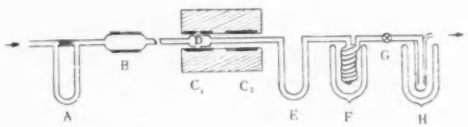

Fig. 1. Flow system.

A Flow meter B Sponge titanium
C_1, C_2 Furnace D Diffusion cell
E Phosphorus pentoxide
F Dry ice trap G Stopcock
H Charcoal trap cooled with dry ice

Each part of the system was made of hard glass except a silica tube in the furnace in which samples were heated, and each part was connected with a polyethylene tube.

Helium gas at a constant flow rate (100 ml./min.) was purified with sponge titanium heated at 800°C to eliminate a trace amount of oxygen. Phosphorus pentoxide was used to remove water in the gas which had swept over a sample. A dry ice trap was set to remove volatile fission products other than rare gases. Xenon-133, which was released, was adsorbed on charcoal cooled with dry ice which was set next to the trap without charcoal. When the charcoal trap was exchanged for a new one at appropriate intervals, a change-over cock was serviceable for the continuous catch of xenon-133 on charcoal.

A typical experiment was as follows. The graphite powder described above was placed in a silica boat which was slid into the silica tube. Then, helium gas was introduced into the system. After confirming that helium gas took the place of air, the tube was slid into Furnace-C_1. The graphite sample was heated at a constant temperature for 30 min. During this period the charcoal trap was exchanged every 5 min. Just 30 min. after the beginning of the heating, the sample together with the tube was slid into Furnace-C_2 whose temperature had been about 50°C higher than that of Furnace-C_1. The trap was exchanged every 2 min. and the sample was heated at a constant temperature for 12 min. The temperature was measured with a platinum-platinum rhodium thermocouple adjacent to the sample. Such a procedure was repeated at a set of increased temperatures.

Making of Heating Curve.—In order to make a heating curve, a graphite sample was heated with a constant increment of temperature and xenon-133 released during a constant period of time was adsorbed on charcoal.

The amount of the released nuclide was plotted versus temperature. The flow system is the same as that shown in Fig. 1 except a furnace and a tube in which a sample was heated. Because the temperature of samples must be continuously increased to temperatures as high as possible, silicon carbide was used as the heater of the furnace.

The sample described above was placed in an alundum boat which was slid into the alundum

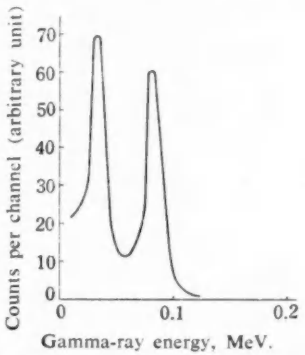

Fig. 2. Gamma-ray spectrum of xenon-133 in a charcoal trap.

tube. Then, helium gas was introduced into the system. After confirming that helium gas took the place of air, the tube was slid into the furnace. The sample was heated with a contsant increment of temperature, 3°C/min. Xenon-133 released was adsorbed charcoal in a trap cooled with dry ice, the trap being exchanged every 10 min.

Activity Measurement.—Activity of xenon-133 adsorbed on charcoal was measured with a RCL 256 channel gamma-ray spectrometer with a well type NaI scintillator (2 inch diameter×1.75). The charcoal was placed in the well, with its trap made of glass, and the activity was measured. The gamma-ray spectrum of xenon-133 is illustrated in Fig. 2.

Results

The absolute value of v_1 and v_2 is not always necessary but the ratio of v_2/v_1 is necessary for determining the activation energy according to Eq. 4. Therefore, when amounts of xenon-133 remaining in graphite are plotted versus diffusion time, the ratio v_2/v_1 is equivalent to a ratio of tangential slopes at a discontinuous point of temperature. A typical plot is shown in Fig. 3. The values obtained from these plots are given in Table II, and the apparent activation energy versus absolute temperature is illustrated in Fig. 4.

Heating curves obtained by another experiment are illustrated in Figs. 5—7. The axis

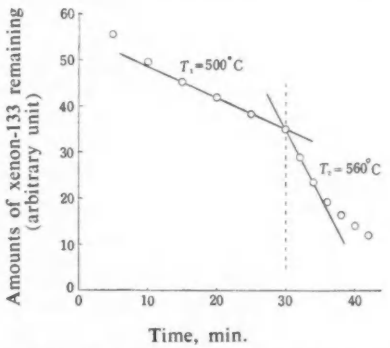

Fig. 3. Isothermal escape rates of xenon-133 in natural graphite-1 at 500 and 560°C.

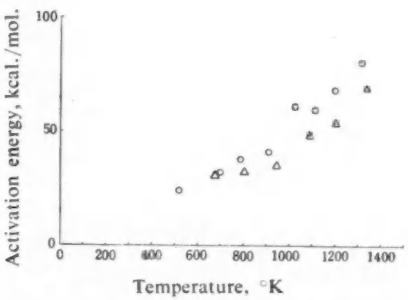

Fig. 4. Apparent activation energy versus temperature.
○ AG △ NG-1

Table II. Activation energies of diffusion of xenon-133 in graphite

AG (Artificial graphite)

T_1 °C	T_2 °C	v_2/v_1	$E+E_D$ kcal./mol.
228	269	5.48	23.3
400	447	4.72	31.3
490	539	4.48	37.4
606	675	6.37	40.6
725	780	4.94	60.7
815	870	3.74	59.2
910	950	2.55	67.7
1023	1082	3.88	80.2

NG-1 (Natural graphite-1)

T_1 °C	T_2 °C	v_2/v_1	$E+E_D$ kcal./mol.
380	418	3.58	30.2
500	560	4.28	32.0
656	696	2.17	34.8
786	840	3.06	48.6
915	956	2.12	53.3
1041	1090	1.81	68.4

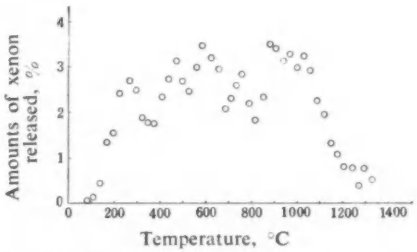

Fig. 5. Heating curve (3°C/min.) of natural graphite-1.

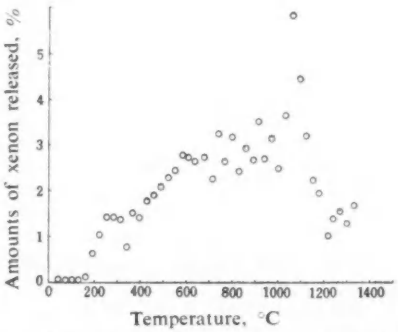

Fig. 6. Heating curve (3°C/min.) of natural graphite-2.

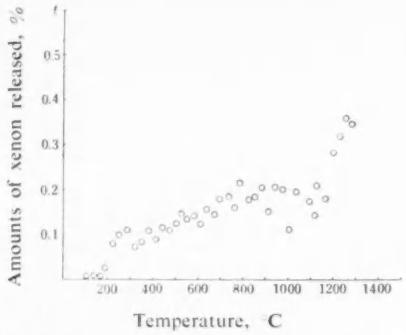

Fig. 7. Heating curve (3 °C/min.) of artificial graphite.

of abscissa is temperature and the axis of ordinate is percent xenon-133 released from graphite every 10 min.

Discussion

In the previous experiment[5], it was observed that the diffusion of xenon consisted of a rapid diffusion and a slow diffusion, and from the latter, the activation energy of the interstitial diffusion was calculated. But it is inadquate to treat the diffusion of xenon in graphite from the slow diffusion alone.

The tendency of the diffusion was observed by Argonne workers[1] and Cubicciotti[3]. The Argonne workers interpreted that there were two mechanisms for the diffusion, a rapid "pore" diffusion and a slow "crystallite" diffusion. However, as pointed out by Cubicciotti, if the above interpretation were correct, there would be a truly rapid diffusion which would eventually give way to a slow diffusion at one temperature; that is, all the rapidly diffusing material would have been gone in a short time and then, an increase in temperature would result in the simple diffusion of the slowly diffusing material. Experimentally, however, it is found that with each increase in temperature there is a rapid escape of xenon. Cubicciotti explains that the initial rapid escape is attributed to a rapid temperature increase of the sample. On the other hand, our experiment on natural graphite-2 showed no striking effect of the rate of temperature increase: the amount (46.3%) of xenon-133 released when the temperature of a graphite sample was increased from room temperature to 800°C in 3 min. and kept constant at 800°C for 90 min. was nearly equal to the amount (41.7%) of xenon-133 released when the temperature of another sample was increased from room temperature to 800°C at a rate of 3°C/min. This fact suggests that the amount of xenon-133 released is mainly determined by a final temperature.

Circles and triangles in Fig. 4 are not on a straight line parallel to the axis of abscissa but on ascending lines, respectively. In other words, the activation energy of the diffusion is not simple but consists of various values, say, 20~40 kcal. at 500 to 1000°K and higher at temperatures over 1000°K. This tendency is the same both in artificial and natural graphite except the fact that the activation energy of diffusion in artificial graphite is a little higher than that in natural graphite.

Heating curves in Figs. 5—7 show the distribution of the amount of released xenon over a wide range of temperature. These figures also indicate the distribution of the energy of xenon in graphite, when the relation shown in Fig. 3 is taken into account. The energy is considered to correspond to E in Eq. 4 because E_D is far smaller than E. From these observations, the fact that the diffusion rate of xenon in natural graphite was greater than that in artificial graphite will be explained as follows. Xenon atoms in natural graphite are distributed more in sites of a low activation energy while xenon atoms in artificial graphite are more in sites of a high activation energy. Therefore, the amount of xenon diffusing out at a temperature is greater in natural graphite than in artificial graphite. Although not studied thoroughly, it is supposed that xenon atoms exist on vacant sites of graphite lattice and that the above mentioned activation energies are determined according to the position of such xenon atoms, because the activation energy of the interlaminar diffusion in graphite is known to be very low. It is obvious by the X-ray diffraction and the electron diffraction methods that artificial graphite is more imperfect than natural graphite. This means that the number of vacancies is larger in artificial graphite than in natural graphite. In this sense, a heating curve is considered to show also the distribution of the vacancies among sites of various energies.

On the basis of discussion described above, a rapid diffusion and a slow diffusion in an isothermal curve are easily interpreted. When a graphite sample is rapidly heated to a certain temperature, a xenon atom existing in a site with an activation energy which corresponds to the temperature diffuses out through the interlaminar space: this is a rapid diffusion. During the maintenance of the temperature, xenon existing in a site with a larger activation energy escapes out with a certain probability: this is a slow diffusion. It is evident that Fick's law can not be applied

to such a system, because the law deals with diffusion only in terms of concentration gradient.

The authors wish to thank Dr. H. Suzuki of Solid State Physics Laboratory of JAERI for helpful discussions.

Division of Chemistry
Japan Atomic Energy Research Institute
Tokai, Ibaraki-ken
(S. Y., S. I., Y. K. & K. S.)

Mitsubishi Atomic Power Industries
Inc. Laboratory
Omiya-shi Saitama-ken
(M. K.)

*Determination of Lanthanum, Samarium and Europium in Manganese Nodules by Neutron Activation**

By Toshi KAWASHIMA, Masumi OSAWA, Yoko MOCHIZUKI and Hiroshi HAMAGUCHI

(Received September 26, 1960)

So far the determination of a trace amount of rare earth elements have primarily been carried out by X-ray fluorometric, emission spectrometric or absorption spectrometric methods; but none of these methods have given satisfactory results. After the atomic pile has become available for wide use, ever growing attention has been paid to the application of radioactivation technique to the determination of many trace elements. A number of reports have proved the validity of the same technique for the determination of a trace amount of rare earth elements because of its selectivity and the high sensitivity.

Brooksbank and Leddicotte[1] determined a number of rare earth elements in biological materials (bones), by making use of the chromatographic separation and successive countings of the eluates after neutron irradiation of the sample. Likewise, Cornish[2] reported the ion exchange separation method. Jakovlev[3] discussed an approach for the determination of the total content of rare earth elements in high purity materials (graphite, beryllium, bismuth and germanium) on the basis of the activity of samarium and europium estimated by analyzing the decay curves, without resorting to chromatographic separation. Nakai et al.[4] reported the determination of dysprosium samarium, and lanthanum in thorium metal and oxide, based on gamma-ray counting of the rare earth fraction obtained by anion exchange separation from the sample irradiated in JRR-1.

Various nuclides are formed when a minute amount of rare earth elements in rocks and meteorites are irradiated with thermal neutrons.

TABLE I. NUCLEAR DATA

Element	Clarke number	Radionuclide	Half life	Activity* dis./sec.
Sc	0.0005	^{46}Sc	85 days	$2.65 \cdot 10^{2}$
Y	0.0028	^{90}Y	64 hr.	$2.3 \cdot 10^{3}$
La	0.0018	^{140}La	40 hr.	$9.0 \cdot 10^{3}$
Ce	0.0046	^{141}Ce	33 days	$3.6 \cdot 10$
		^{143}Ce	33 hr.	$4.1 \cdot 10^{2}$
Pr	0.00055	^{142}Pr	19 hr.	$5.8 \cdot 10^{3}$
Nd	0.0024	^{147}Nd	11.3 days	$6.0 \cdot 10$
		^{149}Nd	2 hr.	$1.9 \cdot 10^{3}$
Sm	0.00065	^{153}Sm	47 hr.	$1.2 \cdot 10^{4}$
Eu	0.00010	^{152}Eu	9.3 hr.	$1.5 \cdot 10^{3}$
Gd	0.00064	^{159}Gd	18 hr.	$7.6 \cdot 10^{2}$
Tb	0.00009	^{160}Tb	73 days	$2.5 \cdot 10$
Dy	0.00045	^{165}Dy	2.3 hr.	$4.7 \cdot 10^{3}$
Ho	0.00011	^{166}Ho	27 hr.	$5.7 \cdot 10^{3}$
Er	0.00025	^{171}Er	7.5 hr.	$6.6 \cdot 10^{2}$
Tm	0.00002	^{170}Tm	120 days	$2.2 \cdot 10$
Yb	0.00027	^{175}Yb	4.2 days	$1.2 \cdot 10^{3}$
		^{177}Yb	1.8 hr.	$6.3 \cdot 10^{3}$
Lu	0.000075	^{177m}Lu	3.7 hr.	$8.3 \cdot 10^{3}$
		^{177}Lu	6.9 days	$8 \cdot 10^{2}$

* A (dps) = Clarke number $\cdot 10^{-2} \cdot Ab.(1/M)6.03 \cdot 10^{23} \cdot \sigma \cdot S$

A: Activity at the end of bombardment
M: Mass number Ab: Isotopic abundance
S: Saturation factor: $(1-e^{-\lambda t})$, $t = 10$ hr.
σ: Neutron capture cross section.

* Presented at the 12th Annual Meeting of the Chemical Society of Japan, Kyoto, April, 1959.

1) W. A. Brooksbank and G. W. Leddicotte, *J. Phys. Chem.*, **57**, 819 (1953).

2) F. W. Cornish, *Brit. Atomic Energy Research Establishment Rept.*, AERE C/R-1224 (1953).

3) J. V. Jakovlev, *Proceedings of International Conference on Peaceful Uses of Atomic Energy, Geneva*, 1955, Paper 632 (USSR), Vol. 15, pp. 54–59; *Anal. Abstr.*, **4**, 1112 (1957).

4) T. Nakai et al., Presented at the 2nd symposium on radiochemistry, Kyoto, Nov., 1958.

Then, the nature and activity of the induced radionuclides which come into question when 1 g. of sample containing rare earth elements in its normal natural abundance ratio is irradiated for 10 hr. with thermal neutrons of its intensity of 10^{11} n/cm^2/sec., are shown in Table I. These radionuclides would decay according to Fig. 1. It is clear that the nuclides which should be considered are lanthanum-140, samarium-153, europium-152 and yttrium-90 when as long as 20 hr. are needed for chemical processing after the end of irradiation.

The gamma ray spectrum of the rare earth fraction would then be considered to be the sum of photopeaks produced by X-rays which are induced by K electron capture, and compton continuums, and photopeaks produced by complete gamma ray absorption and bremsstrahlungs induced by β-rays which are emitted by lanthanum, samarium, europium and long lived nuclides. Therefore, the decay curve obtained by measuring the activity at a fixed base bias under the same counting conditions is expected to be analyzed into a few components. The present paper reports the determination of lanthanum, samarium, and europium in manganese nodules by means of a comparison method based on the counting rate of the respective components analyzed as above.

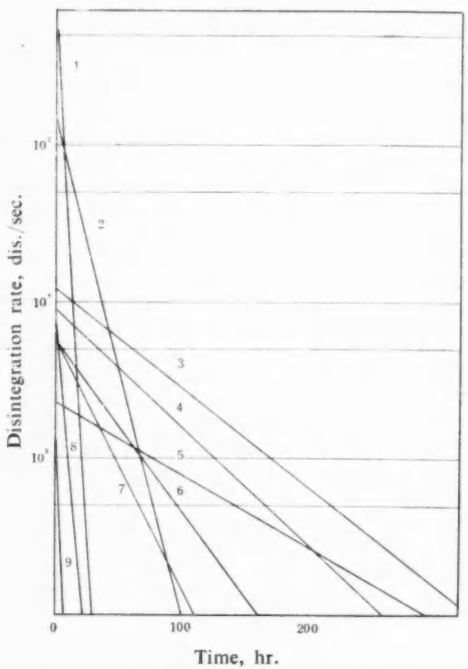

Fig. 1. Relative activities of rare earth radionuclides.

1: 2.3 hr. Dysprosium-165
2: 9.3 hr. Europium-152
3: 47 hr. Samarium-153
4: 40 hr. Lanthanum-140
5: 64 hr. Yttrium-90
6: 27 hr. Holmium-166
7: 19 hr. Praseodymium-142
8: 3.7 hr. Lutetium-177m
9: 1.8 hr. Ytterbium-177

Experimental

Reagents and Samples. — Standard solutions of lanthanum, samarium and europium were prepared by dissolving respective metal oxides in nitric acid. The purity of these oxides listed by Johnson Mathey, was 99.99% for samarium oxide and 99.9% for europium and lanthanum oxides. These reagents were proved to be radiochemically pure by the activation analysis. Uranyl acetate (Merck) solution was used for the standard of uranium. All other chemicals used in this work were of c. p. or reagent grade.

Manganese nodule samples were offered by Professor E. D. Goldberg, Scripps Institution of Oceanography, La Jolla, California, to whom our thanks are due.

Irradition.—Manganese nodule samples of from 200 to 500 mg. were sealed in a silica tube and irradiated along with neutron monitors in the Japan Research Reactor-1 (JRR-1). The reactor was homogeneous, enriched uranium, water moderated and cooled type, and had a neutron flux of around $2\sim3\times10^{11}$ n/cm^2/sec. The flux monitors were prepared by evaporating a known amount (102, 3.5 and 0.35 μg) of lanthanum, samarium and europium in a silica tube or impregnating it into a filter paper wrapped in a vinyl bag. The irradiation lasted intermittently for 2~3 days, 5 hr. each day.

Chemical Separation.—After neutron irradiation and a suitable decay time (about one day), the manganese nodule was dissolved in aqua regia. Any residue was fused with sodium peroxide, dissolved in hydrochloric acid, and added to the main solution. An aliquot of the solution (1/10 of the total volume) was used for the determination of the rare earth elements, and the remainder of the solution was reserved for the determination of elements other than the rare earths. Twenty milligrams of lanthanum carrier was added to the pipetted aliquot and the rare earth activity was carried down with lanthanum fluoride precipitate by adding hydrofluoric acid to the solution. Further purification was achieved by going through the standard lanthanum fluoride cycle[5] three times. The final lanthanum hydroxide precipitate which was decontaminated from any activities other than those of the rare earth elements was then dissolved in hydrochloric acid and diluted to a known volume. An aliquot of this solution was used for γ-ray counting and the remainder for the determination of the

5) N. E. Ballou, "National Nuclear Energy Series, Radiochemical Studies: The Fission Products, Book 3", McGraw-Hill Book Co., Inc., New York (1953), p. 1673.

chemical yield by a conventional gravimetric method[6].

Counting. — The γ-rays and X-rays from the induced radioactive rare earth nuclides were detected and analyzed with the manual sweep scintillation spectrometer (Atomic Instrument Co., Model 510) equipped with a well type*, 1¾ in. by 2 in., sodium iodide (Tl) scintillation crystal. The quantitative analysis for each rare earth element was made by comparing the lanthanum-140, samarium-153 and europium-152 activities of rare earth fraction which is separated from the irradiated manganese nodules with the correspondingly irradiated monitor of the respective element, after measuring the activity of each of the nuclides as mentioned later. Decay measurements of the rare earth activities from the manganese nodule samples and the flux monitors gave the same half-life for each nuclide.

Results and Discussion

The γ-ray spectrum of the rare earth fraction chemically separated and purified is shown in Fig. 2. Individual γ-ray spectra of lanthanum, samarium and europium obtained by the separate irradiation of the respective elements are shown in Fig. 3. These were measured at a channel width of 1 V. with the well type single channel scintillation spectrometer mentioned above. In this work, the counting rate at the peaks of 0.02, 0.09 and 0.5 MeV. for each sample were measured under exactly the same conditions.

Determination of the Lanthanum, Samarium and Europium Activities. — The activity of the rare earth fraction at the peak of 0.5 MeV. is attributed to 40 hr. lanthanum-140 plus long-lived components (Figs. 2 and 3). Therefore, the activity of lanthanum-140 at a given time can be determined by graphical analysis of the

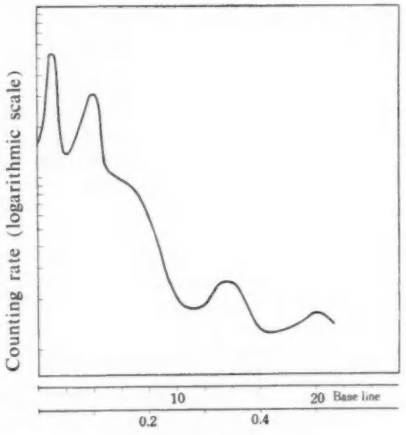

Fig. 2. Gamma-spectrum due to rare earth activities separated from neutron irradiated manganese nodule.

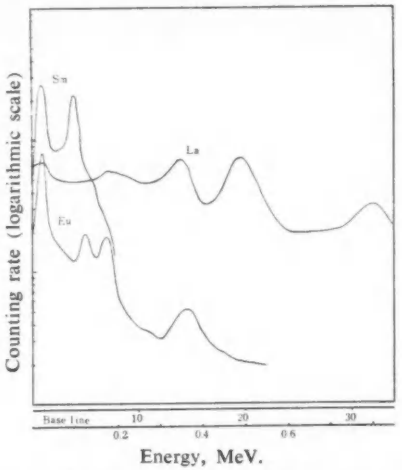

Fig. 3. Gamma-spectra of lanthanum-140, samarium-153 and europium-152.

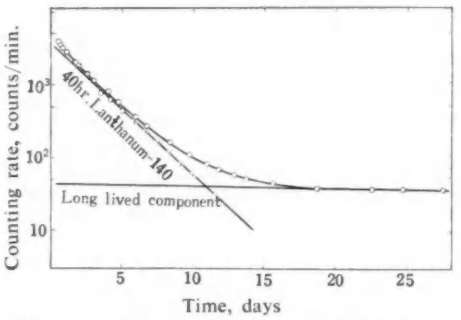

Fig. 4. Analysis of decay curve for the determination of lanthanum.

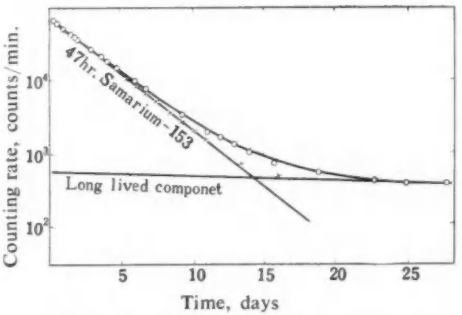

Fig. 5. Analysis of decay curve for the determination of samarium.

6) W. F. Hillebrand, E. F. Lundell, H. A. Bright and J. I. Hoffman, "Applied Inorganic Analysis", 2nd ed. John Wiley & Sons, Inc., New York (1953), p. 550.

* Hole 17mmϕ×80mm, covered with aluminium can.

TABLE II. LANTHANUM, SAMARIUM AND EUROPIUM CONTENT OF MANGANESE NODULES (p. p. m.)

Sample	Location	Depth, m.	La	Sm	Eu
Horizon Guyot MP 26 A-3	19°N 169°W	1440~1540	234	33	9.6
			201	24	7.7
			270	35	9.4
			av. 235	av. 31	av. 8.9
Horizon Guyot MP 25 F-2	19°N 170°W	1870~1920	250	40	11.0
			378	60	19.6
			av. 314	av. 50	av. 15.3
Horizon Nodule	40°N 155°W	5500	357	108	19.6
			250	62	16.6
			av. 303	av. 85	av. 18.1

decay curve, a typical one of which is given in Fig. 4.

Just as in the case of lanthanum mentioned above, the activity of 47 hr. samarium-153 is estimated based on the decay curve at the 0.09 MeV. peak, as shown in Fig. 5.

The activity of around 0.025 MeV. peak is the sum of activities due to europium-152, lanthanum-140, samarium-153 and longer-lived nuclides (Figs. 2 and 3). Therefore, the activity of the 9.3 hr. europium-152 component can be analyzed by the graphical analysis of the decay curve at the peak, an example of which is shown in Fig. 6. If the activity of long-lived component (curve B) plus 40 hr. lanthanum-140 component (curve C) is deducted from the gross decay curve A, we obtain the curve D which corresponds to the composite of the activity of europium and samarium. Here the contribution of lanthanum-140 component (curve C) is calculated by the experimentally determined ratio of the counting rate at the peak of around 0.025 MeV. to that of 0.5 MeV. (the ratio is around 1, see Fig. 3). By analyzing the curve D, the decay curve of 9.3 hr. europium-152, curve E, is obtained.

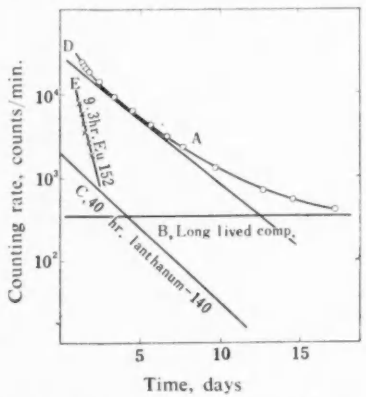

Fig. 6. Analysis of decay curve for determination of europium.

Determination of Lanthanum, Samarium and Europium in Manganese Nodules.—The amounts of lanthanum, samarium and europium in the sample are estimated by comparing the activities of each of the nuclides of the sample determined as above with that of the respective monitor. The results are summarized in Table II.

A possible interference of fission products of uranium in the manganese nodules should be taken into consideration, since lanthanum-140, samarium-153, and many other rare earth nuclides are produced by slow neutron fission of uranium. The interference should not be disregarded particularly in the case of lanthanum-140, because of the high fission yield of mass 140 chain. An experiment to examine this interference was performed by separating and measuring the fission product rare earths from an irradiated known amount of uranium. The uranium assay was carried out by utilizing the activity of fission product barium-140, on an aliquot of the reserved solution mentioned earlier. It was found that the interference with fission product rare earths from the uranium in the samples was negligibly small*.

The overall reproducibility of the method for manganese nodule samples is shown to be about 10~20%. Additional runs would probably increase the reproducibility of the method. As for the sensitivities of the method, as little as 1, 0.02 and 0.01 μg of lanthanum, samarium and europium respectively, could be detemined under the present experimental conditions.

Goldberg and Arrhenius[7], and also Young[8] gave 140 and 220 p.p.m. lanthanum respectively as the average for Pacific pelagic sediments by spectroscopic method. Our data indicate a

* The result of uranium assay will be reported in a later paper. Tatsumoto and Goldberg (*Geochim. et Cosmochim. Acta*, **17**, 201 (1959)) gave 3.9, 3.6, 3.6 p.p.m. in Horizon Nodule by a spectrophotometric method.

7) E. D. Goldberg and G. O. S. Arrhenius, *Geochim. et Cosmochim. Acta*, **13**, 153 (1958).

8) E. J. Young, *Bull. Geol. Soc. Amer.*, **65**, 1329 (1954).

somewhat higher lanthanum content of the manganese nodules than pelagic sediments.

The relative abundance of the three elements was calculated for the three manganese nodules, which are tabulated in Table III. For reference,

TABLE III. RELATIVE ABUNDANCE OF LANTHANUM, SAMARIUM AND EUROPIUM

	Sample	Relative abundance		
		La	Sm	Eu
1a	Horizon Guyot MP 26 A-3	1	0.13	0.038
1b	Horizon Guyot MP 25 F-2	1	0.16	0.049
1c	Horizon Nodule	1	0.28	0.060
2	Crustal rocks (Clarke No.)	1	0.33	0.056
3	Cosmic* (Suess, Urey)	1	0.332	0.093

* Atomic abundance ratio

the abundance ratio of the three elements for crustal rocks, and the cosmic abundance ratio as given by Suess and Urey[9] are also included in Table III. It is seen that no essential differences in the relative abundance of the three rare earth elements are observed among the three different types of materials.

9) H. E. Suess and H. C. Urey, *Revs. Mod. Phys.*, **28**, 53 (1956).

Summary

The gamma spectrometric method has been developed for simultaneous determination of microgram amounts of lanthanum, samarium and europium without chemical separation of each other. The method was based on the chemical separation of rare earth mixtures from neutron irradiated samples and subsequent γ-ray scintillation counting of the isolated rare earth fractions. The sample was irradiated for 2~3 days, 5 hr. each day, in the nuclear reactor JRR-1 at a flux of the order of 10^{11}n/cm^2/sec. The rare earth mixture purified by lanthanum fluoride cycles was used for γ-ray counting at a given pulse height peak. The activity of each component could be evaluated by resolving the decay curves obtained, and the amount calculated by comparing the activity with that of each monitor.

We wish to express our hearty thanks to the staff of the Radiochemistry Group, Japan Atomic Energy Research Institute, for their help in making the irradiation. A part of the expense was defrayed from the Ministry of Education, to which our thanks are due.

Department of Chemistry
Tokyo University of Education
Koishikawa, Tokyo

Photoconductivity of Zinc Oxide under Different Ambient Conditions

By Hiroshi KOKADO, Eiichi INOUE, Takashi YAMAGUCHI and Kenji TAKAHASHI

(Received October 28, 1960)

The existence of a close relationship between photoconduction and oxygen desorption process of zinc oxide has been made clear in some details since Bevan and Anderson's work[1]. The oxygen adsorbed on the surface of zinc oxide seems to produce an acceptor level for conduction electrons and to make a depletion layer under the surface. Destruction of the depletion layer or further formation of the space change layer[2] takes place accompanied by absorption of light, its wavelength is shorter than 4000 Å, and it yields a number of conduction electrons. This model well interprets the peculiarities of the photoconductive process of zinc oxide. Then, one can anticipate that the adsorption of other molecules than oxygen on a surface of zinc oxide too may give a similar or to some extent different effect on the dark- and photo-conduction of the material, depending upon the character of the adsorbant[3].

We have studied the effects of several kinds of ambient molecules on the surface conductivity of zinc oxide at room temperature. The

1) D. J. W. Bevan and J. S. Anderson, *Discussions Faraday Soc.*, No. 8, 238 (1950); D. B. Medved, *J. Chem. Phys.*, **28**, 870 (1958); D. A. Melnick, ibid., **26**, 1136 (1957); W. Ruppel, H. J. Gerritsen and A. Rose, *Helv. Phys. Acta*, **30**, 495 (1957).

2) R. J. Collins and D. G. Thomas, *Phys. Rev.*, **112**, 388 (1958).

3) V. I. Lyahenko and O. V. Snitko, *Trudy Inst. Fiz., Akad. Nauk, Ukr. USSR*, **91**, 1071 (1953); E. K. Putseiko and A. N. Terenin, *Doklady Akad. Nauk SSSR*, **101**, 645 (1955), *Problemy Kinetiki i Kataliza, Akad. Nauk SSSR*, **8**, 53 (1955).

specimens (ca. 20 μ in thickness) were made by depositing zinc oxide powder (Merck's reagent) from an ethanolic suspension on glass plates of 18×18 mm. in size. They possess parallel electrodes that are separated from each other by a gap of 5 mm. Silver paste was used as the electrode material. These specimens showed the values of $10^5 \sim 10^6$ times the initial conductivities measured in air ($10^{-11} \sim 10^{-13}$ ohm^{-1} for 20 V. of applied voltage) when they were kept in vacuum to remove the oxygen adsorbed on the zinc oxide layer. After this treatment, the gases or vapors were introduced onto the specimens and the dark currents were observed after 10 min.

The curves in Fig. 1 show the typical effect of an acceptor (O_2), a donor (NH_3) and a neutral (CO_2) type molecule on the dark

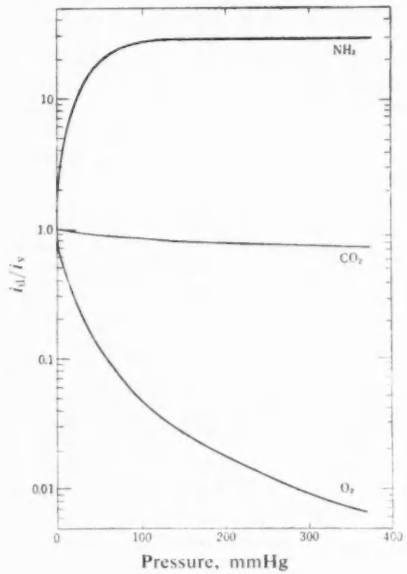

Fig. 1. Influence of the ambient gas on the dark conductivity of zinc oxide.
i_d: Dark current in the gas
i_v: Dark current in vacuum

conductivity. Ammonia was found to be effective on the electronic properties not only in vacuum but in atmospheric air. By pumping the ambient molecules off, the conductivity was unchanged in the case of oxygen, but in the case of ammonia, it returned to the initial value approximately. The behavior of nitrogen was quite similar to that of carbon dioxide and also methylamine to ammonia; otherwise the following three gases behaved as an acceptor type molecules; nitrogen oxide, nitrogen dioxide and methyl ethyl ketone (MEK). However, in the case of MEK, the conductivity was increased partly by taking it off. This seems to suggest that the nature of the adsorption was of somewhat different. Vapors of water, diethyl ether and ethyl alcohol did not change or slightly changed the conductivity of the zinc oxide cell.

As to the photoconductive sensitivity (i_p/i_d in Table I), a remarkable increase was found by adsorption of the electronegative gases such

TABLE I

Gas or vapor	Pressure mmHg	i_d/i_v	i_p/i_d	Decay
O_2	44	$\sim 10^{-2}$	$\sim 10^2$	rapid
NO	45	3×10^{-5}	$10^3 \sim 10^4$	rapid
NO_2	0.3	$<3\times10^{-5}$	$\sim 10^2$	very rapid
MEK	47	$10^{-2} \sim 10^{-3}$	2×10^2	slow
Vacuum	—	—	2~ 3	very slow
CO_2	114	1	2~ 3	very slow
NH_3	42	~10	2~ 3	slow
Pyridine	7.5	$10^{-2} \sim 10^{-4}$	—	—

i_v: Dark current in vacuum
i_d: Dark current in gas or vapor
i_p: Photocurrent in gas or vapor for 10^{12} photons/cm^2 sec. of 3650 Å light from an ultra-high pressure mercury lamp

as oxygen, nitrogen oxide and nitrogen dioxide, while no change was observed by adsorption of carbon dioxide or ammonia type molecules. In Table I, the results of qualitative observations on the rate of current decay after ceasing an irradiation on the cell were also tabulated. It is noteworthy that there exists a parallelism between the chemical activity of the ambient molecules and the rate of the decay process. The active electrons of these molecules may play an important role in the adsorption

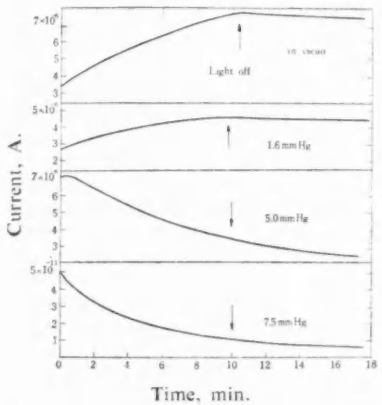

Fig. 2. Photoresponses of the conductivity of zinc oxide in pyridine vapor.

mechanism. MEK having no such active electrons, has only a weak effect to accelerate the decay[4].

The effect of aromatic and aliphatic hydrocarbons and also pyridine on the conductivity of zinc oxide were found to be rather obscure; the conductivity decreased by adsorption of these organic compounds. However, the irradiation on this system did not change the value of its conductivity; it monotonically decreased when an electric field was applied for measurement. This effect was more noticeable if the vapor pressure was increased, as shown in Fig. 2. The nature of this strange phenomenon is not yet clear.

4) By adsorbing ammonia or another donor type molecule too, a little higher decay rate is observed, associated with a greater density of recombination centers, with a greater capture cross section for the recombination, or with both (R. H. Bube, *Phys. Rev.*, **101**, 1668 (1956)).

Graphic Engineering Laboratory
Tokyo Institute of Technology
Meguro-ku, Tokyo

---

*On the Fluorine Shift of Aromatic Fluorine Compounds**

By Teijiro YONEZAWA, Kenichi FUKUI, Hiroshi KATO, Hisao KITANO, Shuzo HATTORI and Shinichiro MATSUOKA

(Received October 24, 1960)

Numerous experimental data on fluorine chemical shifts of various organic compounds have been presented[1-5]. To explain the general trend of these shifts, some empirical interpretations based upon the electronegativity of the atom to which the fluorine is bonded[2], and upon the Hammett constant of a substituent in fluorobenzene have been proposed[3]. These interpretations, however, rest upon no clear basis of electronic configuration around the nucleus.

Ramsey[6] has derived a general expression of nuclear magnetic shielding constant, σ, in a molecule which has no orbital or spin angular momentum and contains only one nucleus of non-zero magnetic moment. The nuclear magnetic shielding is written by his expression

$$A_{v_\lambda}\sigma = \left(\frac{e^2}{3mc^2}\right)\left(0\left|\sum_k \frac{1}{r_k}\right|0\right) - 2A_{v_\lambda}\left[\sum_{n_\lambda'} \frac{1}{E_n - E_0}\left\{(0_\lambda|\sum \mathbf{m}^0{}_{kz}|n_\lambda')\times\left(n_\lambda'\left|\sum_k \frac{\mathbf{m}^0{}_{kz}}{r_k{}^3}\right|0_\lambda\right) + \left(0_\lambda\left|\sum_k \frac{\mathbf{m}^0{}_{kz}}{r_k{}^3}\right|n_\lambda'\right)(n_\lambda'|\sum_k \mathbf{m}^0{}_{kz}|0_\lambda)\right\}\right] \quad (1)$$

where r_k is the distance between the kth electron and the nucleus in question, A_{v_λ} implies an average over all molecular orientations, each of which is specified by the subscript λ; and $\mathbf{m}^0{}_{kz}$ is the z component of the operator for the kth electron

$$\mathbf{m}^0{}_k = \left(\frac{ieh}{4\pi mc}\right)(\mathbf{r}_k \times \nabla_k) \quad (2)$$

The application of this formula to calculate the nuclear magnetic shielding of the nucleus in a complex molecule has been considered to be almost impossible due to the lack of our knowledge of the energies and wave functions of all excited states. Furthermore, as Ramsey[6] pointed out, the formula contains many terms which cancel each other, and this might bring about a considerable error in the numerical calculation.

An important contribution to develop the procedure of obtaining shielding constants was proposed by Saika and Slichter[7]. According to them the screening was divided into three terms.

1. The diamagnetic correction for the atom in question.

* This study was presented at the Symposium on Electronic Structures of Molecules, Tokyo, September, 1959.

1) L. H. Meyer and H. S. Gutowsky, *J. Phys. Chem.*, **57**, 481 (1953).

2) H. S. Gutowsky and C. J. Hoffman, *J. Chem. Phys.*, **19**, 114 (1951).

3) H. S. Gutowsky, D. W. McCall, B. R. McGarvey and L. H. Meyer, *J. Am. Chem. Soc.*, **74**, 4509 (1952).

4) T. Isobe, K. Inukai and K. Ito, *J. Chem. Phys.*, **27**, 1215 (1957); This Bulletin, **33**, 315 (1960).

5) K. Fukui, S. Hattori, T. Yonezawa, R. Kusaka and H. Kitano, *J. Chem. Soc. Japan, Pure Chem. Sec.* (*Nippon Kagaku Zasshi*), **80**, 541 (1959).

6) N. F. Ramsey, *Phys. Rev.*, **78**, 699 (1950).

7) A. Saika and C. P. Slichter, *J. Chem. Phys.*, **22**, 26 (1954).

2. The paramagnetic term for the atom in question.

3. The contribution from other atoms.

Based upon these divisions, they concluded that the F^{19} nuclear magnetic shielding is mainly determined by the paramagnetic contribution of the electrons belonging to the fluorine atom in question. This conclusion was shown to be successful in calculating the chemical shift between HF and F_2. The equation developed by them remained, however, only available for evaluating fluorine shifts in some aliphatic compounds. Further application of their procedure to fluorine shifts in aromatic compounds seems never to have been attempted.

In the present paper, an extension of their analysis to more complex conjugated compounds is presented by using a molecular orbital treatment.

Theoretical

The second order paramagnetic term of Ramsey[6] is approximated referring to the treatment by Saika and Slichter[7]. In the present paper, we have chosen the coordinate system of Fig. 1 whose origin is set at the

Fig. 1. The coordinate system adopted in the present treatment.

fluorine atom in question. Considering the paramagnetic contribution of electrons belonging to the fluorine, the paramagnetic shielding term, σ_p, in a conjugated molecule can be given by the mean of three principal components as

$$\sigma_p = \frac{1}{3}(\sigma_{l-\pi} + \sigma_{l-\sigma} + \sigma_{\sigma-\pi}) \tag{3}$$

These three components are obtained as

$$\begin{aligned}
\sigma_{l-\pi} &= -\left(\frac{eh}{2\pi mc}\right)^2 \left\langle \frac{1}{r^3} \right\rangle \sum^{\text{unocc}} \frac{2}{\varepsilon_i - \varepsilon_l} (c_F^l)^2 \\
\sigma_{l-\sigma} &= -\left(\frac{eh}{2\pi mc}\right)^2 \left\langle \frac{1}{r^3} \right\rangle \frac{2}{\varepsilon_\sigma^* - \varepsilon_l} (a^*)^2 \\
\sigma_{\sigma-\pi} &= -\left(\frac{eh}{2\pi mc}\right)^2 \left\langle \frac{1}{r^3} \right\rangle \left[\sum_i^{\text{unocc}} \frac{2}{\varepsilon_i - \varepsilon_\sigma} \right. \\
&\quad \times \left\{ a^2 (c_F^i)^2 + \sqrt{\frac{2}{3}} abc_1^i c_F^i \right\} \\
&\quad \left. + \sum_j^{\text{occ}} \frac{2}{\varepsilon_\sigma^* - \varepsilon_j} \left\{ (a^*)^2 (c_F^j)^2 + \sqrt{\frac{2}{3}} a^* b^* c_F^j c_1^j \right\} \right]
\end{aligned} \tag{4}$$

respectively, where $\langle 1/r^3 \rangle$ is the average of $1/r^3$ for 2p electron of fluorine, ε_i and ε_l are the energies of the i th π molecular orbital and of the lone pair electrons of the fluorine atom, c_F^i and c_1^i are the coefficients of the i th π electronic LCAO MO, whose energy is $\alpha + \lambda_i \beta$, at the fluorine atom and its adjacent carbon atom, and $\sum^{\text{occ}}$, $\sum^{\text{unocc}}$ indicate summation over all occupied and unoccupied orbitals, respectively. The wave functions of bonding and antibonding C–F σ orbitals, φ_σ and φ_σ^*, whose energies are denoted by ε_σ and ε_σ^* in Eq. 4, respectively, may be expressed by the following linear combinations of two atomic orbitals, χ_F and χ_C, which are the 2p σ AO of fluorine and the sp^2 hybridized orbital of the adjacent carbon atom*.

$$\left.\begin{aligned} \varphi_\sigma &= a\chi_F + b\chi_C \\ \varphi_\sigma^* &= a^*\chi_F + b^*\chi_C \end{aligned}\right\} \tag{5}$$

The coefficients a, b, a^* and b^* are those appearing in Eq. 4. Three components in the right side of Eq. 3, $\sigma_{l-\pi}$, $\sigma_{l-\sigma}$ and $\sigma_{\sigma-\pi}$, can be obtained, as is shown by Eq. 4, by calculating the matrix elements in Eq. 1 between the ground state and the various singlet excited states resulting from one electron transition between MO's designated by each subscript, l, σ and π, denoting the orbital of fluorine lone pairs, C–F σ orbitals and π molecular orbitals, respectively. In the last component $\sigma_{\sigma-\pi}$ which appears only when the π conjugation takes place, the cross term arises from the circumstances that we take account of matrix elements of χ_C and π AO on the adjacent carbon atom in $(0|\mathbf{m}^0_{ky}|n)$ and neglect $(0|\mathbf{m}^0_{ky}/r_k^3|n)$ terms on that carbon, as was done in Ref. 7. Equation 3 is easily shown to coincide with the equation given by Saika and Slichter[7] when one considers that no conjugation takes place. It can be shown also, that Eq. 3 in the present paper is also derivable by an alternative procedure proposed by Pople[8], in which attention was paid to the paramagnetic shielding resulting from the local paramagnetic current of the fluorine.

In the present paper, a chemical shift parameter, δ, is defined as

$$\delta = \frac{H_r - H_c}{H_r} \tag{6}$$

where H_r and H_c are the resonance field for the reference compound and the sample compound, respectively.

The chemical shift, δ, can be represented in terms of the paramagnetic shielding constant obtained by Eq. 3 whenever σ is small and the change of diamagnetic shielding constant can be neglected. Thus the shift between the

* χ_C is written as $\sqrt{1/3}\chi_s + \sqrt{2/3}\chi_{2p\sigma}$, where χ_s and $\chi_{2p\sigma}$ are 2_s and $2_{p\sigma}$ AO's of carbon atom, respectively.

8) J. A. Pople, *Proc. Roy. Soc.*, A239, 541, 550 (1957).

compound in question and the reference one can be expressed as*1

$$\delta = \delta_p(\text{reference}) - \sigma_p(\text{sample}) \tag{7}$$

Numerical Calculation

In order to carry out calculation, the information on the energies of the molecular orbitals and the coefficients involved in Eq. 4 is indispensable. The π molecular orbital energies and the coefficients are settled by the simple LCAO MO method. The values of the Coulomb integrals and the resonance integral representing the characteristics of a fluorine atom and a carbon atom adjacent thereto are taken as

$$\left.\begin{aligned} \alpha_F &= \alpha + 1.8\beta \\ \alpha_{adj} &= \alpha + 0.18\beta \\ \beta_{C-F} &= 0.8\beta \end{aligned}\right\} \tag{8}$$

where α is the Coulomb integral of a carbon atom and β is the resonance integral for a C–C bond in a benzene molecule. The values of α and β are taken to be -7.25 eV. and -2.3 eV., respectively, in numerical calculation*2. Other Coulomb and resonance integrals used for amino and nitro groups in the present calculation are as follows:

$$\alpha_{-NH_2} = \alpha + 0.4\beta$$
$$\beta_{C-NH_2} = 0.4\beta$$
$$\alpha_N = \alpha + \beta$$
$$\alpha_O = \alpha + \beta$$

Since the simple LCAO MO studies for a σ electron system have not been sufficiently copious for providing reliable numerical values of various parameters, an attempt to estimate these parameters is necessary for our calculation. Hereupon, the values of Coulomb and resonance integrals are determined on the basis of some experimental data in the following way. At first, the energies of σ-bonding and antibonding orbitals for the reference compound are put to -14 eV. and -4 eV., respectively. The energy of bonding orbital is equal to the absolute value of ionization potential of an electron localized in a C–F bond in methyl fluoride assigned by McDowell[9]. The energy of the antibonding orbital is estimated by the spectroscopic data on other methyl halides. The molecular orbital coefficients, a and b, are determined from the magnitude of the bond moment, μ, with the aid of simplified formulas*3

$$\mu = \frac{\lambda^2 - 1}{1 + \lambda^2} eR$$
$$a = \frac{-\lambda}{(1+\lambda^2)^{1/2}} \tag{9}$$
$$b = \frac{1}{(1+\lambda^2)^{1/2}}$$

where R is a C–F bond distance, e is the charge of an electron, and $\lambda(\lambda > 0)$ is a coefficient representing the polarity of the molecular orbital. The bond moment, μ, is adopted as 1.51 D and C–F distance as 1.39 Å. Inserting these values into Eq. 9, we obtain: $a = -0.783$ and $b = 0.622$*4. The coefficients a^* and b^* are then obtained as 0.622 and -0.783, respectively.

Coulomb and resonance integrals in a C–F σ electron system might be determined in such a way that in solving the secular determinant these integrals give the values of energies and orbital coefficients estimated above. It may be more reasonable, then, to consider that, as the character of the C–F σ bond alters according to the change of molecular structure, the values adopted for the integrals may change. In this connection it may be recollected that in π electron approximation a π electron is considered to move in a resultant electric field from all other π electrons and the σ skeleton. Hence, in the treatment of σ electrons, the electronic structure is naturally recognized to be affected by π electronic distribution conversely.

Referring to the facts stated above, the Coulomb and resonance integrals available for a C–F σ electron system are expressed as*5

$$\left.\begin{aligned} h_{FF} &= -10.16 - \gamma_F(q_F^0 - q_F) \\ h_{CC} &= -7.84 - \gamma_C(q_C^0 - q_C) \\ h_{CF} &= +4.84 \text{*}6 \end{aligned}\right\} \tag{10}$$

*1 The shielding constant σ is represented by the sum of diamagnetic and paramagnetic shielding constant σ_d, σ_p as $\sigma = \sigma_d + \sigma_p$. Then the shift becomes $\delta = \{\sigma_d(\text{reference}) - \sigma_d(\text{sample})\} + \{\sigma_p(\text{reference}) - \sigma_p(\text{sample})\}$. Neglecting the first term, we obtain Eq. 7.

*2 These values are determined so that the calculated highest occupied orbital energy of fluorobenzene ($\alpha + 0.8441\beta$) becomes equal to the negative value of ionization potential of the compound, 9.19 eV. (V. J. Hammond, W. C. Price, J. P. Teeganand and A. D. Walsh, *Faraday Soc. Discuss.*, **9**, 53 (1950)). The value of α is not so unreasonable compared with the value -7.18 eV. adopted by Mulliken (*Phys. Rev.*, **74**, 736 (1948)). The value of β is equal to that determined by Pariser and Parr (*J. Chem. Phys.* **21**, 767 (1953)).

9) C. A. McDowell and B. A. Cox, *Proc. Roy. Soc.*, **A241**, 194 (1957).

*3 Cf. C. A. Coulson, "Valence", Oxford Univ. (1952), p. 103; In the present formulas, the overlap integral is neglected.

*4 The minus sign of a is determined so as to correspond with the coefficient of bonding σ MO in the present coordinate system (see Fig. 1).

*5 These equations resemble those used in a semi-empirical SCF treatment carried out in a π electron system. (Cf. e. g., R. S. Mulliken et al., *J. Am. Chem. Soc.*, **76**, 4770 (1954)). The present procedure, however, represents a reciprocal interaction of σ electrons with π electrons in a bond.

*6 The exchange integral is taken to be positive since the overlap integral between carbon and fluorine AO's in a C–F σ bond is found to be negative in the present coordinate system (see Fig. 1).

TABLE I. TOTAL π ELECTRON DENSITY, σ-ELECTRONIC ENERGY AND MOLECULAR ORBITAL COEFFICIENT

	q_F	q_C	ε_σ	ε_σ^*	ε_l	a^2	b^2
	1.9330	1.0204	−13.977	−4.023	−10.000	0.6166	0.3834
	1.9318	1.0196	−13.993	−4.033	−10.024	0.6176	0.3824
	1.9306	1.0216	−14.008	−4.043	−10.048	0.6187	0.3813
	1.9268	1.0162	−14.057	−4.075	−10.124	0.6220	0.3780
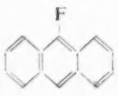	1.9198	1.0128	−14.147	−4.132	−10.264	0.6283	0.3717

TABLE II. TOTAL π ELECTRON DENSITY, σ-ELECTRONIC ENERGY AND MOLECULAR ORBITAL COEFFICIENT

	q_F	q_C	ε_σ	ε_σ^*	ε_l	a^2	b^2
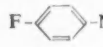	1.9204	0.9686	−14.173	−4.183	−10.252	0.6235	0.3765
	1.9330	1.0204	−13.977	−4.023	−10.000	0.6166	0.3834
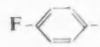	1.9344	1.0342	−13.949	−3.995	− 9.972	0.6165	0.3835
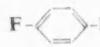	1.9352	1.0410	−13.934	−3.987	− 9.956	0.6164	0.3836

TABLE III. CALCULATED SHIELDING CONSTANTS AND CHEMICAL SHIFTS

	$-\sigma_{l-\sigma}$	$-\sigma_{l-\pi}$	$-\sigma_{\sigma-\pi}$	$-\sigma_p$	δ_{calcd}	δ_{obs} [a]
	165.398	15.761	146.921	1/3×328.080	0	0
	164.590	16.400	146.914	1/3×327.904	−0.06	−0.18
	163.731	16.632	146.875	1/3×327.238	−0.28	−0.26
	161.144	18.462	147.262	1/3×326.868	−0.40	−1.02
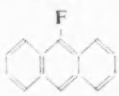	156.305	22.273	147.623	1/3×326.201	−0.63	–

(a) Ref. 5; in units of 10 p. p. m.

TABLE IV. CALCULATED SHIELDING CONSTANTS AND CHEMICAL SHIFTS

	$-\sigma_{l-\sigma}$	$-\sigma_{l-\pi}$	$-\sigma_{\sigma-\pi}$	$-\sigma_p$	δ_{calcd}	δ_{obs} [b]
	159.962	20.738	152.238	1/3×332.938	+1.62	+1.08
	165.398	15.761	146.921	1/3×328.080	0	0
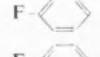	165.453	15.505	145.714	1/3×326.672	−0.47	−0.64
	165.537	15.214	144.889	1/3×325.640	−0.78	−1.46

(b) Ref. 3; in units of 10 p. p. m.

where these matrix elements are represented in units of eV., q_F^0 and q_C^0 denote the total π electron densities at the fluorine and the adjacent carbon atom in the reference, respectively, and q_F and q_C are those in the sample compound. Parameters γ_F and γ_C are tentatively put at 20 and 2, respectively, in the present treatment. Using the integrals in Eq. 10, the energies of bonding and antibonding orbitals as well as the coefficients are calculated.

Finally the energy of lone pair electrons of fluorine, ε_l, is assumed to be*

$$\varepsilon_l = -10 - \gamma_F(q_F^0 - q_F) \qquad (11)$$

in which the second term has a similar meaning in Eq. 10. The value of $\langle 1/r^3 \rangle$ is put at $8.89/a_H^3$, where a_H is the Bohr radius[7].

Result and Discussion

It was discussed qualitatively by the present authors[5] that the two factors, the polarity of C–F bond and the π electron density on fluorine, had a dominant role in determining a paramagnetic term in a conjugated molecule. The two empirical rules were proposed[5], whereby a qualitative analysis of magnetic shielding parameter $\hat{\sigma}$ was made. Further we pointed out that in polycondensed aromatics the magnitude of total π electron more density decreases with the decrease of fluorine chemical shifts, while in some fluorobenzene derivatives this correlation is reversed. More precisely, the fluorine chemical shift seems to be governed by the polarity of a C–F σ bond in fluorobenzene derivatives.

In the present paper an investigation on fluorine chemical shifts in these compounds is made quantitatively by making use of Eqs. 3 and 4.

In Tables I and II, the total densities at the fluorine and the adjacent carbon atom, the energies of bonding and antibonding orbitals, and the values of a^2 and b^2 for benzene derivatives and condensed aromatics are cited. One should note that the polarity of a C–F bond which is measured by the magnitude of a^2 seems to increase with the decrease of q_F in Table I, while in Table II the polarity seems to increase with the increase of q_F.

In Tables III and IV, there are listed three principal components of the paramagnetic shielding constant, the mean of the constants and the calculated values of chemical shift together with observed ones.[3,5] With regard to 9-fluoroanthracene, there are unfortunately no data to be compared with the theoretical result. Though there remain many points to be modified in future, the good agreement observed between the present results and experimental data may be sufficiently valuable to be stressed.

Summary

In order to make a quantitative analysis of the F^{19} magnetic shielding parameters in conjugated molecules, an extension of the idea previously proposed by Saika and Slichter is made. Calculations are carried out with respect to several fluorobenzene derivatives and fluorinated polycondensed aromatic compounds by using the molecular orbital method. The agreement of our calculated shifts with observed shielding data is almost satisfactory.

Faculty of Engineering
Kyoto University
Sakyo-ku, Kyoto
(T. Y., K. F., H. K. & H. K.)

Faculty of Science
Kanazawa University
Kanazawa
(S. H. & S. M.)

* In a rough estimation, it may be assumed that this energy can be obtained by the equation, $\varepsilon_l = -I_F + 1/2(I_F - A_F)$, where I_F and A_F are the ionization potential and the electron affinity of the fluorine in its valence state. Using the published data, $I_F = 17.481$ eV., $A_F = 3.78$ eV., we can obtain $\varepsilon_l = -10.5$ eV. Therefore the value of -10 in Eq. 11 seems not to be so unreasonable.

An LCUAO Treatment of Reactivity in Aromatic Hydrocarbons

By Kenichi FUKUI, Teijiro YONEZAWA, Chikayoshi NAGATA and Yoshimichi KONAKA

(Recieved October 28, 1960)

Several theoretical treatments of reactivity of conjugated molecules have achieved a brilliant develompent in accordance with the progress of the LCAO MO method. In this procedure, the molecular orbital is represented by the linear combination of 2π atomic orbitals. By the use of these coefficients useful indices of reactivity such as electron density[1], bond order[1], and frontier electron density[2] are derived.

On the other hand, a method, the so-called LCUAO MO, in which the molecular orbital is represented by the linear combination of united-atomic orbitals in each bond of a conjugated molecule has been developed by Brown and Matsen[3]. This method is an extension of united-atom approach[4] in hydrogen molecule to conjugated compounds.

This procedure may be considered to supply us more easily with information on the nature of a conjugated double bond if we introduce the frontier electron concept in LCAO MO treatment.

Theoretical

By an ordinary procedure of LCUAO MO method[3], a molecular orbital is written as

$$\psi = \sum_i a_i \phi_i \tag{1}$$

where ϕ_i is the UAO of the ith bond. The secular equation for the system can be obtained from this molecular orbital putting the matrix elements as following.

$$h_{ii} = \int \phi_i^* h \phi_i \mathrm{d}\tau = \alpha$$

$$h_{ij} = \int \phi_i^* h \phi_j \mathrm{d}\tau = \beta \text{ for adjacent bond} \tag{2}$$

$$0 \text{ for non-adjacent bond}$$

where h is the effective one electron hamiltonian, and α and β are the standard Coulomb and resonance integrals in benzene, respectively. Then all the molecular orbital coefficients are determined from the roots of the secular equation by using normalizing condition

$$\sum_i (a_i)^2 = 1 \tag{3}$$

Brown and Matsen[3] has proposed that bond order, P_r, for the rth bond can be obtained by

$$P_r = \sum_j \nu_j (a_r^j)^2 \tag{4}$$

where ν_j is the occupation number for the jth molecular orbital. Then they showed that a good parallelism can be obtained between the bond orders obtained by simple LCAO MO treatment and by the present method.

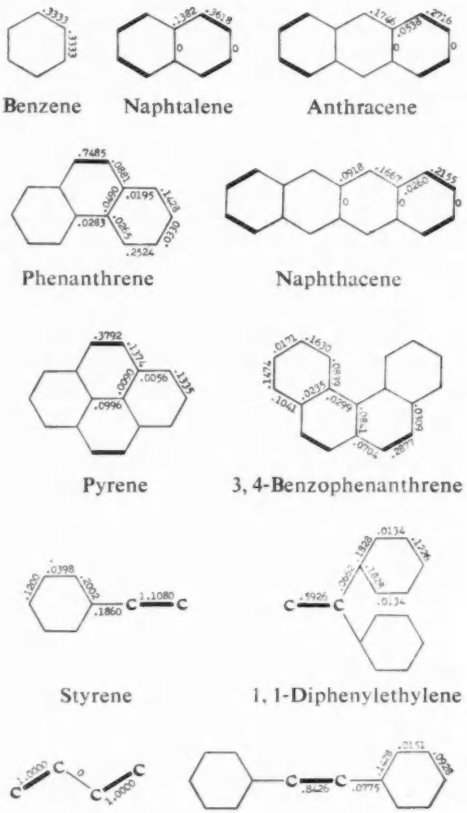

Fig. 1. Electron densities of the highest occupied orbital.

1) H. C. Longuet-Higgins and C. A. Coulson, *Proc. Roy. Soc.*, **A192**, 16 (1947).
2) K. Fukui, T. Yonezawa and H. Shingu, *J. Chem. Phys.*, **20**, 722 (1952); K. Fukui, T. Yonezawa, C. Nagata and H. Shingu, ibid., **22**, 1433 (1954).
3) R. D. Brown and F. A. Matsen, ibid., **21**, 1298 (1953).
4) R. D. Brown, *J. Chem. Soc.*, **1953**, 2615.

TABLE I. REACTIVE BOND IN AROMATIC HYDROCARBONS

Compound	Experimentally most reactive bond*	Bond of largest frontier density	Bond of minimum ortho localization energy**
Benzene	1 : 2	1 : 2	1 : 2
Naphthalene	1 : 2	1 : 2	1 : 2
Anthracene	1 : 2	1 : 2	1 : 2
Phenanthrene	9 : 10	9 : 10	9 : 10
Pyrene	4 : 5	4 : 5	4 : 5
Naphthacene	1 : 2	1 : 2	1 : 2
3,4-Benzophenanthrene (Benzo[*c*]phenanthrene)	5 : 6	5 : 6	5 : 6

* Estimated from the addition reaction of OsO_4, which is considered to be an electrophilic addition taking place simultaneously at the two adjacent carbon atoms.
** Ref. 7.

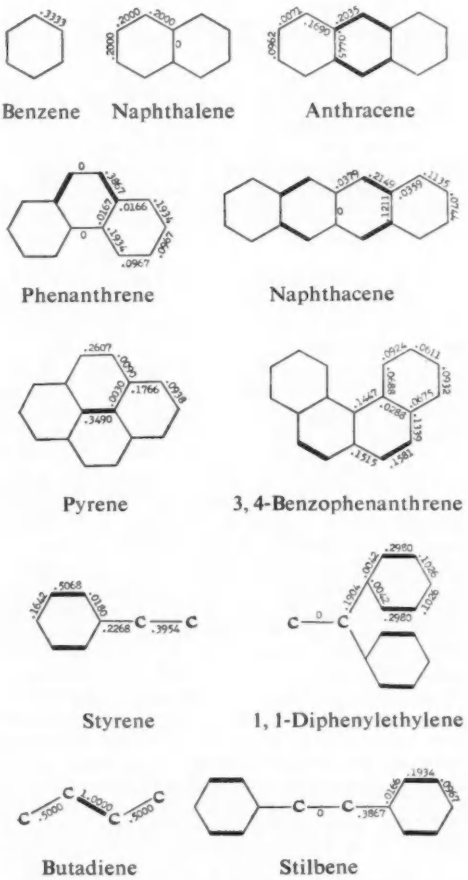

Fig. 2. Electron densities of the lowest vacant orbital.

In these circumstances the investigation is made to elucidate whether or not the frontier electron concept by which the chemical reactivity in conjugated molecules is successfully interpreted may be applicable in LCUAO MO method. The calculation is carried out with respect to benzene, naphthalene, anthracene, naphthacene, pyrene, 3,4-benzophenanthrene (benzo[*c*]phenanthrene), styrene, stilbene and 1,1-diphenylethylene. The electronic distributions of the highest occupied and the lowest vacant orbitals are calculated and indicated in Figs. 1 and 2.

Results and Discussion

The bond of the largest frontier electron density for electrophilic reaction in polycondensed aromatics are indicated in the third column of the Table I. These results may give some information concerning the bond which will play a dominant role in the complex formation of aromatic hydrocarbons with Ag^+ ion[5] or H^+ ion. Furthermore the bond of the largest electron density of the highest occupied orbital in 1,1-diphenylethylene coincides with the position pointed out by Evans and his coworkers[6] in the complex formation of this compound with H^+. In regard to styrene, butadiene and stilbene, calculated results are considered to be reasonable.

On the other hand, the electronic distribution of the lowest vacant orbital shown in Fig. 2 seems to correspond to none of the chemical reactions ever known. But since there exist no experimental data available, we must refrain here from deciding whether the results thus obtained are essentially meaningless or not. But one thing attracts our attention. That is, the most reactive position does not coincide with what is predicted from the electronic distribution of the highest occupied orbital,

5) S. Winstein and H. J. Lucas, *J. Am. Chem. Soc.*, **60**, 836 (1938); R. E. Kofahl and H. J. Lucas, ibid., **76**, 3933 (1954).
6) A. G. Evans, D. M. S. Jones and J. H. Thomas, *J. Chem. Soc.*, **1957**, 104.

while the existing theories of these compounds predict the same position to be most reactive in both electrophilic and nucleophilic additions. A typical one of these theories is the localization theory[7]. This point should be investigated in future.

Faculty of Engineering
Kyoto University
Sakyo-ku, Kyoto

7) E. C. Kooyman and J. A. A. Ketelaar, *Rec. trav. chim.*, **65**, 859 (1946); R. D. Brown, *J. Chem. Soc.*, **1950**, 3249.

Application of RADME to the Chelatometric Determination of Metals Employing the Alternating Current Polarographic Method

By Mutsuo KODAMA

(Received October 6, 1960)

Cadmium- and lead-nitrilotriacetate complexes give rise to two polarographic waves in acetate buffer solution (pH 4.5). The first one is a kinetic wave due to the elecrodeposition of metal ions formed by the dissociation of the complex, and the second is the one due to the direct reduction of complex[1,2]. In ammonia-ammonium nitrate buffer solution, the kinetic currents which originate from the dissociation can also be observed. Owing to the presence of the kinetic current, cadmium and lead can not be titrated with nitrilotriacetic acid (NTA) by employing the usual polarographic method.

In the previous paper, the concentration of copper in an acetate buffer solution of pH 6.0 was determined with NTA by the use of the alternating current polarographic method. In the titration, equivalence points were determined by plotting the peak currents of the alternating current polarograms of copper against the volume of NTA solution added.

The present investigation was directed to the application of rapidly dropping mercury electrode (RADME) to the chelatometric determination of copper, cadmium and lead, using the alternating current polarographic method. At RADME, peak currents due to the electrodeposition of these metal ions which were produced by the dissociation of complexes could not be observed. When RADME is used as an indicator electrode, experimental equivalence points agreed with the stoichiometric equivalence points.

Experimental

Apparatus.—A Yanagimoto Model GA-103 galvarecorder equipped with an automatically scanning potentiometer was employed for the measurements of all current-voltage curves and also for the titrations. The current was determined point by point by manual operation.

Dropping mercury electode (DME) and RADME had the chracteristic features indicated in Table I, the measurements being conducted in air-free 0.1 M potassium chloride solutions with open circuit at 25 ± 0.1°C.

TABLE I. CHARACTERISTICS OF THE ELECTRODES MEASURED IN AIR-FREE 0.1 M POTASSIUM CHLORIDE SOLUTION WITH OPEN CIRCUIT AT 25 ± 0.1°C

	Height of mercury head, cm.	t, sec.	m mg./sec.
DME	70.0	4.02	1.23_7
RADME	60.0	0.35_3	15.54

A simple beaker type cell was used for all measurements. A cell was connected to a saturated calomel electrode (S. C. E.) through a potassium nitrate agar bridge (1.5 kΩ). Semimicroburets of 5 ml. and 10 ml. capacity were used for titrations. During the titrations purified nitrogen gas was passed through the solution to remove dissolved oxygen, prior to the measurements of current-voltage curves and titration curves, which also were conducted after every addition of titrant. All polarographic measurements and titrations were carried out at 25 ± 0.1°C. The cell construction which was used fo rthe alternating current polarographic measurements is shown in Fig. 1. A large platinum electrode was inserted into the solution as the third electrode and this was connected to the anode through a condenser of 100 μF in order to keep the impedance of the electrolysis cell as low as possible.

Reagent. — Nitrilotriacetic acid (NTA) of analytical reagent grade (Wakō Pure Chemical Industries, Ltd.) was used without further purification. The stock solution of NTA was standardized with

1) J. Koryta and I. Kossler, *Collection Czechoslov. Chem. Communs. Suppl.*, **15**, 241 (1950).
2) K. Morinaga and T. Nomura, *J. Chem. Soc. Japan, Pure Chem. Sec. (Nippon Kagaku Zasshi)*, **79**, 200 (1958).

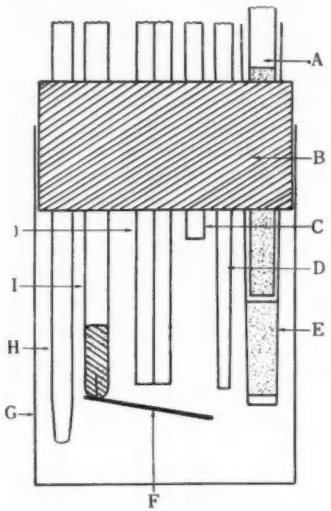

Fig. 1. Cell construction.

A	S. C. E.	F	platinum plate
B	rubber	G	beaker type cell
C	gas outlet	H	gas inlet
D	buret	I	platinum electrode
E	sintered glass	J	DME or RADME

standardized nickel solution[3,4]. Standard solutions of copper, lead and cadmium were prepared from chemicals of analytical reagent grade. The concentration of stock solution was determined gravimetrically[5]. The concentrations of copper and of cadmium were determined by amperometric titration[6,7], using the DME as an indicator electrode. Other chemicals used were all analytical reagent grade. The buffer solutions were prepared by the method described in the previous paper[4].

Results and Discussion

Direct Current (D. C.) Polarography.—Current-voltage curves of cadium-nitrilotriacetate complex were obtained with DME at different heights of mercury column in de-aerated ammonia-ammonium nitrate buffer solution of pH 9.2 containing 0.005% gelatine. The ionic strength was adjusted to 0.7 with potassium nitrate.

As seen from current-voltage curve A (Fig. 2), the mixture of cadmium and nitrilotriacetic acid at the ratio of exactly 1 to 1, gives a polarogram with a small reduction wave of

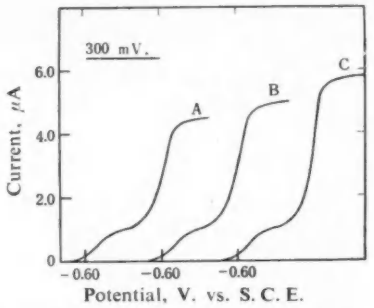

Fig. 2. Current-voltage curves of $1.09_5\times10^{-3}$ M cadmium nitrilotriacetate in an ammonia-ammonium nitrate buffer of pH 9.2 (μ=0.7).

A Height of mercury column, 50 cm.
B Height of mercury column, 70 cm.
C Height of mercury column, 90 cm.

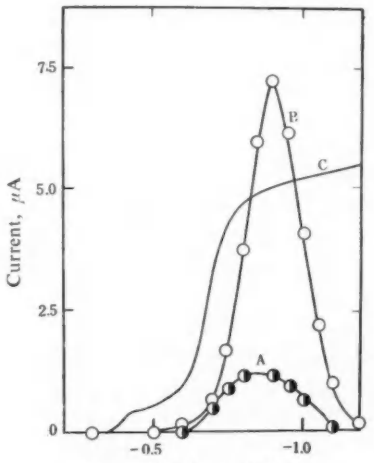

Fig. 3. Current-voltage curves of $1.18_6\times10^{-3}$ M lead-nitrilotriacetate in an ammonia-ammonium nitrate buffer of pH 8.2 (μ=0.7) containig 50 mM tartarate.

A A. C. polarogram at DME
B A. C. polarogram at RADME
C D. C. polarogram at DME

cadmium (-amine complex) ion. Viewed from the experimental results obtained at different heights of mercury column (curves B and C in Fig. 2), the author's explanation that this small prewave must be kinetic in nature, may be justified. Lead-nitrilotriacetate complex in an ammonia-ammonium nitrate buffer solution of pH 8.2 containing 0.005% gelatin (50 mM sodium tartarate was added to avoid the undesirable hydrolysis of lead) also gave the kinetic current (curve C in Fig. 3). The ionic strength was also adjusted to 0.7 with potassium nitrate.

3) M. Kodama, A. Shimizu and H. Terakado, ibid. **81**, 1545 (1960).
4) G. Numaziri, M. Kodama and A. Shimizu, ibid., **81**, 454 (1960).
5) F. P. Treadwell and W. T. Hall, "Analytical Chemistry", Vol. 2 (1953), p. 58.
6) N. Tanaka, I. T. Oiwa and M. Kodama, *Anal. Chem.*, **28**, 1555 (1956).
7) N. Tanaka, M. Kodama, M. Sasaki and M. Sugino, *Japan Analyst (Bunseki Kagaku)*, **6**, 86 (1957).

Alternating Current (A. C.) Polalography.— Alternating current polarograms of cadmium, lead and copper were recorded, using DME or RADME, under the same conditions as those used for direct current polarographic measurements. It was found for lead-nitrilotriacetate complex that the reduction wave of lead ion due to the dissociation of complex entirely disappeared at DME or RADME as shown in Fig. 3 (curves A and B). This phenomenon was also obtained in the reduction of cadmium-nitrilotriacetate complex, when RADME was employed as an indicator electrode (Fig. 4).

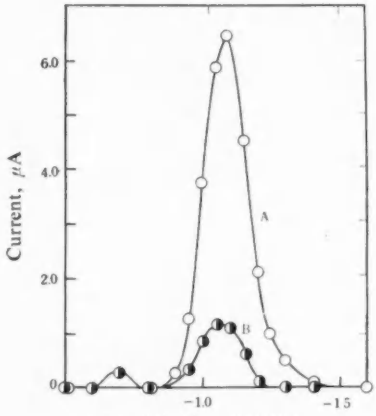

Fig. 4. Alternating current polarograms of $1.09_5\times10^{-3}$ M cadmium-nitrilotriacetate in an ammonia-ammonium nitrate buffer of pH 9.2 ($\mu=0.7$).

A at RADME B at DME

These results may indicate that the rate of the dissociation reaction of metal-nitrilotriacetate complex on the electrode surface is not sufficiently rapid to supply the requisite amount of metal ion to give the kinetic current during the short interval (0.02 sec.) of each alternating current voltage sweep at DME or RADME.

The value of the peak current of metal-nitrilotriacetate conmplex observed at RADME is higher than that observed at DME. In the potential range at which experiments were conducted, the surface-active substance, gelatine, is adsorped on the electrode surface to cover it. The extent of coverage of the rapidly dropping mercury electrode surface differs from that of the ordinary dropping mercury electrode surface, because the drop time of RADME is quite different from that of DME. This difference is related to the extent of inhibition of the electro-oxidation-reduction reaction of complex ion, which may be the reason why the peak current at RADME is higher than that at DME. The adsorption of gelatine on the mercury drop occurs over the entire range of potentials (about +0.4 to −2.0 V. vs. S.C.E.), and the tensammetric peaks due to the adsorption and the desorption of gelatine can not be observed under ordinary experimental conditions. In the case of camphor, however, two tensammetric peaks can be observed at about −0.25 and −1.15 V. vs. S.C.E. The peak in the positive potential region results from the adsorption of camphor, and the peak

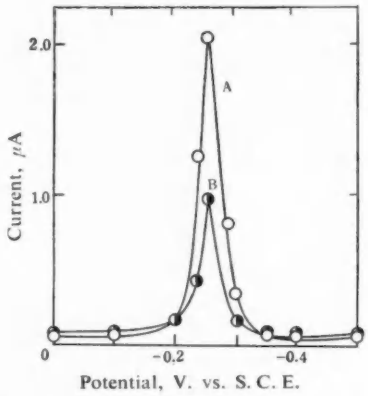

Fig. 5. Alternating current polarograms of 0.5 M KNO_3 solution containing 1.5×10^{-3} M camphor.

A at RADME B at DME

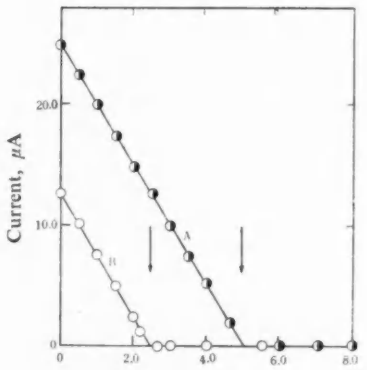

Fig. 6. Titration curves of cadmium with NTA in an ammonia-ammonium nitrate buffer of pH 9.2 ($\mu=0.7$).

A 50 ml. of $1.09_5\times10^{-3}$ M cadmium
B 50 ml. of $5.47_5\times10^{-4}$ M cadmium
Stoichiometric equivalence points are indicated by arrows.

in the negative potential region from the desorption of camphor. The peak currents of positive tensammetric wave of camphor obtained at DME and RADME in the nitrate media are shown in Fig. 5. The value of the peak current observed at RADME differs from that observed at DME. This fact also implies that the extent of coverage of the rapidly dropping mercury electrode surface by the surface-active substance is quite different from that of the dropping mercury electrode surface.

A. C. Poralographic Titrations. — From the above results and the well-known facts[8] that in the reversible case, the A. C. polarographic method is advantageous in the resolution of two component systems and in the determination of low concentration; it seems desirable to employ the A. C. polarographic method to determine the concentration of cadmium or lead with NTA at RADME in an ammnia-ammonium nitrate buffer solution.

Polarographic titration employing the A. C. polarographic method (A. C. polarographic titration) was carried out, under the same conditions as that used for the polarographic measurements, in the concentration range from 1×10^{-3} M to 1×10^{-5} M. Titration curves were obtained by plotting the peak currents due to the electro-reduction of metal ions against the volume of NTA solution added. Typical examples of the titration curves are given in Figs. 6 and 7. These curves were corrected for dilution effect by the addition of titrant. The potential at which the peak currents are given were held constant during the titration. The results of the titration obtained are listed in Tables II and III. Experimental equivalence points agreed with calculated equivalence points satisfactorily. The results of the titration obtained for copper are also listed in Table IV.

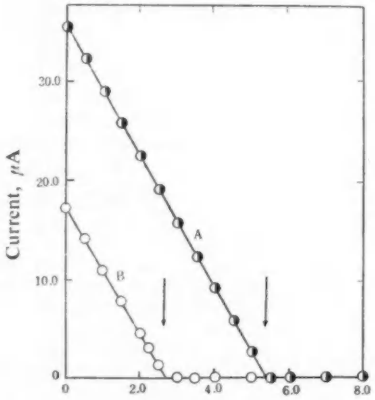

Fig. 7. Titration curves of lead with NTA in an ammonia-ammonium nitrate buffer of pH 9.2 (μ=0.7).

A 50 ml. of $1.18_4\times10^{-3}$ M lead.
B 50 ml. of $5.93_0\times10^{-4}$ M lead.
Stoichiometric equivalence points are indicated by arrows.

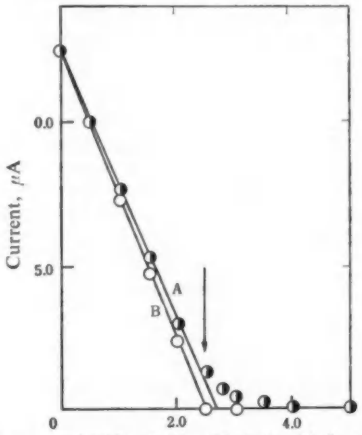

Fig. 8. Titration curves of cadmium with NTA in an ammonia-ammonium nitrate buffer of pH 9.2 (μ=0.77); 50 ml. of $5.47_5\times10^{-4}$ M cadmium.

A 0.4 M ammonia B 0.1 M ammonia

TABLE II. A. C. POLAROGRAPHIC TITRATION OF CADMIUM WITH NTA USING RADME
(INITIAL VOLUME 50 ml.)

Concentration of cadmium, M	Concentration of NTA used for titration, M	NTA required, ml.		Error, %
		Stoichiometric	Experimental	
$1.09_5\times10^{-3}$	$1.09_5\times10^{-2}$	4.98_7	5.00	+0.1
$5.47_5\times10^{-4}$	$1.09_5\times10^{-2}$	2.49_4	2.48	−0.6
$2.73_5\times10^{-4}$	$1.09_5\times10^{-2}$	1.24_7	1.24	−0.6
$1.09_5\times10^{-4}$	$1.09_5\times10^{-3}$	4.98_7	4.96	−0.6
$5.47_5\times10^{-5}$	$1.09_5\times10^{-3}$	2.49_4	2.50	+0.3
$3.28_5\times10^{-5}$	$1.09_5\times10^{-3}$	1.24_7	1.45	−3.0

8) P. Delahay, "New Instrumental Method in Electrochemistry" (1954), p. 176.

TABLE III. A. C. POLAROGRAPHIC TITRATION OF LEAD WITH NTA USING RADME
(INITIAL VOLUME 50 ml.)

Concentration of lead, M	Concentration of NTA used for titration, M	NTA required, ml.		Error, %
		Stoichiometric	Experimental	
$1.18_6\times10^{-3}$	$1.09_5\times10^{-2}$	5.40_0	5.40	0
$5.93_0\times10^{-4}$	$1.09_5\times10^{-2}$	2.70_0	2.69	−0.6
$2.37_4\times10^{-4}$	$1.09_5\times10^{-2}$	1.08_0	1.07	−1.0
$1.18_6\times10^{-4}$	$1.09_5\times10^{-3}$	5.40_0	5.42	−0.4
$5.93_0\times10^{-5}$	$1.09_5\times10^{-3}$	2.70_0	2.72	−0.8
$2.37_4\times10^{-5}$	$1.09_5\times10^{-3}$	1.08_0	1.05	−3.0

TABLE IV. A. C. POLAROGRAPHIC TITRATION OF COPPER WITH NTA USING RADME
(INITIAL VOLUME 50 ml.)

Concentration of copper, M	Concentration of NTA used for titration, M	NTA required, ml.		Error, %
		Stoichiometric	Experimental	
$1.13_0\times10^{-3}$	$1.09_5\times10^{-2}$	5.15_0	5.15	0
$5.65_0\times10^{-4}$	$1.09_5\times10^{-2}$	2.57_5	2.58	−0.2
$2.26_5\times10^{-4}$	$1.09_5\times10^{-2}$	1.03_0	1.02	−1.0
$1.13_0\times10^{-4}$	$1.09_5\times10^{-3}$	5.15_0	5.16	−0.2
$5.65_0\times10^{-5}$	$1.09_5\times10^{-3}$	2.57_5	2.57	−0.2

When a great excess of ammonia is presented in the solution, experimental equivalence points were somewhat greater than the stoichiometrical ones. This fact reveals that the presence of excess ammonia favors the dissociation reaction of the metal-nitrilotriacetate complex (Fig. 8).

Summary

RADME was applied to the chelatometric determination of copper, cadmium and lead with NTA by employing the A. C. polarographic method. At RADME practically no kinetic effects due to the dissociation of metal-nitrilotriacetate complex were observed and the concentration of metal ions could be determined accurately in the concentration range from 1×10^{-3} M to 1×10^{-5} M.

The author thanks Dr. T. Takeshima for reading the manuscript and for advice.

Department of Chemistry
Faculty of Arts and Sciences
Ibaraki University
Watari-machi, Mito

Synthesis of α-Maltosides. I

By Shoji MATSUBARA

(Received October 10, 1960)

Although a large number of glycoside derivatives[1,2] have been synthesized, many attempts to prepare various α-maltoside derivatives have not been promising[3]. At present, non-crystalline phenyl-α-maltoside and methyl-α-maltoside synthesized by Fischer and Bergmann[4], and also by Helferich and Peterson[5] have only been reported. After many trials, the author has succeeded in the synthesis of various α-maltosides.

1) G. Wagner, *Arch. Pharm.*, **290**, 625 (1957).
2) G. Wagner, ibid., **291**, 278 (1958).
3) G. Zemplén, *Ber.*, **60**, 1555 (1935).
4) E. Fischer, M. Bergmann and A. Rabe, ibid., **53**, 2362 (1920).
5) B. Helferich and S. R. Peterson, ibid., **68**, 790 (1935).

The purpose of this study is to obtain some fundamental information concerning the substrate specificity[6-8]; namely, it is to investigate the influence of substituents in the phenyl group on the enzymatic hydrolysis of phenyl-α-maltoside by taka-amylase A[9], and also the mode of interaction of the enzyme activity with structural changes in their substrates. From this point of view, the detailed descriptions of the synthesis are briefly described in this paper.

Experimental

Octaacetylmaltose[3]. — To a solution of 20 g. of anhydrous maltose dissolved in 100 cc. of acetic anhydride, 20 g. of fused sodium acetate was added and the mixture was gently heated. The color of the solution changed from yellow through brown to dark brown. When the violent initial reaction ceased, the solution was heated under stirring for two hours at 100°C in a water bath, poured onto crushed ice, and then diluted with water. The separated yellowish brown oil was allowed to stand overnight in a refrigerator. The crystals which separated out were collected by filtration, dissolved in chloroform, and washed well with water, and dried over anhydrous calcium chloride. The solvent was then evaporated under reduced pressure. The solid was dissolved in hot methanol, filtrated, and the crystalline residue which was obtained from the mother liquor was recrystallized from methanol, giving 14 g. of octaacetylmaltose in the form of colorless crystals, m. p. 158~159°C, $[\alpha]_D^{19} = +124°$ (*c* 1.0, in chloroform).

Heptaacetylphenyl-α-maltoside[4,5]. —The mixture of 68 g. (1 mol.) of octaacetylmaltose, 57 g. (6 mol.) of phenol and 10 g. of fused zinc chloride was heated under violent stirring for two and a half hours at 100°C in a water bath. After cooling, the dark brown oily substance was diluted with water, to remove the zinc chloride. To the solution mixture, benzene was added and the benzene extract was well washed successively with water, with 1 N aqueous sodium hydroxide, with water until it became colorless, and finally dried over anhydrous calcium chloride. The solvent was then evaporated under reduced pressure, leaving a yellowish brown oil. The oily residue was crystallized from 100 cc. of ethanol to give colorless crystals. The crude crystals were combined and recrystallized from ethanol-dioxane mixture (contained 10% dioxane), m. p. 184~184.5°C, $[\alpha]_D^{20} = +170.2°$ (*c* 1.0, in chloroform).

Found: C, 53.92; H, 5.63. Calcd. for $C_{32}H_{40}O_{15}$: C, 53.91; H, 5.66%.

Phenyl-α-maltoside. — A solution of 10 g. of heptaacetylphenyl-α-maltoside dissolved in 100 cc. of a mixture of absolute methanol and chloroform (1 : 1, by volume) was saturated with ammonia gas under cooling. After being kept more than four hours at room temperature, the methanol and ammonia were removed under reduced pressure. The syrupy residue was dissolved in a small quantity of absolute ethanol, and the precipitate was obtained by adding ether. After removing the supernatant solvents, the residue was then successively treated in the same manner as described above to afford pure crystals. The precipitate obtained was combined and washed with ether. This crude crystalline phenyl-α-maltoside was crystallized from absolute ethanol. The yield was 4.75 g., m. p. 202~204°C, $[\alpha]_D^{14.5} = +211°$ (*c* 1.3, in water).

Found: C, 51.57; H, 6.25. Calcd. for $C_{18}H_{26}O_{11}$: C, 51.65; H, 6.27%.

The ultraviolet absorption of the product showed maxima at 266 mμ in water.

Heptaacetyl-*p*-nitrophenyl-α-maltoside. — To a mixture of 20 cc. of glacial acetic acid and 10 cc. of acetic anhydride, 5 g. of heptaacetylphenyl-α-maltoside was added. A mixture of 25 g. of concentrated sulfuric acid (95%) and 25 g. of glacial acetic acid was added under cooling and stirring. Then to this solution, a mixture of 5 g. of nitric acid (sp. gr. 1.38) and 10 cc. of glacial acetic acid was added dropwise, while stirring vigorously. The mixture was kept for four hours at room temperature, and poured into a large amount of ice and water. Within a few minutes a powdery white precipitate was separated, collected, washed completely with water, and dried over anhydrous calcium chloride. The yield of the crude substance was 4.83 g. The crude crystals were recrystallized from absolute ethanol, and the yield of heptaacetyl-*p*-nitrophenyl-α-maltoside was 4.75 g., m. p. 176~178°C, $[\alpha]_D^{14.5} = +223°$ (*c* 1.2, in chloroform).

Found: C, 50.71; H, 5.21; N, 1.83. Calcd. for $C_{32}H_{39}O_{20}N$: C, 50.74; H, 5.19; N, 1.85%.

***p*-Nitrophenyl-α-maltoside.** — The heptaacetyl-*p*-nitrophenyl-α-maltoside was deacetylated by dissolving in absolute methanol (200~300 cc. for 25 g.) and adding a freshly prepared solution of sodium methoxide (from sodium, 10~20 mg., and methanol, 10 cc.). The mixture was kept at room temperature overnight. The methanol was then removed under reduced pressure, and the oily substance was dissolved in 10 cc. of ethanol. The solid was obtained by adding ether, and was then successively treated in the same manner as described above to give pure maltoside crystals which were crystallized to constant melting point using, when possible, a mixture of ethanol-dioxane containing 10% of dioxane. The crude crystals were combined and recrystallized from absolute ethanol/petroleum ether, m. p. 145~146°C, $[\alpha]_D^{14.5} = +265°$ (*c* 1.0, in water).

Found: C, 46.72; H, 5.40; N, 3.04. Calcd. for $C_{18}H_{25}O_{13}N$: C, 46.63; H, 5.44; N, 3.02%.

The ultraviolet absorption of the product showed maxima at 310 mμ in water.

Other Substituted Heptaacetylphenyl-α-maltosides. — The corresponding phenols (0.3~0.4 mol.) and octaacetylmaltose (0.1 mol.) were heated with fused zinc chloride (0.5~2.0 g.) under violent stirring at 110~115°C for 1.5 to 2 hr. The cooled oily product was diluted with water and extracted with

6) R. L. Nath and H. N. Rydon, *Biochem. J.*, **57**, 1 (1954).
7) S. Matsubara, *J. Biochem.*, **49**, 226 (1961).
8) S. Matsubara, ibid., **49**, 232 (1961).
9) S. Matsubara, T. Ikenaka and S. Akabori, ibid., **46**, 425 (1959).

benzene to remove zinc chloride. The benzene solution was washed with water, and then repeatedly with 5% aqueous sodium hydroxide until the washings were colorless. The solution was again washed with water and dried over anhydrous calcium chloride. The solvent was then evaporated under reduced pressure, leaving a dark yellowish brown oil. The oily residue was crystallized from suitable solvents to give colorless crystals. The crude crystals were recrystallized from one more suitable solvent.

Other Substituted Phenyl-α-maltosides. — The other substituted phenyl-α-maltoside was prepared by the same method as with phenyl-α-maltoside. The obtained crude product was recrystallized from suitable solvents.

***o*-Cresyl-α-maltoside.** — Recrystallized from ethanol/ether, m. p. 182~183°C, $[\alpha]_D^{14.5}=+218°$ (*c* 1.0, in water).

Found: C, 52.50; H, 6.45. Calcd. for $C_{19}H_{28}O_{11}$: C, 52.75; H, 6.53%.

The heptaacetyl derivative recrystallized from ethanol, m. p. 175~176°C $[\alpha]_D^{18}=+182°$ (*c* 1.5, in chloroform).

Found: C, 54.60; H, 5.89. Calcd. for $C_{33}H_{42}O_{18}$: C, 54.56; H, 5.83%.

***m*-Cresyl-α-maltoside.**—This was very hydroscopic and resisted all attempts at recrystallization; the product, dried at 100°C in vacuo over P_2O_5, had m. p. 93~98°C, $[\alpha]_D^{15}=+235°$ (*c* 0.5, in water).

Found: C, 51.95; H, 6.42. Calcd. for $C_{19}H_{28}O_{11}$: C, 52.75; H, 6.53%.

The heptaacetyl derivative recrystallized from ethanol, m. p. 135~140°C, $[\alpha]_D^{18}=+185°$ (*c* 1.5, in chloroform).

Found: C, 54.53; H, 5.84. Calcd. for $C_{33}H_{42}O_{18}$: C, 54.56; H, 5.83%.

***p*-Cresyl-α-maltoside.** — Recrystallized from ethanol/ether, m. p. 192~194°C, $[\alpha]_D^{18}=+204°$ (*c* 0.5, in water).

Found: C, 53.02; H, 6.49. Calcd. for $C_{19}H_{28}O_{11}$: C, 52.75; H, 6.53%.

The heptaacetyl derivative recrystallized from ethanol, m. p. 180~181°C, $[\alpha]_D^{18}=+201°$ (*c* 1.0, in chloroform).

Found: C, 54.55; H, 5.81. Calcd. for $C_{33}H_{42}O_{18}$: C, 54.56; H, 5.83%.

***o*-Isopropylphenyl-α-maltoside.** — Recrystallized from ethanol/petroleum ether, m. p. 163~165°C, $[\alpha]_D^{18}=+222°$ (*c* 1.0, in water).

Found: C, 54.57; H, 7.10. Calcd. for $C_{21}H_{32}O_{11}$: C, 54.75; H, 7.01%.

The heptaacetyl derivative recrystallized from ethanol/petroleum ether, m. p. 110~111°C, $[\alpha]_D^{18}=+205°$ (*c* 1.0, in chloroform).

Found: C, 55.67; H, 6.08. Calcd. for $C_{35}H_{46}O_{19}$: C, 55.71; H, 6.15%.

***p*-Isopropylphenyl-α-maltoside.** — Recrystallized from ethanol/petroleum ether, m. p. 175~176°C, $[\alpha]_D^{14.5}=+216°$ (*c* 1.0, in water).

Found: C, 54.71; H, 6.98. Calcd. for $C_{21}H_{32}O_{11}$: C, 54.75; H, 7.01%.

The heptaacetyl derivative recrystallized from ethanol/petroleum ether, m. p. 145~147°C, $[\alpha]_D^{14.5}=+192°$ (*c* 1.0, in chloroform).

Found: C, 55.61; H, 6.21. Calcd. for $C_{35}H_{46}O_{19}$: C, 55.71; H, 6.15%.

***o*-*tert*-Butylphenyl-α-maltoside.** — This was very hydroscopic and resisted all attempts at recrystallization; the product, dried at 100°C in vacuo over P_2O_5, had m. p. 60~65°C, $[\alpha]_D^{18}=+232°$ (*c* 0.5, in water).

Found: C, 54.89; H, 7.18. Calcd. for $C_{22}H_{36}O_{11}$: C, 55.66; H, 7.23%.

The heptaacetyl derivative recrystallized from ethanol/petroleum ether, m. p. 212~214°C, $[\alpha]_D^{18}=+202°$ (*c* 1.15, in chloroform).

Found: C, 56.26; H, 6.28. Calcd. for $C_{36}H_{48}O_{19}$: C, 56.22; H, 6.30%.

***p*-*tert*-Butylphenyl-α-maltoside.** — Recrystallized from ethanol, m. p. 170~172°C, $[\alpha]_D^{18}=+228°$ (*c* 0.62, in water).

Found: C, 55.61; H, 7.20. Calcd. for $C_{22}H_{34}O_{11}$: C, 55.66; H, 7.23%.

The heptaacetyl derivative recrystallized from ethanol/petroleum ether, m. p. 78~80°C, $[\alpha]_D^{18}=+211°$ (*c* 1.32, in chloroform).

Found: C, 56.21; H, 6.26. Calcd. for $C_{36}H_{48}O_{19}$: C, 56.22; H, 6.30%.

***p*-Isoamylphenyl-α-maltoside.** — Recrystallized from ethanol, m. p. 160~163°C, $[\alpha]_D^{18}=+242°$ (*c* 0.65, in water).

Found: C, 56.48; H, 7.47. Calcd. for $C_{23}H_{36}O_{11}$: C, 56.52; H, 7.43%.

The heptaacetyl derivative recrystallized from ethanol/petroleum ether, m. p. 185~187°C, $[\alpha]_D^{18}=+213°$ (*c* 1.2, in chloroform).

Found: C, 56.80; H, 6.44. Calcd. for $C_{37}H_{50}O_{18}$: C, 56.80; H, 6.44%.

***o*-Methoxyphenyl-α-maltoside.** — Recrystallized from ethanol, m. p. 165~166°C, $[\alpha]_D^{14.5}=+184°$ (*c* 0.1, in water).

Found: C, 50.78; H, 6.27. Calcd. for $C_{19}H_{28}O_{12}$: C, 50.87; H, 6.30%.

The heptaacetyl derivative recrystallized from ethanol, m. p. 140~141°C, $[\alpha]_D^{14.5}=+162°$ (*c* 0.1, in chloroform).

Found: C, 53.36; H, 5.65. Calcd. for $C_{33}H_{42}O_{19}$: C, 53.38; H, 5.70%.

***m*-Methoxyphenyl-α-maltoside.** — Recrystallized from ethanol, m. p. 172~175°C, $[\alpha]_D^{14.5}=+193°$ (*c* 0.95, in water).

Found: C, 50.79; H, 6.26. Calcd. for $C_{19}H_{28}O_{12}$: C, 50.87; H, 6.30%.

The heptaacetyl derivative recrystallized from ethanol, m. p. 163~165°C, $[\alpha]_D^{14.5}=+165°$ (*c* 0.95, in chloroform).

Found: C, 52.90; H, 5.59. Calcd. for $C_{33}H_{42}O_{19}$: C, 53.38; H, 5.70%.

***p*-Methoxyphenyl-α-maltoside.** — Recrystallized from ethanol, m. p. 187~189°C, $[\alpha]_D^{14.5}=+201°$ (*c* 0.85, in water).

Found: C, 50.80; H, 6.28. Calcd. for $C_{19}H_{28}O_{12}$: C, 50.87; H, 6.30%.

The heptaacetyl derivative recrystallized from ethanol, m. p. 206~208°C, $[\alpha]_D^{14.5}=+195°$ (*c* 3.1, in chloroform).

Found: C, 53.31; H, 5.78. Calcd. for $C_{33}H_{42}O_{19}$: C, 53.38; H, 5.70%.

***o*-Chlorophenyl-α-maltoside.**—Recrystallized from ethanol, m. p. 193~196°C, $[\alpha]_D^{18}=+165°$ (*c* 0.5, in water).

Found: C, 47.68; H, 5.60; Cl, 7.84. Calcd. for $C_{18}H_{25}O_{11}Cl$: C, 47.72; H, 5.57; Cl, 7.83%.

The heptaacetyl derivative recrystallized from ethanol/petroleum ether, m. p. 195~197°C, $[\alpha]_D^{18}$ = +154° (*c* 2.3, in chloroform).

Found: C, 51.38; H, 5.23; Cl, 4.68. Calcd. for $C_{32}H_{39}O_{18}Cl$: C, 51.44; H, 5.27; Cl, 4.75%.

***p*-Chlorophenyl-α-maltoside.**—Recrystallized from ethanol, m. p. 205~206°C, $[\alpha]_D^{19}$ = +213° (*c* 1.13, in water).

Found: C, 47.70; H, 5.59; Cl, 7.81. Calcd. for $C_{18}H_{25}O_{11}Cl$: C, 47.72; H, 5.57; Cl, 7.83%.

The heptaacetyl derivative recrystallized from ethanol/petroleum ether, m. p. 197~199°C, $[\alpha]_D^{19}$ = +177° (*c* 1.5, in chloroform).

Found: C, 51.43; H, 5.25; Cl, 4.75. Calcd. for $C_{32}H_{39}O_{18}Cl$: C, 51.44; H, 5.27; Cl, 4.75%.

***o*-Nitrophenyl-α-maltoside.** — Recrystallized from ethanol/ether, m. p. 153~155°C, $[\alpha]_D^{14.5}$ = +245° (*c* 1.2, in water).

Found: C, 46.75; H, 5.48; N, 2.95. Calcd. for $C_{18}H_{25}O_{13}N$: C, 46.63; H, 5.44; N, 3.02%.

The heptaacetyl derivative recrystallized from ethanol, m. p. 185~187°C, $[\alpha]_D^{14.5}$ = +222° (*c* 1.5, in chloroform).

Found: C, 50.68; H, 5.15; N, 1.84. Calcd. for $C_{32}H_{39}O_{20}N$: C, 50.74; H, 5.19; N, 1.85%.

***m*-Nitrophenyl-α-maltoside.**—Recrystallized from ethanol/petroleum ether, m. p. 132~136°C, $[\alpha]_D^{14.5}$ = +261° (*c* 2.1, in water).

Found: C, 46.78; H, 5.39; N, 2.95. Calcd. for $C_{18}H_{25}O_{13}N$: C, 46.63; H, 5.44; N, 3.02%.

The heptaacetyl derivative recrystallized from ethanol, m. p. 170~171°C, $[\alpha]_D^{14.5}$ = +234° (*c* 1.8, in chloroform).

Found: C, 50.65; H, 5.11; N, 1.87. Calcd. for $C_{32}H_{39}O_{20}N$: C, 50.74; H, 5.19; N, 1.85%.

α-Naphthyl-, cyclohexyl- and *o*-, *m*-, *p*-Nitrophenyl-α-maltosides. — The mixture of α-naphthol, cyclohexanol, *o*-, *m*-, or *p*-nitrophenol (0.3~0.4 mol.) and octaacetyl-β-maltose (0.1 mol.) were heated with fused zinc chloride (0.5~2.0 g.) and titanic chloride[10] (10 g.) under violent stirring at 110~115°C for 1.5 to 2 hr. by the same method as that described above.

α-Naphthyl - α - maltoside. — Recrystallized from ethanol/ether, m. p. 156~158°C, $[\alpha]_D^{16}$ = +192° (*c* 1.5, in water).

Found: C, 56.41; H, 6.07. Calcd. for $C_{22}H_{28}O_{11}$: C, 56.39; H, 6.03%.

The heptaacetyl derivative recrystallized from ethanol/ether, m. p. 192~194°C, $[\alpha]_D^{16}$ = +185° (*c* 1.5, in chloroform).

Found: C, 56.71; H, 5.53. Calcd. for $C_{36}H_{42}O_{18}$: C, 56.67; H, 5.56%.

Cyclohexyl - α - maltoside. — Recrystallized from ethanol/ether, m. p. 112~115°C, $[\alpha]_D^{16}$ = +211° (*c* 1.5, in water).

Found: C, 50.85; H, 7.63. Calcd. for $C_{18}H_{32}O_{11}$: C, 50.91; H, 7.60%.

The heptaacetyl derivative recrystallized from ethanol, m. p. 152~155°C, $[\alpha]_D^{16}$ = +202° (*c* 1.5, in chloroform).

Found: C, 53.42; H, 6.50. Calcd. for $C_{32}H_{46}O_{18}$: C, 53.46; H, 6.46%.

Alkyl-α-maltosides.—Alkyl-α-maltosides could be prepared by warming maltose with an alcoholic solution of hydrochloric acid. Dry hydrogen chloride was passed into 200 g. of absolute alcohol, with ice cooling and exclusion of moisture, until the increase in weight amounted to 10 g. This solution 20 cc. was then diluted with 980 g. of alcohol, a 0.1% solution of hydrogen chloride being thus obtained. To this solution 50 g. of finely powdered anhydrous maltose was added, and the mixture was warmed at 50°C for forty-two hours, a clear solution being obtained after the first fifteen minutes' warming. It was well to attach a soda-lime tube to the upper end of the condenser, in order to exclude moisture. The clear pale yellow solution was cooled to 0°C, and crystallization was induced by scratching. After standing for two days at 0°C, the first crop was filtered by suction and was washed twice with 100 cc. portions of cold alcohol. The mother liquor and washings were returned to the flask and again warmed for forty-two hours under reflux at 50°C. The liquid was concentrated to 800 cc. and again chilled to 0°C, incubated and allowed to stand at 0°C for two days. The second crop of maltoside so obtained was filtered by suction and washed three times with each 100 cc. portion of cold alcohol. The mother liquor and washings were combined and concentrated to about 300 cc., chilled to 0°C, and again incubated and allowed to stand for two days. The resulting mush of crystals was dissolved in twice its weight of absolute ethanol, and, after standing for two days at 0°C, the third crop of maltoside was filtered. This was recrystallized from 2.5 parts of ethanol. The product was contaminated by slight traces of maltose and possessed a very faint reducing power towards Fehling's solution. For complete purification it was recrystallized (practically with neither loss nor change in melting point) from five parts of absolute ethanol with the use, if necessary, of decolorizing carbon.

Methyl-α-maltoside.—Recrystallized from ethanol, m. p. 201~202°C, $[\alpha]_D^{16}$ = +183° (*c* 1.0, in water).

Found: C, 43.77; H, 6.75. Calcd. for $C_{13}H_{24}O_{11}$: C, 43.80; H, 6.79%.

Isopropyl - α - maltoside. — Recrystallized from ethanol, m. p. 177~179°C, $[\alpha]_D^{16}$ = +166° (*c* 1.0, in water).

Found: C, 46.81; H, 7.32. Calcd. for $C_{15}H_{28}O_{11}$: C, 46.85; H, 7.35%.

***tert* - Butyl - α - maltoside.** — Recrystallized from ethanol, m. p. 188~190°C, $[\alpha]_D^{16}$ = +153° (*c* 1.0, in water).

Found: C, 48.18; H, 7.62. Calcd. for $C_{16}H_{30}O_{11}$: C, 48.21; H, 7.59%.

Isoamyl-α-maltoside. — Recrystallized from ethanol, m. p. 152~155°C, $[\alpha]_D^{16}$ = +143° (*c* 1.5, in water).

Found: C, 49.52; H, 7.80. Calcd. for $C_{17}H_{32}O_{11}$: C, 49.48; H, 7.82%.

Summary

Substituted phenyl-, α-naphthyl-, and cyclohexyl-α-maltosides were prepared from octaacetyl-β-maltose and the corresponding phenols. *p*-Nitrophenyl-α-maltoside was also prepared by

10) A. P. Jansen and P. G. A. B. Wydeveld, *Nature*, **182**, 525 (1958).

another method from the nitration of hepta-acetylphenyl-α-maltoside. Alkyl-α-maltosides were prepared from maltose and corresponding alcohol.

The authors wishes to express his gratitude to Professor Shiro Akabori (Institute for Protein Research, Osaka University) for his helpful advice throughout this work.

Department of Chemistry
Faculty of Science
Osaka University
Nakanoshima, Osaka

Absorption Spectra of Nitrobenzene Derivatives. II. Effect of Solvent on Intramolecular Charge Transfer Spectra of Nitrobenzene Derivatives

By Kimio SEMBA*

(Received September 7, 1960)

In a previous paper[1] intramolecular charge transfer spectra of nitrobenzene derivatives were studied from the viewpoint of Nagakura and Tanaka's theory[2]. These absorption spectra are strongly influenced by solvents and shift toward longer wavelengths for solvents of higher dielectric constant.

Several papers treating of the effect of solvent on the electronic spectra of organic compounds have been published[3]. Recently, Bayliss and McRae[4] discussed the effects in terms of the dipole-, polarization-, and hydrogen bonding forces between solute and solvent molecules. It is not always easy to interpret the solvent effects correctly because these often arise from the resultant of several individual effects reinforcing as well as cancelling each other. It seems certain that hydrogen bonding plays a very important role in the frequency shift, while effects from other origins are no less important, since frequency shifts are observed even in systems containing no hydrogen bonds.

In this paper the role of the electrostatic interaction between solute and solvent molecules in the intramolecular charge transfer spectra of *o*-, *m*- and *p*-nitrophenol, -nitroanisole, -nitroaniline and -nitron-*N*-dimethylaniline was examined on the basis of the general expression proposed by McRae[5] for the solvent effect on absorption spectra. The contribution of hydrogen bonding between solute and solvent molecules was also taken into consideration for some cases.

Experimental

Absorption spectra in the wavelength region 250~400 mμ were obtained by a Hitachi automatic recording spectrophotometer, type EPS-2. Fused quartz cells of 1 cm. path length were used.

Samples of nitrobenzene derivatives were the same ones used in a previous work[1]. Solvents, *n*-hexane, dioxane, cyclohexane, carbon tetrachloride, toluene, benzene, ethyl ether, nitromethane, acetonitrile, methanol, and ethanol, were purified by the method recommended by Weissberger and Proskauer[6], special care having been taken to remove contaminating water.

Result and Discussion

Theoretical Expression for the Solvent Effect. —In current discussions of the solvent effects on electronic absorption spectra the frequency shifts are mainly attributed to dipole, polarization and hydrogen bonding effects. The general formula* derived from the perturbation theory by McRae[5] for solvent-induced spectral shifts can be simplified for the discussion of present results in the following form[7]

* Present address: Research Laboratory, Kurosaki Firebrick Mfg. Co., Ltd., Fujita, Yawata.

1) K. Semba, This Bulletin, 33, 1640 (1960).

2) S. Nagakura and J. Tanaka, *J. Chem. Phys.*, 22, 236 (1954); S. Nagakura, ibid., 23, 1441 (1955).

3) For example: N. D. Coggeshell and E. M. Lang, *J. Am. Chem. Soc.*, 70, 3282 (1948); M. Kasha, *Discussions Faraday Soc.*, 9, 14 (1950); H. McConnell, *J. Chem. Phys.*, 20, 700 (1952); S. Nagakura and H. Baba, *J. Am. Chem. Soc.*, 74, 5693 (1952).

4) N. Bayliss and E. G. McRae, *J. Phys. Chem.*, 58, 1002, 1006 (1954).

5) E. G. McRae, ibid., 61, 562 (1957).

6) A. Weissberger and E. S. Proskauer, "Organic Solvent", Interscience Publishers, Inc., New York (1955).

* Y. Ooshika has also given a similar formula: *J. Phys, Soc. Japan*, 9, 542 (1954).

7) M. Ito, K. Inuzuka and S. Imanishi, *J. Am. Chem. Soc.*, 82, 1317 (1960).

$$\Delta\nu = \text{dispersion term} + B\left[\frac{n_D^2-1}{2n_D^2+1}\right] + C\left[\frac{D-1}{D+2}-\frac{n_D^2-1}{n_D^2+2}\right] + E\left[\frac{D-1}{D+2}-\frac{n_D^2-1}{n_D^2+2}\right]^2 \quad (1)$$

where B, C and E are constants characteristic of the solute molecule,

$$B=\frac{1}{hc}\frac{(\mathbf{M}_{oo}^u)-(\mathbf{M}_{ii}^u)^2}{a^3} \quad (2)$$

$$C=\frac{2}{hc}\frac{(\mathbf{M}_{oo}^u)\,(\mathbf{M}_{oo}^u-\mathbf{M}_{ii}^u)}{a^3} \quad (3)$$

$$E=\frac{6}{hc}\frac{(\mathbf{M}_{oo}^u)\,(\alpha_o^u-\alpha_i^u)}{a^6} \quad (4)$$

$\mathbf{M}_{oo}^u$ and $\mathbf{M}_{ii}^u$ represent the vector dipole moments of the solute molecule in its electronic ground and excited states, respectively, and a is Onsagar's reaction radius of the solute molecule. For the meaning of the various other quantities appearing in these equations McRae's original paper[5] is referred to.

Effect of Electrostatic Interactions.—Absorption maxima (ν_{max}) of *o*-, *m*- and *p*-nitrobenzene derivatives in various solvents are given in Table 1, in which refractive indices and dielectric constants are also given. The *p*-derivative shows only one absorption band which is in the near ultraviolet region due to the intramolecular charge transfer transition. On the other hand, the *o*- and *m*-derivatives show two intramolecular charge transfer bands due to the transitions $H_{x1}\rightarrow V_s$ and $H_{x2}\rightarrow V_s$, as observed in a previous paper[1]. The bands of *o*- and *m*-derivatives at shorter wavelengths in both toluene and benzene solutions can not be observed, because they are covered by solvent absorption bands, hence only the longer-wavelength bands due to the $H_{x1}\rightarrow V_s$ transition are considered.

We shall first consider the effect of non-polar solvents, *n*-hexane, dioxane, carbon tetrachloride, toluene and benzene, in the order of increasing refractive index. It is seen from the table that ν_{max} decreases with the increase in the refractive index of the solvent, with the exception of dioxane. Plots of ν_{max} against $(n_D^2-1)/(2n_D^2+1)$ for these derivatives are shown in Figs. 1—3. For each of these molecules the points for various solvents are approximately on a straight line, with the exception of the point for dioxane.

For non-polar solvents the third and the fourth terms in Eq. 1 may be neglected since $n_D^2 \approx D$, and only the first and the second terms have to be considered. Then, if the first term is much smaller than the second,

Table 1. Absorption maxima of *o*-, *m*- and *p*-nitrobenzene derivatives in various solvents (cm^{-1})

Solvent	n_D	D	*o*-Nitrophenol	*o*-Nitroanisole	*o*-Nitroaniline	*m*-Nitrophenol	*m*-Nitroanisole
n-Hexane	1.375	1.890	36400 28810	39800 32510	37160 26870	37850 32040	38200 31200
Dioxane	1.422	2.209	36420 28560	38690 31240	36160 25020	37090 30390	37160 30620
Cyclohexane	1.426	2.023	36700 28650	39670 32350	36390 26270	38160 31440	38080 31440
Carbon tetrachloride	1.460	2.238	36410 28420	— 31740	36750 25900	38010 31440	37560 30900
Toluene	1.497	2.379	— 28120	— 31290	— 25310	— 30390	— 30390
Benzene	1.501	2.284	— 28040	— 31100	— 25310	— 30690	— 30370

Solvent	*m*-Nitroaniline	*m*-Nitro-*N*-dimethylaniline	*p*-Nitrophenol	*p*-Nitroanisole	*p*-Nitroaniline	*p*-Nitro-*N*-dimethylaniline
n-Hexane	38450* 29060	40310 26120	— 35200	— 34120	— 31240	— 28730
Dioxane	35700* 26800	40020 24840	— 32780	— 32720	— 28080	— 26140
Cyclohexane	37030* 28730	40180 26030	— 35020	— 22890	— 30840	— 28160
Carbon tetrachloride	36620 28240	— 25440	— 34060	— 33380	— 30040	— 27430
Toluene	— 27370	— 24810	— 33210	— 32720	— 28940	— 26170
Benzene	— 27390	— 24560	— 33100	— 32560	— 28890	— 26030

* Absorption shoulder

or if the first term is nearly the equal of these solvents, an approximately linear relation between ν_{max} and $(n_D^2-1)/(2n_D^2+1)$ should hold. Although the frequency shift of absorption caused by non-polar solvents results from the effects of both the first and the second terms in Eq. 1, the second term mainly determines the amount of the shifts, if the first term is small.

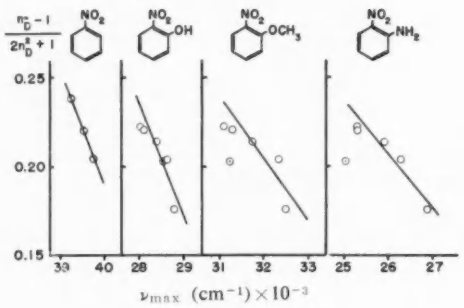

Fig. 1. Relation between $\frac{n_D^2-1}{2n_D^2+1}$ and ν_{max} (longer-wavelength bands) for nitrobenzene and *o*-nitrobenzene derivatives.
(⊙: dioxane, the value n_D for nitrobenzene was used for 250 mμ)

For these nitrobenzene derivatives B in Eq. 2 is negative, indicating that $(\mathbf{M}_{oo}^{u})^2$ is smaller than $(\mathbf{M}_{ll}^{u})^2$, or that the dipole moment values of these derivatives increase in their electronically excited states reached by the absorption transition. The values of B can be evaluated from slopes of the straight lines as apparent in Figs. 1—3 and Table II. The B value for nitrobenzene is evaluated from the data of Bayliss and McRae[4] obtained for *n*-heptane, cyclohexane and carbon tetrachloride. For *p*-nitrobenzene derivatives the B values decrease with the increasing permanent dipole moments of the solute molecules, but for *o*- and *m*-derivatives these relations are not clearly observed. Spectral shifts are also much greater in nitrobenzene derivatives than nitrobenzene.

The present case of a polar solute dissolved in a non-polar solvent corresponds to the case

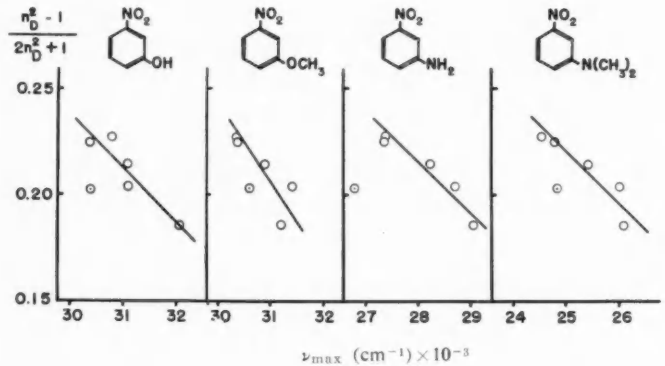

Fig. 2. Ralation between $\frac{n_D^2-1}{2n_D^2+1}$ and ν_{max} (longer-wavelength bands) for *m*-nitrobenzene derivatives. (⊙: dioxane)

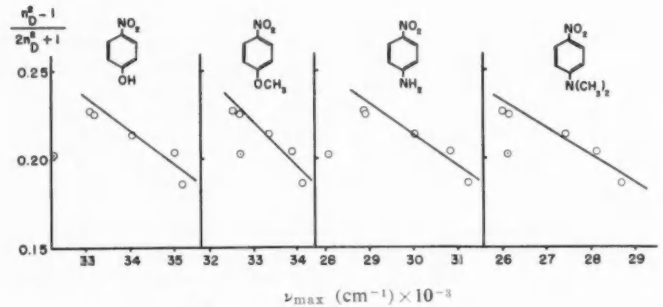

Fig. 3. Relation between $\frac{n_D^2-1}{2n_D^2+1}$ and ν_{max} for *p*-nitrobenzene derivatives. (⊙: dioxane)

TABLE II. EVALUATION OF B VALUES (cm^{-1})

Molecule	B	Ground state dipole moment* (Debye units)
Nitrobenzene	−32000**	3.82∼4.00
o-Nitrophenol	−16000	4.10
o-Nitroanisole	−30000	4.83
o-Nitroaniline	−34000	4.26
m-Nitrophenol	−40000	3.90
m-Nitroanisole	−26000	3.86
m-Nitroaniline	−40000	4.72
m-Nitro-*N*-dimethylaniline	−40000	5.06
p-Nitrophenol	−52000	5.05
p-Nitroanisole	−40000	4.75
p-Nitroaniline	−58000	6.32
p-Nitro-*N*-dimethylaniline	−64000	6.87

* See Ref. 10.
** Evaluated from Bayliss and MaRae's data[4].

III b of Bayliss and McRae's paper[1], in which the solute dipole moment increases during the transition. According to their theory, the forces contributing to the solvation energy are dispersion and dipole-polarization forces (polarization of solvent molecules by the solute dipoles) and the latter is probably greater than the former. When the solute dipole moment increases as the result of the transition, the solvation energy becomes greater in the excited state than in the ground state, and hence absorption maxima are shifted to the red.

It is well known that dioxane behaves differently from other solvents and it can not be regarded as a non-polar solvent here[5,7,8]. Nitrophenol and nitroaniline probably from hydrogen bonds with dioxane and in these systems red shifts due to the hydrogen bonding effect may be expected. However, the anomalous shifts are also observed for nitroanisole and nitro-*N*-dimethylaniline in dioxane solutions, where no hydrogen bonding between solute and solvent molecules can be expected.

Absorption frequency shifts $\Delta\nu_{max}$ due to non-hydrogen bonding polar solvents can be simply expressed in a following form[7]

$$\nu_a-\nu_b=C\left[\frac{D_a-1}{D_a+2}-\frac{D_b-1}{D_b+2}\right]+E\left[\frac{D_a-1}{D_a+2}-\frac{D_b-1}{D_b+2}\right]^2 \quad (5)$$

where ν_a and ν_b are the ν_{max}'s of the solutions in solvents a and b, and D_a and D_b are their respective dielectric constant values. To check this relation we chose ethyl ether with n_D=1.356 and acetonitrile with n_D=1.344 for a and b. Their refractive indices are about the same. Moreover, the absorption spectra of these solvents are similar to each other in the point that they have no strong absorption above 200 mμ, and the dispersion-term contributions from them are expected to be nearly equal[7]. On the other hand, the two solvents have quite different values of dielectric constant, 4.34 for ethyl ether and 37.50 for acetonitrile. Also ethyl ether and nitromethane (n_D=1.382, D=35.87) were used as solvents for *p*-nitro-*N*-dimethylaniline.

Absorption maxima of nitrobenzene, *o*-, *m*- and *p*-nitroanisole and *m*- and *p*-nitro-*N*-dimethylaniline were measured in solvents consisting of ethyl ether and acetonitrile mixed in various proportions*, in which no hydrogen bonding is expected to arise. The results are shown in Figs. 4—9, where for each solute molecule $\Delta\nu_{max}$ for ethyl ether and for the mixed solvents are plotted againt $(D-1)/(D+2)$ of the solvents.

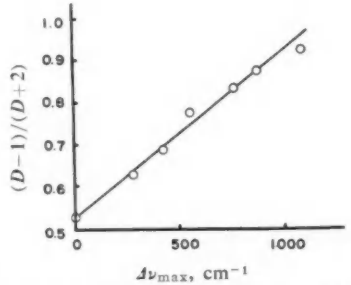

Fig. 4. Relation between $\Delta\nu_{max}$ and $(D-1)/(D+2)$ for nitrobenzene.

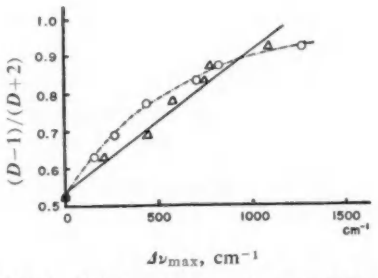

Fig. 5. Relation between $\Delta\nu_{max}$ and $(D-1)/(D+2)$ for *o*-nitroanisole. (○: $H_{x1}\rightarrow V_s$ transiton; △: $H_{x2}\rightarrow V_s$ transition)

* The dielectric constant of a mixed solvent was calculated according to Hoigne and Gaumann[9] by $D=D_0+bW$, where D_0 is the value of dielectric constant of ethyl ether, b the difference of dielectric constant values of ethyl ether and acetonitrile, and W the weight fraction of acetonitrile in the solution.

8) E. Lippert, *Z. Naturforsch.*, **10a**, 541 (1955).

9) J. Hoigne and T. Gaumann, *Helv. Chim. Acta*, **41**, 1933 (1958).

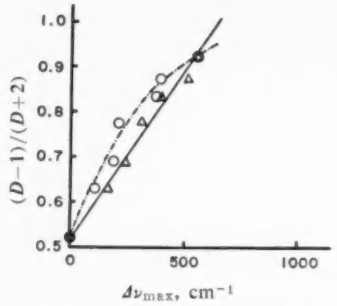

Fig. 6. Relation between $\Delta\nu_{max}$ and $(D-1)/(D+2)$ for *m*-nitroanisole. (○: $H_{x1}\rightarrow V_s$ transition; △: $H_{x2}\rightarrow V_s$ transition)

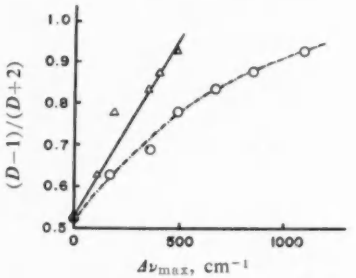

Fig. 7. Relation between $\Delta\nu_{max}$ and $(D-1)/(D+2)$ for *m*-nitro-*N*-dimethylaniline. (○: $H_{x1}\rightarrow V_s$ transition; △: $H_{x2}\rightarrow V_s$ transition)

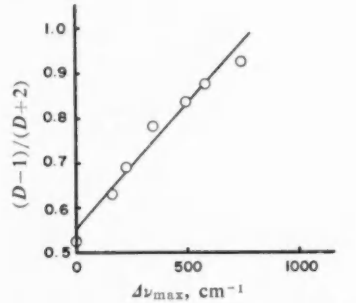

Fig. 8. Relation between $\Delta\nu_{max}$ and $(D-1)/(D+2)$ for *p*-nitroanisole.

For the shorter-wavelength bands of *o*- and *m*-nitrobenzene derivatives which arise from the $H_{x2}\rightarrow V_s$ transition, and also for the intramolecular charge transfer bands of nitrobenzene and *p*-nitrobenzene derivatives, the linear relation holds approximately. However, for all of the longer-wavelength bands of *o*- and *m*-nitrobenzene derivatives arising from $H_{x1}\rightarrow V_s$ transition the plots show obvious curvatures.

These facts indicate that while for the shorter-wavelength bands the shifts are determined only

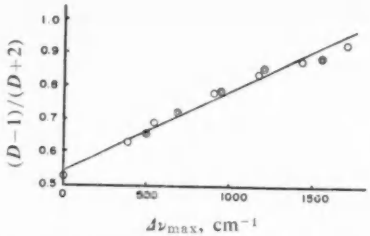

Fig. 9. Relation between $\Delta\nu_{max}$ and $(D-1)/(D+2)$ for *p*-nitro-*N*-dimethylaniline. (○: in ethyl ether and acetonitrile; ◎: in ethyl ether and nitromethane)

by the first term in Eq. 5, for the longer-wavelength bands both the first and the second terms would be responsible. In other words, only the interaction between the permanent dipoles of solute and solvent molecules essentially contribute to the spectral shift for the first case, but for the latter case the interaction between the dipole of the solvent molecules and that induced in the solute molecule also makes possibly an important contribution to the shift.

The values of C in Eq. 5 are easily obtained from the slopes of the straight lines for the shorter-wavelength bands, from which we may calculate* the excited state dipole moment $\mathbf{M}_{ii}^u$, if the values of a are known. Similarly, for the longer-wavelength bands $\mathbf{M}_{ii}^u$ as well as he polarizability differerence $(\alpha_o^u-\alpha_i^u)$ of the solute in its ground and excited states may be estimated from C and E values.

The polarization effect on the spectral shift is apparent only in the $H_{x1}\rightarrow V_s$ transitions of *o*- and *m*-nitrobenzene derivatives. It could not be observed in all other absorption bands investigated. In all cases C and E in Eq. 5 are negative, showing that dipole moment and polarizability are greater in the excited state than in the ground state. This indicates that the stabilization energies arising from the electrostatic interactions between the solute and solvent molecules are much greater in the excited state than in the ground state. Thus, the main factor causing the red shift of these absorption band in polar solvents is the great stabilization in the excited state owing to the electrostatic interaction between the solute and solvent molecules. On the other hand, from the consideration of the obviously important resonance forms of these molecules

* For example, if we assume that a is 4Å for *p*-nitroanisole, the excited state dipole moment $\mathbf{M}_{ii}^u$ can be calculated to be 6.89 D. As its ground state dipole moment is 4.78 D[10], the dipole moment increases by 2.11 D in the excited state.

10) L. G. Wesson, "Tables of Electric Dipole Moments", The Technology Press, M. I. T. (1948).

shown below, the optical absorption may well be accompanied by the excitation of the molecule according to the scheme

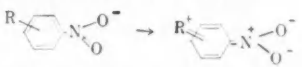

which would contribute largely to the moment of the excited state.

Effect of Hydrogen Bonding.—The hydrogen bonding plays a very important role in the spectral shift of a solution. The hydrogen bonding effect on the absorption spectra of *m*- and *p*-nitrophenol was observed in mixed solvents consisting of *n*-hexane and ethyl ether.

Figs. 10 and 11 show that the absorption maxima are shifted toward the red with an increasing proportion of ethyl ether in the solvent. In each case an isosbestic point is observed. The following hydrogen bonding reaction may be suggested

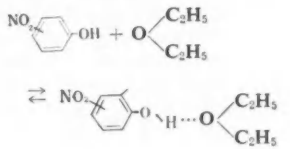

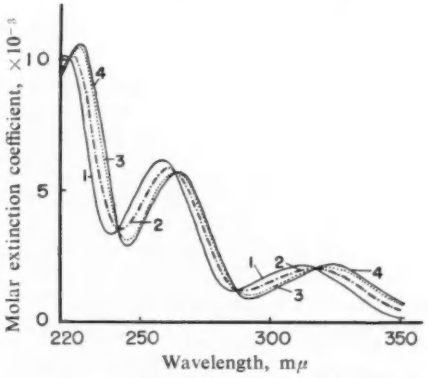

Fig. 10. Absorption curves of *m*-nitrophenol (7.63×10^{-5} mol./l.) in *n*-hexane solution containing ethyl ether at 12°C.
curve 1: *n*-hexane solution (free *m*-nitrophenol)
curve 2: ethyl ether 3.91×10^{-3} mol./l.
curve 3: ethyl ether 7.81×10^{-3} mol./l.
curve 4: calculated curve for bound *m*-nitrophenol

* The equilibrium constant K is calculated as

$$K=\frac{\varepsilon-\varepsilon_A}{\varepsilon'-\varepsilon}\frac{1}{C_B}-\frac{\varepsilon'-\varepsilon_A}{\varepsilon'-\varepsilon}\frac{1}{C_B'}$$

where ε_A is the molar extinction coefficient of free *p*-nitrophenol (curve 1), ε and ε' are those of the mixed solvents for curves 2 and 3, and C_B and C_B' are the concentrations of ethyl ether corresponding to the curves 2 and 3.

** The free energy difference ΔF is calculated as $\Delta F=-RT\ln K$.

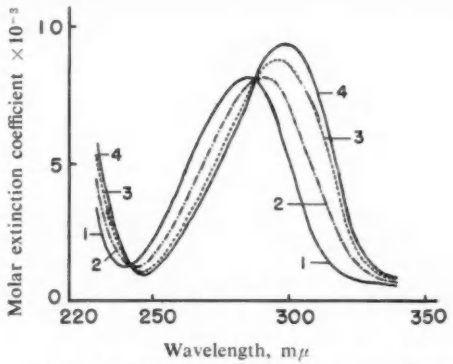

Fig. 11. Absorption curves of *p*-nitrophenol (7.18×10^{-5} mol./l.) in *n*-hexane solution containing ethyl ether at 20°C.
curve 1: *n*-hexane solution (free *p*-nitrophenol)
curve 2: ethyl ether 3.85×10^{-2} mol./l.
curve 3: ethyl ether 1.93×10^{-1} mol./l.
curve 4: calculated curve for bound *p*-nitrophenol

TABLE III. EQUILIBRIUM CONSTANTS AND FREE ENERGY DIFFERENCES FOR *m*- AND *p*-NITROPHENOL

Molecule	Equilibrium constant	Free energy difference (kcal./mol.)
m-Nitrophenol	113.1	−2.6 (12°C)
p-Nitrophenol	24.6	−1.9 (20°C)

From these curves the equilibrium constants* and the free energy differences** are obtained as given in Table III. The equilibrium constant for *m*-nitrophenol is much greater than that for *p*-nitrophenol, indicating that the former requires a very small amount of ethyl ether to reach equilibrium. This may be due to the meta-directing property of the nitro group[1].

For *m*- and *p*-nitroaniline no isosbestic point is clearly observed. This indicates that there is no simple equilibrium relation in the hydrogen bonding reaction. However, their absorption maxima are shifted toward the red with an increasing amount of ethyl ether in the solvents.

Next we shall consider the cases of *p*-nitroanisole and *p*-nitro-*N*-dimethylaniline dissolved in methanol and ethanol. In these systems hydrogen bonds may be expected to be formed between the nitro and the hydroxyl groups, the alcohol molecule playing the role of a proton donor according to the scheme

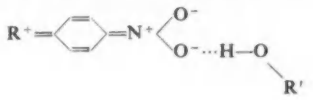

Table IV. Calculated blue-shifts due to $NO_2 \cdots H-O$ (cm^{-1})

Solvent (proton donor)	Nitro-benzene	*o*-Nitro-anisole	*m*-Nitro-anisole	*m*-Nitro-*N*-dimethyl-aniline	*p*-Nitro-anisole	*p*-Nitro-*N*-dimethyl-aniline
Methanol	—	230	150	260	—	—
	130	290	200	330	150	370
Ethanol	—	320	220	250	—	—
	210	270	150	370	280	410

Absorption maxima of *p*-nitroanisole and *p*-nitro-*N*-dimethylaniline are at 32510 and 25540 cm^{-1} in methanol and 32700 and 25700 cm^{-1} in ethanol, respectively. The contribution of electrostatic interactions to the frequency shifts can be evaluated from Eq. 5 as the refractive indices of these alcohols are close to that of ethyl ether or acetonitrile. From the values of C and the dielectric constant for alcohol solutions, the frequency shifts of *p*-nitroanisole relative to the ethyl ether solution can be evaluated as 960 cm^{-1} and as 900 cm^{-1}, and the shifts of *p*-nitro-*N*-dimethylaniline as 1630 and 1520 cm^{-1} for methanol and ethanol, respectively. The experimentally observed shifts for *p*-nitroanisole are 810 and 620 cm^{-1}, and for *p*-nitro-*N*-dimethylaniline 1260 and 1100 cm^{-1}, respectively, for methanol and ethanol. Thus the absorption maximum appears at a shorter wavelength than that expected from only the electrostatic origin in each case. The difference between experimentally observed and calculated frequency shifts may probably be accounted for on the basis of hydrogen bonding between the solute and alcohol molecules. Such differences are observed also for nitrobenzene, *o*- and *m*-nitroanisole, and *m*-nitro-*N*-dimethylaniline as shown in Table IV.

Baba[11] has shown that, if an alcohol molecule plays the role of the proton donor, a blue shift is expected in a $\pi \rightarrow \pi^*$ type transition. The present observed shifts are in good agreement with his theory. Shifts due to hydrogen bonding between the nitro and the hydroxyl groups are estimated as given in Table IV.

11) H. Baba, *Bull. Research Institute of Applied Electricity, Hokkaido University*, **9**, 84 (1957).

Summary

Intramolecular charge transfer spectra of *o*-, *m*- and *p*-nitrobenzene derivatives were measured in solutions with various solvents. Frequency shifts induced by solvents were analyzed on the basis of current theories of solvent effects on absorption spectra. Results show that the frequency shifts in the absorption bands of nitrobenzene derivatives can be interpreted as arising from both the electrostatic and hydrogen bonding interactions.

The author wishes to thank Professor S. Imanishi and Dr. Y. Kanda of Kyushu University for their kind advice and encouragement throughout this investigations and to Dr. M. Ito for his helpful and valuable discussions. The author's thanks are also due to Drs. Y. Kora and T. Ikenoue of Kurosaki Firebrick Mfg. Co. for their kind encouragement.

Department of Chemistry
Faculty of Science
Kyushu University
Hakozaki, Fukuoka

Electronic and Vibrational States of Acrolein

By Kōzō Inuzuka

(Received November 1, 1960)

Eastwood and Snow[1] carried out a vibrational and rotational analysis of the near ultraviolet spetrum of acrolein. Walsh[2] also studied the electronic spectrum of this compound in the vacuum ultraviolet region. Interest in this compound lies partly in the fact that it has a simple skeletal structure containing a system of conjugated double bonds, and that its electronic states can easily be discussed in terms of the MO theory[3]. In a previous paper[4] we studied the n-π^* absorption bands of acrolein as measured with a photoelectric spectrometer. This time the absorption spectrum was measured photographically. In this paper is reported the results of our continued study on the electronic and vibrational states of the molecule. For aiding vibrational analysis, infrared and Raman spectra were also observed, although they have already been measured[5]. Using our new results, more detailed vibrational assignments for the excited state could be made.

Experimental

Acrolein supplied by Tokyo Kasei Kogyo Co. was used. The sample was distilled before measurement. An absorption tube of 40 cm. length provided with quartz windows was used. The spectrum was photographed at various vapor pressures corresponding to temperatures between -25 and 180°C of the tube. The tube with the windows was always kept at temperature about 10°C higher than that of the sample site for purpose of avoiding condensation. A hydrogen or a tungsten lamp was used as the source of the continuum. A Shimadzu type QL-170 spectrograph was used throughout the work. Exposure time from 1 to 20 min. for the tungsten lamp and from 2 to 3 hr. for the hydrogen lamp with a slit width of 20 μ. Fuji process plates were used. Wavelengths were determinined relative to those of iron lines, using a Shimadzu type SR-2 comparator.

For infrared and Raman measurements carbon tetrachloride or ethyl alcohol solution was used. Solvents were purified by Weissberger and Proskauer methods[6]. The Raman spectrograph used was of two dense flint prisms, having the linear dispersion of 24 Å/mm. at 4500 Å. Raman spectrum of acrolein was obtained with ethyl alcohol solution, as acrolein is very unstable chemically under strong irradiation and it was difficult to work with the liquid state. Renewing the sample at about one hour intervals a 12 hr. exposure was made with a slit width of 100 μ. During the exposure filter solution of sodium nitrous oxide was circulated. The infrared absorption was measured with a Hitachi EPI double beam spectrometer with sodium chloride or potassium bromide prism. For acrolein vapor in the sodium chloride region a 10 cm. gas cell was used.

Electronic Transition

Acrolein is a simple aliphatic aldehyde having a system of conjugated double bonds. Electron diffraction study[7] shows that the molecule has a planar *trans*-butadiene-like structure. The molecule thus belongs to the point group Cs and the electronic transitions are all symmetry-allowed. The molecule has four π-electrons and a pair of nonbonding electrons localized on the oxygen atom. Therefore n-π^* and π-π^* transitions are expected to occur. The absorption spectrum of acrolein solution in carbon tetrachloride in the 24993~33324 cm^{-1} region shows a blue shift on addition of ethanol. In ethanol solution the acrolein absorption maximum shifts toward the blue by 400 cm^{-1} relative to carbon tetrachloride solution[4]. The above result suggests the n-π^* nature of this electronic transition. Walsh attributed this transition to a one-electon promotion from the n orbital to the first excited π orbital. His assignment agrees with our calculation[3].

According to the MO theory this first excited state has A′ symmetry, and the lowest state is triplet. Consequently, the vapor absorption begining at 25851 cm^{-1} is assigned to the transition of a nonbonding electron to the first excited singlet state ($^1A'' - {}^1A'$).

Vibrational Analysis

On account of the low Cs symmetry of the molecule, the transition can be of an allowed type. So the 0, 0 band will probably be one

1) E. Eastwood and C. P. Snow, *Proc. Roy. Soc.*, **149A**, 446 (1935).
2) A. D. Walsh, *Trans. Faraday Soc.*, **41**, 498 (1945).
3) K. Inuzuka, This Bulletin, **34**, 6 (1961).
4) K. Inuzuka, ibid., **33**, 678 (1960).
5) M. Aime Cotton, *Compt. rend.*, **208**, 740 (1939).
6) A. Weissberger and E. S. Proskauer, "Organic Solvents", Interscience Publishers, Inc., New York, N. Y. (1955).
7) H. Mackle and L. E. Sutton, *Trans. Faraday Soc.*, **47**, 691 (1951).

of the stronger bands. The development of the spectrum with increasing temperature suggests that the 0, 0 band is surely the strong band at 25851 cm^{-1}. In an earlier work of Eastwood and Snow a band at 25860 cm^{-1} was chosen as the 0, 0 band from rotational analysis, and two progressions of bands with mean separations of 1260 and 500 cm^{-1} respectively were observed. Since our measurement was limited to about 30294 cm^{-1}, the progression corresponding to 1260 cm^{-1} could not be followed further than the second overtone. These bands are accompanied each by a strong subsidary band with the separation of 499 cm^{-1}. In our analysis 1270 cm^{-1} was taken as the interval of the progression. Among the observed bands, nearly 130 in number, some show rotational structures but many are not well defined. It is difficult to interpret correctly all of these observed bands on account of the low symmetry of the molecule, so we give in Table I the position and interpretations only

Table I. Vibrational analysis of ultraviolet absorption spectrum of acrolein vapor

In.	Å	cm^{-1}	Freq. distance from the 0, 0 band	Assignment
vs	3867.2	25851	0	0, 0
vs	3794.0	26350	499	0+499
m	3705.7	26978	1127	0+1127
vs	3686.2	27121	1270	0+1270
vs	3666.6	27265	1414	0+1414
bm	3638.5	27476	1625	499+1127=1626
s	3620.0	27616	1765	1270+499=1769
bs	3601.6	27758	1907	499+1414=1913
m	3538.3	28254	2403	1270+1127=2397
s	3521.3	28391	2540	2(1270)
bm	3502.2	28545	2694	1270+1414=2684
m	3484.1	28693	2842	2(1414)
m	3461.6	28880	3029	2(1270)+499=3039
w	3387.4	29513	3662	2(1270)+1127=3667
w	3369.0	29674	3823	3(1270)
w	3354.1	29806	3955	2(1270)+1414=3954
w	3324.5	30071	4220	3(1414)

vs: very strong, s: strong, bm: broad medium, m: medium, w: weak

for stronger bands. The frequencies of 1270 and 499 cm^{-1} are assigned definitely to two totally symmetric vibrations of type A′ of the lower electronic state. The very weak bands on the longer wavelength side of the 0, 0 band decrease their intensity with decreasing temperature, and the vicinity of 70°C is favorable for their observation. The number of moderately strong bands is small on this side of the 0, 0 band. A sharp band is separated from the 0, 0 band by 145 cm^{-1}, and three fine bands by about 313 cm^{-1}. The latter bands are the ones called by Eastwood and Snow a, b and c bands, although our wavelengths are slightly different from that of Eastwood and Snow.

In addition, there is a series of four bands 24636, 24611, 24577 and 24552 cm^{-1} on the further long wavelength side. Among these bands the second one which is separated from the 0, 0 band by 1240 cm^{-1} is the strongest. On the whole our observation agrees well with that of Eastwood and Snow. Besides these bands, two weak but sharp bands are observed at 24259 and 24240 cm^{-1}. There are no further bands on the red side of these two bands. The bands on the red side of the 0, 0 band having appreciable intencities usually represent fundamental vibrational frequencies of the ground state. From this viewpoint we may assign the two bands separated from the 0, 0 band by 1274 and 1611 cm^{-1}, respectively, to the two frequencies 1270 and 1623 cm^{-1} found in infrared and Raman spectra. Bands other than those described above are tentatively interpreted as combination bands. A band with moderate intensity separated by 1127 cm^{-1} from the 0, 0 band on its shorter wavelength side form a satellite accompanying the stronger 1270 cm^{-1} band. The 1127 cm^{-1} frequency appears also in other combination bands, so that it is reasonable to assume this frequency as a fundamental. There is a very strong band at 27265 cm^{-1} separated by 1414 cm^{-1} from the 0, 0 band. Starting from this band a progression containing two more bands with 1414 cm^{-1} interval is observed. The 1414 cm^{-1} frequency also appears in other combination bands, so that we may assume this to be another fundamental.

Fundamental Vibrational Frequencies

The acrolein molecule, CH_2CHCHO, may belong, at the most, to the point group Cs. As it contains eight atoms, eighteen normal modes of vibration are possible, of which thirteen are of the totally symmetrical A′ type, and the remaining five are of the anti-symmetrical A″ type. Both types are active in infrared and Raman spectra. There will be seven essentially valency type vibrations of the four C–H, one C=C, one C–C and one C=O bonds. Analogously to 1, 3-butadiene[8,9] there will also be an A″ type torsional oscillation about the C–C bond. Another important mode of A′ is the planar deformation of the C=C–C=O skeleton.

8) C. M. Richards and J. R. Nielsen, *J. Opt. Soc., Am.* **40**, 438 (1950).
9) R. S. Rasmussen and R. R. Brattain, *J. Chem. Phys.*, **15**, 131 (1947).

TABLE II. INFRARED AND RAMAN FREQUENCIES OF ACROLEIN MOLECULE (cm^{-1})

Infrared				Raman		Assignment
CCl_4 solution		vapor		EtOH solution		
w	570			w	340	Skeletal bending
				m	574	Skeletal bending
s	910	m	906			
s	959	s	917	w	980	CH and CH_2 wagging
s	982	s	960			
		s	990			
			1147			
s	1152	s	1156	w	1170	CH_2 rocking
			1163			
w	1270	w	1262	m	1272	C-C stretching
			1280			
m	1360	m	1348	s	1360	CH rocking
			1366			
m	1420	m	1410	w	1426	CH_2 deformation
			1427			
m	1617	m	1613	s	1620	C=C stretching
			1632			
vs	1708	vs	1713	vs	1701	C=O stretching
			1727			
m	2700	m	2710			
m	2755	m	2790			
m	2805	m	2810			C-H stretching
w	2990	w	3000			
w	3100	w	3100			
w	3375	w	3388			C=O overtone

The infrared spectrum was measured in the 460~4000 cm^{-1} region, but a weak band at 340 cm^{-1} was found in the Raman spectrum. An analogous band was found in 1, 3-butadiene at 320 cm^{-1} and has been assigned to a skeletal deformation vibration. Therefore we have assigned the Raman band of acrolein at 340 cm^{-1} to an A'' type skeletal deformation vibration. We found a weak band at 570 cm^{-1} in the infrared potassium bromide region, and in the Raman spectrum at 574 cm^{-1}. It may be assigned to an A' type skeletal deformation vibration. In 1, 3-butadiene the corresponding Raman band is at 513 cm^{-1}. Corresponding to the infrared bands in the 900 cm^{-1} region only one Raman band at 980 cm^{-1} was found with very small intensity. This band system may be due to the CH and CH_2 wagging vibrations. The infrared band at 1150 cm^{-1} is strong and sharp, and the corresponding Raman band has exactly the same frequency shift.

This band may be assigned to the rocking vibration of the methylene radical. The Raman band at 1272 cm^{-1} has medium intensity. In infrared two bands appear at 1235 and 1270 cm^{-1}, the former being very weak, and the latter medium strong. We may assign the latter frequency 1270 cm^{-1} to the C-C stretching vibration, in analogy to the 1205 cm^{-1} of 1, 3-butadiene and 1284 cm^{-1} of biacetyl[10]. The value of 1270 cm^{-1} for acrolein might appear too high for the C-C stretching frequency, but it is probably due to the partial double bond character of the bond in this molecule, whose length is 1.46 Å[7], considerably shorter than the normal C-C single bond length 1.53~1.54 Å. The band at 1360 cm^{-1} was observed in both the Raman and infrared spectra with considerable intensity. This frequency may be assigned to the CH rocking vibration. The weak band at 1420 cm^{-1} in infrared and at 1426 cm^{-1} in Raman spectra may be assigned to the CH_2 deformation vibration in analogy to the Raman 1442 cm^{-1} band in 1, 3-butadiene. The C=C stretching frequency is observed as the 1617 cm^{-1} infrared band for solution, as the 1620 cm^{-1} Raman medium strong band. The C=O stretching frequency is observed at 1695~1725 cm^{-1} in solution with two peaks in the infrared and at 1700 cm^{-1} in the Raman spectrum. It is the strongest band in both the spectra, but the Raman frequency seems to have been affected by the solvent. C-H valence vibration bands lying in the 2700~3000 cm^{-1} region were not observed in the Raman spectrum as they may be hidden under excited Hg lines. Result of the vibrational analysis is given in Table II.

In a symmetry-allowed molecular electronic

10) J. W. Sidman and D. S. McClure, *J. Am. Chem. Soc.*, 77, 6471 (1955).

Table II. Fundamental vibrational frequencies (cm^{-1})

Raman (solution)	Infrared (vapor)	Lower state	Upper state	Assignment
1701	1713} 1727}	1720	1270	C=O valence (A′)
1620	1613} 1632}	1623	1414	C=C valence (A′)
1272	1259} 1280}	1270	1127	C-C valence (A′)
570		570	499	C=C-C=O bending (A′)

transition, totally symmetric vibrational frequencies appear generally with large intensities in absorption. In the acrolein spectrum as analyzed above, all of the interval frequencies contained in prominent progressions can be assigned either to fundamental, or to combination frequencies of A′ type vibrational modes of the excited electonic state. In Table III correlations among upper and lower state vibrational frequencies are given. Of these fundamental frequencies those of the upper state of 1270 cm^{-1} and 499 cm^{-1} are the most important in the vapor absorption. The former is observed up to the second overtone (3×1270 cm^{-1}) and is assigned to the C=O stretching mode. The latter frequency is assigned to a skeletal bending mode, as its corresponding lower state frequency is very probably 570 cm^{-1} observed in both Raman and infrared spectra. The very strong band separated from the 0, 0 band by 1414 cm^{-1} may be associated with another fundamental vibration, since we could not analyze so strong a band as a combination or overtone and since, moreover, its frequency separation 1414 cm^{-1} is repeated twice more in forming a prominent progression. In our previous paper[4] this frequency was assigned to the C=C vibration, although a slightly different value was then reported. The 1127 cm^{-1} frequency is observed as satellite bands accompanying each of the 1270 cm^{-1} progression bands. This frequency was not reported in the above cited paper[4]. It can be assigned to the C-C vibration of the excited electronic state in analogy to the biacetyl 1136 cm^{-1} (excited state) and 1284 cm^{-1} (ground state). In acrolein the corresponding lower state frequency is 1270 cm^{-1}.

Summary

The position, blue-shift and theoretical calculation[3] of the state energy of the electronic transition of acrolein in 24241~30294 cm^{-1} region suggest that the transition is of the $n-\pi^*$ type. From the vibrational analysis of acrolein vapor spectrum, it is known that the vapor spectum of acrolein has four progressions corresponding to the C=O, C=C and C-C stretching, and skeletal bending frequency in the lower state.

The author expresses his sincere thanks to Professor S. Imanishi and Dr. Y. Kanda for their kind encouragements throughout this work. He is also indebted to Dr. M. Ito and Mr. R. Shimada for their helpful advice and discussions.

Department of Chemistry
Facutly of Science
Kyushu University
Hakozaki, Fukuoka

Electron Diffraction Investigations on the Molecular Structures of sec-Butyl Chloride and Alcohol

By Mashio YAMAHA and Masato IGARASHI

(Received October 12, 1960)

The molecular structures of propane[1], butane[2] and their chlorine derivatives, such as *n*- and isopropyl chloride[3,4], 1, 2-dichloropropane[5] and *tert*-butyl chloride[6,7] have already been studied by electron diffraction, using the visual method or the sector-microphotometer method. It appears that only a few studies have been done on the molecular structures of alcohols[4,8-10].

In this paper the results of electron diffraction investigation about *sec*-butyl chloride and alcohol using the sector-microphotometer method are described and compared with those of the related compounds.

Experimental

sec-Butyl chloride and alcohol were kindly furnished by Dr. T. Miyazawa, the University of Tokyo. They were the same samples which were used in the spectroscopic studies.

The diffraction patterns were taken at room temperature of about 20°C using an apparatus[11] having an r^2-sector which was rotated rapidly during exposure. The exposures of each set were regulated to be about 2 : 1 in order to apply Karle's method[12]. The camera length was 11.82 cm. and the wavelength of electron was about 0.0567 Å, which was determined by measuring the transmission patterns of gold foil.

The optical densities of the photographic plates were measured by a microphotometer. The plates were rotated rapidly about their centers during scanning. The optical densities were converted to relative intensities by Karle's procedure[12]. A smooth background line was drawn through the intensity curve multiplied by q and the molecular intensity curve $M(q)$ was obtained using the following formula,

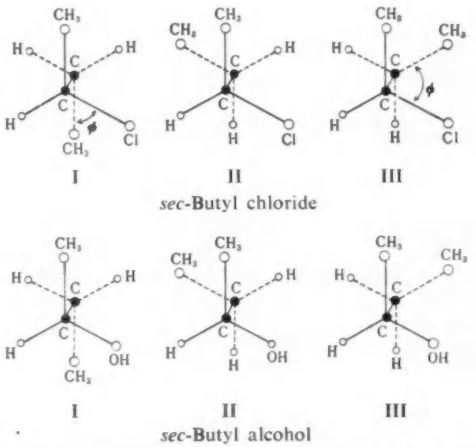

Fig. 1. Rotational isomers of *sec*-butyl chloride and alcohol.

TABLE I. LIST OF MOLECULAR CONSTANTS OF PROPANE, BUTANE AND THIR CHLORINE DERIVATIVES

Molecule	C-C, Å	C-Cl, Å	Angle CCC	Angle CCCl	Reference
Propane	1.54 ±0.02	—	111.5°±3°	—	1
n-Butane	1.539±0.003	—	112°9′ ±9′	—	2
n-Propyl chloride	1.535±0.02	1.775±0.02	109.5°±2.5°	111°±2°	3
Isopropyl chloride	1.55 ±0.02	1.76 ±0.02	109.5°±1.5°	111°±1.5°	4
1, 2-Dichloropropane	1.56 ±0.05	1.79 ±0.035	109.5°(ass.)	108°±4°	5
tert-Butyl chloride	1.54 ±0.01	1.80 ±0.01	111.5°±1°	—	6
tert-Butyl chloride	1.54 ±0.03	1.80 ±0.04	111.5°±1.5°	—	7

1) L. Pauling and L. O. Brockway, *J. Am. Chem. Soc.*, **59**, 1223 (1939).
2) K. Kuchitsu, This Bulletin, **32**, 748 (1959).
3) Y. Morino and K. Kuchitsu, *J. Chem. Phys.*, **28**, 175 (1958).
4) Y. Yamaha, This Bulletin, **27**, 170 (1954).
5) W. Wood and V. Schomaker, *J. Chem. Phys.*, **20**, 555 (1952).
6) O. Bastiansen and L. Smedvik, *Acta Chem. Scand.*, **7**, 653 (1953).
7) J. W. Coutts and R. L. Livingston, *J. Am. Chem. Soc.*, **75**, 1542 (1953).
8) K. Kimura and K. Kubo, *J. Chem. Phys.*, **30**, 151 (1959).
9) M. Kimura, *J. Chem. Soc. Japan, Pure Chem. Sec.* (*Nippon Kagaku Zasshi*), **71**, 18 (1950).
10) V. Schomaker, *Acta Cryst.*, **3**, 46 (1950).
11) K. Kuchitsu, This Bulletin, **30**, 391 (1956).
12) J. Karle and I. L. Karle, *J. Chem. Phys.*, **18**, 957 (1950).

TABLE II. LIST OF MOLECULAR CONSTANTS OF ALCOHOLS

Molecule	C-C, Å	C-O, Å	Reference
Methyl alcohol	—	1.428±0.003	8
Ethyl alcohol	1.54(ass.)	1.48 ±0.04	9
Ethyl alcohol	1.55±0.02	1.43 ±0.02	10
Isopropyl alcohol	1.54±0.02	1.45 ±0.03	4

$$M(q)=(I_T/I_B)-1 \quad (1)$$

where I_T is the total intensity and I_B is the background intensity.

Analysis

The radial distribution curves were calculated by the following equation,

$$f(r) = \sum_{q=0}^{q=85} qM(q)\exp(-aq^2)\sin(\pi qr/10) \quad (2)$$

where $M(q)$ is the experimental molecular intensity obtained from Eq. 1. Here the correction for the non-nuclear scatterings was not made. The artificial damping factor a was chosen so that $\exp(-aq^2)=0.1$ at $q=85$, and $q=(40/\lambda)\sin(\theta/2)$, where θ is the angle of scattering and λ is the wavelength of the electron beam.

In the calculation of the radial distribution curve, the intensity curve below $q=15$ was spliced by the theoretical intensity curve with a constant coefficient. The intensity curve in such a region is hardly affected at all by the bond distance changes of the order 0.01 Å, but considerably affected by the internal rotation around the middle C-C bond (Fig. 1). Several steps of successive approximations were taken in order to make the assumed model practically selfconsistent with the final radial distribution curve.

The theoretical intensity curves were calculated using the following equation,

$$qM_c(q)=\sum_{i,j}(Z_iZ_j/r_{ij})\exp(-b_{ij}q^2)\sin(\pi qr_{ij}/10) \quad (3)$$

where r_{ij} is the interatomic distance between the ith and jth atoms, b_{ij} is its temperature factor which is calculated from the mean amplitude, Z_i is the ith atomic number, except hydrogen, where the effective value 1.25 was used. The mean amplitudes used for the factors b_{ij} are shown in Table III. The theoretical intensity curves of the mixed rotational isomers were considered.

***sec*-Butyl Chloride.**—The radial distribution curve (Fig. 3) has peaks at 1.085, 1.54, 1.80, 2.17, 2.715, 3.23 and 4.15 Å. The first peak is assigned to bonded C-H distances, the second to bonded C-C distances, the third to bonded C-Cl distance with some contributions of nonbonded H···H distances, the fourth to nonbonded C···H distances. The peak of the nonbonded C···H distances, when the fourth peak is resolved into its components, shows that the angles CCH are about 109.5°, if the C-H bond distances are assumed to be 1.09 Å. The fifth peak is mainly resolved into those of nonbonded C···C and C···Cl distances, although it involves some components of the others. If the C-Cl bond distance is assumed to be 1.80 Å, the peak of C···Cl distances shows that the angles CCCl are equal to 109.5°.

In the same way, the peak of C···C distances, although the height is less than that of C···Cl and its position is somewhat uncertain, shows that the angles CCC are about 110~112°. The peak at about 3.23 Å is characteristic of the gauche C···Cl and shows the existence of I or III or both the forms (Fig. 1). The peak shows also that the azimuthal angle ϕ is about 70°C. The peak at 4.15 Å is characteristic of the trans C···Cl and shows the existence of the form II. The peak of gauche C···C overlaps heavily with the other more predominant peaks and the peak of trans C···C is very low, so these two peaks are not so suitable to estimate the amount of forms I and III. As the area under the peak is approximately proportional to Z_iZ_j/r_{ij}, the amount of each form can be found from the area of the characteristic peak and since the areas of trans C···Cl and gauche C···Cl are

TABLE III. MEAN AMPLITUDES USED FOR THE ANALYSIS

Atomic pair	Mean amplitude Å	Atomic pair	Mean amplitude Å
C-C	0.050	O···H	0.114
C-Cl	0.050	H···H	0.135
C-O	0.050	*trans*-C···C	0.070
C-H	0.077	*trans*-C···Cl	0.068
C···C	0.079	*trans*-C···O	0.070
C···Cl	0.073	*gauche*-C···C	0.160
C···O	0.073	*gauche*-C···Cl	0.140
C···H	0.120	*gauche*-C···O	0.140
Cl···H	0.114		

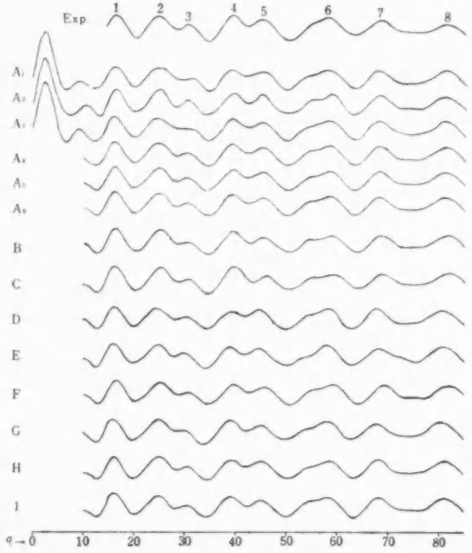

Fig. 2. Intensity curves of *sec*-butyl chloride.

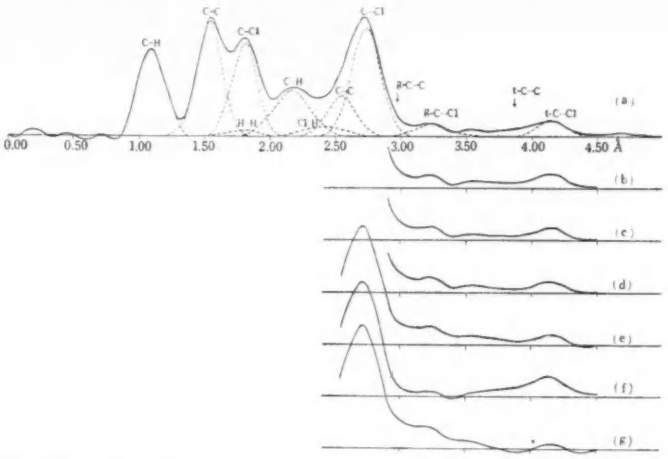

Fig. 3. Radial distribution curves of *sec*-butyl chloride. Spliced theoretical intensity curves below $q=15$ are as follows;

(a) I 50%, II 50%, (b) I 25%, II 50%, III 25%, (c) II 50%, III 50%, (d) I 33%, II 33%, III 33%, (e) I 100%, (f) II 100%, (g) III 100%

affected by the spliced theoretical intensity curves below $q=15$, various ratios of the three forms were tried so that the peaks became almost self consistent with the assumed ratio. The theoretical intensity curves of the forms I and II below $q=15$ are not so different from each other, so the radial distribution curve is not affected very much by the ratio of these two kinds of spliced portions. The ratio of the amounts of the forms I and III could not be obtained unambiguously. Only the ratio of the form II and the sum of the forms I and III was obtained rather definitely.

Its reasonable ratio was about 50%:50%. The radial distribution curves a, b and c are almost selfconsistent with the assumed amounts of the rotational isomers, but d, e, f and g are not selfconsistent (Fig. 3).

Making reference to the results of the radial distribution curve, the theoretical intensity curves of various models were drawn in order to find the best model. The theoretical intensity curves of the three rotational isomers show some different features respectively at about $q=25\sim50$ and among the three, the forms I and III which have gauche C···Cl resemble each other rather than the form II which has trans C···Cl. However the theoretical intensity curve of any one rotational isomer does not fit better with the experimental than that of the mixed one, so for one model of assumed bond distances and bond angles, some mixtures of the rotational isomers I, II and III were examined, but for the most part the ratio, form I: form II=50%: 50% was assumed (Table IV). The intensity curves A_5 and A_6 fit with the experimental better than any other (Fig. 2). Next to them B fits well. Both curves C and D in which the C-Cl bond distance is 1.76 and 1.82 Å, respectively, show very different intensities at maxima 4 and 5 compared with the experimental. So the C-Cl bond distance can be determined to be 1.79 ± 0.015 Å.

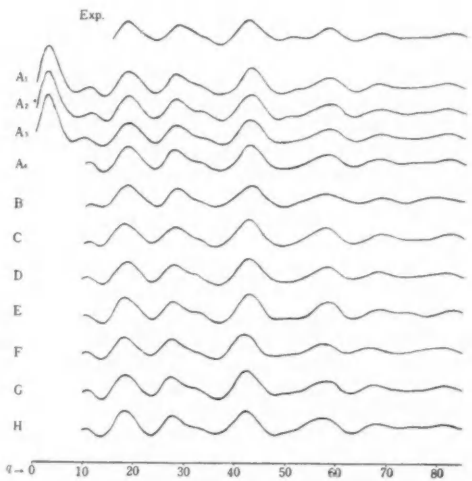

Fig. 4. Intensity curves of *sec*-butyl alcohol.

The intensity curves F and G in which C-C bond distances are 1.52 and 1.56 Å, respectively, have not very different appearances from the experimental, but the $q_{\text{calcd}}/q_{\text{obs}}$ values are not so good as that of 1.54 Å. The C-C bond distances can be considered to be 1.54 ± 0.01 Å. The intensity curves H and I in which C-H bond distances are 1.07 and 1.11 Å, respectively, have different intensity ratios at maxima 4 and 5 compared with the experimental. The C-H bond distances seem to be 1.09 ± 0.015 Å.

***sec*-Butyl Alcohol.**—The radial distribution curve has peaks at 1.06, 1.515, 2.16, 2.485, 2.93 and 3.73 Å (Fig. 5). The first peak is considered to be the resultant of bonded C-H and O-H peaks, the second to be that of bonded C-C and C-O peaks,

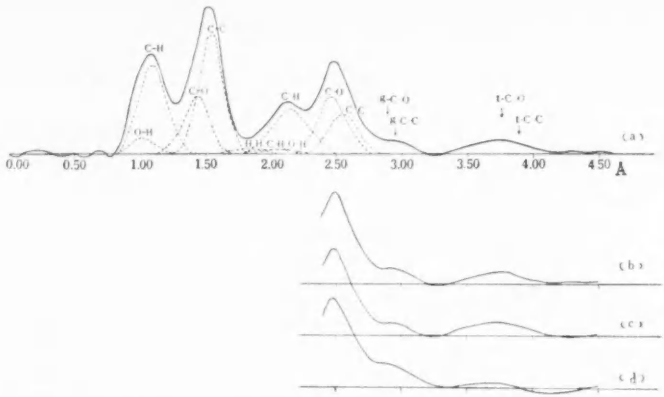

Fig. 5. Radial distribution curves of *sec*-butyl alcohol. Spliced theoretical intensity curves below $q=15$ are as follows;
(a) I 50%, II 50% (b) I 100%, (c) II 100%, (d) III 100%

TABLE IV. MOLECULAR MODELS OF *sec*-BUTYL CHLORIDE AND q_{calcd}/q_{obs} VALUES

Model	C-C Å	C-H Å	C-Cl Å	Angle CCC	Angle CCCl	Percent of rotational isomers I	II	III	Mean value of q_{calcd}/q_{obs}	Average deviation
A_1	1.54	1.09	1.80	109.5°	109.5°	100	0	0	1.004	0.012
A_2	1.54	1.09	1.80	109.5°	109.5°	0	100	0	0.997	0.007
A_3	1.54	1.09	1.80	109.5°	109.5°	0	0	100	—	—
A_4	1.54	1.09	1.80	109.5°	109.5°	33	33	33	0.997	0.006
A_5	1.54	1.09	1.80	109.5°	109.5°	25	50	25	0.999	0.004
A_6	1.54	1.09	1.80	109.5°	109.5°	50	50	0	0.999	0.005
B	1.54	1.09	1.78	109.5°	109.5°	50	50	0	1.006	0.005
C	1.54	1.09	1.76	109.5°	109.5°	50	50	0	—	—
D	1.54	1.09	1.82	109.5°	109.5°	50	50	0	0.991	0.005
E	1.54	1.09	1.80	112°	112°	50	50	0	0.989	0.007
F	1.52	1.09	1.78	109.5°	109.5°	50	50	0	1.014	0.008
G	1.56	1.09	1.80	109.5°	109.5°	50	50	0	0.991	0.008
H	1.54	1.07	1.80	109.5°	109.5°	50	50	0	0.999	0.006
I	1.54	1.11	1.80	109.5°	109.5°	50	50	0	0.997	0.005

TABLE V. MOLECULER MODELS OF *sec*-BUTYL ALCOHOL AND q_{calcd}/q_{obs} VALUES

Model	C-C Å	C-H Å	C-O Å	Angle CCC	Angle CCO	Percent of rotational isomers I	II	III	Mean value of q_{calcd}/q_{obs}	Average deviation
A_1	1.54	1.09	1.43	109.5°	109.5°	100	0	0	1.000	0.009
A_2	1.54	1.09	1.43	109.5°	109.5°	0	100	0	1.005	0.008
A_3	1.54	1.09	1.43	109.5°	109.5°	0	0	100	1.004	0.009
A_4	1.54	1.09	1.43	109.5°	109.5°	50	50	0	1.004	0.013
B	1.54	1.09	1.40	109.5°	109.5°	50	50	0	1.010	0.013
C	1.54	1.09	1.46	109.5°	109.5°	50	50	0	0.996	0.012
D	1.54	1.09	1.43	112°	109.5°	50	50	0	1.001	0.008
E	1.52	1.09	1.43	109.5°	109.5°	50	50	0	1.008	0.006
F	1.56	1.09	1.43	109.5°	109.5°	50	50	0	0.989	0.008
G	1.54	1.07	1.43	109.5°	109.5°	50	50	0	1.004	0.009
H	1.54	1.11	1.43	109.5°	109.5°	50	50	0	1.004	0.008

the third to be that of nonbonded C···cH, C···oH and O···cH peaks, the fourth to be that of nonbonded C···O and C···C peaks. Each of the above peaks consists of two or more components, so it is resolved into its components somewhat arbitrarily. Assuming the mean amplitudes listed in Table III, these peaks were resolved as in Fig. 5. The resolved peaks show that the angles CCH are about 109.5° and the angles CCC and CCO are both slightly greater than 109.5°.

The fifth peak at about 2.93 Å is characteristic of gauche C···O or C···C and the sixth peak at about 3.73 Å is characteristic of trans C···O or C···C. From both the peaks the amount of the rotational isomers are to be obtained. But these peaks are almost entirely controlled by the spliced intensity curves below $q=15$. They can be seen from the fact that the theoretical intensity curves of the rotational isomers above $q=15$ are not very different from each other. Moreover each peak may be constructed respectively from two adjacent components, C···O and C···C, and the resolution into its components is somewhat arbitrary. So it is difficult to determine the amounts of the rotational isomers unambiguously at the present step. It seems, however, that all the three rotational isomers may be present and the form II is predominant among them.

The theoretical intensity curves of various models listed in Table V are drawn in Fig. 4. As the intensity curves of models A, E and F do not show a greatly different appearance compared with the experimental, the C-C bond distances were estimated by the $q_{\text{calcd}}/q_{\text{obs}}$ values as 1.54 ± 0.015 Å (Table V). The intensity curves B and C have slightly different appearances from the experimental at the vicinity $q=50$ and unappropriate $q_{\text{calcd}}/q_{\text{obs}}$ values, so the C-O bond distance is considered to be 1.43 ± 0.02 Å. The intensity curves G and H have not greatly different features and $q_{\text{calcd}}/q_{\text{obs}}$ values compared with A, that the C-H bond distances cannot be determined within small limits of uncertainty. They seem to be 1.09 ± 0.03 Å.

Summary and Discussion

The molecular structures of *sec*-butyl chloride and alcohol have been investigated by the sector and microphotometer method of electron diffraction. The structural information was derived from the radial distribution curves and correlation with the theoretical intensity curves. The results were as follows:

sec-Butyl chloride; C-C $=1.54\pm0.01$ Å, C-Cl $=1.79\pm0.015$ Å, angles CCC $=111\pm1.5°$, angles CCH $\approx 10.95°$, angle CCCl $\approx 109.5°$, the abundance ratio of the rotational isomer in which C···Cl is trans and that in which C···Cl are gauche is about 50% : 50%.

sec-Butyl alcohol; C-C $=1.54\pm0.015$ Å, C-O $=1.43\pm0.02$ Å, C-H $=1.09\pm0.03$ Å, angles CCC and CCO are slightly greater than 109.5°, angles CCH $\approx 109.5°$. The abundance ratio of the rotational isomers could not be determined unambiguously at present.

When the above results are compared with Tables I and II, the C-C bond distances, the angles CCC and CCCl coincide with each other, although the accuracies are somewhat different. The C-Cl bond distance of *sec*-butyl chloride coincides with the results on *n*-propyl chloride[3], 1,2-dichloropropane[5] and *tert*-butyl chloride[6,7], but it is about 0.03 Å longer than that of isopropyl chloride[4].

The C-O bond distance of *sec*-butyl alcohol coincides with most cases of alcohols.

As for the rotational isomers, the abundance ratio was obtained to some extent about *sec*-butyl chloride, but not obtained unambiguously about *sec*-butyl alcohol at the present step.

By the measurement of specific rotation of *D*-*sec*-butyl alcohol, Bernstein and Pedersen[13] have found the amounts of the three rotational isomers to be 42% (form I), 42% (form II), 15.3% (form III), assuming that forms I and II have the same energy and that the form III is less stable (Fig. 1).

The amounts of rotational isomers will be obtained more accurately by the use of a long camera-length of electron diffraction apparatus.

The authors wish to express their hearty thanks to Professor A. Kotera for his kind guidance throughout this work, to Professor Y. Morino, the University of Tokyo, for the use of diffraction apparatus, to Dr. K. Kuchitsu and Dr. E. Hirota, the University of Tokyo, for their kind aid during the experiment and for their calculation by the Punched Card Machine; also to Dr. S. Shibata and Dr. H. Morimoto, Nagoya University, for the microphotometer-tracing.

Department of Chemistry
Faculty of Science
Tokyo University of Education
Koishikawa, Tokyo

13) H. Bernstein and E. E. Pedersen, ibid., 17, 885 (1949).

SHORT COMMUNICATIONS

On the Electromigration in Ion-exchange Papers

By Takeo YAMABE, Manabu SENŌ and Nobuharu TAKAI

(Received March 6, 1961)

In electromigration of ions in ion-exchange papers, which are filter papers impregnated with pulverized ion-exchange resins, we may expect the contribution of ion-exchange adsorption to the electromigration behavior of ions. This behavior of alkaline earth metal ions and amino acid ions will be presented in this communication. This may be the first report dealing with the electrophoretic method using these papers, although some chromatographic experiments have been carried out[1].

The usual apparatus for paper electrophoresis (Toyo Roshi Type C) were used and the ionic mobilities under constant voltages were measured. Ion-exchange papers (Rohm and Haas Co.) were Amberlite SA-2 (sulfonic) and WA-2 (carboxylic), which were used after conditioning with acid, alkali and methanol. For comparison, Toyo Roshi No. 50 was used as an ordinary paper. Systems examined are Mg^{2+}, Ca^{2+}, Sr^{2+} and Ba^{2+} (chloride) supported in 0.05 N hydrochloric acid, sodium chloride or sodium hydroxide, and glycine, glutamic acid and lysine monohydrochloride supported in acetic acid-sodium acetate. For detection of spots of ions, coloration of alkaline earth metal with alizarin-ammonia and that of amino acid with ninhidrin were adopted.

TABLE I. MOBILITIES OF ALKALINE EARTH METAL IONS
10 V./cm., supporting media 0.05 N HCl

	Mobilities, $cm^2/V.\ sec. \times 10^4$			
	Mg^{2+}	Ca^{2+}	Sr^{2+}	Ba^{2+}
Toyo Roshi No. 50	3.1	3.6	3.6	3.9
Amberlite SA-2	0.22	0.33	0.33	0.03
Amberlite WA-2	2.6	3.0	3.0	3.3

TABLE II. MOBILITIES OF AMINO ACID IONS
25 V./cm., supporting media 1 M CH_3COOH

	Mobilities, $cm^2/V.\ sec. \times 10^4$		
	Glycine	Glutamic acid	Lysine
Toyo Roshi No. 50	0.71	0.53	1.27
Amberlite SA-2	0.11	0.09	0.01
Amberlite WA-2	0.66	0.45	0.81

A part of the experimental results is shown in Tables I and II. The ionic electromigration in ion-exchange papers possesses the diminished velocity and tailing, in comparison with the case where the ordinary paper is used. This is remarkable on SA-2 paper which exhibits strong exchange adsorption for cations. It must be noticed that the ionic mobilities decrease in the same order, $Ba^{2+} > Sr^{2+}$, $Ca^{2+} > Mg^{2+}$, on the paper No. 50 as in free solution, but Sr^{2+}, $Ca^{2+} > Mg^{2+} > Ba^{2+}$ on sulfonic SA-2 paper in acidic medium*. This might be ascribed to especially strong affinity of sulfonic acid resin for barium ion, being in accordance with observation in the permselectivity of the ion-selective membrane[2]. On carboxylic WA-2 paper, there is scarecely adsorption effect in acidic medium, where the paper is not in dissociated state. In neutral and alkaline medium, the ionic mobilities have the order, $Ba^{2+} > Sr^{2+} > Mg^{2+} > Ca^{2+}$, e. g., calcium ion is retarded to a great extent. Amino acid ions in acidic medium decrease in migrating velocity on SA-2 (lysine most remarkable), but do not decrease largely on WA-2 which does not dissociate so that the adsorption effect is small.

From the above observation, it was confirmed that the synergetic effect of electromigration and ion-exchange adsorption exerts, and this method offers the practical application to separation of ions and is interesting in connection with the ionic transport behavior across the ion-exchange membranes.

The Institute of Industrial Science
The University of Tokyo
Yayoi-cho, Chiba

1) M. M. Tuckerman, *Anal. Chem.*, 30, 231 (1958); H. R. Roberts and M. G. Kolor, ibid., 31, 565 (1959); H. T. Peterson, Jr., ibid., 31, 1279 (1959).

* In neutral and alkaline medium the similar results are obtained but calcium ion is retarded to some extent.

2) T. Yamabe, M. Senō, T. Tanaka and I. Kamii., This Bulletin, 33, 1740 (1960).

Protection of Amide-Nitrogen for Peptide Synthesis. A Novel Synthesis of Peptides Containing C-Terminal Glutamine

By Shiro AKABORI, Shumpei SAKAKIBARA and Yasutsugu SHIMONISHI

(Received January 11, 1961)

It is known that troublesome side reactions[1] occur in the synthesis of asparagine- or glutaminepeptides due to the instability of the β- or γ-amide groups. Therefore, a suitable protection of amide nitrogen is desirable, in which the protecting group should be easily removable after formation of the peptide bonds. Frankel et al.[2] reported that removal of the benzyl group from N^{β}-benzyl-asparagine was very difficult because of the unexpected stability of the group.

In the present work, glycyl-L-glutamine and L-alanyl-L-glutamine ware prepared using xanthydrol[3] (I) as a protective agent by the following procedures. N^{α}-Cbzo*-N^{γ}-xanthyl-L-glutamine (II) was prepared from N^{α}-cbzo-L-glutamine (III) in glacial acetic acid containing an equimolar amount of I. Yield 80%; m. p. 182~183°C, $[\alpha]_D^{17}-5.7°$ (*c* 5.7, dimethylformamide). Found: C, 66.36; H, 5.55; N, 6.13. Calcd. for $C_{26}H_{24}O_6N_2 \cdot 1/2H_2O$: C, 66.52; H, 5.37; N, 5.97%.

When II was treated with hydrogen bromide in glacial acetic acid, L-glutamine (IV) was recovered in 55% yield. IV had the same optical activity with the glutamine which was obtained directly from the starting material III, m. p. 187°C, $[\alpha]_D^{32.5}+6.4°$ (*c* 2.8, H_2O). It is interesting that N^{γ}-xanthyl-L-glutamine (V) was not obtained from IV and I in acetic acid. The substance V was first obtained by selective hydrogenation of II in ethanol using palladium-charcoal as catalyst; m. p. 222°C (dicomp.). Found: C, 65.71; H, 5.60; N, 8.97. Calcd. for $C_{18}H_{18}O_4N_2$: C, 66.24; H, 5.56; N, 8.58%.

Synthesis of Glycyl-L-glutamine. — N^{α}-Cbzo-N^{γ}-xanthyl-L-glutamine methylester (VI) was prepared from II in dioxane by treatment with diazomethane. Recrystallization of VI from dioxane gave fine colorless needles (80~85%); m. p. 235~235.5°C. Found: C, 68.21; H, 5.58; N, 5.94. Calcd. for $C_{27}H_{26}O_6N_2$: C, 68.34; H, 5.52; N, 5.90%. The cbzo-group was removed by catalytic hydrogenation, and N^{γ}-xanthyl-L-glutamine methylester acetate (VII) was obtained as colorless needles (67%); m. p. 148~148.5°C. Fuond: C, 62.72; H, 6.07; N, 6.90. Calcd. for $C_{21}H_{24}O_6N_2$: C, 62.99; H, 6.04; N, 7.00%. Substance VII was coupled with cbzo-glycine *p*-nitrophenylester (VIII) in anhydrous chloroform[4,5], and cbzo-glycyl-N^{γ}-xanthyl-L-glutamine methylester (IX) was obtained as fine colorless needles after recrystallization from dioxane (70%); m. p. 184°C. Found: C, 65.49; H, 5.64; N, 7.89. Calcd. for $C_{29}H_{29}O_7N_3$: C, 65.52; H, 5.50; N, 7.91%. The product IX was carefully saponified in dioxane using *N*-sodium hydroxide, and cbzo-glycyl-N^{γ}-xanthyl-L-glutamine (X) was obtained. It was recrystallized from methanol-toluene (4 : 1) and water (77%): m. p. 198°C. Found: C, 65.17; H, 5.39; N, 8.04; eq. wt.: Na, 516. Calcd. for $C_{28}H_{27}O_7N_3$: C, 64.98; H, 5.26; N, 8.12%; mol. wt. 517.5. Treatment of X with hydrogen bromide, foffowed by purification by Amberlite IR-4B, gave glycyl-L-glutamine monohydrate (XI) in 70% yield; m. p. 206°C (decomp.). Found: C, 38.02; H, 7.02; N, 19.12. Calcd. for $C_7H_{13}O_4N_3 \cdot H_2O$: C, 38.00; H, 6.84; N, 19.00%. $[\alpha]_D^{15}=-1.8°$ (*c* 3.8, water). Thierfelder[6] reported; m. p. 199~200°C, $[\alpha]_D^{15}-2.47°$ (*c* 4.20, water).

Synthesis of L-Alanyl-L-glutamine. — Cbzo-L-alanyl-N^{γ}-xanthyl-L-glutamine methyl ester (XII) was prepared by coupling cbzo-L-alanine *p*-nitrophenyl ester with VII in the same manner, and was recrystallized from ethanol (90%); m. p. 208°C (decomp.). Found: C, 65.17; H, 5.69; N, 7.79. Calcd. for $C_{30}H_{31}O_7N_3$: C, 66.04; H, 5.73; N, 7.70%. L-Alanyl-L-glutamine monohydrate was obtained from XII by the similar procedure to that of XI, m. p. 214~215°C (decomp.). Found: C, 40.42; H, 7.52; N, 17.82. Calcd. for $C_8H_{15}O_4N_3 \cdot H_2O$: C, 40.84; H, 7.28; N, 17.86%. $[\alpha]_D^{14}=+11.4°$ (*c* 3.70, water).

Detailed results will be published elsewhere.

Institute for Protein Research
Osaka University
Kita-ku, Osaka

1) J. Rudinger, *Angew. Chem.*, **71**, 742 (1959).
2) M. Frankel, Y. Liwschitz and A. Zilkha, *J. Am. Chem. Soc.*, **75**, 3270 (1953).
3) R. F. Phillips et al., *J. Org. Chem.*, **8**, 1355 (1943).
* Cbzo.....carbobenzoxy.
4) R. Schwyzer and P. Sieber, *Angew. Chem.*, **68**, 518 (1956).
5) M. Bodanszky and V. du Vigneaud, *J. Am. Chem. Soc.*, **81**, 5688 (1959).
6) H. Thierfelder et al., *Z. Physiol. Chem.*, **105**, 58 (1919).

Steric Configuration of the α, β-Diaminobutyric Acid Isolated from the Antibiotic Glumamycin

By Masahiko FUJINO, Michitaka INOUE, Jisaburo UEYANAGI and Akira MIYAKE

(Recived February 20, 1961)

Inoue[1] previously isolated α, β-diaminobutyric acid from the acid hydrolysate of glumamycin, an acidic peptide antibiotic. Martin et al.[2] also reported the separation of α, β-diaminobutyric acid from Aspartocin, an antibiotic resembling glumamycin. Although both products seem to have the same configuration from their optical rotation, this has so far not been studied. Inoue has shown[3] that only one β-amino group of the two α, β-diaminobutyric acids* of glumamycin is free.

The configuration of the α-amino group has been studied by conversion of free amino group of glumamycin into a hydroxyl group and subsequent hydrolysis to α-amino-β-hydroxybutyric acid, and that of the β-amino group by oxidation of α, β-diaminobutyric acid to alanine.

Glumamycin was treated with sodium nitrite in 80% acetic acid to convert the free amino group into hydroxyl and the resulting hydroxyglumamycin was hydrolyzed with hydrochloric acid. The reaction mixture was developed on a column of Dowex 50x4 (200 ~ 400 mesh) with ammonium formate buffer (pH 3.4)[4] and the crystals obtained from the threonine fraction of the eluate were recrystallized from aqueous ethanol (Found: C, 40.06; H, 7.81; N, 11.90. Calcd. for $C_4H_9O_3N$: C, 40.33; H, 7.62; 11.76%). The product was found to be a mixture of threonine and allothreonine by paper chromatography with *n*-butalnol·acetone·ammonia·water (50: 6.25: 6.25: 37.5)[5]. However, since the β-position of α, β-diaminobutyric acid of glumamycin may undergo partial Walden inversion under the conditions, it is impossible to decide the configuration of the α-carbon atom directly from the optical rotation of the product. But DNP-L-threonine and DNP-L-allothreonine exhibit the same optical rotation, $[M]_D^{25} = +305°$ (4% sodium bicarbonate)[6]. The above product was converted into its DNP-derivative by the method of Levy[7] and then subjected to chromatography on Amberlite IRC-50 according to the method of Seki[8] to remove the DNP-OH which formed as a by-product. DNP-derivative showed an optical rotation of $[M]_D^{24} = -294° \pm 14$ (*c* 0.48, 4% sodium bicarbonate) and its yield was 92%. This fact shows that above product is a mixture of D-threonine and D-allothreonine, therefore α-carbon atom of α, β-diaminobutyric acid has the D-configuration. Further, as α, β-diaminobutyric acid obtained from the hydrolysate of hydroxy-glumamycin, and that obtained from the hydrolysate of glumamycin have the same optical rotation and physical properties, the two moles of α, β-diaminobutyric acid in glumamycin evidently have the same steric configuration.

Oxidation of α, β-diaminobutyric acid with hydrogen peroxide was conducted by the method of Dakin[9]. Namely, the compound was allowed to react with 2 mol. of 3% hydrogen peroxide at 50°C for one hour. The reaction mixture was passed through a column of Amberlite IR-120, the column was eluted with N-ammonium hydroxide, and the effluent was concentrated to give D-alanine (Found: C, 40.51; H, 7.88; N, 15.44%), $[\alpha]_D^{20} = -16$, (*c* 1, 6 N hydrochloric acid) which was confirmed by infrared spectrum and paper chromatography.

Thus, it was found that the β-carbon atom of α, β-diaminobutyric acid belongs to the D-series, and consequently α, β-diaminobutyric acid takes D-erythro-configuration.

The authors wish to express their sincere thanks to Dr. Satoru Kuwada, the Director of Research Laboratories, Dr. Sueo Tasuoka, Vice Director of Research Laboratories, Dr. Kuniyoshi Tanaka, the Head of 2nd Division of Research Laboratories for their guidance and encouragement.

Research Laboratories
Takeda Chemical Industries, Ltd.
Higashiyodogawa-ku, Osaka

1) M. Inoue et al., This Bulletin, **33**, 1014 (1960).
2) J. H. Martin and W. K. Hausmann, *J. Am. Chem. Soc.*, **60**, 2079 (1960).
3) M. Inoue, in press.
* It is already recognized that glumamycin contains two moles of α, β-diaminobutyric acid and both amino groups of one mole are not free.
4) C. H. W. Hirs, S. Moore and W. H. Stein, *J. Biol. Chem.*, **195**, 669 (1952).
5) K. N. F. Shaw and S. W. Fox, *J. Am. Chem. Soc.*, **75**, 3421 (1953).
6) K. R. Rao and H. A. Sober, ibid., **76**, 1328 (1954).
7) A. L. Levy, *Nature*, **174**, 126 (1954).
8) T. Seki, *Chemistry of Proteins* (*Tokyo*), **4**, 209 (1956).
9) H. D. Dakin, *J. Biol. Chem.*, **1**, 171 (1905); **4**, 63 (1908).

The Structure of Todomatuic Acid. Synthesis of (±)-Dihydro-desoxo-todomatuic Acid

By Masao NAKAZAKI and Sachihiko ISOE

(Received March 6, 1961)

Todomatuic acid, $C_{15}H_{24}O_3$, monocyclic unsaturated keto-acid (m. p. 58.5°C, b. p. 200~215°C/3 mmHg, $[\alpha]_D^{32.5}+85.84°$; semicarbazone, m. p. 193.2~193.7°C), was first isolated by Tuchihashi and Hanzawa[1] on hydrolysis of the high boiling fraction of an oil, obtained as a by-product when *Abies sachalinensis* Mast. (to do matu) was digested with sulfite in pulp industry.

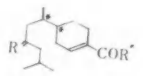

Ia R=O R'=OH
b R=H$_2$ R'=OH
c R=H$_2$ R'=OCH$_3$

The structure Ia was advanced by Momose[2], mainly by the results of oxidative degradation of Ia with potassium permanganate which gave oxalic acid and an acyclic saturated keto-dicarboxylic acid (II), $C_{13}H_{22}O_5$ (semicarbazone, decomp. p. 185~186°C). Further oxidation of II with nitric acid gave isovaleric acid and β-(α-carboxyethyl)glutaric acid. Among various possible structures which satisfy the results of the degradation, Ia was favored because Ia is compatible with the isoprene rule.

In this communication, the synthesis of (±)-dihydro-desoxo-todomatuic acid (Xb) is reported.

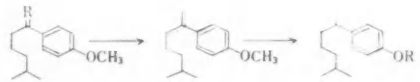

IIIa R=O IV Va R=CH$_3$
b R=OH, CH$_3$ b R=H

(4-Anisyl)-isohexyl ketone (IIIa) (b. p. 131~133°C/1 mmHg; semicarbazone, m. p. 124~125°C) obtained by Friedel-Crafts reaction of anisole with isocaproyl chloride, was converted into IIIb by Grignard reaction with methylmagnesium bromide, and then IIIb was dehydrated by boiling with acetic anhydride to the unsaturated phenol ether IV (b. p. 109~115°C/1 mmHg).

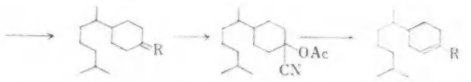

VIa R=OH, H VII VIIIa R=CN
b R=O b R=COOH

Catalytic hydrogenation of IV gave Va (b. p. 107~113°C/1 mmHg), which was hydrolyzed by boiling with hydroiodic acid in acetic acid to afford the phenol Vb (b. p. 127~128°C/1 mmHg). High pressure catalytic hydrogenation of Vb (Raney nickel, 130 atms., 30°C) yielded the alcohol VIa (b. p. 120~121°C/1 mmHg), which was oxidized with potassium dichromate in sulfuric acid to the ketone VIb (b. p. 113~114°C/1 mmHg; semicarbazone, m. p. 149~150°C). The cyanohydrin acetate VII (b. p. 145~147°C/1 mmHg) prepared from VIb with potassium cyanide and acetic anhydride, was pyrolyzed by passing through a heated Pyrex tube(600°C) packed with ceramic Raschig rings to give unsaturated cyanide VIIIa, which was then hydrolyzed to the unsaturated acid VIIIb (b. p. 163~165°C 1 mmHg).

IXa R=OH Xa R=OCH$_3$
b R=OCH$_3$ b R=OH
c R=NHC$_6$H$_5$
(or its antipode) (or its antipode)

Although two racemic forms are expected for the structure VIIIb, the infrared absorption spectrum of synthetic VIIIb was found superimposable on that of (+)-desoxo-todomatuic acid (Ib) (m. p. 59~60°C, $[\alpha]_D^{27}+94.3°$ in ethanol; anilide, m. p. 78~79°C) obtained by Wolff-Kishner reduction of Ia. Catalytic hydrogenation of the methyl ester Ic of natural Ib gave saturated methyl ester IXb in which only one asymmetric center remains.

Heating with sodium methoxide converted IXb into more stable methyl ester Xa, which was hydrolyzed to give (+)-dihydro-desoxo-todomatuic acid (Xb) (b. p. 150~153°C/1 mmHg, n_D^{18} 1.4723, $[\alpha]_D^{27}+14.1°$ in ethanol; anilide Xc, m. p. 115~116°C). Following the same procedure, racemic IXb gave (±)-dihydro-desoxo-todomatuic acid (Xb) (b. p. 152~155°C/1 mmHg, n_D^{18} 1.4723; anilide, Xc

1) R. Tuchihashi and T. Hanzawa, *J. Chem. Soc. Japan, Pure Chem. Sec.* (*Nippon Kagaku Zasshi*), **61**, 1041 (1940).
2) T. Momose, *J. Pharm. Soc. Japan* (*Yakugaku Zasshi*), **61**, 288 (1941).

5

O STATE
IVERSITY
UL 25 1961
Bi....y
CHEMISTRY HALL LIBRARY

昭和33年12月25日 第三種郵便物認可 昭和36年5月8日 印刷 [毎月1回
昭和36年5月15日 発行 15日発行]

BULLETIN
OF THE
CHEMICAL SOCIETY OF JAPAN

Vol. 34 No. 5 May 1961

CONTENTS

General and Physical

The Relation between Reactivity and Selectivity . . . . . Y. OGATA and I. TABUSHI 604
The Crystal Structure of *p*-Aminobenzenearsonic Acid . . . . . A. SHIMADA 639
Mass Spectrometric Study on Absorption of Water Vapor on a Graphite Surface . . H. INOUYE 643
Kolbe's Reaction of Higher Fatty Acids. II. Electrolysis of Lauric Acid by a Pulsating Current with an Artificial Graphite Anode. . . . . R. MATSUDA, T. HISANO and D. KUBOTA 649
An Empirical Method for Estimating Normal Boiling Point and other Physical Properties of Alkene Hydrocarbons . . . . . M. TAMURA, M. KURATA, K. NAKANISHI and I. NAGATA 684
Internal Rotation and Low Frequency Spectra of Esters, Monosubstituted Amides and Polyglycine . . . . . T. MIYAZAWA 691
The Behavior of Fission Products Captured in Graphite Powder by Nuclear Recoil. IV. Further Studies on the Diffusion of Xenon-133 in Graphite . . . . . S. YAJIMA, S. ICHIBA, Y. KAMEMOTO, K. SHIBA and M. KORI 697
Photoconductivity of Zinc Oxide under Different Ambient Conditions. . . . . H. KOKADO, E. INOUE, T. YAMAGUCHI and K. TAKAHASHI 705
On the Fluorine Shift of Aromatic Fluorine Compounds . . . . . T. YONEZAWA, K. FUKUI, H. KATO, H. KITANO, S. HATTORI and S. MATSUOKA 707
A LCUAO Treatment of Reactivity in Aromatic Hydrocarbons . . . . . K. FUKUI, T. YONEZAWA, C. NAGATA and Y. KONAKA 712
Absorption Spectra of Nitrobenzene Derivatives. II. Effect of Solvent on Intramolecular Charge Transfer Spectra of Nitrobenzene Derivatives. . . . . K. SEMBA 722
Electronic and Vibrational States of Acrolein. . . . . K. INUZUKA 729
Electron Diffraction Investigations on the Molecular Structures of *sec*-Butyl Chloride and Alcohol . . . . . M. YAMAHA and M. IGARASHI 733

Analytical and Inorganic

Acid-Base Property and Metal Chelate Formation of 4-(2-Pyridylazo)-resorcinol. . T. IWAMOTO 605
Mineral Content of Mixed Fertilizer. . . . . J. ANDO and S. MATSUNO 678
Determination of Lanthanum, Samarium and Europium in Manganese Nodules by Neutron Activation. . . . . T. KAWASHIMA, M. OSAWA, Y. MOCHIZUKI and H. HAMAGUCHI 701
Application of RADME to the Chelatometric Determination of Metals Employing the Alternating Current Polarographic Method . . . . . M. KODAMA 714

Organic and Biological

A Ring-Chain Tautomerism in the Reaction Products of 3-Aminotropolone and Some Ethoxymethyleneacetates. . . . . T. NOZOE, K. DOI and K. KITAHARA 611
A Note on the Ring-Chain Tautomerism in the Reaction Products of *o*-Aminophenol and Some Ethoxymethyleneacetates. . . . . T. NOZOE and K. DOI 614
On the Structure of 2-Mercaptotropones. . . . . T. NOZOE and K. MATSUI 616
Reaction of Troponoids and Organometallic Compounds. VI. Reaction of Tropone with Grignard Reagents . . . . . T. NOZOE, T. MUKAI and T. TEZUKA 619
Diels-Alder Reaction of Troponoids. II. Adducts of Halotropones and Maleic Anhydride . . . . . T. NOZOE and Y. TOYOOKA 623

(Continued on inside cover)

Published by the Chemical Society of Japan

THE CHEMICAL SOCIETY OF JAPAN
(NIPPON KAGAKUKAI)

Founded in 1948

Successor to the former Chemical Society of Japan founded in 1878 and to the Society of Chemical Industry, Japan founded in 1898.

OFFICERS

San-ichiro MIZUSHIMA, *President*, Director of Tokyo Research Institute Yawata Iron and Steel Co., Ltd.
Yoshikazu HACHIHAMA, *Vice-President*, Osaka University
Kenji IWAMOTO, *Vice-President*, The University of Gunma
Yonezo MORINO, *Vice-President*, The University of Tokyo
Sojiro OKA, *Vice-President*, The University of Tokyo
Hiroshi SOBUE, *Vice-President*, The University of Tokyo

BULLETIN OF THE CHEMICAL SOCIETY OF JAPAN

Editor: Tadao SHIBA, Tokyo Institute of Technology, Tokyo
Assistant Editor: Tadashi SUEHIRO, Gakushuin University, Tokyo
Editorial Board:

Yoshié BANSHO	Hidehiro GOTÔ	Keniti HIGASI
Yoshimasa HIRATA	Hiroo INOKUCHI	Tatsujiro ISHIMORI
Tadashi KAMIKUBO	Michio KOBAYASHI	Ichiro MIYAGAWA
Masazumi NAKAGAWA	Shigeru OAE	Shigeru OHASHI
Kazuo SATAKE	Syûzô SEKI	Osamu SIMAMURA
Yoshitada TOMODA	Iwao YASUMORI	Koshiro YOSHIOKA

(Continued from outside cover)

Reaction of Hydrogen Peroxide on Fatty Acid Esters under Pressure. III. Oxidation of Methyl 9, 10-Dihydroxystearate. . . . . H. KAMEOKA 626
Polymerization of Allyl Chloride by Ziegler's Catalyst . . . . . S. MURAHASHI, S. NOZAKURA and K. HATADA 631
Oxidation of 2-Methyl 5-Ethyl Pyridine to Isocinchomeronic Acid. . . . . T. KATO 636
A New Method for the Preparation of Piperazines. I. Preparation of *N*-Mono-alkyl(-aryl)-piperazines. . . . . K. NAKAJIMA 651
A New Method for the Preparation of Piperazines. II. Preparation of *N, N'*-Disubstituted Piperazines. . . . . K. NAKAJIMA 655
Radiation-induced Reaction in an Aqueous Benzoic Acid Solution. I. Dose and Dose Rate Dependencies of Salicylic Acid, and of Biphenyldicarboxylic Acids . . . . . A. SAKUMOTO and G. TSUCHIHASHI 660
Radiation-induced Reaction in an Aqueous Benzoic Acid Solution. II. Determination of Products by Isotope Dilution Method . . . . . A. SAKUMOTO and G. TSUCHIHASHI 663
Studies on Meso-ionic Compounds. XIII. ψ-2,4-Dihydro-4,5-diphenyl-2-keto-1-oxa-3,4-diazole . . . . . M. HASHIMOTO and M. OHTA 668
Bile Acids and Steroids. XXI. Studies on the Hog Bile Acids (Part 5). On the Oxidation of Epimeric 3, 6-Dihydroxycholanoic Acids with *N*-Bromosuccinimide . . . . . J. KAWANAMI 671
Studies on Organophosphorus Compounds. I. The Reaction of *O,O*-Dimethyl Phosphonate with *p*-Benzoquinone. . . . . Y. NISHIZAWA 688
Synthesis of α-Maltosides. I. . . . . S. MATSUBARA 718

Applied

Kinetics of the Reduction of Selenious Acid by Sulfur Dioxide. I. Reduction in Acidic Solution with Hydrochloric Acid. . . . . K. HAMADA 593
Kinetics of the Reduction of Selenious Acid by Sulfur Dioxide. II. Reduction in Acidic Solution with Sulfuric Acid . . . . . K. HAMADA 596
Kinetics of the Reduction of Selenious Acid by Sulfur Dioxide. III. Application to Recovery and Purification of Selenium in Sulfuric Acid Works. . . . . K. HAMADA 600

Short Communications

On the Electromigration in Ion-exchange Papers . . . . . T. YAMABE, M. SENŌ and N. TAKAI 738
Protection of Amide-Nitrogen for Peptide Synthesis. A Novel Synthesis of Peptides Containing *C*-Terminal Glutamine . . . . . S. AKABORI, S. SAKAKIBARA and Y. SHIMONISHI 739
Steric Configuration of the α, β-Diaminobutyric Acid Isolated from the Antibiotic Glumamycin . . . . . ; M. FUJINO, M. INOUE, J. UEYANAGI and A. MIYAKE 740
The Structure of Todomatuic Acid. Synthesis of (±)-Dihydro-desoxo-todomatuic Acid . . . . . M. NAKAZAKI and S. ISOE 741

*Kinetics of the Reduction of Selenious Acid by Sulfur Dioxide. I. Reduction in Acidic Solution with Hydrochloric Acid**

By Keinosuke HAMADA

(Received February 17, 1960)

Raw materials for the production of selenium depend heavily on a sludge and a copper slime, which are obtained as a by-product of a sulfuric acid factory and a copper refinery, respectively. In order to investigate the behavior of selenium at the sulfuric acid production plant, to increase the yield of selenium recoverable from the sulfuric acid plant source and to establish a simple method for the refining of these raw materials, the following series of studies were undertaken.

Consideration will be given first to the kinetics of the reduction of selenious acid in hydrochloric acid by sulfur dioxide. The percentage completion of these reactions is calculated by weighing the selenium precipitated from a solution. Sulfur dioxide is passed into a solution continuously, so that the reaction is of zero order with respect to sulfur dioxide.

It has been proved that the reduction of selenious acid was of the second order with respect to selenious acid. Furthermore, a general equation was derived for the rate constant of the reaction by studying the effects of hydrogen ion concentration and temperature upon it.

Experimental

Materials.—1.752, 0.736, 0.368 and 0.172 mol./l. aqueous solution of selenious acid were prepared by dissolving extra pure reagent selenious acid in distilled water. On the other hand, 12, 6, 4.5 and 3% (by volume) hydrochloric acid solutions were prepared by diluting the first grade reagent hydrochloric acid (s. g. 1.18~1.19) with distilled water. The pH*1 values of these acid solutions were 0.02, 0.31, 0.42 and 0.59, which corresponded to 0.96, 0.49, 0.38 and 0.26 g. ion/l. of hydrogen ion concentration*2, respectively. Liquid sulfur dioxide was purchased from Befu Chemical Industrial Co.

Measurements.—Experimental solutions were prepared as follows. Ten milliliters of the above aqueous solutions of selenious acid were placed in a 200 ml. measuring flask, which was filled with the above-mentioned dilute hydrochloric acid. The solution was poured into a 300 ml. Erlenmeyer's flask, and kept at a constant temperature within ±0.1°C by a thermostat, and then sulfur dioxide was passed into the solution. The sulfur dioxide was initially passed through a washing bottle filled with water kept at the same constant temperature. Each of the selenious acid solutions was reduced by sulfur dioxide in four kinds of hydrochloric acid solutions at various temperatures.

After a certain period, the contents in an Erlenmeyer's flask was poured into 600 ml. of distilled water. In this way the reaction could be prevented owing to the decrease of the hydrogen ion concentration as well as temperature[1]. Precipitated selenium was filtered with a previously weighed glass filter (1G-4), washed by water, dried at 105~110°C in an air bath and then weighed.

Percentage completion of reaction is expressed with (precipitated selenium/initial selenium in the solution) × 100.

Results and Discussion

Selenious Acid Concentration Dependence of the Reduction of Selenious Acid.—Concentrations of the prepared selenious acid solutions in hydrochloric acid were 0.0876, 0.0368, 0.0184 and 0.0086 mol./l., respectively. At constant temperature (70°C) and constant hydrogen ion concentration (0.49 g. ion/l.), these selenious acid solutions were reduced by sulfur dioxide. The weight of precipitated selenium was converted into percentage completion according to the above expression. Fig. 1 shows the selenious acid concentration dependence of the reduction of selenious acid by plotting the percentage completion against the elapsed time.

The values of half time ($t_{1/2}$) can be obtained from Fig. 1, and these are 100, 260, 460 and 1200 sec., respectively. When a is the initial concentration of selenious acid (mol./l.), p the quantity of reduced selenious acid (equal to precipitated selenium) after time t (in sec.), k_1*3 the rate constant (l. mol^{-1} sec^{-1}), $t_{1/2}$ the half time (sec.), and the reaction is of the nth order with respect to selenious acid, this reaction can be expressed mathematically by

$$-\mathrm{d}(a-p)/\mathrm{d}t=\mathrm{d}p/\mathrm{d}t=k_1(a-p)^n \qquad (1)$$

The solution of Eq. 1 is as follows,

* Presented at the 13th Annual Meeting of the Chemical Society of Japan, Tokyo, April, 1960.

*1 Measured by a pH-meter with 0.01 pH accuracy.

*2 Calculated from pH value.

1) J. W. Mellor: "A Comprehensive Treatise on Inorg. and Theoret. Chem." Vol. X, S, Se, p. 699.

*3 k_1 does not mean the rate constant of first order reaction, but the rate constant of the reduction of selenious acid in hydrochloric acid.

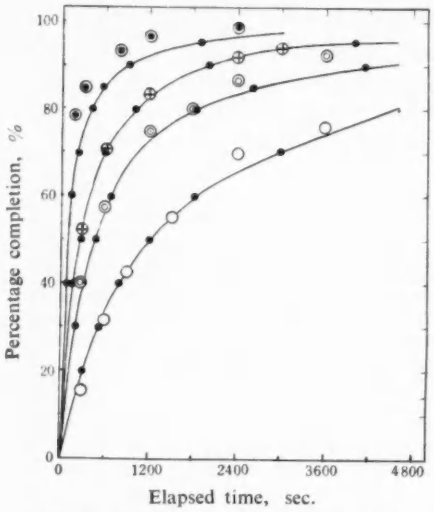

Fig. 1. H_2SeO_3 concn. dependence of the reduction of H_2SeO_3 in HCl at const. $[H^+]$ (0.49 g. ion/l.) and const. temp. (70°C).

- ◉ 0.0876 mol./l.
- ⊕ 0.0368 〃
- ◎ 0.0184 〃
- ○ 0.0086 〃
- • Calculated by Eq. 2, with n equal to 2.

$$t=\{a^{n-1}-(a-p)^{n-1}\}/\{k_1(n-1)\times(a-p)^{n-1}a^{n-1}\} \quad (2)$$

If t is equal to $t_{1/2}$, p is equal to $a/2$. Making these substitutions for t and p in Eq. 2, the result is

$$t_{1/2}=(2^{n-1}-1)/\{k_1(n-1)a^{n-1}\} \quad (3)$$

When the values of the initial concentration of selenious acid and the experimentally determined half time ($t_{1/2}$) are substituted for a and $t_{1/2}$ in Eq. 3, four equations are obtained;

$$1200=(2^{n-1}-1)/\{k_1(n-1)\times 0.0086^{n-1}\} \quad (i)$$

$$460=(2^{n-1}-1)/\{k_1(n-1)\times 0.0184^{n-1}\} \quad (ii)$$

$$260=(2^{n-1}-1)/\{k_1(n-1)\times 0.0368^{n-1}\} \quad (iii)$$

$$100=(2^{n-1}-1)/\{k_1(n-1)\times 0.0876^{n-1}\} \quad (iv)$$

Combining these equations, one can obtain the values of n which are 2.27, 1.82, 2.10, 2.05, 2.07 and 1.98. The mean value of n is 2.05, and from this it can be established that this reaction is one of second order with respect to selenious acid. As n is equal to 2, the values of k_1 can be calculated from the above four equations.

Temperature Dependence of the Reduction of Selenious Acid.—At constant initial concentration of selenious acid (0.0184 mol./l.) and constant hydrogen ion concentration (0.49 g. ion/l.), selenious acid in hydrochloric acid is reduced by sulfur dioxide, when the temperature is at 70, 60, 55 and 50°C. Fig. 2 shows the plot of the percentage completion against the elapsed time based upon the experimental data. As n is equal to 2, and the values of the initial concentration of selenious acid are known and the values of half time can be obtained from Fig. 2, upon making these substitutions for the values for n, a and $t_{1/2}$ in Eq. 3, the rate constants at 70, 60, 55 and 50°C are 0.118, 0.042, 0.020 and 0.012 l. mol^{-1} sec^{-1}, respectively.

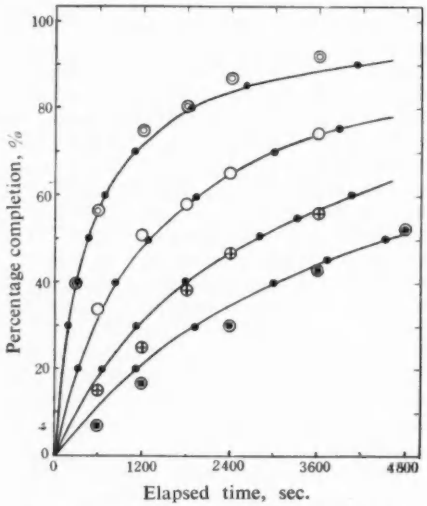

Fig. 2. Temperature dependence of the reduction of H_2SeO_3 at const. $[H_2SeO_3]$ (0.0184 mol./l.) and const. $[H^+]$ (0.49 g. ion/l.).

- ◎ 70°C
- ○ 60°C
- ⊕ 55°C
- ◉ 50°C
- • Calculated by Eq. 2, with n equal to 2.

The influence of temperature on reaction velocity can be derived by plotting the logarithm of the rate constant, $\log k_1$, against the reciprocal of the absolute temperature, $1/T$ (Fig. 3). As Fig. 3 shows that the experimental points fall on a straight line, the energy of activation E can be calculated from the value of the slope in Fig. 3.

The slope is equal to $-E/2.303R$[2]. The slope of the straight line in Fig. 3 is equal to -5.35×10^3, and as R is taken as 1.987 cal. deg^{-1} mol^{-1}, it follows that for the reduction of selenious acid E is 24.5 kcal./mol. Moreover,

2) S. Glasstone, "Elements of Physical Chemistry", Maruzen, Tokyo (1958), p. 607.

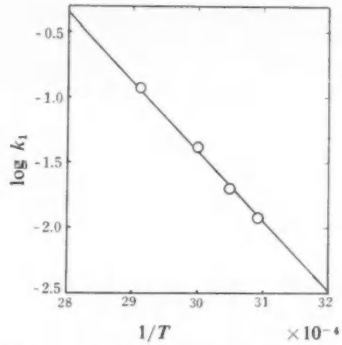

Fig. 3. Arrhenius' plot of the reduction of H_2SeO_3 by SO_2.

the rate constant k_1 is proportional to exp $(-E/RT)$.

Hydrogen Ion Concentration Dependence of the Reduction of Selenious Acid.—At a constant initial concentration of selenious acid (0.0184 mol./l.), the constant temperature (60°C) and various hydrogen ion concentrations (0.26, 0.38, 0.49 and 0.96 g. ion/l.), the selenious acid in hydrochloric acid were reduced by sulfur dioxide. These results are shown in Fig. 4.

Rate constant k_1 can be obtained from Eq. 3. Plotting the rate constant against the square of hydrogen ion concentration, it is seen in Fig. 5 that the experimental points fall on a straight line.

It is evident from Fig. 5 that rate constant k_1 is proportional to $[H^+]^2$.

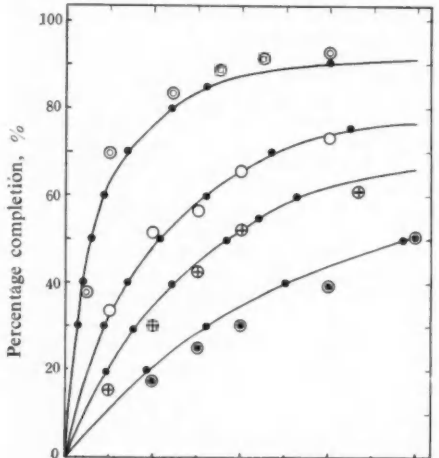

Fig. 4. $[H^+]$ dependence of the reduction of H_2SeO_3 at const. $[H_2SeO_3]$ (0.0184 mol./l.) and const. temp. (60°C).

- ◎ 0.96 g. ion/l.
- ○ 0.49 〃
- ⊖ 0.38 〃
- ◉ 0.26 〃
- • Calculated by Eq. 2, with n equal to 2.

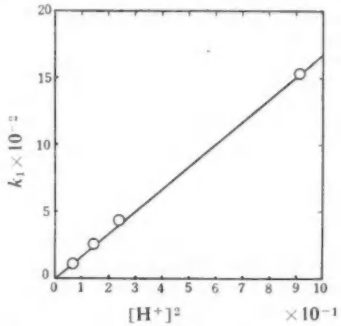

Fig. 5. Plot of k_1 against $[H^+]^2$.

When the temperature is equal to 60°C, hydrogen ion concentration is equal to 0.49 g. ion/l. and the initial concentration of selenious acid is equal to 0.0184 mol./l., the rate constant k_1 is evaluated to be 0.042 l. mol^{-1} sec^{-1}. When these values*4 are adopted, the general Eq. 4 for rate constant can be derived, according to the above-mentioned temperature and hydrogen ion concentration dependence, that is,

$$k_1 = 2.054 \times 10^{15} \times [H^+]^2 \exp(-E/RT) \quad (4)$$

where E is the energy of activation (24.5 kcal./mol.), R the gas constant (1.987 cal. deg^{-1} mol^{-1}) and T the absolute temperature.

Summary

(1) The reduction of selenious acid in hydrochloric acid by sulfur dioxide is a typical second order reaction with respect to selenious acid, while the reaction is of zero order with respect to sulfur dioxide because of the continuous passage of sulfur dioxide through a solution.

(2) The results obtained at 70, 60, 55 and 50°C (a=0.0184 mol./l., $[H^+]$ =0.49 g. ion/l.) give a good Arrhenius plot, leading to the value of 24.5 kcal. mol^{-1} for the energy of activation.

(3) The rate constant of this reaction under a certain condition can be evaluated by the general equation,

$$k_1 = 2.054 \times 10^{15} \times [H^+]^2 \exp(-E/RT)$$

where $[H^+]$ is hydrogen ion concentration, E, the energy of activation and T absolute temperature.

*4 These experimental data are in good accordance with theoretical values (denoted by •) obtained from Eq. 2.

(4) The reduction of selenious acid in sulfuric acid, which will be published in a subsequent paper, is a reversible reaction. The above equation for the rate constant is utilized as a basic equation, in order to determine the rate constant in the forward direction of the reversible reaction.

The author wishes to express his sincere thanks to Dr. H. Negita of the Department of Chemistry, Hiroshima University, for his discussion and advice, and also he wishes to thank Mr. M. Kodama for his assistance.

Department of Chemistry
Faculty of Science
Hiroshima University
Hiroshima

---

*Kinetics of the Reduction of Selenious Acid by Sulfur Dioxide. II. Reduction in Acidic Solution with Sulfuric Acid**

By Keinosuke HAMADA

(Received Feburary 17, 1960)

This paper deals with the kinetics of the reduction of selenious acid in sulfuric acid by sulfur dioxide. Amelin and Yashke[1] investigated the reduction of selenious acid in concentrated sulfuric acid (60~80% by weight), and reported that the reaction was of first order with respect to selenious acid and to sulfur dioxide. The present author has studied the reduction of selenious acid by sulfur dioxide in dilute sulfuric acid, and has obtained different results from that obtained when concentrated sulfuric acid is utilized. The same method as that described in Part I[2] of this series was used. However, since it was found that the reaction in sulfuric acid was reversible, the method of measurements was improved by taking account of the equilibrium in the reversible reaction. The influences of temperature, initial concentration of selenious acid and hydrogen ion concentration on the reaction were investigated, and also general equations were derived for k_2*1 and k_2' which were rate constants of the forward and reverse reactions.

Experimental

Materials. — 0.736, 0.368 and 0.184 mol./l. aqueous solutions of selenious acid were prepared by dissolving extra pure reagent selenious acid in distilled water. Also prepared were 6.0, 4.5, 3.0 and 1.5% (by volume) sulfuric acid by diluting the first grade reagent sulfuric acid (s.g. about 1.84) with distilled water. pH*2 values were 0.08, 0.22, 0.38 and 0.62, and their hydrogen ion concentrations were evaluated to be 0.83, 0.60, 0.42 and 0.24 g. ion/l., respectively. The liquid sulfur dioxide was purchased.

Measurements. — This experiment was performed by means of the same procedures as those reported in Part I[2] of this series except that sulfuric acid was used in place of hydrochloric acid. However, since it was discovered that the reaction in sulfuric acid was reversible, the procedure suitable to this factor was adopted. That is, after the expected time for the reaction had elapsed, the precipitated selenium was filtered with a glass filter (1G-4)*3. Then the selenium was washed with dilute hydrochloric acid and water. Hereafter, the experimental procedures are the same as those in Part I[2] of this series.

Results and Discussion

Selenious Acid Concentration Dependence of the Reduction of Selenious Acid. — Ten milliliters of the three selenious acid solutions were diluted to 200 ml. with 4.5% (by volume) sulfuric acid ($[H^+]=0.60$), the concentrations of the experimental solutions of selenious acid being 0.0092, 0.0184 and 0.0368 mol./l., respectively. These solutions were reduced by sulfur dioxide at constant temperature (60°C). Weights of precipitated selenium were converted into percentage completion, and the plot of the percentage completion against elapsed time (sec.) is shown in Fig. 1.

---

* Presented at the 13th Annual Meeting of the Chemical Society of Japan, Tokyo, April, 1960.

1) A. G. Amelin and E. V. Yashke, *Proc. Acad. Sci. U. S. S. R. Sec. Chem.*, **108**, 313 (1956); *Chem. Abstr.*, **51**, 54g (1957); *Chem. Zentr.*, **128**, 6688 (1957).

2) Part I: This Bulletin, **34**, 593 (1961).

*1 k_2 does not mean the rate constant of the second order reaction, but the rate constant of reaction in sulfuric acid.

*2 Measured by a pH-meter with 0.01 pH accuracy.

*3 Since the present reaction is reversible, diluting reactants with water can not be adopted to stop the process of the reaction. The effects of a reverse reaction appear conspicuously.

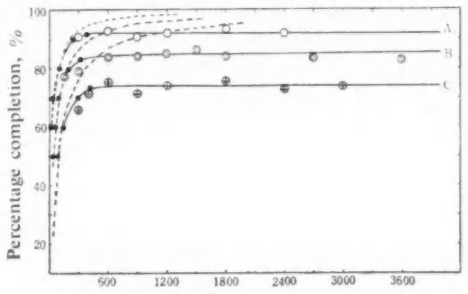

Fig. 1. H_2SeO_3 concn. dependence of the reduction of H_2SeO_3 at const. temp. (60°C) and const. $[H^+]$ (0.60 g. ion/l.).
○ 0.0368 mol./l. ◎ 0.0184 mol./l.
◑ 0.0092 mol./l. • calculated by Eq. 4.
Dotted lines: forward reaction with rate constant obtained from Eq. 1, when reverse reaction does not occur.

Each curve of Fig. 1 reaches an equilibrium, which is very different from the results in hydrochloric acid[2]. It is certain that the present reaction which comes to equilibrium is reversible[3].

The lines estimated from the experiment in the region below 60% completion of reaction are in good accordance with those obtained from Eqs. 1 and 2 based on only the forward reaction[2] (dotted lines).

Accordingly, the effect of the reverse reaction can be neglected in the region below 60% completion, where the reaction appears to be similar to the simple reaction in hydrochloric acid.

Provided that the reaction in sulfuric acid is of the second order with respect to selenious acid as it was in the case of hydrochloric acid, the rate constant k_2 for the forward reaction can be calculated by $t_{1/2}=1/(k_2a)$*1.

In the region below 60% completion, the author could not obtain any experimental data which could discriminate between curves A_1, B_1 and C_1. However, the value of k_2 in the reaction for curve C_1 is calculated to be 1.278 l. mol^{-1} sec^{-1} from $t_{1/2}=1/(k_2a)$, since the half time ($t_{1/2}$) is evaluated to be 85 sec. from the curve C_1 of Fig. 1, which is estimated from the experiment (a=0.0092 mol./l.).

The general equation for the rate constant of the reaction in hydrochloric acid was obtained as follows[2];

$$k_1=2.054\times10^{15}\times[H^+]^2\times\exp(-E/RT)$$
$$(E=24.5\ \text{kcal./mol.})$$

When the experimental conditions for curve C_1, 60°C and 0.60 g. ion/l., are substituted for T and $[H^+]$ in the above equation, the rate constant can be calculated to be 0.0629 l. mol^{-1} sec^{-1}. This value is far below the above-mentioned value (1.278 l. mol^{-1} sec^{-1}), so it has to be multiplied by 20 in order to be in good accordance with the latter value. In this way, the general equation for rate constant k_2 of the forward reaction in sulfuric acid is expressed tentatively as follows:

$$k_2=20\times k_1$$
$$k_2=4.108\times10^{16}\times[H^+]\times\exp(-E/RT)$$
$$(E=24.5\ \text{kcal./mol.}) \qquad (1)$$

The values of k_2 estimated from the experiment in the reaction for curves A_1 and B_1 of Fig. 1 are in accordance with the ones calculated from Eq. 1.

The reverse rate constant k_2' can be obtained by substituting the value of forward rate constant k_2, which is calculated from Eq. 1 in Eq. 3. When k_2 and k_2' are substituted in Eq. 4, the parts of the curves in Fig. 1 are drawn theoretically. The curvatures obtained from the experiment are in good accordance with those drawn by the calculated values from Eq. 4.

From these facts it is concluded that the values of k_2 based on Eq. 1 are correct.

Eq. 1 is derived by assuming that the activation energy E of the reaction in sulfuric acid is equal to the one in hydrochloric acid (E=24.5 kcal./mol.). However, the coefficient of 20 may be due to the difference of the activation energy in each case. Although the energy of activation could not be obtained experimentally, it will be possible for it to be obtained by calculation. The values of k_2 at 60, 50, 40 and 30°C are calculated with Eq. 1 to be 1.258, 0.400, 0.118 and 0.032 l. mol^{-1} sec^{-1}, respectively. The line A of Fig. 3 shows the plotting of the logarithm of k_2 against the reciprocal of the absolute temperature. Each point falls upon a straight line. It follows from the slope of the straight line that the energy of activation is 22.5 kcal./mol. So, Eq. 1 is rewritten as follows:

$$k_2=2.054\times10^{15}\times[H^+]^2\times\exp(-E/RT)$$
$$(E=22.5\ \text{kcal./mol.}) \qquad (1')*3$$

The dotted lines in each figure are obtained from Eqs. 1 and 2,

$$t=p/\{k_2a(a-p)\}=x/\{k_2a(1-x)\}$$
$$(p=ax) \qquad (2)*6$$

3) S. Glasstone, "Elements of Physical Chemistry", Maruzen, Tokyo (1958), p. 600.

*4 Eq. 3 in Part I[2] of this series (as n=2).

*5 Eq. 1′ is the same equation as Eq. 1. But, for the general equation of rate constant, the expression of Eq. 1′ seems to be better than the one of Eq. 1.

*6 Eq. 2 in Part I[2] of this series (as n=2).

where t is the elapsed time (sec.) of reaction, p the reduced quantity of selenious acid (mol./l.) when time t has elapsed, x percentage completion (%) when time t has elapsed, k_2 rate constant (l. mol^{-1} sec^{-1}), and a initial concentration of selenious acid (mol./l.).

The reversible reaction which is of the second order with respect to selenious acid can be expressed mathematically[3] by

$$-\mathrm{d}(a-p)/\mathrm{d}t=\mathrm{d}p/\mathrm{d}t=k_2(a-p)^2-k_2'p^2 \qquad (3)^{4)*7}$$

The solution of Eq. 3 is as follows, ($p=ax$)

$$t=\frac{2.303}{2a\sqrt{k_2k_2'}}\times\log\left|\frac{\{(k_2-k_2')x-k_2-\sqrt{k_2k_2'}\}/(k_2-k_2')x-k_2+\sqrt{k_2k_2'}}{(-\sqrt{k_2k_2'}-k_2)/(\sqrt{k_2k_2'}-k_2)}\right| \qquad (4)$$

The curvatures of the practical lines are drawn according to Eq. 4. Values of k_2' in Eq. 4 can be obtained from Eq. 5.

As the reverse reaction occurs, selenium must be dissolved in dilute sulfuric acid. However, the purchased selenium is not dissolved in dilute sulfuric acid or in basic solution (NH_4OH)*8. This is inconsistent with the fact that the reduction of selenious acid in dilute sulfuric acid is a reversible reaction. This discrepancy can be solved by assuming that α selenium is dissolved in dilute sulfuric acid or in a basic solution, whereas β selenium is not dissolved*8. The purchased selenium is dried at 100~105°C, and is of the β form.

On the contrary, the selenium produced by reducing selenious acid below 99°C is of the α form, because the allotropic transition temperature of selenium from α to β is 99°C[5].

At equilibrium of the reversible reaction, it is evident that $\mathrm{d}p_m/\mathrm{d}t=0$ in Eq. 3 where p_m is the value of p at equilibrium (the value of p at equilibrium is equal to the maximum value of p). When p is equal to $p_m(ax=ax_m)$, Eq. 5 can be derived from Eq. 3 as follows,

$$\mathrm{d}p/\mathrm{d}t=k_2(a-p_m)^2-k_2'p^2_m$$
$$=k_2a^2(1-x_m)^2-k_2'a^2x_m^2=0 \qquad (5)$$

where x_m is the maximum percentage completion at equilibrium. The values of x_m obtained from Fig. 1 are 92, 85 and 74%, respectively. When the values of x_m and k_2 (1.258 l. mol^{-1} sec^{-1}) obtained from Eq. 1 are substituted in Eq. 5, then the values of k_2' can be calculated to be 0.009, 0.039 and 0.155 l. mol^{-1} sec^{-1} for curves A_1, B_1 and C_1 in Fig. 1.

Table I shows the relation between the initial concentration of selenious acid, a, and the reverse rate constant, k_2'.
It is evident from Table I that k_2' is inversely proportional to a^2.

TABLE I. RELATION BETWEEN a^2 AND k_2'

a, mol./l.	x_m, %	k_2	k_2'	$a^2k^{2'}\times10^{-5}$
0.0368	92	1.258	0.009	1.30
0.0184	85	1.258	0.039	1.33
0.0092	74	1.258	0.155	1.24

Temperature Dependence of the Reduction of Selenious Acid. — At constant initial concentration of selenious acid (0.0184 mol./l.) and hydrogen ion concentration (0.60 g. ion/l), selenious acid in sulfuric acid is reduced by sulfur dioxide at different temperatures, 60, 50, 40 and 30°C.

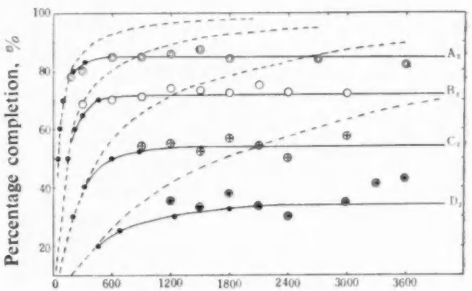

Elapsed time, sec.

Fig. 2. Temp. dependence of the reduction of H_2SeO_3 at const. [H_2SeO_3] (0.0184 mol./l.) and const. [H^+] (0.60 g. ion/l.).
◎ 60°C ○ 50°C ⊕ 40°C ⊙ 30°C
• Calculated by Eq. 4.
Dotted lines: Ref. 2, Fig. 1

4) A. Wattilon and F. Grunderbeck, *Bull. soc. chim. Belges*, **65**, 657 (1956); *Chem. Abstr.*, **51**, 7103 (1957).

*7 Although the precipitated selenium coagulates gradually at a temperature above about 40°C in this experiment, the size of selenium particles prepared at the outset of the reaction is ultramicroscopic or electronmicroscopic. The very fine particles of selenium are dispersed by the passage of sulfur dioxide at the onset of the reaction. The reaction in the reverse direction is one where the dissolving of the precipitated selenium on its surface takes place. When k_s is a rate constant for dissolving the solid and S is the constant dependent on the surface of the solid, k_sSp^2 expresses a rate of the reverse reaction. If S is constant under the present experimental conditions, k_sSp^2 can be expressed by $k_2'p^2$ in Eq. 3. From Figs. 1, 2 and 4, it is seen that the higher the temperature, greater hydrogen ion concentration and initial concentration of selenious acid are, the better are the experimental data in accordance with Eq. 3. If S is variable under all experimental conditions, Eq. 3 can not be derived.

*8 Eq. 6 shows that the lower the hydrogen ion concentration, the higher is the value of k'_2 (rate constant of reverse reaction), i.e., selenium is dissolved in basic solution more easily than in acidic solution. In fact, selenium produced by reducing selenious acid at 60°C disappears by adding basic solution[2](NH_4OH), but selenium dried over 100°C does not dissolve in basic solution.

5) Roger Dolique et al., *Bull. soc. chim. France, Mém.* [5], **10**, 231 (1943); *Chem. Abstr.*, **38**, 6156–8 (1944).

The results are shown in Fig. 2, where the precipitated selenium is converted into percentage completion. The values of k_2 at 60, 50, 40 and 30°C are calculated with Eq. 1 to be 1.258, 0.400, 0.118 and 0.032 l. mol^{-1} sec^{-1}, respectively. The values of x_m at the above temperature can be obtained from Fig. 2, and they are 85, 72, 54 and 34%, respectively. Making these substitutions for k_2 and x_m in Eq. 5, the values of k_2' at each temperature can be calculated to be 0.039, 0.060, 0.086 and 0.121 l. mol^{-1} sec^{-1}.

Line B of Fig. 3 shows the plotting of the logarithm of k_2' against the reciprocal of the absolute temperature ($1/T$). It is evident that experimental points fall upon a straight line. The relation between the rate constant of reverse direction and the temperature can be derived from the straight line B in Fig. 3 as follows.

$$k_2' \propto \exp(-E/RT)$$

The energy of activation E can be calculated to be -8.06 kcal./mol. from the slope of the line B in Fig. 3.

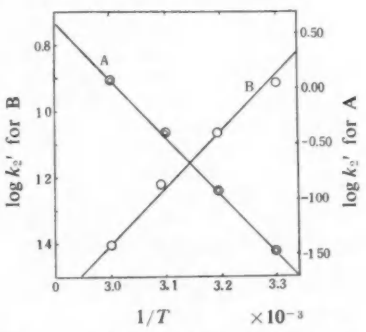

Fig. 3. Arrhenius' plot of the forward and reverse reaction.

Hydrogen Ion Concentration Dependence of the Reduction of Selenious Acid. — At constant initial concentration of selenious acid (0.0184 mol./l.), constant temperature (60°C) and various hydrogen ion concentrations (0.83, 0.60 and 0.042 g. ion/l.), selenious acid in sulfuric acid was reduced by sulfur dioxide.

The results are shown in Fig. 4, where precipitated selenium is converted into a percentage completion. The values of k_2 and k_2' can be calculated from Eqs. 1 and 5, (see Table II).

From Table II, the rate constant of reverse direction, k_2', is inversely proportional to the square of hydrogen ion concentration, $[H^+]^2$. According to the above-mentioned selenious acid concentration, temperature and hydrogen ion concentration dependence of the reverse

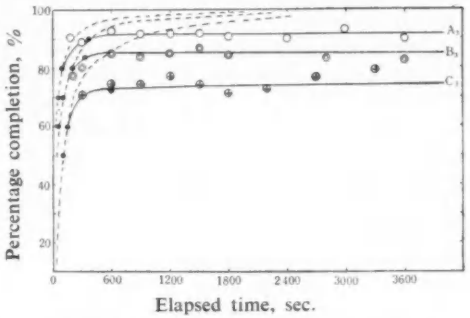

Fig. 4. $[H^+]$ dependence of the reduction of H_2SeO_3 at const. $[H_2SeO_3]$ (0.0184 mol./l.) and const. temp. (60°C).
○ 0.83 g. ion/l. ◎ 0.60 g. ion/l.
⊕ 0.42 g. ion/l. • Calculated by Eq. 4.
Dotted lines: Ref. Fig. 1

TABLE II. RELATION BETWEEN k_2' AND $[H^+]$

$[H^+]$	k_2	x_m, %	k_2'	$[H^+]^2$	$k_2' \times [H^+]^2$ ($\times 10^{-3}$)
0.83	2.408	91.5	0.021	0.689	14.33
0.60	1.258	85.0	0.039	0.369	14.04
0.42	0.617	74.0	0.076	0.176	13.37

reaction, the general equation for the reverse rate constant k_2' can be derived as follows:

$$k_2' = 2.413 \times 10^{-11} \times \{1/(a^2[H^+]^2)\} \times \exp(-E/RT) \qquad (6)$$

where a is the initial concentration of selenious acid, $[H^+]$ hydrogen ion concentration, E activation energy (-8.06×10^3 kcal./mol.), R the gas constant and T the absolute temperature.

Also, the data of curve B_1 in Fig. 1, curve A_2 in Fig. 2 and curve B_3 in Fig. 3 are adopted for the above Eq. 6.

Relation among Rate Constant, Maximum Percentage Completion and Initial Concentration of Selenious Acid.—Fig. 5 shows the plotting maximum percentage completion x_m against

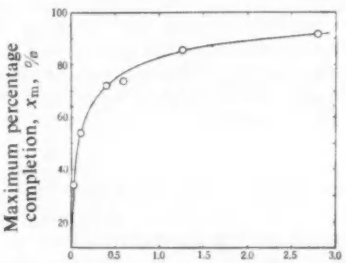

Fig. 5. Plot of maximum percentage (x_m) against forward rate constant (k_2).

forward rate constant k_2 at the constant initial concentration of selenious acid (0.0184 mol./l.). The experimental equation which expresses the relation between x_m and k_2 can be derived from Fig. 5 by

$$x_m = 0.828 \times k_2^{0.114} \quad (\text{at } a = 0.0184 \text{ mol./l.}) \quad (7)$$

When the consideration of initial concentration of selenious acid a is taken into Eq. 7, the relationship between k_2, x_m and a can derived as follows,

$$x_m = 1.306 \times (k_2 \cdot a)^{0.114} \quad (8)$$

Summary

(1) The reduction of selenious acid in sulfuric acid by sulfur dioxide is a reversible reaction, because the reaction has an equilibrium and the process of the reaction is in good accordance with the equation which expressed mathematically the reversible reaction, that is,

$$-d(a-p)/dt = dp/dt = k_2(a-p)^2 - k_2'p^2$$

(2) Up to the present time the rate constant k_2 of the forward reaction was derived by substitution of the experimental data for x_m in the following equation,

$$k_2 = \{2.303x_m/2a(x_m-1)t\} \times \log[(x-x_m)/\{(2x_m-1)x - x_m\}]$$

The general equation for k_2, which does not depend on x_m, has been obtained as follows,

$$k_2 = 2.054 \times 10^{15} \times [H^+]^2 \times \exp(-E/RT)$$
$$(E = 22.5 \text{ kcal./mol.})$$

The rate constant k_2' of the reverse reaction can be calculated by

$$k_2' = 2.413 \times 10^{-11} \times \{1/(a^2[H^+]^2)\} \times \exp(-E/RT) \quad (E = -8.06 \text{ kcal./mol.})$$

(3) It has not previously been reported that α selenium is dissolved in dilute sulfuric acid (below 85% by weight), as shown by the present experimental procedure.

(4) The results obtained from this study are useful in the recovery and refinining of selenium. Then application to the recovery and refining of selenium will be expressed in another succeeding paper.

The author wishes to express his thanks to Dr. H. Negita of the Department of Chemistry, Hiroshima University for helpful discussion, and also he wishes to thank Mr. M. Kodama for his assistance.

Department of Chemistry
Faculty of Science
Hiroshima University
Hiroshima

Kinetics of the Reduction of Selenious Acid by Sulfur Dioxide. III. Application to Recovery and Purification of Selenium in Sulfuric Acid Works

By Keinosuke HAMADA

(Received March 30, 1960)

The greater part of the starting materials for the productions of selenium consists of an anode-slime deposited in the electrolytic refining of copper and a sludge containing selenium recovered in the manufacturing process of sulfuric acid. The latter is called sulfuric acid sludge.

The reaction of selenious acid by sulfur dioxide was found to be a reversible reaction in sulfuric acid. The general equation for the rate constant of the forward reaction and the relation between the rate constant and the maximum percentage completion (maximum yield) were derived in the previous paper[1].

A great deal of sludge has recently been recovered from the mist acid which is a by-product of the manufacture of sulfuric acid, and a very simple and economical method of purification of selenium has been found by means of the application of the experimental results[1].

Application to the Recovery of Selenium in the Mist Acid.—A schematic diagram of the contact process for manufacturing sulfuric acid is shown in Fig. 1. Generally pyrites have about 12.6 parts of selenium per million[2] of pyrites. When pyrite is roasted, the selenium in the

1) Part II; This Bulletin, **34**, 596 (1961).
2) T. Tsuge et al., *J. Agr. Chem. Soc. Japan* (*Nippon Nogei-Kagaku Kaishi*), **23**, 421 (1950).

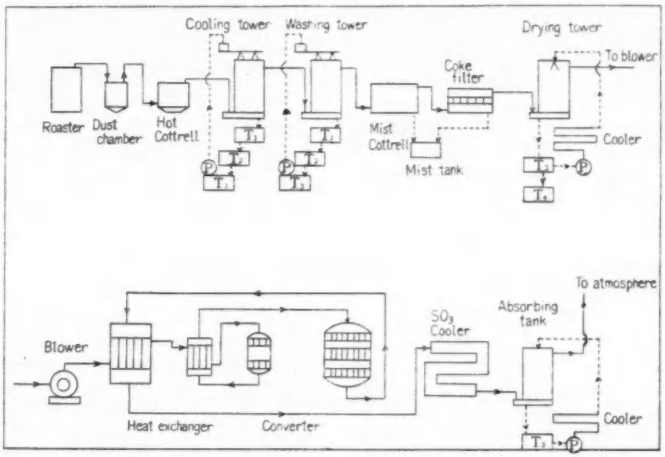

Fig. 1. Schematic diagram of contact process of sulfuric acid.

T_1: Cooling tank T_4: Storage tank —→— Gas
T_2: Precipitating tank Ⓟ: Pump —→-- Acid
T_3: Pump tank

pyrite is oxidized to selenium dioxide. The part of the selenium dioxide is dissolved in the mist acid*, which is excluded from gas by a mist Cottrell and a coke filter, and is brought into a mist tank. The concentration of the mist acid is about 15° Bé (s. g. 1.115) while the acid is saturated with sulfur dioxide. Nevertheless, a large quantity of selenious acid exists in mist acid without being reduced to selenium. This fact can easily by explained according to the results of Part II[1] of this series, as follows. The reaction of selenious acid with sulfur dioxide in sulfuric acid is reversible, and the rate constant of the forward reaction, k_2, is expressed according to the following equation:

$$k_2 = 2.054 \times 10^{15} \times [H^+]^2 \times \exp(-E/RT) \quad (E = 22.5 \text{ kcal./mol.}) \qquad (1)$$

The equation which expresses the relation among rate constant, k_2, maximum percentage completion, x_m, and initial concentration of selenious acid, a, is as follows:

$$x_m = 1.306 \times (k_2 \cdot a)^{0.114} \qquad (2)$$

In these equations, $[H^+]$ is hydrogen ion concentration, T absolute temperature of solution, E the energy of activation, R the gas constant and a initial concentration of selenious acid. It is evident that maximum yield, x_m, depends heavily on temperature at the constant $[H^+]$ and a, according to Eqs. 1 and 2. When the mist acid is heated up to the boiling point, selenium can be precipitated. After heating the mist acid, the selenium content in the mist acid is found to be about 0.00015 mol./l. Ninety-five per cent of selenium in the mist acid can be recovered by only heating the mist acid. Selenium sludge gained from the mist acid has a high content of selenium (about 80%), and a great deal of sludge can be recovered each day, making sludge a useful and plentiful starting substance for the isolation of selenium.

Application to the Purification of Selenium. —Up to the present time, many studies[3-33]

* The mist acid has about 0.003 mol. selenious acid per liter.

3) Z. Littmann, *Z. angew. Chem.*, **19**, 1039 (1906).
4) N. Chikashige et al., Brit. Pat. 134536 (1919).
5) J. Sugie, *Osaka Ind. Lab.*, **1**, No. 1, 1 (1920).
6) T. Shimoi et al., Japan. Pat. 3629 (1920).
7) S. Sugie, *J. Japan Ceram. Assoc.*, **343**, 226 (1921).
8) W. Stahl, *Chemiker-Ztg.*, **50**, 280 (1926).
9) Z. Littmann, ibid., **50**, 704 (1926).
10) A. A. Borkovski et al., *Zavodskaya Lab.*, **3**, 306 (1934); *Chem. Abstr.*, **29**, 1739 (1935).
11) A. R. Lindblad, Brit. Pat. 423084 (1935); Fr. Pat. 777857 (1935); Ger. Pat. 641714 (1937).
12) O. C. Martin et al., U. S. Pat. 2039256 (1936).
13) F. W. Heberlein, Can. Pat. 364133 (1937).
14) C. W. Clark et al., *Am. Inst. Mining Met. Engrs., Tech. pub.*, **982**, 22 (1938).
15) H. C. Dudley, U. S. Pat. 2111112 (1938).
16) M. S. Belskaya, Russ. Pat. 58836 (1941).
17) N. R. Bierly, U. S. Pat. 2349697 (1944).
18) C. W. Clark, U. S. Pat. 2409835 (1946).
19) A. J. Philip et al., U. S. Pat. 2413374 (1946).
20) N. S. Artamonov, U. S. S. R. Pat. 66128 (1946).
21) D. Gardner, U. S. Pat. 2414295 (1947).
22) M. C. Bloom, U. S. Pat. 2414438 (1947).
23) N. V. Philips, Fr. Pat. 930184 (1948).
24) A. Voige et al., Ger. Pat. 800860 (1950).
25) T. Sawaya, Japan. Pat. 18 (1950).
26) K. Krebs, Brit. Pat. 644743 (1950).
27) Y. Terasaki, Japan. Pat. 2560 (1952).
28) N. A. Vaarro, Span. Pat. 207021 (1954).
29) T. Tamura, Japan. Pat. 7052 (1955).
30) K. Okamoto, Japan. Pat. 3508 (1955).
31) N. Imai et al., Japan. Pat. 3108 (1956).
32) Y. E. Lebedeff et al., U. S. Pat. 2775509 (1956).
33) S. Ato et al., *Repts. Sci. Research Inst. (Japan)*, **32**, 27 (1956).

have been performed concerning the purification of selenium, and each method of purification of selenium has had its own characteristics.

In the purification of sulfuric acid sludge, the Stahl[8] and Littmann[9] method was found to be the most suitable. However, the method has some difficulty, the yield is relatively lower (around 85%). The present author has noticed that the yield depended largely on the hydrogen ion concentration and temperature according to Eqs. 1 and 2. Therefore, these two factors were taken into account for their method[8,9] as described subsequently.

Experimental

A great success has been attained in the purification of selenium on the industrial scale by enlarging the experimental procedures. Therefore, the process on an industrial scale will now be described in some detail. Figure 2 shows the schematic diagram of the plant for purification of sulfuric acid sludge according to the new method.

The dried sludge is brought into a reacting vessel, and 20 l. of fuming sulfuric acid (23%) per 1 kg. pure selenium in the sludge is added to the vessel.

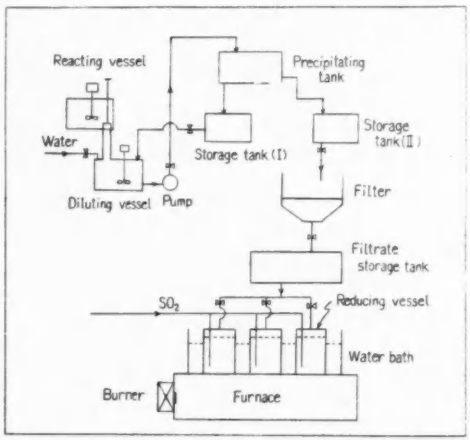

Fig. 2. Schematic diagram of purification plant of selenium.

These mixtures are agitated for two hours with a stirrer. The selenium in the sludge is changed to green selenium anhydro-sulphate ($SeSO_3$) according to the following reaction:

$$Se + H_2SO_4 \cdot SO_3 = SeSO_3 + H_2SO_4$$

Then, 2 l. of nitric acid (62% by weight) per 1 kg. pure selenium in the sludge is added to this green solution, and agitation is continued for one additional hour.

The temperature is increased up to about 120°C, and a yellow solution of selenious acid results as follows.

$$SeSO_3 + 4HNO_3 = H_2SeO_3 + H_2SO_4 + 4NO_2$$

The mixture containing selenious acid is slowly dropped into a diluting vessel, to which 50 l. of water per 1 kg. pure selenium in the sludge has previously been added. The temperature of the solution is elevated up to approximately 140°C, by the heat of the dilution of the fuming sulfuric acid. The excess of nitric acid is released owing to the high temperature. Moreover, 20 l. of water per 1 kg. pure selenium is added to the above solution.

The mixtures in the diluting vessel are pumped up to a precipitating tank, and cooled to the chamber temperature. Solid materials in solution, of course, settle down in this tank. The supernatant is brought into a storage tank (I), and subsequently sent to a filter. The filtrate is introduced into reducing vessels via a filtrate storage tank, and reduced to selenium by some previously water-washed sulfur dioxide (about 6%) used in the manufacture of sulfuric acid. When the solution of selenious acid is reduced, it is kept at bout 70°C*1 in a water bath.

The selenium precipitated in the reducing vessel is removed, washed by water till all traces of sulfuric acid disappear and dried in an air bath at 110°C or lower. The waste solution is 35% (by weight) sulfuric acid, and this solution can be utilized elsewhere in industry.

Results

The purpose of the present study is to find the most suitable method for manufacture of selenium that meets the minimum commercial requirements in the sulfuric acid works.

A 92% yield*2 has been secured and the purity of 99.9% has been obtained according to this new method. Table I shows a few

TABLE I. DATA OF ANALYSIS OF PURIFIED Se AND RAW MATERIALS

	Se, %	Fe	Si	Te	Hg	As	Ag	Pb
Purified Se (A)	99.94	w	w	www	s	nil	ww	nil
Raw material (A)	29.63	ss	s	s	s	ww	s	ss
Purified Se (B)	99.97	w	w	www	w	nil	ww	nil
Raw material (B)	88.99	ss	s	s	w	ww	s	ss

w, weak; ww, very weak; www, trace; s, strong; ss, very strong.

*1 It is evident according to Eqs. 1 and 2[1] that the higher the temperature of the solution is, the greater the yield is. However, the particles of selenium separated at high temperature (about 80°C) are very small. At about 70°C, most particles of the precipitated selenium can pass through a 80~100 mesh sieve, and so they meet commercial requirements. The difference of yield between those at 70°C and at 80°C can hardly be appreciated by the present experiments.

*2 Yield of conventional methods is between 80 and 90%.

examples of analysis*3 of selenium purified by the new method and raw materials.

Table I expresses the relative strength of the lines of emission spectra, except the data for selenium. A remarkable result is shown in Table I, namely, tellurium can be removed without any special effort, but on the contrary, most of the mercury remains in the purified selenium.

Discussion

Selenium in mist acid can be recovered by heating the acid according to the results of Part II[1] of this series.

By improving the Stahl[8] and Littman[9] method according to the results of Part II[1], the simple method for purification of selenium has been found. It was already mentioned in the present paper that this method had many virtues. Especially, it is interesting to note that tellurium can be excluded from the purified selenium without any special steps. According to conventional methods, some special steps were necessary in order to exclude impurities; for example, tellurium. These special processes are: i) using hydrochloric acid[10], ii) ion-exchange resin[34], and iii) distillation[11,15,33,35-39,42]. But it is unnecessary to include any provisions for removal of tellurium in the present method*4[,40,41].

It is the defect of this method that the purity of four nine can not be secured, although that of three nine can be secured. This seems to be caused by the mercury as an impurity.

The author wishes to thank Dr. H. Negita of the Department of Chemistry, Hiroshima University, for the discussion, and also to express hearty thanks to the Factory Manager, E. Yamashita, for the K. Chemical Company of the application of the author's experimental results[1] to the purification of selenium on an industrial scale and the permission to publish the industrial method, also to the staffs of the Department of Sulfuric Acid and Laboratory in the company for their advice and help.

Department of Chemistry
Faculty of Science
Hiroshima University
Hiroshima

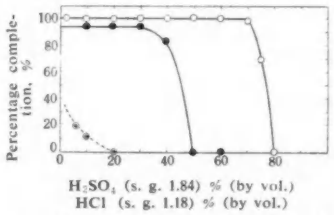

Fig. 3. Reduction of tellurous acid by SO_2.
◉ In acidic soln. with H_2SO_4
● In acidic soln. with (H_2SO_4+10cc. HCl(s. g. 1.18))
○ In acidic soln. with HCl

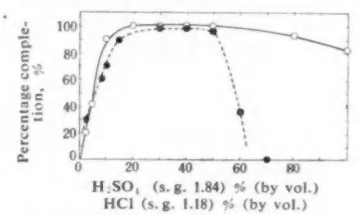

Fig. 4. Reduction of selenious acid by SO_2.
○ In acidic soln. with H_2SO_4
● In acidic soln. with HCl

*3 Selenium is determined by means of gravimetric analysis, while others were determined by spectrochemical analysis.

34) F. Aoi, This Bulletin, **26**, 480 (1953).
35) H. Bode, *Z. anal. Chem.*, **134**, 100 (1951).
36) A. I. Gaev, Russ. Pat. 51200 (1937).
37) N. S. Polvektov, *Microchemie*, **15**, 32 (1934).
38) S. T. Volkov, *Zavodskaya Lab.*, **5**, 1429 (1936); *Chem. Abstr.*, **31**, 6130 (1937).
39) V. K. Zemel, ibid., **5**, 1443 (1936).
40) E. M. Müller, *Z. physik. Chem.*, **100**, 346 (1922).
41) T. L. Pökrovskaya, *Zavodskaya Lab.*, **7**, 15 (1938); *Chem. Abstr.*, **32**, 4101 (1938).
42) T. Takei et al., *Repts. Sci. Research Inst. (Japan)*, **26**, 234 (1950).

*4 It is believed that, tellurium is excluded based on this fact, the higher the concentration of sulfuric acid, the smaller is the rate constant of reduction of tellurous acid in sulfuric acid. This can be guessed by the following simple, qualitative experiment. A solution of tellurous acid of 0.01 mol. per 200 ml. sulfuric acid of many kinds of concentrations were prepared, and left overnight at chamber temperature after being saturated with sulfur dioxide. Fig. 3 shows the plot of the tellurium precipitated (percentage completion) against each concentration of sulfuric acid. One can see that when the concentration of sulfuric acid is above 20% (by volume), tellurium can not be precipitated. Fig. 4 is the same plot as in the case of selenious acid for comparison with Fig. 3.

The Relation between Reactivity and Selectivity

By Yoshiro OGATA and Iwao TABUSHI

(Received July 12, 1960)

Brown and his coworkers have pointed out the existence of the linear relation between the logarithm of the para partial rate factor of toluene, $\log p_f$, which they called a measure of activity of reagent and the selectivity factor which is expressed as the logarithm of ratio of para vs. meta partial rate factor, $\log(p_f/m_f)$[1]. As they have mentioned, the relation can be derived from the Hammett equation and is expressed as

$$\log p_f = \frac{\sigma_p}{\sigma_p - \sigma_m} \log(p_f/m_f) \qquad (1)$$

However, the term of $\log p_f$ is not the reactivity, but the distribution of a given reagent between benzene and toluene, or intermolecular selectivity and it is not surprising that the intermolecular selectivity is proportional to the intramolecular selectivity, $\log(p_f/m_f)$.

The reactivity of a reagent should be expressed as a value related to the rate constant for the reaction between a standard substance and the reagent at a standard condition or k_0. The value of k_0, however, depends on the reaction mechanism, the concentration of the actual attacking species, the environment and conditions. Hence it is difficult to compare the value of k_0 at a standared condition. Nevertheless, as shown in Table I, A-1 and A-2 the qualitative parallelism is sometimes observed between k_0 and the absolute value of ρ or the sensitivity of the rate to the change of substituent in closely related reactions[1c].

If frequency factors are constant, the relative

TABLE I

(A) COMPARISON OF DIFFERENT ATTACKING REAGENTS

A-1) Aromatic alkylation

Reaction	Solvent	$-\rho$	$\log k_0$ l. mol^{-1} sec^{-1}	Ref.
ArH + MeBr, $AlCl_3$	1,2,4-$Cl_3C_6H_3$	3.64	−2.444	6
ArH + MeBr, $GaBr_3$	ArH	3.06	−1.301	7
ArH + EtBr, $GaBr_3$	ArH	2.66	−0.799	7
ArH + *i*-PrBr, $GaBr_3$	ArH	2.54	+2.505	7

A-2) Electrophilic halogenation at 25°C (X; H or CH_3)

Reaction	$-\rho$	$\log k_0$, l. mol^{-1} sec^{-1}	Ref.
C_6H_5X + HClO	7.77	−3.380	8
C_6H_5X + HBrO	6.05	−0.234	9

A-3) Electrophilic addition[10]

Reaction	Products	
	1-Halo-compound	2-Halo-compound
$CH_2=CH-CH_3$ + HClO	$ClCH_2CHOHCH_3$ (90%)	$CH_2OHCHClCH_3$ (10%)
$CH_2=CH-CH_3$ + HCl	None	$CH_3CHClCH_3$
$CH_2=CH-CH_2Cl$ + HClO	$ClCH_2CHOHCH_2Cl$ (30%)	$CH_2OHCHClCH_2Cl$ (70%)
$CH_2=CH-CH_2Cl$ + HCl	None	$CH_3CHClCH_2Cl$

(B) COMPARISON OF DIFFERENT SUBSTRATES

Second-order rate constants of chlorination[11], l. mol^{-1} min^{-1}

R	*p*-Me	H	*m*-NO_2
1. $R-C_6H_4CH=CHCOPh$	800	61	0.23
2. $R-C_6H_4CH=CH-CO_2H$	103	4.9	0.011
k_1/k_2	7.76	12.4	20.9

1) a) H. C. Brown and K. L. Nelson, *J. Am. Chem. Soc.*, **75**, 6292 (1953).
b) H. C. Brown and W. H. Bonner, ibid., **76**, 605 (1954).
c) H. C. Brown and C. W. McGary, Jr., ibid., **77**, 2300 (1955).
d) H. C. Brown and C. R. Smoot, ibid., **78**, 6255 (1956).
e) L. M. Stock and H. C. Brown, ibid., **81**, 3233 (1959), **82**, 1942 (1960).

rate constant of substituted and unsubstituted reactants is expressed as

$$\ln(k/k_0) = -\frac{\Delta H^{\ddagger} - \Delta H_0^{\ddagger}}{RT} = \sigma\rho \qquad (2)$$

Hence it is rational that the absolute value of ρ with constant σ decreases with an increase of temperature[2] which accompanies an increase of the rate constant in the same reaction series. Furthermore, it is supposed from Eq. 2 that the absolute value of $\Delta H^{\ddagger} - \Delta H_0^{\ddagger}$ approaches zero, when both $\Delta H^{\ddagger}$ and $\Delta H_0^{\ddagger}$ approach zero or k_0 becomes very large. Therefore, the ρ value with constant σ tends to decrease with an increase of k_0 under this limitation. Thus the very fast reaction such as protonation have a constant value of rate constants (3×10^{10} l. mol^{-1} sec^{-1} at 18~30°C) or the ρ value of zero[3].

The selectivity may be expressed with either intramolecular selectivity, i.e., orientation, or intermolecular selectivity, i.e., relative rate. Since the former selectivity is proportional to the latter in aromatic compounds[4,5], as shown in Eq. 1, the reactivity-selectivity relation can be tested with any of these selectivities.

Table I shows A) comparison of different attacking reagents and B) comparison of some groups of substrates with different reactivities.

2) H. H. Jaffé, *Chem. Revs.*, **53**, 191 (1953); H. C. Brown and C. W. McGary, Jr., *J. Am. Chem. Soc.*, **77**, 2306 (1955).
3) R. P. Bell, *Quart. Revs.*, **13**, 169 (1959).
4) L. M. Stock and H. C. Brown, *J. Am. Chem. Soc.*, **81**, 2320 (1959).
5) The same is true with aliphatic compounds in which polar effect alone is important.
6) H. Jungk, C. R. Smoot and H. C. Brown, *J. Am. Chem. Soc.*, **78**, 2185 (1956).
7) H. C. Brown and H. Jungk, ibid., **77**, 5584 (1955).
8) P. B. D. de la Mare, J. T. Harvey, M. Hassan and S. Varma, *J. Chem. Soc.*, **1958**, 2756.
9) P. B. D. de la Mare and J. T. Harvey, ibid., **1956**, 36.
10) J. R. Shelton and L. Lee, *J. Org. Chem.*, **25**, 907 (1960). More reactive HClO adds less regularly to substituted ethylenes in comparison with less reactive HCl.
11) P. B. D. de la Mare, *Quart. Revs.*, **3**, 126 (1949).

Summary

The proportionality between $\log p_f$ and $\log(p_f/m_f)$ reported by Brown[1] seems to express the proportionality between inter- and intramolecular selectivities. The standard rate constant k_0 may be a measure for the reagent activity; the parallelism between $1/k_0$ and $|\rho|$ or selectivity is observed in very limited reactions.

Department of Industrial Chemistry
Faculty of Engineering
Kyoto University
Sakyo-ku, Kyoto

*Acid-Base Property and Metal Chelate Formation of 4-(2-Pyridylazo)-resorcinol**

By Toschitake IWAMOTO

(Received January 7, 1960)

4-(2-Pyridylazo)-resorcinol (PAR) has recently been suggested as a water-soluble metal indicator for the EDTA-titration of lead and other metal cations in place of 1-(2-pyridylazo)-2-naphthol (PAN)[1]. The latter forms a colloidal suspension when dissolved in water in the pH range 2 to 13[2], and this fact is one of the disadvantages of the reagent in aqueous systems. The use of PAR as a color reagent in colorimetric analysis[3] and as a metal indicator in precipitation titration[4] and in chelatometric titration[5] has been proposed, all of which is based on the formation of stable colored chelates of PAR with various heavy metals such as lead, cobalt and uranium.

The present paper concerns the acid dissociation of PAR, its chelate formation with some metal cations in aqueous solutions, the stability constant of copper(II)-PAR chelate and the comparison between PAR and PAN as analytical reagent.

The absorption spectra of PAR in aqueous

* Presented partly at the 13th Annual Meeting of the Chemical Society of Japan, Tokyo, April, 1960.
1) P. Wehber, *Z. anal. Chem.*, **158**, 10 (1957); **167**, 186 (1958).
2) B. F. Pease and W. B. Williams, *Anal. Chem.*, **31**, 1044 (1959).
3) F. H. Pollard, P. Hanson and W. J. Geary, *Anal. Chim. Acta*, **20**, 26 (1959).
4) R. Püschel, E. Lassner and R. Scharf, *Z. anal. Chem.*, **163**, 104, 344 (1958); **165**, 401 (1959).
5) E. J. Langmyhr and H. Kristiansen, *Anal. Chim. Acta*, **20**, 524 (1959).

solution at various pH values have been examined, the acid dissociation constants determined by pH-titration and colorimetric method. The composition of the metal chelates of PAR with tervalent iron, bivalent cobalt, nickel, copper, zinc, cadmium, mercury and lead has been determined with the aid of the continuous variation method[6] and the stability constant of copper(II)-PAR chelate determined potentiometrically by pH-titration; its utility in chelatometric analysis was discussed.

Experimental

The PAR used in this study was a sample for test supplied by Dojin Pharmaceutical Laboratories, Kumamoto, Japan.

Found: C, 61.4; H, 4.5; N, 18.7; Calcd. for $C_{11}H_9O_2N_3$: C, 61.1; H, 4.2; N, 19.5[7].

PAR in free acid form is readily soluble in an aqueous alkaline solution. Solubility in water at 10°C was found to be only 5 mg./100 ml.

4-Benzeneazoresorcinol was kindly given by Dr. Yoshio Matsunaga in our laboratory.

A solution of 10^{-2} M potassium hydroxide was prepared by direct dissolution of metallic potassium (E. Merck) in deionized water in a current of nitrogen, and standardized against $1.007_4\times10^{-2}$ M hydrochloric acid. The standard solution of the

Fig. 1. Absorption spectra of PAR.
5×10^{-5} M: 1 cm. silica cell (Cary)

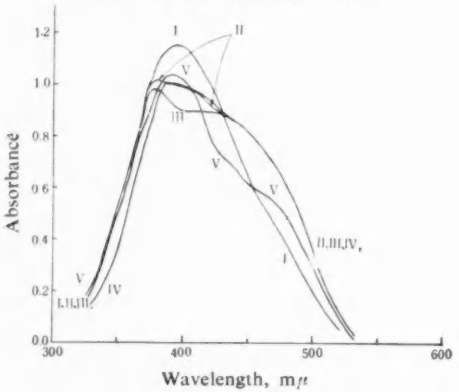

Fig. 1a. Absorption spectra of PAR in acid solutions.

I: 4.7 N HNO_3
II: 3.2 N HNO_3
III: 1.6 N HNO_3
IV: 0.1 N HNO_3
V: pH 3, acetate buffer (0.1 M KNO_3)

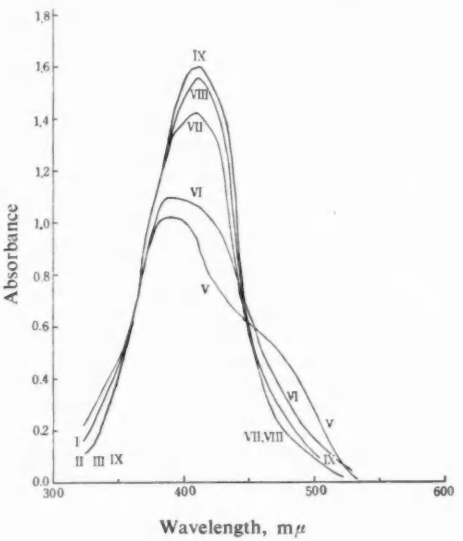

Fig. 1b. Absorption spectra of PAR in neutral solutions.

V: pH 3, acetate buffer
VI: pH 5, acetate buffer
VII: pH 7, phosphate buffer
VIII: pH 9, borax buffer
IX: pH 11, 0.001 N NaOH
(0.1 M KNO_3)

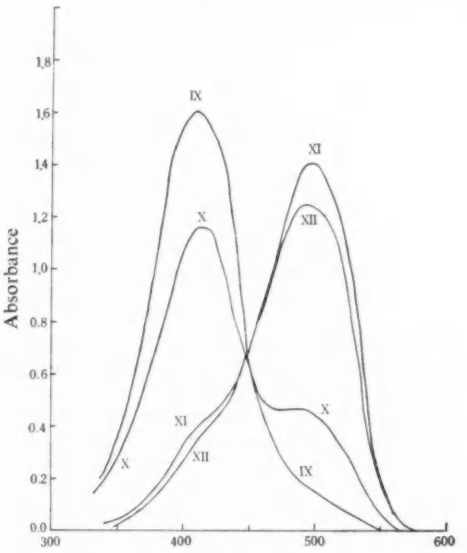

Fig. 1c. Absorption spectra of PAR in alkaline solutions.

IX: 0.001 N NaOH
X: 0.01 N NaOH
(0.1 M KNO_3)
XI: 0.1 N NaOH
XII: 1 N NaOH

6) Y. Shibata, T. Inouye and Y. Nakatsuka, *J. Chem. Soc. Japan (Nippon Kwagaku Kwaishi)*, **42**, 983 (1921); R. Tsuchida, This Bulletin, **10**, 27 (1933). Cf. P. Job, *Ann. chim.*, [10] **9**, 113 (1928).

7) Elementary analysis was performed by Mr. Shozo Masuda in our department. The PAR might contain some impurities (cf. Refs. 2 and 3). The purity of the PAR calculated from the content of nitrogen 18.7/19.5=0.96, agreed with that (0.94) determined by photometric titration with a copper nitrate solution.

acid was prepared by passing a known amount of potassium chloride solution through a column of cation-exchange resin in H-form (Diaion SK #1, analytical grade).

All the other chemicals were of reagent grade, and all metal salts were used as nitrates. Acetate, phosphate and borax buffer, nitric acid, potassium hydroxide and sodium hydroxide solution were used to control the pH. By photometric titrations[7a] with 1.00×10^{-4} M copper nitrate solution, the PAR solutions were standardized after suitable dilution whenever necessary.

The absorption spectra were measured by a Cary Model 11 and a Shimadzu QB-50 spectrophotometer and the colorimetric measurements were done by a Hirama IIb filter electrophotometer. For pH-titrations and pH measurements a Denkishiki DG pH meter equipped with a glass and a calomel electrode was used; the measurements were carried out in a thermostat regulated at 25 ± 0.2°C by circulating water from another large thermostat. During titration the solution was stirred magnetically and bubbled with nitrogen gas through a capillary.

Results and Discussion

Acid Dissociation of PAR.—The absorption spectra of aqueous solutions of PAR depend on the pH values as shown in Fig. 1. The spectra in acid solutions have somewhat complicated aspects which may be caused by the presence of pyridinium form or azo-protonated forms as in case of PAN[2] and some azobenzene derivatives[8]. It can be suggested that an undissociated form a, two kinds of the dissociated forms b and c, and one-protonated form d exist in neutral and alkaline solutions. As the degree of acid dissociation of *o*-hydroxyl group may be lower than that of *p*-hydroxyl group through an intramolecular hydrogen bond formation, the absorption maxima at 390, 410 and 490 mμ can be assigned to a, b and c, respectively, and the broad shoulder from 400 to 470 mμ to d. The existence of these dissociation stages in neutral and alkaline solutions can be supported by similar study on 4-benzeneazoresorcinol. As shown in Fig. 2, in the neutral solution the spectrum has a doublet of 375 and 410 mμ (Curve I)[9]. In the weakly alkaline solutions the absorption maximum shifts to 430 mμ (Curves II and III) and in the more alkaline solution the maximum further shifts to 475 mμ and shows a shoulder at 390 mμ (Curve IV). These properties are analogous to those of PAR.

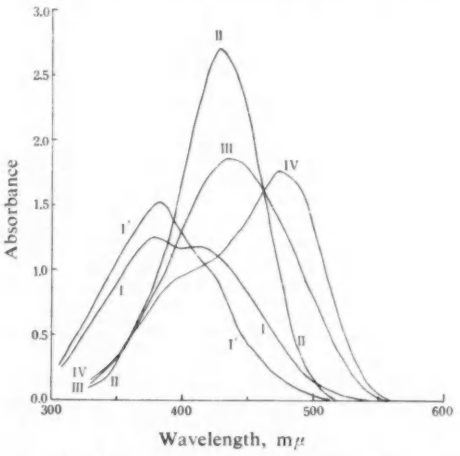

Fig. 2. Absorption spectra of benzeneazoresorcinol.
7×10^{-5} M: 1 cm. silica cell (Cary)
I: 8% ethanol
I': 95% ethanol
II: 4×10^{-4} M borax in 8% ethanol
III: 3×10^{-2} M NaOH in 8% ethanol
IV: 0.7 M NaOH in 8% ethanol

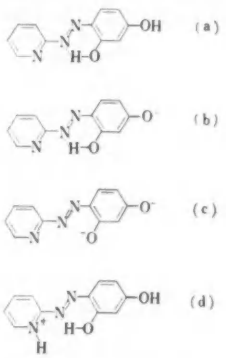

Determination of Acid Dissociation Constants of PAR.—From the pH dependency of the spectra the acid dissociation constants of PAR k_{a_1} and k_{a_2} defined by Eqs. 1 and 2 are estimated as about 10^{-6} and 10^{-12}, respectively.

$$k_{a_1}=\frac{[C_{11}H_8O_2N_3^-]\,[H^+]}{[C_{11}H_9O_2N_3]} \quad (1)$$

$$k_{a_2}=\frac{[C_{11}H_7O_2N_3^{2-}]\,[H^+]}{[C_{11}H_8O_2N_3^-]} \quad (2)$$

In order to obtain more accurate values 100 ml. of 4.72×10^{-5} M PAR solution was titrated with 1.085×10^{-2} M potassium hydroxide solution at 25°C (Fig. 3). One proton caused by the first dissociation was neutralized and k_{a_1} was calculated as 1.48×10^{-6} ($pk_{a_1}=-\log k_{a_1}=5.83$) according to the following equation:

7a) T. Iwamoto, *Japan Analyst (Bunseki Kagaku)*, **10**, 189 (1961).

8) M. T. Rogers, R. W. Campbell, R. W. Maatmann, *J. Am. Chem. Soc.*, **73**, 5122 (1951).

9) The absorption spectrum of 4-benzeneazoresorcinol in an ethanolic solution taken from the late Dr. F. Iimura's unpublished results shows also a singlet maximum at 375 mμ. The splitting may be elucidated in terms of solvent effect.

$$k_{a_1} = \frac{[H^+](aC + [H^+] - [OH^-])}{C - (aC + [H^+] - [OH^-])} \qquad (3)$$

where C stands for the total concentration of PAR and a moles of base added per mole of the acid. Another proton caused by the second dissociation was not liberated under these conditions because of the low value of the second dissociation constant k_{a_2}, as foreseen by the absorption spectra measurements. Then it was approximately determined from absorption measurements of aqueous PAR solutions in the range of pH between 10 and 13.8 with a filter electrophotometer using the filters transparent in the vicinity of 420 and 485 mμ. From the curves in Fig. 4, pk_{a_2} was estimated as 12.5 ($k_{a_2} = 3.2 \times 10^{-13}$).

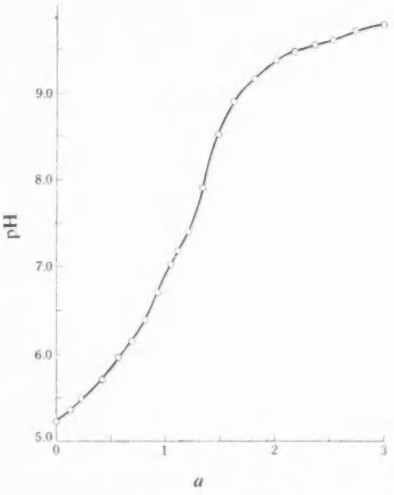

Fig. 3. pH-Titration of PAR free acid.
100 ml. of 5×10^{-5} M PAR solution with 0.01 N KOH solution.
a: moles of base added per mole of acid

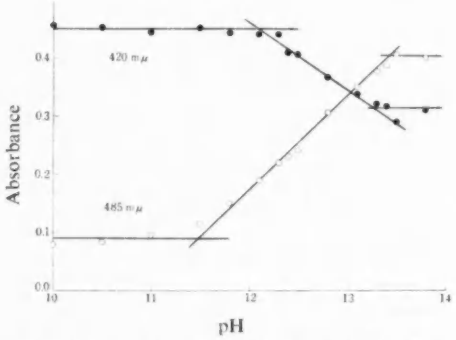

Fig. 4. Absorbance vs. pH of PAR solutions.
5×10^{-6} M PAR, 2 cm glass cell.
Full circle, at 420 mμ; open circle, at 485 mμ

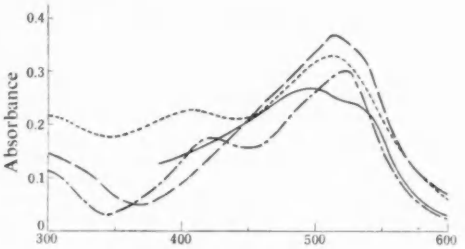

Fig. 5. Absorption spectra of metal-PAR chelates.

—— $Fe(PAR)_2$: 0.6×10^{-5} M pH 4
—— $Co(PAR)_2$: 0.8×10^{-5} M pH 4
---- Cu(PAR): 1.0×10^{-5} M pH 4
---- Pb(PAR): 1.0×10^{-5} M pH 10
1 cm. silica cell (Shimadzu)

TABLE I. COMPOSITIONS AND MOLAR EXTINCTION COEFFICIENTS OF METAL-PAR CHELATES

Metal	Composition	pH	ε at 517 mμ
Fe(III)	1 : 2	4.0	4.2×10^4
Co(II)	1 : 2	4.0	4.2×10^4
Ni(II)	1 : 2	4.0	2.2×10^4
Cu(II)	1 : 1	4.0	3.0×10^4
	1 : 1	10.0	3.2×10^4
Zn(II)	1 : 1	10.0	—
Cd(II)	1 : 1	10.0	—
Hg(II)	1 : 1	10.0	—
Pb(II)	1 : 1	10.0	3.8×10^4

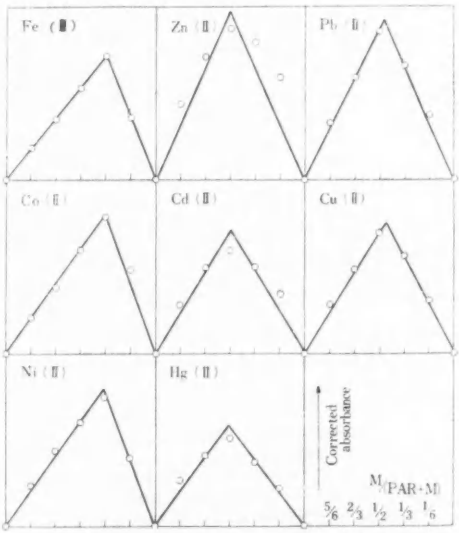

Fig. 6. Graphical determination of the composition of metal-PAR chelates.

Compositions of PAR Chelates of Fe(III), Co(II), Ni(II), Cu(II), Zn(II), Cd(II), Hg(II) and Pb(II).—Wehber[1] and Pollard et al.[3] reported the coloration of the chelates of PAR with various kinds of metals in aqueous solutions. In Fig. 5 are shown a few examples of absorption spectra measured by the present author. The composition of these chelates in aqueous solutions was determined by means of the continuous variation method using the filter photometer with a 517 mμ filter. The results and the molar extinction coefficients of the chelates are given in Table I. In Fig. 6, data are shown graphically. From these data PAR may be considered to act as terdentate ligand having three donor atoms in a plane[10]:

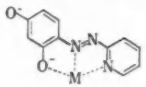

The details of the structure of metal-PAR chelare are now under investigation.

Stability Constant of Copper(II)-PAR Chelate.—In the presence of copper(II)-EDTA chelate, PAR may be applied as a metal indicator to the titration of metal cations which neither form colored chelates with PAR nor react with PAR rapidly and reversibly. To compare the function of the Cu-PAR indicator system with that of Cu-PAN[11], the stability constant of copper(II)-PAR chelate was determined by pH-titration. One hundred ml. of solution containing 4.72×10^{-6} mol. of PAR and the equimolar amount of copper nitrate was titrated with the above-mentioned potassium hydroxide solution. The titration curve shown in Fig. 7 exhibits a marked inflection at $a\simeq2$. Acid dissociation and chelate formation of PAR are as follows:

$$H_2D = H^+ + HD^- \qquad (pk_{a_1}=5.83) \tag{4}$$

$$HD^- = H^+ + D^{2-} \qquad (pk_{a_2}=12.5) \tag{5}$$

$$Cu^{2+} + D^{2-} = CuD^{12)} \tag{6}$$

$$Cu^{2+} + H_2D = 2H^+ + CuD \tag{6'}$$

$$CuD + H^+ = HCuD^+ \tag{7}$$

where H_2D is PAR in undissociated form, HD^- in b form (p. 607) and $HCuD^+$ is one-protonated form of Cu-PAR chelate that may exist in considerably low pH region:

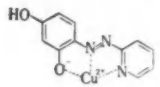

The equilibrium constant for Eq. 6, $k=[CuD]/[Cu^{2+}][D^{2-}]$, gives the stability constant of copper(II)-PAR chelate provided that the activity coefficient of each species is maintained constant. If $k_a'=[H^+][CuD]/[HCuD^+]$ is postulated as the acid dissociation constant for the process reverse to Eq. 7, Eq. 8 gives the relation between k, k_{a_1}, k_{a_2} and the concentration of D^{2-} throughout the titration under the experimental conditions:

$$k[D^{2-}]^2([H^+]^2/k_{a_1}k_{a_2}+[H^+]/k_{a_2}) - [D^{2-}][H^+]^2/k_{a_1}k_{a_2} = (a-1)+[H^+]-[OH^-] \tag{8}$$

where C stands for the total concentration of PAR (=that of Cu^{2+}) and a the moles of base added per mole of PAR.

With the assumption that at adjacent plots of the measurements in the buffer region of the titration curve the value of $[D^{2-}]$ is the same, k was calculated to be 5×10^{11} as the mean value from thirty sets of simultaneous equations derived from Eq. 8. k_a', which can be considered as the second dissociation constant of a hypothetical dibasic acid H_2CuD^{2+},

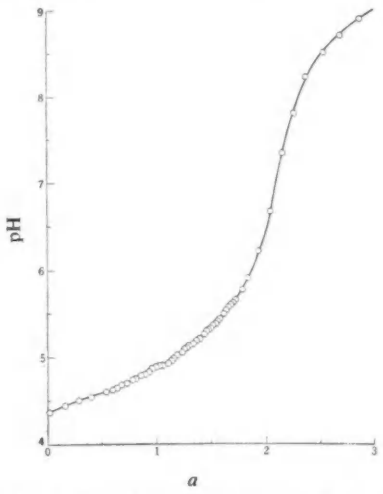

Fig. 7. Titration curve of copper(II)-PAR chelate.
5×10^{-5} M Cu-PAR solution 100 ml. with 0.01 M KOH solution
$\mu=0.1$ M KNO_3, 25°C
a: moles of base added per mole of chelate

10) Y. Muto, This Bulletin, **31**, 1017 (1958); F. Lions and K. V. Martin, *J. Am. Chem. Soc.*, **79**, 2733 (1957); F. Lions and H. A. Goodwin, ibid., **81**, 6415 (1959).

11) H. Flaschka and H. Abdine, *Z. anal. Chem.*, **152**, 77 (1956); *Chemist-Analyst*, **45**, 2 (1956).

12) It is not necessary for CuD to be neutral in charge, for PAR is considered as a terdentate ligand and the coordination requirement of copper(II) atom will be fulfilled by another unidentate anion (e. g. nitrate ion) in the solution.

was determined graphically[13] to be 5×10^{-6} from the titration data.

Analytical Aspects of PAR

Cu-PAR Indicator in EDTA-Titrations.—Pease and Williams[2] have determined the stability constant of copper(II)-PAN chelate to be approximately 10^{16}. This value is considerably greater than that of PAR chelate, 5×10^{11}. Comparing the value for PAN chelate with that for copper(II)-EDTA chelate, 2×10^{18}, they have concluded "this is one reason that the copper(II)-PAN indicator may be successfully used in complexometric titrations of metals with EDTA".

According to Flaschka-Khalafallah's error-equation in visual end-point determination in chelatometric titration, Eq. 9[14], however, it may be concluded that Δp, the deviation of end-point (metal-combined indicator/free indicator=1/9) from equivalence-point, for the above-mentioned copper(II)-EDTA-PAN system is to be +0.04, i.e., the theoretical error is +4% when C_M and C_I were put as 10^{-3} and 10^{-6}, respectively.

$$\Delta p=(9rC_M-0.01C_I-1/9k)/C_M \qquad (9)$$

where C_M: total concentration of metal,
C_I: total concentration of indicator,
k: stability constant of metal-indicator complex,
K: stability constant of metal-complexan, and $r=k/K$.

The error obtained here is contrary to Cheng's observation[15]. To make the error below 0.5%, the stability constant of metal-indicator complex must be below 10^{15}. The value for Cu-PAR satisfies such a requirement. In regards to the relationship of the stability of copper(II)-indicator to that of copper(II)-EDTA, it may be concluded that PAR is a more accurate indicator than PAN provided that the stability constant of Cu-PAN is reliable. Nevertheless, for the practical applications as a titration indicator no remarkable difference between them, except the higher solubility of PAR in water, has yet been found out.

PAR as a Detection Reagent for Heavy Metals.—It must be mentioned that the high absorbancy in the visible region and the water-solubility of PAR chelates favor the detection of heavy metals and very high sensitivity can be achieved. For example, the identification limit of copper(II) in ordinary spot test was found to be 0.01 μg in 0.04 ml. test solution, i.e., limit of dilution is $1:2.5\times10^{-7}$, and that in resin spot test using a few grains of cation-exchange resin Dowex 50W-X8 in H-form as a collector of copper(II)-PAR chelate to be 0.0005 μg ($1:1.3\times10^{-8}$)[16].

Summary

Acid dissociation stages of analytical reagent 4-(2-pyridylazo)-resorcinol (PAR) and metal chelate formation of PAR were investigated by absorption measurements and pH-titrations. The first acid dissociation constant was determined as 1.48×10^{-6} ($pk_{a_1}=5.83$) and the second as 3.2×10^{-13} ($pk_{a_2}=12.5$) at 25°C. PAR forms 1:2 chelate with Fe(III), Co(II) and Ni(II), and forms 1:1 chelate with Cu(II), Zn(II), Cd(II), Hg(II) and Pb(II). The stability constant of copper(II)-PAR chelate was determined as 5×10^{11} at 25°C. Some analytical aspects of PAR were also discussed.

The author wishes to thank Dr. Eiiti Minami, Professor Emeritus, for his interst in this work and Mr. Kunihiko Mizumachi, Lecturer in Rikkio University, for his ardent encouragement and advice in the calculation of the chelate stability constant. He also thanks Dojin Pharmaceutical Laboratories for the gift of the sample of PAR.

Department of Chemistry
Faculty of Science
The University of Tokyo
Hongo, Tokyo

13) S. Glasstone, "An Introduction to Electrochemistry", Van Nostrand Co., New York (1956), p. 401.
14) H. Flaschka and S. Khalafallah, *Z. anal. Chem.*, **156**, 401 (1957).
15) K. L. Cheng, *Anal. Chem.*, **30**, 243 (1958).
16) M. Fujimoto and T. Iwamoto, unpublished results to be reported in detail together with the data for PAN.

A Ring-Chain Tautomerism in the Reaction Products of 3-Aminotropolone and Some Ethoxymethyleneacetates[1]

By Tetsuo Nozoe, Kozo Doi* and Kazuo Kitahara**

(Received April 11, 1960)

Slack and Attridge[2] reported the synthesis of a pyridotropolone (I) by application of the Gould-Jacobs' quinoline synthetic method[3] involving a process of pyrolysis of 5-(β, β-diethoxycarbonylvinylamino)tropolone (II), a condensation product of 5-aminotropolone and ethyl ethoxymethylenemalonate. This kind of synthetic method of pyridotropolones has also been applied to the other 5-aminotropolone derivatives[4] and 4-aminotropolone[5].

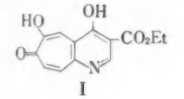

I

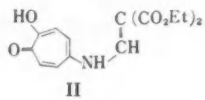

II

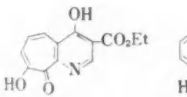

III

IV

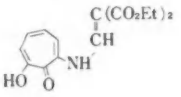

V

In the present series of experiment an attempt was made to prepare a pyridotropolone (III) by application of the similar synthetic method to 3-aminotropolone (IV). Although this objective was not accomplished unfortunately, other interesting observations were made, which are described in this paper.

When 3-aminotropolone (IV) and ethyl ethoxymethylenemalonate were heated, a yellow condensation product of m.p. 138°C was formed in a good yield. Its analytical data agreed with those calculated for the anticipated diethoxycarbonylvinylaminotropolone (V). The ultraviolet absorption spectrum (Fig. 1) of the condensation product seemed to be fairly reasonable for the expected structure V, if the tropolone nucleus and the α, β-unsaturated ester system were to interact through the intermediate nitrogen atom.

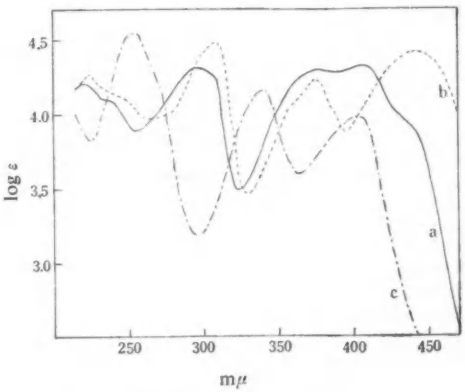

Fig. 1. Ultraviolet absorption spectra.
a) VIII in methanol
b) VIII in 0.01 N sodium hydroxide
c) IV in methanol

However, it has been found that pyrolysis of the above condensation product resulted in formation of not the anticipated pyridotropolone (III) but of another curious substances. Thus, on being heated at 250°C without a solvent, the condensation product afforded oxazolo[5 : 4-b]tropone* (VI) and ethyl malonate. The structure of the former VI was supported from its analytical values, determination of the molecular weight, and the close resemblance of its ultraviolet absorption curve (Fig. 2) to that of the known 2-methyloxazolo [5 : 4-b]-tropone[6] (VII). Ethyl malonate was identified as its dianilide[7].

The foregoing finding makes doubtful the assumption that the condensation product of the aminotropolone and ethoxymethylene-malonate may possess a structure like V. Virtually, the condensation product did not show any coloration with alcoholic ferric chloride and was inert to the action of diazomethane, the facts of which do not give

* Present address: The Chemical Research Institute of Non-Aqueous Solutions, Tohoku University, Sendai.
** Present address: The Research Laboratory, Tokyo Tanabe Pharmaceutical Co., Tokyo.

1) This work in part was presented at the Local Meeting of the Chemical Society of Japan, Yonezawa, June, 1956.
2) R. Slack and C. F. Attridge, *Chem. & Ind.*, **1952**, 471.
3) R. G. Gould and W. A. Jacobs, *J. Am. Chem. Soc.*, **61**, 2890 (1939).
4) K. Yamane, *J. Chem. Soc. Japan, Pure Chem. Sec. (Nippon Kagaku Zasshi)*, **80**, 75 (1959).
5) K. Doi, *Bull. Chem. Research Inst. Non-Aqueous Solns., Tohoku Univ.*, **9**, 19 (1959).
6) Y. Kitahara, *Science Repts. Tohoku Univ., Ser. I*, **40**, 83 (1956).
* Very recently the same authors have reported the another syntheses and some reactions of the oxazolotropone (VI). [This Bulletin, **34**, 312 (1961)].
7) M. Freund, *Ber.*, **17**, 134 (1884).

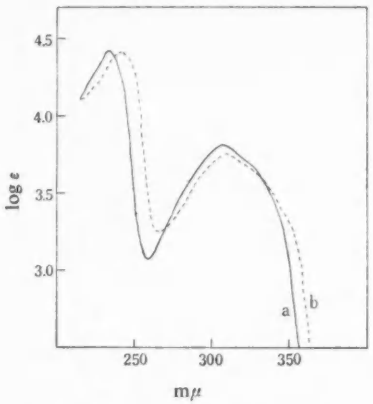

Fig. 2. Ultraviolet absorption spectra.
a) VI in methanol
b) VII in methanol

enough explanation for the condensation product to be a diethoxycarbonylvinylaminotropolone (V).

From the above facts it seems more reasonable to consider that the condensation product has a dihydro-oxazolotropone structure VIII.

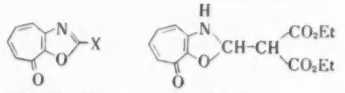

VI: X=H
VII: X=CH_3

VIII

The ultraviolet absorption spectrum of VIII in an alkaline solution shows a red-shift in comparison to that in neutral solution, and this suggests that VIII results in ring-opening to V or IX in an alkaline solution (Fig. 1).

With aid to isolate the chain-isomer V or IX, the condensation product VIII was treated with ethanolic potassium hydroxide, neutralized carefully with dilute mineral acid, and subsequently extracted with chloroform. The fresh extract showed clearly a red coloration with ferric chloride, but the vacuum evaporation of the solvent resulted not in formation of the expected chain-isomer but in recovering of the raw material.

In the condensation reaction of 3-aminotropolone and ethoxymethylenemalonate, it is considered that the anticipated diethoxycarbonylvinylaminotropolone (V) or its isomeric azomethine derivative IX produces at first and spontaneously isomerizes to the ring-isomer VIII. It seems to leave no room for doubt, at any rate, that the condensation product of the aminotropolone and ethoxymethylenemalonate exists in the ring-form of VIII in a neutral state and that it exists in the chain-form of V or IX in an alkaline medium. That the ultraviolet absorption of VIII in methanol solution has maxima in the comparatively longer wavelength regions indicates probably, though not any evidences have been obtained, that VIII is ring-opening to V or IX at least in the condition of the spectral measurement.

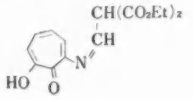

IX

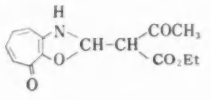

X

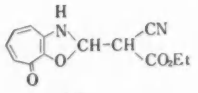

XI

On being heated with ethyl ethoxymethyleneacetoacetate and ethoxymethylenecyanoacetate in place of ethoxymethylenemalonate, 3-aminotropolone (IV) gave readily a condensation product, 2-(ω-acetyl-ω-ethoxy-carbonylmethyl)-2, 3-dihydroöxazolo[5 : 4-b]-tropone[8] (X) and 2-(ω-ethoxycarbonyl-ω-cyanomethyl)-2, 3-dihydroöxazolo[5 : 4-b]tropone (XI), respectively. The structures of these compounds were reasonably supported by the similarities of their ultraviolet absorptions (Fig. 3) to that of VIII and by the formation of the oxazolotropone (VI) by their pyrolysis.

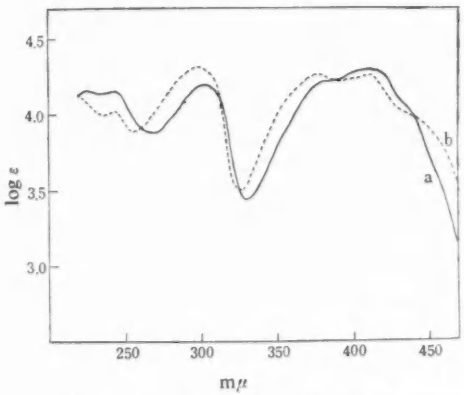

Fig. 3. Ultraviolet absorption spectra.
a) X in methanol
b) XI in methanol

The authors have found that the condensation products of *o*-aminophenol and the above three ethoxymethyleneacetates are also of the

8) Since the description of this work was completed, K. Yamane, *J. Chem. Soc. Japan, Pure Chem. Sec.* (*Nippon Kagaku Zasshi*), **81**, 509 (1960), have reported the synthesis of X by the same sequence.

cyclic structures of the corresponding benzoxazolines, the results of which will be described in the following paper.

Experimental

The ultraviolet absorptions were determined in methanol solution, unless otherwise stated, with a Beckman model DU spectrophotometer.

2-(ω, ω-Diethoxycarbonylmethyl)-2, 3-dihydrooxazolo[5 : 4-b]tropone (VIII).—A mixture of 3-aminotropolone (IV, 1.0 g.) and ethyl ethoxymethylenemalonate (1.7 g.) was heated on an oil bath at 130°C for 30 min. After being cooled at room temperature, the residual solid was recrystallized from ethanol to give the dihydroöxazolotropone (VIII) as yellow leaflets, m. p. 138°C, in nearly quantitative yield.

Found: C, 58.60; H, 5.67; N, 5.05. Calcd. for $C_{15}H_{17}O_6N$: C, 58.63; H, 5.58; N, 4.56%. λ_{max} mμ (log ε): in methanol, 220 (4.33), 295 (4.44), 381 (4.45), 408 (4.45); in 0.01 N sodium hydroxide, 225 (4.34), 310 (4.56), 377 (4.31), 442 (4.49).

The condensation product VIII did not show any coloration with alcoholic ferric chloride and remained inert to the action of diazomethane.

A mixture of VIII (0.3 g.), methanol (10 ml.), sodium hydroxide (0.4 g.) and water (5 ml.) was heated on a water bath at 50°C for 30 min. The orange solution so formed was cooled, neutralized cautiously with dilute hydrochloric acid, and then extracted with chloroform. The extract showed red coloration with ferric chloride, but its evaporation of the solvent under reduced pressure left only starting material VIII.

Oxazolo[5 : 4-b]tropone (VI).—VIII (1.45 g.) was placed in a Claisen flask of small capacity and heated on an oil bath at 230°C for 30 min. Colorless liquid (0.1 g.), which distilled out at 197~199°C and smelled like ethyl malonate, was collected. On being heated at 150°C with excess of aniline, it gave malonic dianilide, m. p. 275°C, undepressed on admixture with an authentic specimen[7]. The distilled residue, after extraction with warm benzene and subsequent evaporation of the solvent, crystallized from cyclohexane to give oxazolotropone (VI, 0.6 g.) as pale yellow prisms, m. p. 151~152°C.

Found: C, 65.60; H, 3.90; N, 9.40; mol. wt. (Rast), 146. Calcd. for $C_9H_5O_2N$: C, 65.30; H, 3.43; N, 9.52%; mol. wt., 147. λ_{max}^{MeOH} mμ (log ε): 235 (4.42), 305 (3.80).

2-(ω-Acetyl-ω-ethoxycarbonylmethyl)-2,3-dihydrooxazolo[5 : 4-b]tropone (X).—A mixture of the aminotropolone (0.7 g.) and ethyl ethoxymethyleneacetoacetate[9] (0.9 g.) was heated at 130°C for 30 min. and the residual solid was crystallized from ethanol to give dihydroöxazolotropone (X) as yellow prisms, m. p. 136°C, in a nearly quantitative yield.

Found: C, 60.69; H, 5.42; N, 5.34. Calcd. for $C_{13}H_{15}O_5N$: C, 60.64; H, 5.45; N, 5.05%. λ_{max}^{MeOH} mμ (log ε): 245 (4.30), 303 (4.35), 415 (4.45).

Pyrolysis of the product (X, 0.54 g.) at 250°C for 30 min. afforded the oxazolotropone (VI, 0.15 g.) and ethyl acetoacetate (50 mg.), identified as its anilide[10].

2-(ω-Ethoxycarbonyl-ω-cyanomethyl)-2,3-dihydrooxazolo[5 : 4-b]tropone (XI).—A mixture of the aminotropolone (140 mg.) and ethyl ethoxymethylenecyanoacetate[11] (170 mg.) was heated at 130°C for 30 min. and the residual solid was crystallized from methanol to give the condensation product (XI) as yellow needles, m. p. 182°C, in nearly quantitative yield.

Found: C, 60.06; H, 4.87; N, 10.86. Calcd. for $C_{13}H_{12}O_4N_2$: C, 59.99; H, 4.64; N, 10.77%. λ_{max}^{MeOH} mμ (log ε): 245 (4.11), 300 (4.41), 378 (4.35), 410 (4.35).

Pyrolysis of XI (0.54 g.) as above described afforded also the oxazolotropone (VI, 0.2 g.) and ethyl cyanoacetate (50 mg.), identified as its amide[12].

The authors express their gratitude to Messrs. S. Ohyama, K. Kato, A. Iwanaga and S. Azumi for microanalyses.

Department of Chemistry
Faculty of Science
Tohoku University
Katahira-cho, Sendai

9) L. Claisen, *Ann.*, **297**, 16 (1897).
10) L. Knorr, ibid., **236**, 75 (1886).
11) M. E. G. deBollemont, *Bull. soc. chim. France*, [3] 25, 20 (1901).
12) B. B. Corson, R. W. Scott and C. E. Vose, "Organic Syntheses," Coll. Vol. I, 173 (1932).

A Note on the Ring-Chain Tautomerism in the Reaction Products of o-Aminophenol and Some Ethoxymethyleneacetates

By Tetsuo Nozoe and Kozo Doi*

(Received August 25, 1960)

In the preceding paper[1], it was shown that the condensation reaction of 3-aminotropolone (I) and ethyl ethoxymethylenemalonate or some ethoxymethyleneacetates afforded, not the anticipated vinylaminotropolone (II), but its ring-tautomer, dihydro-oxazolotropone (III). This conclusion was drawn from the facts that the above condensation products did not show any coloration with ferric chloride test and were inert to the action of diazomethane, and that their pyrolyses resulted in a fragmentation to oxazolo[5:4-b]tropone (IV) and respective acetic acid derivatives. The authors stated, moreover, that the condensation products III probably exist in the chain-forms of II (or their possible azomethine type of isomers) in an alkaline medium.

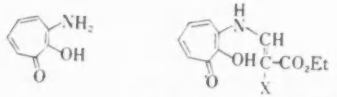

I

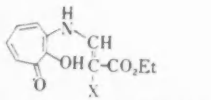

(X=CO_2Et, CN, $COCH_3$)
II

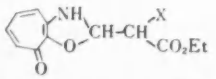

(X=CO_2Et, CN, $COCH_3$)
III

IV

There are not many systematic studies on the ring-chain tautomerism involving a nitrogen atom. Holly and Cope[2] elucidated this problem in the condensation products of *o*-aminobenzyl alcohol or *o*-hydroxybenzylamine with aldehydes or ketones through ultraviolet spectra and molecular refractions. Witkop and Beiler[3] also discussed this tautomerism in the arylidene Schiff bases derived from *o*-aminobenzyl alcohol through the spectral measurements.

From the above point of view, the present authors have felt interest in a possible ring-chain tautomerism between the condensation products of *o*-aminophenol, analogous to 3-aminotropolone (I), and ethoxymethyleneacetates. In this series of experiments, the authors have obtained information similar to that in the case of the aminotropolone; these will be described below in brief.

Condensations of anilines and ethoxymethyleneacetates have been often carried out for many syntheses of quinolines[4] and for identifications of anilines[5], but no report seems to have been made on the condensation of *o*-aminophenol and ethoxymethyleneacetates.

On being heated with ethyl ethoxymethylenemalonate, *o*-aminophenol afforded a condensation product of colorless crystals, m. p. 140~141°C, in a good yield. It did not show any coloration with alcoholic ferric chloride and was inert to the action of diazomethane. As might have been expected from the conclusions in the case of 3-aminotropolone (I), the above experimental results show that the condensation product is not the anticipated vinylaminophenol (V) or its possible isomer of the Schiff base type but is presumably 2-(ω,ω-diethoxycarbonylmethyl)benzoxazoline (VI). The reaction product, moreover, resulted in fission to form benzoxazole and ethyl malonate on pyrolysis, and this fact probably affords a more powerful proof for the assignment of structure VI to the condensation product.

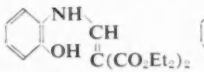

V

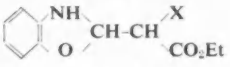

VI: X=CO_2Et
VII: X=$COCH_3$
VIII: X=CN

The ultraviolet absorption of the compound VI in an alkaline solution has maxima at longer wavelength region than in a neutral solution (Fig. 1). This fact indicates probably that the compound VI may exist in the chain-form of V (or its isomeric Schiff base) in an alkaline medium, the conclusion of which is analogous to that of the case in the condensation products of 3-aminotropolone[1].

The use of ethoxymethyleneacetoacetate and ethoxymethylenecyanoacetate, in place of

* Present address: The Chemical Research Institute of Non-Aqueous Solutions, Tohoku University, Sendai.

1) T. Nozoe, K. Doi and K. Kitahara, This Bulletin, **34**, 611 (1961).

2) F. W. Holly and A. C. Cope, *J. Am. Chem. Soc.*, **66**, 1875 (1944).

3) B. Witkop and T. W. Beiler, ibid., **76**, 5589 (1954).

4) R. H. Reitsma, *Chem. Revs.*, **43**, 43 (1948).

5) G. R. Lappin, *J. Chem. Educ.* **28**, 126 (1951).

ethoxymethylenemalonate, in this condensation reaction afforded the respective benzoxazoline VII and VIII in a good yield. These structures were presumed from the facts that their ultraviolet absorptions were similar to that of the compound VI and that their pyrolyses yielded benzoxazole.

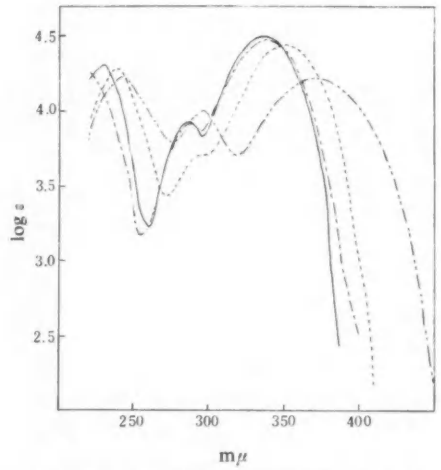

Fig. 1. Ultraviolet absorption spectra in methanol: curve —— VI; curve ---- VII; curve ------ VIII; curve ——— VI in 0.1 N sodium hydroxide solution.

Experimental

The ultraviolet absorptions were measured in methanol, unless otherwise stated, with a Beckman model DU spectrophotometer.

2-(ω, ω-Diethoxycarbonylmethyl)benzoxazoline (VI). — A mixture of *o*-aminophenol (1.1 g.) and ethyl ethoxymethylenemalonate (2.2 g.) was heated on an oil bath at 130°C for 30 min., and then the residual solid was recrystallized from ethanol to form the benzoxazoline VI as colorless prisms, m. p. 140~141°C, in a nearly quantitative yield.

Found: C, 60.11; H, 5.72; N, 5.04. Calcd. for $C_{14}H_{17}O_5N$: C, 60.20; H, 6.14; N, 5.02%.

λ_{max} mμ (log ε): in methanol, 230 (4.30), 286 (3.92), 335 (4.49); in 0.1 N sodium hydroxide, 243 (4.23), 295 (4.00), 370 (4.23).

Pyrolysis of the Compound VI. — The above benzoxazoline VI (5.6 g.) was placed in a Claisen flask with a small capacity and heated on an oil bath at 250°C. Vigorous boiling occurred and colorless liquid distilled out, which was separated into the two fractions by their boiling points at ordinary pressure: a) b. p. 175~185°C, 1.6 g., and b) b. p. 195~199°C, 2.7 g. Fraction (a) was distilled once again and the portion boiled at 180~182°C was collected. The cooled distillate crystallized to give benzoxazole (0.97 g.), alone and mixed m. p. 30~31°C[6]. The fraction (b), with an odor like that of ethyl malonate, afforded malonic dianilide, alone and mixed m. p. 275°C[7], on being heated with excess of aniline at 150°C.

2-(ω-Acetyl-ω-ethoxycarbonylmethyl)benzoxazoline (VII).—A mixture of *o*-aminophenol (1.1 g.) and ethyl ethoxymethyleneacetoacetate (1.9 g.) was heated at 130°C for 20 min. and the residual solid was recrystallized from methanol to give the benzoxazoline (VII) as colorless prisms, m. p. 146~147°C, in a good yield.

Found: C, 62.66; H, 5.98; N, 5.61. Calcd. for $C_{13}H_{15}O_4N$: C, 62.64; H, 6.07; N, 5.62%.

λ_{max}^{MeOH} mμ (log ε): 238 (4.28), 350 (4.45).

VII resulted in the formation of benzoxazole and ethyl acetoacetate, identified as its anilide[8], on pyrolysis at 250°C.

2-(ω-Ethoxycarbonyl-ω-cyanomethyl)benzoxazoline (VIII). — An equimolar mixture of *o*-aminophenol and ethyl ethoxymethylenecyanoacetate was heated at 100°C for 30 min. and the residual solid crystallized from methanol to form the benzoxazoline (VIII) as colorless needles, m. p. 191~192°C, in a good yield.

Found: C, 62.04; H, 5.04; N, 11.90. Calcd. for $C_{12}H_{13}O_3N_2$: C, 62.06; H, 5.21; N, 12.06%.

λ_{max}^{MeOH} mμ (log ε): 287 (3.91), 340 (4.47).

Pyrolysis of the compound VIII at 250°C gave also benzoxazole and ethyl cyanoacetate, identified as its amide[9].

The authors express their gratitude to Professor Yoshio Kitahara, the Chemical Research Institute of Non-Aqueous Solutions of Tohoku University, for his kind advice, to Mr. S. Ohyama and Miss Y. Endo for microanalyses.

Department of Chemistry
Faculty of Science
Tohoku University
Katahira-cho, Sendai

6) A. Ladenburg, *Ber.*, **10**, 1124 (1877).
7) M. Freund, ibid., **17**, 134 (1884).
8) L. Knorr, *Ann.*, **236**, 75 (1886).
9) B. B. Corson, R. W. Scott and C. E. Vose, "Organic Syntheses", Coll. Vol. I (1932), p. 173.

On the Structure of 2-Mercaptotropones

By Tetsuo Nozoe and Kazuo Matsui

(Received August 16, 1960)

2-Mercaptotropone (I) was synthesized in 1953 by Nozoe and his collaborators[1,2]. It comes as reddish orange crystals of m. p. 55°C and the compound was assumed to be present in two tautomeric forms, A and B. Alkylation

(A) (B)

and acylation of I afford only sulfur-substituted derivatives, while reaction with hydrazine gives 2-hydrazinotropone. Bromine easily effects an oxidation to 2,2'-ditroponyl disulfide. These facts suggest a structure A of this compound and this was named 2-mercaptotropone. But further examination on its physicochemical properties as well as those of its homologs suggested that this should rather be a 2-hydroxyl derivative of tropothione, structure B, and details of this work are described herein.

Physical measurements were carried out with 4-isopropyl-2-mercaptotropone (II), 6-isopropyl-2-mercaptotropone (III), 2-methylthiotropone (IV), 4-isopropyl-2-methylthiotropone (V), and 6-isopropyl-2-methylthiotropone (VI)[3], besides the 2-mercaptotropone (I).

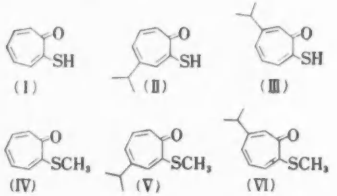

Ultraviolet Absorption Spectra[4].—The ultraviolet absorption spectra of I, II and III are indicated in Fig. 1 and those of IV, V and VI in Fig. 2. As will be seen from these, the spectral curve of 2-mercaptotropones in Fig. 1 shows a fair shift to the longer wavelength side than that of 2-methylthiotropones in Fig. 2, indicating that there is an essential difference in the structure of these two kinds of compounds. This relationship is the same as

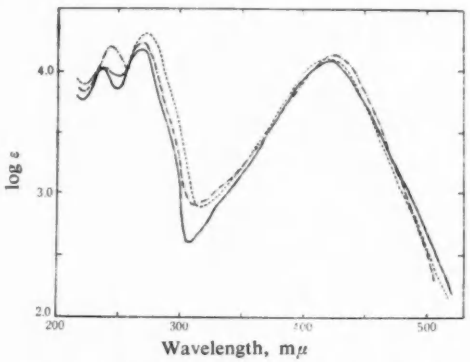

Fig. 1. Ultraviolet absorption spectra in cyclohexane.
——— I ------ II —·—· III

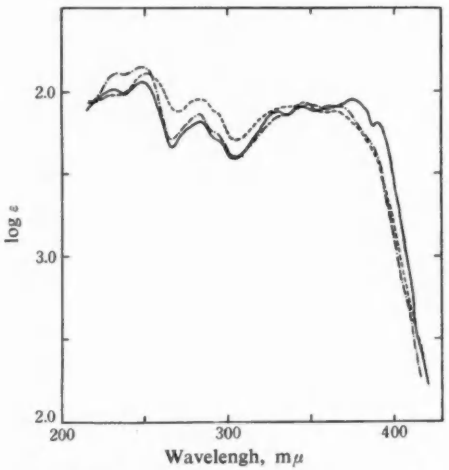

Fig. 2. Ultraviolet absorption spectra in cyclohexane.
——— IV ------ V —·—· VI

that between 2-thiopyridone and its *S*-methyl derivative[5], and if the B type of the structure is assigned to 2-mercaptotropones, the difference in ultraviolet absorptions could be explained as a bathochromic shift due to the C=S group.

1) T. Nozoe, M. Sato and K. Matsui, *Proc. Japan Acad.*, **29**, 22 (1953).
2) Idem, *Sci. Repts. Tohoku Univ., I*, **37**, 211 (1953).
3) K. Matsui, This Bulletin, **33**, 1448 (1960).
4) Measured by a Beckman Model DU spectrophotometer.
5) A. Albert and B. Barlin, "Current Trends in Heterocyclic Chemistry", Butterworths Scientific Publications, London (1958), p. 51.

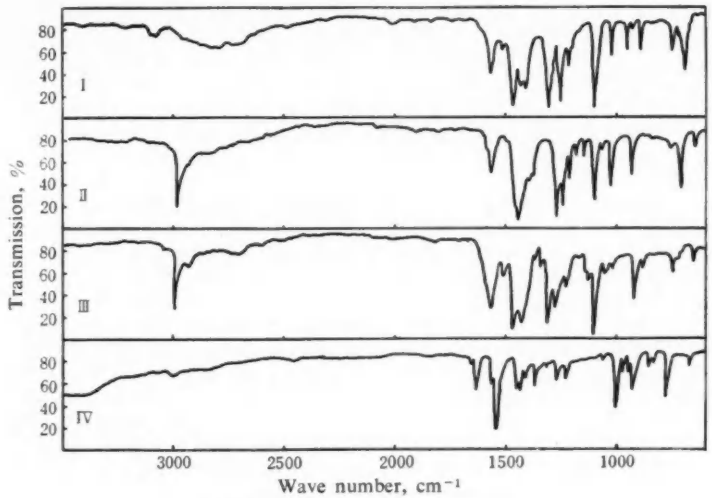

Fig. 3. Infrared absorption spectra.
I in 0.5% CCl_4 soln. II in 0.5% CCl_4 soln.
III in 0.5% CCl_4 soln. IV in KBr-pellet

Infrared Absorption Spectra[2,6]. — Infrared absorption spectra of I, II, III and IV are shown in Fig 3. The absoprtion of IV in the double-bond region is similar to those observed in tropone, 2-methoxytropone, and 2-halotropone[7], but the spectra of I, II and III are quite different from those seen in tropones and tropolones in general. Furthermore, examination of the spectra of I in the 3000 cm^{-1} region indicates the presence of a broad and weak absorption in the region of 3000～2600 cm^{-1}. It is rather appropriate to consider that I takes the structure B and the ν_{OH} absorption has been shifted to lower wave-numbers by chelation, than a shift of ν_{SH} absorption to higher wave-numbers side from the usual absorption at 2600～2550 cm^{-1}.

The absence of a strong absorption assignable to the C=O group in a higher wave-numbers side than 1500 cm^{-1} in the double-bond region also agrees with the structure B and considering Mecke's law[8] the absorption at 1100 cm^{-1} is assumed to correspond to $\nu_{C=S}$.

The same thing may be said of II and III, and 2-mercaptotropones are therefore assumed to take the B of the type structure from infrared absorption spectral examinations.

Nuclear Magnetic Resonance Spectra[9]. — The NMR spectra of I, II, III and IV were measured in carbon tetrachloride solution at 40 Mc./sec. at room temperature, with cyclohexane as the internal reference. The results are indicated in Fig. 4. It should be noted here that in I, II and III, the resonance line of the ring proton appears as two signals, at 280 and 230 c. p. s. Since the ring proton appears as one signal at ca. 240 c. p. s. in tropone and tropolone[10], the small signal at 280 c. p. s. in the considerably lower magnetic field side should be assigned to the ring proton

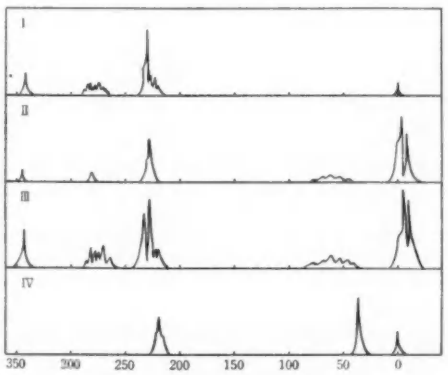

Fig. 4. NMR spectra of I, II, III and IV.

6) Measured by a Perkin-Elmer Model 21 double beam spectrophotometer.
7) S. Kinumaki, K. Aida and Y. Ikegami, *Sci. Repts. Reseach Inst. Tohoku Univ.*, A-8, 264 (1956).
8) R. Mecke, R. Mecke and A. Lüttringhaus, *Chem. Ber.*, **90**, 975 (1957).
9) Measured by a Varian V 4300 B spectrometer.
10) D. Ginsberg, "Chemistry of Non-benzenoid Aromatic Compounds", Interscience Publishers, New York (1959), p. 380.

next to sulfur group. Further, the fact that this is absent in IV suggests that, I, II and III take the B type of the structure, and the signal of proton attached to the carbon next to the C=S group appears in the lower magnetic field side because is it in a different magnetic surrounding from other protons.

The resonance line at ca. 340 c. p. s. in I, II, and III may be assignable to SH group, but the OH line in tropolone appears at ca. 280 c. p. s.[10] This is in reverse of the general observation that the resonance line of SH compounds appears in a higher magnetic field than the corresponding OH compounds[11,12]. This fact also denies the A type of the structure.

pK_a value.—The fact that pK_a value of I (5.89)[13] is smaller than that of tropolone (6.92)[14], is in agreement with the general observation that thiophenols show smaller pK_a value than the corresponding phenols. The difference of I and tropolone is, however, only 1 pK_a unit, and this rather small difference compared with that, ca. 3 pK_a unit[15,16], between thiophenols and phenols might be explained by the assignment of the structure B rather than A to I as follows.

2-Thiopyridones[17] show smaller pK_a values than the corresponding 2-pyridones[18] by ca. 2 pK_a unit, which is presumably due to the difference in inductive and mesomeric effect between the C=S and the C=O group. Similarly, it might be expected that in the case of I, structure B, and the tropolone, the C=S group in I should activate the OH group, more than the C=O group in tropolone does. But spacious and electron-rich sulfur atom induced by these electronic effects of the C=S group, conversely tend to control the liberation of proton in the OH group located close by*, more than does the oxygen atom in tropolone.

As a result of these opposing effects of the C=S group in I, the small pK_a difference between I and tropolone is understandable without inconsistency.

Solubility. — Mercaptans in general are practically insoluble in water, but the solubility of I in water is 0.846 g./l.[13] Such a large degree of solubility also supports the structure B.

The results of the foregoing ultraviolet, infrared, and NMR spectral measurements, pK_a value, and solubility, all indicate the appropriateness of the B type of the structure for 2-mercaptotropones. It has therefore been clarified that, although the compounds behave as A type of the structure during various reactions, they take the B type of the structure in a static state.

Consequently, the conventional structure A for 2-mercaptotropone (I) should be corrected and the structure B, i. e. 2-hydroxytropothione, is forwarded.

The authors are grateful to Tanabe Seiyaku Co., Ltd. for allowing one (Matsui) of the authors to take part in this research at Sendai. The authors' deepest gratitudes are expressed to Dr. T. Isobe and his colleagues, Chemical Institute of Non-Aqueous Solutions, Tohoku University, for their technical cooperation and keen discussion on NMR spectra, and to Mr. Y. Ikegami, the same Institute, for his helpful advices in infrared analyses.

Department of Chemistry
Faculty of Science
Tohoku University
Katahira-cho, Sendai

11) B. P. Dailey and J. N. Shoolery, *J. Am. Chem. Soc.*, **77**, 3977 (1955).
12) L. H. Meyer, A. Saika and H. S. Gutowsky, ibid., **75**, 4567 (1953).
13) N. Yui, *Sci. Repts. Tohoku Univ., I*, **40**, 114 (1956).
14) Idem., ibid., **40**, 50 (1956).
15) G. Schwarzenbach and H. Egli, *Helv. Chim. Acta*, **17**, 1176 (1934).
16) W. H. Fletcher, *J. Am. Chem. Soc.*, **75**, 3784 (1953).
17) R. A. Jones and A. R. Katritzky, *J. Chem. Soc.*, **1958**, 3610.
18) A. Albert and J. N. Phillips, ibid., **1956**, 1294.

* It should be noted here that tropone and tropolone derivatives with the SH group are extremely unstable and undergo dehydrogenative condensation to yield disulfides, unless the SH group is situated at the carbon next to the C=O group and a hydrogen bond between these groups is formed[21].

Reaction of Troponoids and Organometallic Compounds. VI. Reaction of Tropone with Grignard Reagents***

By Tetsuo NOZOE, Toshio MUKAI and Takahiro TEZUKA

(Received August 29, 1960)

It has been known that tropolone methyl ethers undergo reaction with Grignard reagents to give tropone derivatives substituted in the 2-position[1,2]. Considering that tropone, the parent compound of tropolone, possesses some degree of ketonic properties[3], its Grignard reaction is considered to be of interest, but no report has been published on this subject. The present paper describes the reaction of methyl-, isopropyl- and phenylmagnesium halide on tropone and the preparation of tropone derivatives via the products thereby formed.

Applications of two molar equivalents of phenylmagnesium bromide on tropone (I) and subsequent decomposition of the magnesium complex with dilute hydrochloric acid gives an oil II, $C_{13}H_{12}O$; 2, 4-dinitrophenylhydrazone, m. p. 135°C, maleic anhydride adduct, m. p. 147°C. Catalytic reduction of II results in absorption of 2 molar equivalents of hydrogen to form 2-phenylcycloheptanone. The NMR spectrum of II at 40 Mc. (Fig. 1)*** exhibits three sorts of signals due to phenyl (a), vinyl (b) and methylene (c) protons respectively. These observations indicate that II is one of the 2-phenylcycloheptadienone such as A, B or C, formed by ketonization of enolic intermediate III which was produced by 1, 8-addition of the Grignard reagent to the conjugated system in I.

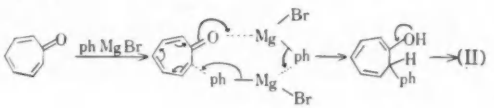

(I) (III)

As in the reaction of Grignard reagents with tropolone methyl ethers, two molar equivalents of the reagent are also necessary in this reaction in order to obtain II in fair yield. This implies that the reaction proceeds through a complex formation between tropone and two molecules of the Grignard reagent, analogous to the cyclic intermediate suggested by Swain and others[4].

The infrared spectrum of II shows a carbonyl band at 1660 cm^{-1} characteristic of the conjugated dienone system[5], implying that II is represented by B or C. The maxima in the ultraviolet spectrum of II, 235 and 315 mμ (log ε: 3.98 and 3.85), also supports this view, and moreover, the bathochromic shift of 23 and 13 mμ compared with cyclohepta-2, 4-dien-1-one[6], 292 mμ (log ε: 3.97) and eucarvone[7], 302 mμ (log ε: 3.82) respectively, indicates that II can be best represented by B rather than C.

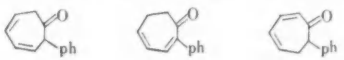

(A) (B) (C)

II absorbs one molar equivalent of bromine in acetic acid to form an oily dibromide e. g. IV, which lacks the intensive maxima above 220 mμ in the ultraviolet spectrum. When IV is heated under reduced pressure, hydrogen bromide is liberated to form the hydrobromide of 2-phenyltropone, m. p. 145~147°C (30%), from which 2-phenyltropone (V)[1] is formed.

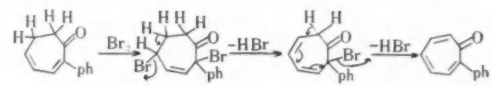

(II) (IV) (V)

Oxidation of II with selenium dioxide or chromium trioxide gives also 2-phenyltropone in 75 and 10% yield respectively.

In an earlier work[8] in this laboratory, it

* Part V: K. Kikuchi, This Bulletin 33, 628 (1960). This report is also Part VI of Tropones.

** Presented before the Local Meeting of the Chemical Society of Japan, Sendai, December, 1958.

1) (a) T. Nozoe, T. Mukai and J. Minegishi, *Proc. Japan Acad.*, 27, 419 (1951); (b) T. Nozoe, T. Mukai and I. Murata, ibid., 28, 142 (1952); (c) T. Nozoe, T. Mukai, J. Minegishi and T. Fujisawa, *Sci. Repts. Tohoku Univ., I*, 37, 388 (1953).

2) (a) K. Kikuchi, *J. Chem. Soc. Japan, Pure Chem. Sec. (Nippon Kagaku Zasshi)*, 77, 1439 (1956); (b) K. Kikuchi, ibid., 81, 505 (1960); (c) K. Kikuchi, This Bulletin, 33, 628 (1960).

3) T. Nozoe, T. Mukai and K. Takase, *Sci. Repts. Tohoku Univ., I*, 39, 164 (1956).

*** All NMR spectra were measured with a Varian V-4300B spectrometer.

4) C. G. Swain and H. B. Boyles, *J. Am. Chem. Soc.*, 73, 871 (1951).

5) Eucarvon shows carbonyl band at 1661 cm^{-1}.

6) E. E. van Tamelen and G. T. H. Hildahl, *J. Am. Chem. Soc.*, 75, 5451 (1953).

7) E. J. Corey and H. J. Burke, ibid., 76, 5257 (1954).

8) (a) T. Nozoe, T. Mukai, M. Ishii and Y. Ikegami, unpublished work; (b) T. Mukai, This Bulletin, 31, 852 (1958).

had been shown that the reaction of phenylmagnesium bromide on 2-phenyltropone afforded colorless plates (VII) $C_{19}H_{16}O$, m. p. 87°C, accompanied by 2,7-diphenyltropone (VIII), both of which gave 2,7-diphenylcycloheptanone on catalytic hydrogenation, but the structure of compound VII remained unestablished. It is likely now that VII has the structure as shown below.

(VII) (VIII)

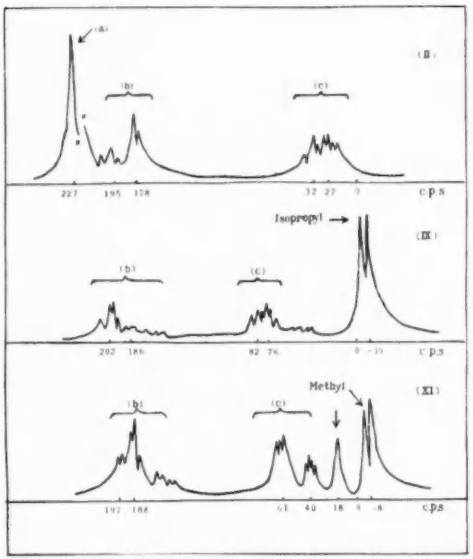

Fig. 1. NMR spectra of 2-phenyl-(II), 2-isopropyl-(IX) and 2-methylcycloheptadienone-(XI) at 40 Mc., relative to cyclohexane as inner reference.

The reaction of tropone with isopropylmagnesium bromide affords a liquid (IX), $C_{10}H_{14}O$, λ_{max} 302 mμ (log ε: 3.31), which absorbs 2 molar equivalents of hydrogen on catalytic hydrogenation to give 2-isopropylcycloheptanone. The NMR spectrum of IX (Fig. 1) also suggests the cycloheptadienone type. Since the infrared spectrum indicates two carbonyl absorption bands at 1705 and 1658 cm^{-1}, it is assumed that IX is a mixture of IXa and IXb (R=*i*-C_3H_7). From the comparison of the absorption intensity in the ultraviolet spectrum of IX at 302 mμ with that of eucarvon (mentioned above), the proportion of IXa to IXb is assumed to be about 2 to 1.

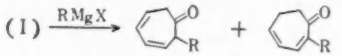

(IXa) R=*i*-C_3H_7 (IXb) R=*i*-C_3H_7
(XIa) R=CH_3 (XIb) R=CH_3

IX adds one molar equivalent of bromine, but the dibromide thereby formed easily loses hydrogen bromide during removal of the solvent to afford an oily product (X) which gives the known 2-amino-7-isopyropyltropone[9] on being treated with hydrazine hydrate, indicating that X is 2-isopropyltropone.

Although the ultraviolet spectrum and the infrared diagram of X are analogous to those of known 2-methyl- and 2-ethyltropone[10], X does not form a picrate, an oxime or a 2,4-dinitrophenylhydrazone by the usual process and this may be due to the steric hindrance of the isopropyl group.

Similarly, the reaction of tropone with methylmagnesium iodide gives an oil (XI), λ_{max} 235 and 298 mμ (log ε: 3.54 and 3.53), whose catalytic hydrogenation produces 2-methylcycloheptanone. Treatment of XI with bromine easily effects bromination-dehydrobromination to give the known 2-methyltropone.

The infrared spectrum of XI exhibits carbonyl bands at 1710 and 1665 cm^{-1} as in the case of IX, and XI is considered to be a mixture of XIa and XIb (R=CH_3). This is also supported by its NMR spectrum (Fig. 1) in which two kinds of signals due to the methyl group appear at +18 c. p. s. (singlet) and −8 c. p. s. (doublet). The former is assumed to come from the methyl group in XIb, whereas the latter is due to the methyl group in XIa. Moreover, the calculation of the areas of two signals due to methyl groups in NMR spectrum and the intensity in the ultraviolet spectrum of XI shows that XIa is more prominent than XIb in that mixture.

Both IX and XI are easily dehydrogenated by the treatment with selenium dioxide to give 2-isopropyl- or 2-methyltropone in 55 and 60% yields, respectively.

It follows, therefore, that the Grignard reaction of tropone is also useful as a general method for the preparation of tropone derivatives.

After the present work had been completed, it was learned very recently that Closs and Closs[11] had obtained a compound XII (R=H or CH_3) from the reaction of methyllithium on tropone or 2-methyltropone. They also

9) T. Nozoe et al., unpublished work.
10) T. Mukai, *J. Chem. Soc. Japan, Pure Chem. Sec.* (*Nippon Kagaku Zasshi*), **79**, 1547 (1958).
11) G. L. Closs and L. E. Closs, Abstracts of Papers, National Meeting of the American Chemical Society, Cleveland, April, 1960.

(XII)

obtained similar compounds by the application of methylene chloride and methyllithium on phenol or cresol, but details are not available. Our results in which the conjugated dienones with the double bond in position different from that in XII (R=H) has been obtained, would be due to a migration of the double bond during the decomposition of the magnesium complex with dilute hydrochloric acid.

Experimental[12]

2-Phenylcycloheptadienone (II).—A solution of 3.0 g. of tropone in 40 ml. of absolute ether was added dropwise at 0°C with stirring to 2.2 mol. equiv. of Grignard reagent prepared from 10.3 g. of bromobenzene and 1.5 g. of magnesium in 40 ml. of absolute ether. After additional stirring for half an hour, the reaction mixture was decomposed with 1 N hydrochloric acid, extracted with ether, washed with water and dried over anhydrous sodium sulfate. Removal of the solvent afforded 7.5 g. of crude oil, whose distillation in vacuo gave 4.35 g. (84%) of pale yellow oil (II), b. p. 139～145°C (3 mmHg), n_D^{16} 1.4890, λ_{max}^{MeOH} 235 mμ (log ε: 3.98), 315 mμ (log ε: 3.85). For analysis, this oil was redistilled to give b. p. 143～145°C (3 mmHg).

Found: C, 84.31; H, 6.38. Calcd. for $C_{13}H_{12}O$: C, 84.75; H, 6.57%.

Application of 1.0 and 1.5 molar equivalents of the Grignard reagent on tropone afforded II in 30% and 75% yields with the recovery of tropone (35 and 3% respectively).

2,4-Dinitrophenylhydrazone, m. p. 134～135°C, λ_{max}^{MeOH} 375 mμ (log ε: 4.15).

Found: C, 62.54; H, 4.31; N, 15.08. Calcd. for $C_{19}H_{16}O_2N_4$: C, 62.63; H, 4.43; N, 15.38%.

Catalytic Reduction of 2-Phenylcycloheptadienone (II).—A solution of 300 mg. of II in 4.5 ml. of ethanol was hydrogenated at 1 atm. and 18°C with prereduced palladium-carbon catalyst. After 125 min., 87 ml. (2.4 mol. equiv.) of hydrogen was absorbed. Removal of the catalyst and evaporation of the solvent afforded 300 mg. of an oil, which gave semicarbazone m. p. 150～151.5°C, undepressed on admixture with an authentic sample of 2-phenylcycloheptanone semicarbazone[13].

Bromination of 2-Phenylcycloheptadienone (II).—A solution of bromine in acetic acid (88 mg./0.5 ml.) was added dropwise at 0°C to a solution of 100 mg. of II in 5 ml. of acetic acid, by which 1.2 mol. equiv. of bromine was absorbed. After stirring for one hour, the reaction mixture was diluted with water, extracted with benzene, washed with water and dried over anhydrous sodium sulfate. Removal of the solvent at room temperature under reduced pressure gave 200 mg. of brown oil, a chromatographic purification of which on alumina afforded dibromide IV as a viscous oil.

Found: C, 44.76; H, 3.34. Calcd. for $C_{13}H_{12}OBr_2$: C, 45.36; H, 3.51%.

2-Phenyltropone.—a) The dibromide (200 mg.) obtained above was heated at 80°C under reduced pressure (20 mmHg) overnight. The resultant residue was extracted with benzene, washed with water and dried. Evaporation of the solvent and chromatographic purification on alumina yielded 2-phenyltropone (70 mg.) as a reddish oil. On treatment of this oil (70 mg.) with hydrazine hydrate, crystals (20 mg.), m. p. 200～202°C were obtained. Recrystallization from benzene gave yellow needles, m. p. 203～204°C, identical with authentic 2-amino-7-phenyltropone[1].

b) II (1 g.) was brominated in acetic acid and the reaction mixture was treated as described above. On removal of the solvent at 80°C, 400 mg. of 2-phenyl tropone as colorless needles, m. p. 145～147°C*, which showed almost identical ultraviolet absorption maximum with that of 2-phenyltropone. This hydrobromide (200 mg.) was heated at 100°C under reduced pressure (20 mmHg) for 2 hr. and subsequently sublimed to afford 90 mg. of yellow needles, m. p. 82～83°C, undepressed on admixture with authentic 2-phenyltropone.

Dehydrogenation of II with Selenium Dioxide.—A solution of 200 mg. of II in 2 ml. of dioxane was heated under reflux with selenium dioxide (140 mg.) for 7 hr. The deposited selenium (30 mg.) was filtered off and the filtrate was concentrated. The resultant residue was dissolved in benzene, washed successively with saturated sodium bicarbonate solution and water, and dried. On removal of the solvent, 150 mg. (75%) of crystals, m. p. 70～75°C was obtained. Recrystallization from benzene and chromatographic purification on alumina gave yellow prisms, m. p. 83～84°C, identical with 2-phenyltropone.

Oxidation of II with Chromium Trioxide.—A solution of 1.9 g. of II in 6 ml. of pyridine was added to pyridine-chromic acid complex (1 g. CrO_3/10 ml. pyridine) at 15～20°C. After stirring for 10 hr. and standing for another 12 hr. at room temperature, the reaction mixture was treated with methanol to decompose excess of chromium trioxide, neutralized with concentrated hydrochloric acid, extracted with chloroform, washed with water and dried. Removal of the solvent and subsequent purification on alumina gave 70 mg. of an oil. Treatment of this oil (70 mg.) with hydrazine hydrate by usual way afforded 20 mg. of crystals, m. p. 198～202°C. Recrystallization from benzene gave yellow prisms, m. p. 206～207°C, identical with 2-amino-7-phenyltropone[1].

Diels-Alder Reaction of II.—A mixture of 200 mg. of II and 130 mg. (1.2 mol. equiv.) of maleic anhydride in 2 ml. of dry benzene was heated under reflux for 11 hr. On removal of the solvent 200 mg. of an oil was obtained which on standing for 10 days, gave 70 mg. of crystals, m. p. 145～170°C. Recrystallization from benzene gave white needles, m. p. 186～187°C.

Found: C, 71.88; H, 4.53. Calcd. for $C_{17}H_{14}O_4$: C, 70.33; H, 4.86%. λ_{max}^{MeOH} 295 mμ (log ε: 2.43).

12) All the melting points are not crroected.

* On exposure in the air it decomposed to an oil.

2-Isopropylcycloheptadienone (IX).—A solution of 5 g. of tropone in 50 ml. of absolute ether was added at 0°C to a 2.2 mol. equiv. of Grignard reagent prepared from 13.36 g. of isopropyl bromide and 2.50 g. of magnesium in 40 ml. of absolute ether. The reaction mixture was treated as in the case of II. The resultant residue was distilled in vacuo to give three fractions: i) b. p. below 70°C (4 mmHg) n_D^{15} 1.4870, 0.5 g.; ii) b. p. 70~75°C (4 mmHg), n_D^{15} 1.4850, 4.4 g. (62%); iii) b. p. above 75°C (4 mmHg), small amount.

Found [for fraction (ii)]: C, 79.51; H, 9.05. Calcd. for $C_{10}H_{14}O$: C, 79.95; H, 9.39%.

Hydrogenation of IX.—2-Isopropylcycloheptadienone (IX) (300 mg.) was hydrogenated in 5 ml. of acetic acid at 1 atm. and 18°C with 10 mg. of prereduced platinum oxide catalyst. Ninty-five milliliters of hydrogen (2.0 mol. equv.) was taken up within 80 min. After removal of the catalyst, the mother liquor was diluted with water, extracted with petroleum ether, washed and dried. On evaporation of the solvent, 250 mg. of an oil was remained, which afforded semicarbazone, m. p. 170.5~171.5°C, undepressed on admixture with that of 2-isopropylcycloheptanone[13].

Formation of 2-Isopropyltropone (X) by Bromination of IX.—Bromine in carbon tetrachloride was added to a solution of 650 mg. of IX in 6.5 ml. of carbon tetrachloride by which 1.0 mol. equiv. bromine was absorbed. The reaction mixture was treated as in the case of II. Residual oil thus obtained was purified through its hydrochloride and then chromatographed on alumina, by which 160 mg. of brown oil was obtained. An ethanolic solution of this oil (160 mg.) was heated under reflux with 0.23 ml. of 80% hydrazine hydrate for 1 hr. Removal of the solvent followed by chromatography on alumina gave 100 mg. of crystals m. p. 40~50°C, λ_{max}^{MeOH} 242, 336, 399 mμ, identical with that of 2-amino-7-isopropyltropone[9]. Hydrolysis of this crystals (100 mg.) with potassium hydroxide in aqueous ethanol afforded 60 mg. of an oil, having identical R_f value with that of α-thujaplicin.

Formation of 2-Isopropyltropone (X) by Dehydrogenation of IX with Selenium Dioxide.—A solution of 1 g. of IX in 10 ml. of dioxane was heated under reflux with 440 mg. (1.2 mol. equiv.) of selenium dioxide for 1 hr. The reaction mixture was filtered to remove deposited selenium (150 mg.) which contains tarry matter and the mother liquor was concentrated. The resultant residue was dissolved in ether, washed with dilute silver nitrate solution and water, and dried. Removal of the solvent and subsequent distillation gave 550 mg. of an oil, b. p. ca. 80°C (2 mmHg), λ_{max}^{MeOH} 233 mμ (log ε: 4.37), 312 mμ (log ε: 3.90). Heating of this oil (100 mg.) with 80% hydrazine hydrate (0.25 ml.) for 2 hr. under reflux afforded 90 mg. of yellow crystals, m. p. 40~60°C. Recrystallization from a mixture of benzene and petroleum ether gave yellow prisms, m. p. 88°C, undepressed on admixture with 2-amino-7-isopropyltropone[9].

13) S. Seto, *Sci. Repts. Tohoku Univ.*, I, 37, 292 (1953).

2-Methylcycloheptadienone (XI).—A solution of 2.4 g. of tropone in 30 ml. of absolute ether was added to 2.2 mol. equiv. of Grignard reagent prepared from 7.5 g. of methyl iodide and 1.2 g. of magnesium, at 0°C and the reaction mixture was treated as in the case of II. On evaporation of the solvent, 1.7 g. of pale yellow oil was obtained. Distillation in vacuo gave three fractions: i) b. p. below 60°C (2 mmHg), trace; ii) b. p. 60~65°C (2 mmHg), 1.0 g. (38%), n_D^{14} 1.480; iii) b. p. above 65°C (2 mmHg), trace.

Found [for fraction (ii)]: C, 77.42; H, 8.04. Calcd. for $C_8H_{10}O$: C, 78.65; H, 8.25%.

Hydrogenation of XI.—XI (500 mg.) in 10 ml. of acetic acid was hydrogenated at 1 atm. and 18°C with prereduced platinum oxide. After 100 min., 122 ml. (2.2 mol. equiv.) of hydrogen was absorbed. The catalyst was removed by filtration and the filtrate was diluted with water, extracted with petroleum ether, washed and dried. Removal of the solvent gave a volatile oil, which gave semicarbazone, m. p. 118°C on allowing to stand with semicarbazide for 20 days at room temperature, undepressed 2-methylcycloheptanone[14].

2-Methyltropone by Bromination of XI.—To a solution of 500 mg. of XI in 10 ml. of carbon tetrachloride was added with stirring a solution of bromine into carbon tetrachloride, by which 1.4 mol. equiv. of bromine was easily absorbed. Treatment of the reaction mixture as in the case of IX afforded 500 mg. (60%) of crystals, decomp. 135°C, λ_{max}^{MeOH} 232, 315 mμ, similar with that of 2-methyltropone hydrochloride. Neutralization of these crystals (100 mg.) with saturated sodium bicarbonate solution gave an oil, which afforded picrate, m. p. 126~127°C (60 mg.). Recrystallization from ethanol gave yellow crystals, m. p. 127~128°C, undepressed on admixture with those of 2-methyltropone[10].

Formation of 2-Methyltropone by Dehydrogenation of XI with Selenium Dioxide.—A solution of 300 mg. of XI in 3 ml. of dioxane was refluxed with 163 mg. (1.2 mol. equiv.) of selenium dioxide for half an hour. Deposited selenium contaminated with tar (80 mg.) was filtered off and similar treatment of the mother liquor as in the case of X afforded 180 mg. of an oil (60%) which gave picrate m. p. 127~128°C, identical with that of 2-methyltropone[10].

The authors thank to Professor T. Isobe for NMR spectra measurement and his kind discussions thereof. Expenses for the present series of experiments were defrayed by a Grant in Aid for Scientific Research from the Ministry of Education.

Department of Chemistry
Faculty of Science
Tohoku University
Katahira-cho, Sendai

14) D. N. Adamson and J. Kenner, *J. Chem. Soc.*, 1939, 181.

Diels-Alder Reaction of Troponoids. II[1]*. Adducts of Halotropones and Maleic Anhydride*

By Tetsuo Nozoe and Yasuo Toyooka

(Received on October 17, 1960)

The Diels-Alder reaction of tropone and maleic anhydride has been reported from our laboratory[1]. Tropone gives a normal endo-cis adduct I more readily than tropolone, presumably owing to the property of enhanced unsaturation.

In the present paper the authors wish to report the Diels-Alder reactions of halotropones. It was found that 2-chloro- and 2-bromotropone give normal adducts in good yield, whilst 2, 7-dibromo- and 2, 4, 7-tribromotropone fail to give the adducts resulting in the complete recovery of the materials started with.

Results

The heating of 2-chlorotropone or 2-bromotropone with two molar equivalents of maleic anhydride in dry xylene effected reaction, affording the adduct II or III in a yield of around 65~85%. The ultraviolet absorption spectra of II and III are shown in Fig. 1.

Catalytic hydrogenation of the adduct, II or III, in ethyl acetate with palladium charcoal as a catalyst, results in the absorption of three molar equivalents of hydrogen respectively both forming the same halogen-free tetrahydro compound IV, which showed no depression of the melting point on admixture with each other and with tetrahydro compound obtained from I. These facts not only offer an important clue to the structure of II and III but also prove the configurations of II and III being the same as I. Actually the infrared spectrum of IV obtained from II or III coincides perfectly with the one of tetrahydro compound obtained from I.

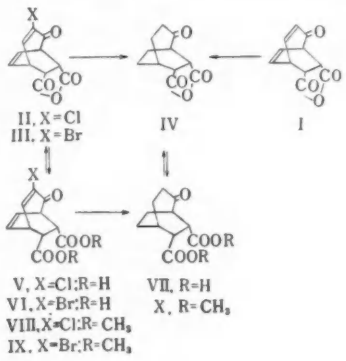

Treatment of the adduct II or III with hot water results in facile hydrolysis and dibasic acid V or VI is formed. The acids V and VI are known to be dibasic from their analytical value and titration. The decomposition points of V and VI are the same as the melting points of II and III respectively. These are considered to be due to the facial dehydrations of V and VI. Actually the heating of V and VI at 200~220°C under a reduced pressure result in the formations of II and III and such facts naturally indicate that the two carboxyls are in cis configuration.

The halogen-free tetrahydro compound IV is also easily hydrolyzed and forms a dibasic acid VII which undergoes facile dehydration as in the case of V and VI. Catalytic hydrogenation of unsaturated dibasic acids V or VI in water, with palladium charcoal as a catalyst, results in absorption of three molar equivalents of hydrogen to form VII. Methylation of these three dibasic acids, V, VI and VII, with diazomethane affords dimethyl esters, VIII, IX and X. It has been found, however, that the reactions of V and VI with excess diazomethane also afford compounds VIII of $C_{14}H_{15}O_5N_2Cl$ and IX of $C_{14}H_{15}O_5N_2Br$. These compounds seem to be the same ones obtained in the case of dibasic acid of I and to have a pyrazol ring at the double bond of $\alpha\beta$-unsaturated ketone system[1]. All of the dimethyl esters, VIII, IX and X, easily form crystalline 2, 4-dinitrophenylhydrazones.

Bromination of the adduct II or III in aqueous solution by the method of Alder-Stein results in addition to the double bond and bromolactone XI or XII is obtained in a good yield. Titration of XI and XII shows them to be a monobasic acid, and the presence of a carboxyl and a γ-lactone is also indicated from the infrared spectral values listed in Table I.

1) Part I of this series: T. Nozoe, T. Mukai, T. Nagase and Y. Toyooka, This Bulletin, 33, 1247 (1960).

Table I. Infrared spectral values of several adducts and their derivatives (cm^{-1})

	I	II	III	Bromo-γ-lactone of I	XI	XII
5-Membered acid anhydride ($\nu_{C=O}$)	1840 1780	1875 1850 1785	1875 1840 1785			
αβ-Unsaturated ketone ($\nu_{C=O}$)	1665	1690	1680	1675	1685	1685
C=C of αβ-unsaturated ketone ($\nu_{C=C}$)	1625	1630 1605	1630 1595		1655 1615	1610
γ-Lactone ($\nu_{C=O}$)				1770	1780	1780
Carboxylic acid $\nu_{C=O}$				1745	1710	1735
Carboxylic acid ν_{OH}				3320	3300	3350

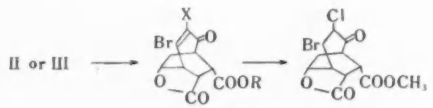

XI, X=Cl;R=H
XII, X=Br;R=H
XIII, X=Cl;R=CH_3

XIV

Methylation of XI with diazomethane afforded monomethyl ester XIII. Catalytic hydrogenation of XIII on palladium charcoal in ethyl acetate results in absorption one molar equivalent of hydrogen and crystalline saturated bromolactone XIV is formed.

Discussion

Bathochromic shifts in the ultraviolet maxima of II and III, 12~19 mμ, respectively, from that of I, are best explained by the α-substitution of halogen on the αβ-unsaturated carbonyl system, in accordance with Woodwards' rule (calcd. values: 242 mμ for II, 250 mμ. for III).

Similar kinds of shifts are observed in the infrared spectra (cf. Table I). It is safely assumed, therefore, that the addition of maleic anhydride has taken place at C-4 and C-7 of 2-halotropone.

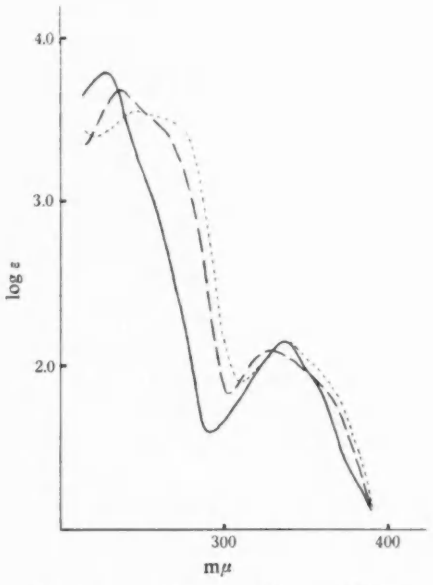

Fig. 1. —— (I) –– (II) ---- (III).

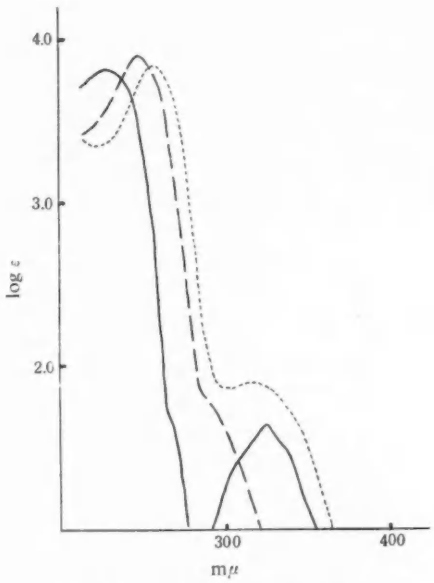

Fig. 2. —— Bromo-γ-lactone of (I) –– (XI) ---- (XII).

It is clear from the foregoing experiments, that both II and III have the endo-cis configuration. Thus tetrahydro compound IV obtained by catalytic hydrogenation II and III is identical with the tetrahydro compound from I.

Products, XI and XII, formed by Alder-Steins' bromination of II and III still have $\alpha\beta$-unsaturated carbonyl system (cf. Fig. 2) indicating that the addition of BrOH occurred on the isolated double bond. This is also supported by the strong band at 1780 cm^{-1} (γ-lactone) in both XI and XIII in their infrared spectra (cf. Table I).

Thus, the structure of bromolactones must be like the ones indicated in the figures.

Experimental

Preparation of Adduct II.—The solution which contained 2.80 g. of 2-chlorotropone and 3.90 g. of maleic anhydride dissolved in 40 cc. of dry xylene was refluxed on an oil bath (175~180°C) for 24 hr. Standing overnight at room temperature, 3.18 g. of pale yellow seeds were separated. Several recrystallizations afforded colorless needles, m. p. 208~209°C.

Found: C, 55.58; H, 2.90. Calcd. for $C_{11}H_7O_4Cl$: C, 55.35; H, 2.09%.

Preparation of IV.—To the solution of 720 mg. of II dissolved in 80 cc. of ethyl acetate, 500 mg. of 5% palladium charcoal was added and was hydrogenated at ordinary temperature and pressure. The absorption of hydrogen was quite slow and 203 cc. of hydrogen (3 mol. equiv.) was absorbed for 2 days. After filtration of the catalyst the solvent was distilled off completely, the residue afforded colorless small needles, m. p. 191~192°C, 320 mg. by several recrystallizations from acetone-ethyl acetate mixture.

Found: C, 63.48; H, 5.63. Calcd. for $C_{11}H_{12}O_4$: C, 63.45; H, 5.81%. λ_{max}^{MeOH} mμ (log ε): 291 (1.80).

Mixed melting point test with the tetrahydro adduct of I showed no depression.

Preparation of V.—Warming the suspension of 640 mg. of II in 50 cc. water on a boiling water bath, II was gradually dissolved. After evaporation to half volume and cooling in an ice bath, 620 mg. of V, as colorless leaflets separated. Although V has the same melting point to II, it melted in saturated sodium bicarbonate solution with effervescence, and neutralization titration value coincided to the dibasic one.

Found: C, 48.19; H, 3.97. Calcd. for $C_{11}H_{11}O_6Cl$: 48.09; H, 4.03%. λ_{max}^{MeOH} mμ (log ε): 248 (3.60), 337 (2.19).

Heating of V in phosphorus pentoxide vacuum desiccator for two days, V changed to II.

Preparation of VIII.—To the solution of 550 mg. of V dissolved in 30 cc. of ethyl acetate, two molar equivalents of diazomethane ethereal solution was added dropwise. After several hours the solvent was distilled off completely, the residue afforded colorless fine powders, m. p. 165~169°C, 550 mg. Several recrystallizations gave colorless fine crystals, m. p. 172~173°C, 410 mg.

Found: C, 54.87; H, 4.87. Calcd. for $C_{13}H_{13}O_5Cl$: C, 58.87; H, 4.60%. λ_{max}^{MeOH} mμ (log ε): 240 (3.74), 330 (1.01).

2,4-Dinitrophenylhydrazone of VIII.—To the solution of 80 mg. of VIII dissolved in 10 cc. of methanol, the mixture of 60 mg. of 2,4-dinitrophenylhydrazine, 0.1 cc. of concentrated sulfuric acid, 0.4 cc. of water and 1.3 cc. of methanol was added, then was refluxed on a water bath for 1.5 hr. Cooling in an ice bath 80 mg. of deep red fine crystals were separated. Several recrystallizations from a small amount of methanol afforded deep red fine crystals, m. p. 154°C, 50 mg.

Found: C, 50.86; H, 3.79; N, 12.38. Calcd. for $C_{19}H_{17}O_8N_4$: C, 49.09; H, 3.69; N, 12.05%. λ_{max}^{MeOH} mμ (log ε): 261 (4.05), 370 (4.42).

Preparation of VII. — (A) *By Catalytic Hydrogenation of V.*—To the solution of 550 mg. of V dissolved in 70 cc. of water, 50 mg. of 5% palladium charcoal was added and the mixture was hydrogenated at ordinary temperature and pressure. The absorption of hydrogen was slow and 139 cc. (3.1 mol. equiv.) of hydrogen was absorbed. After the catalyst was filtered, off the solvent was removed completely, the residue afforded colorless powders (VII), d. p. 172.5°C, 350 mg. by several recrystallizations from small amount of water.

Found: C, 58.39; H, 5.94. Calcd. for $C_{11}H_{14}O_5$: C, 58.40; H, 6.24%. λ_{max}^{MeOH} mμ (log ε): 292 (1.81).

(B) *By Hydrolysis of IV.*—Two hundred milligrams of IV was dissolved in 10 cc. of water, and then the solution was condensed to 1/3 volume on a boiling water bath. Colorless powders (VII), d. p. 173°C, 150 mg. were separated out on cooling.

Either VII obtained by (A) or (B) changed to IV on heating at 150°C in vacuum phosphorus pentoxide desiccator.

Preparation of X.—To the solution of 270 mg. of VII dissolved in 4 cc. of methanol, two molar equivalents of diazomethane ethereal solution was added dropwise. After several hours the solvent was removed completely, the residue afforded pale yellow oil, which failed to crystallize.

2,4-Dinitrophenylhydrazone of X. — The solution which contained 250 mg. of X and 200 mg. of 2,4-dinitrophenyl hydrazine dissolved in 5 cc. of methanol, 0.5 cc. of concentrated sulfuric acid, and 0.5 cc. of water was refluxed on a water bath for 1 hr. Orange crystals were separated. Several washings with hot methanol raised the melting point to 89°.

Found: C, 52.23; H, 4.90; N, 12.94. Calcd. for $C_{19}H_{22}O_8N_4$: C, 52.53; H, 5.10; N, 12.90%. λ_{max}^{MeOH} mμ (log ε): 229 (4.19), 361 (4.33).

Bromination of V: Preparation of XI.—To the solution of 550 mg. of V dissolved in 40 cc. of water, 320mg. of bromine was added dropwise under stirring. The color of the solution changed slowly to pale yellow and then colorless crystals were separated. After standing overnight 160 mg. of XI, d. p. 243°C, in colorless granules were obtained.

Found: C, 39.37; H, 2.27. Calcd. for $C_{11}H_8O_5BrCl$: C, 39.37; H, 2.41%.

Preparation of XIII.—To the solution of 440 mg. of XI dissolved in 20 cc. of ethyl acetate the calculated amount of diazomethane ethereal solution was added dropwise. After several hours the solvent

was removed and residue gave colorless crystals, m. p. 195~198°C, 450 mg. Several recrystallizations from methanol raised the melting point to 201~202°C.

Found: C, 41.40; H, 2.88. Calcd. for $C_{12}H_{10}O_5 \cdot BrCl$: C, 41.23; H, 2.88%.

Preparation of XIV.—To the solution of 250 mg. of XIII dissolved in 60 cc. of ethyl acetate, 100 mg. of 5% palladium charcoal was added and the mixture was hydrogenated at ordinary temperature and pressure. Eighteen cc. of hydrogen was absorbed (1.15 mol. equiv.). After filtration of the catalyst the solvent was distilled off, the residue afforded colorless powders, m. p. 219~222°C, 240 mg. Several recrystallizations from methanol raised the melting point to 230~232°C.

Found: C, 41.25, H, 3.17. Calcd. for $C_{12}H_{12}O_5 \cdot BrCl$: C, 40.99; H, 3.44%.

Preparation of III.—The solution which contained 370 mg. of 2-bromotropone and 400 mg. of maleic anhydride dissolved in 4 cc. of dry xylene was refluxed on an oil bath for 13 hr. Standing overnight in a cool place yellow crystals, m. p. 223~228°C, 410 mg. were separated. Recrystallization from acetone-ethyl acetate mixture raised the melting point to 232~233°C (350 mg.).

Found: C, 46.78; H, 2.40. Calcd. for $C_{11}H_7O_4Br$: C, 46.67; H, 2.49%.

Hydrolysis of III.—After dissolving 200 mg. of III in 10 cc. of water, the solution was evaporated to 1/2 volume on a boiling water bath. Colorless scales, d. p. 233°C, 180 mg. were separated on cooling.

Found: C, 44.00; H, 2.86. Calcd. for $C_{11}H_9O_5Br$: C, 43.88; H, 3.10%. λ_{max}^{MeOH} mμ (log ε): 248 (3.60), 337 (2.16).

Bromination of VI.—To the solution of 570 mg. of VI dissolved in 100 cc. of water, 320 mg. of bromine was added dropwise at room temperature under stirring. After standing overnight colorless granules, d. p. 246°C, 500 mg. were separated. Several recrystallizations from methanol-ethyl acetate mixture afforded colorless crystals, d. p. 257°C, 320 mg.

Found: C, 34.85; H, 2.04. Calcd. for $C_{11}H_8O_2Br_2$: C, 34.77; H, 2.12%.

Organic Chemical Laboratory
Chemical Institute
Faculty of Science
Katahira-cho, Sendai

Reaction of Hydrogen Peroxide on Fatty Acid Esters under Pressure. III. Oxidation of Methyl 9, 10-Dihydroxystearate

By Hiromu KAMEOKA

(Received June 4, 1960)

The reaction of hydrogen peroxide on methyl oleate[1] and on saturated fatty acid methyl esters[2] under pressure has already been reported in detail. The present research was carried out with the intention of finding the kinds of compounds formed by the action of hydrogen peroxide on methyl 9, 10-dihydroxystearate produced by the oxidation of methyl oleate with potassium permanganate and of following up the course of the reaction in the oxidation with hydrogen peroxide as mentioned above.

When methyl oleate is oxidized under pressure by the use of hydrogen peroxide, the position between 9 and 10 having a double bond is oxidized. In this case, however, the formation of 9, 10-dihydroxystearic acid is not observed, but substances coming from cutting off the carbon chain of methyl oleate at the position between 9 and 10 are formed. Moreover, various lower homologues of monobasic and dibasic fatty acid are formed. These are presumably produced by the oxidation at the other position of the carbon chain.

Expecting that the position between 9 and 10 where a double bond exists initially in methyl oleate is most liable to be oxidized in the oxidation of methyl 9, 10-dihydroxystearate and consequently C_9-aldehyde and C_9-fatty acid may be formed with relatively good yields. Methyl 9, 10-dihydroxystearate was subjected to the action of a 30% hydrogen peroxide solution under pressure.

The results obtained in this reaction were like those in the oxidation of saturated fatty acid methyl esters under a similar condition, excepting that the position between 9 and 10 was oxidized.

Experimental

Methyl 9, 10-Dihydroxystearate.—Commercial oleic acid was separated into solid acid and liquid acid through the lead-salt-ethanol process. The liquid acid was converted into lithium salt. This

1) H. Kameoka, *J. Chem. Soc. Japan, Ind. Chem. Sec.* (*Kogyo Kagaku Zasshi*), **63**, 741 (1960).
2) H. Kameoka, ibid., **63**, 744 (1960).

lithium salt, insoluble in a 50% ethanol solution, was filtered out and then changed to free fatty acid. The free fatty acid was subjected to the fractional distillation in a current of carbon dioxide gas three times. The distillate at the distillation temperature of 163~165°C/1 mmHg was oxidized in an aqueous alkaline solution of potassium permanganate, and sulfur dioxide gas was passed into the solution. After filtrating the aqueous solution, the remaining white substance was thoroughly washed with petroleum ether. This substance was recrystallized from a solution of 80% ethanol several times. The resulting crystalline substance having its melting point at 131~132°C and its neutralization value at 177.0 was esterified with methanol and sulfuric acid. The ester was recrystallized from an 80% ethanol solution once more. The ester thus prepared had an acid value 0.0, a saponification value 167.2, a hydroxyl value 334.5 and a melting point 104~105°C, and it was used as the sample of this research.

Hydrogen Peroxide.—A 30% solution was used.

Reaction under Pressure.—The sample (methyl 9, 10-dihydroxystearate) and a 30% hydrogen peroxide solution were enclosed in an autoclave (a capacity of 100 cc.) made of stainless steel, having an electromagnetic stirrer. The initial pressure in each test was maintained at 0 kg./cm². By heating the autoclave, the inside temperature and pressure of it were raised. In this case, heating was controlled in such a way that it may take about 1.5 hr. to reach the temperature shown in Table I, and the pressure was also raised up to the values given in Table I. The reaction time indicates the length of time held within the range of these temperatures and pressures. The conditions of reaction are shown in Table I.

Treatment of the Reaction Products. — Having been allowed to stand overnight after the completion of the reaction, the autoclave was opened. The reaction mixture was taken into a separating funnel. The interior of the autoclave was then thoroughly washed with distilled water and petroleum ether. The washing solutions used were also taken into the separating funnel. The content in the separating funnel was extracted with petroleum ether. In this way the content was separated into the soluble portion [A] and the insoluble portion [B].

As the petroleum ether soluble portion [A], a rather viscous oily substance was obtained after entirely removing the petroleum ether by distillation. This substance, after its constants were measured,

Table I. Conditions of reaction

Reaction No.	Sample wt., g.	30% H_2O_2 g.	Initial press. kg./cm²	Press. kg./cm²	Temp. °C	Final press. kg./cm²	Reaction time min.	Stir. r. p. m.
1	5.0	50	0	65~ 80	100~110	40	90	60
2	5.0	50	0	110~120	130~140	75	120	60
3	5.0	60	0	130~145	138~146	65	120	60
4	5.0	50	0	115~120	145~155	70	180	60
5	6.8	50	0	110~125	145~155	65	180	60
6	10.2	50	0	100~110	125~140	60	120	60
7	10.2	50	0	120~135	140~150	60	180	60

Table II. Table of the systematic separation of the reaction products

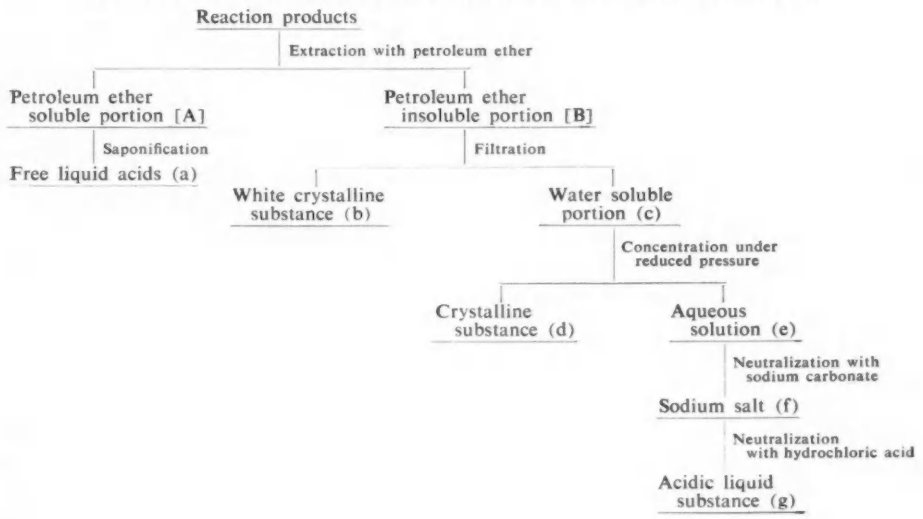

TABLE III. FRACTION (a). FREE ACID (Reaction No. 7, sample of fractional dist. 1.8 g.)

Fraction No.	Temp. of dist., °C/mmHg	Yield g.	N. v.	R_f value	Fatty acids detected
1	~170	0.2	605.3	* 0.69, 0.82	C_3, C_4-monobasic
2	170~210	0.3	461.9	* 0.82, 0.90, 0.96	C_4, C_6, C_9-monobasic
3	120~140/15	0.6	365.6	* 0.90, 0.95 △ 0.59	C_6, C_9-monobasic C_9-monobasic
4	140~160/15	0.4	305.3	△ 0.66, 0.59, 0.54	C_8, C_9, C_{10}-monobasic
5	160~170/15	0.2	279.6	△ 0.54, 0.44	C_{10}, C_{12}-monobasic
6	Residue	0.1	—	△ 0.44	C_{12}-monobasic

Paper chromatography: * Monobasic C_2~C_9-fatty acid, through the hydroxamic acid process[3]. —One-dimensional ascending method; development solvent, butanol saturated with water; filter paper, Toyo. No. 2; development temperature, 30°C; coloring matter, 10% ferric chloride-ethanol solution. △ Members above monobasic C_9-fatty acid, through the 2,4-dinitrophenylhydrazide process[4]. —One-dimensional ascending method; development solvent, methanol-acetic acid-tetraline; stationary phase, tetraline; filter paper, Toyo. No. 2; development temperature, 30°C; coloring matter, 0.5 N potassium hydroxide ethanol solution.

TABLE IV. FRACTION (d). CRYSTALLINE SUBSTANCE
(through fractional crystallization, sample 2.5 g.)

Cryst., No.	Yield, g.	N. v.	M. p., °C	R_f value	Fatty acids detected
1	0.8	943.9	180~183	□ 0.67	C_4-dibasic
2	1.2	763.5	150~153	□ 0.88	C_6-dibasic
3	0.4	651.0	110~131	□ 0.88 ○ 0.48	C_6-dibasic C_9-dibasic
4	0.1	—	—	□ 0.89 ○ 0.48	C_6-dibasic C_9-dibasic

Paper chromatography: □ Dibasic C_2~C_6-fatty acid, through the chloroform-acetic acid-water process[5]. —One-dimensional ascending method; development solvent, chloroform-acetic acid-water; filter paper, Toyo. No. 2; development temperature, 20°C; coloring matter, 0.1% bromocresol-green-ethanol solution. ○ Members above dibasic C_6-fatty acid, through the petroleum ether-chloroform-acetic acid process[6]. —One-dimensional ascending method; development solvent, petroleum ether-chloroform-acetic acid; filter paper, Toyo. No. 2; development temperature, 20°C; coloring matter, 0.1% bromocresolgreen-ethanol solution.

was saponified to convert it into free fatty acids (a).

The petroleum ether insoluble portion [B] was spontaneously separated to a white crystalline substance (b) and a water-soluble portion (c). The crystalline substance b, which was filtered out from c, was washed with distilled water several times and the washing water used was added to c. The whole of c was concentrated under 20 mmHg pressure. In this case c was separated into an aqueous solution (e) and the crystalline substance (d). The aqueous solution (e) showing itself to be acidic was neutralized by the use of a 1% aqueous solution of sodium carbonate. By concentrating this solution, a solid sodium salt (f) was obtained. The salt f was acidified with hydrochloric acid, and then extracted with a large amount of ether. After removing the ether by distillation, an acidic liquid substance (g) was obtained. Examination was made about the substances separated through the process mentioned above respectively. In Table II, the treating procedure of the reaction products are represented.

Petroleum Ether Soluble Portion [A]. — This portion is a rather viscous oily substance and is fragrant. It being presumable that pelargonic aldehyde produced by the breakage between the positions of 9 and 10 may exist in the portion A, this portion was tested to see whether it may form an adduct of sodium bisulfite by the ordinary process or not. However, this test did not give any positive result. Then, a 2 N hydrochloric acid solution of 2,4-dinitrophenylhydrazine was added to the portion A. In this case, a very small amount of yellowish orange precipitates was obtained, the amount of which was not sufficient for identification.

This portion A was next converted to the free acid by saponification with a 5% alcoholic potassium hydroxide solution. The free acid thus obtained was subjected to fractional distillation and the constants of the distillates were measured. The result of Reaction No. 7 is given in Table III.

Each of the portion A obtained in Reactions No. 1—No. 6 was similarly subjected to fractional distillation. Almost the same result as that of Reaction No. 7 was obtained. Moreover, as the hydroxyl value of the portion A was all zero, this portion has no hydroxy compound.

3) Y. Inoue and M. Noda, *J. Japan Oil Chemist's Soc.* (*Yukagaku*), **1**, 136 (1952).
4) Y. Inoue and M. Noda, *Bull. Agr. Chem. Soc. Japan*, **19**, 214 (1955).
5) M. Kobayashi, *J. Japan Oil Chemist's Soc.* (*Yukagaku*), **4**, 53 (1955).
6) M. Kobayashi, ibid., **5**, 85 (1956).

Table V. Fraction (g). Acidic liquid substance
(sample of the fractional distillation, 1.5 g.)

Fraction No.	Temp. of dist., °C	Yield g.	N. v.	R_f value	Fatty acids detected
1	~120	0.5	930.6	* 0.50	C_2-monobasic
2	120~145	0.4	759.6	* 0.50, 0.68	C_2, C_3-monobasic
3	145~165	0.4	633.0	* 0.68, 0.82	C_3, C_4-monobasic
4	Residue	0.2	595.1	* 0.82	C_4-monobasic

Paper chromatography: * Hydroxamic acid process[3].

Petroleum Ether Insoluble Portion [B].—*Crystalline Substance (d) Contained in the Water Soluble Portion (c).*—The substance is assumed to be dibasic acid from its good solubility in water, and good crystallizable property. This crystalline substance was fractionally crystallized from a 10% ethanol solution, and the crystals shown in Table IV were obtained in the case of Reaction No. 7.

The fraction d obtained in Reactions No. 1—No. 6 was similarly subjected to the fractional crystallization with almost the same result as that mentioned above. In cases of the oxidizing conditions as in Reactions No. 1, No. 3 and No. 6, the formation of low members of dibasic acid such as C_2 and C_3 was observed.

Each acid thus separated has nearly an equal neutralization value to the corresponding pure acid. Furthermore, no depression of the melting point was observed when each acid was subjected to the mixed melting point determination.

The Sodium Salt (f) and the Acidic Liquid Substance (g).—The substance g obtained from the salt f was fractionally distilled, and inquiries were made about the respective fractions. The result of Reaction No. 7 is shown in Table V.

In the result shown above, the neutralization values of fractions No. 1, No. 2 and No. 3 were nearly equal to those of acetic, propionic and butyric acids, 934.5, 757.4 and 637.1, respectively. Accordingly it may be confirmed that the main components of these fractions are acetic, propionic and butyric acids. The results of the fractional distillation of g obtained in Reactions No. 1—No. 6 were almost the same as the above. Furthermore, from the result of paper chromatography[3] (hydroxamic acid process: R_f value 0.90) it was observed that small quantities of monobasic C_6 fatty acid were contained in g obtained in Reactions No. 1—No. 3.

White Crystalline Substance (b).—This substance is insoluble in water and petroleum ether. From its saponification value, hydroxyl value and melting point in addition to the insolubility nature mentioned above, this substance seemed to be non-oxidized methyl 9,10-dihydroxy stearate (Table VI). Furthermore, because of its slightly higher acid value and the considerably wide range of its melting point, the formation of free 9,10-dihydroxystearic acid due to the partial hydrolysis of the ester is presumable. Accordingly, this was saponified, and the melting point of 130~132°C and the neutralization value of 175~176 were obtained for the resulting acid. No depression of the melting point was observed when mixed with 9,10-dihydroxystearic acid. Moreover, the substance b was subjected to paper chromatography[5,6]. No existence of dibasic acid in it, however, was observed.

Results

The yields and constants of the separated substances, and the results concerning them in paper chromatography are summarized in Table VI.

As shown in Table VI, lower members of monobasic acid were mainly detected in the portion A. Water soluble lower members of monobasic and dibasic acid and unchanged methyl 9, 10-dihydroxystearate were detected in the portion B. Further, it was found that under the reaction conditions as in Reactions No. 3, No. 4 and No. 5, more than 80% of the methyl 9, 10-dihydroxystearate used was oxidized.

Discussion

In the present experiments, the reaction products, except the nonoxidized substance, had no hydroxyl value. This fact indicates that the hydroxyl group of the initial sample was removed during the oxidation with hydrogen peroxide.

Furthermore, from the fact that monobasic C_9-acid and dibasic C_9-acid were present in the portion A and also in the fraction d, it is clear that the positions of 9 and 10 where the hydroxyl group was initially located are oxidized. The production of the only small quantity of C_9-compounds by breakage at this position is probably explained by the consideration that this position is first attacked by oxygen and C_9-compounds are produced, but the resulting substances are immediately oxidized, and the compounds of smaller carbon numbers are formed. It is evident that lower monobasic acids than C_{10} are liable to be oxidized with hydrogen peroxide[7]. Alternatively, it is considered that other positions of the carbon chain are simultaneously split by the oxidation. This fact is clearly found from the formation of C_{12}, C_{10}-acids and/or lower acids. In case

7) H. Kameoka, ibid., 9, 351 (1960).

TABLE VI. REACTION PRODUCTS

Reaction No.	Petroleum ether soluble portion [A]			Petroleum ether insoluble portion [B]											
				Water soluble portion (c)							White crystalline substance (b)				
				Crystalline substance (d)			Aqueous solution (e)								
								Acidic liquid substance, g.							
	Yield g.	N. v.	Fatty acids detected *, △	Yield g.	N. v.	Acids detected □, ○	Na-salt (f) g.	Yield g.	N. v.	Acids detected, *	Weight g.	A. v.	S. v.	M. p., °C	Acids detected
1	1.5	235.7	C_{18}, C_{12}, C_{10}, C_9, C_8, C_6, C_4-monobasic	0.6	589.3	C_2, C_3, C_4, C_6, C_9-dibasic	1.3	0.3	320.9	C_2, C_3, C_4, C_6-monobasic	2.5	72.1	177.6	110～119	Methyl 9,10-dihydroxy-stearate
2	1.0	307.1	C_{18}, C_{12}, C_{10}, C_9, C_8, C_6, C_4-monobasic	1.1	659.9	C_4, C_6, C_9-dibasic	1.9	1.0	559.7	C_2, C_3, C_4, C_6-monobasic	1.7	55.8	188.4	89～ 96	〃
3	1.2	346.1	C_{12}, C_{10}, C_9, C_8, C_4, C_3, C_2-monobasic	1.8	603.2	C_2, C_3, C_4, C_6, C_9-dibasic	2.8	1.4	735.2	C_2, C_3, C_4, C_6-monobasic	0.5	43.0	186.8	94～104	〃
4	1.2	306.6	C_{12}, C_{10}, C_9, C_8, C_4, C_3, C_2-monobasic	1.7	594.8	C_4, C_6, C_9-dibasic	1.9	0.9	783.6	C_2, C_3, C_4-monobasic	1.0	47.1	180.6	88～104	〃
5	1.7	321.5	C_{12}, C_{10}, C_9, C_8, C_6, C_4, C_3-monobasic	2.1	615.0	C_4, C_6, C_9-dibasic	2.8	1.4	755.0	C_2, C_3, C_4-monobasic	1.4	39.8	176.5	92～104	〃
6	1.9	331.2	C_{12}, C_{10}, C_9, C_8, C_6, C_4-monobasic	2.0	605.1	C_3, C_4, C_6, C_9-dibasic	3.4	1.7	743.0	C_2, C_3, C_4-monobasic	4.3	40.5	179.8	93～104	〃
7	2.3	332.4	C_{12}, C_{10}, C_9, C_8, C_6, C_4, C_3-monobasic	3.2	590.6	C_4, C_6, C_9-dibasic	3.8	1.8	780.6	C_2, C_3, C_4-monobasic	2.5	43.6	181.5	89～104	〃

Paper chromatography: * hydroxamic acid process[3]; △ 2,4-dinitrophenylhydrazide process[4]; □ chloroform-acetic acid-water process[5]; ○ petroleum ether-chloroform-acetic acid process[6].

of the formation of C_{12}, C_{10}-acids, hydroxy acids were not obtained. The mechanism concerning no formation of hydroxy acid has not yet been available.

The formation of considerably large amount of C_4- and C_6-dibasic acids was observed. These products should result from (i) the further oxidation of the substances produced by the breakage of the bond between 9 and 10, and (ii) the secondary oxidation of monobasic C_{12}- and C_{10}-acids which are produced by the direct oxidation of methyl 9, 10-dihydroxystearate. The formation of considerably quantities of dibasic acids will be ascribed to the oxidation of the methyl group of the lower monobasic acids produced by the direct oxidation mentioned above. Moreover, in case of the oxidizing conditions as in Reactions No. 1, No. 3 and No. 6, the formation of lower members of dibasic acid such as C_2 and C_3 was recognized. These C_2- and C_3-dibasic acids may probably be formed under other conditions of reaction. Because of the easy decomposition of these dibasic acids, however, they will be decomposed when the reaction conditions are intense. Furthermore, it is considered that the formation of various lower homologues of fatty acid is due to the same oxidation course as that of the saturated fatty acid methyl ester[2] irrespective of the hydroxyl groups present in the sample molecule.

In short, in the oxidation of methyl 9, 10-dihydroxystearate with hydrogen peroxide, the following reactions will be presumed. That is, the positions 9, 10 containing hydroxyl groups are first oxidized, and the products of such oxidation are subjected to the secondary oxidation, and also there occurs the other reaction following the course of the oxidation similar to that of the saturated acid.

Summary

Methyl 9, 10-dihydroxystearate is oxidized with a 30% hydrogen peroxide solution, under such conditions as the mole ratio of methyl 9, 10-dihydroxystearate to hydrogen peroxide is one to fifteen or more, the reaction time 2 hr., the temperature 138～155°C, and the pressure 110～145 kg./cm^2. Also, it was recognized that 80% or more of methyl 9, 10-dihydroxystearate was oxidized.

As the oxidation products, acetic, propionic, butyric, caproic, caprilic, pelargonic, caprinic and lauric acids were obtained as monobasic acids, and oxalic, malonic, succinic, adipic and azelaic acids were also produced as dibasic acids. Especially, succinic and adipic acids were obtained with good yield.

The author wishes to express his hearty thanks to Professor N. Hirao for his kind guidance and encouragement for the present work.

Faculty of Science and Engineering
Kinki University
Fuse-shi, Osaka

---

*Polymerization of Allyl Chloride by Ziegler's Catalyst**

By Shunsuke MURAHASHI, Shun'ichi NOZAKURA and Kōichi HATADA

(Received July 11, 1960)

In recent years many papers have been published on the stereospecific polymerization of α-olefins by Ziegler's catalyst. However it is well known that the catalyst, by itself, has little effect on the stereospecific polymerization of monomers containing any heteroatom, such as oxygen, nitrogen, sulfur or halogen, except only vinyl butyl ether, a stereospecific polymerization of which was found by Natta[1].

An attempt was made on the polymerization by Ziegler's type catalysts with allyl chloride as a monomer containing heteroatom. Since allyl chloride was first polymerized by Staudinger[2] to a syrupy low polymer, many investigations were done on the polymerization of this monomer, but no solid polymer has been obtained due to the "degradative chain transfer"[3] in its radical polymerization.

By Ziegler's type catalysts allyl chloride

* Presented at the 5th Meeting on High Polymer Chemistry, Kōbe, June, 1959.

1) G. Natta et al., *Angew. Chem.*, **71**, 205 (1959).

2) H. Staudinger and Th. Tleitmann, *Ann.*, **488**, 92 (1930).

3) P. D. Bartlett and R. Alschul, *J. Am. Chem. Soc.*, **67**, 812, 816 (1945). F. M. Lewis and F. R. Mayo, *J. Am. Chem. Soc.*, **76**, 457 (1954).

reacted rather rapidly at low temperatures with evolution of hydrogen chloride and gave a solid polymeric material. In the polymer produced the chlorine content was very much reduced for polyallyl chloride $[C_3H_5Cl]_n$ and indications of some unsaturation were observed. It was found that the polymerization took place only with catalysts having Al-Cl bond. Furthermore, the polymerization was accelerated by the presence of a small amount of benzene, which incorporated in the polymer.

On the basis of these results it was concluded that the polymerization of allyl chloride with Ziegler's type catalysts does not proceed by an anionic mechanism which is characteristic of these catalysts, but occurs with a some Friedel-Crafts type reaction caused by compounds such as Et_2AlCl, $EtAlCl_2$ or $AlCl_3$ formed in the reaction mixture. Also a cationic mechanism is likely to contribute simultaneously to the polymerization.

Similar results were obtained with the polymerization using allyl fluoride, allyl bromide, and 3, 3, 3-trichloropropene-1 as the monomer, respectivey.

Experimental

Materials. — *Allyl Chloride.* — Commercial allyl chloride was purified by distillation and a fraction of b. p. 44.0~45.0°C was used.

Allyl Bromide. — Synthesized according to Kamm and Marvel[4]. B. p. 70°C.

Allyl Iodide. — Prepared from allyl chloride and sodium iodide as described by Letsinger and Traynham[5]. B. p. 48°C/108 mmHg.

Allyl Fluoride.—Prepared from silver fluoride and allyl iodide[6], and collected in a trap cooled in a dry ice-acetone bath. An infrared absorption spectrum of the gaseous sample was shown in Fig. 2.

3,3,3-Trichloro-1-propene. (*Nippon Soda Co.*). — Distilled and a fraction of b. p. 50~53°C/80 mmHg was used.

n-Hexane. — Purified in the usual manner and stored over metallic sodium.

Triethylaluminum. — Supplied by Mitsui Chem. Ind. Co. and was used as a solution in *n*-heptane.

Titanium Tetrachloride.—Supplied by Osaka Titanium Co. and was used as a solution in *n*-heptane.

Apparatus. — A 50 ml. five-necked flask[7] fitted with a thermometer, a stirrer, a nitrogen gas inlet tube and two silicone rubber caps was used as the polymerization vessel. Catalyst components, monomer, and solvent were introduced into the vessel through rubber caps with a hypodermic syringe.

Preparation of Catalysts.—After the vessel was flushed by dry nitrogen, 20 ml. of *n*-hexane and 0.25 g. of titanium tetrachloride were introduced. With boiling the mixture gently, 0.15 g. of $AlEt_3$ was slowly added dropwise, and heating was continued for further 5 min. and cooled. After precipitating the solid catalyst complex the supernatant liquid was removed by a syringe under dry nitrogen. The catalyst was washed three times with 20 ml. of *n*-hexane, and then 20 ml. of *n*-hexane and 0.15 g. of $AlEt_3$ was added.

Other catalysts of Ziegler's type were prepared in the same manner but the wash procedure was omitted.

Polymerization. — The catalyst was cooled to the polymerization temperature in a dry ice-acetone bath and with stirring the monomer was slowly added dropwise. The reaction was exothermic and the heat evolved spontaneously at or after the addition of the monomer, when deep cooling was required to keep the temperature constant. After three to five hours the reaction was stopped by adding 10 ml. of methanol containing a small amount of hydrochloric acid and the polymer was precipitated by pouring the mixture into about 300 ml. of methanol. After standing overnight the polymer was collected and washed with methanol, and dried in vacuo. The polymer was reprecipitated from its benzene solution by methanol.

Allyl fluoride was polymerized as follows. The monomer gas was introduced by a gas inlet tube bubbling through the catalyst suspension and the unreacted monomer was recycled through a trap cooled in dry ice-acetone bath.

Double Bond Titration of Polymer. — A known amount of polymer (about 0.05 g.) was dissolved in 8 ml. of carbon tetrachloride in a 100 ml. glass stoppered flask and 2 ml. of 0.5 N bromate-bromide solution and 1.3 ml. of 10% sulfuric acid were added. After shaking the mixture vigorously for three minutes 2 ml. of 20% aqueous potassium iodide solution were added and again the mixture was shaken vigorously for a minute. The liberated iodine was titrated by 0.1 N sodium thiosulfate solution with starch as an indicator.

Reduction of Polymer with $LiAlH_4$.—A polymer of allyl chloride (0.25 g.) polymerized by $AlEt_3$-$TiCl_4$ catalyst and containing 20.81% by weight of chlorine was reacted with 0.4 g. of $LiAlH_4$ in 30 ml. tetrahydrofuran. The reaction was carried out under dry nitrogen in a sealed tube with shaking for 150 hr. at 60°C. After cooling, the reaction mixture was poured into methanol containing nitric acid to decompose excess $LiAlH_4$. The precipitated polymer was collected, washed with methanol and dried in vacuo. The chlorine content of the product was 7.56% (by wt.).

Results

The results were summarized in Tables I, II and III.

During the polymerization, especially in its initial stage, usually a sudden increase in temperature of the reaction mixture and a evolution of hydrogen chloride were observed, while the color of the catalyst turned to reddish brown gradually.

4) O. Kamm and C. S. Marvel, "Organic Syntheses", Coll. Vol. I, (1956), p. 27.
5) R. L. Letsinger and J. G. Traynham, *J. Am. Chem. Soc.*, **70**, 2818 (1948).
6) M. H. Meslans, *Compt. rend.*, **111**, 882 (1890).
7) S. Murahashi, S. Nozakura, M. Sumi and K. Hatada, This Bulletin, **32**, 1094 (1959).

TABLE I. POLYMERIZATION OF ALLYL CHLORIDE WITH ZIEGLER'S CATALYST

Monomer: 5 ml. (4.70 g.), Catalyst: $AlEt_3$ 0.30 g. + $TiCl_4$ 0.25 g. ($AlEt_3/TiCl_4$=2 mol./mol.), Solvent: *n*-Hexane.

Polymerization			Polymer				
Temp. °C	Time hr.	Solvent ml.	Yield %	Cl-content*1 %	M. p. °C	η_{sp}/C*5 dl./g.	Double bond mol./C_3-unit
20	3	15	29.3	12.53*2	73~ 75	0.043	0.16
0	5	20	9.9	20.61	80~ 81	0.035	—
−10	5	20	9.1	19.55	85~ 86	0.040	—
−20	5	20	9.6	21.40*3	89~ 91	—	0.17
−30	5	45	7.1	18.26*4	105~108	0.081	0.13
−70	170	20	1.5	22.25	73~ 75	—	—

*1 Theoretical value for poly(allyl chloride) $[-CH_2-CH(CH_2Cl)-]_n$: 46.33%.
*2 C, 74.64%; H, 9.20%; corresponding to $C_3H_{4.4}Cl_{0.17}$.
*3 C, 69.30%; H, 8.71%; corresponding to $C_3H_{4.5}Cl_{0.32}$.
*4 C, 73.21%; H, 8.66%; corresponding to $C_3H_{4.3}Cl_{0.25}$.
*5 Benzene solution (C=0.5 g./dl.) at 30°C.

TABLE II. POLYMERIZATION OF ALLYLHALIDES WITH ZIEGLER'S CATALYST

Catalyst: $AlEt_3$ 0.30 g. + $TiCl_4$ 0.25 g. ($AlEt_3/TiCl_4$=2 mol./mol.)
Solvent: *n*-Hexane.

Monomer ml.	Polymerization		Solvent ml.	Polymer				
	Temp. °C	Time hr.		Yield g.	Halogen content, % Found	Halogen content, % Theoretical	M. p. °C	η_{sp}/C(30°C) dl./g.
CH_2=CH-CH_2F 1.0*1	50	45	20	0.030	—	31.63	—	—
3.2*1	25	7	25	0.050	3.2		97~ 98	—
1.2*1	−20	2.5	25	0.030	1.5		75~ 77	—
CH_2=CH-CH_2Br 3.5	−20	5	20	0.255	30.00*2	66.05	85~ 87	0.025
CH_2=CH-CH_2I 3.0	−20	5	20	trace	—	75.55	—	—
CH_2=CH-CCl_3 2.0	20	5	20	0.180	35.28	73.14	135~140	—

*1 The quantities were shown as volumes at −80°C.
*2 C, 61.14%; H, 7.49%; corresponding to $C_3H_{4.4}Br_{0.22}$. Double bond 0.12 mol./C_3-unit.

The polymer obtained was a powder colored in faint yellow, having a melting point between 70~110°C and soluble in benzene, toluene, and tetrahydrofuran. Generally the chlorine content of the polymer was less than a half of the theoretical value (46.33%) for polyallyl chloride $[-CH_2-CH(CH_2Cl)-]_n$. The low viscosity of the polymer solution is indicative of the fairly low molecular weight of the polymer.

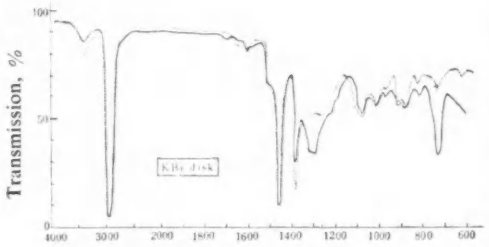

Fig. 1. Infrared absorption spectra of the polymer of allyl chloride (——) and its reduction product with $LiAlH_4$ (·····).

Infrared spectra of a typical sample of the polymer and of its reduction product by lithium aluminum hydride were shown in Fig. 1. The absorption bands arising from C-Cl linkage appeared at 730 cm^{-1} and about 1300 cm^{-1}, and the intensities were decreased with the reduced polymer. At 1378 cm^{-1} and 1460 cm^{-1} are located the absorption bands due to the presence of methyl and methylene groups, respectively. The former increased its intensity relatively to the latter by the reduction of the polymer, indicating the presence of $-CH_2Cl$ groups in the polymer. The bands in a region between 800 cm^{-1} and 1000 cm^{-1} seems to be characteristic of various types of double bonds. In addition to this spectral data the double bond titration of the polymer showed about 0.15 mol. unsaturations per monomer unit in general (Tabel I).

These polymers were shown to be amorphous by their X-ray diffractions.

The chlorine content of the polymer was independent of the polymerization temperature in the range between 0°C and −70°C, while the conversion was strongly depressed at −70°C. The melting point of the polymer and its solution viscosity in benzene decreased slightly with raising the polymerization temperature (Table I).

The polymerizations of allyl fluoride, allyl bromide and 3, 3, 3-trichloro-1-propene by $AlEt_3$-$TiCl_4$ catalyst gave similar solid polymers as obtained from allyl chloride and their halogen contents were also much less than the theoretical values calculated for the monomeric units (Table II). The polymers of allyl fluoride and allyl bromide gave the similar infrared absorption spectra as that given by the polymer of allyl chloride, but the very weak band at 1070 cm^{-1} was considered to be of the C–F linkage in the former polymer (Fig 2). The band appeared to arise from the C–Br linkage was located at 569 cm^{-1} in the polymer of allyl bromide.

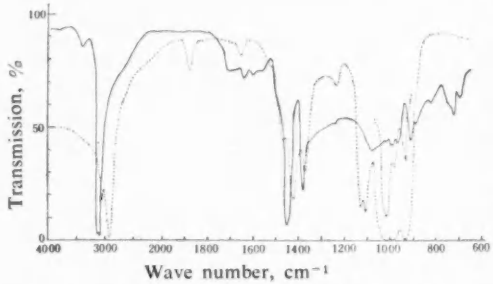

Fig. 2. Infrared absorption spectra of gaseous allyl fluoride (·····) and its polymer (—— KBr disk).

Allyl iodide gave no polymer by $AlEt_3$-$TiCl_4$ catalyst under the same condition as in the polymerization of allyl chloride.

Various types of catalysts were examined for the polymerization of allyl chloride (Table III). Among the Ziegler's type catalysts used, all the compounds having Al–Cl linkage, either the linkage was original or formed from the catalyst components, were capable of polymerizing allyl chloride. However, the catalysts such as $AlEt_3$-$Ti(OBu)_4$, LiBu-$TiCl_4$ and $ZnEt_2$ (ether solution)-$TiCl_4$ gave no polymer under similar or even more drastic conditions. It should be noted, however, that the catalyst prepared from $AlEt_3 \cdot Et_2O$ and $TiCl_4$ hardly polymerized allyl chloride, although the catalyst might have possibly Al–Cl linkage in it.

Of the catalyst for cationic polymerization, what possessed Al–Cl linkage also functioned as catalyst for the polymerization of allyl chloride, while no polymer was obtained with $TiCl_4$ and $BF_3 \cdot Et_2O$. On the other hand, all the basic catalysts examined, such as LiBu, $ZnEt_2$(ether solution) and $AlEt_3$, had no catalytic activity for the polymerization.

It was found that an addition of benzene to the reaction mixture caused remarkable increase in the polymer yield (Table III) and also in the evolution of hydrogen chloride during the polymerization. An infrared absorption spectrum of the yielded polymer (Fig. 3) showed absorption bands due to skeletal vibrations of a benzene ring at 1605

TABLE III. POLYMERIZATION OF ALLYL CHLORIDE WITH VARIOUS CATALYSTS

Monomer: 3.5 ml., Solvent: *n*-Hexane 25 ml., Polymerization temperature: −20°C, Polymerization time: 5 hr.

Catalyst*6	Benzene g.	Polymer: Yield %	Cl-content %	M. p. °C	η_{sp}/C*5 dl./g.	Double bond (mol./C_3-unit)
$AlEt_3$-$TiCl_3$	0	5.0*1	14.79	94∼ 95	0.050	—
$AlEt_3$-$VOCl_3$	0	6.4	18.71	86∼ 89	0.043	—
$AlEt_3 \cdot Et_2O$-$TiCl_4$	0	0.8	—	—	—	—
Et_2AlCl-$TiCl_4$	0	10.8	19.20	83∼ 85	0.050	—
Et_2AlCl-$TiCl_4$	1.0	31.6*2	16.77	116∼118	0.093	0.08
Et_2AlCl	0	4.4	23.87	84∼ 85	0.036	—
Et_2AlCl	1.3	29.6*3	15.05	99∼102	0.072	0.06
$AlCl_3$	0	9.9	23.60	79∼ 80	0.033	—
$AlCl_3$	1.0	44.7*4	17.66	—	—	—

*1 Reaction time: 4 hr.

*2, *3, *4 Benzene-insoluble fractions were 31.7, 11.5, and 16.8%, based on the total amounts of polymers, respectively. The following data described above were obtained on the soluble fractions.

*5 Benzene solution (C=0.5 g./dl.) at 30°C.

*6 The ratios of the two components were unity, except 0.2 of $AlEt_3/TiCl_3$.

cm^{-1} and 1498 cm^{-1}, indicating an existence of a benzene ring in the polymer chain. Furthermore, a part of this polymer was not soluble in any usual organic solvents and had no melting point even above 300°C, and was assumed to be a cross-linked polymer through benzene nuclei. The soluble fraction of this polymer had a higher melting point, a higher solution viscosity and a lower chlorine content, compared with the polymer formed under the same condition but without benzene.

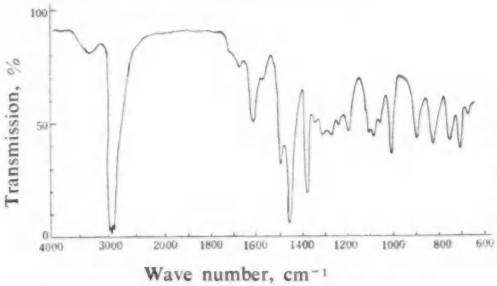

Fig. 3. Infrared absorption spectrum of the polymer of allyl chloride polymerized in the presence of benzene. KBr disk.

Discussion

The results mentioned above reveals that the following features are involved in the polymerization of allyl chloride with Ziegler's type catalyst: a) An evolution of hydrogen chloride during the polymerization and a strongly reduced chlorine content of the resulting polymer. b) Only compounds containing Al–Cl bond such as Et_2AlCl, $EtAlCl_2$ and $AlCl_3$ function to polymerize allyl chloride. These compounds are powerful catalysts of Friedel-Crafts reaction. c) A marked increase in conversion with an addition of benzene to the system and an incorporation of benzene to the resulting polymer. d) An existence of double bonds in the polymer.

On the basis of these facts it is proposed that the Friedel-Crafts type reactions 1, 2 and 3 caused by a compound containing Al–Cl bond is essential in the polymerization of allyl chloride by Ziegler's type catalyst. It seems to be possible that a minor contribution of ordinary cationic processes 1 and 4 is involved and causes some complication in the reaction.

$$CH_2{=}CH{-}CH_2Cl + \overset{|}{Al}{-}Cl \longrightarrow CH_2{=}CH{-}\overset{+}{C}H_2\left[Cl{-}\overset{|}{Al}{-}Cl\right]^- \quad (1)$$

$$CH_2{=}CH{-}\overset{+}{C}H_2\left[Cl{-}\overset{|}{Al}{-}Cl\right]^- + CH_2{=}CH{-}CH_2Cl \longrightarrow CH_2{=}CH{-}CH_2{-}CH{=}CH{-}\overset{+}{C}H_2\left[Cl{-}\overset{|}{Al}{-}Cl\right]^- + HCl \quad (2)$$

or

$$CH_2{=}CH{-}CH_2{-}\underset{\underset{CH_2}{\|}}{C}{-}\overset{+}{C}H_2\left[Cl{-}\overset{|}{Al}{-}Cl\right]^- + HCl \quad (3)$$

$$CH_2{=}CH{-}\overset{+}{C}H_2\left[Cl{-}\overset{|}{Al}{-}Cl\right]^- + CH_2{=}CH{-}CH_2Cl \longrightarrow CH_2{=}CH{-}CH_2{-}CH_2{-}\overset{+}{C}H(CH_2Cl)\left[Cl{-}\overset{|}{Al}{-}Cl\right]^- \quad (4)$$

The reaction may proceed in such a manner as follows: a slow first stage of the reaction catalyzed by a small amount of original species having Al–Cl linkage, such as Et_2AlCl, $EtAlCl_2$ or $AlCl_3$, is followed by a faster reaction owing to a gradual accumulation of these catalyst compound generated by a reaction between $AlEt_3$ and hydrogen chloride liberated during the polymerization, and this finally leads to a violent rise of temperature of the reaction mixture.

The fact that the polymerization is strongly accelerated by adding a small amount of benzene to the system is a further evidence for the Friedel-Crafts type mechanism of the polymerization reaction. The benzene may undergo a variety of reaction, thus forming cross-linkages in some extent between polymer chains and giving a rather large amount of insoluble fraction of the polymer.

Methyl groups in the polymer may be produced by the reactions as following scheme.

$$\sim\!\!\sim\underset{\underset{CH_2}{|}}{C}\sim\!\!\sim \xrightarrow{HCl} \sim\!\!\sim\underset{\underset{CH_3}{|}}{\overset{\overset{Cl}{|}}{C}}\sim\!\!\sim$$

$$\sim\!\!\sim\underset{\underset{CH_2Cl}{|}}{CH}\sim\!\!\sim \xrightarrow{Et_3Al\ etc.} \sim\!\!\sim\underset{\underset{CH_3}{|}}{CH}\sim\!\!\sim \quad \text{or} \quad \sim\!\!\sim\underset{\underset{C_3H_7}{|}}{CH}\sim\!\!\sim$$

In the case of $AlEt_3{\cdot}Et_2O{-}TiCl_4$ catalyst, these components may also produce any compound such as Et_2AlCl, $EtAlCl_2$ or $AlCl_3$, but etherated. It is considered that the coordinated ether reduces the ionic character of the Al–Cl bond so strongly that the compound can not function as a catalyst for the Friedel-Crafts type reaction.

The authors wish to thank Mitsui Chem. Ind. Co. for the generous supply of triethylaluminum and Osaka Titanium Co. for titanium tetrachloride.

Department of Chemistry
Faculty of Science
Osaka University
Nakanoshima, Osaka

Oxidation of 2-Methyl 5-Ethyl Pyridine to Isocinchomeronic Acid

By Tokio KATO

(Received August 26, 1960)

In the preparation of isocinchomeronic acid (ICA) from 2-methyl 5-ethyl pyridine (MEP), several kinds of oxidizing reagents, such as sulfuric acid[1], selenium peroxide[2], nitric acid[3] and cupric nitrate[4] have been used. Cupric nitrate (with or without nitric acid) is said to give the highest yield of ICA among them, where this process consumes a large quantity of nitrate or nitric acid (more than 10 mol. as NO_2 to 1 mol. MEP oxidized).

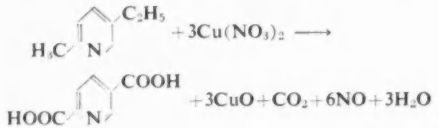

MEP can not be oxidized with molecular oxygen as in the case of *p*-xylene with catalysts such as cobalt or manganese acetates. But the combined use of oxygen (a little more than theoretical moles for the oxidation of MEP) with cupric nitrate was found to be effective to obtain ICA (through its cupric salt) with a yield higher than 85 ml. % to MEP consumed, where the used cupric nitrate was easily recovered and reused.

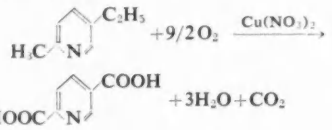

Experimental

Materials.—MEP of more than 98% purity was purchased from Carbide and Carbon Chem. Co. Ltd., and used without purification. Its specifications are as following; specific gravity (20°/20°), 0.918～0.922; b. p., 171～181°C (760 mmHg); water content, less than 0.2% by weight. Reaction vessel was 1 l. auto-clave (18 : 8 stainless steel) with magnetic stirrer.

Oxidation.—MEP, cupric nitrate (as 200 cc. aqueous solution) and oxygen were charged in the

TABLE I. REACTION VARIABLE IN THE OXIDATION OF MEP.

Exp. No.	MEP mol.	$Cu(NO_3)_2$[a] mol.	Charged mol. ratio $Cu(NO_3)_2$/MEP	N_2[d]+O_2 atm.	O_2% by vol.	Duration min.[b] 180～200°C	200～230°C
1	0.149	0.79	5.30	Not charged		10	200
2	〃	0.476	3.20	〃		〃	〃
3	〃	0.155	1.04				
4	0.197	0.203	〃	〃		〃	〃
5	0.149	0.103	0.69	50	54	〃	130
6	〃	0.155	1.04	〃	55	3	100
7	〃	0.103[c5]	0.69	〃	53	10	180
8	0.198	0.155	0.77	58	56	5	85
9	〃	〃 [c8]	〃	〃	48	3	90
10	〃	〃 [c9]	〃	〃	42	〃	120
11	0.197	0.203	1.04	〃	45	5	130
12	〃	〃	〃	〃	40	5	120
13	〃	〃	〃	50	44	〃	160
14	〃	〃	〃	53	50	30	95
15	〃	〃	〃	60	54	240	0
16	0.296	〃	0.69	90	48	30	180
17	〃	〃 [c16]	〃	80	53	20	150

a) Used as 200 cc. aqueous solution in each experiments.
b) See Figs. 1, 2 and 3.
c) Recovered $Cu(NO_3)_2$ charged c5), c8), c9) and c16) mean recovered ones in Exps. No. 5, 8, 9 and 16 respectively.
d) Measured at 20°C before heating the vessel.

1) T. E. Jordan, *Ind. Eng. Chem.*, **44**, 332 (1952).
2) D. Jercher, *Chem. Ber.*, **88**, 156 (1955).
3) U. S. Pat. 2524957 (1950).
4) U. S. Pat. 2552268 (1951).

Table II. Results of experiments in Table I

Exp. No.	O_2 Consumed moles	mol. ratio O_2/MEP	CO_2 Produced moles	mol. ratio CO_2/MEP	Cupric Isocinchomronate moles×2[a],	yield[b] %	ICA Yield[b] %
1	Not charged		0.18	1.2	Not charged		87
2	〃		0.17	1.1	〃		40
3	〃		0.19	1.3	〃		7
4	〃		0.20	1.0	〃		0
5	0.70	4.7	0.13	0.9	0.133	89	84
6	0.76	5.1	0.12	0.8	0.127	85	80
7	0·68	4.6	0.20	1.3	0.138	92	87
8	0.83	4.2	0.18	0·9	0.179	90	85
9	0.75	3.8	0.22	1.1	0.174	88	83
10	0.76	〃	0.24	1.2	0.179	90	85
11	0.87	4.4	0.20	1.0	0.180	91	86
12	0.80	3.9	0.16	0.8	〃	〃	〃
13	0.74	3.8	0.25	1.3	0.177	90	85
14	0.82	4.2	0.24	1.2	0.182	92	87
15	0.84	4.3	0.23	〃	0.181	〃	〃
16	1.27	〃	0.36	〃	0.278	94	88
17	1.25	4.2	0.33	1.1	0.279	〃	〃

a) 1 mol. of cupric salt is prepared from 2 mol. of MEP
b) Based upon consumed moles of MEP

Table III. Formation of ICA from its cupric salt

Exp. No.	Aqueous soln. of NaOH Concn. of NaOH % by wt.	gr.	Mol. ratio NaOH/ICA	Conditions Temp. °C	Duration hr.	ICA Moles	Yield[a] % by wt.
1	10	300	4.9	95	1.0	0.141	93
2	〃	200	3.3	〃	〃	0.143	94
3	〃	100	1.6	〃	〃	0.064	42
4	〃	〃	〃	〃	3.0	0.053	35
5	5	400	3.3	〃	1.0	0.145	95
6	〃	300	2.5	〃	〃	0.143	94
7	〃	〃	〃	75	〃	0.144	95

a) Based upon the cupric salt consumed, and in each Exp. 0.076 mol. (30.0 g.) of the cupric salt was used.

autoclave, where oxygen was diluted to less than 60% by volume with nitrogen. In some experiment, oxygen was not charged, in order to compare their results with that of other experiments, in which oxygen was used. The vessel was heated and its temperature was kept at 180~230°C, until oxygen was sufficiently absorbed to the oxidate and its pressure stopped dropping.

After the vessel was cooled to room temperature, the content of oxygen and carbon dioxide in the blowing gas was measured. The reaction product was filtered, where the deposit obtained was submitted to elementary analysis after being washed with water and dried in an air oven.

A certain quantity of the deposit was mixed and stirred with hot alkali aqueous solution, and copper was filtered off as cupric oxide from the solution.

Sodium salt of ICA (very soluble in water) formed in the filtrate was neutralized with concentrated aqueous hydrochloric acid, and white deposit liberated at pH 1.8~2.0, was also submitted to elementary analysis after being washed with water and dried in the air oven.

Results and Discussion

Reaction variables in the oxidation of MEP and their results were shown in Tables I and II respectively.

With no oxygen charged as in Exps. 1—4, the cupric salt of I.C.A. in the reaction product was not pure, being mixed with other cupric salts such cupric oxide, cupric hydroxide, and cupric nitrite.

Furthermore the yield of ICA fell markedly with decrease of cupric nitrate charged.

In Exps. 5—17 with oxygen used, the deposits obtained were uniformly found to be pure cupric isocinchomeronate (2 mol. of isocinchomeronate combined with 1 mol. of Cu^{2+}).

Found: C, 42.09; H, 2.22; N, 7.02; Cu, 16.25. Calcd. for $(C_7H_3O_4N)_2Cu$: C, 42.49; H, 2.04; N, 7.08; Cu 16.05%.

With decrease of cupric nitrate charged, the yield was not lowerd (always not less than

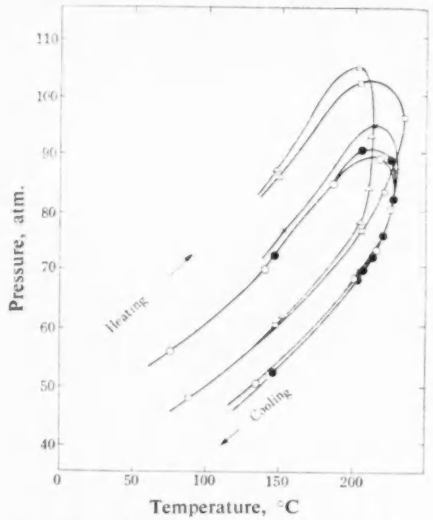

Fig. 1. Absorption of oxygen in the oxidation of MEP.
(Exp. Nos. 5—9) plotted per 30 min.
—○— No. 5 —△— No. 8
—×— 〃 6 —□— 〃 9
—●— 〃 7

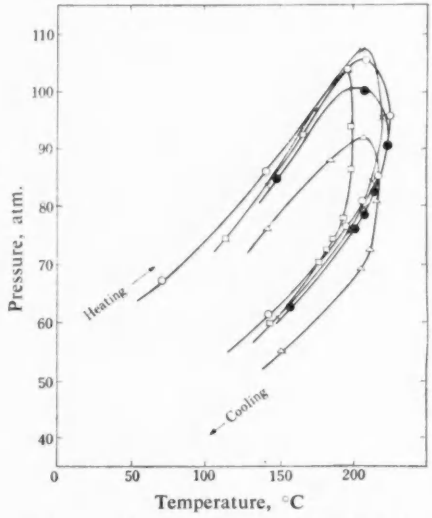

Fig. 2. Absorption of oxygen in the oxidation of MEP.
(Exp. Nos. 10—15) plotted per 30 min.
—○— No. 10 —△— No. 14
—×— 〃 11, 12 —□— 〃 15
—●— 〃 13

85 mol.% to MEP consumed), and any trace of nitrogen oxide or nitrogen dioxide was not detected in the reaction product and blowing gas. Cupric nitrate used was easily

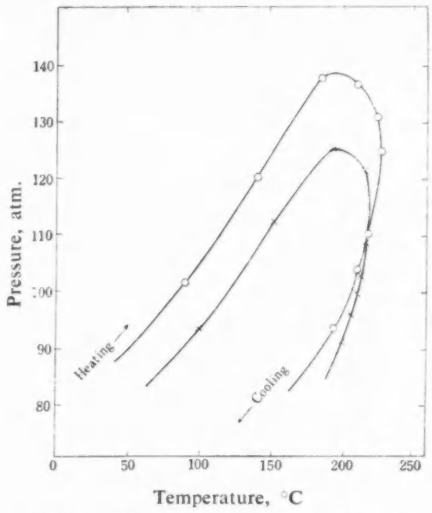

Fig. 3. Absorption of oxygen in the oxidation of MEP.
(Exp. 16 and 17) plotted per 30 min.
—○— No. 16 —×— No. 17

recovered by cupric oxide or cupric hydroxide being dissolved in the recovered filtrate and it was reused as in Exps. 7, 9, 10 and 17.

As shown in Figs. 1, 2 and 3, oxygen was absorbed at 180~230°C, where overheating was found to cause violent explosion. Molar ratio of oxygen consumed and carbon dioxide formed to that of MEP oxidized were approximately consistent to the theoretical values, 4.5 and 1.0 respectively. Based upon the results in Tables I, II and Figs. 1—3, the oxidation of MEP to cupric isocinchomeronate is considered to proceed as following;

$$C_2H_5(C_5NH_3)CH_3+9/2\,O_2+1/2\,Cu(NO_3)_2 \rightarrow$$
$$1/2(HOOC_5NH_3COO)_2Cu+3H_2O+CO_2+HNO_3$$

and oxygen only is consumed to oxidize MEP.

ICA prepared from its cupric salt, as shown in Table III, and its dimethyl ester melted at 237 and 164°C respectively, both of which agree with the values in the literature[5].

Isocinchomeronic acid in Table II.

Found: C, 49.98; H, 2.96; N, 8.34. Calcd. for $C_7H_5O_4N$: C, 50.34; H, 3.01; N, 8.38%.

The author is grateful to Dr. H. Sobue, Professor of Tokyo University, Dr. A. Tomita, Chief of the Laboratory Institute, and Dr. Y. Tsunoda for their valuable advice.

Laboratory Institute
Tokai Electrode Mfg. Co.
Fujisawa, Kanagawa-ken

5) Beilstein, Band 12, p. 154, 155.

*The Crystal Structure of p-Aminobenzenearsonic Acid**

By Akira SHIMADA

(Received August 6, 1960)

The crystal structure of benzenearsonic acid has recently been reported by the present author[1] to reveal the molecular configuration of an organoarsenic compound and the hydrogen-bond formation in this crystal. In connection with the above work, the crystal structure of *p*-aminobenzenearsonic acid, $H_2N \cdot C_6H_4AsO(OH)_2$, was undertaken as a part of a program concerned with the crystal chemistry of organoarsenic compounds.

This study has another interest, since the sodium salt of this acid has always proved of great value in medicine under the name of "Atoxyl".

Experimental

Suitable crystals for X-ray work were selected from the specimens kindly prepared and supplied by Professor H. Nakata of Konan University. They were colorless, transparent needles with a long dimension in the *b* direction. Oscillation and Weissenberg photographs were taken with Cu K_α radiation, and they showed that the unit cell is monoclinic with the following dimensions:

a=7.35 Å, b=6.35 Å, c=8.81 Å, and β=101°

It was already shown by Gilta[2] that this crystal belongs to the monoclinic system with the axial ratios, $a:b:c=1.162276:1:1.393499$, and the monoclinic angle, $\beta=101°20'$. The axial ratios given above by the morphological method can be compared with, 1.157 : 1 : 1.387, the values derived by the X-ray measurement. Two formula units per unit cell results in a calculated density 1.786 g. cm^{-3}**.

The only extinction rule was found for $(0k0)$ with k odd, which indicates the probable space group $P2_1$ with the fact that a symmetry plane is not permissible, and this was confirmed in the course of the structure analysis. All the intensities were estimated visually with a calibrated scale, by making use of the mutiple-film technique. The data were recorded from small crystals [cross sections with rectangular dimensions; 0.18×0.11 mm. for $(h0l)$, and 0.09×0.21 mm. for $(0kl)$], and

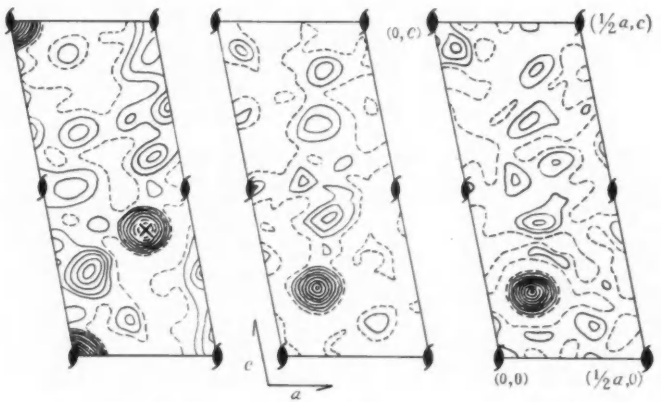

Fig. 1. (a) The Patterson projection, $P(UW)$, along the *b* axis, the rotation peak due to arsenic atoms being marked by a cross. Contours at arbitrary scale. (b) The minimum function, $M_2(XZ)$, derived from the rotation peak in Fig. 1a. (c) The electron-density projection, $\rho_1(XZ)$, for comparison with $M_2(XZ)$ in Fig. 1b. Contours at arbitrary scale.

* The major part of this paper was read at the 13th Annual Meeting of the Chemical Society of Japan, Tokyo, April, 1960.

1) A. Shimada, This Bulletin, **32**, 309 (1959); A. Shimada, ibid., **33**, 301 (1960).

2) G. Gilta, *Bull. soc. chim. Belges*, **32**, 19 (1923).

** The density was measured to be 1.9571 g. cm^{-3} by Lorenz and Schmidt (*Z. anorg. u. allgem. Chem.* **112**, 269 (1920)), and the author obtained the value of 1.85 g. cm^{-3} by floatation in bromoform and carbon tetrachloride mixture. These observed values are higher than the calculated value, but it seems certain that the unit cell contains two formula units.

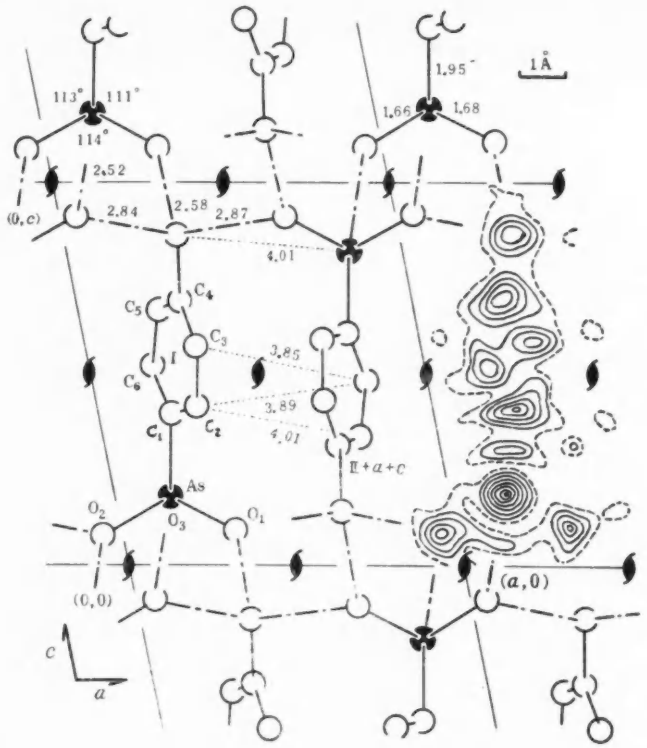

Fig. 2. The structure and the electron-density projection along the *b* axis, with bond angles, intra- and intermolecular distances (Å). Contours at intervals of $2\,e\,Å^{-2}$, starting at $2\,e\,Å^{-2}$ (broken lines), except the arsenic atom, where contours are at intervals of $10\,e\,Å^{-2}$. Dot-dash lines indicate hydrogen bonds.

no absorption corrections were applied. The corrections for polarization and Lorentz factors were made in the usual way.

Structure Determination

The structure has been determined by making use of the heavy atome technique. The Patterson projection $P(UW)$ onto the (010) plane was first synthesized, because the b axis is the shortest and the projection of the structure has a center of symmetry. This Patterson projection $P(UW)$, as shown in Fig. 1a, seemed to give some clues to the outline of molecules due to vectors from the heavy arsenic atom to the lighter atoms in addition to the location of the arsenic atom due to the large rotation peak near the origin. Consequently, we set up the minimum function $M_2(XZ)$ based upon this rotation peak. At the same time, the electron-density projection $\rho_1(XZ)$ was synthesized, the Fourier terms being the observed structure amplitudes whose signs were determined only by the coordinates of an arsenic atom. It will be seen that there is a good correspondence between $M_2(XZ)$ and $\rho_1(XZ)$ as shown in Figs. 1b and 1c, and they are sufficient to give the approximate coordinates of lighter atoms. With these maps as a start, a sequence of electron-density projections were synthesized to make clear all of the atomic positions except hydrogen atoms.

Although the projection onto (100) plane has no center of symmetry, the electron-density projections were constructed by the successive refining, referring to the Patterson projection onto (100) plane and the refined electron-density projection onto (010) plane. The final electron-density projections are shown in Figs. 2 and 3, and the final coordinates are listed in Table I, being refined by the difference syntheses at later stages.

In the calculation of structure factors, McWeeny's scattering curves[3] for nitrogen

3) R. McWeeny, *Acta Cryst.*, **4**, 513 (1951).

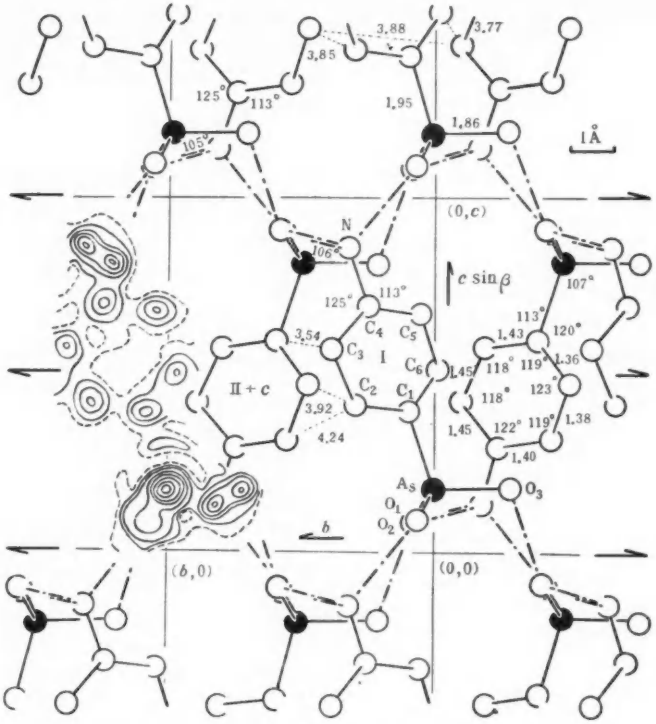

Fig. 3. The structure and the electron-density projection along the a axis, with bond angles, intra- and intermolecular distances (Å). Contours at intervals of $2\,e\,Å^{-2}$, starting at $2\,e\,Å^{-2}$ (broken lines), except the vicinity of the arsenic atom, where contours above $6\,e\,Å^{-2}$ are at intervals of $10\,e\,Å^{-2}$. Dot-dash lines indicate hydrogen bonds.

Table I. Atomic coordinates

Atom	x/a	y/b	z/c
As	0.163_2	0	0.183_1
O_1	0.338	0.063	0.093
O_2	−0.041	0.078	0.086
O_3	0.156	−0.293	0.185
C_1	0.213	0.093	0.398
C_2	0.299	0.295	0.418
C_3	0.331	0.386	0.572
C_4	0.298	0.254	0.698
C_5	0.234	0.047	0.675
C_6	0.184	−0.028	0.523
N	0.327	0.318	0.863

atom, of "valence states" for carbon atom and of $1/3(f^{\parallel}+2f^{\perp})$ for oxygen atom were used, while the scattering curve given by Berghuis et al.[4] was used for arsenic atom. An isotropic temperature factor was estimated to be $2.7\,Å^2$ for all atoms. R indicates for the final coordinates were 13.0 and 14.9% for $(h0l)$ and $(0kl)$ respectively, excluding terms too weak to be observed. The comparison of observed structure factors with calculated ones is shown in Fig. 4.

4) J. Berghuis, I. M. Haanappel, M. Poters, B. O. Loopstra, C. H. MacGillavry and A. L. Veenendaal, ibid., 8, 478 (1955).

Description of the Structure

The general nature of the structure is shown in Figs. 2 and 3, which are b and a axis projections for this crystal. The arsenic atom is surrounded by a group consisting of three oxygen atoms, O_1, O_2 and O_3 of the arsonic acid and one carbon atom C_1 of the benzene ring. The average As–O distance is 1.73 Å, and the As–C distance is 1.95 Å. The disposition of bonds from the arsenic atom appears to be nearly tetrahedral, the angles between the bonds being abnut 109°. The benzene ring is planar and the average distance between adjacent carbon atoms is 1.41 Å, individual values ranging from 1.36 to 1.45 Å. The N–C distance is 1.49 Å and the nitrogen atom is found to lie on the plane of a benzene ring

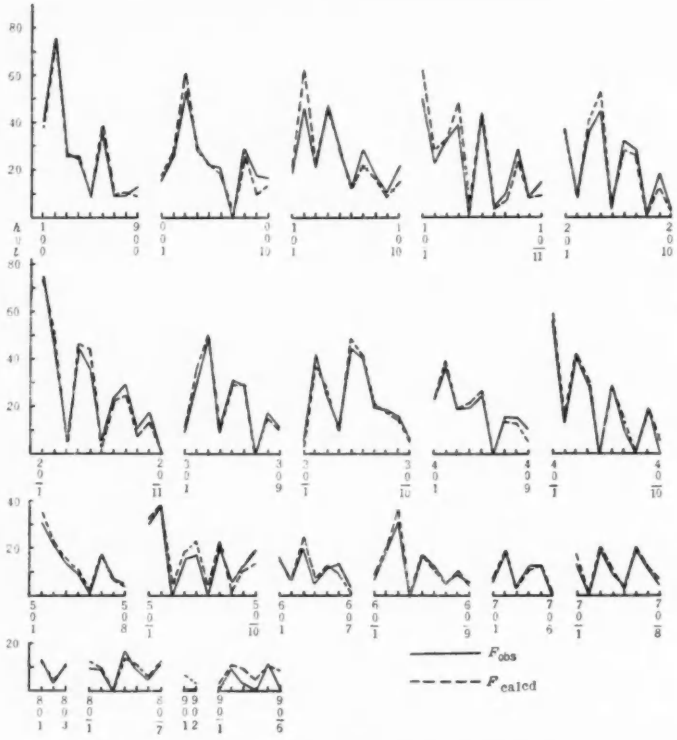

Fig. 4. (a) Comparison of observed and calculated structure factors, F($h0l$).

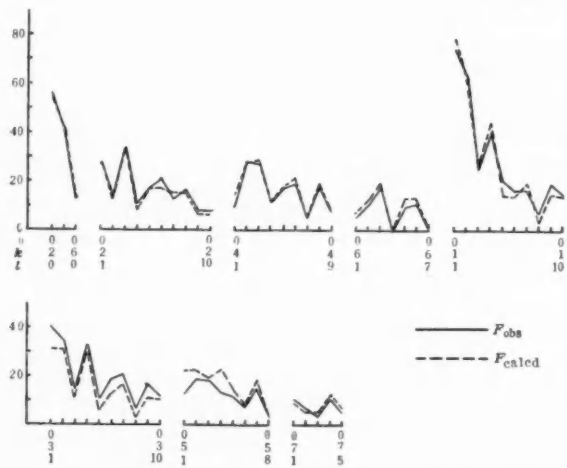

Fig. 4. (b) Comparison of observed and calculated structure factors, F($0kl$).

within the limit of experimental error.

The molecules are held together by a beautiful network of hydrogen bonds. These are four hydrogen atoms available for hydrogen bonding in an asymmetric unit. Two of them come from the *p*-amino group, two come from the arsonic group. There is one hydrogen bond between oxygen atoms and there are three hydrogen bonds between oxygen and nitrogen atoms. The hydrogen bond, with a length 2.52 Å from the atom O_2 of molecule I to the atom O_3 of molecule II, links molecules with each other to form endless chains along the screw axis perpendicular to the (010) plane. The nitrogen atom in the *p*-amino group of the molecule I forms three hydrogen bonds, the first with a length 2.84 Å to the atom O_2 of the molecule II$+c$ (molecule displaced by the unit vector c), the second with a length 2.58 Å to the atom O_1 of the molecule I$+c$, and the third with a length 2.87 Å to the atom O_1 of the molecule II$+a+c$. These three hydrogen bonds connect the endless chains through benzene rings to form a three dimensional net work. This triple hydrogen-bond formation of a nitrogen atom will suggest that one of hydrogen atoms is transferred from an arsonic acid group to the *p*-amino group. On this basis, the formula of the molecule should be written as $NH_3^+ \cdot C_6H_4 \cdot AsO_2(OH)^-$, which indicates that the molecule is in the zwitterion form in the crystal. This conclusion will be supported by the fact that this acid is strictly monobasic[5].

There is no seriously short van der Waals contact in this structure. The shortest distance between nighboring molecules, 3.51 Å, is found between the atom O_2 of the molecule I and the arsenic atom of the molecule II. There is also a contact at 3.54 Å between the atom O_1 of the molecule I and the atom C_1 of the molecule II$+a+c-b$. The shortest contact between adjacent benzene rings occurs at 3.54 Å between the atom C_1 of the molecule I and the atom C_3 of the molecule II$+a+c-b$. Other intermolecular distances exceed 3.55 Å. A comparison of this structure with that of the benzenearsonic acid is interesting. They are closely similar in having endless chains formed by the hydrogen bonds between arsonic acid groups, while in *p*-aminobenzenearsonic acid there are additional hydrogen bonds to connect these chains. This difference in mode of packing will explain why the crystal of *p*-aminobenzenearsonic acid has no cleavage, in contrast to that of benzenearsonic acid which shows cleavages along endless chains.

The author wishs to express his sincere thanks to Professor I. Nitta and Professor T. Watanabé of Osaka University for their helpful advice, and to Professor H. Nakata of Konan University for supplying the specimens.

Department of Chemistry
Faculty of Science
Osaka City University
Kita-ku, Osaka

5) A. E. Goddard, "A Text-book of Inorganic Chemistry", Vol. XI., Part II, Charles Griffin and Co., London (1930), p. 179.

Mass Spectrometric Study on Adsorption of Water Vapor on a Graphite Surface

By Hokotomo Inouye

(Received September 17, 1959)

Although it is of interest in connection with the study of the adsorption of gas on a solid surface to know what sorts of ions are formed by electron bombardment at the surface, there are few mass spectrometric studies on the subject.

By electron bombardment at surface, ions are formed both on the surface and in the gas phase. Therefore, it is important to distinguish the ions which are formed from adsorbed molecules on the surface from those formed simultaneously in the space adjacent to the surface. For this purpose the author has devised a method to know places of formation of ions by analyzing their peak shapes obtained by means of a single focusing mass spectrometer with a modified ionization chamber.

Plumlee and Smith[1] found that O^+ was

1) R. H. Plumlee and L. P. Smith, *J. Appl. Phys.*, 21, 811 (1950).

emitted from an electron-bombarded molybdenum surface by means of a mass spectrometer with the ionization chamber of special structure. However, the author's method may be simpler and give more precise results than Plumlee's method.

The results obtained by application of the author's method to the ions formed by electron bombardment at a graphite surface covered with adsorbed water vapor are described below.

Experimental

In Fig. 1 is shown the schematic diagram of the mass spectrometer used in the present work. The

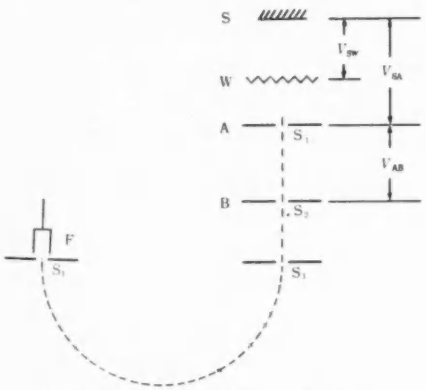

Fig. 1. Schematic diagram of the mass spectrometer.

repeller is replaced by a solid surface, S, to be studied. A hot filament, W, for an electron source is placed between S and the drawing-out electrode, A. Thermoelectrons emitted from W are accelerated by a potential difference V_{SW} and strike S, forming ions on the surface and also in the space between the surface and the place where the potential corresponds to the ionization potential of a gas molecule. A part of these ions is drawn out of the slit S_1 of A by a definite potential difference V_{SA} and is accelerated by the variable potential difference V_{AB} for voltage scanning. Ions formed at different places in the ionization chamber, even if they have the same m/e, acquire different energies from V_{SA}, and hence, for scanning all of them, V_{AB} should be varied over a certain range. Thus the peak shape of the ions will be determined by their distribution in the ionization chamber.

Peak Shape of the Ions Formed on the Surface.—If all the ions of one kind are emitted from the surface with zero initial kinetic energy, the only value, ${}_{S}V_{AB}$, of V_{AB} will be sufficient to bring the ions to the exit slit, S_4, of the analyzer. The peak shape will be a symmetrical one characteristic of the instrument (Peak 1). Now, let V_s be the total accelerating potential ($V_{SA}+{}_{S}V_{AB}$) for the apex of this peak.

If the ion has a certain initial kinetic energy V_0 and the angle between its direction and the normal to the surface is θ, V_{AB} bringing the ion to S_4 is ${}_{S}V_{AB}-V_0\cos\theta$, since it has the energy of $V_{SA}+V_0\cos\theta$ at S_1. As the directional divergency of the ion beam at S_3 is small owing to the geometry of the instrument, the position of the peak apex can be determined only by the energy divergency, or the distribution of θ, among the ions passing through S_3. Some ions formed even with great values of θ are able to enter the analyzer through S_3. The value of θ of the most abundant ions in this distribution is assumed to be θ_m. Then the peak apex will move from V_s by $V_0\cos\theta_m$ towards the lower potential side on the potential axis representing $V_{SA}+V_{AB}$. The peak shape also depends on the directional distribution of the ions at formation and on the geometry of the instrument. Generally, the peak width is broader than that of the ions with zero initial kinetic energy (Peak 2).

If the magnitude of the initial kinetic energy extends over a certain range, this distribution will also affect the position and shape of the peak.

Peak Shape of the Ions Formed in the Gas Phase.—If the energy of an electron emitted from W becomes equal to the ionization potential J of a gas molecule at P on the way to S, the molecule in the space between P and S will be ionized by a collision with the electron. The number of ions formed per unit volume, the unit electronic current and the unit time is given by the product of the ionization probability and the density of the gas molecules. Ionization probability increases with the increasing energy of the incident electron and decreases after reaching the maximum. Therefore, the number of the ions formed along the electron path increases from zero at P up to the maximum at S, provided that the applied accelerating potential V_{SW} of the electron is higher than J and lower than the value corresponding to the maximum probability.

Even if the ions thus formed are supposed to have zero initial kinetic energy, they acquire different energies from V_{SA} according to the places of their formation; thus, a wide range of V_{AB} is necessary for scanning all of them. When V_{AB} is equal to ${}_{S}V_{AB}$ the ions formed just before S can arrive at S_4, and at greater values of V_{AB} those formed at places distant from S arrive at S_4. The amount of the ions formed just before S is maximum, and it decreases as the distance of the place of the

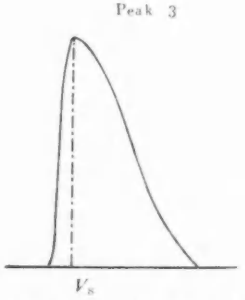

Fig. 2. Peak of the ions formed in the gas phase.

ion formation from S increases. Therefore, the peak has its apex at V_S, and its slope at the higher potential side is more gentle than that at the lower potential side as shown in Fig. 2 (Peak 3).

If V_{SW} is higher than the value corresponding to the maximum probability, the place of the maximum ion formation moves from the surface toward P. So the apex moves from V_S toward the higher potential side (Peak 4 in Fig. 3).

If the ions have some initial energies, the peak will be broadened also toward the lower potential side similarly to Peak 2, provided that any ion striking upon the surface underwent an elastic reflection. It may, however, be difficult to distinguish this peak from Peak 3.

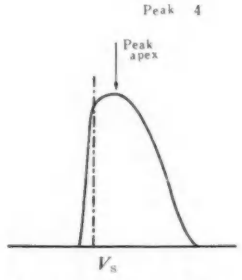

Fig. 3. Peak of the ions formed in the gas phase at V_{SW} exceeding the value correspondi.g to the maximum ionization probability.

Peaks of the Ions Formed Both on the Surface and in the Gas Phase.—If an adsorbed gas is ionized in the gas phase after desorption as neutral molecules or atoms, the peak of the ions will have a shape quite similar to Peak 3. However, it is able to be distimguished from the peak of the ions due to the molecules originally present in the gas phase, because for the former peak the height is proportional to the square of the electronic current but for the latter it is directly proportional to the electronic current[2].

If the adsorbed gas is removed not only directly as ions from the surface but also as neutral molecules or atoms giving the ions of the same m/e afterwards, two kinds of peaks will result either from superposition of Peaks 1 and 3, or from that of Peaks 2 and 3.

(A) All the ions of the same m/e formed on the surface and in the gas phase are supposed to have no initial kinetic energy. Since Peak 1 is obtained for the former and Peak 3 for the latter, the observed peak will be one that results from superposition of both peaks as shown in Fig. 4 (Peak 5).

If V_{SW} higher than the value corresponding to the maximum ionization probability is applied, the observed peak has a shape such as is shown in Fig. 5 (Peak 6), since Peak 4 takes the place of Peak 3 in Fig. 4. Thus, detection of the ions formed on the surface will become easier.

2) Y. Ohta, *J. Chem. Soc. Japan, (Nippon Kwagaku Kwaisi)*, **64**, 849, 986 (1943).

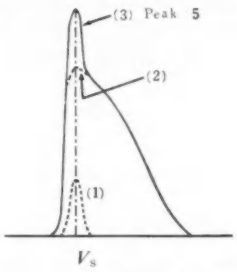

Fig. 4. Peaks of the ions of the same m/e formed simultaneously on the surface and in the gas phase with no initial kinetic energy. (1): peak of the ions formed on the surface, (2): peak of the ions formed in the gas phase, (3): the compounded peak of 1 and 2.

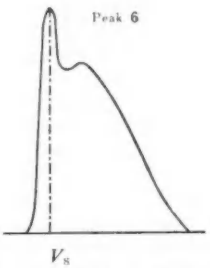

Fig. 5. Peak of the ions of the same m/e formed simultaneously on the surface and in the gas phase by application of V_{SW} higher than the value corresponding to the maximum ionization probability.

(B) If the ions formed on the surface have a fairly high initial kinetic energy but those formed in the gas phase have little, Peak 2 is obtained for the former and Peak 3 for the latter. The compounded peak is such as is shown in Fig. 6 (Peak 7). However, in some cases this peak may be indistinguishable from Peak 2 or Peak 5.

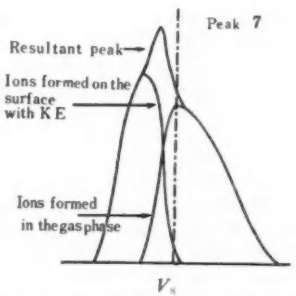

Fig. 6. Peak of the ions formed simultaneously on the surface with an initial kinetic energy and in the gas phase without initial kinetic energy

As described above, the shapes of ion peaks are different from one another according to the places of their formation and to the presence of the initial kinetic energy. From the shape of the peak one may be able to know the place of formation of the ions and also, though not so exactly, to estimate their initial kinetic energy.

Experimental Results

Ions found in the present work have m/e of $1(H^+)$, $2(H_2^+)$, $17(HO^+)$, $18(H_2O^+)$, $28(CO^+)$, and $183\sim186$. The peaks of these ions are shown in Figs. 7—12. Besides them a group of ions which is supposed to be formed from grease vapor is found.

1) H_2O^+ and HO^+.—As the peak of H_2O^+ has a similar shape to Peak 3 in Fig. 2, this ion is supposed to be formed in the gas phase.

The peak shape of HO^+ appears to be similar to Peak 7 rather than to Peak 3. Thus, some of them may be formed on the surface with kinetic energy. However, for the present, HO^+ is supposed to be formed only from water molecules in the gas phase, owing to the fact that the observed relative intensity of HO^+ to H_2O^+ is not greatly different from the result, i.e., 1:4 which Tate and others[3] have obtained on water vapor by voltage scanning, and that it is difficult because of their low intensity to judge certainly whether the peak is similar to Peak 7 or not.

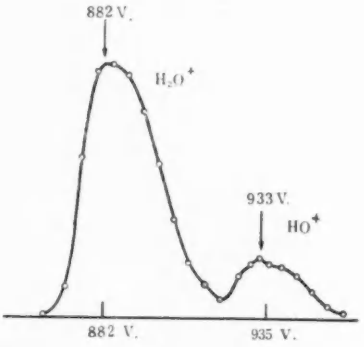

Fig. 7. H_2O^+ and HO^+. Figures on the potential axis indicate the normal position of the peak apex of the ion.

No measurement has yet been carried out to certify whether these ions are due to residual water vapor or due to the molecules desorbed by electron bombardment.

2) H_2^+.—As shown in Figs. 8 and 9, the peak shape is similar to Peak 5 in Fig. 4 when V_{SW} is 50 V. and to Peak 6 in Fig. 5 when it is 100 V. The ions are supposed to be formed both on the surface and in the gas phase and neither of them is supposed to have any initial kinetic energy.

3) M. M. Mann, A. Hustrulid and J. T. Tate, *Phys. Rev.*, 58, 340 (1940).

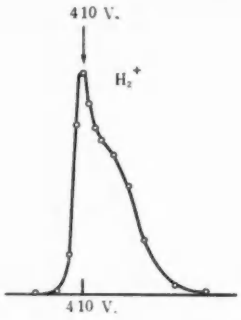

Fig. 8. H_2^+ when V_{SW} is 50 V.

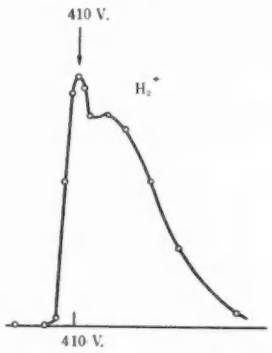

Fig. 9. H_2^+ when V_{SW} is 100 V.

3) H^+.—As the peak has a similar shape, as shown in Fig. 10, to that of Peak 7, the ions are formed both on the surface and in the gas phase, and, at least, those formed on the surface seem to have a certain initial kinetic energy.

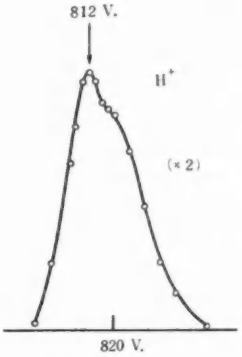

Fig. 10. H^+.

The position of the peak apex of Fig. 8 corresponds to the total accelerating potential of H_2^+ leaving the surface without initial kinetic energy. From the value, 410 V., for the apex of H_2^+, the position of the apex of H^+, peak is calculated to be 820 V., whereas the observed value is 812. Hence, it is shifted by 8 V. towards the lower potential side. This shift will be due to the initial kinetic energy of H^+ from the surface.

Now, if the peak of the ions formed in the gas phase is assumed to be curve 1*1 of Fig. 11 and is deducted from the observed curve 3, then curve 2 will result. This curve corresponds to the peak of the ions leaving the surface with initial kinetic energy, the value of which is calculated*2 from the position of the apex to be 10 V.*3

4) CO^+.—Ions of m/e 28 correspond to CO^+ or N_2^+, but they are concluded to be CO^+ and not N_2^+, since N^+ (m/e 14) has not been found.

From the peak shape these ions are considered to consist of those formed in the gas phase and of those leaving the surface with kinetic energy, the value of which, however, would be small.

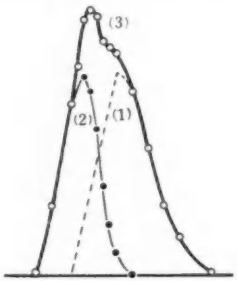

Fig. 11. H^+ peak divided into the component peaks.

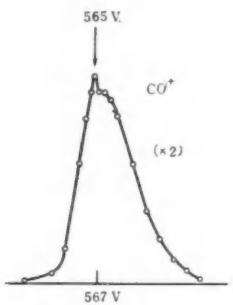

Fig. 12. CO^+.

5) Ions of m/e 183~186.—The behavior of this group of ions is very different from that of any other ion, and hence they are not supposed to be grease vapor ions but possibly W^+ which is produced by electron impact on tungsten vapor evaporating from the heated tungsten filament for the electron source. However, they have not yet been confirmed as such, because the resolving power of the instrument is not sufficient to determine exactly of what m/e of ions they consist.

Consideration

Despite the fact that hydrogen and carbon monoxide were not introduced into the apparatus on purpose, it was found that H_2^+, H^+ and CO^+ were formed both on the surface and in the gas phase. Therefore, these ions must be formed from the water vapor adsorbed on graphite.

According to the results obtained by the thermal method on adsorption of water vapor on a carbon surface[4,5], H_2 will be desorbed from the surface even at room temperatures, and the gas removed from the surface at lower temperatures containing CO_2 and a smaller quantity of CO. At higher temperatures CO is increased. These facts are considered to suggest that the reaction of water with carbon gives adsorbed H_2 and two types of surface oxides of carbon; one that readily decomposes even by evacuation at room temperatures to give CO_2 and the other that is more stable and decomposes at higher temperatures with evolution of CO.

Thus, formation of H_2^+ and other ions both on the surface and in the gas phase may be interpreted as follows:

By electron bombardment upon the graphite surface covered with adsorbed water vapor, some of the adsorbed H_2 molecules may leave the surface directly as H_2^+, and others give H_2^+ in the gas phase by successive electron impact after desorption as neutral gaseous molecules. H_2^+ formed in the gas phase does not possess initial kinetic energy. Also H_2^+ directly leaving the surface will not have initial kinetic energy if the potential curves of the adsorbed H_2 molecules are not very different from those of gaseous H_2 molecules.

If the more stable surface oxide is assumed to take a configuration such that CO rather

*1 In the curve (1) the peak width due to the instrument is taken into consideration.

*2 As the θ distribution of the amount of the ions passing through S_3 is unknown, the amount of the ions emitted along the axis of the slit system is assumed to be maximum ($\theta_m=0$).

*3 Several possible peaks were tried as curve (1), but always 10 V. was obtained.

4) R. N. Smith, C. Pierce and C. D. Joel, *J. Phys. Chem.*, **58**, 298 (1954).

5) P. H. Emmett, *Chem. Revs.*, **43**, 69 (1948).

than O is adsorbed on the surface after the apparatus is sufficiently evacuated, it can be removed as CO or CO^+ by electron bombardment.

H^+ formed in the gas phase may originate from H_2 or H leaving the surface by electron bombardment and, in addition, from gaseous water molecules and grease vapor. However, most of them are probably due to dissociative ionization of H_2 or ionization of H, since the contribution of H^+ from the last two origins to the total H^+ current is small.

H^+ from the surface may also be due to the adsorbed H_2 which resulted from water adsorbed on the graphite surface.

According to the potential curves of higher energy states of H_2 molecules, there is the state of unstable H_2^{2+} at 46 V. higher than the normal state, and this H_2^{2+} gives two H^+'s, each with kinetic energy of about 7 V., after spontaneous dissociation. Also at 28 V. higher, there is the unstable $^2\Sigma_u$ state of H_2^+. It is dissociated into H and H^+, each with kinetic energy of about 5 V. Increased energy of the incident electrons can increase this energy up to about 7 V.[6].

If the electronic states of the adsorbed H_2 are not greatly different from those of the gaseous molecule, there is sufficient possibility of transition of the adsorbed H_2 to unstable H_2^+ or H_2^{2+}, because the energy V_{sw} of the incident electrons is at least 50 V. When these unstable molecular ions are dissociated, if it is assumed that only one H^+ leaves the surface and the other H^+ or H is bound to the surface, the leaving H^+ will carry all of the initial energy of 10~15 V. for two particles.

Such being the case, and taking into consideration the presence of the directional distribution at formation, the presence of H^+ leaving the surface with kinetic energy of about 10 V. will, at least qualitatively, be explainable.

It has also been supposed that some of surface oxides formed from adsorbed water on a graphite surface might have OH-radicals[1]. If that is the case, formation of HO^+ on the surface will be possible. However, it was not confirmed in this work as mentioned in Experimental Results 1).

6) H. S. W. Massey and E. H. S. Burhop, "Electronic and Ionic Impact Phenomena", Oxford University Press (1952), p. 231.

Summary

Peak shapes in mass spectra obtained by voltage scanning using a mass spectrometer with such a modified ionization chamber as that described above are characterized by the places of formation and the initial kinetic energy of the ions. Thus, from the shape of the peak, one may be able to decide the place of formation of the ions and, though not so precisely, to estimate their initial kinetic energy.

When the method was applied to the ions formed by electron bombardment at a graphite surface covered with adsorbed water vapor, it was found that (1) H_2O^+ and HO^+ were formed from residual or desorbed H_2O only in the gas phase, (2) H_2^+, H^+ and CO^+ were formed both on the surface and in the gas phase, and (3) H^+ which formed on the surface had the initial kinetic energy of about 10 V. These results will confirm the fact that the adsorbed water molecule is dissociated into adsorbed H_2 and surface oxide of carbon that probably takes a configuration such that CO is adsorbed on the surface.

The author wishes to express his hearty thanks to Professor Nobuji Sasaki of Kyoto University for his guidance throughout the course of this work.

Department of Chemistry
Faculty of Literature and Sciences
Kochi University
Kochi

*Kolbe's Reaction of Higher Fatty Acids. II. Electrolysis of Lauric Acid by a Pulsating Current with an Artificial Graphite Anode**

By Ryoichi MATSUDA, Takeo HISANO and Daishiro KUBOTA

(Received August 27, 1960)

In the previous paper[1] a study of electrolysis of lauric acid was reported with respect to the relation between the current efficiency of Kolbe's reaction and the anodic current density as well as the alkalinity of the electrolyte, and it was thereby conculded that nickel anode behaved almost similarly to platinum one towards Kolbe's reaction of lauric acid. In connection with the above mentioned result it was undertaken to study behaviors of other anode materials concerning the electrolysis of lauric acid in the present paper.

In Exp. 1 artificial graphite, lead, tantalum, molybdenum, tungsten and iron anodes were employed for electrolysis by direct current, but none of these anodes gave rise to Kolbe's reaction of lauric acid. Accordingly a pulsating current was applied instead of a direct current with the same anodes as those mentioned above, and it was found that only the artificial graphite anode was suitable for Kolbe's reaction. The other anodes were not desirable, being either unable to get the current flow or dissolved partly or entirely in the electrolyte solution. In Exp. 2 the effect of the anodic current density of the pulsating current upon the current efficiency of Kolbe's reaction in the electrolysis with an artificial graphite anode was studied, and comparison was made with the corresponding case employing direct current reported in the previous paper. Exp. 3 dealt with the effect of alkalinity of the electrolyte on the current efficiency of Kolbe's reaction and the result was compared with the corresponding case of the previous paper to discuss the mechanism of Kolbe's reaction.

Experimental

The electrolytic vessel was the same as described in the previous paper. Four electrolytic solutions were prepared, each of them containing 1 mol. lauric acid and different portion of potassium hydroxide in a mixture of 800 cc. ethanol and 550 cc. water: thus solutions A, B, C and D contained 0.25, 0.5, 0.75 and 1.00 mol. potassium hydroxide respectively and 1 mol. lauric acid. Each electrolysis was conducted with 40 cc. electrolyte at 40°C. In each case 2200 coulombs of either direct or pulsating current were supplied, this quantity of electricity being nearly 90% of that electrochemically equivalent to the lauric acid present in the solution. The pulsating current was generated by a mercury filled Tunger rectifier, and consisted of half-waves of an approximately perfect sinnusoidal curve. The frequency was 60 cycles per second.

Results and Discussion

Experiment 1.—Artificial graphite, lead, tantalum, molybdenum, tungsten and iron were used as anode to investigate the influence of anode material on Kolbe's reaction. The anode was a square plate 1×1 cm. except that of tungsten having a spiral form made of a wire 0.5 mm. of diameter and 15 cm. long. The cathode in each case was a square plate with the effective surface area ten times as large as the anode, and stood face to face with the latter. The anodic current density was 0.4~1.0 amp./cm². The result is summarised in Tables I and II.

Table I. Behaviors of various anodes in the electrolysis with direct current

Anode	C	Pb	Ta	Mo	W	Fe
Cathode	C	Pb	Ni	Ni	Ni	Fe
Current	none	none	none	flow	flow	flow
Kolbe's reaction	none	none	none	none	none	none

Table II. Behaviors of various anodes in the electrolysis with pulsating current

Anode	C	Pb	Ta	Mo	W	Fe
Cathode	C	Pb	Ni	Ni	Ni	Fe
Current	flow	flow	none	—	flow	flow
Kolbe's reaction	partly occurred	none	none	—	none	none

Graphite Anode.—The artificial graphite anode was coupled with a cathode of the same material. When direct current was applied through the circuit, its intensity decreased with unexpected rapidity, e. g., the initial amperage of 80 m amp. decaying to 5 m amp. in ten minutes. No appreciable change of the anode surface was observed during this period. When pulsating current was applied in place of direct current through the electrolyte which had just been treated with the latter, a stationary current was observed at 3 V. A fresh solution was then electrolyzed with pulsating current, and 0.87 g. docosane was obtained with a small amount of alcohol. The content of the vessel after electrolysis was heated with potassium carbonate and filtered. The precipitate was made alkaline with potassium carbonate solution and extracted with ether. The ethereal extract was concentrated and distilled under

* D. Kubota's graduation thesis at Tokushima University.

1) T. Mizuta, T. Hisano and R. Matsuda, This Bulletin, 33, 700 (1960).

reduced pressure, and the resulted 0.75 g. of the fraction with K_7=110~130°C was tested by diazo and Bittre color reactions. By both reactions the alcohol was detected. The anode surface was not changed in its appearance by either current. According to Kunugi[2] the use of the artificial graphite anode brought about 11~12% current efficiency of Kolbe's reaction when acetic acid was electrolyzed with direct current.

Lead Anode.—Direct current did not flow through the lead anode coupled with a lead cathode, neither changed the surface of the former electrode. However, by applying the pulsating current at 20~23 V., the current of 0.6 amp. was observed to pass, and the anode was entirely dissolved in the electrolyte solution after some thirty minutes.

Tantalum Anode.—The tantalum anode was coupled with a nickel cathode. Neither direct nor pulsating current flowed and no apparent change of the anode occurred.

Molybdenum Anode.—The molybdenum anode was entirely dissolved in the solution by direct current at 12~13.5 V.

Tungsten Anode.—The tungsten anode was coupled with a nickel cathode, and direct current flowed through it, but neither Kolbe's reaction nor any change of the anode occurred. Pulsating current flowed too, but it did not give rise to Kolbe's reaction.

Iron Anode.—Both direct and pulsating currents flowed through the iron anode which was coupled with an iron cathode. The anode was partly dissolved in the solution, but no Kolbe's reaction occurred. The reaction is, however, reported[2] to take place to a small extent when acetic acid is electrolyzed with the same anode as above mentioned by direct current.

Experiment 2. As the electrolysis by pulsating current with the artificial graphite anode was the only case which was found to be suitable for Kolbe's reaction in Exp. 1, the influence of current density upon the current efficiency was investigated under such condition as mentioned above. As shown in Fig. 1 the increase of current density of the pulsating current favored the current efficiency of Kolbe's reaction. Exp. 2 of the previous paper which dealt with the influenceof current density of direct current upon the current efficiency of Kolbe's reaction showed that there was a similar tendency. In comparing these two cases of electrolysis, however, it is to be born in mind that the solution of the present experiment is more concentrated with respect to potassium hydroxide than the other, and also that higher concentration with respect to the alkali is disadvantageous to the current efficiency of Kolbe's reaction irrespective of the nature of the current. In dealing with the current density of the artificial graphite anode itsporosity has to be taken into consideration.

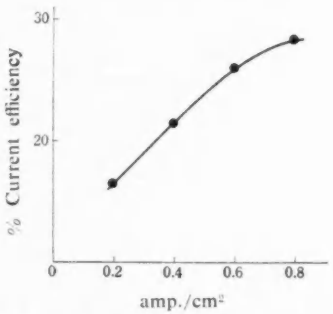

Fig. 1. Influence of anodic current density of pulsating current on docosane production.

Experiment 3. The influence of alkalinity of the electrolyte solutions upon Kolbe's reaction with the artificial graphite anode by pulsating current was studied and the result is shown in Fig. 2.

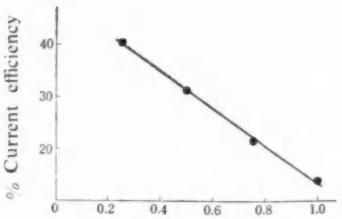

Fig. 2. Influence of alkalinity of solution on docosane production.

Corresponding cases with platinum and nickel anodes by direct current were described in the previous paper. When these two electrolyses are compared with the present case, it is seen that there is a common tendency between them that the current efficiency of Kolbe's reaction decreases linearly with increasing alkalinity. When the alkalinity is the highest one, the current efficiencies of the three cases are close to each other. With the decrease of alkalinity the current efficiency with the artificial graphite anode increases more slowly than the other two. At any rate it is evident that Kolbe's reaction of lauric acid has a close relationship with the alkalinity or the hydrogen ion concentration of the electrolyte solution. Matsuda[3] pointed out that there is an important relationship between Kolbe's reaction and hydrogen ion concentration when the aqueous solution of acetic acid is electrolyzed.

The authors wish to express their thanks to Nippon Oils and Fats Co., Ltd. who kindly offered them the lauric acid.

Department of Applied Chemistry
Faculty of Engineering
Tokushima University
Tokushima

2) T. Kunugi, *J. Electrochem. Soc. Japan (Denkikagaku)*, **20**, 208 (1952).

3) B. Matsuda, This Bulletin, **7**, 18, 297 (1932).

A New Method for the Preparation of Piperazines. I. Preparation of N-Mono-alkyl(-aryl)-piperazines

By Kazuo NAKAJIMA

(Received October 8, 1960)

For the preparation of piperazine and its derivatives a number of methods have been proposed up to the present by several investigators[1]. Because of the complexity and the poor yield, these methods still leave much to be desired. Many trials, therefore, have been made by the present author to find out a new convenient route to these compounds. And, after all, it was found that a compound of the general formula A gives a piperazine derivative B under the elimination of an ester C, when it is heated at 200~300°C, according to the following Eq. 1.

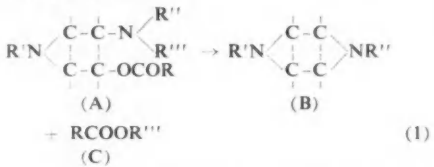

(A) (B) (C) (1)

In this equation, R′ and R″ represent alkyl, aralkyl, cycloalkyl, aryl or acyl groups which are destined to remain in the molecule of B after the fission. R‴ also may be an alkyl, aralkyl or cycloalkyl group (equal to or lower than R″), but neither aryl nor acyl group, for these groups are incapable of being removed as a part of the ester C. RCO– in A and in C is an acyl group, but, in fact, it is restricted to the easily available acetyl.

As can be seen from Eq. 1, this reaction seems to be quite a new type of reaction, i. e. the cyclization under the elimination of an ester*.

The actual procedure of this reaction consists in heating the compound A above 200°C, the conditions being arranged so that the ester C can be distilled over as it is formed during the heating, and in fractionating the resulting piperazine B under reduced pressure. Generally speaking from the data of the series of the experiments, the yields are fairly good.

The adequate selections of R′, R″ and R‴ in A make it possible to synthesize various compounds of piperazine-ring system.

As a part of synthetical works in the field of piperazines by the new route, synthesis of *N*-mono-alkyl(-aryl)-piperazines is dealt with in the present paper.

Synthesis of *N*-Mono-alkyl(-aryl)-piperazines.—The full course of synthesis of *N*-mono-alkyl-(-aryl)-piperazines (V) from *N*, *N*-disubstituted ethylenediamines (I) is represented by the following Eq. 2.

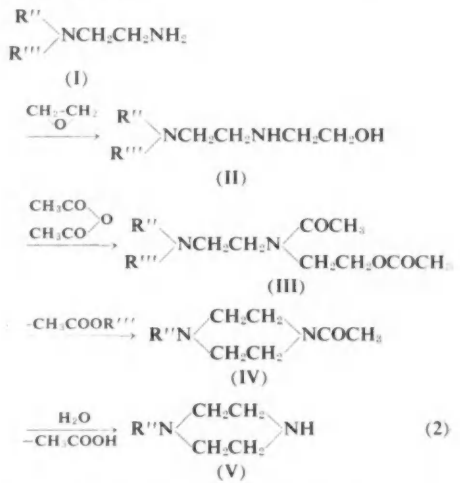

(I) (II) (III) (IV) (V) (2)

N, *N*-Disubstituted ethylenediamines (I)[2] are converted into *N*, *N*-disubstituted aminoethyl ethanolamines (II) by the action of ethylene oxide or ethylene chlorohydrin. In this reaction considerable quantities of *N*, *N*-disubstituted aminoethyl diethanolamines are formed, from which II can be isolated by fractionation under

1) D. S. Pratt and C. O. Young, *J. Am. Chem. Soc.*, **40**, 1428 (1918); W. B. Martin and A. E. Martell, ibid., **70**, 1817 (1948); T. S. Moore, H. Boyle and V. M. Thorne, *J. Chem. Soc.*, **1929**, 39; R. Baltzly, J. S. Buck, E. Lorz and W. Schön, *J. Am. Chem. Soc.*, **66**, 263 (1944), K. E. Hamlin et al., ibid., **71**, 2731 (1949); R. Baltzly, ibid., **76**, 1164 (1954); T. Ishiguro, E. Kitamura and M. Matsumura, *J. Pharm. Soc. Japan* (*Yakugaku Zasshi*), **73**, 1110 (1953); **74**, 1162 (1954); **75**, 1370 (1955).

* A similar type of reaction has also been found and will be discussed in detail later in a separate article.

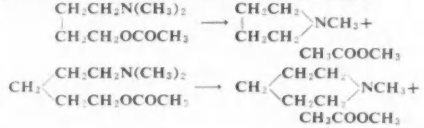

2) K. Nakajima, *J. Chem. Soc. Japan, Pure Chem. Sec.* (*Nippon Kagaku Zasshi*), **81**, 499, 961, 1131, 1477 (1960).

Table I. Properties of $HN\langle^{CH_2CH_2N(R'')R'''}_{CH_2CH_2OH}$

Comp. No.	R''	R'''	Phys. form (color)	M. p. °C	B. p., °C/mmHg† 10	20	50	100	760	N, % Found	Calcd.	Picrate M. p. °C	Platinichloride Dec. p., °C	Pt, % Found	Calcd.
1	CH_3	CH_3	Mob. l. (colorless)		80	97	118	135	205	21.02	21.19	200 (dec.)	214	35.67	35.99
2	C_2H_5	C_2H_5	〃		113	132	152	170	235	17.51	17.48	90	*		
3	n-C_3H_7	n-C_3H_7	〃		134	153	178	199	266	14.86	14.88	140	*		
4	i-C_3H_7	i-C_3H_7	〃		116	135	160	181	248	14.77	14.88	175	*		
5	n-C_4H_9	n-C_4H_9	Oily l. (colorless)		150	164	188	208	280	13.01	12.95	*	*		
6		CH_3	〃		168	186	210	230	302	14.14	13.98	*	*		
7			〃		220	236	264	286 (dec.)		10.32	10.44	193	212	28.78	28.76
8		CH_3	〃		182	199	222	244	317	14.33	14.42	153	*		
9		C_2H_5	Wh. sld. (colorless)	42	192	208	231	252	323	13.30	13.45	120	195	37.40	31.56

† uncorrected
* not obtained in crystalline form.
Key to abbreviation: Phys. = physical; mob. l. = mobile liquid; wh. sld. = white solid; dec. p. = decomposition point.

Table II. Properties of $CH_3CON\langle^{CH_2CH_2N(R'')R'''}_{CH_2CH_2OCOCH_3}$

Comp. No.	R''	R'''	Phys. form (color)	B. p., °C/mmHg† 6	8	10	20	50	100	760	N, % Found	Calcd.	Picrate M. p. °C	Platinichloride Dec. p., °C	Pt, % Found	Calcd.
1	CH_3	CH_3	Oily l. (colorless)	140	147	152	170	188	205		13.05	12.95	185	167 (melt)	31.01	31.17
2	C_2H_5	C_2H_5	〃	164	174	180	192	212 (dec.)			11.52	11.47	*	*		
3	n-C_3H_7	n-C_3H_7	〃	182	189	194	210 (dec.)				10.27	10.28	195	198		
4	i-C_3H_7	i-C_3H_7	〃	170	176	182	194 (dec.)				10.12	10.28	220	*		
5	n-C_4H_9	n-C_4H_9	〃	189	296	202	216 (dec.)				9.30	9.33	*	209	19.50	19.30
6		CH_3	〃	192	203	210	227 (dec.)				9.89	9.90	*	*		
7			〃	240 (dec.)	250 (dec.)						7.75	7.95	*	*		
8		CH_3	〃	211	218	224	243	270	291 (dec.)		10.21	10.06	*	*		
9		C_2H_5	〃	216	224	232	251	274	295 (dec.)		9.51	9.58	*	*		

reduced pressure. Some physical properties of II are summarized in Table I.

The second stage is the acetylation of the secondary amino and hydroxyl group in II, which can be effected by two equivalent amounts of acetic anhydride. The reaction proceeds spontaneously with the evolution of heat, and the subsequent distillation under reduced pressure gives III almost in a quantitative yield.

Some physical properties of III are shown in Table II.

On the third stage, III is submitted to the thermal decomposition, which leads to IV and the ester. As outlined in the introduction, distillation of the ester formed during the heating, and subsequent vacuum-fractionation of IV remaining in the flask are the procedures sufficient to give a pure product for the present synthetic purpose.

Table III. Properties of $CH_3CON\langle^{CH_2CH_2}_{CH_2CH_2}\rangle NR''$

Comp. No.	R''	Phys. form (color)	M. p. °C	B. p., °C/mmHg† 10	20	50	100	760	N, % Found	Calcd.	Picrate M. p. °C	Platinichloride Dec. p., °C	Pt, % Found	Calcd.
1	CH_3	Mob. l. (colorless)						168	19.50	19.70	280 (dec.)	270	28.02	28.10
2	C_2H_5	〃		118	138	160	182	254	17.93	17.93	115	227	27.44	27.01
3	n-C_3H_7	〃		133	151	175	194	265	16.30	16.45	212 (dec.)	*		
4	i-C_3H_7	〃		124	146	171	193	263	16.27	16.45	*	*		
5	n-C_4H_9	〃		146	165	190	210	280	15.11	15.20	190 (dec.)	*		
6,7		Oily l. (colorless)		186	202	226	248	320	13.09	13.31	*	*		
8,9		Cryst. (colorless)	75	206	225	251	270	347	13.67	13.71	*	230	23.93	23.83

Table IV. Properties of $HN\langle^{CH_2CH_2}_{CH_2CH_2}\rangle NR''$

Comp. No.	R''	Phys. form (color)	B. p., °C/mmHg† 10	20	50	100	760	N, % Found	Calcd.	Picrate M. p. °C	Platinichloride Dec. p., °C	Pt, % Found	Calcd.
1	CH_3	Mob. l. (colorless)			44	66	137	28.02	27.97	270 (dec.)	275	28.11	28.25
2	C_2H_5	〃		40	64	84	157	24.42	24.53	250 (dec.)	280	37.34	37.23
3	n-C_3H_7	〃	47	65	89	110	180	22.00	21.85	228	260	36.18	36.23
4	i-C_3H_7	〃	44	63	87	103	173	21.78	21.85	240 (dec.)	266	36.24	36.23
5	n-C_4H_9	〃	84	101	123	141	208	19.43	19.70	250 (dec.)	250	35.22	35.34
6,7		Oily l. (colorless)	116	135	158	177	248	16.45	16.65	225 (dec.)	260	33.40	33.76
8,9		Oily l. (yellowish)	139	154	178	180	272	17.30	17.27	150	259	33.99	34.10

As would be anticipated, β-(*N*-methyl-*N*-cyclohexylaminoethyl)-acetaminoethyl acetate (Table II, No. 6) and β-(*N*, *N*-dicyclohexylaminoethyl)-acetaminoethyl acetate (Table II, No. 7) give the same product, *N*-cyclohexyl-*N'*-acetyl-piperazine (Table III, No. 6, 7) under elimination of methyl acetate or cyclohexyl acetate respectively (Eq. 3). The same applies to the case of β-(*N*-methyl-*N*-phenylaminoethyl)-acetaminoethyl acetate (Table II, No. 8) and β-(*N*-ethyl-*N*-phenylaminoethyl)-acetaminoethyl acetate (Table II, No. 9), *N*-phenyl-*N*-acetyl-piperazine (Table III, No. 8, 9) being equally formed (Eq. 4).

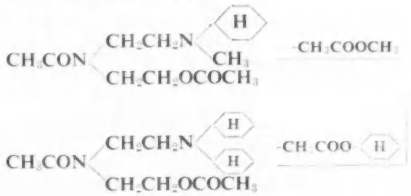

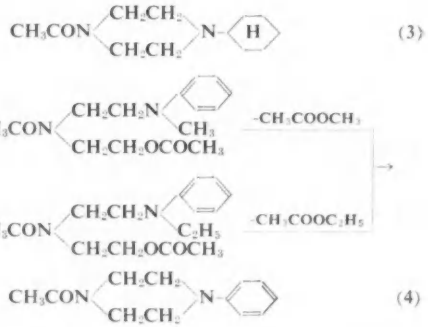

Some physical properties of IV are shown in Table III.

The last stage is the de-acetylation of IV. It may be effected easily by heating the acetyl piperazines with an equal volume of 6 N hydrochloric acid under reflux for 2 hr. The *N*-mono-substituted piperazines thus prepared are a colorless liquid, readily soluble in water

with an exception of *N*-phenyl-piperazine.

Some physical properties of V are cited in Table IV.

The reaction mixture of II and acetic anhydride can conveniently be submitted to the thermal decomposition without isolation of the acetylated compounds.

Experimental

***N*-(β-Diethylaminoethanol)-aminoethanol (Table I. No. 2).**—Ethylene oxide, generated by dropping 150 g. of 33% sodium hydroxide solution from a pressure-compensated dropping funnel upon a boiling mixture of 100 g. of ethylene chlorohydrin and 50 g. of water under reflux, is passed in a solution of 116 g. (1 mol.) of *N*,*N*-diethylethylenediamine in about 80 g. of methyl alcohol. Contineous shaking and cooling by cold water facilitate the absorption of ethylene oxide in the reaction mixture.

The gain of weight of the reaction mixture will be 44~50 g., and indicates that about one mole of ethylene oxide thereby can be brought into the reaction.

By distillation under atmospheric pressure, about 60 g. of *N*,*N*-diethylethylenediamine (b. p. 150~165°C) is recovered, and by fractionation under reduced pressure, about 50 g. of *N*-β-diethylaminoethylethanolamine, b. p. 113°C/10 mmHg, or 130°C/20 mmHg, and about 40 g. of *N*-β-diethylaminoethyldiethanolamine, b. p. 165°C/10mmHg, or 184°C/20 mmHg are obtained.

Ethylene chlorohydrin may be used instead of ethylene oxide as follows. Forty grams of ethylene chlorohydrin (0.5 mol.) is gradually added from a dropping funnel onto 116 g. (1 mol.) of *N*,*N*-diethylethylenediamine heated under reflux, thereby the reaction proceeds immediately at the rate of addition of the ethylene chlorohydrin. When the addition is complete, the reaction mixture is heated up to 200°C and maintained at this temperature for a while. Owing to the separation of hydrochloride of *N*,*N*-diethylethylenediamine, the reaction mixture is solidified. A hot solution of 30 g. (approx. 0.5 mol.) of potassium hydroxide in 80 cc. of methyl alcohol is gradually added to the reaction mixture with stirring. The precipitate of potassium chloride is removed by filtration and washed with a small quantity of methyl alcohol. After methyl alcohol has been removed from the filtrate and washings, 75 g. of *N*,*N*-diethylethylenediamine is recovered. The residual liquid is submitted to distillation under reduced pressure, whereby 45~50 g. of *N*-β-diethylaminoethylethanolamine and 25~30 g. of *N*-β-diethylaminoethyldiethanolamine are obtained.

***N*-(β-Diethylaminoethyl)-acetaminoethyl Acetate (Table II, No. 2).**—This compound can be obtained by addition of 23 g. (0.22 mol.) of acetic anhydride to 13 g. of *N*-β-diethylaminoethylethanolamine. Acetic acid and an excess of acetic anhydride are distilled off and the residue is distilled under reduced pressure, the expected acetate is collected at 175~177°C/10 mmHg, as a colorless oily liquid —yield 20~21 g. (about 90%).

The practical procedure in this piperazine-synthesis can be carried out so that the reaction mixture of *N*-β-disubstituted-aminoethylethanolamine and acetic anhydride is directly submitted to the thermal decomposition, the isolation of the acetylated compounds being omitted. The techniques here required are quite the same as in use of pure acetates isolated.

***N*-Ethyl-*N'*-acetyl-piperazine (Table III, No. 2).**—Twenty grams of *N*-β-diethylaminoethylacetaminoethyl acetate is heated in a Claisen flask, with a thermometer inserted through the straight neck so deep in the liquid as to read the internal reaction temperature and another thermometer fixed in the side neck of the flask. When the internal temperature reaches up above 250°C, the liquid turns brown in color and the boiling begins with the decomposition into *N*-ethyl-*N'*-acetyl-piperazine and ethyl acetate, which distills over as it is formed.

When the thermal decomposition is complete, the internal temperature is practically settled to a constant, i. e. 250~260°C.

On distillation, pure *N*-ethyl-*N'*-acetyl-piperazine comes over at 252~256°C as a colorless liquid—yield about 7 g. (Ca. 80%).

***N*-Ethyl-piperazine (Table IV, No. 2).**—*N*-Ethyl-*N'*-acetyl-piperazine (5 g.) is heated with 5 cc. of 20% hydrochloric acid under reflux for 2 hr. After the excess of hydrochloric acid has been distilled off, the resulting solution is made alkaline with a sodium hydroxide solution, and extracted with ether in a continuous extractor. The ether layer is dried over anhydrous sodium sulfate, the ether is removed, and the residue is distilled. About 3 g. of pure *N*-ethyl-piperazine is obtained as a colorless liquid b. p. 155~157°C—yield about 90%.

The author wishes to express his sincere gratitude to Professor Ryozo Goto (Kyoto University) for his kind guidance throughout the course of this work.

Kyoto Works
Teikoku Chemical Industry Co., Ltd.
Nakagyo-ku, Kyoto

A New Method for the Preparation of Piperazines. II. Preparation of N, N'-Disubstituted Piperazines

By Kazuo NAKAJIMA

(Received September 20, 1960)

A new method for preparing piperazine derivatives has been proposed by the author in the preceding paper[1]. The present paper deals with the preparation of some *N*, *N'*-disubstituted piperazines by this method. The procedure consists in treating an *N*, *N'*, *N'*-trisubstituted *N*-β-aminoethylethanolamine of the general formula A with acetic anhydride to yield an *O*-acetyl derivative B, followed by heating at 200~300°C to split into the desired *N*, *N'*-disubstituted piperazine C, and an acetic ester D, as is seen in the following Scheme 1;

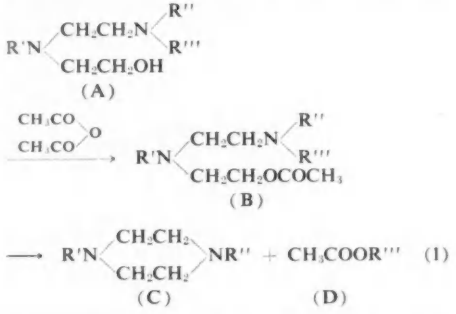

In the scheme, R' and R'' are alkyl, aralkyl, cycloalkyl or aryl group, whereas R''' is the same group as R'' or a lower alkyl, aralkyl or cycloalkyl group.

If R', R'' and R''' are chosen appropriately, it is possible to synthesize a variety of *N*, *N'*-disubstituted piperazines.

The properties of *N*, *N'*, *N'*-trisubstituted *N*-β-aminoethylethanolamines, which are used as the starting material, of their *O*-acetyl derivatives and of the end-products, *N*, *N'*-disubstituted piperazines are summarized in Tables I, II and III respectively.

Many proposals have been made hitherto for the preparation of *N*, *N'*-disubstituted piperazines. Among the compounds of this series listed in Table III, *N*, *N'*-dimethyl-, *N*, *N'*-diethyl-, *N*, *N'*-di-*n*-propyl-, *N*-methyl-*N'*-phenyl, *N*-ethyl-*N'*-phenyl- and *N*, *N'*-diphenyl-piperazine are known.

The compounds I_1*, I_2, I_3 and I_4, where R', R'' and R''' are the same, are easily prepared through alkylation of *N*-β-aminoethylethanolamine.

The alkylation can be achieved by using alkyl halide, but the methylation is also readily accomplished with formic acid and formalin by the Eschweiler-Clarke procedure.

In the Experimental Part, the synthesis of *N*, *N'*, *N'*-trimethyl-*N*-β-aminoethylethanolamine (I_1) by the latter procedure and that of *N*, *N'*, *N'*-tri-*n*-butyl-*N*-β-aminoethylethanolamine (I_4) by the use of *n*-butyl bromide were examplified. The compounds, I_1, I_2, I_3 and I_4 are colorless oily liquids, the first two of which are miscible with water and the latter two are sparingly soluble in water.

As expressed in Scheme 2, the compounds I_5 to I_{11} were synthesized by the action of ethylene oxide or ethylene chlorohydrin on *N*, *N'*-disubstituted ethylenediamines, followed by the introduction of R' group.

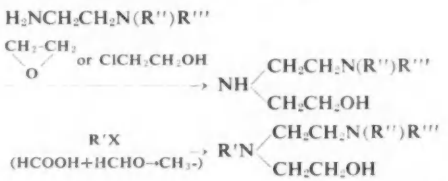

(2)

The preparation and properties of some of *N*-β-disubstituted aminoethylethanolamines have been shown in the preceding paper.

In the Experimental Part, the synthesis of (I_5) by the Eschweiler-Clarke procedure and that of (I_{10}) by the use of an alkyl halide have been illustrated.

The products thus obtained are colorless or yellowish oily liquids, sparingly soluble in water, with the exception of I_5 and I_6 which are freely soluble.

In compounds I_{12} and I_{13}, group R' is cyclohexyl. An attempt was made to introduce this by cyclohexyl bromide, but the formation of a considerable quantity of cyclohexene resulted in a low yield of I_{12} or I_{13}. In I_{14} and I_{15}, R' is a phenyl group.

I_{14} and I_{15} were therefore prepared from *N*-phenyl-*N*-β-aminoethylethanolamine.

1) K. Nakajima, This Bulletin, **34**, 651 (1961).

* I_1 indicates compound 1 in Table I.

TABLE I. PROPERTIES OF $R'N\langle^{CH_2CH_2N(R'')R'''}_{CH_2CH_2OH}$

Comp. No.	R'	R''	R'''	Phys. form (color)	B. p., °C/mmHg 10	20	50	100	760	N, % Found	Calcd.	Picrate M. p. °C	Platinichloride Dec. p. °C	Pt, % Found	Calcd.
1	CH_3	CH_3	CH_3	Oily liq. (colorless)	84	100	122	142	206	19.15	19.16	229 (dec.)	215	34.75	35.08
2	C_2H_5	C_2H_5	C_2H_5	〃	115	130	154	174	237	15.09	14.88	*	227	32.75	32.61
3	n-C_3H_7	n-C_3H_7	n-C_3H_7	〃	142	157	180	199	266	12.30	12.16	164	227	30.39	30.47
4	n-C_4H_9	n-C_4H_9	n-C_4H_9	〃	162	180	204	225	295	10.31	10.28	*	220	28.35	28.59
5	CH_3	C_2H_5	C_2H_5	〃	90	110	134	155	225～226	15.98	16.08	218	215	33.39	33.40
6	n-C_3H_7	C_2H_5	C_2H_5	〃	117	135	159	180	250	13.70	13.85	163	225	31.80	31.87
7	n-C_4H_9	C_2H_5	C_2H_5	〃	129	158	170	192	262～263	12.63	12.95	66	215	31.26	31.15
8	$C_6H_5CH_2$–	C_2H_5	C_2H_5	〃	176	195	220	241	308	11.08	11.19	98	210	29.14	29.55
9	CH_3	n-C_4H_9	n-C_4H_9	〃	127	145	169	190	260	12.10	12.16	*	228	30.60	30.63
10	C_2H_5	C_6H_5	CH_3	Syrupy (colorless)	179	190	216	235	305	12.54	12.60	130	red.		
11	CH_3	C_6H_5	C_2H_5	〃	182	200	225	244	315	12.60	12.60	*	*		
12	H	CH_3	CH_3	〃	150	165	189	210	280	12.97	13.07	158	*		
13	H	C_2H_5	C_2H_5	〃	167	185	209	230	Ca. 290 (dec.)	11.21	11.56	*	190	30.10	29.91
14	C_6H_5	CH_3	CH_3	〃	170	195	219	240	310 (dec.)	13.36	13.45	*	red.		
15	C_6H_5	C_2H_5	C_2H_5	〃	180	197	222	242	313 (dec.)	11.60	11.85	115	red.		
16	C_6H_5	C_6H_5	$-CH_2-CH_2-OH$	Viscous (colorless)	264	282	311	330 (dec.)		9.24	9.33	141	147	27.45	27.47

* Not obtained in crystalline form.

Key to abbreviation: Phys. form = physical form; liq. = liquid; dec. p. = decomposition point; red. = Platinichloride was reduced; mob. liq. = mobile liquid.

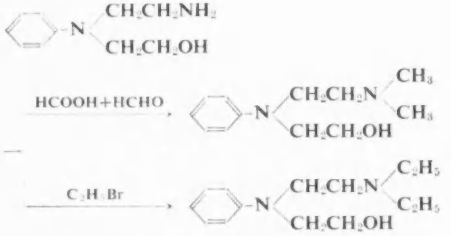

In the Experimental Part, synthesis of *N*-(β-diethylaminoethyl)-*N*-cyclohexylethanolamine (I_{12}) is cited.

The next step of this piperazine-synthesis is the formation of *O*-acetyl compounds from the *N*, *N'*, *N'*-trisubstituted *N*-β-aminoethylethanolamines with acetic anhydride. By the careful fractional distillation of the reaction mixture under reduced pressure the *O*-acetyl derivatives are obtained in an almost theoretical yield. However, the distillation must be carried out under fairly low pressure, say 10 mmHg, in order to obtain the *O*-acetyl compounds in a pure form, because they have a tendency to undergo decomposition over 200°C to piperazine derivatives. For any practical purpose, the *O*-acetyl compounds need not be isolated. The yields of piperazines are 70 to 95 per cent.

In the preparation of the compounds III_1 to III_{15} from the corresponding *O*-acetyl compounds, methyl acetate or ethyl acetate is formed. From II_{16}, however, ethylene diacetate is formed.

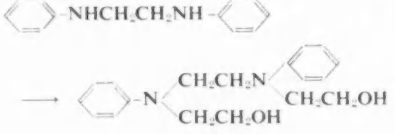

(I_{16})

TABLE II. PROPERTIES OF $R'N\langle^{CH_2CH_2N(R'')R'''}_{CH_2CH_2OCOCH_3}$

Comp. No.	R'	R''	R'''	Phys. form (color)	M. p. °C	B. p., °C/mmHg 10	20	50	100	760	N, % Found	Calcd.	Picrate M. p. °C	Platinichloride Dec. p. °C	Pt, % Found	Calcd.
1	CH_3	CH_3	CH_3	Oily liq. (colorless)		102	119	140	159	Ca. 220 (dec.)	14.58	14.88	263	222	32.49	32.62
2	C_2H_5	C_2H_5	C_2H_5	〃		125	142	166	186	Ca. 230 (dec.)	12.11	12.16	141	224	30.35	30.47
3	n-C_3H_7	n-C_3H_7	n-C_3H_7	〃		148	167	191	210	Ca. 256 (dec.)	10.22	10.28	134	222	28.35	28.59
4	n-C_4H_9	n-C_4H_9	n-C_4H_9	〃		167	185	209	230	229 (dec.)	8.80	8.91	125	223	26.90	26.93
5	CH_3	C_2H_5	C_2H_5	〃		104	124	148	170	240 (dec.)	13.10	12.95	163	166	31.23	31.16
6	n-C_3H_7	C_2H_5	C_2H_5	〃		127	146	169	190 (dec.)		11.50	11.46	105	208	29.70	29.82
7	n-C_4H_9	C_2H_5	C_2H_5	〃		128	157	180	202 (dec.)		10.71	10.89	125	222	29.40	29.19
8		C_2H_5	C_2H_5	〃		180	200	225	(dec.)		9.32	9.58	132	220	27.80	27.78
9	CH_3	n-C_4H_9	n-C_4H_9	〃		156	172	195	216	(dec.)	10.11	10.23	149	233	28.70	28.59
10	C_2H_5		CH_3	Viscous (colorless)		196	215 (dec.)				10.59	10.60	98	red.		
11	CH_3		C_2H_5	〃		190	210 (dec.)				11.09	10.60	132	221	28.96	28.94
12		CH_3	CH_3	〃		142	160	184	205	(dec.)	10.72	10.93	Ca. 290	215	29.20	29.28
13		C_2H_5	C_2H_5	〃		170	190	214	235 (dec.)		9.77	9.85	185	210	28.01	28.11
14		CH_3	CH_3	〃		195	219	240 (dec.)			11.36	11.19	*	red.		
15		C_2H_5	C_2H_5	〃		240	250 (dec.)				10.12	10.06	160	232		
16			$-CH_2CH_2OCOCH_3$	Cryst. 76 (colorless)		(243/3 mmHg dec.)					7.20	7.29	140	202	24.80	24.56

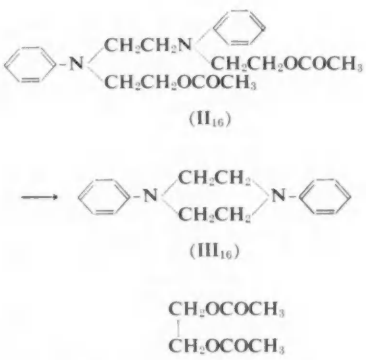

(II_{16}) ⟶ (III_{16})

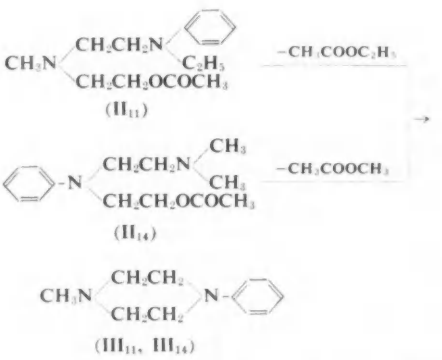

(II_{11}) → (II_{14}) → (III_{11}, III_{14})

II_{11} and II_{14} give the same product with liberation of ethyl acetate and methyl acetate respectively. This is also the case with II_{10} and II_{15}.

In the Experimental Part, preparations of *N*, *N'*-dimethylpiperazine (III_1), *N*-methyl-*N'*-phenylpiperazine (III_{11}), and *N*, *N'*-diphenylpiperazine (III_{16}) have been cited.

Table III. Properties of $R'N\langle^{CH_2CH_2}_{CH_2CH_2}\rangle NR''$

Comp. No.	R'	R''	Phys. form (color)	M. p. °C	B. p., °C/mmHg 10	20	50	100	760	N, % Found	Calcd.	Picrate M. p. °C	Platinichloride Dec. p. °C	Pt, % Found	Calcd.
1	CH_3	CH_3	Mob. liq. (colorless)				40	62	132	29.51	24.53	280 (dec.)	Ca. 270	37.25	37.23
5	CH_3	C_2H_5	〃			36	61	82	151～153	21.70	21.85	255 (dec.)	248	36.35	36.26
9	CH_3	n-C_4H_9	〃		62	81	105	126	196	18.03	17.93	Ca. 240 (dec.)	280	38.45	34.46
12	CH_3		Oily liq. (colorless)		111	131	155	196	246	15.42	15.37	224 (dec.)	257	33.00	32.95
{11 {14	CH_3		Viscous (yellowish)	35	133	150	175	196	266	15.80	15.90	Ca. 210	245	32.99 33.10	33.29
2	C_2H_5	C_2H_5	Oily liq. (colorless)		37	56	80	101	171～173	19.77	19.70	Ca. 250 (dec.)	263	35.32	35.34
6	C_2H_5	n-C_3H_7	〃		52	76	94	115	188	19.82	19.93	235	225	34.45	34.46
7	C_2H_5	n-C_4H_9	〃		76	95	119	140	210	16.24	16.45	230	260	33.50	33.63
8	C_2H_5		〃		150	170	194	208	278	13.40	13.71	147	260	31.63	31.77
13	C_2H_5		〃		134	152	177	197	268	14.12	14.27	220	258	32.03	32.18
{10 {15	C_2H_5		Viscous (yellowish)		150	170	144	215	285	14.62	14.72	164	245	32.52 32.57	32.51
3	n-C_3H_7	n-C_3H_7	Oily liq. (colorless)		74	93	117	138	207～209	16.47	16.45	258 (dec.)	275	33.70	33.63
4	n-C_4H_9	n-C_4H_9	〃		99	127	152	173	243	14.17	14.12	245 (dec.)	Ca. 280	32.05	32.08
16			Cryst. (colorless)	163	226	242	266	288	(dec.)	11.75	11.76	192	245	30.09	30.10

Experimental

N,N',N'-Trimethyl-N-β-aminoethylethanolamine (I_1).—To a mixture of 52 g. (0.5 mol.) of N-β-aminoethylethanolamine and 350 g. of 80% formic acid, heated under reflux, was added 175 g. of formalin (30%) dropwise from a dropping funnel.

A vigorous reaction set in with the evolution of carbon dioxide.

When the addition of formalin was complete, the reaction mixture was boiled under reflux until no more gas was evolved (about 6 hr.). After an addition of 150 ml. of hydrochloric acid (approx. 6 N), the solution was evaporated to dryness under reduced pressure on a steam bath.

To the resulting solid, was added 200 g. of 30% sodium hydroxide solution.

The solution was extracted with ether using a continuous extraction apparatus, until no more volume diminution of the aqueous layer was observed. After the removal of the ether, the residue was distilled fractionally. From the etherial solution there was obtained by the fractinal distillation 58～64 g. of I_1, a colorless oily liquid, b. p. 206°C, in an 80% yield.

This compound is readily miscible with water, alcohol, acetone and benzene; d_4^{20} 0.9044. The hydrochloride is colorless crystals, m. p. 187°C.

N,N',N'-Tri-n-butyl-N-β-aminoethylethanolamine (I_4).—In a three-necked flask equipped with a reflux condenser, a thermometer and a dropping funnel, was placed 52 g. (0.5 mol.) of N-β-aminoethylethanolamine, and heating was commenced.

When the temperature rose to about 100°C, 37 g. (0.25 mol.) of n-butyl bromide was carefully added from the dropping funnel.

When the addition was complete, the temperature of the reaction mixture was raised to about 180°C, and then the mixture was allowed to stand to cool. A hot solution of 14 g. of potassium hydroxide in 30 ml. of methyl alcohol was poured in, shaking well. The crystals of potassium bromide were separated by filtration, and washed with a small amount of methyl alcohol.

From the filtrate methyl alcohol and water were distilled off. The distillation was discontinued when the temperature of the residue in the flask reached 150°C.

This procedure was repeated twice, using 18.5 g. (0.125 mol.) of n-butyl bromide and 7 g. (0.125 mol.) of potassium hydroxide in 30 ml. of methyl alcohol the first time, and 10 g. of n-butyl bromide and 8 g.

of potassium hydroxide in 20 ml. of methyl alcohol in the second. I_4 was purified by distillation under reduced pressure. There was obtained about 110 g. of I_4 (approx. 80%) as a colorless oily liquid, b. p. 162°C/10 mmHg or 180°C/20 mmHg.

Almost the same yields were obtained with I_2 and I_3 in a manner similiar to that described above.

***N*-Methyl-*N*-(β-diethylaminoethyl) ethanolamine** (I_5). — Forty grams (0.25 mol.) of *N*-(β-diethylamino-ethyl)ethanolamine was mixed with 40 g. of formic acid (80%). With boiling under reflux, 25 g. of formalin was added dropwise.

The reaction was carried out in the same manner as in I_1. The yield of I_5, b. p. 225~226°C, was 35 g. (80%).

Similarly, *N*-methyl-*N*-(β-di-*n*-butylaminoethyl)-ethanolamine (I_9) could be prepared from *N*-(β-di-*n*-butylaminoethyl)ethanolamine.

***N*-Ethyl-*N*-(β-methylamino-ethyl) ethanolamine** (I_{10}). —In a pressure vessel, 22 g. (0.5 mol.) of ethylene oxide dissolved in 50 ml. of methyl alcohol was added to 76 g. (0.5 mol.) of *N*-methyl-*N*-phenylethylenediamine and the mixture was allowed to stand until an exothermal but not violent reaction was complete.

Fractional distillation of this reaction mixture under reduced pressure gave about 30 g. of *N*-(β-methylanilinoethyl)ethanolamine, boiling at 182°C/10 mmHg, 199°C/20 mmHg, or 317°C/760 mmHg. From the fore-run of the distillation, about 20 g. of unchanged starting material, *N*-methyl-*N*-phenylethylenediamine, was recovered (b. p. 124°C/10 mmHg, 142°C/20 mmHg, 257°C/760 mmHg). From the after-run, about 40 g. of *N*-(β-methylanilinoethyl)-diethanolamine was obtained in the form of colorless oily liquid boiling at 208°C/10 mmHg or 231°C/20 mmHg.

For the purpose of preparing I_{10}, a mixture of 19.5 g. (0.1 mol.) of *N*-(β-methylanilino-ethyl)-ethanolamine and 11 g. (0.1 mol.) of ethyl bromide was heated under reflux.

After completion of the vigorous reaction, the reaction mixture was neutralized by adding a sodium hydroxide solution using phenolphthalein as the indicator. The oily layer was separated and distilled under reduced pressure.

There was obtained about 18 g. of I_{10}, as a colorless oily liquid boiling at 179°C/10 mmHg or 190°C/20 mmHg in an 80% yield.

***N*-(β-Diethylamino-ethyl)-*N*-cyclohexylethanolamine** (I_{13}). — A mixture of 18 g. (0.1 mol.) of *N*-(β-aminoethyl)-*N*-cyclohexylethanolamine (a colorless oily liquid, b. p. 162°C/10 mmHg, 181°C/20 mmHg, or 295°C/760 mmHg), and 11 g. (0.1 mol.) of ethyl bromide was heated under reflux. After a vigorous reaction had subsided, the cooled reaction mixture was made alkaline with 30% sodium hydroxide solution using phenolphthalein as the indicator.

The oily product that separated was shaken with an equal volume of water**, and distilled fractionally.

About 18 g. of I_{13} was obtained as acolorless oily liquid, boiling at 167°C/10 mmHg or 185°C/20 mmHg.

** There is no appreciable difference between the boiling point of the starting material and that of I_{13}. But the former is miscible with water at any proportion, and the latter is sparingly soluble in it. The separation depends upon this difference of solubility.

***N*, *N'*-(Bis-β-hydroxxethyl)-*N*, *N'*-diphenylethylenediamine** (I_{16}).—To 42 g. (0.2 mol.) of *N*,*N'*-diphenylethylenediamine was added 18 g. (0.4 mol.) of ethyleneoxide dissolved in 50 ml. of methyl alcohol. After being stored in a refrigerator for two days, the mixture was distilled. At 264°C/10 mmHg or 282°C/20 mmHg. I_{16} was distilled off quantitatively as a colorless and strongly viscous liquid. The melting point of its picrate was 141°C, and that of its platinichloride 147°C.

***N*-Methyl-*N*-(β-dimethylamino-ethyl) aminoethyl Acetate** (II_1).—Acetic anhydride (12.5 g.) was added to 14.5 g. (0.1 mol.) of I_1. By fractional distillation of the mixture, II_1 was obtained at 119°C/20 mmHg, or 140°C/50 mmHg as a colorless oily liquid. The yield was 17 g. (approx. 90%).

***N*,*N'*-Dimethylpiperazine** (III_1).—II_1 was placed in a Claisen flask equipped with a thermometer inserted through the straight neck to indicate the internal temperature and another thermometer fixed in the side neck to detect the distilling temperature.

Distillation was carefully carried out. At the beginning, the temperature of the content remained at about 206°C, the boiling point of II_1. As the decomposition of II_1 proceeded, the internal temperature gradually fell, and the distillation of the methyl acetate began. After the theoretical amount of methyl acetate had distilled over, *N*,*N'*-dimethylpiperazine was collected at 110~140°C.

Redistillation gave the pure product boiling at 130~132°C. The yield was 90% or greater.

***N*-Ethyl-*N'*-phenylpiperazine** (III_{15}).—A reaction mixture of 25 g. (0.1 mol.) of *N*-(β-diethylamino-ethyl)-*N*-phenylethanolamine (I_{15}) and 12 g. (0.12 mol.) of acetic anhydride was distilled in the same manner as in the preceding example.

After acetic acid formed and the excess acetic anhydride had distilled out, the temperature of the content increased gradually, reaching 300°C at one time. But as the decomposition proceeded, the internal temperature fell somewhat and ethyl acetate began to distill off at 80~100°C. After completion of the decomposition, the resulting brown liquid was purified by vacuum distillation. This purification furnished about 15 g. of III_{15} in an 80% yield as a yellowish viscous liquid.

***N*, *N'*-Diphenylpiperazine** (III_{16}). — Acetic anhydride(25 g.; ca. 0.24 mol.) was added to 30 g. (0.1 mol.) of I_{16}. The reaction mixture was submitted to distillation in the same manner as in the preceding example with the object of decomposing it into III_{16} and ethylenediacetate, which distilled out 180~190°C. The residual material was further distilled under reduced pressure. Recrystallization of the solidified distillate from methyl alcohol afforded about 18 g. of III_{16} in colorless crystals, m. p. 163°C. The yield was about 80% of the theory.

The author is deeply grateful to Professor Ryozo Goto, Kyoto University, for giving much helpful advice and encouragement during the course of this work.

Kyoto Works
Teikoku Chemical Industry Co., Ltd.
Nakagyo-ku, Kyoto

Radiation-induced Reaction in an Aqueous Benzoic Acid Solution. I. Dose and Dose Rate Dependencies of Salicylic Acid, and of Biphenyldicarboxylic Acids

By Akihisa SAKUMOTO and Gen-ichi TSUCHIHASHI

(Received July 28, 1960)

Reactive species such as hydrogen atoms and hydroxyl radicals, and so-called "molecular" products hydrogen and hydrogen peroxide from water are yielded by the actions of ionizing radiation on aqueous solutions. Hydrogen atoms and hydroxyl radicals in these species react rapidly with many solutes dissolved in solutions. The reaction of many organic compounds with these reactive species has been studied by a number of workers.

The radiation-induced reaction of an aqueous benzoic acid solution was studied first by Weiss[1] using X-rays, and recently by Downes[2] using very weak Co 60 gamma rays source. Little attention had been paid by earlier workers to the effect of dissolving oxygen occurring in the reactions when solutions of organic compounds were irradiated by ionizing radiations. The presence of molecular oxygen during irradiation, however, would lead not only to the quantitative differences in the efficiency of the oxidative process but also to some qualitative differences in the reaction products.

In the present work, the radiation-induced reaction of an aqueous benzoic acid solution with, and without, molecular oxygen has been studied and does and dose rate dependencies of the yield of salicylic acid, and of biphenyldicarboxylic acids produced have been examined at high dose and high dose rate, using 10 kc. Co-60 source of the Japan Atomic Energy Research Institute[3].

Experimental

Materials. — Benzoic acid used in this work, obtained from a commercial source, was purified by recrystallization four times from ethanol, m. p. 122°C (uncorrected). Demineralized water was used to prepare a benzoic acid solution. Nitrogen to remove the oxygen contained in sample solutions was purified by letting it bubble through slightly acidified vanadyl sulfate solution[4]. Bomb oxygen was used without further purification.

Preparation of Solutions.—Solutions were 0.300% with regard to benzoic acid, and the pH was not specially adjusted. In order to prepare an oxygen free solution, oxygen contained in the solution was driven off by letting purified nitrogen bubble through for two hours. After this treatment, the concentration of oxygen in the solution is estimated to be lower than 1.9×10^{-5} mol./l.[5] Solutions were charged in 30 ml. test tubes, fitted with glass stoppers. The irradiation vessels were cleaned with cleaning solution, rinsed several times, and then washed with distilled water.

Saturation of oxygen during the irradiation was held by continuous bubbling of bomb oxygen in the sample solution. ($[O_2]$ was measured to be 1.2×10^{-3} mol./l.)[5]

Irradiation. — Both solutions with and without molecular oxygen were irradiated with gamma rays from 10 kc. Co-60 source with absorbed dose from 6.2×10^5 to 1.1×10^7 r and with dose rate from 2.7×10^4 to 3.9×10^5 r/hr. at room temperature. Dose rates were measured by means of both ferrous—ferric[6] and ceric-cerous[7] dosimeters, and the amount of energy absorbed in the solutions was calculated using G-values of Fe^{2+} oxidized to Fe^{3+} being 15.5 and of Ce^{4+} reduced to Ce^{3+} being 2.45.

Determination of Salicylic Acid. — The determination of salicylic acid was carried out by colourimetry. After adjusting the pH of the irradiation solution which, if necessary, was filtered off, between 2.5 and 2.8 by means of 50% acetic acid—3% ammonium acetate buffer, an adequate of 1% ferric chloride solution was added to give salicylic acid complex. The absorbance of salicylic acid complex was measured spectrophotometrically at 530 mμ.

Determination of Biphenyldicarboxylic Acids.— Irradiation in the absence of oxygen gave biphenyldicarboxylic acids as precipitate. The precipitate including three isomers of biphenyldicarboxylic acids was separated from the solution using the ultracentrifuge. The collected precipitate was dried for five hours at 80~85°C. Yields of biphenyldicarboxylic acids were determined gravimetrically. Biphenyldicarboxylic acids did not precipitate in the case of irradiation with oxygen.

1) J. Weiss, H. Leobl and G. Stein, *J. Chem. Soc.*, **1951**, 405.
2) A. M. Downes, *Auster. J. Chem.*, **2**, 155 (1958).
3) A. Danno et al., The 7th Hot Laboratories and Equipment Conference, Cleveland (1959), pp. 349~360.
4) L. Meites and J. Meites, *Anal. Chem.*, **20**, 984 (1948).
5) H. Hotta, A. Terakawa and S. Ōno, This Bulletin, **33**, 442 (1960).
6) G. R. A. Johnson and J. Weiss, *Proc. Roy. Soc.*, **A240**, 189 (1957).
7) For example, T. Rigg, G. Stein and J. Weiss, ibid., **A211**, 375 (1952).

Results and Discussion

Aqueous solutions of benzoic acid were irradiated with Co-60 gamma rays at a fixed absorbed dose of 3.8×10^{5} r by varying dose rate from 2.7×10^{4} to 3.9×10^{5} r/hr. The yield of salcylic acid produced is plotted against the dose rate in Figs. 1 and 2, in which Fig. 1 shows the case of oxygen saturated solutions and Fig. 2 the case of oxygen free solutions. As is shown in these figures, the yield of salicylic acid is decreasing with increasing dose rate in both systems. The yield of salicylic acid in the presence of oxygen was about ten times greater than that in the absence of oxygen.

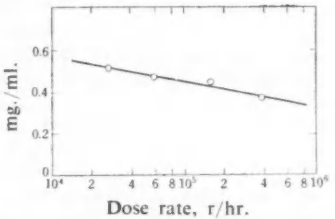

Fig. 1. Yields of salicylic acid produced in oxygen saturated solutions against dose rate. Dose is constant, 3.8×10^{6} r.

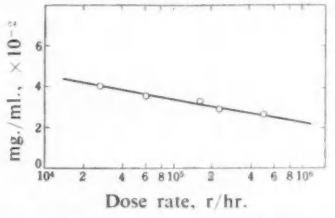

Fig. 2. Yields of salicylic acid produced in oxygen free solutions against dose rate. Dose is constant, 3.8×10^{6} r.

Dose dependence of the yield of salicylic acid by a varying absorbed dose from 6.2×10^{5} to 1.1×10^{7} r at a fixed dose rate of 1.6×10^{5} r/hr. is shown in Figs. 3 and 4, where Fig. 3 shows the system of oxygen saturated and Fig. 4 shows the system of oxygen free solution. Two curves show the same trend that the yield of salicylic acid at high dose is not linearly increasing with the absorbed dose, but gradually increases to approach some constant value. Salicylic acid was produced in both with, and without, molecular oxygen solutions, but biphenyldicarboxylic acids were not observed in the oxygen saturated solutions.

Absorbed dose and dose rate dependencies of yields of biphenyldicarboxylic acids were also studied. Figure 5 shows the plot of yields of biphenyldicarboxylic acids against dose rate.

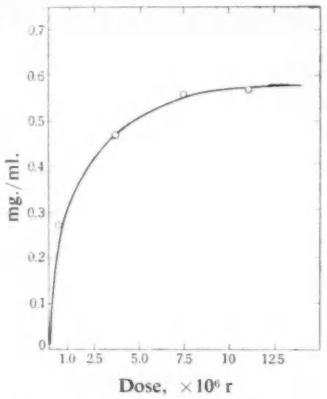

Fig. 3. Yields of salicylic acid produced in oxygen saturated solutions against dose. Dose rate is constant, 1.6×10^{5} r/hr.

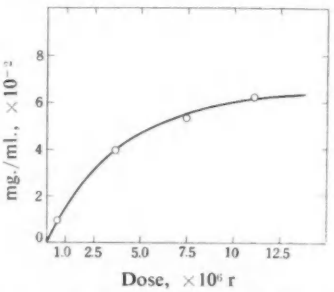

Fig. 4. Yields of salicylic acid produced in oxygen free solutions against dose. Dose rate is constant, 1.6×10^{5} r/hr.

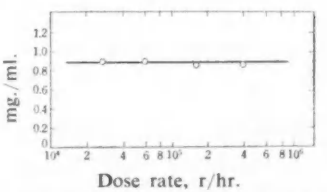

Fig. 5. Yields of biphenyldicarboxylic acid produced in oxygen free solutions against dose rate. Dose is constant, 3.8×10^{6} r.

In this case, the absorbed dose was constant at 3.8×10^{6} r. The yield of the dimer was constant independently of dose rates and $G=0.94$ was obtained. Figure 6 shows yields of biphenyldicarboxylic acids against the absorbed dose, which were produced when irradiation was carried out at a fixed dose rate of 1.6×10^{5} r/hr. As is shown in this figure, yields of biphenyldicarboxylic acids have a linear relationship with the absorbed dose. This relationship is quite different from that of the

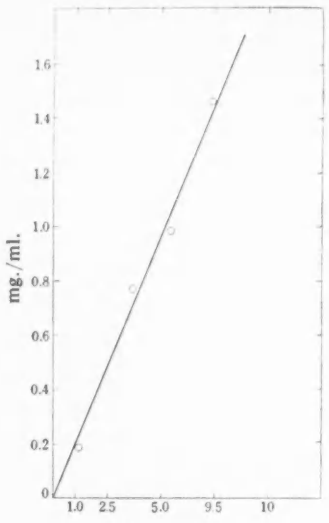

Fig. 6. Yields of biphenyldicarboxylic acid produced in oxygen free solutions against dose. Dose rate is constant, 1.6×10^5 r/hr.

yield of salicylic acid as is shown in Figs. 3 and 4.

Basing on the above results, the mechanism of the radiation-induced reaction in an aqueous solution of benzoic acid is assumed as follows.

In the present experiment, the concentration of benzoic acid was 3.0 mg./ml. of solution. At this relatively low concentration, the direct-hit effects of benzoic acid by gamma rays can be neglected. Water is decomposed by ionizing radiation into hydrogen atom, hydroxyl radical, hydrogen peroxide and hydrogen[8].

$$H_2O \text{ -W→ } H\cdot,\ HO\cdot,\ H_2O_2,\ H_2 \qquad (1)$$

Accordingly, the radiation-induced reaction in a dilute aqueous solution is assumed to be initiated by reactive species such as the hydrogen atom and/or the hydroxyl radical produced from the radiolytic decomposition of water.

When water containing molecular oxygen was irradiated, the hydrogen atom produced according to Eq. 1 reacts rapidly with dissolving oxygen giving the hydroperoxy radical[9].

$$H\cdot + O_2 \rightarrow HO_2\cdot \qquad (2)$$

Owing to this reaction, the concentration of hydrogen atom in the presence of oxygen may be considerably lower than that in the absence of oxygen.

If this fact is taken into consideration, radiation-induced reaction in an aqueous solution containing molecular oxygen must be initiated by the hydroxyl radical and/or the hydroperoxy radical formed according to Eq. 2. However, it should be noticed that the hydroperoxy radical is assumed to have less oxidizing power than the hydroxyl radical on thermodynamic grounds because the bond dissociation energy of hydrogen peroxide, D(H–O_2H), calculated to be 90 kcal./mol., is smaller than that of water, D(H–OH), calculated to be 118 kcal./mol.[10]

Therefore, the hydroperoxy radical appears to be unreactive directly towards benzoic acid. From these reasons, it would be reasonable to consider that the disappearance of benzoic acid in an aqueous solution is initiated by hydrogen-abstraction with the hydroxyl radical produced from radiolytic decomposition of water.

Dehydrogenation of ring hydrogen of benzoic acid, giving hydroxycarbonylphenyl radical as an intermediate, can be followed by a two reaction process: first, the reaction of this radical with hydroxyl radical to form salicylic acid which shows the hydroxylation of ortho-position of benzoic acid, and second, the dimerization of these radicals to produce biphenyldicarboxylic acid as follows.

Biphenyldicarboxylic acids including all kinds of their isomers are insoluble in water giving a pale yellow precipitate and consequently do not suffer from further reaction. The yield of these acids is independent on the dose rate as is shown in Fig. 5, and has a first order relationship with the absorbed dose in the range of the present work (up to 1.1×10^7 r) as is shown in Fig. 6. These results signify that the formation of hydroxycarbonylphenyl radical produced as an intermediate according to Eq. 3 is linearly dependent on the absorbed dose.

8) A. O. Allen and H. A. Schwarz, Proceedings of the Second United Nations International Conference on the Peaceful Uses of Atomic Energy, **29**, 30 (1958).

9) P. Riesz and E. J. Hart, *J. Phys. Chem.*, **63**, 858 (1959).

10) J. Weiss, *Internat. J. Appl. Radiation Isotopes*, **6**, 52 (1959).

Hydroxylation of benzoic acid takes place in all possible positions. Accordingly, three isomers of hydroxybenzoic acid may be formed. In the present work, the yield of only isomer, *o*-hydroxybenzoic acid, i. e. salicylic acid, was determined. The yield of salicylic acid at high dose does not show a linear relationship with absorbed dose, but increases gradually with increasing absorbed dose as is shown in Figs. 3 and 4. On the other hand, it is evident from the experimental results of Weiss[1] that the yield of the acid at the low dose (up to 5×10^4 E. U. in his work) has a linear relationship with the absorbed dose. It would seem, therefore, that the trend of the dose-yield curve of salicylic acid at the high dose in the present work may suggest further hydroxylation of salicylic acid to give di-hydroxybenzoic acids and the formation of these acids being more and more remarkable with increasing absorbed dose.

When irradiation of an aqueous solution containing molecular oxygen was carried out, hydroxylation of benzoic acid increased remarkably in comparison with that of the molecular oxygen free solution and the dimerization of hydrocarbonylphenyl radical did not occur. Therefore, the mechanism in this case must be mentioned compared to the different mechanism described above.

If a sufficient amount of molecular oxygen exists in an aqueous solution, it reacts easily with the hydroxycarbonylphenyl radical, as well as the hydrogen, and this reaction results finally in the formation of salicylic acid.

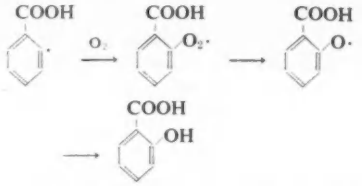

(6)

Consequently, the dimerization of the hydroxycarbonylphenyl radical was suppressed. Concerning the formation of salicylic acid in the presence of molecular oxygen, there is the possibility also of the reaction,

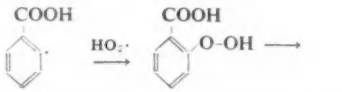

(7)

which can also lead to the eventual formation of salicylic acid. The contribution of this reaction is assumed to be small, because the concentration of oxygen is greater than that of hydroperoxy radical, provided that the reaction rate of the reaction 6 is of the same order as that of 7.

The authors wish to express hearty thanks to Professor Kenjiro Kimura, a director of the Institute, and Dr. A. Danno for their kind encouragement and discussion throughout the entire course of this study.

Division of Radiation Applications
Japan Atomic Energy Research Institute
Tokai, Ibaraki-ken

Radiation-induced Reaction in an Aqueous Benzoic Acid Solution. II. Determination of Products by Isotope Dilution Method

By Akihisa Sakumoto and Gen-ichi Tsuchihashi

(Received August 3, 1960)

In the preceding paper*, dose and dose rate dependencies of the yield of salicylic acid, and of biphenyldicarboxylic acids were studied in the presence or the absence of molecular oxygen when aqueous solutions of benzoic acid were irradiated with Co-60 gamma rays. In the presence of molecular oxygen, the yield of salicylic acid was greater than that in the absence of molecular oxygen and biphenyldicarboxylic acids was not produced, whereas in the absence of melecular oxygen the main products were biphenyldicarboxylic acids. In the preceding paper, the isomers of hydroxybenzoic and biphenyldicarboxylic acids produced in the solution could not be identified.

The determination of 2-, 3- and 4-hydroxybenzoic acid and biphenyl as reaction products was carried out by Weiss and his collaborators

* Part I: A. Sakumoto and G. Tsuchihashi, This Bulletin, 34, 660 (1961).

using paper chromatography[1]. Recently, Downes separated the isomers of monohydroxybenzoic acids from benzoic acid, and the isomers of dihydroxybenzoic acids from salicylic acid as reaction products by radioactive assay and radiochromatography[2].

In the present work, an isotope dilution method was applied in order to determine the reaction products in the radiolysis of aqueous solutions of benzoic acid (carboxyl-^{14}C) in the presence or the absence of molecular oxygen. From the results obtained, a mechanism of the radiation-induced reaction will be discussed.

Experimental

Materials.—Benzoic acid (carboxyl-^{14}C) was synthesized from phenylmagnesium bromide and $^{14}CO_2$ by Grignard reaction[3]. This acid was purified by recrystallization from ethanol-water to give a constant specific activity. The specific activity of the acid was 2.289×10^{-2} mc./mol.

Each isomer of biphenyldicarboxylic acid used for the carrier of the isotope dilution method was synthesized according to the method cited in the literatures[4,5]. Each compound was purified by recrystallization except 4,4'-biphenyldicarboxylic acid which was purified by precipitation four times from dilute alkaline solution of it. The melting points** of the isomers were as follows: 2,2'-, 228.0~228.5°C; 3,3'-, 356~357°C. 4,4'-Biphenyldicarboxylic acid did not melt.

Commercial grade 2-, 3-, 4-hydroxybenzoic acid and 2,3-, 2,4-, 2,5-, 2,6-dihydroxybenzoic acid were also purified by recrystallization. The melting points** of the isomers were as follows; 2-, 157~158.5°C; 3-, 200~200.5°C; 4-, 213~213.5°C; 2,3-, 205~206°C; 2,4-, 212.5~213°C; 2,5-, 199~200°C; 2,6-, 149~151°C.

Preparation of Solution.—The preparation of 0.300% aqueous benzoic acid (carboxyl-^{14}C) solution was carried out by dissolving it in demineralized water. The pH of the solution was not specially adjusted. The irradiation samples of both oxygen free and saturated solution were prepared as described in the preceding paper.

Irradiations.—The irradiation vessels and method have been described in the preceding paper. In the present work, irradiations were carried out at the dose rate of 1.6×10^5 r/hr. and the absorbed dose of 4.0×10^6 r in the presence of molecular oxygen and at the dose rate of 1.7×10^5 r/hr. and the absorbed dose of 4.3×10^6 r in the absence of molecular oxygen at room temperature. The measurement of the absorbed dose was carried out according to the method as described in Part I.

Radioactive Assay of Irradiation Products.—Determination of the yield of irradiation products was carried out as follows. An adequate of analyzing carrier which was weighed accurately was added to an aliquot of irradiated solution, and then dissolved. After the solution was cooled to precipitate the added carrier, the precipitate was filtered off and purified several times by recrystallization to offer a constant counting rate after oxidation to barium carbonate.

Purification of 4,4'-biphenyldicarboxylic acid, being insoluble in ordinary organic solvents, was carried out by dissolving it in dilute sodium hydroxide and reprecipitating it by adding dilute hydrochloric acid.

The isotope dilution method was also applied in order to determine unreacted benzoic acid (carboxyl-^{14}C) left in the solution after irradiation. After the addition of non-active benzoic acid, the purification of the acid was carried out by recrystallization six time from ethanol-water and then by sublimation three or five times.

Each sample purified was oxidized according to the Van Slyke-Folch oxidation method[6]. Carbon dioxide liberated after oxidation of a purified sample was absorbed by 0.74 N sodium hydroxide solution and then precipitated as barium carbonate by adding 17.6% barium chloride-2.5% ammonium chloride solution.

The resulting barium carbonate was filtered off, washed with ethanol and dried. The specific activity of barium carbonate was measured at infinite thickness by a Tracerlab. T.G.C.-14 counter.

Results

Isomers of hydroxybenzoic acid and biphenyldicarboxylic acid were assayed as products when

TABLE I. YIELDS OF PRODUCTS IN OXYGEN FREE SOLUTION OF BENZOIC ACID (CARBOXYL-^{14}C) IRRADIATED WITH Co-60 GAMMA RAYS

Product	Weight mg./ml.	Yield %	*G*-Value
2-Hydroxybenzoic acid	0.040	1.3	0.066
3-Hydroxybenzoic acid	0.047	1.6	0.077
4-Hydroxybenzoic acid	0.056	1.9	0.092
2,2'-Biphenyldicarboxylic acid	0.41	14	0.38
3,3'-Biphenyldicarboxylic acid	0.072	2.4	0.068
4,4'-Biphenyldicarboxylic acid	0.30	10	0.28
Benzoic acid*	1.86	62	
—Benzoic acid**	1.14	38	1.88

Dose, 4.3×10^6 r, dose rate, 1.7×10^5 r/hr.

* Unchanged benzoic acid (carboxyl-^{14}C) in the irradiated solution.

** The disappearance of benzoic acid (carboxyl-^{14}C), calculated from the amount of unchanged benzoic acid (carboxyl-^{14}C).

1) J. Weiss, H. Loeble and G. Stein, *J. Chem. Soc.*, 1951, 405.
2) A. M. Downes, *Austr. J. Chem.*, 2, 154 (1951).
3) W. G. Dauben and P. E. Yankwich, *Anal. Chem.*, 19, 828 (1947).
4) "Organic Syntheses", Coll. Vol. I (1948), p. 222.
5) F. Ullman and O. Löwenthal, *Ann.*, 332, 72 (1904).
** The melting point of each compound is uncorrected.
6) D. D. Van Slyke and H. Folch, *J. Biol. Chem.*, 136, 509 (1940).

an aqueous solution of benzoic acid (carboxyl-^{14}C) irradiated in oxygen free solution. Results obtained are summarized in Table I shown as the yield and *G*-value of each reaction product. In Table I, benzoic acid indicates unchanged benzoic acid (carboxyl-^{14}C) which is left in the irradiated solution. *G*-Value of the disappearance of benzoic acid (carboxyl-^{14}C) shown as (-benzoic acid) in Table I, calculated from the amount of unchanged benzoic acid (carboxyl-^{14}C), is 1.88. The ratio of produced hydroxybenzoic acids and biphenyldicarboxylic acids is approximately 1 : 3. The *G*-value ratio of each hydroxybenzoic acid and each biphenyldicarboxylic acid will be discussed in the following section.

When irradiation was carried out in the presence of oxygen, the yield of products was quantitatively and qualitatively different from those in the absence of oxygen. 2, 3-, 2, 4-, 2, 5- and 2, 6-Dihydroxy benzoic acid are produced in place of isomers of biphenyldicarboxylic acid. The total amount of dihydroxy benzoic acids is 0.31 as *G*-value, being about one fifth of mono-hydroxybenzoic acids. Table II shows the yield and *G*-value of products in the oxygen saturated solution. In this case, *G*-value of 2, 2'-biphenyldicarboxylic acid, the most abundant isomer in the irradiation of oxygen free solution, was estimated to be lower than 0.0003. Therefore, a noticeable amount of isomers of biphenyldicarboxylic acid was not observed in an oxygen saturated solution.

Table II. Yields of products in oxygen saturated solution of benzoic acid (carboxyl-^{14}C) irradiated with Co-60 gamma rays

Product	Weight mg./ml.	Yield %	*G*-value
2-Hydroxybenzoic acid	0.45	15	0.79
3-Hydroxybenzoic acid	0.16	5.4	0.29
4-Hydroxybenzoic acid	0.37	12	0.65
2,3-Dihydroxy-benzoic acid	0.072	2.4	0.12
2,4-Dihydroxy-benzoic acid	0.056	1.9	0.088
2,5-Dihydroxy-benzoic acid	0.060	2.0	0.096
2,6-Dihydroxy-benzoic acid	0.0036	0.12	0.0057
Benzoic acid*	1.31	61	
−Benzoic acid**	1.19	39	2.12
2,2'-Biphenyl-dicarboxylic acid	2.9×10^{-4}		0.0003

Dose, 4.0×10^{6} r, dose rate, 1.6×10^{5} r/hr.
* Unchanged benzoic acid (carboxyl-^{14}C) in the irradiated solution.
** The disappearance of benzoic acid (carboxyl-^{14}C) calculated from the amount of unchanged benzoic acid (carboxyl-^{14}C).

Discussion

The mechanism of radiation-induced reaction of an aqueous solution of organic compound has been studied by a number of workers. The primary process of the reaction is assumed to be radiolytic decomposition of water. Recently, Burton and his collaborators proposed the following *G*-values for the species[7].

$$H_2O \rightsquigarrow H\cdot,\ HO\cdot,\ H_2,\ H_2O_2 \qquad (1)$$
$$G = 3.70\ \ 2.93\ \ 0.39\ \ 0.78$$

These values will be used in the following discussion.

From the present results of radioactive assay, some information about the initial step of the radiation-induced reaction is obtained. As is shown in Tables I and II, *G*-values of the disappearence of benzoic acid were 2.12 in the presence of molecular oxygen and 1.88 in the absence of molecular oxygen. These values agree fairly well with each other in spite of irradiation conditions being different.

This agreement signifies that dissolving oxygen does not affect the initial step of the decomposition of benzoic acid. It would be, therefore, reasonable to consider that in both cases the initial stage of the reaction is initiated by the attack of the same radical on the benzoic acid molecule.

Hydrogen atom in the reactive species produced from water reacts easily with dissolving oxygen forming hydroperoxy radical in the presence of oxygen.

$$H\cdot + O_2 \rightarrow HO_2\cdot \qquad (2)$$

If the decomposition of benzoic acid is initiated by the hydrogen atom, it is impossible to explain the *G*-value of the decomposition of benzoic acid being almost of the same value regardless of the dissolving of oxygen. Consequently, a hydroxyl radical must be considered to be the only radical which can attack benzoic acid.

Based on the above reasons, the disappearence of benzoic acid in an aqueous solution is considered to be initiated by hydrogen-abstraction of hydroxyl radical as is proposed in the previous paper:

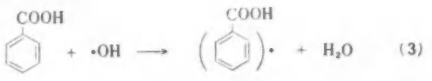

(3)

The concentration of hydroxycarbonylphenyl radical as an intermediate in the reaction must

7) K. C. Kurien, P. V. Phung and M. Burton, *Radiation Research*, **11**, 283 (1959).

TABLE III. *G*-VALUE OF INTERMEDIATE RADICAL

Condition	Hydroxyl radical: Used for hydrogen-abstraction	Hydroxyl radical: Used for combination with H. C. P. radical	Total	H. C. P. radical*1
Oxygen free	$G(H)$*2 $+2G(B)$*3 $=1.7$	$G(H)=0.24$	1.94	$G(H)+2G(B)=1.7$
Oxygen saturated	$G(H)+2G(D)$*4 $=2.3$	zero	2.3	$G(H)+G(D)=2.0$

*1 H. C. P. radical is hydroxycarbonylphenyl radical
*2 The total *G*-value of hydroxybenzoic acids
*3 The total *G*-value of biphenyldicarboxylic acids
*4 The total *G*-value of dihydroxybenzoic acids
The *G*-value of hydroxyl radical produced in the primary process is 2.92[7].

be of the same value in both cases, because the *G*-value of hydroxyl radical produced primarily from radiolytic decomposition of water is constant of 2.93 regardless of whether with or without oxygen.

In spite of the constant *G*-value of the disappearance of benzoic acid, the products of the reaction in the presence of oxygen were quite different from those in the absence of oxygen. In the former case hydroxybenzoic acids were the predominant products, whereas biphenyldicarboxylic acids were the main products in the latter case.

In the absence of oxygen, the total *G*-value of biphenyldicarboxylic acid as main product was 0.73, whereas that of hydroxybenzoic acid was 0.24. Hydroxybenzoic acid may be produced by the combination reaction of hydroxyl radical with hydroxycarbonylphenyl radical:

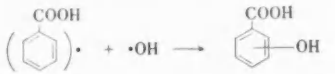

(4)

In this case, the amount of hydroxyl radical concerned in the hydroxylation of benzoic acid might be two fold of the amount of hydroxybenzoic acid, and so the *G*-value of this radical participating in the reaction will be calculated to be 0.48, and subsequently, the *G*-value of hydroxycarbonylphenyl radical produced in the reaction as an intermediate might be 0.24.

On the other hand, there are two possibilities of the formation of biphenyldicarboxylic acids from hydroxycarbonylphenyl radical. If biphenyldicarboxylic acids are produced by the substitution reaction of hydroxycarbonylphenyl radical as in the following,

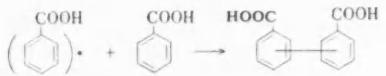

(5)

the disappearance of benzoic acid in this case would be considerably greater than that in the presence of oxygen as mentioned below. It is because the same yield of hydroxycarbonylphenyl radical is proposed in both cases. Accordingly, the formation of biphenyldicarboxylic acids can be attributed to the dimerization of hydroxycarbonylphenyl radical.

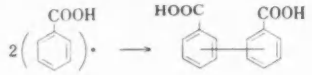

(6)

In this case, the amount of hydroxycarbonylphenyl radical converted into biphenyldicarboxylic acids is two times as much as that of biphenyldicarboxylic acid. If the predominant process of the reaction is the dimerization of hydroxycarbonylphenyl radicals, the total amount of hydroxycarbonylphenyl radical is 1.70 as calculated in Table III.

In the presence of molecular oxygen, hydroxybenzoic acids were predominant products. Noticeable amount of biphenyldicarboxylic acid was not observed. The *G*-value of 2, 2′-biphenyldicarboxylic acid, the most abundant isomer in the absence of molecular oxygen, was reduced to the value of 0.0003. Therefore, it would be unlikely that hydroxybenzoic acid in the presence of molecular oxygen is produced by the combination reaction of hydroxycarbonylphenyl radical with a hydroxyl radical, because the formation of hydroxybenzoic acid by this type of the reaction would be, without fail, accompanying the formation of biphenyldicarboxylic acid as in the case of oxygen free solution.

Hydroxycarbonylphenyl radical produced according to Eq. 3 reacts easily with dissolving oxygen to give a hydroxycarbonylphenylperoxy radical. It is, in general, considered that aromatic peroxide is very unstable. Consequently, the peroxy radical would decompose spontaneously into the phenoxy radical and then the reaction results finally in the formation of monohydroxybenzoic acid as is shown in the following:

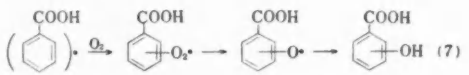

(7)

The formation of dihydroxybenzoic acids as minor products may be also explained by the

same sequence starting from mono-hydroxybenzoic acid instead of benzoic acid. For example, the following sequence is given for 2, 3-dihydroxybenzoic acid:

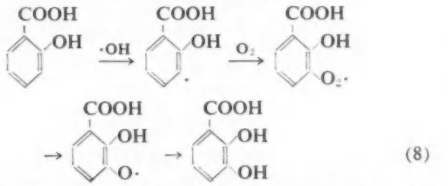

(8)

The above mechanism is supported by the radiation-induced reaction of an aqueous ethanol solution by Weiss and collaborators[8]. They found butane-2, 3-diol as main products in the irradiation of an oxygen free solution,

$$CH_3\cdot CH_2OH \xrightarrow{HO\cdot} CH_3\cdot\dot{C}HOH$$

$$\rightarrow CH_3\cdot \underset{OH}{\overset{|}{C}}H\cdot \underset{OH}{\overset{|}{C}}H\cdot CH_3$$

but, in the presence of oxygen, the dimerization of these radicals was completely suppressed, and acetaldehyde was formed as a predominant product. In this case, they proposed the formation of the peroxy radical ($CH_3\cdot \underset{O_2\cdot}{\overset{|}{C}}HOH$) as an intermediate in the reaction.

$$CH_3\cdot\dot{C}HOH \xrightarrow{O_2} CH_3\cdot \underset{O_2\cdot}{\overset{|}{C}}HOH \rightarrow CH_3CHO$$

Table III shows the *G*-value of intermediate radicals produced in systems both with and without molecular oxygen. Based on the mechanism given by Eqs. 3, 7 and 8, the *G*-values of hydroxyl and hydroxycarbonylphenyl radicals as an intermediate in the presence of oxygen are calculated to be 2.3 and 2.0, respectively, as is shown in the Table III. The total *G*-value of reacting hydroxyl radical is close to that of hydroxyl radical produced in the primary process (1). Accordingly, it is likely that the most of the hydroxyl radicals formed in the primary process of the reaction react with benzoic acid giving the reaction products. The *G*-value of both hydroxyl and hydroxycarbonylphenyl radicals estimated here are greater in the presence of oxygen than in its absence.

There remain, therefore, some possibilities of the formation of hydroxyl radicals from hydroperoxy radicals produced according to Eq. 2 as follows:

$$2HO_2\cdot \rightarrow H_2O_2 + O_2 \qquad (9)$$

$$H_2O_2 \rightarrow 2HO\cdot \qquad (10)$$

Some information for the orientation of the hydroxycarbonylphenyl radical is obtained from the experimental values. *G*-Value of 2-, 3- and 4-hydroxycarbonylphenyl radical produced in the absence of oxygen are calculated to be 0.83, 0.21 and 0.65, respectively, basing on the yields of products summerized in Table I. Thus, the *G*-value ratio of 2-: 3-: 4-hyroxycarbonylphenyl radical is 1 : 0.26 : 0.79.

On the other hand, *G*-values of hydroxybenzoic acid, in the presence of oxygen, were 0.79, 0.29 and 0.65 for 2-, 3-, 4-isomer, respectively. In this case, the present authors can not predict any *G*-values of intermediate hydroxy, hydroxycarbonylphenyl radical isomers 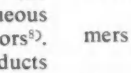 produced from mono-hydroxybenzoic acids. If the formation of dihydroxybenzoic acid, being much smaller than that of mono-hydroxybenzoic acid, might be neglected, the *G*-value ratio calculated as 1 : 0.37 : 0.82 for 2-: 3-: 4-hydroxycarbonylphenyl radical in the presence of molecular oxygen agrees fairly well with that in the absence of molecular oxygen. The easiness of the abstraction of ring hydrogen of benzoic acid by hydroxyl radical is shown, basing on the *G*-value ratio of 2-, 3- and 4-hydroxycarbonylphenyl radical, in the following.

ortho > para > meta

It seems also likely that this agreement supports the above postulate that the reaction is initiated by hydrogen-abstraction reaction of hydroxyl radical without regard to dissolving oxygen.

The ratio of hydroxybenzoic acids obtained by Weiss and his collaborators was approximately 5 : 2 : 10 for 2-: 3-: 4-hydroxybenzoic acid in the solution containing molecular oxygen, whereas the ratio was 6 : 4 : 10 under the condition of with insufficient quantity of available oxygen. In their results, the para-isomer was major component[1]. On the other hand, the ratio of mono-hydroxybenzoic acids obtained by Downes was approximately 9 : 5 : 4 for 2-: 3-: 4-hydroxybenzoic acid[2]. In this case, the ortho-isomer was a major component as well as in the present results, although a different ratio was obtained. These different ratios of products may be attributed rather to the different analytical method, the radiation energies or the experimental conditions such as temperature or concentration than to the different dose rate.

We wish to express our thanks to Professor K. Kimura for his kind guidance and Dr. A. Danno for his many helpful discussions.

Division of Radiation Applications
Japan Atomic Energy Research Institute
Tokai, Ibaraki-ken

8) G. G. Jayson, G. Scholes and J. Weiss, *J. Chem. Soc.*, 1957, 1358.

Studies on Meso-ionic Compounds. XIII[1]. *ψ-2, 4-Dihydro-4, 5-diphenyl-2-keto-1-oxa-3, 4-diazole**

By Mutsuko HASHIMOTO and Masaki OHTA

(Received October 20, 1960)

Since Earl et al.[2] synthesized in 1935 3-phenylsydnone (I; R=Ph, R'=H), many studies on meso-ionic compounds have been carried out especially with sydnones I, whereas not any meso-ionic compound of type II which differs from the sydnones in the reversal of the –CO–O– grouping is yet known, and we have therefore undertaken a general study of this new meso-ionic system.

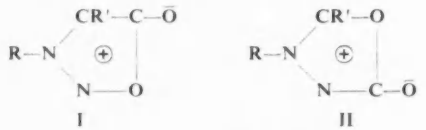

VI; R=R'=C_6H_5
IX; R=CH_3, R'=C_6H_5

Fig. 1

Attempts to prepare the compound II were already made by Baker et al.[3] in 1950. Their attempts were mainly based on methods by which the dithio-analogues III had been prepared[4], and the failure of their syntheses was due in several cases to the instability of carbamic acids. On the assumption that iso-cyanate IV might cyclise to the compound II, the reaction of the hydrochloride of *N*-benzoyl-*N*-phenylhydrazine with carbonyl chloride in boiling toluene was also tried, but they obtained *N*, *N'*-di(benzanilido)urea alone.

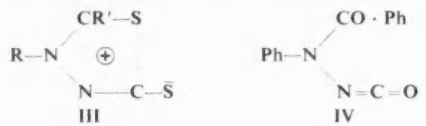

Fig. 2

On the other hand, Hoegerle[5] reported that *N*-aminopyridone-(2) was subjected to the action of carbonyl chloride in chloroform in the presence of potassium carbonate to give the compound V in which the meso-ionic ring in question forms part of a polycyclic system.

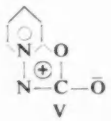

Fig. 3

Now we treated *N*-benzoyl-*N*-phenylhydrazine with carbonyl chloride under the same conditions as Hoegerle used and recrystallized the product from dry benzene obtaining a crystalline solid $C_{18}H_{16}O_2N_2$, m. p. 161~162°C. This, if formulated as $3 \cdot C_{14}H_{10}O_2N_2$, C_6H_6, would correspond to the required meso-ionic compound VI incorporating benzene. Heating the crystalline solid at 100°C under reduced pressure for four days removed benzene from it to afford white crystals, m. p. 165~166°C, which gave analytical figures indicative of the formula $C_{14}H_{10}O_2N_2$.

A comparison of the infrared spectrum of the compound with that of its precursor, *N*-benzoyl-*N*-phenylhydrazine, led us to assign it the structure VI. That is: (1) the disappearance of bands at 3338 and 3278 cm^{-1} in the precursor, arising from NH stretching, (2) the lack of the characteristic band for iso-cyanate group, and (3) the shift of Amide I band in the precursor at 1625 cm^{-1} towards a band at 1755 cm^{-1}, which corresponds closely with the ester-carbonyl bands in sydnones listed by Earl et al.[6] and Fugger et al.[7] We therefore designated the compound VI as *ψ*-2, 4-dihydro-4, 5-diphenyl-2-keto-1-oxa-3, 4-diazole following the systematic nomenclature proposed by Baker et al.[8]

The *ψ*-oxadiazole VI is insoluble in absolute ethanol at room temperature, but on heating it converts into ethyl *N*-benzoyl-*N*-phenylhydrazinoformate (VII). When refluxed with cyclohexanol in dry benzene for 6 hr. VI gives

1) Part XII: M. Hashimoto and M. Ohta, This Bulletin, **33**, 1394 (1960).

* Presented at the Local Meeting of the Chemical Society of Japan, Hokkaido, July, 1960.

2) J. C. Earl and A. W. Mackney, *J. Chem. Soc.*, **1935**, 899.

3) W. Baker, W. D. Ollis and V. D. Poole, ibid., **1950**, 1547.

4) M. Busch et al., *Ber.*, **28**, 2635 (1895); *J. pr. Chem.*, **60**, 218, 228, 231, 236 (1899); **67**, 201, 202, 246, 250, 257 (1903); W. Baker et al., *J. Chem. Soc.*, **1951**, 289.

5) K. Hoegerle, *Helv. Chim. Acta*, **41**, 548 (1958).

6) J. C. Earl et al., *J. Chem. Soc.*, **1951**, 2207.

7) J. Fugger et al., *J. Am. Chem. Soc.*, **77**, 1845 (1955).

8) W. Baker, W. D. Ollis and V. D. Poole, *J. Chem. Soc.*, **1949**, 311.

cyclohexyl *N*-benzoyl-*N*-phenylhydrazinoformate (VIII). Heating VI with *N*-benzoyl-*N*-phenylhydrazine at 100°C for 20 min. affords

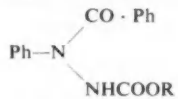

VII; $R=C_2H_5$
VIII; $R=C_6H_{11}$

Fig. 4

N, *N'*-di(benzanilido)urea, which has a lower melting point by 10°C than that reported by Baker et al., but gives the correct analytical values. The same product is also obtained on treatment of VI with boiling water for 3 hr. When heated with aniline at 100°C for 15 min., VI gives 1-benzoyl-1, 4-diphenylsemicarbazide. On treatment with concentrated aqueous ammonia or aqueous dimethylamine, VI gives not the corresponding semicarbazides, but benzamide or *N*-benzoyl-*N*-phenylhydrazine, respectively.

These reactions which suggest the presence of a iso-cyanate group in a molecule were also observed in the polycyclic analogue V[5]. However, the fact that V can be recrystallized from ethanol but VI suffers a ring fission from hot ethanol indicates that VI is less stable than V.

By acid hydrolysis, VI regenerates *N*-benzoyl-*N*-phenylhydrazine. The probable mechanism of the above described hydrolysis is shown in

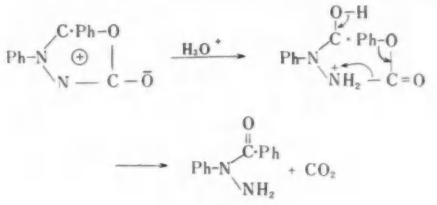

Fig. 5

Fig. 5 after that of acid hydrolysis of sydnones proposed by Baker et al.[9] Unlike sydnones**, *N*-benzoyl-*N*-phenylhydrazine obtained here is unaffected by acid and therefore no further degradation towards phenylhydrazine and benzoic acid might occur.

By alkaline hydrolysis, VI affords phenylhydrazine and benzoic acid. This observation could best be accounted for, if it is considered that the hydrolysis of lactonic group of VI produces unstable intermediate *N'*-carboxy-*N*-benzoyl-*N*-phenylhydrazine and this immediately decomposes to phenylhydrazine and benzoic acid.

Besides the above diphenyl derivative VI, attempts to prepare some analogues were frustrated except *ψ*-2, 4-dihydro-4-methyl-5-phenyl-2-keto-1-oxa-3, 4-diazole (IX) by the inaccessibility of *α*-acylhydrazines. The compound IX was prepared, in very poor yield, by the same treatment of *N*-benzoyl-*N*-methylhydrazine as that used for VI. Recrystallization from dry benzene afforded colorless needles, m. p. 150°C, which gave analytical figures indicative of the formula $C_9H_8O_2N_2$ (IX). Owing to the poor yield both of *N*-benzoyl-*N*-methylhydrazine and of IX, we obtained too small a quantity of IX to examine its infrared spectrum or to perform various reactions similar to those to which diphenyl derivative VI was subjected.

Experimental

N-Benzoyl-N-phenylhydrazine.—A mixture of *N'*-acetyl-*N*-benzoyl-*N*-phenylhydrazine (5 g.), concentrated sulfuric acid (5 ml.), water (25 ml.) and ethanol (35 ml.) was refluxed for 2 hr. Silky needles which separated on cooling were filtered off, suspended in plenty of water and neutralized with sodium carbonate affording colorless prisms (3.1 g.), m. p. 66°C. Recrystallization from dilute ethanol raised m. p. to 78°C (the reported melting point is 69~70°C.[10]).

Found: N, 13.03. Calcd. for $C_{13}H_{12}ON_2$: N, 13.20%.

ψ-2, 4-Dihydro-4, 5-diphenyl-2-keto-1-oxa-3, 4-diazole (VI).—To a solution of *N*-benzoyl-*N*-phenylhydrazine (2 g.) in chloroform (200 ml.) was added finely powdered, anhydrous potassium carbonate (20 g.) and then a violent stream of carbonyl chloride was introduced with vigorous stirring at −7°C for 10 min. After it has been kept standing overnight, reaction mixture was allowed to reflux for 30 min. and sediments were removed. The filtrate was evaporated and the residue was recrystallized from dry benzene to give colorless lancets (1.71 g.), m. p. 161~162°C, which incorporate benzene.

Found: C, 72.16; H, 4.80; N, 10.98. Calcd. for $C_{45}H_{36}O_6N_6$ ($3\cdot C_{14}H_{10}O_2N_2$, C_6H_6): C, 72.72; H, 4.53; N, 10.66%.

When this compound was heated at 100°C under reduced pressure, benzene was removed affording white crystals, m. p. 165~166°C.

Found: C, 70.72; H, 4.52; N, 11.62. Calcd. for $C_{14}H_{10}O_2N_2$: C, 70.58; H, 4.23; N, 11.76%.

Ethyl N-Benzoyl-N-phenylhydrazinoformate (VII).—(a) A solution of VI (0.35 g.) in absolute ethanol (10 ml.) was warmed on a water bath and after 3 hr. evaporated under reduced pressure to give white powder (0.37 g.), m. p. 132°C. Recrystallization from dilute ethanol gave colorless

9) W. Baker and W. D. Ollis, *Quart. Rev.*, **11**, 22 (1957).
** When heated with aqueous acid, the sydnones give *N*-substituted hydrazine, carboxylic acid and carbon dioxide. The interesting production of *α*-acylhydrazine is observed only when 3-phenylsydnone is treated with one molecular proportion of water and hydrogen bromide.

10) O. Widman, *Ber.*, **26**, 947 (1893).

needles, m. p. 135~136°C, undepressed by admixture with the authentic sample prepared by route (b).

Found: C, 67.18; H, 5.92; N, 10.03. Calcd. for $C_{16}H_{16}O_2N_2$: C, 67.59; H, 5.67; N, 9.85%.

(b) To a solution of *N*-benzoyl-*N*-phenylhydrazine in ether was added equimolar ethyl chloroformate and the solid which separated was filtered off and recrystallized from dilute ethanol affording colorless needles, m. p. 136°C (Found: N, 9.95%).

Cyclohexyl *N*-Benzoyl-*N*-phenylhydrazinoformate (VIII).—A mixture of VI (0.5 g.), cyclohexanol (1 ml.) and dry benzene (20 ml.) was refluxed for 6 hr., evaporated under reduced pressure and the residue washed with ether and recrystallized twice from dilute dioxane to give colorless needles, m. p. 138~139°C.

Found: N, 8.05. Calcd. for $C_{20}H_{22}O_3N_2$: N, 8.28%.

***N*, *N'*-Di(benzanilido)urea.**—(a) *N*-Benzoyl-*N*-phenylhydrazine (1 g.) and VI (0.5 g.) were finely powdered, mixed up and kept at 100°C for 20 min. The cooled, hard solid was washed thoroughly with ether and further twice with hot chloroform (yield, 0.82 g.). Recrystallization from pyridine gave a white powder, m. p. 263°C (decomp.) (the reported melting point is 274°C[3]).

Found: C, 72.21; H, 5.33; N, 12.81. Calcd. for $C_{27}H_{22}O_3N_4$: C, 72.00; H, 4.89; N, 12.44%.

(b) VI (0.5 g.) was refluxed with water (20 ml.) with stirring for 3 hr. The precipitate was filtered off, washed with chloroform, dried (0.25 g.) and recrystallized from pyridine giving a white powder, m. p. 263.5°C (decomp.) (Found: C, 71.89; H, 4.93; N, 12.76%).

1-Benzoyl-1, 4-diphenylsemicarbazide.—VI (0.5 g.) was dissolved in purified aniline (1 ml.), heated at 100°C for 15 min. and then the solid which deposited was collected, washed with ether (yield, 0.6 g.) and recrystallized from dilute ethanol affording colorless needles, m. p. 210~211°C.

Found: C, 72.27; H, 5.37; N, 12.82. Calcd. for $C_{20}H_{17}O_2N_3$: C, 72.49; H, 5.17; N, 12.68%.

Reaction of VI with Aqueous Ammonia.—VI (1 g.) was added to concentrated aqueous ammonia (40 ml.) and stirred vigorously. After 3~4 hr. complete dissolution occurred, a pale orange color developing. After it has been kept standing at room temperature for 2 days, the reaction mixture was evaporated under reduced pressure and the residue with a smell of phenylhydrazine was collected, washed with ether, dried (yield, 0.14 g.) and recrystallized from a little water giving colorless needles, m. p. 126~127°C, undepressed by admixture with authentic benzamide.

Found: N, 11.64. Calcd. for C_7H_7ON: N, 11.57%.

Reaction of VI with Aqueous Dimethylamine.—VI (0.5 g.) was added to 40% aqueous dimethylamine (10 ml.) and stirred vigorously. After 15 min. complete dissolution occurred, an orange color developing. After it has been kept standing at room temperature for 5 days, the reaction mixture was evaporated under reduced pressure to give the residual oil which solidified on addition of concentrated hydrochloric acid. Recrystallization from ethanol-ether yielded colorless needles, m. p. 192~193°C (decomp.), which showed the positive Beilstein test.

Found: N, 11.46. Calcd. for $C_{13}H_{13}ON_2Cl$: N, 11.27%.

The authentic sample prepared by the action of concentrated hydrochloric acid on *N*-benzoyl-*N*-phenylhydrazine had m. p. 191~193°C (decomp.) (Found: N, 11.12%).

Acid Hydrolysis.—When VI (1 g.) was warmed with 10% aqueous hydrochloric acid on a water bath, complete dissolution did not occur but the form of crystallization gradually changed. The precipitate was filtered off, dried (0.66 g.) and recrystallized from water affording colorless needles, m. p. 199°C (decomp.), which showed the positive Beilstein test.

Found: C, 62.60; H, 5.49; N, 10.89. Calcd. for $C_{13}H_{13}ON_2Cl$: C, 62.78; H, 5.23; N, 11.3%.

Alkaline Hydrolysis.—VI (1 g.) was readily dissolved in 10% aqueous sodium hydroxide. After 45 min. the solution was acidified to give colorless leaflets (0.39 g.), m. p. 122°C, undepressed by admixture with authentic benzoic acid. The acidic filtrate was neutralized and extracted with ether. The extract was dried with sodium sulfate and evaporated to give an oily product, from which on addition of aqueous oxalic acid the oxalate of phenylhydrazine was obtained.

***ϕ*-2, 4-Dihydro-4-methyl-5-phenyl-2-keto-1-oxa-3,4-diazole (IX).**—To a solution of *N*-benzoyl-*N*-methylhydrazine (3.5 g.), prepared by Michaelis' method[11], in chloroform (600 ml.) was added finely powdered, anhydrous potassium carbonate (60 g.) and then a violent stream of carbonyl chloride was introduced with vigorous stirring at −5~−8°C for 10 min. After it has been kept standing overnight, the reaction mixture was refluxed for 30 min. and sediments were removed. The filtrate was evaporated to give very viscous oil with a strong smell of benzoyl chloride. Addition of ether afforded a small amount of crystalline solid, which was collected and recrystallized from dry benzene giving colorless needles, m. p. 150°C.

Found: C, 61.55; H, 4.88; N, 16.15. Calcd. for $C_9H_8O_2N_2$: C, 61.36; H, 4.58; N, 15.90%.

We are indebted to Dr. Asaji Kondo for microanalyses and to Dr. Tadashi Sato for infrared spectroscopic work.

Laboratory of Organic Chemistry
Tokyo Institute of Technology
Meguro-ku, Tokyo

11) A. Michaelis and E. Hadanck, ibid., **41**, 3288 (1908).

Bile Acids and Steroids. XXI[1]. *Studies on the Hog Bile Acids (Part 5)*[1]. *On the Oxidation of Epimeric 3,6-Dihydroxycholanoic Acids with N-Bromosuccinimide*[*1]

By Jun'ichi KAWANAMI

(Received September 30, 1960)

Previously, it was described that α-hyodeoxycholic acid is selectively oxidized at C-3 with *N*-bromosuccinimide (NBS) to give 3-oxo-6α-hydroxy-5β-cholanoic acid[2], whereas it has been reported earlier by Wieland[3] that it was preferentially oxidized at C-6 with chromic acid. From this reverse result, it was of interest to investigate the oxidation of epimeric 3,6-dihydroxy-5β-cholanoic acids with NBS. Oxidation was carried out in both dioxane-water (9:1) and acetone-water (7:3) in order to obtain information depending on polarity of the solvent and with 1 and 2 molar equivalents of NBS respectively in order to obtain information depending on selectivity. As seen in Table I, the order of susceptibility to oxidation obtained from the results was as follows:

$$6\beta > 3\beta \ \& \ 3\alpha > 6\alpha \quad (A/B: \text{cis})$$

The 6β-hydroxyl group was most rapidly oxidized, the 6α-hydroxyl group was not attacked and the ease of oxidation of both the 3β- and the 3α-hydroxyl groups were in between. However, the difference between 3β- and 3α-hydroxyl group was not definable in such an experiment. Although there is a method in which the reagent such as NBS is volumetrically titrated, it is presumed to complicate the results on account of two factors, both a consumption by the substrates and a decomposition by the solvent. Therefore, the author examined the oxidation using the absorption band at 1720 cm^{-1} corresponding to the carbonyl group of the six-membered ketone in the infrared spectrum. This band is so strong that it is useful for determination. Since the reaction itself was assumed to be very complicated as mentioned above, it was most reliable to use the optical densities of the six-membered carbonyl band in the infrared spectrum for this purpose. In this case, as methyl 3-oxo-6α-hydroxy-5β-cholanoate was oily, it was unsuitable for preparing the calibration curve. Consequently, methyl lithocholate[7] and methyl 3β-hydroxy-5β-cholanoate[8] were used as starting materials. Ester is also suitable to avoid the overlap of the acid carbonyl band with the six-membered ketone band in the infrared spectrum. As the six-membered carbonyl band was further somewhat overlapped with that of

TABLE I. THE POSITION ATTACKED AND THE YIELD IN EACH EPIMER

Solvent	Dioxane-Water (9:1)		Acetone-Water (7:3)	
Mol. equiv. of NBS	1	2	1	2
Reaction time at room temperature (20±2°C)	1.5 hr.	1.5 hr.	Overnight	4 days
3α, 6α	3(27.2%)	3(30.1%)	3(41.7%)	3(61.8%)
3β, 6α[4]	3(21.3%)	3(45.7%)	3(31%)	3(62.5%)
3β, 6β[5]	6(77%)	6(56.6%)	6(77.5%)	6(55%)
		3,6(14.3%)		3,6(19.3%)
3α, 6β[6]	6(70%)	6(60%)	6(70%)	6(59.4%)
		3,6(7.5%)		3,6(16%)

*1 The rest is abbreviated as NBS.

1) Part XX: J. Kawanami, This Bulletin, **34**, 509 (1961).

2) K. Takeda and J. Kawanami, *J. Biochem. (Japan)*, **40**, 477 (1953).

3) H. Wieland and E. Dane, *Z. Physiol. Chem.*, **212**, 41 (1932).

4) β-Hyodeoxycholic acid was prepared from 3-oxo-6α-hydroxy-5β-cholanoic acid according to Moffett method. (R. B. Moffett and W. Hoehn, *J. Am. Chem. Soc.*, **69**, 1995 (1947)).

5) Synthesis of 3β, 6β-dihydroxy-5β-cholanoic acid was described in the preceding part XX.

6) 3α, 6β-Dihydroxy-5β-cholanoic acid was prepared from methyl 3α-acetoxy-6-oxo-5β-cholanoate according to Moffett method. (R. B. Moffett and W. Hoehn, *J. Am. Chem. Soc.*, **68**, 1855 (1946)). This compound was also prepared in good yield by using sodium borohyride in place of Raney nickel.

7) Methyl lithocholate was prepared from cholic acid according to the usual method. (S. Sarel and Y. Yanuka, *J. Org. Chem.*, **24**, 2018 (1959)).

8) Methyl 3β-hydroxy-5β-cholanoate was prepared from both Methyl 3-oxo-cholanoate and Methyl 3α-tosyloxy-5β-cholanoate according to Fieser's and Reindel's method respectively. (F. Reindel and K. Niederlandre, *Ber.*, **68**, 1243 (1935); L. F. Fieser and J. C. Babcock, *J. Am. Chem. Soc.*, **74**, 5474 (1952)).

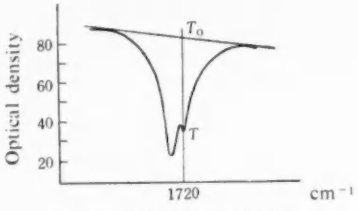

Fig. 1. Baseline method.

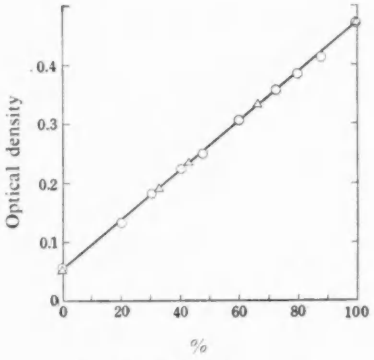

Fig. 2. Calibration curve.
—○— 3α-epimer; —△— 3β-epimer

the ester group, T_0 was estimated according to the baseline method (Fig. 1).

The calibration curve was made by using a variety of mixtures consisting of each methyl 3β- or 3α-hydroxy-5β-cholanoate and methyl 3-oxo-5β-cholanoate. As shown in Fig. 2, the calibration curve plotting the relationship between the optical density and the concentration ($W/W\%$) of the oxidation product, 3-oxo-5β-cholanoate to each of methyl 3β- or 3α-hydroxy-5β-cholanoate, formed a straight line which indicated its usefulness for a quantitative analysis. The values thus obtained are shown in Tables II and III. Then, the

TABLE II. RELATIONSHIP BETWEEN OPTICAL DENSITY AND RATIO ($W/W\%$) OF THE 3-OXO DERIVATIVE TO THE 3α-EPIMER

Percentage of 3-oxo deriv.	3-Oxo mg.	3α-OH mg.	CCl_4 + Sample mg.	W %	$\overline{T}_0$	$\overline{T}$
0	0	5.0	589.0	0.850	88.3	79.4
20	0.8	3.2	472.0	0.848	87.8	67.7
30	1.8	4.2	717.2	0.838	87.6	61.7
40	2.0	3.0	604.0	0.828	88.0	57.9
48	4.5	4.9	1163.1	0.807	87.7	55.2
60	3.0	2.0	594.0	0.842	87.7	48.5
72	4.3	1.7	704.5	0.852	87.3	43.5
80	4.0	1.0	588.0	0.850	87.3	41.3
87.4	6.9	1.0	942.9	0.837	87.1	39.6
100	6.3	0	792.4	0.795	87.2	36.6

TABLE III. RELATIONSHIP BETWEEN OPTICAL DENSITY AND RATIO ($W/W\%$) OF THE 3-OXO DERIVATIVE TO THE 3β-EPIMER

Percentage of 3-oxo deriv.	3-Oxo mg.	3β-OH mg.	Sample $+CCl_4$ mg.	W %	$\overline{T}_0$	$\overline{T}$
0	0	7.2	897.3	0.801	87.8	80.0
33.3	2.7	5.4	924.9	0.875	87.7	60.0
43.4	3.7	4.9	948.9	0.908	87.4	53.6
66.7	6.2	3.1	1081.8	0.859	87.1	45.5
100	6.3	0	792.4	0.795	87.2	36.6

TABLE IV. RELATIONSHIP BETWEEN THE YIELD OF OXIDATION PRODUCTS AND TIME AT 25°C

No.*	t min.	Sample mg.	Sample $+CCl_4$ mg.	W %	D	Yield
1	30	45.5	5342.3	0.851	—	—
2	30	46.2	5490.0	0.841	—	—
3	50	41.2	4850.6	0.850	0.122	20
4	50	45.0	5305.0	0.848	0.105	15
5	70	35.0	4099.5	0.854	0.183	38
6	70	44.3	5215.3	0.851	0.144	27
7	90	44.6	5232.6	0.852	0.257	60
8	90	44.0	5171.0	0.850	0.227	51.5

* Odd numbers are from the 3β-epimer and even numbers from the 3α-epimer.

TABLE V. THE OXIDATION OF BOTH EPIMERS FOR 60 min. AT 25°C

Starting material	Sample mg.	Sample $+CCl_4$ mg.	W %	D	Yield of 3-oxo deriv. %
3β	41	4.919	0.831	0.262	63.8
3α	43.5	5.050	0.862	0.219	48.3

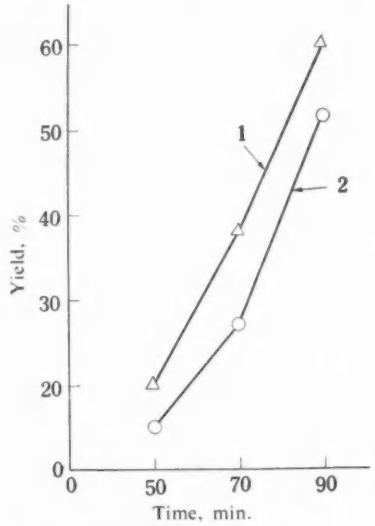

Fig. 3. Relationship between time and yield in each epimer.
(1) 3β-epimer; (2) 3α-epimer

oxidation of epimeric methyl 3-hydroxy-5β-cholanoates was carried out with 1.3 molar equivalents of NBS in dioxane-water (9:1) solution at 25°C. There is a marked difference in the yield between 3β- and 3α-hydroxyl derivatives (Fig. 3). The values obtained are shown in Tables IV and V. Accordingly, the order of susceptibility to oxidation obtained from the results described above was as follows:

$$6\beta(a) > 3\beta(a) > 3\alpha(e) > 6\alpha(e) \quad (A/B: \text{cis})$$

In order to obtain the further support on the influence of steric factors in this reaction, the oxidation of two 3,6-dihydroxy-5α-cholanoic acid (3β,6β-dihydroxy-5α-cholanoic acid and 3β,6α-dihydroxy-5α-cholanoic acid) was examined. The oxidation was carried out as in the previous case. While the oxidation of the former gave a 6-oxo derivative, the oxidation of the latter gave a 3-oxo derivative. From these results in A/B-trans series, the 6β-hydroxy group was also rapidly oxidized but the 6α-hydroxyl group was not affected under such a condition and the ease of oxidation of the 3β-hydroxyl group was in between. Accordingly, the order of the susceptibility to the oxidation of hydroxyl groups in A/B-trans series was also as follows:

$$6\beta(a) > 3\beta(e) > 6\alpha(e) \quad (A/B: \text{trans})$$

Discussion on the Reaction Mechanism

Prior to considering the reaction mechanism of oxidation with NBS from the above result, the outline of reports on the reaction mechanism of chromic acid oxidation should be described. Westheimer and Nicolaides[9] minutely studied the reaction mechanism of chromic acid oxidation and they found that the rate-determining step is not the formation of a chromate ester but the cleavage of the carbon hydrogen bond.

$$(A) \quad R_2CHOH + HCrO_4^- + H^+ \overset{\text{fast}}{\rightleftarrows} R_2CHOCrO_3H + H_2O$$

$$(B) \quad R_2\underset{\underset{H}{|}}{C}-O-CrO_3H + H_2O \xrightarrow{\text{slow}} R_2C{=}O + [HCrO_3^-] + H_3O^+$$

Barton[10] found that the conformational factor determined nearly always the order of reactivity in oxidation among several hydroxyl groups and established a general rule that an axial alcohol is ordinarily more susceptible than the corresponding equatorial alcohol. There are, however, some cases in which an equatorial alcohol having a less accessible axial carbon hydrogen bond is faster oxidized than an axial alcohol (e.g. compare equatorial 11α-hydroxyl with 3-axial hydroxyl group). Schreiber and Eschenmoser[11] measuring the reaction rates of oxidation of a number of hydroxy-5α-cholestanes, confirmed again a general rule proposed by Barton and further defined a second factor determining reaction rates. That is, the transformation of the tetrahedral carbon of an alcoholic (or chromate ester) group to a trigonal carbonyl carbon often eliminates some or all of the repulsive interactions leading to instability. The reaction rates are thus dependent upon the extent of decrease in such interactions. A example in A/B-trans series is as follows:

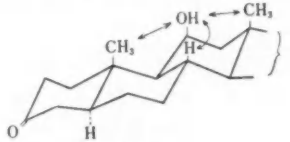

Fig. 4

As seen in Fig. 4, the 11β-hydroxyl group is under steric strain from the repulsions between the four groups, 11β-hydroxyl, C-10-methyl, C-13-methyl and 8β-hydrogen. Relief of this strain provides a driving force sufficient to promote the oxidation.

On the other hand, oxidation with reagents such as *N*-bromosuccinimide or *N*-bromoacetamide has been less clear from both mechanistic and conformational view points[12]. On the basis of the studies described above, the reaction mechanism of oxidation with NBS could be considered. The order of susceptibility to oxidation of the epimeric 3,6-dihydroxycholanoic acids with NBS was as follows:

$$(C) \quad 6\beta(a) > 3\beta(a) > 3\alpha(e) > 6\alpha(e) \quad (A/B: \text{cis})$$

$$(D) \quad 6\beta(a) > 3\beta(e) > 6\alpha(e) \quad (A/B: \text{trans})$$

On the other hand, the order in chromic acid oxidation of hydroxy-5α-cholestanes by Schreiber at the corresponding position was as follows:

$$(E) \quad 6\beta(a) > 3\alpha(a) > 6\alpha(e) > 3\beta(e)$$
$$[36]^* \quad [3.0]^* \quad [2.0]^* \quad [1.0]^* \quad (A/B: \text{trans})$$

* Relative rates to 3β-hydroxy-5α-cholestane.

From the results on the oxidation of α-hyodeoxycholic acid with chromic acid, there are also the following positions.

9) F. H. Westheimer and N. Nicolaides, ibid., **71**, 25 (1949).
10) D. H. R. Barton, *Experientia*, **6**, 316 (1950); *J. Chem. Soc.*, **1953**, 1027.
11) J. Schreiber and A. Eschenmoser, *Helv. Chim. Acta*, **38**, 1929 (1955).
12) H. J. E. Loenthal, *Tetrahedron*, **6**, 269 (1959).

(F) $6\alpha(e) > 3\alpha(e)$ (A/B: cis)

Compared with the above cited four expressions C, D, E and F, it is analogous in conformational view in accord with the Barton rule. In other words, an axial alcohol is more susceptible to oxidation than the corresponding equatorial epimer ($6\beta > 6\alpha$, $3\beta > 3\alpha$: A/B cis). Accordingly, in the case of the axial hydroxyl group, it is clear that the oxidation with NBS proceeds likewise to chromic acid oxidation, because both intermediates similarly have a more accessible C–H bond (equatorial) and a repulsive intermediate ester (axial). The concept described above will be also supported by the following examples.

cholestane-3β, 5α, 6β-triol—
6-oxo derivative[13]

3β, 6β-dihydroxy-5α-cholanoic acid—
6-oxo derivative*2

5α-cholestane-3β, 7α-diol—
7-oxo derivative[14]

11β-hydroxytigogenine—11-oxo derivative[15]

11β-hydroxyprogesterone—
11-oxo derivative[16]

(11α-hydroxyprogesterone was not affected under same condition).

On the other hand, in the series of the generally less reactive equatorial hydroxyl group, e.g. in the case of α-hyodeoxycholic acid, the order with NBS was the reverse of that with chromic acid as seen in expressions C and F. This difference is supposed to depend on a driving force in the intermediate, because it is clear that the conformation of C–H bond (e.g. the 6β-H in Figs. 5 and 6) is equivalent in each case. In the chromic acid oxidation, the intermediate ester has a strong driving force which is derived from both a large space-claim ("Raumbeanspruchung") and an inductive factor (Fig. 5). On the other hand, in the oxidation with NBS, it is assumed that the intermediate ester has a little driving force which resulted from a smaller space-claim and from almost no inductive factor. (Fig. 6). The further explanation was as follows: in the chromic acid oxidation, since the 6β-hydrogen suffers the driving force sufficient to promote the reaction as mentioned above, it can be more easily eliminated than the 3β-hydrogen, whereas in the case of NBS, the driving force of the intermediate hypohalite is very insufficient. For this reason, an attack of the base on a hydrogen atom attached to the hydroxyl carbon is indispensable for the promotion of the reaction as well as the elimination of this hydrogen. Consequently, it may be deduced that the most important factor in the oxidation of the less reactive equatorial alcohol with NBS depends upon the extent of easiness of the proximity of base to the C–H bond of the alcoholic carbon being oxidized. Therefore, in the oxidation of α-hyodeoxycholic acid with NBS, the 3α-hydroxyl group is more easily oxidized than the 6α-hydroxyl group owing to the vulnerability of the 3β-hydrogen. This concept may be further supported by the fact that the less accessible C–H bonds such as in the 6α- or 11α-alcohol are not affected.

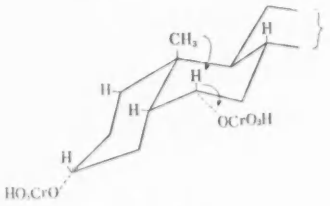

Fig. 5

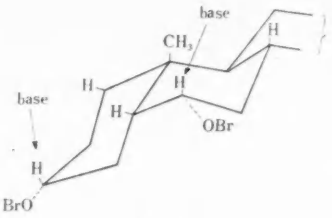

Fig. 6

Examples which show the concept described above are as follows:

3β, 6α-dihydroxy-5α-cholanoic acid—
3-oxo derivative*2

5β-androstane-3α, 11α, 17β-triol—
3, 17-dioxo derivative[17]

11α-hydroxypregnane-3, 20-dione is recovered unchanged after treatment with *t*-butylhypochlorite.

3β, 11α-dihydroxy-5α-pregnan-20-one—
3, 20-dioxo derivative[18]

That desoxycholic acid was not affected with

13) L. F. Fieser and S. Rajagopalan, *J. Am. Chem. Soc.*, **71**, 3938 (1949).
*2 See experimental part.
14) L. F. Fieser and S. Rajagopalan, ibid., **74**, 3309 (1952).
15) S. G. Brooks, J. S. Hunt, A. G. Long and B. Mooney, *J. Chem. Soc.*, **1957**, 1175.
16) A. R. Hanze, G. S. Fonken, A. V. McIntosch, A. M. Searcy and R. H. Levin, *J. Am. Chem. Soc.*, **76**, 3179 (1954).
17) H. L. Herzog, M. Jevnik, and E. B Hershberg, ibid., **75**, 269 (1953).
18) O. Mancera, J. Romo, F. Sondheimer, G. Rosenkranz and C. Djerassi, *J. Org. Chem.*, **17**, 1066 (1952).

NBS in aqueous acetone or in aqueous sodium hydrogen carbonate[19] but with NBA in aqueous *t*-butanol[20], certainly appears to be governed principally by steric effects coupled with size of the reagent and solvating power of the solvent. Thereupon, all hydroxyl groups in which α-hydrogen permits the approach of the base, should be oxidized and this theory was also supported by the following examples.

Ethyl 3β, 5β, 19-trihydroxyetianate—3-oxo derivative[21]

Methyl 3α-hydroxy-9α, 11α-epoxy-5β-cholanoate—3-oxo derivative[22]

The hydroxyl group at C_3 in samogenine[23] (I) and in desoxycholic acid[19] (II), however, was not affected with NBS The reason is not clear in details but it perhaps depends upon the intermediate permitting no release of α-hydrogen on account of vicinal effect or another interactions.

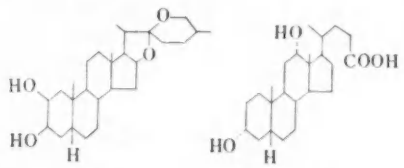

(I) (II)

Experimental[24]

Oxidation of Epimeric 3, 6-Dihydroxy-5β-cholanoic Acids with NBS—General procedure of oxidation was performed by almost the same means as the method previous described[2].

1) The Case of α-Hydroxycholic Acid.—*1.1) With 1 Molar Equivalent of NBS in Dioxane-Water.*—A mixture consisting of α-hyodeoxycholic acid (761 mg.), dioxane-water (9 : 1) (15 ml.) and NBS. (380 mg.; 1.1 mol. equiv.) was allowed to stand for 1.5 hr. at room temperature (18°C). The mixture was changed from colorless to yellow and to orange successively in coloration. To the solution, 10% of aqueous sodium bisulfite was added. The ether extract was washed well with water and evaporated to dryness to afford oil (920 mg.) which was followed by esterification with methanol (4 ml.) and 10% of methanolic hydrochloric acid (0.5 ml.) overnight at room temperature. The ether extract, after isolation in the usual way, gave a yellow oil (777 mg.) which was chromatographed on alumina to afford methyl 3-oxo-6α-hydroxy-5β-cholanoate 3-acetal, 237 mg. (27.2%), m. p. 153~154°C. Identity was established by a mixed melting point and the infrared spectrum with the authentic sample. Infrared spectrum: ν_{max} 3564 (OH); 1724 cm^{-1} (C=O).

Found: C, 72.10; H, 10.30. Calcd. for $C_{27}H_{46}O_5$: C, 71.96; H, 10.29%.

1.2) With 2 Molar Equivalents of NBS in Dioxane-Water.—A mixture consisting of α-hyodeoxycholic acid (605 mg.), dioxane-water (9 : 1) (10 ml.) and NBS (600 mg.; 2.2 mol. equiv.) was treated as in the previous case. The mixture gave methyl 3-oxo-6α-hydroxy-5β-cholanoate 3-acetal, m. p. 152~153°C, 209 mg. (30.1%). This compound was identified by a mixed melting point and the infrared spectrum with the authentic sample.

1.3) With 1 Molar Equivalent of NBS in Acetone-Water.—A mixture consisting of α-hyodeoxycholic acid (579 mg.), acetone-water (7 : 3) (13 ml.) and NBS (290 mg.; 1.1 mol. equiv.) was treated as in the previous case after being allowed to stand overnight at room temperature to furnish crystals, 224 mg., m. p. 146~151°C. The residue from the filtrate was chromatographed on alumina in the usual manner to afford the acetal with m. p. 149~151°C (53 mg.). Total yield were 41.7%. This sample was also identical in a mixed melting point and the infrared spectrum.

1.4) With 2 Molar Equivalents of NBS in Acetone-Water.—The mixture consisting of α-hyodeoxycholic acid (929 mg.), pyridine (500 mg.), acetone-water (7 : 3) (20 ml.) and NBS (926 mg.; 2.2 mol. equiv.) was treated in a way similar to that of the case in the preceding section after being kept for four days at room temperature (20°C) to give the acetal with m. p. 150~152°C (660 mg.; 61.8%). Identity was established by a mixed melting point and the infrared spectrum. Found: C, 72.16; H, 10.26%.

2) The Case of β-Hyodeoxycholic Acid.—*2.1) With 1 Molar Equivalent of NBS in Dioxane-Water.*—After treatment as in the case of section 1.1 the above acetal with m. p. 152~153°C was obtained in 21.3% yield. This compound was identical with the authentic methyl 3-oxo-6α-hydroxy-5β-cholanoate 3-acetal in a mixed melting point and the infrared spectrum.

2.2) With 2 Molar Equivalents of NBS in Dioxane-Water.—Treatment as in the case of section 1.2 afforded the acetal with m. p. 150~152°C in 45.7% yield. Identification was carried out by a mixed melting point and the infrared spectrum.

2.3) With 1 Molar Equivalent of NBS in Acetone-Water.—Treatment similar to that in the case of section 1.3 gave the acetal with m. p. 150~152°C in 31% yield. This compound was also identified

19) L. F. Fieser and S. Rajagopalan, *J. Am. Chem. Soc.*, **71**, 3535 (1949).
20) H. Reich and T. Reichstein, *Helv. Chim. Acta*, **26**, 562 (1943).
21) P. Herzig and M. Ehrenstein, *J. Org. Chem.*, **17**, 713 (1952).
22) L. F. Fieser and S. Rajagopalan, *J. Am. Chem. Soc.*, **73**, 118, 5252 (1951).
23) H. Ōsaka, private communication.
24) All melting points are uncorrected. Infrared spectra were recorded in Nujol Mulls with a "Koken DS 301" double beam infrared spectrophotometer, unless otherwise noted, and the ultraviolet spectra were taken in 95% ethanol solution using a "Hitachi EPS 2" spectrophotometer. Optical rotations were determined in a 1-dm. tube for chloroform solutions, unless otherwise specified. Alumina used for chromatography in this experiment was Merk's reagent grade standardized according to Brockmann and the chromatography was usually performed according to the method described by T. Reichstein. (T. Reichstein and W. Schoppee, *Diss. Faraday Soc.*, **1949**, 305) Extracts were dried over anhydrous sodium sulfate before evaporation unless stated otherwise.

by a mixed melting point and the infrared spectrum.

2.4) With 2 Molar Equivalents of NBS in Acetone-Water.—Isolation similar to that in the case of section 1.4 furnished the acetal with m. p. 148~150°C in 62.5% yield. Identity was established by a mixed melting point and the infrared spectrum.

3) The Case of 3β, 6β-Dihydroxy-5β-cholanoic Acid.—In this experiment, methyl 3β, 6β-dihydroxy-5β-cholanoate was used on account of insolubility of its acid in acetone-water (7 : 3).

3.1) With 1 Molar Equivalent of NBS in Dioxane-Water.—A mixture consisting of methyl 3β, 6β-dihydroxy-5β-cholanoate (350 mg.), dioxane-water (9 : 1) (10 ml.) and NBS (169 mg.; 1.1 mol. equiv.) was allowed to stand for 1.5 hr. at room temperature (22°C). To the solution, 10% of aqueous sodium bisulfite was added to decolorize it. The extract with ether was washed well with water and evaporated to dryness to yield orange oil (494 mg.) which was acetylated with pyridine (4 ml.) and acetic anhydride (4 ml.) under reflux for 2 hr. After cooling, the mixture was carefully diluted with water to afford crystals which were collected, washed throughly with water and recrystallized from methanol to methyl 3β-acetoxy-6-oxo-5α-cholanoate, 235 mg., scales, m. p. 156~158°C. Ether extraction from the above aqueous and methanolic filtrate afforded a yellow oil (156 mg.) which was followed by chromatography on alumina. The eluate with petroleum ether-benzene (2 : 8 and 1 : 1) and benzene gave the above 6-oxo derivative with m. p. 157.5~158°C (61 mg.). Total yield was 77%. This compound was identified by a mixed melting point and the infrared spectrum with the authentic methyl 3β-acetoxy-6-oxo-5α-cholanoate. $[\alpha]_D^{24} = -14 \pm 2°$ (*c* 1.038). Infrared spectrum: ν_{max} 1730, 1710 (C=O); 1252, 1239, 1169, 1039 cm^{-1} (C-O).

Found: C, 72.65; H, 9.48. Calcd. for $C_{27}H_{42}O_5$: C, 72.61; H, 9.48%.

3.2) With 2 Molar Equivalents of NBS in Dioxane-Water.—A mixture consisting of methyl 3β, 6β-dihydroxy-5β-cholanoate (347 mg.) dioxane-water (9 : 1) (10 ml.) and NBS (320 mg.; 2.1 mol. equiv.) was treated as in the previous subsection to give an orange oil (413 mg.) which was followed by chromatography on alumina. The eluate with benzene-petroleum ether (1 : 1), benzene and benzene-chloroform (9 : 1) furnished methyl 3β-acetoxy-6-oxo-5α-cholanoate, 216 mg. (56.6%), scales, m. p. 158~159°C. This was identical with the above specimen in a mixed melting point and the infrared spectrum. The benzene-chloroform (8 : 2 and 1 : 1) elution afforded methyl 3,6-dioxo-5α-cholanoate, 49 mg. (14.3%), m. p. 146~148°C. Zimmermann test gave cherry-red coloration. Infrared spectrum: ν_{max} 1745, 1711 cm^{-1} (C=O).

Found: C, 74.19; H, 9.58. Calcd. for $C_{25}H_{38}O_4$: C, 74.59; H, 9.52%.

3.3) With 1 Molar Equivalent of NBS in Acetone-Water.—Isolation as in the section 3.1 after being kept overnight at room temperature (18°C) gave methyl 3β-acetoxy-6-oxo-5α-cholanoate, m. p. 157~158°C in 77.5% yield. Zimmermann test was negative. This compound was also identical with the above specimen by a mixed melting point and the infrared spectrum.

3.4) With 2 Molar Equivalents of NBS in Acetone-Water.—Treatment as in the previous case furnished methyl 3β-acetoxy-6-oxo-5α-cholanoate, m. p. 157~158°C in 55% yield from the elution with benzene-petroleum ether (1 : 1) and benzene, and methyl 3,6-dioxo-5α-cholanoate, m. p. 148°C in 19.3% yield from the benzene-chloroform (9 : 1) eluate. These samples were also identified by a mixed melting point and the infrared spectrum.

4) The Case of 3α, 6β-Dihydroxy-5β-cholanoic Acid.—*4.1) With 1 Molar Equivalent of NBS in Dioxane-Water.*—To a solution of 3α, 6β-dihydroxy-5β-cholanoic acid (377 mg.) in dioxane-water (9 : 1) (10 ml.), NBS (188 mg.; 1.1 mol. equiv.) was added and kept for 1.5 hr. at room temperature (20±2°C). Isolation, esterification with ethereal diazomethane and acetylation in the usual way gave methyl 3α-acetoxy-6-oxo-5β-cholanoate as prisms, m. p. 150~153°C, 260 mg. $[\alpha]_D^{17} = -21 \pm 2°$ (*c* 1.052, dioxane). Infrared spectrum: ν_{max} 1703 (C=O); 1241, 1230, 1164, 1036, 1026 cm^{-1} (C-O).

Found: C, 72.62; H, 9.59. Calcd. for $C_{27}H_{42}O_5$: C, 72.61; H, 9.48%.

By chromatography on alumina, the filtrate from the above crystals gave further 6-oxo derivative, 40 mg., m. p. 155~165°C (from methanol), a mixture of 5α- and 5β-series.

Found: C, 72.71; H, 9.53%. Total yield was 70%.

4.2) With 2 Molar Equivalents of NBS in Dioxane-Water.—Isolation in the usual way gave a mixture of 6-oxo derivative in 5α- and 5β-series with m. p. 143~147°C in 60% yield from the eluate with benzene-petroleum ether (1 : 1), benzene and benzene-chloroform (9 : 1). Infrared spectrum: ν_{max} 1741, 1712 (C=O); 1249, 1175, 1025 cm^{-1} (C-O).

Found: C, 72.75; H, 9.43. Calcd. for $C_{27}H_{42}O_5$: C, 72.61; H, 9.48%.

The benzene-chloroform (8 : 2 and 1 : 1) eluate gave methyl 3,6-dioxo-5α-cholanoate, m. p. 146~148°C, in 7.5% yield. Infrared spectrum: ν_{max} 1740, 1710 (C=O); 1171 cm^{-1} (C-O).

Found: C, 74.19; H, 9.64. Calcd. for $C_{25}H_{38}O_4$: C, 74.59; H, 9.52%.

4.3) With 1 Molar Equivalent of NBS in Acetone-Water.—The methyl ester was used in this case because the acid was not dissolved in acetone-water (7 : 3). Treatment as in section 3.3 gave 6-oxo derivative, m. p. 150~155°C, in 70% yield. The identification was carried out by a mixed melting point and the infrared spectrum.

Found: C, 72.55; H, 9.64%.

4.4) With 2 Molar Equivalents of NBS in Acetone-Water.—Reaction and isolation as in section 3.4 afforded 6-oxo derivatives in 5α- and 5β-series with m. p. 155~160°C and m. p. 169~170°C, respectively in 59.4% yield from the eluate with benzene and benzene-chloroform (9 : 1). Zimmermann test was negative. Identity was established by a mixed melting point and the infrared spectrum.

Found: C, 72.92; H, 9.57%.

Benzene-chloroform (9 : 1) elution gave methyl 3,6-dioxo-5β-cholanoate, m. p. 128~129°C, in 16% yield. Infrared spectrum: ν_{max} 1739, 1712 (C=O), 1171 cm^{-1} (C-O).

Found: C, 74.07; H, 9.44%.

Oxidation of 3β, 6α-Dihydroxy-5α-cholanoic Acid[*3]. — To a solution of 3β,6α-dihydroxy-5α-cholanoic acid (140 mg.) and pyridine (37.3 mg.) in acetone (1.96 ml.) and water (0.84 ml.) was added NBS (82.5 mg.; 1.3 mol. equiv.). The resulting mixture was refluxed for 4.5 hr., and then the solvent was removed under reduced pressure to the point of distinct turbidity. After a large volume of water was added, the precipitate was collected and dried. This crude keto acid (46 mg.) was recrystallized from acetone to afford 3-oxo-6α-hydroxy-5α-cholanoic acid, fine needles, m. p. 195~197°C (20 mg.). Zimmermann test was positive. $[\alpha]_D^{32} = +4 \pm 2°$ (*c* 1.059, pyridine).

Found: C, 73.21; H, 9.85. Calcd. for $C_{24}H_{38}O_4$: C, 73.80; H, 9.81%.

The above crude acid was esterified with ethereal diazomethane to yield its methyl ester, melting at 90~97°C undefinitely. Zimmermann test was positive. $[\alpha]_D^{27} = +55 \pm 2°$ (*c* 1.038). Infrared spectrum: $\nu_{max}^{CHCl_3}$ 3524 (OH); 1731, 1711 cm^{-1} (C=O).

Found: C, 72.86; H, 10.04. Calcd. for $C_{25}H_{40}O_4 \cdot 1/2H_2O$: C, 72.61; H, 9.91%.

Acetylation of this methyl ester gave methyl 3-oxo-6α-acetoxy-5α-cholanoate, plates, m. p. 115~116°C (from ether-petroleum ether). Zimmermann test was positive. $[\alpha]_D^{33} = +48 \pm 4°$ (*c* 0.608)[*4]. Infrared spectrum: $\nu_{max}^{CHCl_3}$ 1729, 1712 (C=O); 1249, 1175, 1024 cm^{-1} (C-O).

Found: C, 72.92; H, 9.81. Calcd. for $C_{27}H_{42}O_5$: C, 72.61; H, 9.48%.

Oxidation of 3β, 6β-Dihydroxy-5α-cholanoic Acid[*5]. — To a solution of 3β,6β-dihydroxy-5α-cholanoic acid (73 mg.) in acetone (6 ml.), water (1 ml.) and methanol (1.5 ml.), was added NBS (75 mg.; 2.3 mol. equiv.). After the resulting mixture was kept for 3 hr. at room temperature, aqueous sodium bisulfite was added, and the extract with ether was washed with water and evaporated to furnish needles with m. p. 235~237°C. This crude acid was recrystallized from acetone to methyl 3β-hydroxy-6-oxo-5α-cholanoic acid, m. p. 244~245°C, 23 mg. Zimmermann test was negative. Ultraviolet spectrum: λ_{max}^{EtOH} 287 mμ (ε=45). Infrared spectrum: ν_{max} 1727, 1689 cm^{-1} (C=O).

Found: C, 73.61; H, 9.68. Calcd. for $C_{24}H_{38}O_4$: C, 73.80; H, 9.81%.

Its methyl ester was obtained as scales from methanol, melting at 93~95°C. Acetylation of this methyl ester furnished methyl 3β-acetoxy-6-oxo-5α-cholanoate, m. p. 155~157°C, scales. A mixed melting point with methyl 3α-acetoxy-6-oxo-5β-cholanoate with m. p. 156~157°C was melted at 130~135°C. $[\alpha]_D^{32} = -9 \pm 2°$ (*c* 0.91, methanol).

Found: C, 72.62; H, 9.45. Calcd. for $C_{27}H_{42}O_5$: C, 72.61; H, 9.48%.

*3 Synthesis of this compound was described in preceding part XX.

*4 Optical rotation of methyl 3-oxo-6α-acetoxy-5β-cholanoate was as follows: $[\alpha]_D^{31} = -29 \pm 2°$ (*c* 1.057).

*5 As optical rotation of this compound had not been reported, it was measured by the author and its value was found to be as follows: $[\alpha]_D^{33} = -0.1 \pm 2°$ (*c* 1.057, pyridine).

Spectroscopic Determination of the Order of Reactivity in the Oxidation of Methyl 3β- and 3α-Hydroxy-5β-cholanoate with NBS. — *Measurement.*—For the measurement of the optical densities, a "Koken DS 301" (double beam) was used. Infrared spectra were measured by used of a 0.25 mm. cell and at the concentration of about 37% transmission of carbonyl stretching absorption band of the ester group which was controlled by dilution. The speed in the measurements was adjusted to 50 cm^{-1} per 36 sec. at about 1700 cm^{-1} for the purpose of a quantitative analysis. The optical densities of carbonyl band at 1720 cm^{-1} in carbon tetrachloride solution was calculated by the base line method (Fig. 1). T_0 and T were a mean value of three measurements.

Procedure. — A mixture consisting of 3-hydroxy compounds (210 mg.), NBS (126 mg.; 1.3 mol. equiv.) and dioxane-water (9:1) (22 ml.) in a 50 ml. reaction flask with stopper was allowed to stand at 25°C with use of thermostat. Each 5 ml. of the reaction mixture was pipetted at various times and the reaction in each aliquot was stopped with aqueous sodium bisulfite, extracted with ether and successively washed with water, soda and water (ten times). The ethereal layers were evaporated and finally dried in vacuo for 12 hr. at 60°C. The obtained residue (about 45 mg.) was dissolved in so much carbon tetrachloride as to make an adequate concentration giving optical density of the carbonyl band in the ester group at about 37% transmission. The yield of the oxidation product was estimated from the calibration curve prepared above (Fig. 2). These values are shown in Tables IV and V (Fig. 3).

Summary

(1) The order of susceptibility of the hydroxyl groups in epimeric 3,6-dihydroxy-cholanoic acids to the oxidation with NBS was determined and the results were as follows:

6β(a) > 3β(a) > 3α(e) > 6α(e) (A/B: cis)

6β(a) > 3β(e) > 6α(e) (A/B: trans)

(2) Reaction mechanism of the oxidation with NBS was discussed.

The author is particularly indebted to Dr. K. Takeda, Director of this Laboratory, for his discussions and encouragement during this work. The author gratefully acknowledges many helpful discussions with Dr. W. Nagata. Thanks are also due to Mr. Y. Matsui for infrared spectral measurements, to Messers T. Ieki, K. Miyahara, K. Daikatsu, T. Takaoka and Miss. U. Kasugai for elementary analyses and to Mr. T. Iwata for measurements of optical rotation.

Research Laboratory
Shionogi & Co., Ltd.
Imafuku, Amagasaki, Hyogo

Mineral Content of Mixed Fertilizer

By Jumpei ANDO and Seiichi MATSUNO

(Received September 28, 1960)

Recently in Japan nearly 1200000 tons of mixed fertilizer has been produced yearly by the following process:—calcium superphosphate, ammonium sulfate and potassium chloride are mixed, ammoniated so as to neutralize the free phosphoric acid in superphosfate, granulated between 3 and 20 meshes with sprayed water, dried in a rotary drier so as to have 2~3% free water, cooled to 40~60°C by rotary cooler, kept in storage pile for days or weeks and then packed. Ikeno[1] reported that ammonium syngenite and monoammonium phosphate were formed in 8-8-7 mixed fertilizer. No other report is found concerning the fertilizer.

In the present work the mineral content of the products having various $N : P_2O_5 : K_2O$ ratios and reactions during the production process were investigated so as to clarify the cause of caking of products which often takes place in the storage pile, the action of water in the products which must be known for calculation of material balance, and other problems concerning the fertilizer have been studied.

Experimental and Results

Mineral Content of Products.—It was clarified by X-ray diffraction that commercial mixed fertilizers (Table I) were mainly composed of potassium ammonium syngenite (crystalline solution of potassium syngenite $K_2SO_4 \cdot CaSO_4 \cdot H_2O$ and ammonium syngenite $[(NH_4)_2SO_4 \cdot CaSO_4 \cdot H_2O]$, monoammoniumpotassium phosphate (crystalline solution of monoammonium phosphate $NH_4H_2PO_4$ and monopotassium phosphate KH_2PO_4), ammonium chloride and calcium sulfate anhydride. The minerals used as raw materials such as monocalcium phosphate monohydrate, ammonium sulfate and potassium chloride were not at all or were only slightly detected in the products. The amount of these minerals in the products was determined by X-ray diffractometer using spinel $MgO \cdot Al_2O_3$ as inner standard.

Synthesis of Standard Samples.—a) *Inner Standard.*—By preliminary tests it was found that spinel $MgO \cdot Al_2O_3$ was suitable as inner standard. A mixture of equal mole of refined magnesia and alumina was heated for 30 min. at 1600~1670°C. Spinel was formed almost completely. The product contained very few other minerals.

b) *Calcium Sulfate Anhydride.*—Calcium carbonate was treated with concentrated sulfuric acid.

c) *Syngenite.*—Ammonium sulfate or potassium sulfate or various mixtures of both of these was mixed with a theoretical amount of calcium sulfate anhydride and excess of water, heated at 45°C on a water bath and dried. Addition of water and drying were repeated until the single salts disappeared and syngenite or a homogeneous crystalline solution of syngenite was formed.

d) *Monoammoniumpotassium Phosphate.*—Monoammonium phosphate and monopotassium phosphate were mixed at various ratios, the mixture being wet with water, heated at 45°C on water bath

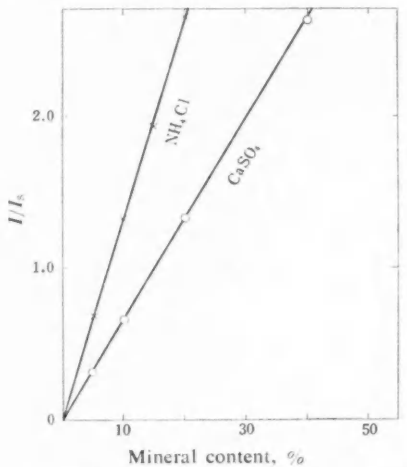

Fig. 1. Calibration curves of ammonium chloride and calcium sulfate anhydride.

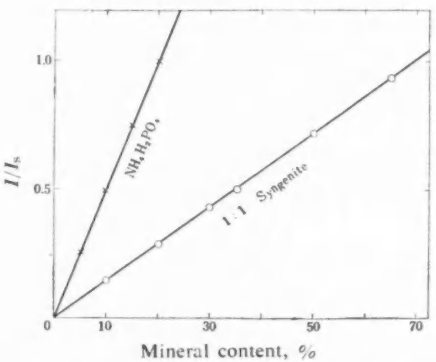

Fig. 2. Calibration curves of monoammonium phosphate and 1 : 1 syngenite.

1) R. Ikeno and Y. Shimomura, *J. Chem. Soc. Japan, Ind. Chem. Sec.* (*Kogyo Kagaku Zasshi*), **63**, 78 (1960).

and dried. A homogeneous crystalline solution was formed easily.

Method of Determination.—The Amount of each salt was determined measuring the diffraction peaks of the following angle (2θ by Cu ray): spinel 36.8°, crystalline solution of syngenite around 9°, monoammoniumpotassium phosphate around 16.6°, ammonium chloride 32.6°, calcium sulfate anhydride 25.4°, ammonium sulfate 20.4° and potassium chloride 28.3°. One handred parts of a mixture of 1 : 1 syngenite (crystalline solution of ammonium and potassium syngenite 1 : 1 by weight), monoammonium phosphate, ammonium chloride and calcium sulfate anhydride were mixed with 25 parts

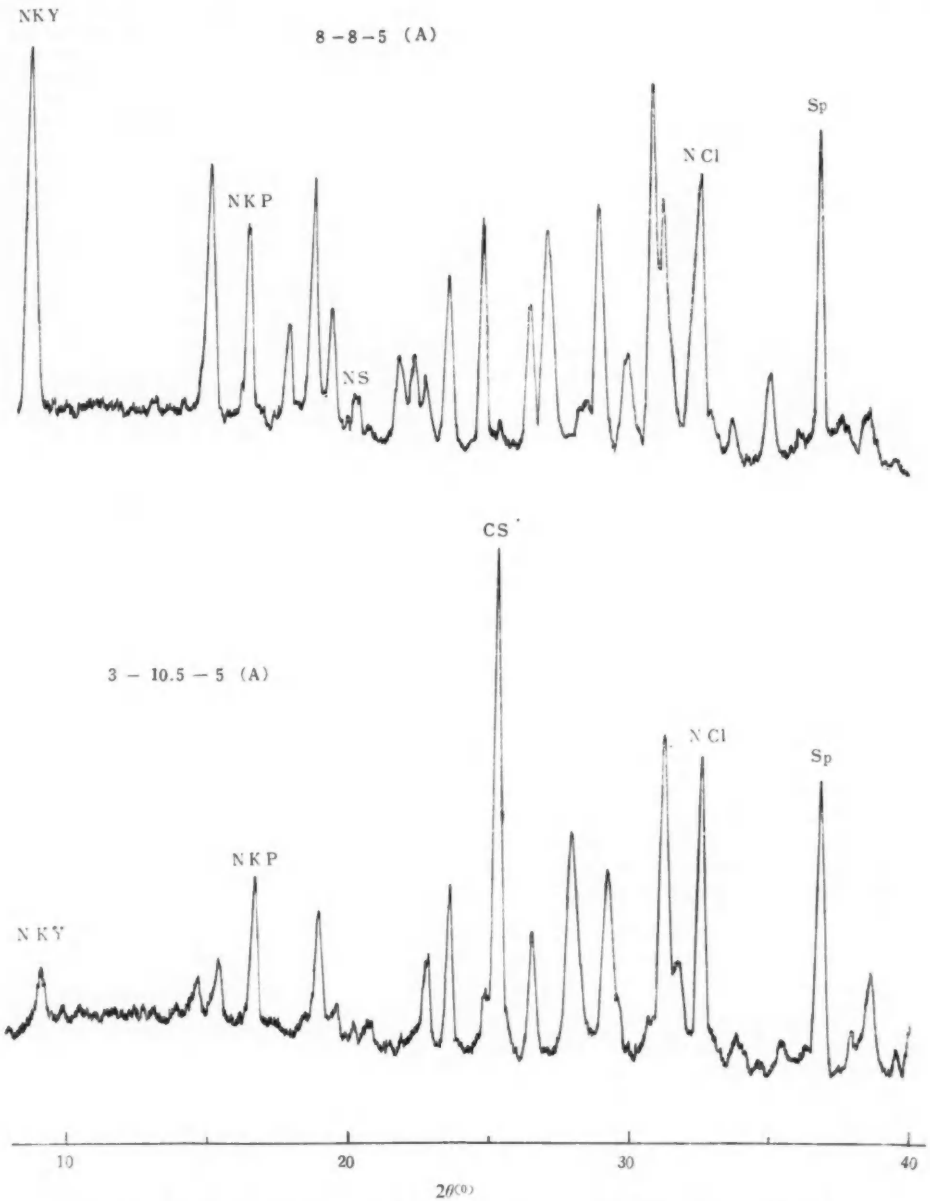

Fig. 3. X-ray diffraction patterns of mixtures of commercial fertilizers, 100 parts, and spinel, 25 parts (Cu ray, Ni filter).

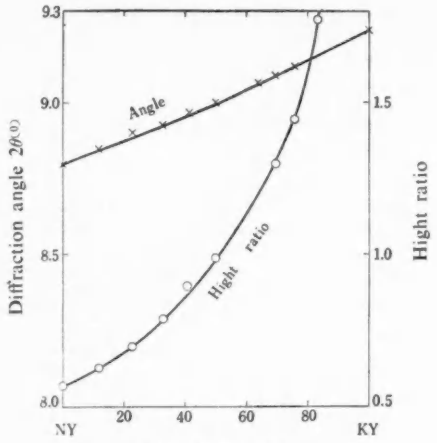

Fig. 4. Relation between weight ratio of ammonium syngenite (NY) component and potassium syngenite (KY) component in their crystalline solution and diffraction angle of center of the peak and also the ratio of height of the peak of 1 : 1 syngenite and that of other syngenite.

of spinel and were recorded by X-ray diffractometer. Calibration curves thus obtained are illustrated in Figs. 1 and 2.

One hundred parts of mixed fertilizer and 25 parts of spinel were mixed and recorded by X-ray diffractometer (Fig. 3). The content of ammonium chloride and of calcium sulfate anhydride were determined by Fig. 1.

Figure 4 or 6 was plotted by measurement of various crystalline solution of syngenite or phosphate. The NH_4/K ratio and amount of syngenite or phosphate in commercial fertilizer were determined using the relations of Figs. 2 and 4 or 6.

Results of determination of commercial fertilizer are shown in Table I. These samples contained 1~3% free water measured by weight loss on heating for 3 hr. at 100°C (Table II). A small part of salt was dissolved in the water and was not determined by X-ray. A sample 3-10-10 (C) contained a considerable amount of potassium chloride which was not detected in other samples. The samples contained less than 3% ammonium sulfate. No monocalcium phosphate monohydrate was detected in any sample. Considering these facts together with the results of Table II it is known that the quantitative analysis by X-ray was performed fairly accurately.

Reactions during Production Process.—Mixed fertilizer 8-8-6 was prepared in the laboratory under conditions similar to that of a large scale plant.

TABLE I. MINERAL CONTENT (%) OF COMMERCIAL MIXED FERTILIZER PRODUCED IN THREE PLANTS (A, B and C)

Sample	$CaSO_4$	NH_4Cl	NKP			NKY			Total
			Sum	NP	KP	Sum	NY	KY	
8-8-5 (A)	1.7	6.5	12.5	11.9	0.6	58.8	41.2	17.6	81.0
6-9.5-5 (A)	12.3	6.7	14.8	14.1	0.7	44.8	28.0	16.8	78.6
3-10.5-5 (A)	27.5	8.5	15.6	11.2	4.4	24.6	5.7	18.9	76.2
8-8-5 (B)	6.7	6.5	14.1	14.1	0	51.8	36.2	15.6	80.7
8-8-6 (C)	3.4	7.2	14.7	14.3	0.4	66.4	41.5	24.9	91.7
8-7-8 (C)	3.3	10.5	12.2	12.0	0.2	65.8	33.2	32.6	91.8
6-9-6 (C)	20.1	7.5	14.8	13.8	1.0	47.7	25.3	22.4	90.1
8-7-8 (C)	3.4	11.5	13.1	12.9	0.2	57.3	30.4	26.9	85.3
3-10-10 (C)	31.6	5.7	21.6	15.0	6.6	25.3	4.8	20.5	84.2

NP=monoammonium phosphate, KP=monopotassium phosphate,
NKP=crystalline solution of NP and KP, NY=ammonium syngenite, KY=potassium syngenite,
NKY=crystalline solution of NY and KY

TABLE II. COMPARISON OF N, P_2O_5 AND K_2O CONTENT DETERMINED BY CHEMICAL ANALYSIS (G) AND BY X-RAY ANALYSIS (X) OF TABLE I

Sample	N		P_2O_5		K_2O		Free water
	X	G	X	G	X	G	
8-8-5 (A)	6.88	8.76	7.65	8.79	5.55	5.56	3.0
6-9.5-5 (A)	5.92	6.96	9.07	10.34	5.35	5.53	3.1
3-10.5-5 (A)	4.07	4.05	9.21	10.61	7.26	7.68	5.5
8-8-5 (B)	6.46	8.50	8.70	9.10	4.74	5.31	1.4
8-8-6 (C)	7.11	8.33	9.04	9.10	7.70	6.25	0.8
8-7-8 (C)	7.00	8.01	7.54	7.53	9.98	10.01	1.9
6-9-6 (C)	5.78	6.02	9.03	9.10	7.16	7.20	2.2
8-7-8 (C)	7.13	8.70	8.10	8.12	8.25	8.60	0.9
3-10-10 (C)	3.72	3.80	12.70	11.46	6.47	10.70	2.5

The mineral content of samples during the course of preparation was determined by X-ray. Samples of each process in a large scale plant were investigated, too.

Superphosphate (−20 mesh, P_2O_5 17.56%, free water 12.02%) 356 g., potassium chloride (red colored, −42 mesh) 73.5 g. and ammonium sulfate (−42 mesh) 266 g. were mixed and put in a porcelain rotary drum (26×26 cm.). After 74 cc. of 4.75% aqueous ammonia and 15 cc. of water were sprayed the mixture was granulated between 4 and 10 mesh and dried in an air oven at 130°C for 15, 30, 45 and 60 min. Fifty grams of the sample dried for 60 min. (containing 2.91% free water) was put in a 50 cc. stoppered bottle and kept at 50°C for 5 days and then at room temperature for 10 days. The mineral content of samples just after mixing, granulation, drying and keeping for each time were determined by X-ray. The free water of samples was measured by weight loss on drying powdered samples for 3 hr. at 100°C.

It was known by preliminary tests that when the sample containing much water was powdered finely and recorded by X-ray a remarkable change took place in the sample during this procedure. In order to determine the mineral content of samples without the change during analytical procedure the samples were washed with pure ethyl alcohol, filtered, dried at room temperature in vacuum desiccator in several minutes and tested by X-ray diffractometer. In this case the free water of samples was eliminated and the salts dissolved in the water were crystallized. The mineral content of the original sample was calculated multiplying the value of X-ray analysis by (100-free water %)/100. The results are shown in Fig. 7.

Figure 7 illustrates that the following chemical reactions take place partly soon after the mixing of raw materials and extensively by the addition of ammonia and water.

$$Ca(H_2PO_4)_2 \cdot H_2O + (NH_4)_2SO_4 = 2NH_4H_2PO_4 + CaSO_4 + H_2O \quad \text{.....(1)}$$

$$(NH_4)_2SO_4 + CaSO_4 + H_2O + (NH_4)_2SO_4 \cdot CaSO_4 \cdot H_2O \quad \text{.....(2)}$$

$$CaSO_4 \cdot 1/2H_2O + (NH_4)_2SO_4 + 1/2H_2O = (NH_4)_2SO_4 \cdot CaSO_4 \cdot H_2O \quad \text{.....(3)}$$

$$H_3PO_4 + NH_4OH = NH_4H_2PO_4 + H_2O \quad \text{.....(4)}$$

$$2KCl + (NH_4)_2SO_4 = K_2SO_4 + 2NH_4Cl \quad \text{.....(5)}$$

$$K_2SO_4 + Ca(H_2PO_4)_2 \cdot H_2O = 2KH_2PO_4 + CaSO_4 + H_2O \quad \text{.....(6)}$$

$$K_2SO_4 + CaSO_4 + H_2O = K_2SO_4 \cdot CaSO_4 \cdot H_2O \quad (7)$$

$$mKH_2PO_4 + nNH_4H_2PO_4 \rightarrow \text{crystalline solution} \quad \text{.....(8)}$$

$$r[(NH_4)_2SO_4 \cdot CaSO_4 \cdot H_2O] + s(K_2SO_4 \cdot CaSO_4 \cdot H_2O) \rightarrow \text{crystalline solution} \quad \text{.....(9)}$$

$$2KH_2PO_4 + (NH_4)_2SO_4 \cdot CaSO_4 \cdot H_2O = 2NH_4H_2PO_4 + K_2SO_4 \cdot CaSO_4 \cdot H_2O \quad (10)$$

Potassium sulfate formed by reaction 5 reacts

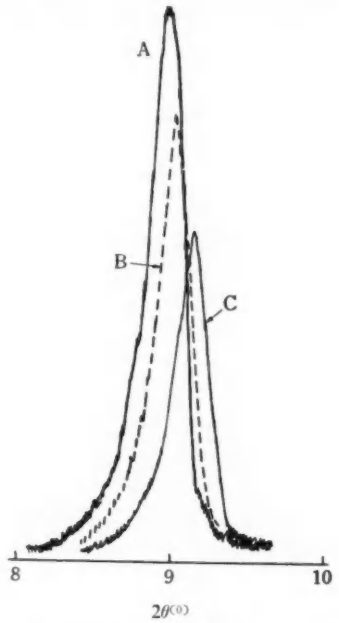

Fig. 5. Change of diffraction peak of crystalline solution of syngenite.
Weight ratios of ammonium and potassium syngenite are: A 66 : 34; B 50 : 50; C 24 : 76.

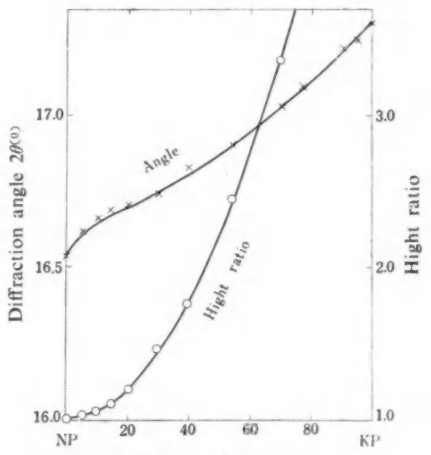

Fig. 6. Relation between weight ratio of monoammonium phosphate (NP) component and monopotassium phosphate (KP) component in their crystalline solution and diffraction angle of center of the peak and also the ratio of height of the peak of NP and that of the crystalline solution.

immediately to form potassium syngenite (7) and monopotassium phosphate(6) and does not actually exist in samples. Reactions 1–9 were almost completed when the granules were dried for 15 min. in a 130°C oven. At this time the free water of the sample was 8.52%.

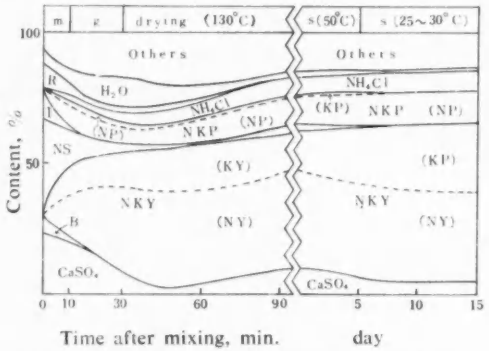

Fig. 7. Change of mineral content of samples in the midst of production process.
m=mixing, g=granulation, s=storing in sealed bottles, R=KCl, I=$Ca(H_2PO_4)_2 \cdot H_2O$, NP=$NH_4H_2PO_4$, KP=KH_2PO_4, NKP=crystalline solution of NP and KP, NS=$(NH_4)_2SO_4$, KY=$K_2SO_4 \cdot CaSO_4 \cdot H_2O$, NY=$(NH_4)_2SO_4 \cdot CaSO_4 \cdot H_2O$, NKY=crystalline solution of NY and KY, B=$CaSO_4 \cdot 1/2H_2O$.

It was clarified that by further drying a part of syngenite was decomposed to form calcium sulfate anhydride and ammonium sulfate. When dried for 60 min. the free water of the sample was 2.91% and the content of ammonium sulfate and calcium sulfate anhydride increased to a fair extent (Fig. 7). After being stored for days in a sealed bottle at 50°C the free water and those minerals decreased to form syngenite and the grains of the sample slightly adhered to each other forming a cake. When the granulated sample was dried at 120°C for 60 min. the free water content of the sample was 4.32%. Decomposition of syngenite took place similarly. After being stored for days at 50°C the grains adhered to each other more firmly than they did in the above sample.

The reaction 10 took place gradually and continued even in storing at room temperature. By this reaction NH_4/K ratio of crystalline solution of syngenite decreased and that of monophosphate increased.

Samples of 8–8–5 mixed fertilizer in the midst of each process of large scale production were tested in the same way. It was clarified that the above reactions took place similarly but often more slowly than in the laboratory test, perhaps because the raw materials were not mixed so well as in the laboratory. A greater amount of calcium sulfate anhydride and ammonium sulfate and less syngenite were contained in the sample before piling. The sample after being piled and caked contained a very small amount of free water and these salts.

Thermal Decomposition of Syngenite.—Figure 8 illustrates the weight loss of synthetic ammonium and potassium syngenite and crystalline solution of equal weight of the two when heated at a rate of 3~4°C/min. Ammonium syngenite was decomposed over 110°C. Over 160°C ammonium sulfate was volatilized. 1 : 1 syngenite or potassium syngenite was decomposed over 120°C or 240°C respectively. The syngenite contained in commercial fertilizer 8–8–6 or 8–8–5 resembled 1 : 1 syngenite and was not decomposed by heating for hours at 120°C. Ammonium syngenite was not decomposed by heating for hours at 100°C. However, it was clarified that the syngenite just after its formation in mixed fertilizer e.g. just after the granulation or at the begining of drying was partly decomposed

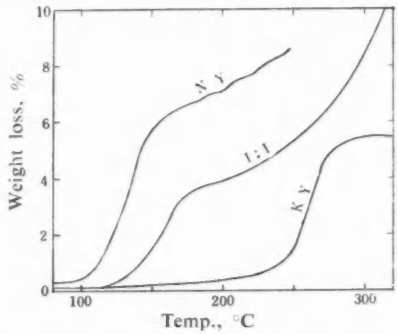

Fig. 8. Thermal decomposition of syngenite.
NY=ammonium syngenite, KY=potassium syngenite, 1 : 1=crystalline solution of the two 1 : 1 by weight.

even by heating at 100°C, perhaps because syngenite crystals had not grown well and a small amount of impurities such as HPO_4^{2-} instead of SO_4^{2-} was contained in the crystal.

To determine exactly the free water content of such samples by heating at 100°C, the amount of crystallization water lost by the heating must also be measured determining the amount of syngenite decomposed.

Discussion

It seems that syngenite, especially ammonium-rich syngenite plays an important role concerning the caking of products in a storage pile. In the preparation of standard samples it was observed that potassium rich syngenite was formed quickly and had little tendency of hardening and that ammonium-rich syngenite was formed slowly and hardened. Moreover, ammonium-rich syngenite is apt to decompose on drying and recrystallize during piling.

It has been known that mixed fertilizers such as 8–7–8, 8–8–6 and 8–8–5 are apt to form a hard cake and that the fertilizers such as 3–10–10, 3–10.5–5 etc. have little tendency of caking in a storage pile. This is attributable to the fact that the latter contain less and the former much ammonium syngenite component.

In large scale plants the granules are often dried in shorter time at a higher temperature than was done in the laboratory experiment. Thermal decomposition of syngenite must take place remarkably on the surface of grains which are dried enough and reach a high temperature. Free water remains in the inner part of the grains and gradually disperses to the surface to cause the recrystallization of syngenite and the caking of products. By the crystallization of syngenite the free water content of the products is reduced and a part of the salts dissolved in the water is crystallized promoting the formation of a hard cake.

The reaction 10 takes place successively in a storage pile. When the raw materials were not powdered finely or mixed well, reactions 1–9 are not completed before piling but occur continuously in the storage pile. All of these reactions are promoted by free water in the granules.

In order to prevent the caking of products (1) free water of the granules must be reduced as far as possible by drying, (2) drying at high temperature must be avoided so as to depress the thermal decomposition of syngenite, (3) the raw materials had better be powdered and mixed well so that the reactions 1–9 are almost finished before piling, and (4) the dried sample had better be cooled to a lower temperature. Of course it is desirable not to pile the products too high.

It was observed that ammonium chloride was volatilized slightly by heating at 130°C. In the drier of the large scale plant a small amount of ammonium chloride must be volatilized. Also for this reason the granules must not be dried at a high temperature.

Measurement of the amount of free and crystallization water of the products is nesessary for calculation of material balance. It was clarified that water of crystallization was contained only in syngenite and that its amount could be measured by X-ray determination of syngenite. The free water content of products stored for more than a week after granulation could be measured almost exactly by drying the samples for 3 hr. at 100°C. To measure the free water content of samples soon after production by the above method the loss of crystallization water by the drying must also be measured, determining the amount of syngenite before and after the drying. By such a method the material balance of mixed fertilizer could be calculated exactly.

Summary

The mineral content of mixed fertilizer produced with calcium superphosphate, ammonium sulfate and potassium chloride and also the reactions during the production process were investigated by X-ray diffraction.

It was observed that remarkable reactions took place between monocalcium phosphate, calcium sulfate, ammonium sulfate and potassium chloride by the addition of water for granulation. At the beginning of drying of the wet granules these minerals almost disappeared to form ammonium chloride and crystalline solutions of ammonium and potassium syngenite and those of monoammonium and monopotassium phosphate.

The syngenite thus formed decomposed partly by further drying and again formed while the product was placed in a storage pile. It seems that the caking of the product which often occurs in a storage pile is caused mainly by the crystallization of syngenite which decreases the amount of free water in the product and makes other salts crystallize at the same time.

Thanks are extended to Kurehakagakukogyo Co., Ltd., Nihonsuisokogyo Co., Ltd. and Nissankagakukogyo Co., Ltd. for samples of mixed fertilizer, and to Mr. T. Noguchi of Kurehakagakukogyo Co., Ltd. for assistance with chemical analyses.

Department of Industrial Chemistry
Faculty of Engineering
Chuo University
Bunkyo-ku, Tokyo

An Empirical Method for Estimating Normal Boiling Point and other Physical Properties of Alkene Hydrocarbons

By Mikio TAMURA, Michio KURATA, Koichiro NAKANISHI[*1] and Isamu NAGATA[*2]

(Received October 20, 1960)

The structural variation in the physical properties of alkene hydrocarbons is determined by the number and relative position of double bonds and side chains in the molecule. Owing to the presence and mutual influence of two different kinds of chemical bonds and side chains, correlation between properties and molecular structure is far more complicated than that in the case of isoparaffins, for which an elaborate set of structural parameters can be successfully used[1,2]. Although a few attempts were made to correlate the boiling point[3,4] or critical constants[5,6] with the molecular structure of alkenes, no extensive method has been established at the present stage.

In this paper, an empirical relation between the physical properties of lincar and branched alkenes and their molecular structure is proposed. The "effective carbon number" method which has been used for isoparaffins in the previous report[2] is again adopted. As will be shown later, a characteristic constant called "effective carbon number" can be defined for all the alkene hydrocarbons. Thus, this effective carbon number is first calculated by the proposed equation and then, by the use of a previously presented nomogram[2], the normal boiling point and other physical properties of the alkenes can be estimated from the knowledge of the structural formula alone.

Effective Carbon Number

When the boiling points of normal paraffins are plotted against the number of carbon atoms, a family of curves for different pressures is obtained. Then, reading the boiling points of a given alkene on these curves, one can obtain a set of values of an "effective number" of carbon atoms, each corresponding to every different pressure. These sets of values for several alkenes obtained by this procedure are listed in Table I together with the used values of the boiling point[7,8], where a reasonable constancy of the values is observed over a considerably wide range of pressure. This effective number of carbon atoms depending on the structural feature of each compound but not on the external condition is called the "effective carbon number" and hereafter denoted by n^*. It is shown that the proper assignment of the n^* value is advantageous not only for the estimation of the boiling point of the alkenes at various external pressures but also for that of other physical properties such as the critical constants, as in the case of isoparaffins[2].

TABLE I. CONSTANCY OF EFFECTIVE CARBON NUMBER OF ALKENES AT VARIOUS EXTERNAL PRESSURES

Compound	Pressure, mmHg	10	20	60	200	400	760
1-Butene	T_b[7] (°C)	−81.5	−72.89	−57.15	−36.10	−21.62	−6.26
	n^*	3.88	3.87	3.86	3.86	3.86	3.85
2-Methylpropene	T_b[7] (°C)	−81.95	−73.37	−57.664	−36.666	−22.227	−6.900
	n^*	3.87	3.85	3.84	3.85	3.84	3.84
1,3-Butadiene	T_b[8] (°C)	−79.7	−71.0	−55.1	−33.9	−19.3	−4.5
	n^*	3.92	3.93	3.93	3.90	3.89	3.86

*1 Present address: Department of Industrial Chemistry, Faculty of Engineering, Shinshu University, Nagano.
*2 Present address: Department of Chemical Engineering, Kyoto University, Kyoto.

1) H. Wiener, *J. Am. Chem. Soc.*, **69**, 17 (1947).
2) K. Nakanishi, M. Kurata and M. Tamura, *J. Chem. & Eng. Data*, **5**, No. 2, 210 (1960).
3) W. J. Taylor, J. M. Pignocco and F. D. Rossini, *J. Research Natl. Bur. Standards*, **34**, 413 (1945).
4) C. W. Beck and L. Y. Beck, *Ind. Eng. Chem.*, **51**, 223 (1959).
5) G. V. Michael and G. Thodos, *Chem. Eng. Progr. Symposium Series* No. 7, **49**, 131 (1953).
6) G. Thodos, *A. I. Ch. E. Journal*, **1**, 165 (1955).
7) F. D. Rossini, K. S. Pitzer, R. L. Arnett and G. C. Pimentel, "Selected Values of Physical and Thermodynamic Properties of Hydrocarbons and Related Compounds", American Petroleum Institute Research Project 44, Carnegie Press, Pittsburgh, Pa. (1953).
8) D. R. Stull, *Ind. Eng. Chem.*, **39**, 517 (1947).

Structural Units

The molecular structure of alkenes can be specified by the number and the relative position of double bonds and those of branching units. Therefore, if the mutual influence among these units is properly estimated, the deviation of the effective carbon number from the real one may be expressed as a linear combination of several factors, each corresponding to a double bond or a branching unit. Although various kinds of methods for such factorization would be possible, only the linear factorization is used here because of its simplicity for practical purposes.

The following four groups of carbon atoms are adopted as the structural units of alkenes: i. e. (I) double bond existing in the linear portion of the molecule, (II) double bond attached to branching atoms, (III) trifunctional branching and (IV) tetrafunctional branching. Schematically, these are

(I) $-C=C-$, (II) $-C=\underset{\displaystyle C}{\underset{|}{C}}-C-$ or $-\underset{\displaystyle C}{\underset{|}{C}}-\underset{\displaystyle C}{\underset{|}{C}}=\underset{\displaystyle C}{\underset{|}{C}}-C-$,

(III) $-\underset{\displaystyle C}{\underset{|}{C}}-C-C-$ and (IV) $-\underset{\displaystyle C}{\underset{|}{\overset{\displaystyle C}{\overset{|}{C}}}}-C-C-$

For each of the four structural units, the following equation is obtained after some troublesome analysis of available boiling point data:

$$\Delta n_{\mathrm{I}} = 0.24 - 0.12b_1 + 0.05b_2 \quad (1)$$

$$\Delta n_{\mathrm{II}} = 0.24 - 0.08b_1 + 0.07b_2 \quad (2)$$

$$\Delta n_{\mathrm{III}} = 0.28 - 0.06c_2 + 0.06c_3 \quad (3)$$

$$\Delta n_{\mathrm{IV}} = 0.73 - 0.14c_2 + 0.05c_3 \quad (4)$$

The difference of the effective carbon number n^* from the real carbon number n is then given by the sum of these contributions,

$$\Delta n = n - n^* = \sum_{\mathrm{I}} \Delta n_{\mathrm{I}} + \sum_{\mathrm{II}} \Delta n_{\mathrm{II}} + \sum_{\mathrm{III}} \Delta n_{\mathrm{III}} + \sum_{\mathrm{IV}} \Delta n_{\mathrm{IV}} \quad (5)$$

where the summation extends over all structural units of each type. The four parameters, b_1, b_2, c_2 and c_3, in Eqs. 1 to 4 are defined as follows:

- b_1—the number of carbon-carbon bonds adjacent to the double bond.
- b_2—the number of carbon-carbon bonds (single and double) next but one to the double bond.
- c_2—the number of the second neighbor carbon atoms of the branching point (tertiary or quaternary carbon atom).
- c_3—the number of the third neighbor carbon atoms of the branching point (tertiary or quaternary carbon atom).

As is easily seen, the intrinsic contribution of the structural unit I, III and IV is represented by the first term of Eqs. 1, 3 and 4, respectively, while two other terms which represent the contribution of adjacent carbon atoms to each structural unit are introduced to take the mutual correlation of the structural units into account. The choice of type II as an independent structural unit is also due to the fact that the correlation of the double bond with the branching is so strong that it can not be treated separately.

It is obvious from the definition that the effective carbon number of isoparaffins is given by

$$n^* = n - \sum_{\mathrm{III}} (0.28 - 0.06c_2 + 0.06c_3) - \sum_{\mathrm{IV}} (0.73 - 0.14c_2 + 0.05c_3) \quad (6)$$

The accuracy of this equation is of the same degree as that of Eq. 41 in the previous paper[2], which is expressed in terms of the Wiener parameters[1].

Example of Calculation

The present method consists of the following two procedures:

(1) Effective carbon number n^* is calculated by Eq. 5. Only the structural formula of alkene in question is required.

(2) The vapor pressure-temperature relationship, the critical constants and the heat of vaporization at normal boiling point can be read on nomogram[2] by using the value of n^* just obtained.

For clear understanding of the method, calculation of the normal boiling point of 3, 5, 5-trimethyl-1-hexene is presented as an example.

3, 5, 5-Trimethyl-1-hexene

$$C^1=C^2-\underset{\displaystyle C^7}{\underset{|}{C^3}}-C^4-\underset{\displaystyle C^9}{\underset{|}{\overset{\displaystyle C^8}{\overset{|}{C^5}}}}-C^6$$

This compound contains the aforementioned structural units of I, III and IV types. The unit of type I is attached to one carbon-carbon bond to be counted as b_1, say C^2–C^3, and to two bonds to be counted as b_2, say C^3–C^4 and C^3–C^7; hence

$$\Delta n_{\mathrm{I}} = 0.24 - 0.12 \times 1 + 0.05 \times 2 = 0.22$$

The structural unit of type III or tertiary carbon atom C^3 has two second neighbors, say C^1 and C^5, and three third neighbors, say C^6, C^8 and C^9, hence

$$\Delta n_{\mathrm{III}} = 0.28 - 0.06 \times 2 + 0.06 \times 3 = 0.34$$

Quaternary carbon atom C^5 has one second neighbor, C^3, and two third neighbors, C^2 and C^7, and so

$$\Delta n_{\mathrm{IV}} = 0.73 - 0.14 \times 1 + 0.05 \times 2 = 0.69$$

TABLE II. NORMAL BOILING POINT OF MONOALKENES

Compound	Normal boiling point T°_{b}, °C		Effective carbon number, n^*	
	Obs.[9]	Calcd.	Obs.	Calcd.
Ethylene	−103.7	−104.0	1.76	1.76
Propylene	−47.7	−47.0	2.86	2.88
1-Butene	−6.3	−6.0	3.85	3.83
2-Butene	1.	2.0	4.04	4.00
2-Methylpropene	−6.9	−2.0	3.84	3.92
1-Pentene	29.9	30.0	4.83	4.83
2-Pentene	36.1	34.0	5.00	4.95
2-Methyl-2-butene	38.6	36.0	5.07	5.00
2-Methyl-1-butene	31.2	31.0	4.86	4.85
3-Methyl-1-butene	20.1	20.0	4.55	4.56
1-Hexene	63.5	63.0	5.83	5.83
2-Hexene	68.2	67.0	5.98	5.95
3-Hexene(*trans*)	67.1	65.0	5.93	5.90
2-Methyl-1-pentene	62.2	63.0	5.80	5.85
3-Methyl-1-pentene	54.2	56.0	5.54	5.62
4-Methyl-1-pentene	53.9	54.0	5.53	5.55
2-Methyl-2-pentene	65.0	66.0	5.88	5.93
3-Methyl-2-pentene	68.0	66.0	5.97	5.93
4-Methyl-2-pentene	57.0	56.0	5.60	5.62
2-Ethyl-1-butene	64.7	62.0	5.76	5.78
2,3-Dimethyl-1-butene	55.6	51.0	5.58	5.46
3,3-Dimethyl-1-butene	41.2	41.0	5.14	5.14
2,3-Dimethyl-2-butene	73.	71.0	6.1	6.08
1-Heptene	93.6	93.0	6.83	6.83
2-Heptene	98.5	97.0	7.00	6.95
3-Heptene	95.6	95.0	6.90	6.90
2,3,3-Trimethyl-1-butene	77.9	77.0	6.30	6.26
1-Octene	121.3	120.0	7.83	7.83
2-Isopropyl-3-methyl-1-butene	113.6	100.0	7.55	7.08
1-Nonene	146.9	147.0	8.84	8.83
2,3,3,4-Tetramethyl-1-pentene	133.2	133.0	8.30	8.32
1-Decene	170.6	170.0	9.84	9.83
2,3,3,4,4-Pentamethyl-1-pentene	158.8	157.0	9.33	9.27

n^*_{obs}=Effective carbon number at normal boiling point (cf. Table I)
n^*_{calcd}=Calculated value by Eq. 5

Thus, the summing up of the above three Δn_j's gives,

$$\Delta n = 0.22 + 0.34 + 0.69 - 1.25$$

$$\text{or} \quad n^* = 9 - 1.25 = 7.75$$

Then, using the nomogram[2], 118°C is obtained for the normal boiling point which is to be compared with the observed value 119.4°C[9].

Comparison with Experimental Data

A test of the present method by the procedure described in the last section was carried out for 188 monoalkenes and 46 dialkenes.

The average deviation of the calculated values of normal boiling point of the monoalkenes from the literature values[9,10] was as small as 2.5°C, with the maximum deviation −17°C for 2-*tert*-butyl-3,3-dimethyl-1-butene. Only ten percent of the tested compounds showed an error higher than 5°C. Table II shows about 30 examples of this test.

In the case of dialkenes with no "conjugated double bond", the average deviation of the normal boiling point was found to be about 2.4°C, the maximum deviation was −11°C for 1,4-heptadiene, and the deviation was less than 5°C for 87 percent of the tested compounds. Table III shows the results for typical examples.

In the presence of the conjugated double

9) G. Egloff, "Physical Constants of Hydrocarbons" Vol. V, Reinhold Publishing Corporation, New York, (1953).

10) S. W. Ferris, "Handbook of Hydrocarbons", Academic Press Inc., New York (1955).

Table III. Normal boiling point of dialkenes

Compound	Normal boiling point T^0_b, °C		Effective carbon number, n^*	
	Obs.[10]	Calcd.	Obs.	Calcd.
1,4-Hexadiene	65.	61.0	5.88	5.78
1,5-Hexadiene	59.5	58.0	5.70	5.66
2-Methyl-1,4-pentadiene	56.	59.0	5.60	5.70
3-Methyl-1,4-pentadiene	55.	49.0	5.57	5.40
1,4-Heptadiene	100.8	90.0	7.10	6.73
1,5-Heptadiene	94.3	91.0	6.85	6.78
2-Methyl-1,5-hexadiene	92.1	89.0	6.78	6.68
3-Methyl-1,5-hexadiene	80.5	82.0	6.39	6.46
5-Methyl-1,4-hexadiene	91.8	91.0	6.77	6.76
2,4-Dimethyl-1,4-pentadiene	81.3	89.0	6.41	6.70
1,7-Octadiene	117.5	116.0	7.69	7.66
3-Methyl-1,5-heptadiene	110.5	112.0	7.44	7.51
2-Methyl-1,6-heptadiene	115.6	116.0	7.65	7.68
2,4-Dimethyl-1,5-heptadiene	132.1	134.0	8.29	8.41
2,6-Dimethyl-2,6-octadiene	166.9	169.0	9.67	9.86

n^*_{obs} = Effective carbon number at normal boiling point (cf. Table I)
n^*_{calcd} = Calculated value by Eq. 5

Table IV. Comparison of calculated critical constants and heat of vaporization with literature values

Compound	Effective carbon number, n^*	Critical temperature °K			Critical pressure atm.			Heat of vaporization (kcal./mol.) at T^0_b		at 25°C	
	Calcd.	Obs.[7]	Calcd.	Thodos[5]	Obs.[7]	Calcd.	Thodos[5]	Obs.[7]	Calcd.	Obs.[7]	Calcd.
Ethylene	1.76	282.4	—	290.3	50.0	—	50.7	3.24	—	—	—
Propylene	2.88	365.0	363.0	367.3	45.6	43.0	45.7	4.40	4.36	—	3.27
1-Butene	3.83	419.6	415.0	425.3	39.7	37.0	39.8	5.24	5.14	4.87	4.70
2-Butene (*cis*)	4.00	430.2	424.0	429.3	41.	38.0	37.4	5.58	5.27	5.30	4.95
(*trans*)				426.3			37.3	5.44		5.15	
2-Methylpropene	3.92	417.9	422.0	425.2	39.5	36.0	40.4	5.29	5.22	4.92	4.84
1-Pentene	4.83	474.2	461.0	471.4	40.	34.0	35.2	—	5.95	—	6.02
2-Pentene	4.95	475.6	466.0	471.5	40.4	34.0	32.9	—	6.05	—	6.19
2-Methyl-2-butene	5.00	470.2	468.0	471.2	34.	33.0	33.2	—	6.09	—	6.06
2-Methyl-1-butene	4.85	—	462.0	471.6	—	34.0	35.6	—	5.97	—	6.25
3-Methyl-1-butene	4.56	464.8	450.0	—	33.9	35.0	—	—	5.75	—	5.69

bond, Eq. 5 fails to express the difference of the effective carbon number of compounds from the real carbon number. However, the effective carbon number itself can also be defined for this type of compound (see Table I), and a conventional procedure is possible. That is, if one boiling point datum is available, n^* can be obtained on nomogram without the aid of Eq. 5.

Table IV shows the comparison of the estimated values of critical temperature, critical pressure and heat of vaporization with the observed values[7], where the critical constants estimated by the Thodos' method[5,6] are also given for comparison.

The application of Eq. 6 to isoparaffins is also satisfactory, though the results are not given here*3. It is especially favorable for the estimation of the heat of vaporization at normal boiling point and the critical temperature.

*3 Details of the results will be published elsewhere.

Summary

A method of estimating the structural variation in the boiling point and other physical properties of alkenes is developed. By this method, all properties are expressed in terms of a structural constant called the "effective carbon number" which depends on the number and relative position of double bonds and those of side chains but not on external variables such as the temperature. An empirical equation is presented to correlate the effective carbon number with molecular structure. By combining the use with the previously presented nomogram*4, it is proved to be quite

*4 Copies of original drawing of the nomogram will be sent upon request.

useful for rapid evaluation of various properties including the temperature-vapor pressure relationship and the critical constants.

Department of Industrial Chemistry
Faculty of Engineering
Kyoto University
Sakyo-ku, Kyoto

Studies on Organophosphorus Compounds. I. The Reaction of O,O-Dimethyl Phosphonate with p-Benzoquinone

By Yoshihiko NISHIZAWA

(Received September 1, 1960)

It is well known that phosphonates* having phosphorus-hydrogen linkage react with the carbonyl groups as aldol-condensation to produce α-hydroxy phosphonate[1]:

$$C_6H_5CHO + HP(O)(OH)_2 \rightarrow C_6H_5CH(OH)P(O)(OH)_2$$

Ville[2] and Marie[3] studied this reaction with various ketones and aldehydes from 1889 to 1904.

Recently, it has been well known that Dipterex[4] was prepared by this reaction of *O,O*-dimethyl phosphonate with chloral, which proved to be very useful as an insecticide.

$$(CH_3O)_2P(O)H + OHC\cdot CCl_3 \rightarrow (CH_3O)_2P(O)\underset{\displaystyle OH}{\underset{|}{C}}HCCl_3$$

Furthermore, Sallman et al.[5] have reported that *O,O*-dialkyl phosphonates react with α,α'-dihalo-ketones to produce α-hydroxy-β,β'-dihalo phosphonates which are also useful as an insecticide.

The products of this reaction, α-hydroxy-β-halo phosphonates, have not only the agricultural usefulness but also a very interesting property which is that the phosphonates are changed to vinyl phosphorates under the presence of alkaline[6-8].

$$(CH_3O)_2P(O)\underset{\displaystyle OH}{\underset{|}{C}}H\cdot CCl_3 \xrightarrow{NaOH} (CH_3O)_2P(O)CH{=}CCl_2$$

Thus, the reaction of phosphonate having the phosphorus-hydrogen linkage with carbonyl groups of aldehydes or ketones were studied widely, but the reaction with the carbonyl group of benzoquinone has not been reported yet.

During the course of an investigation of organophosphorus compounds, the present author found that the reaction of *O,O*-dimethyl phosphonate with carbonyl group of *p*-benzoquinone did not produce the usual α-hydroxy phosphonate but the phosphorate having *p*-hydroxy-phenyl group.

The reaction of two moles ratio of *O,O*-dimethyl phosphonate with one mole ratio of *p*-benzoquinone produced undistillable pale yellow oil. This product was purified by acetone and ligroin. The refractive index and the infrared absorption spectrum of this product was not changed by the purification using silica-gel column-chromatography. So, it was considered that this product was a pure substance. The microanalytical data of this product showed that this product was composed of one mole ratio of *O,O*-dimethyl phosphonate and one mole ratio of *p*-benzoquinone. Moreover, the reaction product of one mole ratio of *O,O*-dimethyl phosphonate and one mole ratio of *p*-benzoquinone showed the same refractive index, infrared absorption spectrum and microanalytical data as the above product.

$$n(CH_3O)_2P(O)H + O{=}\langle\bigcirc\rangle{=}O \rightarrow$$

(I) (II)

$$(CH_3O)_2P(O)O{-}\langle\bigcirc\rangle{-}OH$$

(III)

* Phosphorus compounds in this paper were named according to the Drake Comittee's Report (*Chem. Eng. News*, **30**, 4515 (1952)).

1) G. N. Kosolapoff, "Organophosphorus Compounds", Jhon Wiley & Sons. (1950), p. 129.
2) J. Ville, *Compt. rend.*, **107**, 659 (1888); **109**, 71 (1890); **110**, 384 (1890).
3) C. Marie, ibid., **133**, 219, 818 (1901); **134**, 286, 847 (1902); **135**, 106, 1118 (1902); **136**, 48, 234, 508 (1903); **137**, 124 (1903); **138**, 1707 (1904).
4) W. Lovenz, U. S. Pat. 2701225.
5) R. Sallman, D. R. Pat. 1000364.
6) W. F. Barthel, *J. Am. Chem. Soc.*, **77**, 2424 (1955).
7) W. Lorenz, ibid., **77**, 2554 (1955).
8) W. Perkow, D. R. Pat. 1024945.

n is 1 or 2 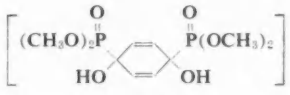

The infrared absorption spectrum of this product III did not show the absorption bands of the carbonyl group of *p*-benzoquinone, but strong absorption bands of phenyl group (1450, 1510 cm^{-1})[9], P=O (1265 cm^{-1})[9] and P–O–C (Arom) linkages (1205 cm^{-1})[9] were observed. (see Fig. 1).

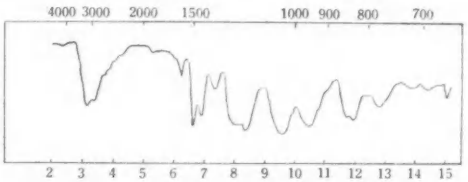

Fig. 1 The infrared spectrum of *O*, *O*-dimethyl-*O*-(*p*-hydroxy-phenyl)phosphorate (III) (liquid).

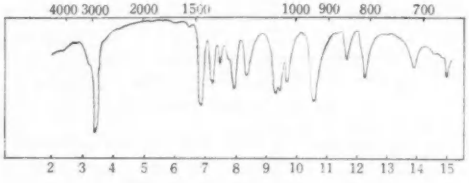

Fig. 2 The infrared spectrum of *O*, *O*-dimethyl-*O*-(4-hydroxy-2, 3, 5, 6-tetrachloro-phenyl)phosphorate (IV) (in Nujol).

Moreover, the product showed the color reaction of phenol by ferric chloride and a hydrolysis of the product produced hydroquinone.

From the above results, it was presumed that the reaction of *O*, *O*-dimethyl phosphonate with the carbonyl group of *p*-benzoquinone did not produce the usual α-hydroxy phosphonate but 4-hydroxy-phenyl phosphorate (III).

In the above experiments, there remained uncertainty whether the product is the pure material or not, because the product is an undistillable oil. However, the above presumption against the above experimental results was confirmed by the reaction of *O*, *O*-dimethyl phosphonate with chloranil. The reaction of one or two moles ratio of *O*, *O*-dimethyl phosphonate with one mole ratio of chloranil produced the same crystals which melt at 237~239°C.

9) L. J. Bellamy, "The Infrared Spectra of Complex Molecules"; Jhon Wiley & Sons. (1958).

The melting point of these crystals coincided with that of *O*, *O*-dimethyl-*O*-(4-hydroxy-2, 3, 5, 6-tetrachlorophenyl)phosphorate (IV) which was prepared by Ramirez's method[10] and the mixed melting point did not decrease.

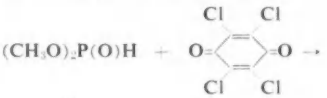

(I)

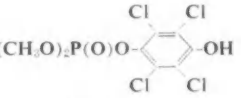

(IV)

It seems that the above reactions have different mechanism from the usual reactions of phosphonate with carbonyl groups of aldehydes and ketones.

It is considered that *O*, *O*-dialkyl phosphonate have polymerized form of two or three molecules by hydrogen bonding at the free state[11-13], but in aldol type reactions, the hydrogen atom is released easily as proton and the phosphonate becomes the phosphite-form[14]:

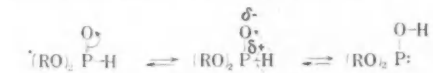

Therefore, when the phosphonate reacts with the aldehydes or ketones, this hydrogen atom cuts itself off as proton from phosphite molecule and the phosphite group reacts with the electrophilic carbon atom of carbonyl group just as the aldehyde group in aldol condensation does.

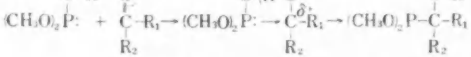

When the phosphonate reacts with the carbonyl group which has an ethylenic double bond in conjugated system, the phosphorus atom links the β-carbon atom of carbonyl group[15]. This reaction might be explained by the same mechanism as above.

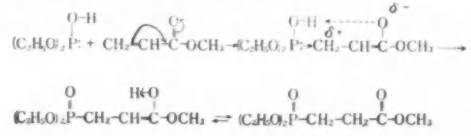

10) F. Ramirez, *J. Am. Chem. Soc.*, **81**, 587 (1959).
11) B. A. Arbuzov, *Doklady Akad. Nauk S. S. S. R.*, **54**, 599 (1946).
12) B. A. Arbuzov, ibid., **54**, 787 (1946).
13) B. A. Arbuzov, ibid., **55**, 31 (1947).
14) M. Murakami, "Hanno-Yuukikagaku", Asakura-Syoten (1949), p. 316.
15) E. C. Ladd, Can. Pat. 509034.

If the reaction of the phosphonate with the quinone has the same ionic mechanism, it may be considered that the quinone have the formula IIIA as excited resonance form[16]. According to this mechanism, it is normal that the phosphorus atom attacks the carbon atom of the quinone nucleus.

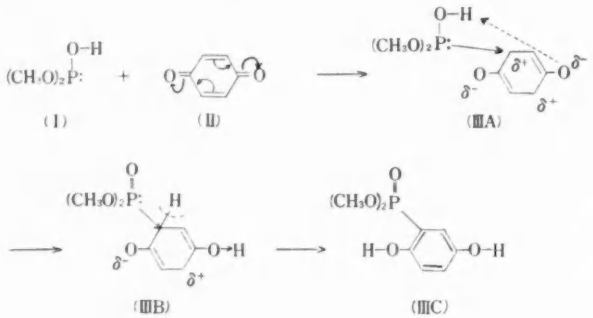

(I) (II) (IIIA) (IIIB) (IIIC)

In fact, hydrogen halides, benzene sulfonic acids or xanthic acids react with quinone and link the carbon atom of quinone nucleus according to the above mechanism[16]. But the reaction of phosphonate can not be explained by the above mechanism, since the experimental facts show the production of the phosphorate.

On the other hand, it is well known that the reaction of trialkyl phosphites with α-halocarbonyl compounds does not produce the phosphonates as in Arbuzov's reaction but phosphorates as in Perkow's reaction[17].

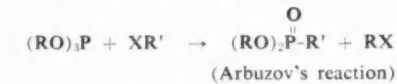

(Arbuzov's reaction)

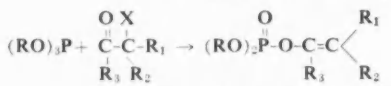

(Perkow's reaction)

On the above reaction mechanism, Allen[18] and Pudovik[19] have reported that the trialkyl phosphites attack the electrophilic carbon atom of carbonyl group and then the phosphorus atom forms the oxide ring as the intermediate:

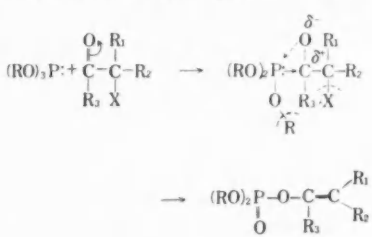

In the reaction of *O,O*-dimethyl phosphonate with *p*-benzoquinone, it is considered that the reaction mechanism is the same as above, namely, phosphite group attacks the nucleophilic carbon atom of quinone nucleus and then the phosphorus atom forms the oxide ring as intermediate because there is a carbonyl group at α-position.

Accordingly, the phosphorus atom cuts itself off from the quinone nucleus instead of eliminating the hydrogen atom and then the phosphorate is produced.

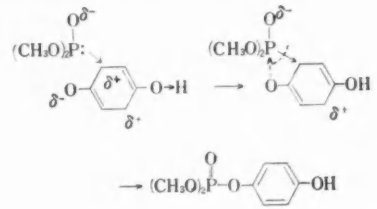

(III)

It is well explained by this mechanism that the phosphonate reacts with *p*-benzoquinone by 1:1 mole ratio and does not produce the α-hydroxy phosphonate but produces phosphorate and, moreover, when the water is presented in this reaction, hydroquinone is produced.

Namely, in the presence of water, the phosphorus atom forms the oxide ring between the oxygen atom of water instead of the oxygen atom of quinone. So, Perkow's rearrangement occurs between the phosphonate and the water.

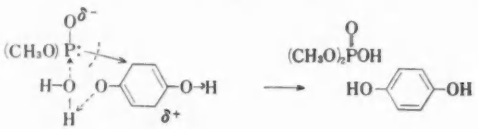

16) M. Murakami, "Hanno-Yuukikagaku", Asakura-Syoten. (1949), p. 351.
17) W. Perkow, *Chem. Ber.*, **88**, 662 (1955).
18) J. Allen, *J. Am. Chem. Soc.*, **77**, 2871 (1955).
19) A. N. Pudovik, *J. Gen. Chem., USSR*, **26**, 2503 (1956).

Experimental

Reaction of *O*, *O*-Dimethyl Phosphonate with *p*-Benzoquinone.—To a solution of 15 g. of *p*-benzoquinone and 0.5 g. of triethylamine in 45 ml. of dioxane was gradually added under cooling by water 32.0 g. of *O*, *O*-dimethyl phosphonate. After the addition, the reaction mixture was stirred for 7 hr. at 70°C and then allowed to stand over night at room temperature. The reaction mixture was condensed in vacuo (0.3 mmHg) at 60°C, 30.0 g. of the pale yellow oil was obtained.

This oil was dissolved in acetone and then ligroin was added gradually. The upper layer was separated by decantation, and the lower layer was concentrated in vacuo. The viscous oil was obtained and yielded 25.0 g. (83%) n_D^{26} 1.5205.

Found: P, 14.3. Calcd. for $C_8H_{11}O_5P$: P, 14.2%.

The same reaction using 16.5 g. of *O*, *O*-dimethyl phosphonate instead of 32.0 g. of *O*, *O*-dimethyl phosphonate, produced 23.8 g. of same oil.

Hydrolysis of *O*, *O*-Dimethyl-*O*-(4-hydroxy-phenyl)phosphorate (III).—The mixture of 10.0 g. of *O*, *O*-dimethyl-*O*-(4-hydroxy-phenyl)phosphorate (III) and 30 ml. of 8% hydrochloric acid was heated at 80°C for 50 hr. The water layer was extracted continuously with ether and then the ether layer was dried over anhydrous sodium sulfate. After removal of the ether, the residue was recrystallized from benzene.

Four grams of *p*-hydroquinone was obtained and melted at 170~171°C. The melting point of a mixture of the hydroquinone and the authentic specimen did not decrease.

Reaction of *O*, *O*-Dimethyl Phosphonate with Chloranil.—To a solution of 24.6 g. of chloranil in 250 ml. of dioxane was added by drop-wise 11.0 g. of *O*, *O*-dimethyl phosphonate under cooling with ice water. After the addition, the reaction mixture was stirred for 5 hr. at 80°C and then cooled. The reaction mixture was concentrated under a reduced pressure and the crude crystals were precipitated. The crystals were recrystallized from methanol, melted at 237~239°C. and yielded 22.0 g. (61%). A mixture of these crystals and the authentic *O*, *O*-dimethyl-*O*-(4-hydroxy-2, 3, 5, 6-tetrachloro-phenyl)-phosphorate which was prepared by Ramirez's method[10] melted at 238~239°C.

Found: P, 9.2; Cl, 39.73. Calcd. for $C_8H_7Cl_4O_5P$: P, 8.7; Cl, 39.88%.

Reaction of *O*, *O*-Dimethyl Phosphonate with *p*-Benzoquinone under the Presence of Water.—The solution of 15 g. of *p*-benzoquinone in 100 ml. of methanol which contained 5% water was added to the solution of 16.5 g. of *O*, *O*-dimethyl phosphonate in 50 ml. of benzene. After the reaction mixture was stirred, benzene, water and alcohol were removed and then the residue was extracted continuously with ether. The ether layer was dried over anhydrous sodium sulfate. After removal of the ether, the residue was recrystallized from benzene and 10.8 g. of the hydroquinone was obtained and melted at 171~172°C.

The author wishes to express his thanks to Professor Shinichirou Fujise and Professor Tarou Yamazaki of Tohoku University for helpful suggestions in the preparation of this manuscript. He also wishes to thank to the Sumitomo Chem. Co. Ltd., for permission to publish this work. He is indebted to his co-workers in the microanalytical section in this laboratory. He also wishes to express his thanks to Mr. M. Nakagawa for his earnest assistance.

Sumitomo Chemical Co., Ltd.
Osaka Works
Konohana-ku, Osaka

Internal Rotation and Low Frequency Spectra of Esters, Monosubstituted Amides and Polyglycine

By Tatsuo MIYAZAWA*

(Received September 20, 1960)

Monosubstituted amides, polypeptides and proteins have been known to exhibit several prominent bands characteristic to the –CONH– group. The bands at about 3300 cm^{-1} and 3100 cm^{-1} are now considered to be due to the Fermi resonance between the fundamental N–H stretching vibration and the first overtone of the amide II vibration[1]. The amide I (1650 cm^{-1}), the amide II (1550 cm^{-1}), and the amide III (1250 cm^{-1}) vibrations involve the C=O stretching, the C–N stretching and the N–H in-plane bending modes. These vibrations have long been subjects of controversy; however, their nature has finally been elucidated

* Present address: Institute for Protein Research, Osaka University, Kita-ku, Osaka.

1) R. M. Badger and A. D. E. Pullin, *J. Chem. Phys.*, 22, 1142 (1954); T. Miyazawa, *J. Mol. Spectroscopy*, 4, 168 (1960).

by a normal coordinate treatment of *N*-methylacetamide[2]. The amide IV (650 cm^{-1}), the amide V (750 cm^{-1}), and the amide VI (600 cm^{-1}) bands have been found to be due primarily to the O=C–N bending[3], the N–H out-of-plane bending[4], and the C=O out-of-plane bending modes[5], respectively. The torsional vibration (the amide VII) around the C–N bond is directly related to the potential barrier hindering internal rotation about the C–N bond. For the molecule of *N*-methylformamide the band at 356 cm^{-1} has been assigned to this torsional mode[5].

Internal rotation around the C–N bond of the peptide group is one of the most important factors in determining the conformation or the secondary structure of polypeptides and proteins. Since biological activities of proteins are closely related to their secondary structures an extended spectroscopic study of the hindering potential was undertaken. The torsional vibrations in the low frequency region were assigned and normal coordinate treatments were made of the out-of-plane vibrations for the purpose of determining the potential barrier.

Monosubstituted amides exhibit infrared spectra analogous to those of esters and the analyses of the spectra of esters provide useful information in studving amide spectra. It may be remarked that esters and monosubstituted amides are isoelectronic with each other and, in addition, the mass of NH is not very different from the mass of the oxygen atom. Therefore spectroscopic studies were made of esters as well as of the monosubstituted amides in question.

Internal Rotation around the C–O Bond of Esters

Electron diffration studies of the molecular structures of methyl formate and methyl acetate were made by O'Gorman et al.[6] and the molecule was found to be in the cis form

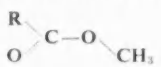

(R=H or CH_3)

The observed diffraction haloes were in accord with a structure slightly twisted from the planar structure by an internal rotation angle of about 25°. More recently the structure of methyl formate, however, was precisely determined by a microwave absorption measurement and the molecule was established to be in the planar cis form[7]. In the present study, therefore, the infrared spectra of esters will be discussed in terms of the planar cis structure.

Infrared spectra of methyl formate and methyl acetate in the gaseous state and in nonpolar solutions have been measured by Wilmshurst[8] in the region above 300 cm^{-1}. In the present work the measurements were extended out to 190 cm^{-1} so that the torsional frequencies might be observed.

Infrared Absorption Measurements.—For the measurements in the region 400～190 cm^{-1} a Perkin Elmer Model 12C spectrometer equipped with a cesium iodide prism[9] was used. Infrared spectra of methyl formate were measured in the gaseous state, in the solid nitrogen matrix, and in the crystalline state. The vapor spectra were obtained at room temperature with a 10 cm. gas cell and the gas pressure was 30 or 156 mmHg. The observed spectra are shown in Figs. 1 and 2A. A strong band was observed at 325 cm^{-1} with shoulders at about 305 cm^{-1} and at 340 cm^{-1}, in agreement with a previous result[8]. No other strong band, however, was observed below 300 cm^{-1}. The matrix spectra were recorded at 20°K for the molar ratio (N_2 : ester) of 32 or 100, where 140 micromoles of the ester sample was dispersed in the matrix over an area of about 2 cm^2. The nitrogen gas used as the matrix material was purified by passing over copper at 600°C and then through a liquid nitrogen bath. The experimental technique of the matrix isolation method was described before[10]. The observed matrix spectra are shown in Fig. 2B. Two prominent bands were observed at

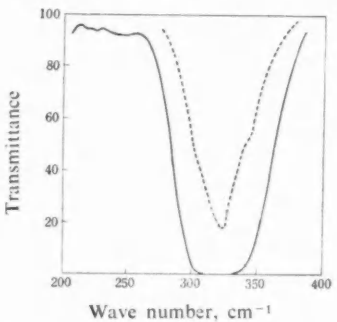

Fig. 1. Infrared spectra of methyl formate vapor, solid line : p=156 mmHg, broken line : p=30 mmHg.

2) T. Miyazawa, T. Shimanouchi and S. Mizushima, *J. Chem. Phys.*, **29**, 611 (1958).
3) T. Miyazawa, T. Shimanouchi and S. Mizushima, ibid., **24**, 408 (1956); T. Miyazawa, *J. Chem. Soc. Japan, Pure Chem. Sec. (Nippon Kagaku Zasshi)*, **77**, 171, 321, 526 (1956).
4) H. K. Kessler and G. B. B. M. Sutherland, *J. Chem. Phys.*, **21**, 570 (1953).
5) D. E. DeGraaf and G. B. B. M. Sutherland, ibid., **26**, 716 (1957).
6) J. M. O'Gorman, Wm. Shand and V. Schomaker, *J. Am. Chem. Soc.*, **72**, 4222 (1950).
7) R. F. Curl, *J. Chem. Phys.*, **30**, 1529 (1959).
8) J. K. Wilmshurst, *J. Mol. Spectroscopy*, **1**, 201 (1957).
9) T. Miyazawa, *J. Chem. Phys.*, **29**, 421 (1958).
10) E. D. Becker and G. C. Pimentel, ibid., **25**, 224 (1956).

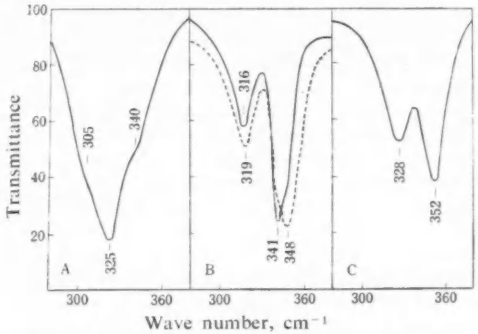

Fig. 2. Infrared spectra of methyl formate. A: vapor, B: matrix (solid line: molar ratio=100, broken line: ratio=32), C: crystal.

316 and 341 cm^{-1} for the molar ratio of 100 and these peaks shifted to 319 and 348 cm^{-1} for a lower ratio of 32. In preparing the crystalline specimen the ester gas was sprayed on a cesium bromide window kept at 140°K and the frozen sample was once slowly warmed up to a temperature slightly below the sublimation point allowing enough time for annealing and then cooled to 150°K for the absorption measurement. The observed crystalline spectrum is shown in Fig. 2C. Two bands were observed at 328 and 352 cm^{-1}, corresponding to the matrix bands at 319 and 348 cm^{-1}, respectively.

Infrared measurements in the vapor phase at room temperature were also made in the region 250~170 cm^{-1} by the use of the grating spectrometer described by Bohn et al.[11] The path length of the vapor cell was 70 cm.; however, no band of methyl formate vapor was observed at a gas pressure of 50~100mmHg. On the other hand a fairly strong band of methyl acetate was observed at 213 cm^{-1} with a gas pressure of 53 mmHg as shown in Fig. 3.

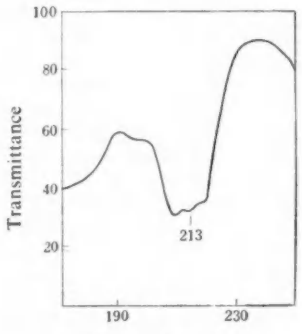

Fig. 3. Infrared spectrum of methyl acetate vapor.

Vibrational Assignment of Methyl Formate. —The vibrational modes of methyl formate expected in the region below 400 cm^{-1} are the C–O–methyl bending mode and the twisting modes around the ester C–O bond and around the O–methyl bond. The strong vapor band at 325 cm^{-1} corresponds to the fairly strong polarized Raman line at 332 cm^{-1} in the liquid state and may be assigned to the C–O–methyl bending mode. The twisting frequencies depend of course upon the potential barrier hindering internal rotation. The three-fold potential barrier of the O–methyl bond has been determined to be 1150±100 cal./mol.[7] and the corresponding twisting frequency will be of the order of 150 cm^{-1}. On the other hand the potential barrier of the ester C–O bond may be of the same order of height as the barrier, 10 kcal./mol., of formic acid monomer[12] and the corresponding twisting frequency may well be in the region 400~200 cm^{-1}. Excepting the 325 cm^{-1} band assigned to the C–O–methyl bending mode, however, no other band with more than 5% absorption was observed with the cell length of 10 cm. and with the gas pressure of 150 mmHg. It may be noted that the 325 cm^{-1} band has a rather peculiar contour, suggesting the possibility of the overlapping of the bands due to the C–O–methyl bending mode and due to the C–O torsional mode.

In the solid matrix the complications arising from rotational fine structures are absent. In the case of formic acid[12] the O=C–O bending mode and the C–O twisting mode exhibit a vibration-rotation band with complicated contour in the vapor phase, whereas in the matrix the two frequencies were resolved. Therefore the matrix isolation technique was used in the present case of methyl formate and the vapor band at 325 cm^{-1} was resolved into two distinct peaks in the nitrogen matrix. In order to establish the fact that these peaks are due to the two vibrational modes, C–O–methyl bending and C–O twisting of a single species, the effect of the molar ratio was observed (see Fig. 2B). On decreasing the molar ratio from 100 to 32, however, the relative intensities of the two peaks did not change appreciably, and these two peaks may now be assigned to the two modes mentioned above. It was not possible to decide which of the two peaks in the matrix was due to the twisting mode. Nevertheless the frequency of 325 cm^{-1} may be taken to be the twisting frequency in the vapor phase.

11) C. R. Bohn, N. K. Freeman, W. D. Gwinn, J. L. Hollenberg and K. S. Pitzer, ibid., 21, 719 (1953).

12) T. Miyazawa and K. S. Pitzer, ibid., 30, 1076 (1959).

Vibrational Assignment of Methyl Acetate.—The molecule of methyl acetate has three skeletal in-plane bending modes and one skeletal out-of-plane bending mode. The Raman lines or the infrared bands at 640, 433, 303 and 610 cm^{-1} have been assigned to these skeletal modes[8,13]. In the region below 400 cm^{-1} three torsional frequencies are expected, one around the ester C–O bond, one around the O–methyl bond, and the last one around the C–methyl bond. As in the case of methyl formate the torsional frequency around the O–methyl bond will be of the order of 150 cm^{-1}. The potential barrier around the C–methyl bond of methyl acetate has not been determined as yet; however, it will not be too different from the value of 483±25 cal./mol. as found for acetic acid monomer[14]. The corresponding torsional frequency will be of the order of 100 cm^{-1}. The observed infrared band of methyl acetate at 213 cm^{-1} is most reasonably assigned to the torsional mode around the ester C–O bond. The reduced moment of inertia for the internal rotation is greater for methyl acetate than for methyl formate and thus a torsional frequency somewhat lower than 325 cm^{-1} of methyl formate may be expected for methyl acetate.

Normal Coordinate Treatment of Out-of-plane Vibrations. — In order to estimate the twofold potential barrier of the ester C–O bond the normal coordinate treatments were made of the out-of-plane vibrations of methyl formate and methyl acetate. The methyl groups of these esters were treated as single dynamic units. The symmetry coordinates and the inverse kinetic energy matrix were derived previously[12]. The bond lengths used in the calculation were r(C=O) = 1.22 Å, r(C–O) = 1.36 Å, r(O–methyl) = 1.46 Å, r(C–H) = 1.07 Å and r(C–methyl) = 1.52 Å, and all the valence angles were taken to be 120° for simplicity.

The out-of-plane potential function was expressed in terms of the out-of-plane bending constant for the three bonds of the carbonyl carbon atom, H_Ω, the torsional potential constant for the ester C–O bond, H_θ, and the interaction constant, $H_{\Omega\theta}'$. In the case of formic acid monomer[12] the interaction constant $H_{\Omega\theta}' = -0.00_5$ has been found to be negligible as compared to the potential constants, $H_\Omega = 0.58_2$ and $H_\theta = 0.13_1$. In the present treatments of esters the interaction constant was neglected. In calculating the torsional potential constant the correction for the anharmonicity of the two-fold torsional potential function, $V = V_2 \cdot (1-\cos 2\theta)/2$ was made to the observed torsional frequency. The correction $\nu_0 - \nu$ is equal to $h/8\pi^2 c I_r$ where h is Planck's constant, c the light velocity, and I_r the reduced moment of inertia for intramolecular rotation[12]. The values of the correction were calculated to be 6 and 3 cm^{-1} for the cis form and the trans form of methyl formate and 2 cm^{-1} for both the cis form and trans form of methyl acetate. The CH out-of-plane bending frequency of 1019 cm^{-1} and the corrected torsional frequency of 331 cm^{-1} were used for the calculation of the potential constants of $H_\Omega = 0.55_3$ and $H_\theta = 0.18_2$ (in unit of 10^{-11} erg). Then the two-fold potential barrier of methyl formate was found to be 13.1 kcal./mol. The potential constants of methyl acetate were calculated to be $H_\Omega = 0.533$ and $H_\theta = 0.221$ from the skeletal out-of-plane bending frequency of 607 cm^{-1} and the corrected torsional frequency of 215 cm^{-1}. The two-fold potential barrier of methyl acetate was found to be 15.9 kcal./mol. It may be noted that the potential barriers of esters are higher than those of formic acid (10 kcal./mol.) and of acetic acid (10 kcal./mol.)[15].

Trans Form of Esters.—The trans isomer of formic acid monomer has been found by the infrared spectra in the vapor phase, and the energy of the trans isomer has been found to be 2 kcal./mol. higher than the more abundant cis isomer[12]. The normal coordinate treatment of the out-of-plane vibrations was also made of the trans form of methyl formate as an aid in assigning the bands due to the trans form. Since the torsional potential constant of the trans isomer has been found to be the same as that of the cis isomer in the case of formic acid, the potential function of the cis form of methyl formate was also used for the treatment of the trans form. The C–H out-of-plane bending frequency and the torsional frequency were calculated to be 1053 and 233 cm^{-1}, respectively. As shown in Fig. 1, however, no band with more than 5% absorption has been observed in the vicinity of 233 cm^{-1}. From the intensity of the 325 cm^{-1} band, the abundance ratio trans/cis was estimated to be less than 1% and the energy difference between the two forms is considered to be greater than 2.7 kcal./mol.

The relaxation absorption of sound in liquid ethyl formate has been ascribed to the rotational isomerism around the ester C–O bond[16]. Actually, however, there is also the rotational isomerism around the O–CH_2 bond of ethyl formate, and the hindering potential previously estimated from the ultrasonic studies may not be compared with the present results.

13) T. Miyazawa, *J. Chem. Soc. Japan, Pure Chem. Sec.* (*Nippon Kagaku Zasshi*), **77**, 619 (1956).
14) W. J. Tabor, *J. Chem. Phys.*, **27**, 974 (1957).
15) T. Miyazawa, unpublished.
16) J. Karpovich, *J. Chem. Phys.*, **22**, 1767 (1954); D. Tabuchi, ibid., **28**, 1014 (1958).

Internal Rotation around the C–N Bond of the Peptide Group

The stable conformation of the peptide group has been established to be the planar trans form by Mizushima et al.[17] The vibrational analysis of *N*-methyl acetamide and *N*-methyl formamide will therefore be made with the planar trans structure,

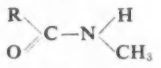

***N*-Methylacetamide.**—The vibrational assignment as well as the normal coordinate treatment of the in-plane vibrations have been made[2,3,13] and the nature of the skeletal bending vibrations at 436 and 289 cm^{-1} have already been elucidated. The Raman spectrum of liquid *N*-methylacetamide has been carefully measured by Sugita[18] and a new weak line has been observed at 206 cm^{-1}. Since the methyl torsional frequencies around the C–methyl bond and around the N–methyl bond will be lower than 150 cm^{-1} as in the case of methyl acetate, the Raman line at 206 cm^{-1} is most reasonably assigned to the torsional frequency around the C–N bond of the peptide group. It may be noted that this frequency is not very different from the corresponding frequency 213 cm^{-1} of methyl acetate.

In the present study an approximate normal coordinate treatment of the out-of-plane vibrations was made, treating the methyl groups and the NH group as single dynamic units. The bond lengths used were the same as those used in the treatment of the in-plane vibrations[2]. Because of the approximate nature of the present treatment, the correction for the anharmonicity of the torsional frequency was not made. From the observed skeletal out-of-plane bending frequency of 600 cm^{-1} (the amide VI band) and the torsional frequency of 206 cm^{-1} the potential constants were calculated to be $H_\Omega = 0.50_8$ and $H_\theta = 0.19_5$, and then the two-fold potential barrier was estimated to be 14 kcal./mol. The bond order of the C–N bond of the peptide group may be estimated to be 0.3~0.4 from the torsional potential constant as in the case of formic acid. This value agrees with the bond order 0.3~0.4 derived from the bond distances.

***N*-Methylformamide.** — Infrared and Raman spectra of liquid *N*-methylformamide have been measured by DeGraaf and Sutherland[5]. The polarized Raman line at 302 cm^{-1} has been assigned to the C–N–methyl skeletal bending vibration and the depolarized line at 356 cm^{-1} to the torsional vibration around the peptide C–N bond. These frequencies correspond to the frequency of 325 cm^{-1} observed for methyl formate.

The normal coordinate treatment of the out-of-plane vibrations of *N*-methylformamide was made as in the case of *N*-methylacetamide. The C–H bond length was taken as 1.07 Å and the other lengths were the same as those of *N*-methylacetamide. From the C–H out-of-plane bending frequency[3] of 1015 cm^{-1} and the torsional frequency of 356 cm^{-1} the potential constants were calculated to be $H_\Omega = 0.53_2$ and $H_\theta = 0.20_2$. This torsional potential constant corresponds to the potential barrier of 14 kcal./mol.

The two-fold potential barrier of the C–N bond of the peptide group has been estimated by Pauling and Corey[19] to be about 30 kcal./mol. As the results of the present spectroscopic studies, however, the values of the potential barrier of *N*-methylacetamide and *N*-methylformamide were both found to be about 14 kcal./mol., and this lower value is to be used in discussing the relative stabilities of the various conformations of a polypeptide chain.

Low Frequency Infrared Spectra of Polyglycine I and II

Infrared absorption spectra have been widely used in studying the conformations of polymer chains. In the case of polypeptide chains the correlations between the chain conformations and the amide I and II frequencies were first noticed by Elliott and Ambrose[20]; that is to say the folded conformation exhibits the amide I and II bands at about 1650 and 1540 cm^{-1} whereas the extended conformation exhibits the bands at 1630 and 1520 cm^{-1}. Recently these correlations were given theoretical interpretations and were refined and extended to cover the random coil conformation, the α helix, the antiparallel-chain extended conformation, and the parallel-chain extended conformation as well as Nylon 66[21]. These refined correlations, although useful for synthetic polypeptides and certain fibrous proteins, may not be too dependable in proteins exhibiting ill-defined amide I and II bands[22]. Therefore it should be worthwhile to find out other characteristic bands whose frequencies change more sensitively than do the amide I and II bands.

17) S. Mizushima, T. Shimanouchi, S. Nagakura, K. Kuratani, T. Tsuboi, H. Baba and O. Fujioka, *J. Am. Chem. Soc.*, **72**, 3490 (1950).
18) T. Sugita, unpublished.
19) L. Pauling and R. B. Corey, *Proc. Nat. Acad. Sci.*, **37**, 251 (1951).
20) A. Elliott and E. J. Ambrose, *Nature*, **165**, 921 (1950).
21) T. Miyazawa, *J. Chem. Phys.* **32**, 1647 (1960); T. Miyazawa and E. R. Blout, *J. Am. Chem. Soc.*, **83**, 712 (1961).
22) M. Beer, G. B. B. M. Sutherland, K. N. Tanner and D. L. Wood, *Proc. Royal Soc.*, **A249**, 147 (1959).

The N–H stretching vibration is localized in the N–H bond and involves only the nitrogen in the main chain of polypeptides. Its frequency, then, will not change appreciably with the chain conformation. On the other hand the torsional mode around the peptide C–N bond involves the C_α–C–N–C_α atoms in the main chain and its frequency is expected to be most sensitive to the conformational change of the chain. In this connection normal coordinate treatments of the skeletal vibrations of the polymers of the type, $(-CH_2-)_n$ and $(-CH_2-O-)_n$, have been made, and in fact the low frequencies primarily due to the torsional modes have been found to change most sensitively with the chain conformation[23].

Polyglycine has been known to exist in two forms[24]; polyglycine I is in the antiparallel-chain extended conformation and polyglycine II is in the helical conformation with three-fold screw axis[21,24,25]. In the present study the infrared spectra of these two forms of polyglycine were measured as Nujol paste in the region 400~190 cm^{-1}. The samples used were kindly given by Mr. Tsuchiya of the University of Tokyo. As shown in Fig. 4 polyglycine I exhibits a band at 217 cm^{-1}. This frequency appears to correspond to the frequency of 206 cm^{-1} observed for *N*-methylacetamide and is most reasonably assigned to the torsional mode around the C–N bond of the antiparallel-chain extended conformation. On the other hand polyglycine II* exhibits the corresponding band at 365 cm^{-1}. It is remarkable to note that the torsional frequency of polyglycine I is almost doubled by the transformation to polyglycine II. The amide VII band is thus found to be most sensitive to the conformation of polypeptide chains. It would be worth while to find out more extensive correlations between the various conformations and the infrared spectra in the low frequency region.

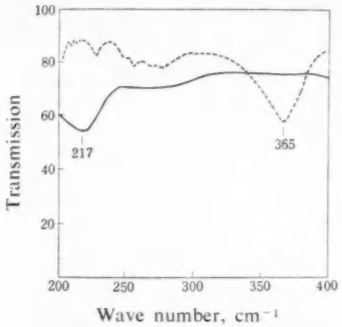

Fig. 4. Infrared spectra of polyglycine I (solid line) and polyglycine II (broken line).

The author wishes to thank Professor K. S. Pitzer of the University of California for his interest and encouragement and to Mr. Shoji Tsuchiya of the University of Tokyo for generously supplying the samples of polyglycine. The present work was partly supported by the American Petroleum Institute Research Project 50.

Department of Chemistry
University of California
Berkeley, California, U. S. A.

Institute for Protein Research
Osaka University
Kita-ku, Osaka

23) T. Miyazawa, *Spectrochim. Acta*, **16**, 1231, 1233 (1960); *J. Chem. Phys.*, in press.
24) C. H. Bamford, L. Brown, E. M. Cant, A. Elliott, W. E. Hanby and B. R. Malcolm, *Nature*, **176**, 396 (1955).
25) F. H. C. Crick and A. Rich, ibid., **176**, 780 (1955).

* The weak peaks observed in the region 200~280 cm^{-1} are presumably due to water vapor.

The Behavior of Fission Products Captured in Graphite Powder by Nuclear Recoil. IV. Further Studies on the Diffusion of Xenon-133 in Graphite

By Seishi YAJIMA, Sumio ICHIBA, Yuichiro KAMEMOTO, Koreyuki SHIBA and Masaharu KORI

(Received September 3, 1960)

Several papers have been published on the diffusion of fission products in graphite[1-7]. Only artificial graphite in a form similar to a fuel element, a disk or a pellet, was used in those experiments. On the other hand, the authors have studied the diffusion of fission products in many kinds of graphite such as amorphous carbon, artificial graphite, and natural graphite. The diffusion of xenon[6], iodine[7], and tellurium[7] in graphite was previously reported. However, more recent study by the authors suggests that in the determination of activation energy of diffusion in such a complicated material as graphite the use of Fick's law is not entirely satisfactory and that fission products in graphite have many energy states. Consequently, this experiment has been undertaken to determine the diffusion rate of fission product xenon-133 in graphite and the distribution of xenon-133 among such energy states as mentioned above.

Theoretical Consideration

In general, the escape rate v of fission products captured in imperfections with energy E is given by

$$v = -\frac{dn}{dt} = -\int \frac{n(x,y,t)}{a(x,y)} dx dy \nu \times \exp[-(E_D+E)/kT] \quad (1)$$

where

$n(x,y,t)$: number of fission products captured in a small region between x and $x+dx$, and y and $y+dy$.

$a(x,y)$: number of jumps of fission products required to escape from the graphite.

E_D : activation energy of diffusion of fission products.

T : temperature in °K.

ν : frequency of vibration of a fission product in the graphite.

k : Boltzmann constant.

If an isothermal escape rate of a fission product in a sample is determined at T_1,

$$v_1 = -\int \frac{n_1(x,y,t)}{a(x,y)} dx dy \nu \times \exp[-(E_D+E)/kT_1] \quad (2)$$

After time t, if T_1 is instantly increased to T_2 and an isothermal escape rate is determined at the temperature,

$$v_2 = -\int \frac{n_2(x,y,t)}{a(x,y)} dx dy \nu \times \exp[-(E_D+E)/kT_2] \quad (3)$$

When being extrapolated to t, n_1 is equal to n_2. Then,

$$\ln(v_2/v_1) = \frac{E_D+E}{k}\frac{T_2-T_1}{T_1T_2} \quad (4)$$

or

$$E_D+E = \frac{2.303\,kT_1T_2}{T_2-T_1}\log(v_2/v_1) \quad (4')$$

When the fission products are caught in imperfection distributed over various energy states of graphite, Eq. 4 must be carefully applied to the calculation of activation energies. As Mugnuson et al.[8] discussed, however, if the difference of temperature T_1 and T_2 is taken as small as possible, the most important activation energy of the diffusion of fission products within the range of T_1 and T_2 is calculated according to Eq. 4.

Experimental

Preparation of Samples.—A mixture of 1 g. of graphite powder and 60 mg. of uranium dioxide was irradiated with thermal neutrons[1] (thermal

1) D. Schulz, "Summary Report for January, February, and March, 1947", ANL-4006, Sec. I. 6, 62 (Oct. 3, 1947).
2) C. A. Smith and C. T. Young, "Diffusion of Fission Fragments from Uranium-Impregnated Graphite", NAA-SR-72 (May 4, 1951).
3) D. Cubicciotti, "The Diffusion of Xenon from Uranium Carbide-Impregnated Graphite", NAA-SR-194 (Oct. 13, 1952).
4) C. T. Young and C. A. Smith, "Preliminary Experiments on Fission Product Diffusion from Uranium-Impregnated Graphite in the Range 1800~2200°C", NAA-SR-232 (March 25, 1953).
5) L. B. Doyle, "High-Temperature Diffusion of Individual Fission Element from Uranium Carbide-Impregnated Graphite", NAA-SR-255 (Sept. 11, 1953).
6) T. Nakai, S. Yajima, K. Shiba, J. Osugi and D. Shinoda, This Bulletin 33, 497 (1960).
7) S. Yajima, S. Ichiba, Y. Kamemoto and K. Shiba, ibid., 34, 493 (1961).
8) G. D. Mugnuson, W. Palmer and J. S. Koehler, *Phys. Rev.*, **109**, 1990 (1958).

neutron flux, about 5×10^{11} neutrons/cm^2/sec.) for five hours in an experimental hole of JRR-1 reactor. After irradiation the mixture was treated with a hot 4 N nitric acid solution to dissolve uranium dioxide and neptunium-239 produced. In order to measure the activity of xenon-133 without any influence of other fission xenon nuclides and iodine-133, the irradiated graphite samples were cooled for four days before use.

Particle sizes of graphite samples used in this experiment and the analytical data on impurities are shown in Table I.

TABLE I. PARTICLE SIZES OF GRAPHITE SAMPLES AND ANALYTICAL DATA OF IMPURITIES

	Sample		
	AG (Artificial graphite)	NG-1 (Natural graphie-1)	NG-2 (Natural graphite-2)
Particle size (micron)	30	1	50
Impurity			
Ash (total)	0.07%	0.3%	0.8%
SiO_2	250 p.p.m.	220 p.p.m.	3700 p.p.m.
Al_2O_3	210	60	3500
Fe_2O_3	130	24	300
MgO	15	24	100
CaO	70	36	300
V_2O_5	—	0.12	0.5
MnO	—	—	—
Na_2O	20	12	25
K_2O	15	12	20
NiO	—	0.06	—
ThO_2	—	2.4	—
CuO	—	—	—
B_2O_5	0.1	0.02	0.5

Determination of Activation Energy.—A flow system is illustrated in Fig. 1. Furnace-C_1 and Furnace-C_2 consisted of an alundum tube with a nichrome winding. The temperature of the furnaces could be increased to 1150°C and kept constant at a temperature with a transformer. The temperature was measured with a platinum-platinum rhodium thermocouple. The temperature of Furnace-C_2 was always kept about 50°C higher than that of Furnace-C_1.

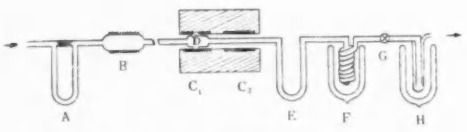

Fig. 1. Flow system.

A Flow meter B Sponge titanium
C_1, C_2 Furnace D Diffusion cell
E Phosphorus pentoxide
F Dry ice trap G Stopcock
H Charcoal trap cooled with dry ice

Each part of the system was made of hard glass except a silica tube in the furnace in which samples were heated, and each part was connected with a polyethylene tube.

Helium gas at a constant flow rate (100 ml./min.) was purified with sponge titanium heated at 800°C to eliminate a trace amount of oxygen. Phosphorus pentoxide was used to remove water in the gas which had swept over a sample. A dry ice trap was set to remove volatile fission products other than rare gases. Xenon-133, which was released, was adsorbed on charcoal cooled with dry ice which was set next to the trap without charcoal. When the charcoal trap was exchanged for a new one at appropriate intervals, a change-over cock was serviceable for the continuous catch of xenon-133 on charcoal.

A typical experiment was as follows. The graphite powder described above was placed in a silica boat which was slid into the silica tube. Then, helium gas was introduced into the system. After confirming that helium gas took the place of air, the tube was slid into Furnace-C_1. The graphite sample was heated at a constant temperature for 30 min. During this period the charcoal trap was exchanged every 5 min. Just 30 min. after the beginning of the heating, the sample together with the tube was slid into Furnace-C_2 whose temperature had been about 50°C higher than that of Furnace-C_1. The trap was exchanged every 2 min. and the sample was heated at a constant temperature for 12 min. The temperature was measured with a platinum-platinum rhodium thermocouple adjacent to the sample. Such a procedure was repeated at a set of increased temperatures.

Making of Heating Curve.—In order to make a heating curve, a graphite sample was heated with a constant increment of temperature and xenon-133 released during a constant period of time was adsorbed on charcoal.

The amount of the released nuclide was plotted versus temperature. The flow system is the same as that shown in Fig. 1 except a furnace and a tube in which a sample was heated. Because the temperature of samples must be continuously increased to temperatures as high as possible, silicon carbide was used as the heater of the furnace.

The sample described above was placed in an alundum boat which was slid into the alundum

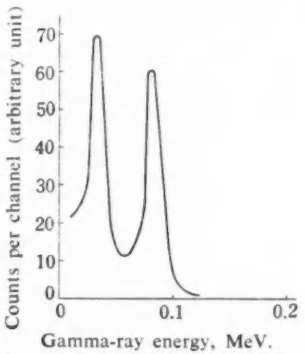

Fig. 2. Gamma-ray spectrum of xenon-133 in a charcoal trap.

tube. Then, helium gas was introduced into the system. After confirming that helium gas took the place of air, the tube was slid into the furnace. The sample was heated with a contsant increment of temperature, 3°C/min. Xenon-133 released was adsorbed charcoal in a trap cooled with dry ice, the trap being exchanged every 10 min.

Activity Measurement.—Activity of xenon-133 adsorbed on charcoal was measured with a RCL 256 channel gamma-ray spectrometer with a well type NaI scintillator (2 inch diameter×1.75). The charcoal was placed in the well, with its trap made of glass, and the activity was measured. The gamma-ray spectrum of xenon-133 is illustrated in Fig. 2.

Results

The absolute value of v_1 and v_2 is not always necessary but the ratio of v_2/v_1 is necessary for determining the activation energy according to Eq. 4. Therefore, when amounts of xenon-133 remaining in graphite are plotted versus diffusion time, the ratio v_2/v_1 is equivalent to a ratio of tangential slopes at a discontinuous point of temperature. A typical plot is shown in Fig. 3. The values obtained from these plots are given in Table II, and the apparent activation energy versus absolute temperature is illustrated in Fig. 4.

Heating curves obtained by another experiment are illustrated in Figs. 5—7. The axis

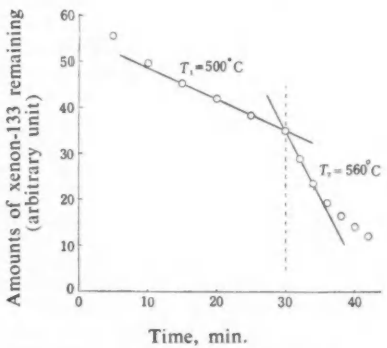

Fig. 3. Isothermal escape rates of xenon-133 in natural graphite-1 at 500 and 560°C.

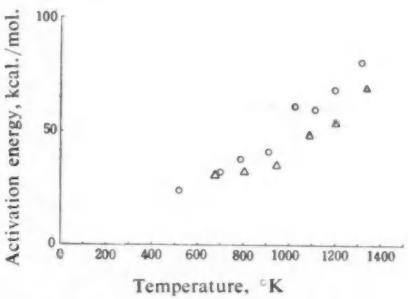

Fig. 4. Apparent activation energy versus temperature.
○ AG △ NG-1

TABLE II. ACTIVATION ENERGIES OF DIFFUSION OF XENON-133 IN GRAPHITE

AG (Artificial graphite)

T_1 °C	T_2 °C	v_2/v_1	$E+E_D$ kcal./mol.
228	269	5.48	23.5
400	447	4.72	31.5
490	539	4.48	37.4
606	675	6.37	40.6
725	780	4.94	60.7
815	870	3.74	59.2
910	950	2.55	67.7
1023	1082	3.88	80.2

NG-1 (Natural graphite-1)

T_1 °C	T_2 °C	v_2/v_1	$E+E_D$ kcal./mol.
380	418	3.58	30.2
500	560	4.28	32.0
656	696	2.17	34.6
786	840	3.06	48.6
915	956	2.12	53.3
1041	1090	1.81	68.4

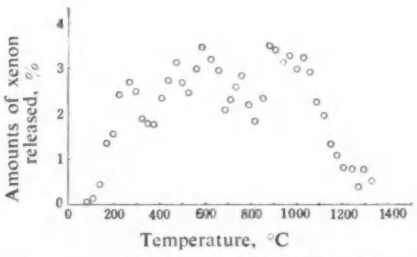

Fig. 5. Heating curve (3°C/min.) of natural graphite-1.

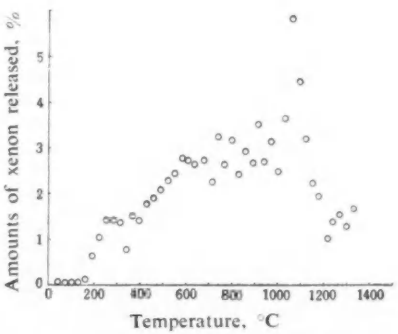

Fig. 6. Heating curve (3°C/min.) of natural graphite-2.

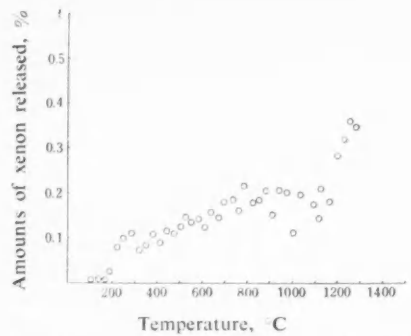

Fig. 7. Heating curve (3°C/min.) of artificial graphite.

of abscissa is temperature and the axis of ordinate is percent xenon-133 released from graphite every 10 min.

Discussion

In the previous experiment[6], it was observed that the diffusion of xenon consisted of a rapid diffusion and a slow diffusion, and from the latter, the activation energy of the interstitial diffusion was calculated. But it is inadquate to treat the diffusion of xenon in graphite from the slow diffusion alone.

The tendency of the diffusion was observed by Argonne workers[1] and Cubicciotti[3]. The Argonne workers interpreted that there were two mechanisms for the diffusion, a rapid "pore" diffusion and a slow "crystallite" diffusion. However, as pointed out by Cubicciotti, if the above interpretation were correct, there would be a truly rapid diffusion which would eventually give way to a slow diffusion at one temperature; that is, all the rapidly diffusing material would have been gone in a short time and then, an increase in temperature would result in the simple diffusion of the slowly diffusing material. Experimentally, however, it is found that with each increase in temperature there is a rapid escape of xenon. Cubicciotti explains that the initial rapid escape is attributed to a rapid temperature increase of the sample. On the other hand, our experiment on natural graphite-2 showed no striking effect of the rate of temperature increase: the amount (46.3%) of xenon-133 released when the temperature of a graphite sample was increased from room temperature to 800°C in 3 min. and kept constant at 800°C for 90 min. was nearly equal to the amount (41.7%) of xenon-133 released when the temperature of another sample was increased from room temperature to 800°C at a rate of 3°C/min. This fact suggests that the amount of xenon-133 released is mainly determined by a final temperature.

Circles and triangles in Fig. 4 are not on a straight line parallel to the axis of abscissa but on ascending lines, respectively. In other words, the activation energy of the diffusion is not simple but consists of various values, say, 20~40 kcal. at 500 to 1000°K and higher at temperatures over 1000°K. This tendency is the same both in artificial and natural graphite except the fact that the activation energy of diffusion in artificial graphite is a little higher than that in natural graphite.

Heating curves in Figs. 5—7 show the distribution of the amount of released xenon over a wide range of temperature. These figures also indicate the distribution of the energy of xenon in graphite, when the relation shown in Fig. 3 is taken into account. The energy is considered to correspond to E in Eq. 4 because E_D is far smaller than E. From these observations, the fact that the diffusion rate of xenon in natural graphite was greater than that in artificial graphite will be explained as follows. Xenon atoms in natural graphite are distributed more in sites of a low activation energy while xenon atoms in artificial graphite are more in sites of a high activation energy. Therefore, the amount of xenon diffusing out at a temperature is greater in natural graphite than in artificial graphite. Although not studied thoroughly, it is supposed that xenon atoms exist on vacant sites of graphite lattice and that the above mentioned activation energies are determined according to the position of such xenon atoms, because the activation energy of the interlaminar diffusion in graphite is known to be very low. It is obvious by the X-ray diffraction and the electron diffraction methods that artificial graphite is more imperfect than natural graphite. This means that the number of vacancies is larger in artificial graphite than in natural graphite. In this sense, a heating curve is considered to show also the distribution of the vacancies among sites of various energies.

On the basis of discussion described above, a rapid diffusion and a slow diffusion in an isothermal curve are easily interpreted. When a graphite sample is rapidly heated to a certain temperature, a xenon atom existing in a site with an activation energy which corresponds to the temperature diffuses out through the interlaminar space: this is a rapid diffusion. During the maintenance of the temperature, xenon existing in a site with a larger activation energy escapes out with a certain probability: this is a slow diffusion. It is evident that Fick's law can not be applied

to such a system, because the law deals with diffusion only in terms of concentration gradient.

The authors wish to thank Dr. H. Suzuki of Solid State Physics Laboratory of JAERI for helpful discussions.

Division of Chemistry
Japan Atomic Energy Research Institute
Tokai, Ibaraki-ken
(S. Y., S. I., Y. K. & K. S.)

Mitsubishi Atomic Power Industries
Inc. Laboratory
Omiya-shi Saitama-ken
(M. K.)

*Determination of Lanthanum, Samarium and Europium in Manganese Nodules by Neutron Activation**

By Toshi KAWASHIMA, Masumi OSAWA, Yoko MOCHIZUKI and Hiroshi HAMAGUCHI

(Received September 26, 1960)

So far the determination of a trace amount of rare earth elements have primarily been carried out by X-ray fluorometric, emission spectrometric or absorption spectrometric methods; but none of these methods have given satisfactory results. After the atomic pile has become available for wide use, ever growing attention has been paid to the application of radioactivation technique to the determination of many trace elements. A number of reports have proved the validity of the same technique for the determination of a trace amount of rare earth elements because of its selectivity and the high sensitivity.

Brooksbank and Leddicotte[1] determined a number of rare earth elements in biological materials (bones), by making use of the chromatographic separation and successive countings of the eluates after neutron irradiation of the sample. Likewise, Cornish[2] reported the ion exchange separation method. Jakovlev[3] discussed an approach for the determination of the total content of rare earth elements in high purity materials (graphite, beryllium, bismuth and germanium) on the basis of the activity of samarium and europium estimated by analyzing the decay curves, without resorting to chromatographic separation. Nakai et al.[4] reported the determination of dysprosium samarium, and lanthanum in thorium metal and oxide, based on gamma-ray counting of the rare earth fraction obtained by anion exchange separation from the sample irradiated in JRR-1.

Various nuclides are formed when a minute amount of rare earth elements in rocks and meteorites are irradiated with thermal neutrons.

TABLE I. NUCLEAR DATA

Element	Clarke number	Radionuclide	Half life	Activity* dis./sec.
Sc	0.0005	^{46}Sc	85 days	$2.65 \cdot 10^{2}$
Y	0.0028	^{90}Y	64 hr.	$2.3 \cdot 10^{3}$
La	0.0018	^{140}La	40 hr.	$9.0 \cdot 10^{3}$
Ce	0.0046	^{141}Ce	33 days	$3.6 \cdot 10$
		^{143}Ce	33 hr.	$4.1 \cdot 10^{5}$
Pr	0.00055	^{142}Pr	19 hr.	$5.8 \cdot 10^{3}$
Nd	0.0024	^{147}Nd	11.3 days	$6.0 \cdot 10$
		^{149}Nd	2 hr.	$1.9 \cdot 10^{5}$
Sm	0.00065	^{153}Sm	47 hr.	$1.2 \cdot 10^{4}$
Eu	0.00010	^{152}Eu	9.3 hr.	$1.5 \cdot 10^{5}$
Gd	0.00064	^{159}Gd	18 hr.	$7.6 \cdot 10^{2}$
Tb	0.00009	^{160}Tb	73 days	$2.5 \cdot 10$
Dy	0.00045	^{165}Dy	2.3 hr.	$4.7 \cdot 10^{5}$
Ho	0.00011	^{166}Ho	27 hr.	$5.7 \cdot 10^{3}$
Er	0.00025	^{171}Er	7.5 hr.	$6.6 \cdot 10^{2}$
Tm	0.00002	^{170}Tm	120 days	$2.2 \cdot 10$
Yb	0.00027	^{175}Yb	4.2 days	$1.2 \cdot 10^{3}$
		^{177}Yb	1.8 hr.	$6.3 \cdot 10^{3}$
Lu	0.000075	^{177m}Lu	3.7 hr.	$8.3 \cdot 10^{3}$
		^{177}Lu	6.9 days	$8 \cdot 10^{2}$

* A (dps) = Clarke number $\cdot 10^{-2} \cdot Ab.(1/M)6.03 \cdot 10^{23} \cdot \sigma \cdot S$

A: Activity at the end of bombardment
M: Mass number Ab: Isotopic abundance
S: Saturation factor: $(1-e^{-\lambda t})$, $t = 10$ hr.
σ: Neutron capture cross section.

* Presented at the 12th Annual Meeting of the Chemical Society of Japan, Kyoto, April, 1959.

1) W. A. Brooksbank and G. W. Leddicotte, *J. Phys. Chem.*, **57**, 819 (1953).
2) F. W. Cornish, *Brit. Atomic Energy Research Establishment Rept.*, AERE C/R-1224 (1953).
3) J. V. Jakovlev, *Proceedings of International Conference on Peaceful Uses of Atomic Energy, Geneva*, 1955, Paper 632 (USSR), Vol. 15, pp. 54–59; *Anal. Abstr.*, **4**, 1112 (1957).
4) T. Nakai et al., Presented at the 2nd symposium on radiochemistry, Kyoto, Nov., 1958.

Then, the nature and activity of the induced radionuclides which come into question when 1 g. of sample containing rare earth elements in its normal natural abundance ratio is irradiated for 10 hr. with thermal neutrons of its intensity of 10^{11} n/cm^2/sec., are shown in Table I. These radionuclides would decay according to Fig. 1. It is clear that the nuclides which should be considered are lanthanum-140, samarium-153, europium-152 and yttrium-90 when as long as 20 hr. are needed for chemical processing after the end of irradiation.

The gamma ray spectrum of the rare earth fraction would then be considered to be the sum of photopeaks produced by X-rays which are induced by K electron capture, and compton continuums, and photopeaks produced by complete gamma ray absorption and bremsstrahlungs induced by β-rays which are emitted by lanthanum, samarium, europium and long lived nuclides. Therefore, the decay curve obtained by measuring the activity at a fixed base bias under the same counting conditions is expected to be analyzed into a few components. The present paper reports the determination of lanthanum, samarium, and europium in manganese nodules by means of a comparison method based on the counting rate of the respective components analyzed as above.

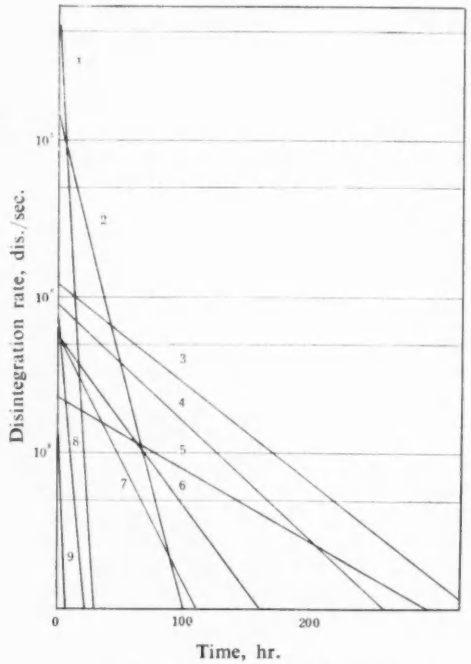

Fig. 1. Relative activities of rare earth radionuclides.

1: 2.3 hr. Dysprosium-165
2: 9.3 hr. Europium-152
3: 47 hr. Samarium-153
4: 40 hr. Lanthanum-140
5: 64 hr. Yttrium-90
6: 27 hr. Holmium-166
7: 19 hr. Praseodymium-142
8: 3.7 hr. Lutetium-177m
9: 1.8 hr. Ytterbium-177

Experimental

Reagents and Samples. — Standard solutions of lanthanum, samarium and europium were prepared by dissolving respective metal oxides in nitric acid. The purity of these oxides listed by Johnson Mathey, was 99.99% for samarium oxide and 99.9% for europium and lanthanum oxides. These reagents were proved to be radiochemically pure by the activation analysis. Uranyl acetate (Merck) solution was used for the standard of uranium. All other chemicals used in this work were of c. p. or reagent grade.

Manganese nodule samples were offered by Professor E. D. Goldberg, Scripps Institution of Oceanography, La Jolla, California, to whom our thanks are due.

Irradition.—Manganese nodule samples of from 200 to 500 mg. were sealed in a silica tube and irradiated along with neutron monitors in the Japan Research Reactor-1 (JRR-1). The reactor was homogeneous, enriched uranium, water moderated and cooled type, and had a neutron flux of around $2\sim3\times10^{11}$ n/cm^2/sec. The flux monitors were prepared by evaporating a known amount (102, 3.5 and 0.35 μg) of lanthanum, samarium and europium in a silica tube or impregnating it into a filter paper wrapped in a vinyl bag. The irradiation lasted intermittently for 2~3 days, 5 hr. each day.

Chemical Separation.—After neutron irradiation and a suitable decay time (about one day), the manganese nodule was dissolved in aqua regia. Any residue was fused with sodium peroxide, dissolved in hydrochloric acid, and added to the main solution. An aliquot of the solution (1/10 of the total volume) was used for the determination of the rare earth elements, and the remainder of the solution was reserved for the determination of elements other than the rare earths. Twenty milligrams of lanthanum carrier was added to the pipetted aliquot and the rare earth activity was carried down with lanthanum fluoride precipitate by adding hydrofluoric acid to the solution. Further purification was achieved by going through the standard lanthanum fluoride cycle[5] three times. The final lanthanum hydroxide precipitate which was decontaminated from any activities other than those of the rare earth elements was then dissolved in hydrochloric acid and diluted to a known volume. An aliquot of this solution was used for γ-ray counting and the remainder for the determination of the

5) N. E. Ballou, "National Nuclear Energy Series, Radiochemical Studies: The Fission Products, Book 3", McGraw-Hill Book Co., Inc., New York (1953), p. 1673.

chemical yield by a conventional gravimetric method[6].

Counting. — The γ-rays and X-rays from the induced radioactive rare earth nuclides were detected and analyzed with the manual sweep scintillation spectrometer (Atomic Instrument Co., Model 510) equipped with a well type*, 1¾ in. by 2 in., sodium iodide (Tl) scintillation crystal. The quantitative analysis for each rare earth element was made by comparing the lanthanum-140, samarium-153 and europium-152 activities of rare earth fraction which is separated from the irradiated manganese nodules with the correspondingly irradiated monitor of the respective element, after measuring the activity of each of the nuclides as mentioned later. Decay measurements of the rare earth activities from the manganese nodule samples and the flux monitors gave the same half-life for each nuclide.

Results and Discussion

The γ-ray spectrum of the rare earth fraction chemically separated and purified is shown in Fig. 2. Individual γ-ray spectra of lanthanum, samarium and europium obtained by the separate irradiation of the respective elements are shown in Fig. 3. These were measured at a channel width of 1 V. with the well type single channel scintillation spectrometer mentioned above. In this work, the counting rate at the peaks of 0.07, 0.09 and 0.5 MeV. for each sample were measured under exactly the same conditions.

Determination of the Lanthanum, Samarium and Europium Activities. — The activity of the rare earth fraction at the peak of 0.5 MeV. is attributed to 40 hr. lanthanum-140 plus long-lived components (Figs. 2 and 3). Therefore, the activity of lanthanum-140 at a given time can be determined by graphical analysis of the

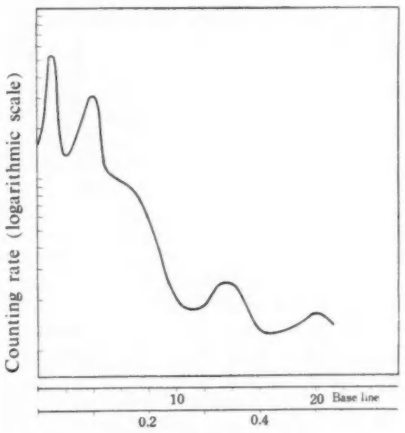

Fig. 2. Gamma-spectrum due to rare earth activities separated from neutron irradiated manganese nodule.

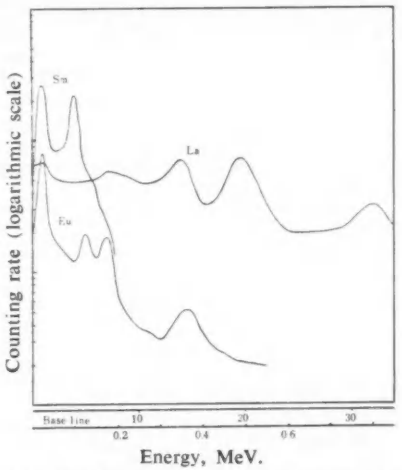

Fig. 3. Gamma-spectra of lanthanum-140, samarium-153 and europium-152.

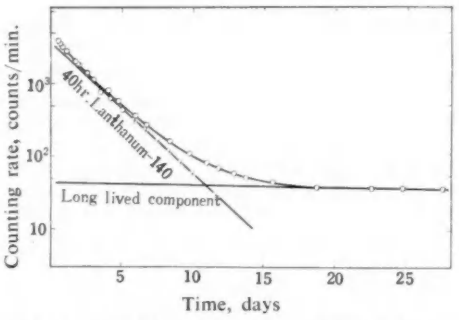

Fig. 4. Analysis of decay curve for the determination of lanthanum.

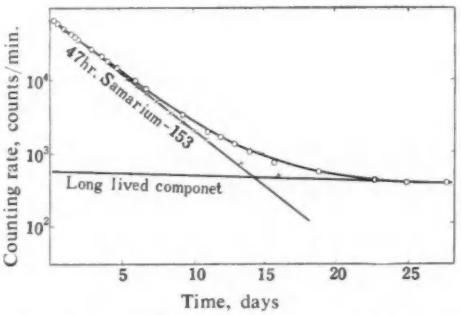

Fig. 5. Analysis of decay curve for the determination of samarium.

6) W. F. Hillebrand, E. F. Lundell, H. A. Bright and J. I. Hoffman, "Applied Inorganic Analysis", 2nd ed. John Wiley & Sons, Inc., New York (1953), p. 550.

* Hole 17mmϕ×80mm, covered with aluminium can.

TABLE II. LANTHANUM, SAMARIUM AND EUROPIUM CONTENT OF MANGANESE NODULES (p. p. m.)

Sample	Location	Depth, m.	La	Sm	Eu
Horizon Guyot MP 26 A-3	19°N 169°W	1440~1540	234	33	9.6
			201	24	7.7
			270	35	9.4
			av. 235	av. 31	av. 8.9
Horizon Guyot MP 25 F-2	19°N 170°W	1870~1920	250	40	11.0
			378	60	19.6
			av. 314	av. 50	av. 15.3
Horizon Nodule	40°N 155°W	5500	357	108	19.6
			250	62	16.6
			av. 303	av. 85	av. 18.1

decay curve, a typical one of which is given in Fig. 4.

Just as in the case of lanthanum mentioned above, the activity of 47 hr. samarium-153 is estimated based on the decay curve at the 0.09 MeV. peak, as shown in Fig. 5.

The activity of around 0.025 MeV. peak is the sum of activities due to europium-152, lanthanum-140, samarium-153 and longer-lived nuclides (Figs. 2 and 3). Therefore, the activity of the 9.3 hr. europium-152 component can be analyzed by the graphical analysis of the decay curve at the peak, an example of which is shown in Fig. 6. If the activity of long-lived component (curve B) plus 40 hr. lanthanum-140 component (curve C) is deducted from the gross decay curve A, we obtain the curve D which corresponds to the composite of the activity of europium and samarium. Here the contribution of lanthanum-140 component (curve C) is calculated by the experimentally determined ratio of the counting rate at the peak of around 0.025 MeV. to that of 0.5 MeV. (the ratio is around 1, see Fig. 3). By analyzing the curve D, the decay curve of 9.3 hr. europium-152, curve E, is obtained.

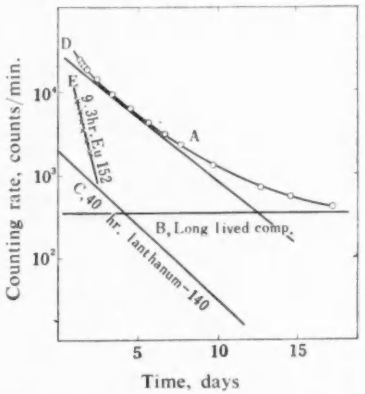

Fig. 6. Analysis of decay curve for determination of europium.

Determination of Lanthanum, Samarium and Europium in Manganese Nodules.—The amounts of lanthanum, samarium and europium in the sample are estimated by comparing the activities of each of the nuclides of the sample determined as above with that of the respective monitor. The results are summarized in Table II.

A possible interference of fission products of uranium in the manganese nodules should be taken into consideration, since lanthanum-140, samarium-153, and many other rare earth nuclides are produced by slow neutron fission of uranium. The interference should not be disregarded particularly in the case of lanthanum-140, because of the high fission yield of mass 140 chain. An experiment to examine this interference was performed by separating and measuring the fission product rare earths from an irradiated known amount of uranium. The uranium assay was carried out by utilizing the activity of fission product barium-140, on an aliquot of the reserved solution mentioned earlier. It was found that the interference with fission product rare earths from the uranium in the samples was negligibly small*.

The overall reproducibility of the method for manganese nodule samples is shown to be about 10~20%. Additional runs would probably increase the reproducibility of the method. As for the sensitivities of the method, as little as 1, 0.02 and 0.01 μg of lanthanum, samarium and europium respectively, could be detemined under the present experimental conditions.

Goldberg and Arrhenius[7], and also Young[8] gave 140 and 220 p.p.m. lanthanum respectively as the average for Pacific pelagic sediments by spectroscopic method. Our data indicate a

* The result of uranium assay will be reported in a later paper. Tatsumoto and Goldberg (*Geochim. et Cosmochim. Acta*, **17**, 201 (1959)) gave 3.9, 3.6, 3.6 p. p. m. in Horizon Nodule by a spectrophotometric method.

7) E. D. Goldberg and G. O. S. Arrhenius, *Geochim. et Cosmochim. Acta*, **13**, 153 (1958).

8) E. J. Young, *Bull. Geol. Soc. Amer.*, **65**, 1329 (1954).

somewhat higher lanthanum content of the manganese nodules than pelagic sediments.

The relative abundance of the three elements was calculated for the three manganese nodules, which are tabulated in Table III. For reference,

TABLE III. RELATIVE ABUNDANCE OF LANTHANUM, SAMARIUM AND EUROPIUM

	Sample	Relative abundance		
		La	Sm	Eu
1a	Horizon Guyot MP 26 A-3	1	0.13	0.038
1b	Horizon Guyot MP 25 F-2	1	0.16	0.049
1c	Horizon Nodule	1	0.28	0.060
2	Crustal rocks (Clarke No.)	1	0.33	0.056
3	Cosmic* (Suess, Urey)	1	0.332	0.093

* Atomic abundance ratio

the abundance ratio of the three elements for crustal rocks, and the cosmic abundance ratio as given by Suess and Urey[9] are also included in Table III. It is seen that no essential differences in the relative abundance of the three rare earth elements are observed among the three different types of materials.

9) H. E. Suess and H. C. Urey, *Revs. Mod. Phys.*, **28**, 53 (1956).

Summary

The gamma spectrometric method has been developed for simultaneous determination of microgram amounts of lanthanum, samarium and europium without chemical separation of each other. The method was based on the chemical separation of rare earth mixtures from neutron irradiated samples and subsequent γ-ray scintillation counting of the isolated rare earth fractions. The sample was irradiated for 2~3 days, 5 hr. each day, in the nuclear reactor JRR-1 at a flux of the order of 10^{11}n/cm^2/sec. The rare earth mixture purified by lanthanum fluoride cycles was used for γ-ray counting at a given pulse height peak. The activity of each component could be evaluated by resolving the decay curves obtained, and the amount calculated by comparing the activity with that of each monitor.

We wish to express our hearty thanks to the staff of the Radiochemistry Group, Japan Atomic Energy Research Institute, for their help in making the irradiation. A part of the expense was defrayed from the Ministry of Education, to which our thanks are due.

Department of Chemistry
Tokyo University of Education
Koishikawa, Tokyo

Photoconductivity of Zinc Oxide under Different Ambient Conditions

By Hiroshi KOKADO, Eiichi INOUE, Takashi YAMAGUCHI and Kenji TAKAHASHI

(Received October 28, 1960)

The existence of a close relationship between photoconduction and oxygen desorption process of zinc oxide has been made clear in some details since Bevan and Anderson's work[1]. The oxygen adsorbed on the surface of zinc oxide seems to produce an acceptor level for conduction electrons and to make a depletion layer under the surface. Destruction of the depletion layer or further formation of the space change layer[2] takes place accompanied by absorption of light, its wavelength is shorter than 4000 Å, and it yields a number of conduction electrons. This model well interprets the peculiarities of the photoconductive process of zinc oxide. Then, one can anticipate that the adsorption of other molecules than oxygen on a surface of zinc oxide too may give a similar or to some extent different effect on the dark- and photo-conduction of the material, depending upon the character of the adsorbant[3].

We have studied the effects of several kinds of ambient molecules on the surface conductivity of zinc oxide at room temperature. The

1) D. J. W. Bevan and J. S. Anderson, *Discussions Faraday Soc.*, No. 8, 238 (1950); D. B. Medved, *J. Chem. Phys.*, **28**, 870 (1958); D. A. Melnick, ibid., **26**, 1136 (1957); W. Ruppel, H. J. Gerritsen and A. Rose, *Helv. Phys. Acta*, **30**, 495 (1957).

2) R. J. Collins and D. G. Thomas, *Phys. Rev.*, **112**, 388 (1958).

3) V. I. Lyahenko and O. V. Snitko, *Trudy Inst. Fiz., Akad. Nauk, Ukr. USSR*, **91**, 1071 (1953); E. K. Putseiko and A. N. Terenin, *Doklady Akad. Nauk SSSR*, **101**, 645 (1955), *Problemy Kinetiki i Kataliza, Akad. Nauk SSSR*, **8**, 53 (1955).

specimens (ca. 20 μ in thickness) were made by depositing zinc oxide powder (Merck's reagent) from an ethanolic suspension on glass plates of 18×18 mm. in size. They possess parallel electrodes that are separated from each other by a gap of 5 mm. Silver paste was used as the electrode material. These specimens showed the values of $10^5 \sim 10^6$ times the initial conductivities measured in air ($10^{-11} \sim 10^{-13}$ ohm^{-1} for 20 V. of applied voltage) when they were kept in vacuum to remove the oxygen adsorbed on the zinc oxide layer. After this treatment, the gases or vapors were introduced onto the specimens and the dark currents were observed after 10 min.

The curves in Fig. 1 show the typical effect of an acceptor (O_2), a donor (NH_3) and a neutral (CO_2) type molecule on the dark

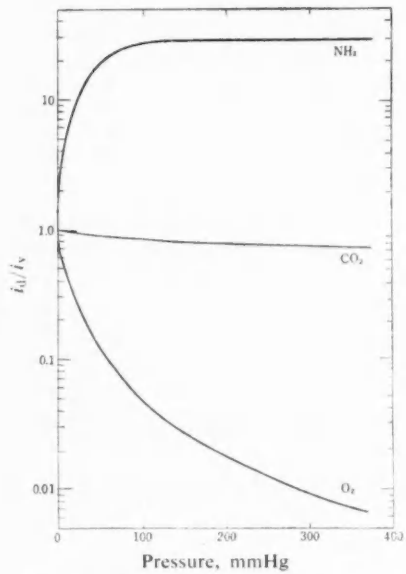

Fig. 1. Influence of the ambient gas on the dark conductivity of zinc oxide.
i_d: Dark current in the gas
i_v: Dark current in vacuum

conductivity. Ammonia was found to be effective on the electronic properties not only in vacuum but in atmospheric air. By pumping the ambient molecules off, the conductivity was unchanged in the case of oxygen, but in the case of ammonia, it returned to the initial value approximately. The behavior of nitrogen was quite similar to that of carbon dioxide and also methylamine to ammonia; otherwise the following three gases behaved as an acceptor type molecules; nitrogen oxide, nitrogen dioxide and methyl ethyl ketone (MEK). However, in the case of MEK, the conductivity was increased partly by taking it off. This seems to suggest that the nature of the adsorption was of somewhat different. Vapors of water, diethyl ether and ethyl alcohol did not change or slightly changed the conductivity of the zinc oxide cell.

As to the photoconductive sensitivity (i_p/i_d in Table I), a remarkable increase was found by adsorption of the electronegative gases such

TABLE I

Gas or vapor	Pressure mmHg	i_d/i_v	i_p/i_d	Decay
O_2	44	$\sim 10^{-2}$	$\sim 10^2$	rapid
NO	45	3×10^{-5}	$10^3 \sim 10^4$	rapid
NO_2	0.3	$<3\times10^{-5}$	$\sim 10^2$	very rapid
MEK	47	$10^{-2} \sim 10^{-3}$	2×10^2	slow
Vacuum	—	—	2~ 3	very slow
CO_2	114	1	2~ 3	very slow
NH_3	42	~10	2~ 3	slow
Pyridine	7.5	$10^{-2} \sim 10^{-4}$	—	—

i_v: Dark current in vacuum
i_d: Dark current in gas or vapor
i_p: Photocurrent in gas or vapor for 10^{12} photons/cm^2 sec. of 3650 Å light from an ultra-high pressure mercury lamp

as oxygen, nitrogen oxide and nitrogen dioxide, while no change was observed by adsorption of carbon dioxide or ammonia type molecules. In Table I, the results of qualitative observations on the rate of current decay after ceasing an irradiation on the cell were also tabulated. It is noteworthy that there exists a parallelism between the chemical activity of the ambient molecules and the rate of the decay process. The active electrons of these molecules may play an important role in the adsorption

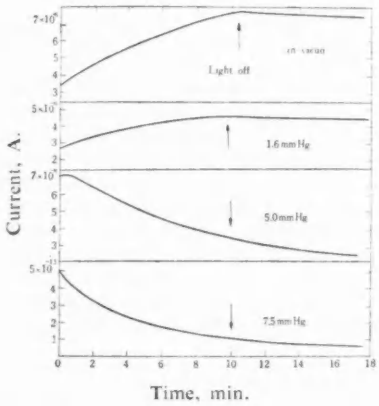

Fig. 2. Photoresponses of the conductivity of zinc oxide in pyridine vapor.

mechanism. MEK having no such active electrons, has only a weak effect to accelerate the decay[4].

The effect of aromatic and aliphatic hydrocarbons and also pyridine on the conductivity of zinc oxide were found to be rather obscure; the conductivity decreased by adsorption of these organic compounds. However, the irradiation on this system did not change the value of its conductivity; it monotonically decreased when an electric field was applied for measurement. This effect was more noticeable if the vapor pressure was increased, as shown in Fig. 2. The nature of this strange phenomenon is not yet clear.

Graphic Engineering Laboratory
Tokyo Institute of Technology
Meguro-ku, Tokyo

4) By adsorbing ammonia or another donor type molecule too, a little higher decay rate is observed, associated with a greater density of recombination centers, with a greater capture cross section for the recombination, or with both (R. H. Bube, *Phys. Rev.*, **101**, 1668 (1956)).

---

*On the Fluorine Shift of Aromatic Fluorine Compounds**

By Teijiro YONEZAWA, Kenichi FUKUI, Hiroshi KATO, Hisao KITANO, Shuzo HATTORI and Shinichiro MATSUOKA

(Received October 24, 1960)

Numerous experimental data on fluorine chemical shifts of various organic compounds have been presented[1-5]. To explain the general trend of these shifts, some empirical interpretations based upon the electronegativity of the atom to which the fluorine is bonded[2], and upon the Hammett constant of a substituent in fluorobenzene have been proposed[3]. These interpretations, however, rest upon no clear basis of electronic configuration around the nucleus.

Ramsey[6] has derived a general expression of nuclear magnetic shielding constant, σ, in a molecule which has no orbital or spin angular momentum and contains only one nucleus of non-zero magnetic moment. The nuclear magnetic shielding is written by his expression

$$\begin{aligned} A_{v_\lambda}\sigma = & \left(\frac{e^2}{3mc^2}\right)\left(0\left|\sum_k \frac{1}{r_k}\right|0\right) \\ & - 2A_{v_\lambda}\left[\sum_{n_\lambda'} \frac{1}{E_n - E_0}\left\{(0_\lambda|\sum \mathbf{m}^0{}_{kz}|n_\lambda')\right.\right. \\ & \times\left(n_\lambda'\left|\sum_k \frac{\mathbf{m}^0{}_{kz}}{r_k^3}\right|0_\lambda\right) \\ & \left.\left. + \left(0_\lambda\left|\sum_k \frac{\mathbf{m}^0{}_{kz}}{r_k^3}\right|n_\lambda'\right)(n_\lambda'|\sum_k \mathbf{m}^0{}_{kz}|0_\lambda)\right\}\right] \end{aligned} \tag{1}$$

where r_k is the distance between the kth electron and the nucleus in question, A_{v_λ} implies an average over all molecular orientations, each of which is specified by the subscript λ; and $\mathbf{m}^0{}_{kz}$ is the z component of the operator for the kth electron

$$\mathbf{m}^0{}_k = \left(\frac{ieh}{4\pi mc}\right)(\mathbf{r}_k \times \nabla_k) \tag{2}$$

The application of this formula to calculate the nuclear magnetic shielding of the nucleus in a complex molecule has been considered to be almost impossible due to the lack of our knowledge of the energies and wave functions of all excited states. Furthermore, as Ramsey[6] pointed out, the formula contains many terms which cancel each other, and this might bring about a considerable error in the numerical calculation.

An important contribution to develop the procedure of obtaining shielding constants was proposed by Saika and Slichter[7]. According to them the screening was divided into three terms.

1. The diamagnetic correction for the atom in question.

* This study was presented at the Symposium on Electronic Structures of Molecules, Tokyo, September, 1959.

1) L. H. Meyer and H. S. Gutowsky, *J. Phys. Chem.*, **57**, 481 (1953).

2) H. S. Gutowsky and C. J. Hoffman, *J. Chem. Phys.*, **19**, 114 (1951).

3) H. S. Gutowsky, D. W. McCall, B. R. McGarvey and L. H. Meyer, *J. Am. Chem. Soc.*, **74**, 4509 (1952).

4) T. Isobe, K. Inukai and K. Ito, *J. Chem. Phys.*, **27**, 1215 (1957); This Bulletin, **33**, 315 (1960).

5) K. Fukui, S. Hattori, T. Yonezawa, R. Kusaka and H. Kitano, *J. Chem. Soc. Japan, Pure Chem. Sec.* (*Nippon Kagaku Zasshi*), **80**, 541 (1959).

6) N. F. Ramsey, *Phys. Rev.*, **78**, 699 (1950).

7) A. Saika and C. P. Slichter, *J. Chem. Phys.*, **22**, 26 (1954).

2. The paramagnetic term for the atom in question.

3. The contribution from other atoms.

Based upon these divisions, they concluded that the F^{19} nuclear magnetic shielding is mainly determined by the paramagnetic contribution of the electrons belonging to the fluorine atom in question. This conclusion was shown to be successful in calculating the chemical shift between HF and F_2. The equation developed by them remained, however, only available for evaluating fluorine shifts in some aliphatic compounds. Further application of their procedure to fluorine shifts in aromatic compounds seems never to have been attempted.

In the present paper, an extension of their analysis to more complex conjugated compounds is presented by using a molecular orbital treatment.

Theoretical

The second order paramagnetic term of Ramsey[6] is approximated referring to the treatment by Saika and Slichter[7]. In the present paper, we have chosen the coordinate system of Fig. 1 whose origin is set at the

Fig. 1. The coordinate system adopted in the present treatment.

fluorine atom in question. Considering the paramagnetic contribution of electrons belonging to the fluorine, the paramagnetic shielding term, σ_p, in a conjugated molecule can be given by the mean of three principal components as

$$\sigma_p=\frac{1}{3}(\sigma_{l-\pi}+\sigma_{l-\sigma}+\sigma_{\sigma-\pi}) \tag{3}$$

These three components are obtained as

$$\begin{aligned}
\sigma_{l-\pi}&=-\left(\frac{eh}{2\pi mc}\right)^2\left\langle\frac{1}{r^3}\right\rangle\sum^{\text{unocc}}\frac{2}{\varepsilon_i-\varepsilon_l}(c_F^{\,l})^2\\
\sigma_{l-\sigma}&=-\left(\frac{eh}{2\pi mc}\right)^2\left\langle\frac{1}{r^3}\right\rangle\frac{2}{\varepsilon_\sigma^*-\varepsilon_l}(a^*)^2\\
\sigma_{\sigma-\pi}&=-\left(\frac{eh}{2\pi mc}\right)^2\left\langle\frac{1}{r^3}\right\rangle\left[\sum_i^{\text{unocc}}\frac{2}{\varepsilon_i-\varepsilon_\sigma}\right.\\
&\quad\times\left\{a^2(c_F^{\,i})^2+\sqrt{\frac{2}{3}}abc_1^{\,i}c_F^{\,i}\right\}\\
&\quad\left.+\sum_j^{\text{occ}}\frac{2}{\varepsilon_\sigma^*-\varepsilon_j}\left\{(a^*)^2(c_F^{\,j})^2+\sqrt{\frac{2}{3}}a^*b^*c_F^{\,j}c_1^{\,j}\right\}\right]
\end{aligned} \tag{4}$$

respectively, where $\langle 1/r^3\rangle$ is the average of $1/r^3$ for 2p electron of fluorine, ε_i and ε_l are the energies of the ith π molecular orbital and of the lone pair electrons of the fluorine atom, $c_F^{\,i}$ and $c_1^{\,i}$ are the coefficients of the ith π electronic LCAO MO, whose energy is $\alpha+\lambda_i\beta$, at the fluorine atom and its adjacent carbon atom, and $\sum^{\text{occ}}$, $\sum^{\text{unocc}}$ indicate summation over all occupied and unoccupied orbitals, respectively. The wave functions of bonding and antibonding C–F σ orbitals, φ_σ and φ_σ^*, whose energies are denoted by ε_σ and ε_σ^* in Eq. 4, respectively, may be expressed by the following linear combinations of two atomic orbitals, χ_F and χ_C, which are the 2p σ AO of fluorine and the sp^2 hybridized orbital of the adjacent carbon atom*.

$$\left.\begin{aligned}\varphi_\sigma&=a\chi_F+b\chi_C\\ \varphi_\sigma^*&=a^*\chi_F+b^*\chi_C\end{aligned}\right\} \tag{5}$$

The coefficients a, b, a^* and b^* are those appearing in Eq. 4. Three components in the right side of Eq. 3, $\sigma_{l-\pi}$, $\sigma_{l-\sigma}$ and $\sigma_{\sigma-\pi}$, can be obtained, as is shown by Eq. 4, by calculating the matrix elements in Eq. 1 between the ground state and the various singlet excited states resulting from one electron transition between MO's designated by each subscript, l, σ and π, denoting the orbital of fluorine lone pairs, C–F σ orbitals and π molecular orbitals, respectively. In the last component $\sigma_{\sigma-\pi}$ which appears only when the π conjugation takes place, the cross term arises from the circumstances that we take account of matrix elements of χ_C and π AO on the adjacent carbon atom in $(0|\mathbf{m}^0{}_{ky}|n)$ and neglect $(0|\mathbf{m}^0{}_{ky}/r_k^3|n)$ terms on that carbon, as was done in Ref. 7. Equation 3 is easily shown to coincide with the equation given by Saika and Slichter[7] when one considers that no conjugation takes place. It can be shown also, that Eq. 3 in the present paper is also derivable by an alternative procedure proposed by Pople[8], in which attention was paid to the paramagnetic shielding resulting from the local paramagnetic current of the fluorine.

In the present paper, a chemical shift parameter, δ, is defined as

$$\delta=\frac{H_r-H_c}{H_r} \tag{6}$$

where H_r and H_c are the resonance field for the reference compound and the sample compound, respectively.

The chemical shift, δ, can be represented in terms of the paramagnetic shielding constant obtained by Eq. 3 whenever σ is small and the change of diamagnetic shielding constant can be neglected. Thus the shift between the

* χ_C is written as $\sqrt{1/3}\chi_s+\sqrt{2/3}\chi_{2p\sigma}$, where χ_s and $\chi_{2p\sigma}$ are 2_s and $2_{p\sigma}$ AO's of carbon atom, respectively.

8) J. A. Pople, *Proc. Roy. Soc.*, A239, 541, 550 (1957).

compound in question and the reference one can be expressed as*1

$$\delta = \delta_p(\text{reference}) - \sigma_p(\text{sample}) \tag{7}$$

Numerical Calculation

In order to carry out calculation, the information on the energies of the molecular orbitals and the coefficients involved in Eq. 4 is indispensable. The π molecular orbital energies and the coefficients are settled by the simple LCAO MO method. The values of the Coulomb integrals and the resonance integral representing the characteristics of a fluorine atom and a carbon atom adjacent thereto are taken as

$$\left.\begin{aligned} \alpha_F &= \alpha + 1.8\beta \\ \alpha_{adj} &= \alpha + 0.18\beta \\ \beta_{C-F} &= 0.8\beta \end{aligned}\right\} \tag{8}$$

where α is the Coulomb integral of a carbon atom and β is the resonance integral for a C–C bond in a benzene molecule. The values of α and β are taken to be -7.25 eV. and -2.3 eV., respectively, in numerical calculation*2. Other Coulomb and resonance integrals used for amino and nitro groups in the present calculation are as follows:

$$\alpha_{-NH_2} = \alpha + 0.4\beta$$
$$\beta_{C-NH_2} = 0.4\beta$$
$$\alpha_N = \alpha + \beta$$
$$\alpha_O = \alpha + \beta$$

Since the simple LCAO MO studies for a σ electron system have not been sufficiently copious for providing reliable numerical values of various parameters, an attempt to estimate these parameters is necessary for our calculation. Hereupon, the values of Coulomb and resonance integrals are determined on the basis of some experimental data in the following way. At first, the energies of σ-bonding and antibonding orbitals for the reference compound are put to -14 eV. and -4 eV., respectively. The energy of bonding orbital is equal to the absolute value of ionization potential of an electron localized in a C–F bond in methyl fluoride assigned by McDowell[9]. The energy of the antibonding orbital is estimated by the spectroscopic data on other methyl halides. The molecular orbital coefficients, a and b, are determined from the magnitude of the bond moment, μ, with the aid of simplified formulas*3

$$\mu = \frac{\lambda^2 - 1}{1 + \lambda^2} eR$$
$$a = \frac{-\lambda}{(1+\lambda^2)^{1/2}} \tag{9}$$
$$b = \frac{1}{(1+\lambda^2)^{1/2}}$$

where R is a C–F bond distance, e is the charge of an electron, and $\lambda(\lambda > 0)$ is a coefficient representing the polarity of the molecular orbital. The bond moment, μ, is adopted as 1.51 D and C–F distance as 1.39 Å. Inserting these values into Eq. 9, we obtain: $a = -0.783$ and $b = 0.622$*4. The coefficients a^* and b^* are then obtained as 0.622 and -0.783, respectively.

Coulomb and resonance integrals in a C–F σ electron system might be determined in such a way that in solving the secular determinant these integrals give the values of energies and orbital coefficients estimated above. It may be more reasonable, then, to consider that, as the character of the C–F σ bond alters according to the change of molecular structure, the values adopted for the integrals may change. In this connection it may be recollected that in π electron approximation a π electron is considered to move in a resultant electric field from all other π electrons and the σ skeleton. Hence, in the treatment of σ electrons, the electronic structure is naturally recognized to be affected by π electronic distribution conversely.

Referring to the facts stated above, the Coulomb and resonance integrals available for a C–F σ electron system are expressed as*5

$$\left.\begin{aligned} h_{FF} &= -10.16 - \gamma_F(q_F^0 - q_F) \\ h_{CC} &= -7.84 - \gamma_C(q_C^0 - q_C) \\ h_{CF} &= +4.84^{*6} \end{aligned}\right\} \tag{10}$$

*1 The shielding constant σ is represented by the sum of diamagnetic and paramagnetic shielding constant σ_d, σ_p as $\sigma = \sigma_d + \sigma_p$. Then the shift becomes $\delta = \{\sigma_d(\text{reference}) - \sigma_d(\text{sample})\} + \{\sigma_p(\text{reference}) - \sigma_p(\text{sample})\}$. Neglecting the first term, we obtain Eq. 7.

*2 These values are determined so that the calculated highest occupied orbital energy of fluorobenzene ($\alpha + 0.844\beta$) becomes equal to the negative value of ionization potential of the compound, 9.19 eV. (V. J. Hammond, W. C. Price, J. P. Teeganand and A. D. Walsh, *Faraday Soc. Discuss.*, **9**, 53 (1950)). The value of α is not so unreasonable compared with the value -7.18 eV. adopted by Mulliken (*Phys. Rev.*, **74**, 736 (1948)). The value of β is equal to that determined by Pariser and Parr (*J. Chem. Phys.* **21**, 767 (1953)).

9) C. A. McDowell and B. A. Cox, *Proc. Roy. Soc.*, **A241**, 194 (1957).

*3 Cf. C. A. Coulson, "Valence", Oxford Univ. (1952), p. 103; In the present formulas, the overlap integral is neglected.

*4 The minus sign of a is determined so as to correspond with the coefficient of bonding σ MO in the present coordinate system (see Fig. 1).

*5 These equations resemble those used in a semi-empirical SCF treatment carried out in a π electron system. (Cf. e. g., R. S. Mulliken et al., *J. Am. Chem. Soc.*, **76**, 4770 (1954)). The present procedure, however, represents a reciprocal interaction of σ electrons with π electrons in a bond.

*6 The exchange integral is taken to be positive since the overlap integral between carbon and fluorine AO's in a C–F σ bond is found to be negative in the present coordinate system (see Fig. 1).

TABLE I. TOTAL π ELECTRON DENSITY, σ-ELECTRONIC ENERGY AND MOLECULAR ORBITAL COEFFICIENT

	q_F	q_C	ε_σ	ε_σ^*	ε_l	a^2	b^2
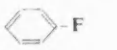	1.9330	1.0204	−13.977	−4.023	−10.000	0.6166	0.3834
	1.9318	1.0196	−13.993	−4.033	−10.024	0.6176	0.3824
	1.9306	1.0216	−14.008	−4.043	−10.048	0.6187	0.3813
	1.9268	1.0162	−14.057	−4.075	−10.124	0.6220	0.3780
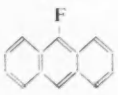	1.9198	1.0128	−14.147	−4.132	−10.264	0.6283	0.3717

TABLE II. TOTAL π ELECTRON DENSITY, σ-ELECTRONIC ENERGY AND MOLECULAR ORBITAL COEFFICIENT

	q_F	q_C	ε_σ	ε_σ^*	ε_l	a^2	b^2
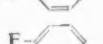	1.9204	0.9686	−14.173	−4.183	−10.252	0.6235	0.3765
	1.9330	1.0204	−13.977	−4.023	−10.000	0.6166	0.3834
	1.9344	1.0342	−13.949	−3.995	− 9.972	0.6165	0.3835
	1.9352	1.0410	−13.934	−3.987	− 9.956	0.6164	0.3836

TABLE III. CALCULATED SHIELDING CONSTANTS AND CHEMICAL SHIFTS

	$-\sigma_{l-\sigma}$	$-\sigma_{l-\pi}$	$-\sigma_{\sigma-\pi}$	$-\sigma_p$	δ_{calcd}	δ_{obs} [a]
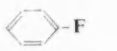	165.398	15.761	146.921	1/3×328.080	0	0
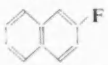	164.590	16.400	146.914	1/3×327.904	−0.06	−0.18
	163.731	16.632	146.875	1/3×327.238	−0.28	−0.26
	161.144	18.462	147.262	1/3×326.868	−0.40	−1.02
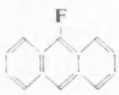	156.305	22.273	147.623	1/3×326.201	−0.63	—

(a) Ref. 5; in units of 10 p. p. m.

TABLE IV. CALCULATED SHIELDING CONSTANTS AND CHEMICAL SHIFTS

	$-\sigma_{l-\sigma}$	$-\sigma_{l-\pi}$	$-\sigma_{\sigma-\pi}$	$-\sigma_p$	δ_{calcd}	δ_{obs} [b]
	159.962	20.738	152.238	1/3×332.938	+1.62	+1.08
	165.398	15.761	146.921	1/3×328.080	0	0
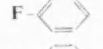	165.453	15.505	145.714	1/3×326.672	−0.47	−0.64
	165.537	15.214	144.889	1/3×325.640	−0.78	−1.46

(b) Ref. 3; in units of 10 p. p. m.

where these matrix elements are represented in units of eV., q_F^0 and q_C^0 denote the total π electron densities at the fluorine and the adjacent carbon atom in the reference, respectively, and q_F and q_C are those in the sample compound. Parameters γ_F and γ_C are tentatively put at 20 and 2, respectively, in the present treatment. Using the integrals in Eq. 10, the energies of bonding and antibonding orbitals as well as the coefficients are calculated.

Finally the energy of lone pair electrons of fluorine, ε_l, is assumed to be*

$$\varepsilon_l = -10 - \gamma_F(q_F^0 - q_F) \qquad (11)$$

in which the second term has a similar meaning in Eq. 10. The value of $\langle 1/r^3 \rangle$ is put at $8.89/a_H^3$, where a_H is the Bohr radius[7].

Result and Discussion

It was discussed qualitatively by the present authors[5] that the two factors, the polarity of C–F bond and the π electron density on fluorine, had a dominant role in determining a paramagnetic term in a conjugated molecule. The two empirical rules were proposed[5], whereby a qualitative analysis of magnetic shielding parameter σ was made. Further we pointed out that in polycondensed aromatics the magnitude of total π electron more density decreases with the decrease of fluorine chemical shifts, while in some fluorobenzene derivatives this correlation is reversed. More precisely, the fluorine chemical shift seems to be governed by the polarity of a C–F σ bond in fluorobenzene derivatives.

In the present paper an investigation on fluorine chemical shifts in these compounds is made quantitatively by making use of Eqs. 3 and 4.

In Tables I and II, the total densities at the fluorine and the adjacent carbon atom, the energies of bonding and antibonding orbitals, and the values of a^2 and b^2 for benzene derivatives and condensed aromatics are cited. One should note that the polarity of a C–F bond which is measured by the magnitude of a^2 seems to increase with the decrease of q_F in Table I, while in Table II the polarity seems to increase with the increase of q_F.

In Tables III and IV, there are listed three principal components of the paramagnetic shielding constant, the mean of the constants and the calculated values of chemical shift together with observed ones.[3,5] With regard to 9-fluoroanthracene, there are unfortunately no data to be compared with the theoretical result. Though there remain many points to be modified in future, the good agreement observed between the present results and experimental data may be sufficiently valuable to be stressed.

Summary

In order to make a quantitative analysis of the F^{19} magnetic shielding parameters in conjugated molecules, an extension of the idea previously proposed by Saika and Slichter is made. Calculations are carried out with respect to several fluorobenzene derivatives and fluorinated polycondensed aromatic compounds by using the molecular orbital method. The agreement of our calculated shifts with observed shielding data is almost satisfactory.

Faculty of Engineering
Kyoto University
Sakyo-ku, Kyoto
(T. Y., K. F., H. K. & H. K.)

Faculty of Science
Kanazawa University
Kanazawa
(S. H. & S. M.)

* In a rough estimation, it may be assumed that this energy can be obtained by the equation, $\varepsilon_l = -I_F + 1/2(I_F - A_F)$, where I_F and A_F are the ionization potential and the electron affinity of the fluorine in its valence state. Using the published data, $I_F = 17.481$ eV., $A_F = 3.78$ eV., we can obtain $\varepsilon_l = -10.5$ eV. Therefore the value of -10 in Eq. 11 seems not to be so unreasonable.

An LCUAO Treatment of Reactivity in Aromatic Hydrocarbons

By Kenichi FUKUI, Teijiro YONEZAWA, Chikayoshi NAGATA and Yoshimichi KONAKA

(Recieved October 28, 1960)

Several theoretical treatments of reactivity of conjugated molecules have achieved a brilliant develompent in accordance with the progress of the LCAO MO method. In this procedure, the molecular orbital is represented by the linear combination of 2π atomic orbitals. By the use of these coefficients useful indices of reactivity such as electron density[1], bond order[1], and frontier electron density[2] are derived.

On the other hand, a method, the so-called LCUAO MO, in which the molecular orbital is represented by the linear combination of united-atomic orbitals in each bond of a conjugated molecule has been developed by Brown and Matsen[3]. This method is an extension of united-atom approach[4] in hydrogen molecule to conjugated compounds.

This procedure may be considered to supply us more easily with information on the nature of a conjugated double bond if we introduce the frontier electron concept in LCAO MO treatment.

Theoretical

By an ordinary procedure of LCUAO MO method[3], a molecular orbital is written as

$$\phi = \sum_i a_i \phi_i \qquad (1)$$

where ϕ_i is the UAO of the ith bond. The secular equation for the system can be obtained from this molecular orbital putting the matrix elements as following.

$$h_{ii} = \int \phi_i^* h \phi_i \mathrm{d}\tau = \alpha$$

$$h_{ij} = \int \phi_i^* h \phi_j \mathrm{d}\tau = \beta \text{ for adjacent bond} \qquad (2)$$

$$0 \text{ for non-adjacent bond}$$

where h is the effective one electron hamiltonian, and α and β are the standard Coulomb and resonance integrals in benzene, respectively. Then all the molecular orbital coefficients are determined from the roots of the secular equation by using normalizing condition

$$\sum_i (a_i)^2 = 1 \qquad (3)$$

Brown and Matsen[3] has proposed that bond order, P_r, for the rth bond can be obtained by

$$P_r = \sum_j \nu_j (a_r^j)^2 \qquad (4)$$

where ν_j is the occupation number for the jth molecular orbital. Then they showed that a good parallelism can be obtained between the bond orders obtained by simple LCAO MO treatment and by the present method.

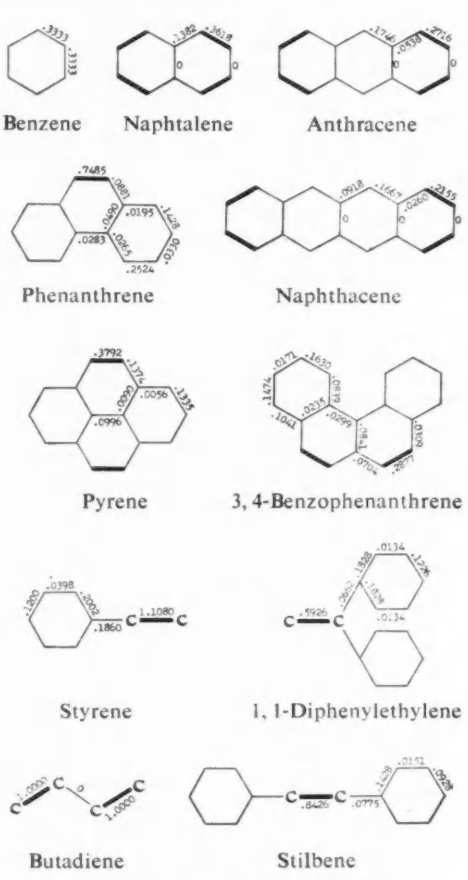

Fig. 1. Electron densities of the highest occupied orbital.

1) H. C. Longuet-Higgins and C. A. Coulson, *Proc. Roy. Soc.*, **A192**, 16 (1947).
2) K. Fukui, T. Yonezawa and H. Shingu, *J. Chem. Phys.*, **20**, 722 (1952); K. Fukui, T. Yonezawa, C. Nagata and H. Shingu, ibid., **22**, 1433 (1954).
3) R. D. Brown and F. A. Matsen, ibid., **21**, 1298 (1953).
4) R. D. Brown, *J. Chem. Soc.*, **1953**, 2615.

TABLE I. REACTIVE BOND IN AROMATIC HYDROCARBONS

Compound	Experimentally most reactive bond*	Bond of largest frontier density	Bond of minimum ortho localization energy**
Benzene	1 : 2	1 : 2	1 : 2
Naphthalene	1 : 2	1 : 2	1 : 2
Anthracene	1 : 2	1 : 2	1 : 2
Phenanthrene	9 : 10	9 : 10	9 : 10
Pyrene	4 : 5	4 : 5	4 : 5
Naphthacene	1 : 2	1 : 2	1 : 2
3,4-Benzophenanthrene (Benzo[*c*]phenanthrene)	5 : 6	5 : 6	5 : 6

* Estimated from the addition reaction of OsO_4, which is considered to be an electrophilic addition taking place simultaneously at the two adjacent carbon atoms.
** Ref. 7.

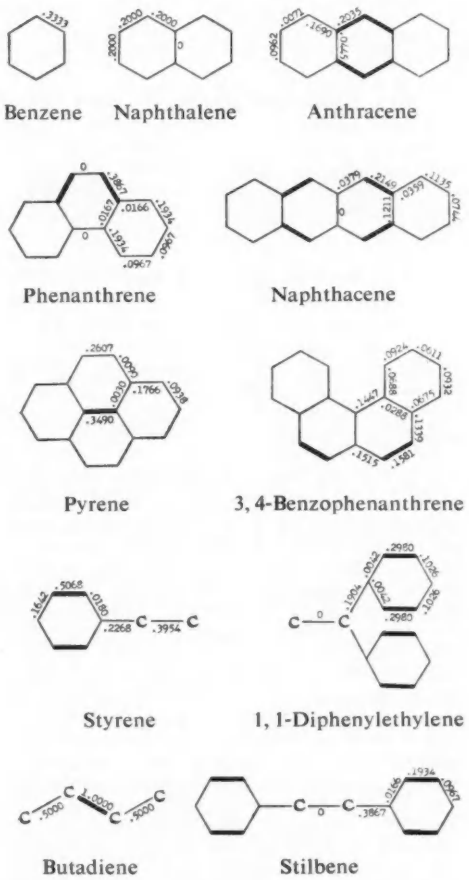

Fig. 2. Electron densities of the lowest vacant orbital.

In these circumstances the investigation is made to elucidate whether or not the frontier electron concept by which the chemical reactivity in conjugated molecules is successfully interpreted may be applicable in LCUAO MO method. The calculation is carried out with respect to benzene, naphthalene, anthracene, naphthacene, pyrene, 3,4-benzophenanthrene (benzo[*c*]phenanthrene), styrene, stilbene and 1,1-diphenylethylene. The electronic distributions of the highest occupied and the lowest vacant orbitals are calculated and indicated in Figs. 1 and 2.

Results and Discussion

The bond of the largest frontier electron density for electrophilic reaction in polycondensed aromatics are indicated in the third column of the Table I. These results may give some information concerning the bond which will play a dominant role in the complex formation of aromatic hydrocarbons with Ag^+ ion[5] or H^+ ion. Furthermore the bond of the largest electron density of the highest occupied orbital in 1,1-diphenylethylene coincides with the position pointed out by Evans and his coworkers[6] in the complex formation of this compound with H^+. In regard to styrene, butadiene and stilbene, calculated results are considered to be reasonable.

On the other hand, the electronic distribution of the lowest vacant orbital shown in Fig. 2 seems to correspond to none of the chemical reactions ever known. But since there exist no experimental data available, we must refrain here from deciding whether the results thus obtained are essentially meaningless or not. But one thing attracts our attention. That is, the most reactive position does not coincide with what is predicted from the electronic distribution of the highest occupied orbital,

5) S. Winstein and H. J. Lucas, *J. Am. Chem. Soc.*, **60**, 836 (1938); R. E. Kofahl and H. J. Lucas, ibid., **76**, 3933 (1954).
6) A. G. Evans, D. M. S. Jones and J. H. Thomas, *J. Chem. Soc.*, **1957**, 104.

while the existing theories of these compounds predict the same position to be most reactive in both electrophilic and nucleophilic additions. A typical one of these theories is the localization theory[7]. This point should be investigated in future.

Faculty of Engineering
Kyoto University
Sakyo-ku, Kyoto

7) E. C. Kooyman and J. A. A. Ketelaar, *Rec. trav. chim.*, **65**, 859 (1946); R. D. Brown, *J. Chem. Soc.*, **1950**, 3249.

Application of RADME to the Chelatometric Determination of Metals Employing the Alternating Current Polarographic Method

By Mutsuo KODAMA

(Received October 6, 1960)

Cadmium- and lead-nitrilotriacetate complexes give rise to two polarographic waves in acetate buffer solution (pH 4.5). The first one is a kinetic wave due to the elecrodeposition of metal ions formed by the dissociation of the complex, and the second is the one due to the direct reduction of complex[1,2]. In ammonia-ammonium nitrate buffer solution, the kinetic currents which originate from the dissociation can also be observed. Owing to the presence of the kinetic current, cadmium and lead can not be titrated with nitrilotriacetic acid (NTA) by employing the usual polarographic method.

In the previous paper, the concentration of copper in an acetate buffer solution of pH 6.0 was determined with NTA by the use of the alternating current polarographic method. In the titration, equivalence points were determined by plotting the peak currents of the alternating current polarograms of copper against the volume of NTA solution added.

The present investigation was directed to the application of rapidly dropping mercury electrode (RADME) to the chelatometric determination of copper, cadmium and lead, using the alternating current polarographic method. At RADME, peak currents due to the electrodeposition of these metal ions which were produced by the dissociation of complexes could not be observed. When RADME is used as an indicator electrode, experimental equivalence points agreed with the stoichiometric equivalence points.

Experimental

Apparatus.—A Yanagimoto Model GA-103 galvarecorder equipped with an automatically scanning potentiometer was employed for the measurements of all current-voltage curves and also for the titrations. The current was determined point by point by manual operation.

Dropping mercury electode (DME) and RADME had the chracteristic features indicated in Table I. the measurements being conducted in air-free 0.1 M potassium chloride solutions with open circuit at 25 ± 0.1°C.

TABLE I. CHARACTERISTICS OF THE ELECTRODES MEASURED IN AIR-FREE 0.1 M POTASSIUM CHLORIDE SOLUTION WITH OPEN CIRCUIT AT 25 ± 0.1°C

	Height of mercury head, cm.	t, sec.	m mg./sec.
DME	70.0	4.02	1.23_7
RADME	60.0	0.35_3	15.54

A simple beaker type cell was used for all measurements. A cell was connected to a saturated calomel electrode (S. C. E.) through a potassium nitrate agar bridge (1.5 kΩ). Semimicroburets of 5 ml. and 10 ml. capacity were used for titrations. During the titrations purified nitrogen gas was passed through the solution to remove dissolved oxygen, prior to the measurements of current-voltage curves and titration curves, which also were conducted after every addition of titrant. All polarographic measurements and titrations were carried out at 25 ± 0.1°C. The cell construction which was used fo rthe alternating current polarographic measurements is shown in Fig. 1. A large platinum electrode was inserted into the solution as the third electrode and this was connected to the anode through a condenser of 100 μF in order to keep the impedance of the electrolysis cell as low as possible.

Reagent. — Nitrilotriacetic acid (NTA) of analytical reagent grade (Wakō Pure Chemical Industries, Ltd.) was used without further purification. The stock solution of NTA was standardized with

1) J. Koryta and I. Kossler, *Collection Czechoslov. Chem. Communs. Suppl.*, **15**, 241 (1950).
2) K. Morinaga and T. Nomura, *J. Chem. Soc. Japan, Pure Chem. Sec. (Nippon Kagaku Zasshi)*, **79**, 200 (1958).

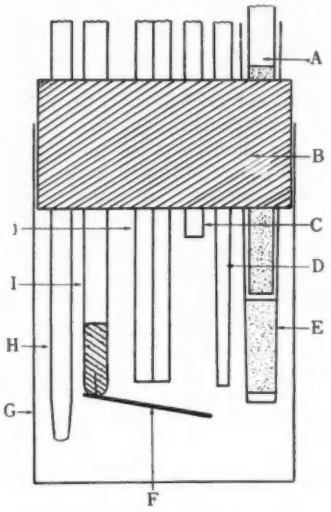

Fig. 1. Cell construction.

A	S. C. E.	F	platinum plate
B	rubber	G	beaker type cell
C	gas outlet	H	gas inlet
D	buret	I	platinum electrode
E	sintered glass	J	DME or RADME

standardized nickel solution[3,4]. Standard solutions of copper, lead and cadmium were prepared from chemicals of analytical reagent grade. The concentration of stock solution was determined gravimetrically[5]. The concentrations of copper and of cadmium were determined by amperometric titration[6,7], using the DME as an indicator electrode. Other chemicals used were all analytical reagent grade. The buffer solutions were prepared by the method described in the previous paper[4].

Results and Discussion

Direct Current (D. C.) Polarography.—Current-voltage curves of cadium-nitrilotriacetate complex were obtained with DME at different heights of mercury column in de-aerated ammonia-ammonium nitrate buffer solution of pH 9.2 containing 0.005% gelatine. The ionic strength was adjusted to 0.7 with potassium nitrate.

As seen from current-voltage curve A (Fig. 2), the mixture of cadmium and nitrilotriacetic acid at the ratio of exactly 1 to 1, gives a polarogram with a small reduction wave of

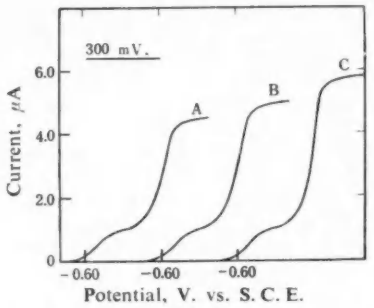

Fig. 2. Current-voltage curves of $1.09_8\times10^{-3}$ M cadmium nitrilotriacetate in an ammonia-ammonium nitrate buffer of pH 9.2 ($\mu=0.7$).

A Height of mercury column, 50 cm.
B Height of mercury column, 70 cm.
C Height of mercury column, 90 cm.

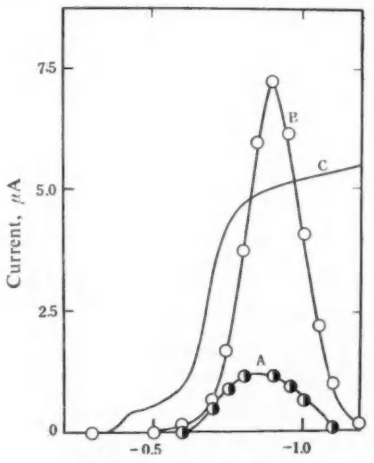

Fig. 3. Current-voltage curves of $1.18_6\times10^{-3}$ M lead-nitrilotriacetate in an ammonia-ammonium nitrate buffer of pH 8.2 ($\mu=0.7$) containig 50 mM tartarate.

A A. C. polarogram at DME
B A. C. polarogram at RADME
C D. C. polarogram at DME

cadmium (-amine complex) ion. Viewed from the experimental results obtained at different heights of mercury column (curves B and C in Fig. 2), the author's explanation that this small prewave must be kinetic in nature, may be justified. Lead-nitrilotriacetate complex in an ammonia-ammonium nitrate buffer solution of pH 8.2 containing 0.005% gelatin (50 mM sodium tartarate was added to avoid the undesirable hydrolysis of lead) also gave the kinetic current (curve C in Fig. 3). The ionic strength was also adjusted to 0.7 with potassium nitrate.

3) M. Kodama, A. Shimizu and H. Terakado, ibid. **81**, 1545 (1960).
4) G. Numaziri, M. Kodama and A. Shimizu, ibid., **81**, 454 (1960).
5) F. P. Treadwell and W. T. Hall, "Analytical Chemistry", Vol. 2 (1953), p. 58.
6) N. Tanaka, I. T. Oiwa and M. Kodama, *Anal. Chem.*, **28**, 1555 (1956).
7) N. Tanaka, M. Kodama, M. Sasaki and M. Sugino, *Japan Analyst* (*Bunseki Kagaku*), **6**, 86 (1957).

Alternating Current (A. C.) Polalography.— Alternating current polarograms of cadmium, lead and copper were recorded, using DME or RADME, under the same conditions as those used for direct current polarographic measurements. It was found for lead-nitrilotriacetate complex that the reduction wave of lead ion due to the dissociation of complex entirely disappeared at DME or RADME as shown in Fig. 3 (curves A and B). This phenomenon was also obtained in the reduction of cadmium-nitrilotriacetate complex, when RADME was employed as an indicator electrode (Fig. 4).

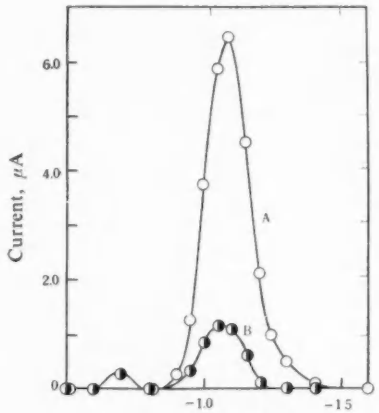

Fig. 4. Alternating current polarograms of $1.09_5\times10^{-3}$ M cadmium-nitrilotriacetate in an ammonia-ammonium nitrate buffer of pH 9.2 (μ=0.7).
A at RADME B at DME

These results may indicate that the rate of the dissociation reaction of metal-nitrilotriacetate complex on the electrode surface is not sufficiently rapid to supply the requisite amount of metal ion to give the kinetic current during the short interval (0.02 sec.) of each alternating current voltage sweep at DME or RADME.

The value of the peak current of metal-nitrilotriacetate conmplex observed at RADME is higher than that observed at DME. In the potential range at which experiments were conducted, the surface-active substance, gelatine, is adsorped on the electrode surface to cover it. The extent of coverage of the rapidly dropping mercury electrode surface differs from that of the ordinary dropping mercury electrode surface, because the drop time of RADME is quite different from that of DME. This difference is related to the extent of inhibition of the electro-oxidation-reduction reaction of complex ion, which may be the reason why the peak current at RADME is higher than that at DME. The adsorption of gelatine on the mercury drop occurs over the entire range of potentials (about +0.4 to −2.0 V. vs. S.C.E.), and the tensammetric peaks due to the adsorption and the desorption of gelatine can not be observed under ordinary experimental conditions. In the case of camphor, however, two tensammetric peaks can be observed at about −0.25 and −1.15 V. vs. S.C.E. The peak in the positive potential region results from the adsorption of camphor, and the peak

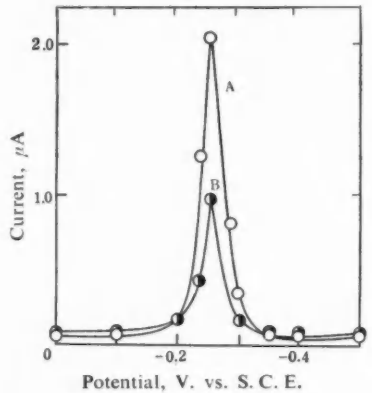

Fig. 5. Alternating current polarograms of 0.5 M KNO_3 solution containing 1.5×10^{-3} M camphor.
A at RADME B at DME

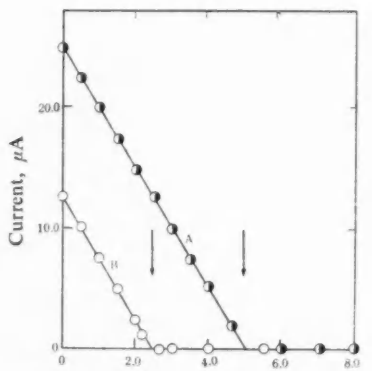

Fig. 6. Titration curves of cadmium with NTA in an ammonia-ammonium nitrate buffer of pH 9.2 (μ=0.7).
A 50 ml. of $1.09_5\times10^{-3}$ M cadmium
B 50 ml. of $5.47_5\times10^{-4}$ M cadmium
Stoichiometric equivalence points are indicated by arrows.

in the negative potential region from the desorption of camphor. The peak currents of positive tensammetric wave of camphor obtained at DME and RADME in the nitrate media are shown in Fig. 5. The value of the peak current observed at RADME differs from that observed at DME. This fact also implies that the extent of coverage of the rapidly dropping mercury electrode surface by the surface-active substance is quite different from that of the dropping mercury electrode surface.

A. C. Poralographic Titrations. — From the above results and the well-known facts[8] that in the reversible case, the A. C. polarographic method is advantageous in the resolution of two component systems and in the determination of low concentration; it seems desirable to employ the A. C. polarographic method to determine the concentration of cadmium or lead with NTA at RADME in an ammnia-ammonium nitrate buffer solution.

Polarographic titration employing the A. C. polarographic method (A. C. polarographic titration) was carried out, under the same conditions as that used for the polarographic measurements, in the concentration range from 1×10^{-3} M to 1×10^{-5} M. Titration curves were obtained by plotting the peak currents due to the electro-reduction of metal ions against the volume of NTA solution added. Typical examples of the titration curves are given in Figs. 6 and 7. These curves were corrected for dilution effect by the addition of titrant. The potential at which the peak currents are given were held constant during the titration. The results of the titration obtained are listed in Tables II and III. Experimental equivalence points agreed with calculated equivalence points satisfactorily. The results of the titration obtained for copper are also listed in Table IV.

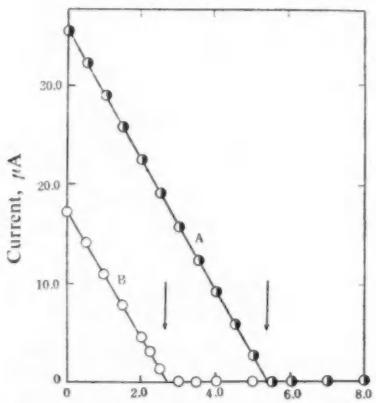

Fig. 7. Titration curves of lead with NTA in an ammonia-ammonium nitrate buffer of pH 9.2 ($\mu=0.7$).

A 50 ml. of $1.18_5\times10^{-3}$ M lead.
B 50 ml. of $5.93_0\times10^{-4}$ M lead.
Stoichiometric equivalence points are indicated by arrows.

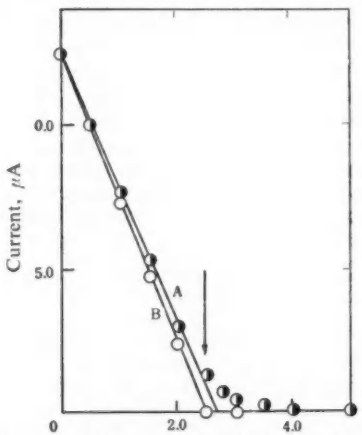

Fig. 8. Titration curves of cadmium with NTA in an ammonia-ammonium nitrate buffer of pH 9.2 ($\mu=0.77$); 50 ml. of $5.47_5\times10^{-4}$ M cadmium.

A 0.4 M ammonia B 0.1 M ammonia

TABLE II. A. C. POLAROGRAPHIC TITRATION OF CADMIUM WITH NTA USING RADME
(INITIAL VOLUME 50 ml.)

Concentration of cadmium, M	Concentration of NTA used for titration, M	NTA required, ml.		Error, %
		Stoichiometric	Experimental	
$1.09_5\times10^{-3}$	$1.09_5\times10^{-2}$	4.98_7	5.00	+0.1
$5.47_5\times10^{-4}$	$1.09_5\times10^{-2}$	2.49_4	2.48	−0.6
$2.73_5\times10^{-4}$	$1.09_5\times10^{-2}$	1.24_7	1.24	−0.6
$1.09_5\times10^{-4}$	$1.09_5\times10^{-3}$	4.98_7	4.96	−0.6
$5.47_5\times10^{-5}$	$1.09_5\times10^{-3}$	2.49_4	2.50	+0.3
$3.28_5\times10^{-5}$	$1.09_5\times10^{-3}$	1.24_7	1.45	−3.0

8) P. Delahay, "New Instrumental Method in Electrochemistry" (1954), p. 176.

TABLE III. A. C. POLAROGRAPHIC TITRATION OF LEAD WITH NTA USING RADME
(INITIAL VOLUME 50 ml.)

Concentration of lead, M	Concentration of NTA used for titration, M	NTA required, ml.		Error, %
		Stoichiometric	Experimental	
$1.18_6\times10^{-3}$	$1.09_8\times10^{-2}$	5.40_0	5.40	0
$5.93_0\times10^{-4}$	$1.09_8\times10^{-2}$	2.70_0	2.69	−0.6
$2.37_4\times10^{-4}$	$1.09_8\times10^{-2}$	1.08_0	1.07	−1.0
$1.18_6\times10^{-3}$	$1.09_8\times10^{-3}$	5.40_0	5.42	+0.4
$5.93_0\times10^{-5}$	$1.09_8\times10^{-3}$	2.70_0	2.72	+0.8
$2.37_4\times10^{-5}$	$1.09_8\times10^{-3}$	1.08_0	1.05	−3.0

TABLE IV. A. C. POLAROGRAPHIC TITRATION OF COPPER WITH NTA USING RADME
(INITIAL VOLUME 50 ml.)

Concentration of copper, M	Concentration of NTA used for titration, M	NTA required, ml.		Error, %
		Stoichiometric	Experimental	
$1.13_0\times10^{-3}$	$1.09_8\times10^{-2}$	5.15_0	5.15	0
$5.65_0\times10^{-4}$	$1.09_8\times10^{-2}$	2.57_5	2.58	+0.2
$2.26_5\times10^{-4}$	$1.09_8\times10^{-2}$	1.03_0	1.02	−1.0
$1.13_0\times10^{-3}$	$1.09_8\times10^{-3}$	5.15_0	5.16	+0.2
$5.65_0\times10^{-5}$	$1.09_8\times10^{-3}$	2.57_5	2.57	−0.2

When a great excess of ammonia is presented in the solution, experimental equivalence points were somewhat greater than the stoichiometrical ones. This fact reveals that the presence of excess ammonia favors the dissociation reaction of the metal-nitrilotriacetate complex (Fig. 8).

Summary

RADME was applied to the chelatometric determination of copper, cadmium and lead with NTA by employing the A. C. polarographic method. At RADME practically no kinetic effects due to the dissociation of metal-nitrilotriacetate complex were observed and the concentration of metal ions could be determined accurately in the concentration range from 1×10^{-3} M to 1×10^{-5} M.

The author thanks Dr. T. Takeshima for reading the manuscript and for advice.

Department of Chemistry
Faculty of Arts and Sciences
Ibaraki University
Watari-machi, Mito

Synthesis of α-Maltosides. I

By Shoji MATSUBARA

(Received October 10, 1960)

Although a large number of glycoside derivatives[1,2] have been synthesized, many attempts to prepare various α-maltoside derivatives have not been promising[3]. At present, non-crystalline phenyl-α-maltoside and methyl-α-maltoside synthesized by Fischer and Bergmann[4], and also by Helferich and Peterson[5] have only been reported. After many trials, the author has succeeded in the synthesis of various α-maltosides.

1) G. Wagner, *Arch. Pharm.*, **290**, 625 (1957).
2) G. Wagner, ibid., **291**, 278 (1958).
3) G. Zemplén, *Ber.*, **60**, 1555 (1935).
4) E. Fischer, M. Bergmann and A. Rabe, ibid., **53**, 2362 (1920).
5) B. Helferich and S. R. Peterson, ibid., **68**, 790 (1935).

The purpose of this study is to obtain some fundamental information concerning the substrate specificity[6-8]; namely, it is to investigate the influence of substituents in the phenyl group on the enzymatic hydrolysis of phenyl-α-maltoside by taka-amylase A[9], and also the mode of interaction of the enzyme activity with structural changes in their substrates. From this point of view, the detailed descriptions of the synthesis are briefly described in this paper.

Experimental

Octaacetylmaltose[3]. — To a solution of 20 g. of anhydrous maltose dissolved in 100 cc. of acetic anhydride, 20 g. of fused sodium acetate was added and the mixture was gently heated. The color of the solution changed from yellow through brown to dark brown. When the violent initial reaction ceased, the solution was heated under stirring for two hours at 100°C in a water bath, poured onto crushed ice, and then diluted with water. The separated yellowish brown oil was allowed to stand overnight in a refrigerator. The crystals which separated out were collected by filtration, dissolved in chloroform, and washed well with water, and dried over anhydrous calcium chloride. The solvent was then evaporated under reduced pressure. The solid was dissolved in hot methanol, filtrated, and the crystalline residue which was obtained from the mother liquor was recrystallized from methanol, giving 14 g. of octaacetylmaltose in the form of colorless crystals, m. p. 158~159°C, $[\alpha]_D^{19} = +124°$ (*c* 1.0, in chloroform).

Heptaacetylphenyl-α-maltoside[4,5]. — The mixture of 68 g. (1 mol.) of octaacetylmaltose, 57 g. (6 mol.) of phenol and 10 g. of fused zinc chloride was heated under violent stirring for two and a half hours at 100°C in a water bath. After cooling, the dark brown oily substance was diluted with water, to remove the zinc chloride. To the solution mixture, benzene was added and the benzene extract was well washed successively with water, with 1 N aqueous sodium hydroxide, with water until it became colorless, and finally dried over anhydrous calcium chloride. The solvent was then evaporated under reduced pressure, leaving a yellowish brown oil. The oily residue was crystallized from 100 cc. of ethanol to give colorless crystals. The crude crystals were combined and recrystallized from ethanol-dioxane mixture (contained 10% dioxane), m. p. 184~184.5°C, $[\alpha]_D^{20} = +170.2°$ (*c* 1.0, in chloroform).

Found: C, 53.92; H, 5.63. Calcd. for $C_{32}H_{40}O_{15}$: C, 53.91; H, 5.66%.

Phenyl-α-maltoside. — A solution of 10 g. of heptaacetylphenyl-α-maltoside dissolved in 100 cc. of a mixture of absolute methanol and chloroform (1 : 1, by volume) was saturated with ammonia gas under cooling. After being kept more than four hours at room temperature, the methanol and ammonia were removed under reduced pressure. The syrupy residue was dissolved in a small quantity of absolute ethanol, and the precipitate was obtained by adding ether. After removing the supernatant solvents, the residue was then successively treated in the same manner as described above to afford pure crystals. The precipitate obtained was combined and washed with ether. This crude crystalline phenyl-α-maltoside was crystallized from absolute ethanol. The yield was 4.75 g., m. p. 202~204°C, $[\alpha]_D^{14.5} = +211°$ (*c* 1.3, in water).

Found: C, 51.57; H, 6.25. Calcd. for $C_{18}H_{26}O_{11}$: C, 51.65; H, 6.27%.

The ultraviolet absorption of the product showed maxima at 266 mμ in water.

Heptaacetyl-*p*-nitrophenyl-α-maltoside. — To a mixture of 20 cc. of glacial acetic acid and 10 cc. of acetic anhydride, 5 g. of heptaacetylphenyl-α-maltoside was added. A mixture of 25 g. of concentrated sulfuric acid (95%) and 25 g. of glacial acetic acid was added under cooling and stirring. Then to this solution, a mixture of 5 g. of nitric acid (sp. gr. 1.38) and 10 cc. of glacial acetic acid was added dropwise, while stirring vigorously. The mixture was kept for four hours at room temperature, and poured into a large amount of ice and water. Within a few minutes a powdery white precipitate was separated, collected, washed completely with water, and dried over anhydrous calcium chloride. The yield of the crude substance was 4.83 g. The crude crystals were recrystallized from absolute ethanol, and the yield of heptaacetyl-*p*-nitrophenyl-α-maltoside was 4.75 g., m. p. 176~178°C, $[\alpha]_D^{14.5} = +223°$ (*c* 1.2, in chloroform).

Found: C, 50.71; H, 5.21; N, 1.83. Calcd. for $C_{32}H_{39}O_{20}N$: C, 50.74; H, 5.19; N, 1.85%.

***p*-Nitrophenyl-α-maltoside.** — The heptaacetyl-*p*-nitrophenyl-α-maltoside was deacetylated by dissolving in absolute methanol (200~300 cc. for 25 g.) and adding a freshly prepared solution of sodium methoxide (from sodium, 10~20 mg., and methanol, 10 cc.). The mixture was kept at room temperature overnight. The methanol was then removed under reduced pressure, and the oily substance was dissolved in 10 cc. of ethanol. The solid was obtained by adding ether, and was then successively treated in the same manner as described above to give pure maltoside crystals which were crystallized to constant melting point using, when possible, a mixture of ethanol-dioxane containing 10% of dioxane. The crude crystals were combined and recrystallized from absolute ethanol/petroleum ether, m. p. 145~146°C, $[\alpha]_D^{14.5} = +265°$ (*c* 1.0, in water).

Found: C, 46.72; H, 5.40; N, 3.04. Calcd. for $C_{18}H_{25}O_{13}N$: C, 46.63; H, 5.44; N, 3.02%.

The ultraviolet absorption of the product showed maxima at 310 mμ in water.

Other Substituted Heptaacetylphenyl-α-maltosides. — The corresponding phenols (0.3~0.4 mol.) and octaacetylmaltose (0.1 mol.) were heated with fused zinc chloride (0.5~2.0 g.) under violent stirring at 110~115°C for 1.5 to 2 hr. The cooled oily product was diluted with water and extracted with

6) R. L. Nath and H. N. Rydon, *Biochem. J.*, **57**, 1 (1954).
7) S. Matsubara, *J. Biochem.*, **49**, 226 (1961).
8) S. Matsubara, ibid., **49**, 232 (1961).
9) S. Matsubara, T. Ikenaka and S. Akabori, ibid., **46**, 425 (1959).

benzene to remove zinc chloride. The benzene solution was washed with water, and then repeatedly with 5% aqueous sodium hydroxide until the washings were colorless. The solution was again washed with water and dried over anhydrous calcium chloride. The solvent was then evaporated under reduced pressure, leaving a dark yellowish brown oil. The oily residue was crystallized from suitable solvents to give colorless crystals. The crude crystals were recrystallized from one more suitable solvent.

Other Substituted Phenyl-α-maltosides. — The other substituted phenyl-α-maltoside was prepared by the same method as with phenyl-α-maltoside. The obtained crude product was recrystallized from suitable solvents.

***o*-Cresyl-α-maltoside.** — Recrystallized from ethanol/ether, m. p. 182~183°C, $[\alpha]_D^{14.5}=+218°$ (*c* 1.0, in water).

Found: C, 52.50; H, 6.45. Calcd. for $C_{19}H_{28}O_{11}$: C, 52.75; H, 6.53%.

The heptaacetyl derivative recrystallized from ethanol, m. p. 175~176°C $[\alpha]_D^{18}=+182°$ (*c* 1.5, in chloroform).

Found: C, 54.60; H, 5.89. Calcd. for $C_{33}H_{42}O_{18}$: C, 54.56; H, 5.83%.

***m*-Cresyl-α-maltoside.**—This was very hydroscopic and resisted all attempts at recrystallization; the product, dried at 100°C in vacuo over P_2O_5, had m. p. 93~98°C, $[\alpha]_D^{17}=+235°$ (*c* 0.5, in water).

Found: C, 51.95; H, 6.42. Calcd. for $C_{19}H_{28}O_{11}$: C, 52.75; H, 6.53%.

The heptaacetyl derivative recrystallized from ethanol, m. p. 135~140°C, $[\alpha]_D^{18}=+185°$ (*c* 1.5, in chloroform).

Found: C, 54.53; H, 5.84. Calcd. for $C_{33}H_{42}O_{18}$: C, 54.56; H, 5.83%.

***p*-Cresyl-α-maltoside.** — Recrystallized from ethanol/ether, m. p. 192~194°C, $[\alpha]_D^{18}=+204°$ (*c* 0.5, in water).

Found: C, 53.02; H, 6.49. Calcd. for $C_{19}H_{28}O_{11}$: C, 52.75; H, 6.53%.

The heptaacetyl derivative recrystallized from ethanol, m. p. 180~181°C, $[\alpha]_D^{18}=+201°$ (*c* 1.0, in chloroform).

Found: C, 54.55; H, 5.81. Calcd. for $C_{33}H_{42}O_{18}$: C, 54.56; H, 5.83%.

***o*-Isopropylphenyl-α-maltoside.** — Recrystallized from ethanol/petroleum ether, m. p. 163~165°C, $[\alpha]_D^{18}=+222°$ (*c* 1.0, in water).

Found: C, 54.57; H, 7.10. Calcd. for $C_{21}H_{32}O_{11}$: C, 54.75; H, 7.01%.

The heptaacetyl derivative recrystallized from ethanol/petroleum ether, m. p. 110~111°C, $[\alpha]_D^{18}=+205°$ (*c* 1.0, in chloroform).

Found: C, 55.67; H, 6.08. Calcd. for $C_{35}H_{46}O_{18}$: C, 55.71; H, 6.15%.

***p*-Isopropylphenyl-α-maltoside.** — Recrystallized from ethanol/petroleum ether, m. p. 175~176°C, $[\alpha]_D^{14.5}=+216°$ (*c* 1.0, in water).

Found: C, 54.71; H, 6.98. Calcd. for $C_{21}H_{32}O_{11}$: C, 54.75; H, 7.01%.

The heptaacetyl derivative recrystallized from ethanol/petroleum ether, m. p. 145~147°C, $[\alpha]_D^{14.5}=+192°$ (*c* 1.0, in chloroform).

Found: C, 55.61; H, 6.21. Calcd. for $C_{35}H_{46}O_{18}$: C, 55.71; H, 6.15%.

***o*-*tert*-Butylphenyl-α-maltoside.** — This was very hydroscopic and resisted all attempts at recrystallization; the product, dried at 100°C in vacuo over P_2O_5, had m. p. 60~65°C, $[\alpha]_D^{18}=+232°$ (*c* 0.5, in water).

Found: C, 54.89; H, 7.18. Calcd. for $C_{22}H_{36}O_{11}$: C, 55.66; H, 7.23%.

The heptaacetyl derivative recrystallized from ethanol/petroleum ether, m. p. 212~214°C, $[\alpha]_D^{18}=+202°$ (*c* 1.15, in chloroform).

Found: C, 56.26; H, 6.28. Calcd. for $C_{36}H_{48}O_{18}$: C, 56.22; H, 6.30%.

***p*-*tert*-Butylphenyl-α-maltoside.** — Recrystallized from ethanol, m. p. 170~172°C, $[\alpha]_D^{18}=+228°$ (*c* 0.62, in water).

Found: C, 55.61; H, 7.20. Calcd. for $C_{22}H_{34}O_{11}$: C, 55.66; H, 7.23%.

The heptaacetyl derivative recrystallized from ethanol/petroleum ether, m. p. 78~80°C, $[\alpha]_D^{18}=+211°$ (*c* 1.32, in chloroform).

Found: C, 56.21; H, 6.26. Calcd. for $C_{36}H_{48}O_{18}$: C, 56.22; H, 6.30%.

***p*-Isoamylphenyl-α-maltoside.** — Recrystallized from ethanol, m. p. 160~163°C, $[\alpha]_D^{18}=+242°$ (*c* 0.65, in water).

Found: C, 56.48; H, 7.47. Calcd. for $C_{23}H_{36}O_{11}$: C, 56.52; H, 7.43%.

The heptaacetyl derivative recrystallized from ethanol/petroleum ether, m. p. 185~187°C, $[\alpha]_D^{18}=+213°$ (*c* 1.2, in chloroform).

Found: C, 56.80; H, 6.44. Calcd. for $C_{37}H_{50}O_{18}$: C, 56.80: H, 6.44%.

***o*-Methoxyphenyl-α-maltoside.** — Recrystallized from ethanol, m. p. 165~166°C, $[\alpha]_D^{14.5}=+184°$ (*c* 0.1, in water).

Found: C, 50.78; H, 6.27. Calcd. for $C_{19}H_{28}O_{12}$: C, 50.87; H, 6.30%.

The heptaacetyl derivative recrystallized from ethanol, m. p. 140~141°C, $[\alpha]_D^{14.5}=+162°$ (*c* 0.1, in chloroform).

Found: C, 53.36; H, 5.65. Calcd. for $C_{33}H_{42}O_{19}$: C, 53.38; H, 5.70%.

***m*-Methoxyphenyl-α-maltoside.** — Recrystallized from ethanol, m. p. 172~175°C, $[\alpha]_D^{14.5}=+193°$ (*c* 0.95, in water).

Found: C, 50.79; H, 6.26. Calcd. for $C_{19}H_{28}O_{12}$: C, 50.87; H, 6.30%.

The heptaacetyl derivative recrystallized from ethanol, m. p. 163~165°C, $[\alpha]_D^{14.5}=+165°$ (*c* 0.95, in chloroform).

Found: C, 52.90; H, 5.59. Calcd. for $C_{33}H_{42}O_{19}$: C, 53.38; H, 5.70%.

***p*-Methoxyphenyl-α-maltoside.** — Recrystallized from ethanol, m. p. 187~189°C, $[\alpha]_D^{14.5}=+201°$ (*c* 0.85, in water).

Found: C, 50.80; H, 6.28. Calcd. for $C_{19}H_{28}O_{12}$: C, 50.87; H, 6.30%.

The heptaacetyl derivative recrystallized from ethanol, m. p. 206~208°C, $[\alpha]_D^{14.5}=+195°$ (*c* 3.1, in chloroform).

Found: C, 53.31; H, 5.78. Calcd. for $C_{33}H_{42}O_{19}$: C, 53.38; H, 5.70%.

***o*-Chlorophenyl-α-maltoside.**—Recrystallized from ethanol, m. p. 193~196°C, $[\alpha]_D^{18}=+165°$ (*c* 0.5, in water).

Found: C, 47.68; H, 5.60; Cl, 7.84. Calcd. for $C_{18}H_{25}O_{11}Cl$: C, 47.72; H, 5.57; Cl, 7.83%.

The heptaacetyl derivative recrystallized from ethanol/petroleum ether, m. p. 195~197°C, $[\alpha]_D^{18}$ = +154° (*c* 2.3, in chloroform).

Found: C, 51.38; H, 5.23; Cl, 4.68. Calcd. for $C_{32}H_{39}O_{19}Cl$: C, 51.44; H, 5.27; Cl, 4.75%.

***p*-Chlorophenyl-α-maltoside.**—Recrystallized from ethanol, m. p. 205~206°C, $[\alpha]_D^{19}$ = +213° (*c* 1.13, in water).

Found: C, 47.70; H, 5.59; Cl, 7.81. Calcd. for $C_{18}H_{25}O_{11}Cl$: C, 47.72; H, 5.57; Cl, 7.83%.

The heptaacetyl derivative recrystallized from ethanol/petroleum ether, m. p. 197~199°C, $[\alpha]_D^{19}$ = +177° (*c* 1.5, in chloroform).

Found: C, 51.43; H, 5.25; Cl, 4.75. Calcd. for $C_{32}H_{39}O_{19}Cl$: C, 51.44; H, 5.27; Cl, 4.75%.

***o*-Nitrophenyl-α-maltoside.** — Recrystallized from ethanol/ether, m. p. 153~155°C, $[\alpha]_D^{14.5}$ = +245° (*c* 1.2, in water).

Found: C, 46.75; H, 5.48; N, 2.95. Calcd. for $C_{18}H_{25}O_{13}N$: C, 46.63; H, 5.44; N, 3.02%.

The heptaacetyl derivative recrystallized from ethanol, m. p. 185~187°C, $[\alpha]_D^{14.5}$ = +222° (*c* 1.5, in chloroform).

Found: C, 50.68; H, 5.15; N, 1.84. Calcd. for $C_{32}H_{39}O_{20}N$: C, 50.74; H, 5.19; N, 1.85%.

***m*-Nitrophenyl-α-maltoside.**—Recrystallized from ethanol/petroleum ether, m. p. 132~136°C, $[\alpha]_D^{14.5}$ = +261° (*c* 2.1, in water).

Found: C, 46.78; H, 5.39; N, 2.95. Calcd. for $C_{18}H_{25}O_{13}N$: C, 46.63; H, 5.44; N, 3.02%.

The heptaacetyl derivative recrystallized from ethanol, m. p. 170~171°C, $[\alpha]_D^{14.5}$ = +234° (*c* 1.8, in chloroform).

Found: C, 50.65; H, 5.11; N, 1.87. Calcd. for $C_{32}H_{39}O_{20}N$: C, 50.74; H, 5.19; N, 1.85%.

***α*-Naphthyl-, cyclohexyl- and *o*-, *m*-, *p*-Nitrophenyl-α-maltosides.** — The mixture of α-naphthol, cyclohexanol, *o*-, *m*-, or *p*-nitrophenol (0.3~0.4 mol.) and octaacetyl-β-maltose (0.1 mol.) were heated with fused zinc chloride (0.5~2.0 g.) and titanic chloride[10] (10 g.) under violent stirring at 110~115°C for 1.5 to 2 hr. by the same method as that described above.

α-Naphthyl-α-maltoside. — Recrystallized from ethanol/ether, m. p. 156~158°C, $[\alpha]_D^{16}$ = +192° (*c* 1.5, in water).

Found: C, 56.41; H, 6.07. Calcd. for $C_{22}H_{25}O_{11}$: C, 56.39; H, 6.03%.

The heptaacetyl derivative recrystallized from ethanol/ether, m. p. 192~194°C, $[\alpha]_D^{16}$ = +185° (*c* 1.5, in chloroform).

Found: C, 56.71; H, 5.53. Calcd. for $C_{36}H_{42}O_{18}$: C, 56.67; H, 5.56%.

Cyclohexyl-α-maltoside. — Recrystallized from ethanol/ether, m. p. 112~115°C, $[\alpha]_D^{16}$ = +211° (*c* 1.5, in water).

Found: C, 50.85; H, 7.63. Calcd. for $C_{18}H_{32}O_{11}$: C, 50.91; H, 7.60%.

The heptaacetyl derivative recrystallized from ethanol, m. p. 152~155°C, $[\alpha]_D^{16}$ = +202° (*c* 1.5, in chloroform).

Found: C, 53.42; H, 6.50. Calcd. for $C_{32}H_{46}O_{18}$: C, 53.46; H, 6.46%.

Alkyl-α-maltosides.—Alkyl-α-maltosides could be prepared by warming maltose with an alcoholic solution of hydrochloric acid. Dry hydrogen chloride was passed into 200 g. of absolute alcohol, with ice cooling and exclusion of moisture, until the increase in weight amounted to 10 g. This solution 20 cc. was then diluted with 980 g. of alcohol, a 0.1% solution of hydrogen chloride being thus obtained. To this solution 50 g. of finely powdered anhydrous maltose was added, and the mixture was warmed at 50°C for forty-two hours, a clear solution being obtained after the first fifteen minutes' warming. It was well to attach a soda-lime tube to the upper end of the condenser, in order to exclude moisture. The clear pale yellow solution was cooled to 0°C, and crystallization was induced by scratching. After standing for two days at 0°C, the first crop was filtered by suction and was washed twice with 100 cc. portions of cold alcohol. The mother liquor and washings were returned to the flask and again warmed for forty-two hours under reflux at 50°C. The liquid was concentrated to 800 cc. and again chilled to 0°C, incubated and allowed to stand at 0°C for two days. The second crop of maltoside so obtained was filtered by suction and washed three times with each 100 cc. portion of cold alcohol. The mother liquor and washings were combined and concentrated to about 300 cc., chilled to 0°C, and again incubated and allowed to stand for two days. The resulting mush of crystals was dissolved in twice its weight of absolute ethanol, and, after standing for two days at 0°C, the third crop of maltoside was filtered. This was recrystallized from 2.5 parts of ethanol. The product was contaminated by slight traces of maltose and possessed a very faint reducing power towards Fehling's solution. For complete purification it was recrystallized (practically with neither loss nor change in melting point) from five parts of absolute ethanol with the use, if necessary, of decolorizing carbon.

Methyl-α-maltoside.—Recrystallized from ethanol, m. p. 201~202°C, $[\alpha]_D^{16}$ = +183° (*c* 1.0, in water).

Found: C, 43.77; H, 6.75. Calcd. for $C_{13}H_{24}O_{11}$: C, 43.80; H, 6.79%.

Isopropyl-α-maltoside. — Recrystallized from ethanol, m. p. 177~179°C, $[\alpha]_D^{16}$ = +166° (*c* 1.0, in water).

Found: C, 46.81; H, 7.32. Calcd. for $C_{15}H_{28}O_{11}$: C, 46.85; H, 7.35%.

***tert*-Butyl-α-maltoside.** — Recrystallized from ethanol, m. p. 188~190°C, $[\alpha]_D^{16}$ = +153° (*c* 1.0, in water).

Found: C, 48.18; H, 7.62. Calcd. for $C_{16}H_{30}O_{11}$: C, 48.21; H, 7.59%.

Isoamyl-α-maltoside. — Recrystallized from ethanol, m. p. 152~155°C, $[\alpha]_D^{16}$ = +143° (*c* 1.5, in water).

Found: C, 49.52; H, 7.80. Calcd. for $C_{17}H_{32}O_{11}$: C, 49.48; H, 7.82%.

Summary

Substituted phenyl-, α-naphthyl-, and cyclohexyl-α-maltosides were prepared from octaacetyl-β-maltose and the corresponding phenols. *p*-Nitrophenyl-α-maltoside was also prepared by

10) A. P. Jansen and P. G. A. B. Wydeveld, *Nature*, **182**, 525 (1958).

another method from the nitration of hepta-acetylphenyl-α-maltoside. Alkyl-α-maltosides were prepared from maltose and corresponding alcohol.

The authors wishes to express his gratitude to Professor Shiro Akabori (Institute for Protein Research, Osaka University) for his helpful advice throughout this work.

Department of Chemistry
Faculty of Science
Osaka University
Nakanoshima, Osaka

Absorption Spectra of Nitrobenzene Derivatives. II. Effect of Solvent on Intramolecular Charge Transfer Spectra of Nitrobenzene Derivatives

By Kimio SEMBA*

(Received September 7, 1960)

In a previous paper[1] intramolecular charge transfer spectra of nitrobenzene derivatives were studied from the viewpoint of Nagakura and Tanaka's theory[2]. These absorption spectra are strongly influenced by solvents and shift toward longer wavelengths for solvents of higher dielectric constant.

Several papers treating of the effect of solvent on the electronic spectra of organic compounds have been published[3]. Recently, Bayliss and McRae[4] discussed the effects in terms of the dipole-, polarization-, and hydrogen bonding forces between solute and solvent molecules. It is not always easy to interpret the solvent effects correctly because these often arise from the resultant of several individual effects reinforcing as well as cancelling each other. It seems certain that hydrogen bonding plays a very important role in the frequency shift, while effects from other origins are no less important, since frequency shifts are observed even in systems containing no hydrogen bonds.

In this paper the role of the electrostatic interaction between solute and solvent molecules in the intramolecular charge transfer spectra of *o*-, *m*- and *p*-nitrophenol, -nitroanisole, -nitroaniline and -nitron-*N*-dimethylaniline was examined on the basis of the general expression proposed by McRae[5] for the solvent effect on absorption spectra. The contribution of hydrogen bonding between solute and solvent molecules was also taken into consideration for some cases.

Experimental

Absorption spectra in the wavelength region 250~400 mμ were obtained by a Hitachi automatic recording spectrophotometer, type EPS-2. Fused quartz cells of 1 cm. path length were used.

Samples of nitrobenzene derivatives were the same ones used in a previous work[1]. Solvents, *n*-hexane, dioxane, cyclohexane, carbon tetrachloride, toluene, benzene, ethyl ether, nitromethane, acetonitrile, methanol, and ethanol, were purified by the method recommended by Weissberger and Proskauer[6], special care having been taken to remove contaminating water.

Result and Discussion

Theoretical Expression for the Solvent Effect. —In current discussions of the solvent effects on electronic absorption spectra the frequency shifts are mainly attributed to dipole, polarization and hydrogen bonding effects. The general formula* derived from the perturbation theory by McRae[5] for solvent-induced spectral shifts can be simplified for the discussion of present results in the following form[7]

* Present address: Research Laboratory, Kurosaki Firebrick Mfg. Co., Ltd., Fujita, Yawata.

1) K. Semba, This Bulletin, **33**, 1640 (1960).

2) S. Nagakura and J. Tanaka, *J. Chem. Phys.*, **22**, 236 (1954); S. Nagakura, ibid., **23**, 1441 (1955).

3) For example: N. D. Coggeshell and E. M. Lang, *J. Am. Chem. Soc.*, **70**, 3282 (1948); M. Kasha, *Discussions Faraday Soc.*, **9**, 14 (1950); H. McConnell, *J. Chem. Phys.*, **20**, 700 (1952); S. Nagakura and H. Baba, *J. Am. Chem. Soc.*, **74**, 5693 (1952).

4) N. Bayliss and E. G. McRae, *J. Phys. Chem.*, **58**, 1002, 1006 (1954).

5) E. G. McRae, ibid., **61**, 562 (1957).

6) A. Weissberger and E. S. Proskauer, "Organic Solvent", Interscience Publishers, Inc., New York (1955).

* Y. Ooshika has also given a similar formula: *J. Phys, Soc. Japan*, **9**, 542 (1954).

7) M. Ito, K. Inuzuka and S. Imanishi, *J. Am. Chem. Soc.*, **82**, 1317 (1960).

$$\Delta\nu = \text{dispersion term} + B\left[\frac{n_D^2-1}{2n_D^2+1}\right] + C\left[\frac{D-1}{D+2}-\frac{n_D^2-1}{n_D^2+2}\right] + E\left[\frac{D-1}{D+2}-\frac{n_D^2-1}{n_D^2+2}\right]^2 \quad (1)$$

where B, C and E are constants characteristic of the solute molecule,

$$B=\frac{1}{hc}\frac{(\mathbf{M}_{oo}^u)-(\mathbf{M}_{ii}^u)^2}{a^3} \quad (2)$$

$$C=\frac{2}{hc}\frac{(\mathbf{M}_{oo}^u)\,(\mathbf{M}_{oo}^u-\mathbf{M}_{ii}^u)}{a^3} \quad (3)$$

$$E=\frac{6}{hc}\frac{(\mathbf{M}_{oo}^u)\,(\alpha_o^u-\alpha_i^u)}{a^6} \quad (4)$$

$\mathbf{M}_{oo}^u$ and $\mathbf{M}_{ii}^u$ represent the vector dipole moments of the solute molecule in its electronic ground and excited states, respectively, and a is Onsagar's reaction radius of the solute molecule. For the meaning of the various other quantities appearing in these equations McRae's original paper[5] is referred to.

Effect of Electrostatic Interactions.—Absorption maxima (ν_{max}) of *o*-, *m*- and *p*-nitrobenzene derivatives in various solvents are given in Table 1, in which refractive indices and dielectric constants are also given. The *p*-derivative shows only one absorption band which is in the near ultraviolet region due to the intramolecular charge transfer transition. On the other hand, the *o*- and *m*-derivatives show two intramolecular charge transfer bands due to the transitions $H_{x1}\rightarrow V_8$ and $H_{x2}\rightarrow V_8$, as observed in a previous paper[1]. The bands of *o*- and *m*-derivatives at shorter wavelengths in both toluene and benzene solutions can not be observed, because they are covered by solvent absorption bands, hence only the longer-wavelength bands due to the $H_{x1}\rightarrow V_8$ transition are considered.

We shall first consider the effect of non-polar solvents, *n*-hexane, dioxane, carbon tetrachloride, toluene and benzene, in the order of increasing refractive index. It is seen from the table that ν_{max} decreases with the increase in the refractive index of the solvent, with the exception of dioxane. Plots of ν_{max} against $(n_D^2-1)/(2n_D^2+1)$ for these derivatives are shown in Figs. 1—3. For each of these molecules the points for various solvents are approximately on a straight line, with the exception of the point for dioxane.

For non-polar solvents the third and the fourth terms in Eq. 1 may be neglected since $n_D^2 \approx D$, and only the first and the second terms have to be considered. Then, if the first term is much smaller than the second,

Table I. Absorption maxima of *o*-, *m*- and *p*-nitrobenzene derivatives in various solvents (cm^{-1})

Solvent	n_D	D	*o*-Nitrophenol	*o*-Nitroanisole	*o*-Nitroaniline	*m*-Nitrophenol	*m*-Nitroanisole
n-Hexane	1.375	1.890	36400 28810	39800 32510	37160 26870	37850 32040	38200 31200
Dioxane	1.422	2.209	36420 28560	38690 31240	36160 25020	37090 30390	37160 30620
Cyclohexane	1.426	2.023	36700 28650	39670 32350	36390 26270	38160 31440	38080 31440
Carbon tetrachloride	1.460	2.238	36410 28420	— 31740	36750 25900	38010 31440	37560 30900
Toluene	1.497	2.379	— 28120	— 31290	— 25310	— 30390	— 30390
Benzene	1.501	2.284	— 28040	— 31100	— 25310	— 30690	— 30370

Solvent	*m*-Nitroaniline	*m*-Nitro-*N*-dimethylaniline	*p*-Nitrophenol	*p*-Nitroanisole	*p*-Nitroaniline	*p*-Nitro-*N*-dimethylaniline
n-Hexane	38450* 29060	40310 26120	—	—	—	—
Dioxane	35700* 26800	40020 24840	— 32780	— 32720	— 28080	— 26140
Cyclohexane	37030* 28730	40180 26030	— 35020	— 22890	— 30840	— 28160
Carbon tetrachloride	36620 28240	— 25440	— 34060	— 33380	— 30040	— 27430
Toluene	— 27370	— 24810	— 33210	— 32720	— 28940	— 26170
Benzene	— 27390	— 24560	— 33100	— 32560	— 28890	— 26030

* Absorption shoulder

or if the first term is nearly the equal of these solvents, an approximately linear relation between ν_{max} and $(n_D^2-1)/(2n_D^2+1)$ should hold. Although the frequency shift of absorption caused by non-polar solvents results from the effects of both the first and the second terms in Eq. 1, the second term mainly determines the amount of the shifts, if the first term is small.

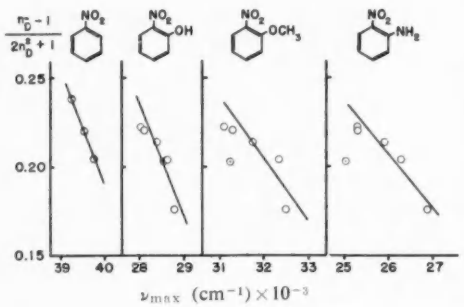

Fig. 1. Relation between $\frac{n_D^2-1}{2n_D^2+1}$ and ν_{max} (longer-wavelength bands) for nitrobenzene and *o*-nitrobenzene derivatives. (⊙: dioxane, the value n_D for nitrobenzene was used for 250 mμ)

For these nitrobenzene derivatives B in Eq. 2 is negative, indicating that $(\mathbf{M}_{oo}^{u})^2$ is smaller than $(\mathbf{M}_{ii}^{u})^2$, or that the dipole moment values of these derivatives increase in their electronically excited states reached by the absorption transition. The values of B can be evaluated from slopes of the straight lines as apparent in Figs. 1—3 and Table II. The B value for nitrobenzene is evaluated from the data of Bayliss and McRae[4] obtained for *n*-heptane, cyclohexane and carbon tetrachloride. For *p*-nitrobenzene derivatives the B values decrease with the increasing permanent dipole moments of the solute molecules, but for *o*- and *m*-derivatives these relations are not clearly observed. Spectral shifts are also much greater in nitrobenzene derivatives than nitrobenzene.

The present case of a polar solute dissolved in a non-polar solvent corresponds to the case

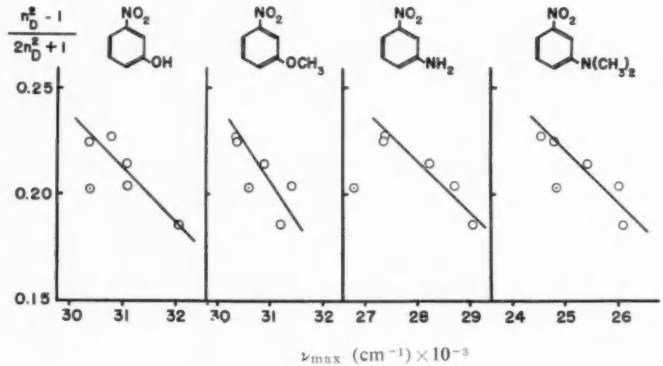

Fig. 2. Ralation between $\frac{n_D^2-1}{2n_D^2+1}$ and ν_{max} (longer-wavelength bands) for *m*-nitrobenzene derivatives. (⊙: dioxane)

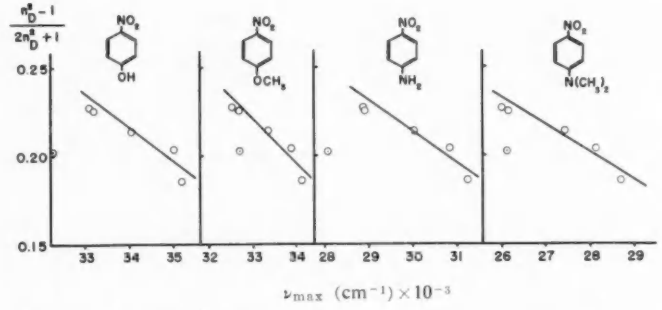

Fig. 3. Relation between $\frac{n_D^2-1}{2n_D^2+1}$ and ν_{max} for *p*-nitrobenzene derivatives. (⊙: dioxane)

TABLE II. EVALUATION OF B VALUES (cm^{-1})

Molecule	B	Ground state dipole moment* (Debye units)
Nitrobenzene	−32000**	3.82~4.00
o-Nitrophenol	−16000	4.10
o-Nitroanisole	−30000	4.83
o-Nitroaniline	−34000	4.26
m-Nitrophenol	−40000	3.90
m-Nitroanisole	−26000	3.86
m-Nitroaniline	−40000	4.72
m-Nitro-*N*-dimethylaniline	−40000	5.06
p-Nitrophenol	−52000	5.05
p-Nitroanisole	−40000	4.75
p-Nitroaniline	−58000	6.32
p-Nitro-*N*-dimethylaniline	−64000	6.87

* See Ref. 10.
** Evaluated from Bayliss and MaRae's data[4].

III b of Bayliss and McRae's paper[4], in which the solute dipole moment increases during the transition. According to their theory, the forces contributing to the solvation energy are dispersion and dipole-polarization forces (polarization of solvent molecules by the solute dipoles) and the latter is probably greater than the former. When the solute dipole moment increases as the result of the transition, the solvation energy becomes greater in the excited state than in the ground state, and hence absorption maxima are shifted to the red.

It is well known that dioxane behaves differently from other solvents and it can not be regarded as a non-polar solvent here[5,7,8]. Nitrophenol and nitroaniline probably from hydrogen bonds with dioxane and in these systems red shifts due to the hydrogen bonding effect may be expected. However, the anomalous shifts are also observed for nitroanisole and nitro-*N*-dimethylaniline in dioxane solutions, where no hydrogen bonding between solute and solvent molecules can be expected.

Absorption frequency shifts $\Delta\nu_{max}$ due to non-hydrogen bonding polar solvents can be simply expressed in a following form[7]

$$\nu_a-\nu_b=C\left[\frac{D_a-1}{D_a+2}-\frac{D_b-1}{D_b+2}\right]+E\left[\frac{D_a-1}{D_a+2}-\frac{D_b-1}{D_b+2}\right]^2 \quad (5)$$

where ν_a and ν_b are the ν_{max}'s of the solutions in solvents a and b, and D_a and D_b are their respective dielectric constant values. To check this relation we chose ethyl ether with n_D= 1.356 and acetonitrile with n_D=1.344 for a and b. Their refractive indices are about the same. Moreover, the absorption spectra of these solvents are similar to each other in the point that they have no strong absorption above 200 mμ, and the dispersion-term contributions from them are expected to be nearly equal[7]. On the other hand, the two solvents have quite different values of dielectric constant, 4.34 for ethyl ether and 37.50 for acetonitrile. Also ethyl ether and nitromethane (n_D=1.382, D=35.87) were used as solvents for *p*-nitro-*N*-dimethylaniline.

Absorption maxima of nitrobenzene, *o*-, *m*- and *p*-nitroanisole and *m*- and *p*-nitro-*N*-dimethylaniline were measured in solvents consisting of ethyl ether and acetonitrile mixed in various proportions*, in which no hydrogen bonding is expected to arise. The results are shown in Figs. 4—9, where for each solute molecule $\Delta\nu_{max}$ for ethyl ether and for the mixed solvents are plotted againt $(D-1)/(D+2)$ of the solvents.

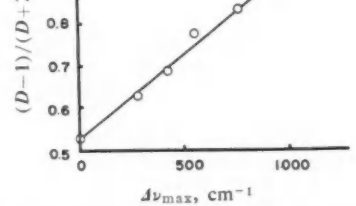

Fig. 4. Relation between $\Delta\nu_{max}$ and $(D-1)/(D+2)$ for nitrobenzene.

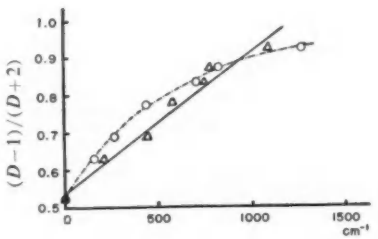

Fig. 5. Relation between $\Delta\nu_{max}$ and $(D-1)/(D+2)$ for *o*-nitroanisole. (○: $H_{x1}\rightarrow V_s$ transiton; △: $H_{x2}\rightarrow V_s$ transition)

8) E. Lippert, *Z. Naturforsch.*, **10a**, 541 (1955).

* The dielectric constant of a mixed solvent was calculated according to Hoigne and Gaumann[9] by $D=D_0+bW$, where D_0 is the value of dielectric constant of ethyl ether, b the difference of dielectric constant values of ethyl ether and acetonitrile, and W the weight fraction of acetonitrile in the solution.

9) J. Hoigne and T. Gaumann, *Helv. Chim. Acta*, **41**, 1933 (1958).

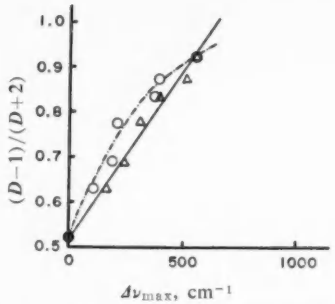

Fig. 6. Relation between $\Delta\nu_{max}$ and $(D-1)/(D+2)$ for *m*-nitroanisole. (○: $H_{x1}\rightarrow V_s$ transition; △: $H_{x2}\rightarrow V_s$ transition)

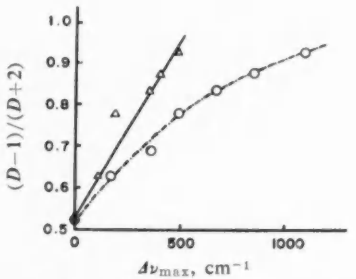

Fig. 7. Relation between $\Delta\nu_{max}$ and $(D-1)/(D+2)$ for *m*-nitro-*N*-dimethylaniline. (○: $H_{x1}\rightarrow V_s$ transition; △: $H_{x2}\rightarrow V_s$ transition)

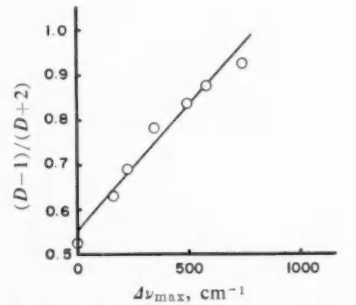

Fig. 8. Relation between $\Delta\nu_{max}$ and $(D-1)/(D+2)$ for *p*-nitroanisole.

For the shorter-wavelength bands of *o*- and *m*-nitrobenzene derivatives which arise from the $H_{x2}\rightarrow V_s$ transition, and also for the intramolecular charge transfer bands of nitrobenzene and *p*-nitrobenzene derivatives, the linear relation holds approximately. However, for all of the longer-wavelength bands of *o*- and *m*-nitrobenzene derivatives arising from $H_{x1}\rightarrow V_s$ transition the plots show obvious curvatures.

These facts indicate that while for the shorter-wavelength bands the shifts are determined only

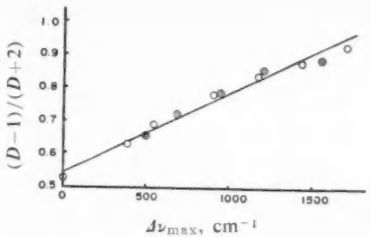

Fig. 9. Relation between $\Delta\nu_{max}$ and $(D-1)/(D+2)$ for *p*-nitro-*N*-dimethylaniline. (○: in ethyl ether and acetonitrile; ◎: in ethyl ether and nitromethane)

by the first term in Eq. 5, for the longer-wavelength bands both the first and the second terms would be responsible. In other words, only the interaction between the permanent dipoles of solute and solvent molecules essentially contribute to the spectral shift for the first case, but for the latter case the interaction between the dipole of the solvent molecules and that induced in the solute molecule also makes possibly an important contribution to the shift.

The values of C in Eq. 5 are easily obtained from the slopes of the straight lines for the shorter-wavelength bands, from which we may calculate* the excited state dipole moment $\mathbf{M}_{ii}^{u}$, if the values of a are known. Similarly, for the longer-wavelength bands $\mathbf{M}_{ii}^{u}$ as well as he polarizability differerence $(\alpha_o^u-\alpha_i^u)$ of the solute in its ground and excited states may be estimated from C and E values.

The polarization effect on the spectral shift is apparent only in the $H_{x1}\rightarrow V_s$ transitions of *o*- and *m*-nitrobenzene derivatives. It could not be observed in all other absorption bands investigated. In all cases C and E in Eq. 5 are negative, showing that dipole moment and polarizability are greater in the excited state than in the ground state. This indicates that the stabilization energies arising from the electrostatic interactions between the solute and solvent molecules are much greater in the excited state than in the ground state. Thus, the main factor causing the red shift of these absorption band in polar solvents is the great stabilization in the excited state owing to the electrostatic interaction between the solute and solvent molecules. On the other hand, from the consideration of the obviously important resonance forms of these molecules

* For example, if we assume that a is 4Å for *p*-nitroanisole, the excited state dipole moment M_{ii}^{u} can be calculated to be 6.89 D. As its ground state dipole moment is 4.78 D[10], the dipole moment increases by 2.11 D in the excited state.

10) L. G. Wesson, "Tables of Electric Dipole Moments", The Technology Press, M. I. T. (1948).

shown below, the optical absorption may well be accompanied by the excitation of the molecule according to the scheme

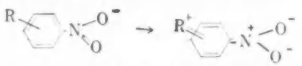

which would contribute largely to the moment of the excited state.

Effect of Hydrogen Bonding.—The hydrogen bonding plays a very important role in the spectral shift of a solution. The hydrogen bonding effect on the absorption spectra of *m*- and *p*-nitrophenol was observed in mixed solvents consisting of *n*-hexane and ethyl ether.

Figs. 10 and 11 show that the absorption maxima are shifted toward the red with an increasing proportion of ethyl ether in the solvent. In each case an isosbestic point is observed. The following hydrogen bonding reaction may be suggested

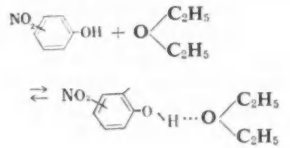

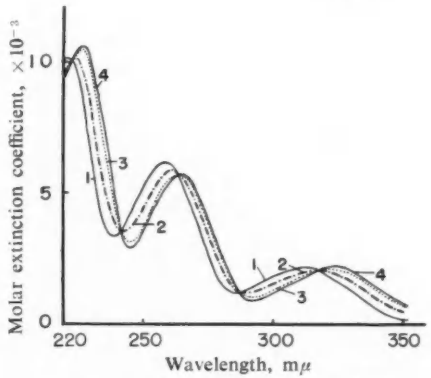

Fig. 10. Absorption curves of *m*-nitrophenol (7.63×10^{-5} mol./l.) in *n*-hexane solution containing ethyl ether at 12°C.
curve 1: *n*-hexane solution (free *m*-nitrophenol)
curve 2: ethyl ether 3.91×10^{-3} mol./l.
curve 3: ethyl ether 7.81×10^{-3} mol./l.
curve 4: calculated curve for bound *m*-nitrophenol

* The equilibrium constant K is calculated as

$$K=\frac{\varepsilon-\varepsilon_A}{\varepsilon'-\varepsilon}\frac{1}{C_B}-\frac{\varepsilon'-\varepsilon_A}{\varepsilon'-\varepsilon}\frac{1}{C_B'}$$

where ε_A is the molar extinction coefficient of free *p*-nitrophenol (curve 1), ε and ε' are those of the mixed solvents for curves 2 and 3, and C_B and C_B' are the concentrations of ethyl ether corresponding to the curves 2 and 3.

** The free energy difference ΔF is calculated as $\Delta F=-RT\ln K$.

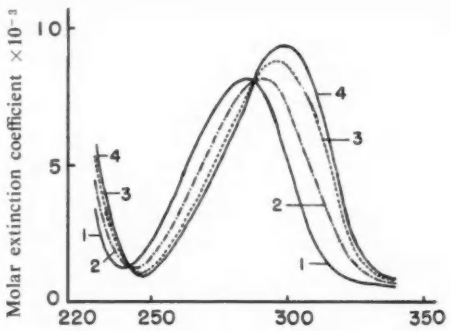

Fig. 11. Absorption curves of *p*-nitrophenol (7.18×10^{-5} mol./l.) in *n*-hexane solution containing ethyl ether at 20°C.
curve 1: *n*-hexane solution (free *p*-nitrophenol)
curve 2: ethyl ether 3.85×10^{-2} mol./l.
curve 3: ethyl ether 1.93×10^{-1} mol./l.
curve 4: calculated curve for bound *p*-nitrophenol

TABLE III. EQUILIBRIUM CONSTANTS AND FREE ENERGY DIFFERENCES FOR *m*- AND *p*-NITROPHENOL

Molecule	Equilibrium constant	Free energy difference (kcal./mol.)
m-Nitrophenol	113.1	−2.6 (12°C)
p-Nitrophenol	24.6	−1.9 (20°C)

From these curves the equilibrium constants* and the free energy differences** are obtained as given in Table III. The equilibrium constant for *m*-nitrophenol is much greater than that for *p*-nitrophenol, indicating that the former requires a very small amount of ethyl ether to reach equilibrium. This may be due to the meta-directing property of the nitro group[1].

For *m*- and *p*-nitroaniline no isosbestic point is clearly observed. This indicates that there is no simple equilibrium relation in the hydrogen bonding reaction. However, their absorption maxima are shifted toward the red with an increasing amount of ethyl ether in the solvents.

Next we shall consider the cases of *p*-nitroanisole and *p*-nitro-*N*-dimethylaniline dissolved in methanol and ethanol. In these systems hydrogen bonds may be expected to be formed between the nitro and the hydroxyl groups, the alcohol molecule playing the role of a proton donor according to the scheme

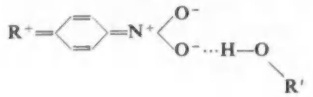

Table IV. Calculated blue-shifts due to $NO_2 \cdots H-O$ (cm^{-1})

Solvent (proton donor)	Nitro-benzene	*o*-Nitro-anisole	*m*-Nitro-anisole	*m*-Nitro-*N*-dimethyl-aniline	*p*-Nitro-anisole	*p*-Nitro-*N*-dimethyl-aniline
Methanol	—	230	150	260	—	—
	130	290	200	330	150	370
Ethanol	—	320	220	250	—	—
	210	270	150	370	280	410

Absorption maxima of *p*-nitroanisole and *p*-nitro-*N*-dimethylaniline are at 32510 and 25540 cm^{-1} in methanol and 32700 and 25700 cm^{-1} in ethanol, respectively. The contribution of electrostatic interactions to the frequency shifts can be evaluated from Eq. 5 as the refractive indices of these alcohols are close to that of ethyl ether or acetonitrile. From the values of C and the dielectric constant for alcohol solutions, the frequency shifts of *p*-nitroanisole relative to the ethyl ether solution can be evaluated as 960 cm^{-1} and as 900 cm^{-1}, and the shifts of *p*-nitro-*N*-dimethylaniline as 1630 and 1520 cm^{-1} for methanol and ethanol, respectively. The experimentally observed shifts for *p*-nitroanisole are 810 and 620 cm^{-1}, and for *p*-nitro-*N*-dimethylaniline 1260 and 1100 cm^{-1}, respectively, for methanol and ethanol. Thus the absorption maximum appears at a shorter wavelength than that expected from only the electrostatic origin in each case. The difference between experimentally observed and calculated frequency shifts may probably be accounted for on the basis of hydrogen bonding between the solute and alcohol molecules. Such differences are observed also for nitrobenzene, *o*- and *m*-nitroanisole, and *m*-nitro-*N*-dimethylaniline as shown in Table IV.

Baba[11] has shown that, if an alcohol molecule plays the role of the proton donor, a blue shift is expected in a $\pi \rightarrow \pi^*$ type transition. The present observed shifts are in good agreement with his theory. Shifts due to hydrogen bonding between the nitro and the hydroxyl groups are estimated as given in Table IV.

11) H. Baba, *Bull. Research Institute of Applied Electricity, Hokkaido University*, **9**, 84 (1957).

Summary

Intramolecular charge transfer spectra of *o*-, *m*- and *p*-nitrobenzene derivatives were measured in solutions with various solvents. Frequency shifts induced by solvents were analyzed on the basis of current theories of solvent effects on absorption spectra. Results show that the frequency shifts in the absorption bands of nitrobenzene derivatives can be interpreted as arising from both the electrostatic and hydrogen bonding interactions.

The author wishes to thank Professor S. Imanishi and Dr. Y. Kanda of Kyushu University for their kind advice and encouragement throughout this investigations and to Dr. M. Ito for his helpful and valuable discussions. The author's thanks are also due to Drs. Y. Kora and T. Ikenoue of Kurosaki Firebrick Mfg. Co. for their kind encouragement.

Department of Chemistry
Faculty of Science
Kyushu University
Hakozaki, Fukuoka

Electronic and Vibrational States of Acrolein

By Kōzō Inuzuka

(Received November 1, 1960)

Eastwood and Snow[1] carried out a vibrational and rotational analysis of the near ultraviolet spetrum of acrolein. Walsh[2] also studied the electronic spectrum of this compound in the vacuum ultraviolet region. Interest in this compound lies partly in the fact that it has a simple skeletal structure containing a system of conjugated double bonds, and that its electronic states can easily be discussed in terms of the MO theory[3]. In a previous paper[4] we studied the n-π^* absorption bands of acrolein as measured with a photoelectric spectrometer. This time the absorption spectrum was measured photographically. In this paper is reported the results of our continued study on the electronic and vibrational states of the molecule. For aiding vibrational analysis, infrared and Raman spectra were also observed, although they have already been measured[5]. Using our new results, more detailed vibrational assignments for the excited state could be made.

Experimental

Acrolein supplied by Tokyo Kasei Kogyo Co. was used. The sample was distilled before measurement. An absorption tube of 40 cm. length provided with quartz windows was used. The spectrum was photographed at various vapor pressures corresponding to temperatures between -25 and 180°C of the tube. The tube with the windows was always kept at temperature about 10°C higher than that of the sample site for purpose of avoiding condensation. A hydrogen or a tungsten lamp was used as the source of the continuum. A Shimadzu type QL-170 spectrograph was used throughout the work. Exposure time from 1 to 20 min. for the tungsten lamp and from 2 to 3 hr. for the hydrogen lamp with a slit width of 20 μ. Fuji process plates were used. Wavelengths were determinined relative to those of iron lines, using a Shimadzu type SR-2 comparator.

For infrared and Raman measurements carbon tetrachloride or ethyl alcohol solution was used. Solvents were purified by Weissberger and Proskauer methods[6]. The Raman spectrograph used was of two dense flint prisms, having the linear dispersion of 24 Å/mm. at 4500 Å. Raman spectrum of acrolein was obtained with ethyl alcohol solution, as acrolein is very unstable chemically under strong irradiation and it was difficult to work with the liquid state. Renewing the sample at about one hour intervals a 12 hr. exposure was made with a slit width of 100 μ. During the exposure filter solution of sodium nitrous oxide was circulated. The infrared absorption was measured with a Hitachi EPI double beam spectrometer with sodium chloride or potassium bromide prism. For acrolein vapor in the sodium chloride region a 10 cm. gas cell was used.

Electronic Transition

Acrolein is a simple aliphatic aldehyde having a system of conjugated double bonds. Electron diffraction study[7] shows that the molecule has a planar *trans*-butadiene-like structure. The molecule thus belongs to the point group Cs and the electronic transitions are all symmetry-allowed. The molecule has four π-electrons and a pair of nonbonding electrons localized on the oxygen atom. Therefore n-π^* and π-π^* transitions are expected to occur. The absorption spectrum of acrolein solution in carbon tetrachloride in the 24993$\sim$33324 cm^{-1} region shows a blue shift on addition of ethanol. In ethanol solution the acrolein absorption maximum shifts toward the blue by 400 cm^{-1} relative to carbon tetrachloride solution[4]. The above result suggests the n-π^* nature of this electronic transition. Walsh attributed this transition to a one-electon promotion from the n orbital to the first excited π orbital. His assignment agrees with our calculation[3].

According to the MO theory this first excited state has A′ symmetry, and the lowest state is triplet. Consequently, the vapor absorption begining at 25851 cm^{-1} is assigned to the transition of a nonbonding electron to the first excited singlet state ($^1A'' - {}^1A'$).

Vibrational Analysis

On account of the low Cs symmetry of the molecule, the transition can be of an allowed type. So the 0, 0 band will probably be one

1) E. Eastwood and C. P. Snow, *Proc. Roy. Soc.*, **149A**, 446 (1935).
2) A. D. Walsh, *Trans. Faraday Soc.*, **41**, 498 (1945).
3) K. Inuzuka, This Bulletin, **34**, 6 (1961).
4) K. Inuzuka, ibid., **33**, 678 (1960).
5) M. Aime Cotton, *Compt. rend.*, **208**, 740 (1939).
6) A. Weissberger and E. S. Proskauer, "Organic Solvents", Interscience Publishers, Inc., New York, N. Y. (1955).
7) H. Mackle and L. E. Sutton, *Trans. Faraday Soc.*, **47**, 691 (1951).

of the stronger bands. The development of the spectrum with increasing temperature suggests that the 0, 0 band is surely the strong band at 25851 cm^{-1}. In an earlier work of Eastwood and Snow a band at 25860 cm^{-1} was chosen as the 0, 0 band from rotational analysis, and two progressions of bands with mean separations of 1260 and 500 cm^{-1} respectively were observed. Since our measurement was limited to about 30294 cm^{-1}, the progression corresponding to 1260 cm^{-1} could not be followed further than the second overtone. These bands are accompanied each by a strong subsidary band with the separation of 499 cm^{-1}. In our analysis 1270 cm^{-1} was taken as the interval of the progression. Among the observed bands, nearly 130 in number, some show rotational structures but many are not well defined. It is difficult to interpret correctly all of these observed bands on account of the low symmetry of the molecule, so we give in Table I the position and interpretations only

TABLE I. VIBRATIONAL ANALYSIS OF ULTRAVIOLET ABSORPTION SPECTRUM OF ACROLEIN VAPOR

In.	Å	cm^{-1}	Freq. distance from the 0, 0 band	Assignment
vs	3867.2	25851	0	0, 0
vs	3794.0	26350	499	0+499
m	3705.7	26978	1127	0+1127
vs	3686.2	27121	1270	0+1270
vs	3666.6	27265	1414	0+1414
bm	3638.5	27476	1625	499+1127=1626
s	3620.0	27616	1765	1270+499=1769
bs	3601.6	27758	1907	499+1414=1913
m	3538.3	28254	2403	1270+1127=2397
s	3521.3	28391	2540	2(1270)
bm	3502.2	28545	2694	1270+1414=2684
m	3484.1	28693	2842	2(1414)
m	3461.6	28880	3029	2(1270)+499=3039
w	3387.4	29513	3662	2(1270)+1127=3667
w	3369.0	29674	3823	3(1270)
w	3354.1	29806	3955	2(1270)+1414=3954
w	3324.5	30071	4220	3(1414)

vs: very strong, s: strong, bm: broad medium, m: medium, w: weak

for stronger bands. The frequencies of 1270 and 499 cm^{-1} are assigned definitely to two totally symmetric vibrations of type A′ of the lower electronic state. The very weak bands on the longer wavelength side of the 0, 0 band decrease their intensity with decreasing temperature, and the vicinity of 70°C is favorable for their observation. The number of moderately strong bands is small on this side of the 0, 0 band. A sharp band is separated from the 0, 0 band by 145 cm^{-1}, and three fine bands by about 313 cm^{-1}. The latter bands are the ones called by Eastwood and Snow a, b and c bands, although our wavelengths are slightly different from that of Eastwood and Snow.

In addition, there is a series of four bands 24636, 24611, 24577 and 24552 cm^{-1} on the further long wavelength side. Among these bands the second one which is separated from the 0, 0 band by 1240 cm^{-1} is the strongest. On the whole our observation agrees well with that of Eastwood and Snow. Besides these bands, two weak but sharp bands are observed at 24259 and 24240 cm^{-1}. There are no further bands on the red side of these two bands. The bands on the red side of the 0, 0 band having appreciable intencities usually represent fundamental vibrational frequencies of the ground state. From this viewpoint we may assign the two bands separated from the 0, 0 band by 1274 and 1611 cm^{-1}, respectively, to the two frequencies 1270 and 1623 cm^{-1} found in infrared and Raman spectra. Bands other than those described above are tentatively interpreted as combination bands. A band with moderate intensity separated by 1127 cm^{-1} from the 0, 0 band on its shorter wavelength side form a satellite accompanying the stronger 1270 cm^{-1} band. The 1127 cm^{-1} frequency appears also in other combination bands, so that it is reasonable to assume this frequency as a fundamental. There is a very strong band at 27265 cm^{-1} separated by 1414 cm^{-1} from the 0, 0 band. Starting from this band a progression containing two more bands with 1414 cm^{-1} interval is observed. The 1414 cm^{-1} frequency also appears in other combination bands, so that we may assume this to be another fundamental.

Fundamental Vibrational Frequencies

The acrolein molecule, CH_2CHCHO, may belong, at the most, to the point group Cs. As it contains eight atoms, eighteen normal modes of vibration are possible, of which thirteen are of the totally symmetrical A′ type, and the remaining five are of the anti-symmetrical A″ type. Both types are active in infrared and Raman spectra. There will be seven essentially valency type vibrations of the four C–H, one C=C, one C–C and one C=O bonds. Analogously to 1, 3-butadiene[8,9] there will also be an A″ type torsional oscillation about the C–C bond. Another important mode of A′ is the planar deformation of the C=C–C=O skeleton.

8) C. M. Richards and J. R. Nielsen, *J. Opt. Soc., Am.* 40, 438 (1950).
9) R. S. Rasmussen and R. R. Brattain, *J. Chem. Phys.*, 15, 131 (1947).

TABLE II. INFRARED AND RAMAN FREQUENCIES OF ACROLEIN MOLECULE (cm^{-1})

Infrared				Raman		Assignment
CCl_4 solution		vapor		EtOH solution		
w	570			w	340	Skeletal bending
				m	574	Skeletal bending
s	910	m	906			
s	959	s	917	w	980	CH and CH_2 wagging
s	982	s	960			
		s	990			
			1147			
s	1152	s	1156	w	1170	CH_2 rocking
			1163			
w	1270	w	1262	m	1272	C–C stretching
			1280			
m	1360	m	1348	s	1360	CH rocking
			1366			
m	1420	m	1410	w	1426	CH_2 deformation
			1427			
m	1617	m	1613	s	1620	C=C stretching
			1632			
vs	1708	vs	1713	vs	1701	C=O stretching
			1727			
m	2700	m	2710			
m	2755	m	2790			
m	2805	m	2810			C–H stretching
w	2990	w	3000			
w	3100	w	3100			
w	3375	w	3388			C=O overtone

The infrared spectrum was measured in the 460~4000 cm^{-1} region, but a weak band at 340 cm^{-1} was found in the Raman spectrum. An analogous band was found in 1, 3-butadiene at 320 cm^{-1} and has been assigned to a skeletal deformation vibration. Therefore we have assigned the Raman band of acrolein at 340 cm^{-1} to an A'' type skeletal deformation vibration. We found a weak band at 570 cm^{-1} in the infrared potassium bromide region, and in the Raman spectrum at 574 cm^{-1}. It may be assigned to an A' type skeletal deformation vibration. In 1, 3-butadiene the corresponding Raman band is at 513 cm^{-1}. Corresponding to the infrared bands in the 900 cm^{-1} region only one Raman band at 980 cm^{-1} was found with very small intensity. This band system may be due to the CH and CH_2 wagging vibrations. The infrared band at 1150 cm^{-1} is strong and sharp, and the corresponding Raman band has exactly the same frequency shift.

This band may be assigned to the rocking vibration of the methylene radical. The Raman band at 1272 cm^{-1} has medium intensity. In infrared two bands appear at 1235 and 1270 cm^{-1}, the former being very weak, and the latter medium strong. We may assign the latter frequency 1270 cm^{-1} to the C–C stretching vibration, in analogy to the 1205 cm^{-1} of 1, 3-butadiene and 1284 cm^{-1} of biacetyl[10]. The value of 1270 cm^{-1} for acrolein might appear too high for the C–C stretching frequency, but it is probably due to the partial double bond character of the bond in this molecule, whose length is 1.46 Å[7], considerably shorter than the normal C–C single bond length 1.53~1.54 Å. The band at 1360 cm^{-1} was observed in both the Raman and infrared spectra with considerable intensity. This frequency may be assigned to the CH rocking vibration. The weak band at 1420 cm^{-1} in infrared and at 1426 cm^{-1} in Raman spectra may be assigned to the CH_2 deformation vibration in analogy to the Raman 1442 cm^{-1} band in 1, 3-butadiene. The C=C stretching frequency is observed as the 1617 cm^{-1} infrared band for solution, as the 1620 cm^{-1} Raman medium strong band. The C=O stretching frequency is observed at 1695~1725 cm^{-1} in solution with two peaks in the infrared and at 1700 cm^{-1} in the Raman spectrum. It is the strongest band in both the spectra, but the Raman frequency seems to have been affected by the solvent. C–H valence vibration bands lying in the 2700~3000 cm^{-1} region were not observed in the Raman spectrum as they may be hidden under excited Hg lines. Result of the vibrational analysis is given in Table II.

In a symmetry-allowed molecular electronic

10) J. W. Sidman and D. S. McClure, *J. Am. Chem. Soc.*, 77, 6471 (1955).

Table II. Fundamental vibrational frequencies (cm^{-1})

Raman (solution)	Infrared (vapor)	Lower state	Upper state	Assignment
1701	1713} 1727}	1720	1270	C=O valence (A′)
1620	1613} 1632}	1623	1414	C=C valence (A′)
1272	1259} 1280}	1270	1127	C-C valence (A′)
570		570	499	C=C-C=O bending (A′)

transition, totally symmetric vibrational frequencies appear generally with large intensities in absorption. In the acrolein spectrum as analyzed above, all of the interval frequencies contained in prominent progressions can be assigned either to fundamental, or to combination frequencies of A′ type vibrational modes of the excited electonic state. In Table III correlations among upper and lower state vibrational frequencies are given. Of these fundamental frequencies those of the upper state of 1270 cm^{-1} and 499 cm^{-1} are the most important in the vapor absorption. The former is observed up to the second overtone (3×1270 cm^{-1}) and is assigned to the C=O stretching mode. The latter frequency is assigned to a skeletal bending mode, as its corresponding lower state frequency is very probably 570 cm^{-1} observed in both Raman and infrared spectra. The very strong band separated from the 0, 0 band by 1414 cm^{-1} may be associated with another fundamental vibration, since we could not analyze so strong a band as a combination or overtone and since, moreover, its frequency separation 1414 cm^{-1} is repeated twice more in forming a prominent progression. In our previous paper[4] this frequency was assigned to the C=C vibration, although a slightly different value was then reported. The 1127 cm^{-1} frequency is observed as satellite bands accompanying each of the 1270 cm^{-1} progression bands. This frequency was not reported in the above cited paper[1]. It can be assigned to the C-C vibration of the excited electronic state in analogy to the biacetyl 1136 cm^{-1} (excited state) and 1284 cm^{-1} (ground state). In acrolein the corresponding lower state frequency is 1270 cm^{-1}.

Summary

The position, blue-shift and theoretical calculation[3] of the state energy of the electronic transition of acrolein in 24241～30294 cm^{-1} region suggest that the transition is of the $n-\pi^*$ type. From the vibrational analysis of acrolein vapor spectrum, it is known that the vapor spectum of acrolein has four progressions corresponding to the C=O, C=C and C-C stretching, and skeletal bending frequency in the lower state.

The author expresses his sincere thanks to Professor S. Imanishi and Dr. Y. Kanda for their kind encouragements throughout this work. He is also indebted to Dr. M. Ito and Mr. R. Shimada for their helpful advice and discussions.

Department of Chemistry
Facutly of Science
Kyushu University
Hakozaki, Fukuoka

Electron Diffraction Investigations on the Molecular Structures of sec-Butyl Chloride and Alcohol

By Mashio YAMAHA and Masato IGARASHI

(Received October 12, 1960)

The molecular structures of propane[1], butane[2] and their chlorine derivatives, such as *n*- and isopropyl chloride[3,4], 1, 2-dichloropropane[5] and *tert*-butyl chloride[6,7] have already been studied by electron diffraction, using the visual method or the sector-microphotometer method. It appears that only a few studies have been done on the molecular structures of alcohols[4,8-10].

In this paper the results of electron diffraction investigation about *sec*-butyl chloride and alcohol using the sector-microphotometer method are described and compared with those of the related compounds.

Experimental

sec-Butyl chloride and alcohol were kindly furnished by Dr. T. Miyazawa, the University of Tokyo. They were the same samples which were used in the spectroscopic studies.

The diffraction patterns were taken at room temperature of about 20°C using an apparatus[11] having an r^3-sector which was rotated rapidly during exposure. The exposures of each set were regulated to be about 2 : 1 in order to apply Karle's method[12]. The camera length was 11.82 cm. and the wavelength of electron was about 0.0567 Å, which was determined by measuring the transmission patterns of gold foil.

The optical densities of the photographic plates were measured by a microphotometer. The plates were rotated rapidly about their centers during scanning. The optical densities were converted to relative intensities by Karle's procedure[12]. A smooth background line was drawn through the intensity curve multiplied by q and the molecular intensity curve $M(q)$ was obtained using the following formula,

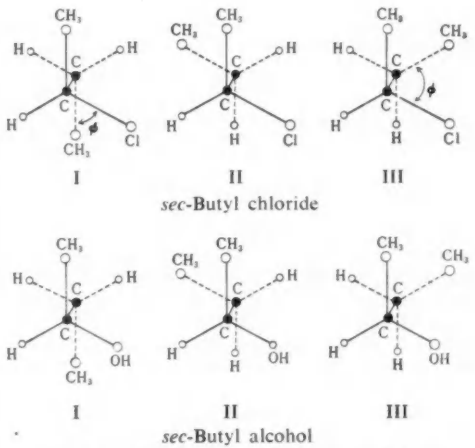

Fig. 1. Rotational isomers of *sec*-butyl chloride and alcohol.

TABLE I. LIST OF MOLECULAR CONSTANTS OF PROPANE, BUTANE AND THIR CHLORINE DERIVATIVES

Molecule	C-C, Å	C-Cl, Å	Angle CCC	Angle CCCl	Reference
Propane	1.54 ±0.02	—	111.5°±3°	—	1
n-Butane	1.539±0.003	—	112°9′ ±9′	—	2
n-Propyl chloride	1.535±0.02	1.775±0.02	109.5°±2.5°	111°±2°	3
Isopropyl chloride	1.55 ±0.02	1.76 ±0.02	109.5°±1.5°	111°±1.5°	4
1, 2-Dichloropropane	1.56 ±0.05	1.79 ±0.035	109.5°(ass.)	108°±4°	5
tert-Butyl chloride	1.54 ±0.01	1.80 ±0.01	111.5°±1°	—	6
tert-Butyl chloride	1.54 ±0.03	1.80 ±0.04	111.5°±1.5°	—	7

1) L. Pauling and L. O. Brockway, *J. Am. Chem. Soc.*, **59**, 1223 (1939).
2) K. Kuchitsu, This Bulletin, **32**, 748 (1959).
3) Y. Morino and K. Kuchitsu, *J. Chem. Phys.*, **28**, 175 (1958).
4) Y. Yamaha, This Bulletin, **27**, 170 (1954).
5) W. Wood and V. Schomaker, *J. Chem. Phys.*, **20**, 555 (1952).
6) O. Bastiansen and L. Smedvik, *Acta Chem. Scand.*, **7**, 653 (1953).
7) J. W. Coutts and R. L. Livingston, *J. Am. Chem. Soc.*, **75**, 1542 (1953).
8) K. Kimura and K. Kubo, *J. Chem. Phys.*, **30**, 151 (1959).
9) M. Kimura, *J. Chem. Soc. Japan, Pure Chem. Sec. (Nippon Kagaku Zasshi)*, **71**, 18 (1950).
10) V. Schomaker, *Acta Cryst.*, **3**, 46 (1950).
11) K. Kuchitsu, This Bulletin, **30**, 391 (1956).
12) J. Karle and I. L. Karle, *J. Chem. Phys.*, **18**, 957 (1950).

TABLE II. LIST OF MOLECULAR CONSTANTS OF ALCOHOLS

Molecule	C-C, Å	C-O, Å	Reference
Methyl alcohol	—	1.428±0.003	8
Ethyl alcohol	1.54(ass.)	1.48 ±0.04	9
Ethyl alcohol	1.55±0.02	1.43 ±0.02	10
Isopropyl alcohol	1.54±0.02	1.45 ±0.03	4

$$M(q)=(I_T/I_B)-1 \quad (1)$$

where I_T is the total intensity and I_B is the background intensity.

Analysis

The radial distribution curves were calculated by the following equation,

$$f(r)=\sum_{q=0}^{q=85} qM(q)\exp(-aq^2)\sin(\pi qr/10) \quad (2)$$

where $M(q)$ is the experimental molecular intensity obtained from Eq. 1. Here the correction for the non-nuclear scatterings was not made. The artificial damping factor a was chosen so that $\exp(-aq^2)=0.1$ at $q=85$, and $q=(40/\lambda)\sin(\theta/2)$, where θ is the angle of scattering and λ is the wavelength of the electron beam.

In the calculation of the radial distribution curve, the intensity curve below $q=15$ was spliced by the theoretical intensity curve with a constant coefficient. The intensity curve in such a region is hardly affected at all by the bond distance changes of the order 0.01 Å, but considerably affected by the internal rotation around the middle C-C bond (Fig. 1). Several steps of successive approximations were taken in order to make the assumed model practically selfconsistent with the final radial distribution curve.

The theoretical intensity curves were calculated using the following equation,

$$qM_c(q)=\sum_{i,j}(Z_iZ_j/r_{ij})\exp(-b_{ij}q^2)\sin(\pi qr_{ij}/10) \quad (3)$$

where r_{ij} is the interatomic distance between the ith and jth atoms, b_{ij} is its temperature factor which is calculated from the mean amplitude, Z_i is the ith atomic number, except hydrogen, where the effective value 1.25 was used. The mean amplitudes used for the factors b_{ij} are shown in Table III. The theoretical intensity curves of the mixed rotational isomers were considered.

***sec*-Butyl Chloride.**—The radial distribution curve (Fig. 3) has peaks at 1.085, 1.54, 1.80, 2.17, 2.715, 3.23 and 4.15 Å. The first peak is assigned to bonded C-H distances, the second to bonded C-C distances, the third to bonded C-Cl distance with some contributions of nonbonded H···H distances, the fourth to nonbonded C···H distances. The peak of the nonbonded C···H distances, when the fourth peak is resolved into its components, shows that the angles CCH are about 109.5°, if the C-H bond distances are assumed to be 1.09 Å. The fifth peak is mainly resolved into those of nonbonded C···C and C···Cl distances, although it involves some components of the others. If the C-Cl bond distance is assumed to be 1.80 Å, the peak of C···Cl distances shows that the angles CCCl are equal to 109.5°.

In the same way, the peak of C···C distances, although the height is less than that of C···Cl and its position is somewhat uncertain, shows that the angles CCC are about 110~112°. The peak at about 3.23 Å is characteristic of the gauche C···Cl and shows the existence of I or III or both the forms (Fig. 1). The peak shows also that the azimuthal angle ϕ is about 70°C. The peak at 4.15 Å is characteristic of the trans C···Cl and shows the existence of the form II. The peak of gauche C···C overlaps heavily with the other more predominant peaks and the peak of trans C···C is very low, so these two peaks are not so suitable to estimate the amount of forms I and III. As the area under the peak is approximately proportional to Z_iZ_j/r_{ij}, the amount of each form can be found from the area of the characteristic peak and since the areas of trans C···Cl and gauche C···Cl are

TABLE III. MEAN AMPLITUDES USED FOR THE ANALYSIS

Atomic pair	Mean amplitude Å	Atomic pair	Mean amplitude Å
C-C	0.050	O···H	0.114
C-Cl	0.050	H···H	0.135
C-O	0.050	*trans*-C···C	0.070
C-H	0.077	*trans*-C···Cl	0.068
C···C	0.079	*trans*-C···O	0.070
C···Cl	0.073	*gauche*-C···C	0.160
C···O	0.073	*gauche*-C···Cl	0.140
C···H	0.120	*gauche*-C···O	0.140
Cl···H	0.114		

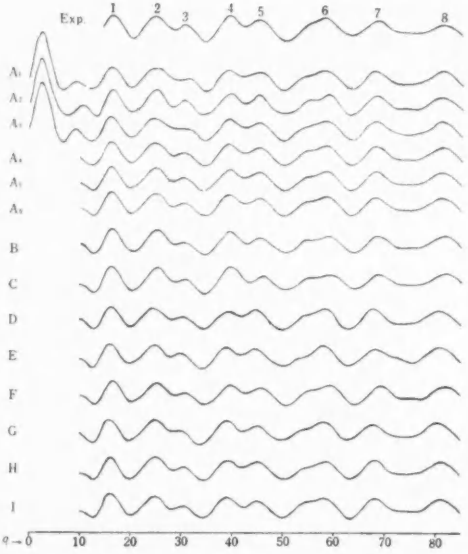

Fig. 2. Intensity curves of *sec*-butyl chloride.

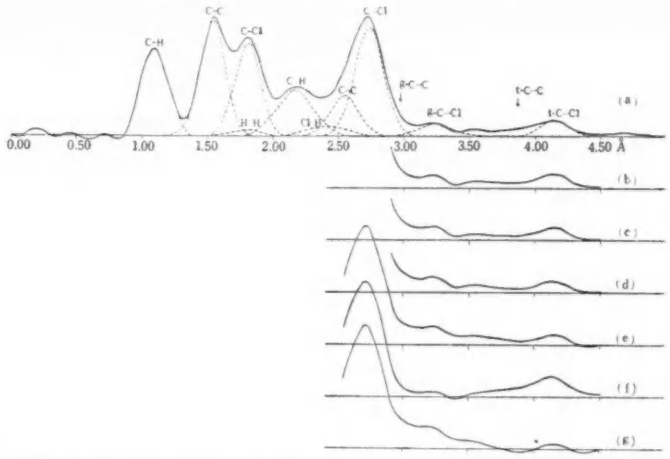

Fig. 3. Radial distribution curves of *sec*-butyl chloride. Spliced theoretical intensity curves below $q=15$ are as follows;

(a) I 50%, II 50%, (b) I 25%, II 50%, III 25%, (c) II 50%, III 50%, (d) I 33%, II 33%, III 33%, (e) I 100%, (f) II 100%, (g) III 100%

affected by the spliced theoretical intensity curves below $q=15$, various ratios of the three forms were tried so that the peaks became almost self consistent with the assumed ratio. The theoretical intensity curves of the forms I and II below $q=15$ are not so different from each other, so the radial distribution curve is not affected very much by the ratio of these two kinds of spliced portions. The ratio of the amounts of the forms I and III could not be obtained unambiguously. Only the ratio of the form II and the sum of the forms I and III was obtained rather definitely.

Its reasonable ratio was about 50%: 50%. The radial distribution curves a, b and c are almost selfconsistent with the assumed amounts of the rotational isomers, but d, e, f and g are not selfconsistent (Fig. 3).

Making reference to the results of the radial distribution curve, the theoretical intensity curves of various models were drawn in order to find the best model. The theoretical intensity curves of the three rotational isomers show some different features respectively at about $q=25\sim50$ and among the three, the forms I and III which have gauche C···Cl resemble each other rather than the form II which has trans C···Cl. However the theoretical intensity curve of any one rotational isomer does not fit better with the experimental than that of the mixed one, so for one model of assumed bond distances and bond angles, some mixtures of the rotational isomers I, II and III were examined, but for the most part the ratio, form I: form II=50%: 50% was assumed (Table IV). The intensity curves A_5 and A_6 fit with the experimental better than any other (Fig. 2). Next to them B fits well. Both curves C and D in which the C-Cl bond distance is 1.76 and 1.82 Å, respectively, show very different intensities at maxima 4 and 5 compared with the experimental. So the C-Cl bond distance can be determined to be 1.79±0.015 Å.

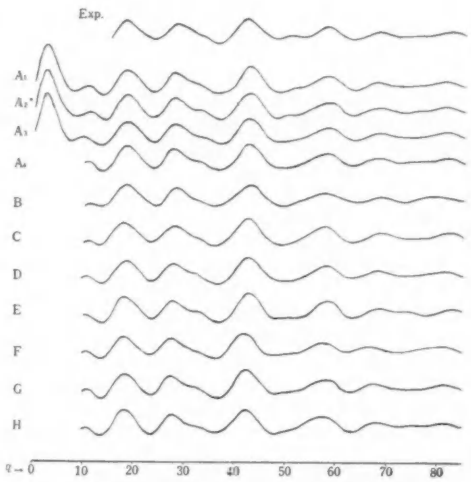

Fig. 4. Intensity curves of *sec*-butyl alcohol.

The intensity curves F and G in which C-C bond distances are 1.52 and 1.56 Å, respectively, have not very different appearances from the experimental, but the q_{calcd}/q_{obs} values are not so good as that of 1.54 Å. The C-C bond distances can be considered to be 1.54±0.01 Å. The intensity curves H and I in which C-H bond distances are 1.07 and 1.11 Å, respectively, have different intensity ratios at maxima 4 and 5 compared with the experimental. The C-H bond distances seem to be 1.09±0.015 Å.

***sec*-Butyl Alcohol.**—The radial distribution curve has peaks at 1.06, 1.515, 2.16, 2.485, 2.93 and 3.73 Å (Fig. 5). The first peak is considered to be the resultant of bonded C-H and O-H peaks, the second to be that of bonded C-C and C-O peaks,

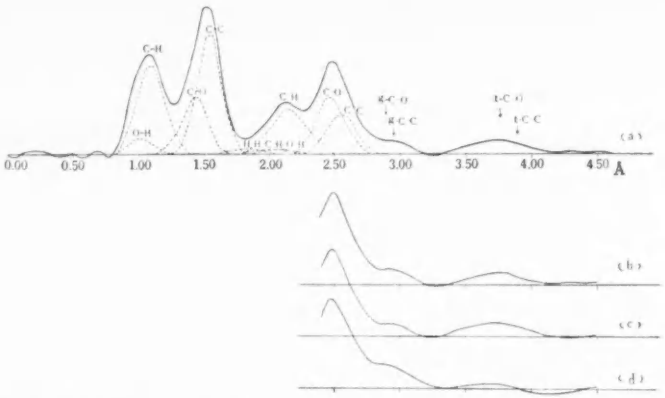

Fig. 5. Radial distribution curves of *sec*-butyl alcohol. Spliced theoretical intensity curves below $q=15$ are as follows;
(a) I 50%, II 50% (b) I 100%, (c) II 100%, (d) III 100%

TABLE IV. MOLECULAR MODELS OF *sec*-BUTYL CHLORIDE AND q_{calcd}/q_{obs} VALUES

Model	C-C Å	C-H Å	C-Cl Å	Angle CCC	Angle CCCl	Percent of rotational isomers I	II	III	Mean value of q_{calcd}/q_{obs}	Average deviation
A_1	1.54	1.09	1.80	109.5°	109.5°	100	0	0	1.004	0.012
A_2	1.54	1.09	1.80	109.5°	109.5°	0	100	0	0.997	0.007
A_3	1.54	1.09	1.80	109.5°	109.5°	0	0	100	—	—
A_4	1.54	1.09	1.80	109.5°	109.5°	33	33	33	0.997	0.006
A_5	1.54	1.09	1.80	109.5°	109.5°	25	50	25	0.999	0.004
A_6	1.54	1.09	1.80	109.5°	109.5°	50	50	0	0.999	0.005
B	1.54	1.09	1.78	109.5°	109.5°	50	50	0	1.006	0.005
C	1.54	1.09	1.76	109.5°	109.5°	50	50	0	—	—
D	1.54	1.09	1.82	109.5°	109.5°	50	50	0	0.991	0.005
E	1.54	1.09	1.80	112°	112°	50	50	0	0.989	0.007
F	1.52	1.09	1.78	109.5°	109.5°	50	50	0	1.014	0.008
G	1.56	1.09	1.80	109.5°	109.5°	50	50	0	0.991	0.008
H	1.54	1.07	1.80	109.5°	109.5°	50	50	0	0.999	0.006
I	1.54	1.11	1.80	109.5°	109.5°	50	50	0	0.997	0.005

TABLE V. MOLECULER MODELS OF *sec*-BUTYL ALCOHOL AND q_{calcd}/q_{obs} VALUES

Model	C-C Å	C-H Å	C-O Å	Angle CCC	Angle CCO	Percent of rotational isomers I	II	III	Mean value of q_{calcd}/q_{obs}	Average deviation
A_1	1.54	1.09	1.43	109.5°	109.5°	100	0	0	1.000	0.009
A_2	1.54	1.09	1.43	109.5°	109.5°	0	100	0	1.005	0.008
A_3	1.54	1.09	1.43	109.5°	109.5°	0	0	100	1.004	0.009
A_4	1.54	1.09	1.43	109.5°	109.5°	50	50	0	1.004	0.013
B	1.54	1.09	1.40	109.5°	109.5°	50	50	0	1.010	0.013
C	1.54	1.09	1.46	109.5°	109.5°	50	50	0	0.996	0.012
D	1.54	1.09	1.43	112°	109.5°	50	50	0	1.001	0.008
E	1.52	1.09	1.43	109.5°	109.5°	50	50	0	1.008	0.006
F	1.56	1.09	1.43	109.5°	109.5°	50	50	0	0.989	0.008
G	1.54	1.07	1.43	109.5°	109.5°	50	50	0	1.004	0.009
H	1.54	1.11	1.43	109.5°	109.5°	50	50	0	1.004	0.008

the third to be that of nonbonded C···cH, C···oH and O···cH peaks, the fourth to be that of nonbonded C···O and C···C peaks. Each of the above peaks consists of two or more components, so it is resolved into its components somewhat arbitrarily. Assuming the mean amplitudes listed in Table III, these peaks were resolved as in Fig. 5. The resolved peaks show that the angles CCH are about 109.5° and the angles CCC and CCO are both slightly greater than 109.5°.

The fifth peak at about 2.93 Å is characteristic of gauche C···O or C···C and the sixth peak at about 3.73 Å is characteristic of trans C···O or C···C. From both the peaks the amount of the rotational isomers are to be obtained. But these peaks are almost entirely controlled by the spliced intensity curves below $q=15$. They can be seen from the fact that the theoretical intensity curves of the rotational isomers above $q=15$ are not very different from each other. Moreover each peak may be constructed respectively from two adjacent components, C···O and C···C, and the resolution into its components is somewhat arbitrary. So it is difficult to determine the amounts of the rotational isomers unambiguously at the present step. It seems, however, that all the three rotational isomers may be present and the form II is predominant among them.

The theoretical intensity curves of various models listed in Table V are drawn in Fig. 4. As the intensity curves of models A, E and F do not show a greatly different appearance compared with the experimental, the C-C bond distances were estimated by the $q_{\text{calcd}}/q_{\text{obs}}$ values as 1.54 ± 0.015 Å (Table V). The intensity curves B and C have slightly different appearances from the experimental at the vicinity $q=50$ and unappropriate $q_{\text{calcd}}/q_{\text{obs}}$ values, so the C-O bond distance is considered to be 1.43 ± 0.02 Å. The intensity curves G and H have not greatly different features and $q_{\text{calcd}}/q_{\text{obs}}$ values compared with A, that the C-H bond distances cannot be determined within small limits of uncertainty. They seem to be 1.09 ± 0.03 Å.

Summary and Discussion

The molecular structures of *sec*-butyl chloride and alcohol have been investigated by the sector and microphotometer method of electron diffraction. The structural information was derived from the radial distribution curves and correlation with the theoretical intensity curves. The results were as follows:

sec-Butyl chloride; C-C $=1.54\pm0.01$ Å, C-Cl $=1.79\pm0.015$ Å, angles CCC $=111\pm1.5°$, angles CCH $\approx 10.95°$, angle CCCl $\approx 109.5°$, the abundance ratio of the rotational isomer in which C···Cl is trans and that in which C···Cl are gauche is about 50% : 50%.

sec-Butyl alcohol; C-C $=1.54\pm0.015$ Å, C-O $=1.43\pm0.02$ Å, C-H $=1.09\pm0.03$ Å, angles CCC and CCO are slightly greater than 109.5°, angles CCH $\approx 109.5°$. The abundance ratio of the rotational isomers could not be determined unambiguously at present.

When the above results are compared with Tables I and II, the C-C bond distances, the angles CCC and CCCl coincide with each other, although the accuracies are somewhat different. The C-Cl bond distance of *sec*-butyl chloride coincides with the results on *n*-propyl chloride[3], 1,2-dichloropropane[5] and *tert*-butyl chloride[6,7], but it is about 0.03 Å longer than that of isopropyl chloride[4].

The C-O bond distance of *sec*-butyl alcohol coincides with most cases of alcohols.

As for the rotational isomers, the abundance ratio was obtained to some extent about *sec*-butyl chloride, but not obtained unambiguously about *sec*-butyl alcohol at the present step.

By the measurement of specific rotation of *D-sec*-butyl alcohol, Bernstein and Pedersen[13] have found the amounts of the three rotational isomers to be 42%(form I), 42%(form II), 15.3%(form III), assuming that forms I and II have the same energy and that the form III is less stable (Fig. 1).

The amounts of rotational isomers will be obtained more accurately by the use of a long camera-length of electron diffraction apparatus.

The authors wish to express their hearty thanks to Professor A. Kotera for his kind guidance throughout this work, to Professor Y. Morino, the University of Tokyo, for the use of diffraction apparatus, to Dr. K. Kuchitsu and Dr. E. Hirota, the University of Tokyo, for their kind aid during the experiment and for their calculation by the Punched Card Machine; also to Dr. S. Shibata and Dr. H. Morimoto, Nagoya University, for the microphotometer-tracing.

Department of Chemistry
Faculty of Science
Tokyo University of Education
Koishikawa, Tokyo

13) H. Bernstein and E. E. Pedersen, ibid., **17**, 885 (1949).

SHORT COMMUNICATIONS

On the Electromigration in Ion-exchange Papers

By Takeo YAMABE, Manabu SENŌ and Nobuharu TAKAI

(Received March 6, 1961)

In electromigration of ions in ion-exchange papers, which are filter papers impregnated with pulverized ion-exchange resins, we may expect the contribution of ion-exchange adsorption to the electromigration behavior of ions. This behavior of alkaline earth metal ions and amino acid ions will be presented in this communication. This may be the first report dealing with the electrophoretic method using these papers, although some chromatographic experiments have been carried out[1].

The usual apparatus for paper electrophoresis (Toyo Roshi Type C) were used and the ionic mobilities under constant voltages were measured. Ion-exchange papers (Rohm and Haas Co.) were Amberlite SA-2 (sulfonic) and WA-2 (carboxylic), which were used after conditioning with acid, alkali and methanol. For comparison, Toyo Roshi No. 50 was used as an ordinary paper. Systems examined are Mg^{2+}, Ca^{2+}, Sr^{2+} and Ba^{2+} (chloride) supported in 0.05 N hydrochloric acid, sodium chloride or sodium hydroxide, and glycine, glutamic acid and lysine monohydrochloride supported in acetic acid-sodium acetate. For detection of spots of ions, coloration of alkaline earth metal with alizarin-ammonia and that of amino acid with ninhidrin were adopted.

TABLE I. MOBILITIES OF ALKALINE EARTH METAL IONS
10 V./cm., supporting media 0.05 N HCl

	Mobilities, $cm^2/V. sec. \times 10^4$			
	Mg^{2+}	Ca^{2+}	Sr^{2+}	Ba^{2+}
Toyo Roshi No. 50	3.1	3.6	3.6	3.9
Amberlite SA-2	0.22	0.33	0.33	0.03
Amberlite WA-2	2.6	3.0	3.0	3.3

TABLE II. MOBILITIES OF AMINO ACID IONS
25 V./cm., supporting media 1 M CH_3COOH

	Mobilities, $cm^2/V. sec. \times 10^4$		
	Glycine	Glutamic acid	Lysine
Toyo Roshi No. 50	0.71	0.53	1.27
Amberlite SA-2	0.11	0.09	0.01
Amberlite WA-2	0.66	0.45	0.81

A part of the experimental results is shown in Tables I and II. The ionic electromigration in ion-exchange papers possesses the diminished velocity and tailing, in comparison with the case where the ordinary paper is used. This is remarkable on SA-2 paper which exhibits strong exchange adsorption for cations. It must be noticed that the ionic mobilities decrease in the same order, $Ba^{2+} > Sr^{2+}$, $Ca^{2+} > Mg^{2+}$, on the paper No. 50 as in free solution, but Sr^{2+}, $Ca^{2+} > Mg^{2+} > Ba^{2+}$ on sulfonic SA-2 paper in acidic medium*. This might be ascribed to especially strong affinity of sulfonic acid resin for barium ion, being in accordance with observation in the permselectivity of the ion-selective membrane[2]. On carboxylic WA-2 paper, there is scarecely adsorption effect in acidic medium, where the paper is not in dissociated state. In neutral and alkaline medium, the ionic mobilities have the order, $Ba^{2+} > Sr^{2+} > Mg^{2+} > Ca^{2+}$, e. g., calcium ion is retarded to a great extent. Amino acid ions in acidic medium decrease in migrating velocity on SA-2 (lysine most remarkable), but do not decrease largely on WA-2 which does not dissociate so that the adsorption effect is small.

From the above observation, it was confirmed that the synergetic effect of electromigration and ion-exchange adsorption exerts, and this method offers the practical application to separation of ions and is interesting in connection with the ionic transport behavior across the ion-exchange membranes.

The Institute of Industrial Science
The University of Tokyo
Yayoi-cho, Chiba

1) M. M. Tuckerman, *Anal. Chem.*, 30, 231 (1958); H. R. Roberts and M. G. Kolor, ibid., 31, 565 (1959); H. T. Peterson, Jr., ibid., 31, 1279 (1959).

* In neutral and alkaline medium the similar results are obtained but calcium ion is retarded to some extent.

2) T. Yamabe, M. Senō, T. Tanaka and I. Kamii., This Bulletin, 33, 1740 (1960).

Protection of Amide-Nitrogen for Peptide Synthesis. A Novel Synthesis of Peptides Containing C-Terminal Glutamine

By Shiro AKABORI, Shumpei SAKAKIBARA and Yasutsugu SHIMONISHI

(Received January 11, 1961)

It is known that troublesome side reactions[1] occur in the synthesis of asparagine- or glutaminepeptides due to the instability of the β- or γ-amide groups. Therefore, a suitable protection of amide nitrogen is desirable, in which the protecting group should be easily removable after formation of the peptide bonds. Frankel et al.[2] reported that removal of the benzyl group from N^{β}-benzyl-asparagine was very difficult because of the unexpected stability of the group.

In the present work, glycyl-L-glutamine and L-alanyl-L-glutamine ware prepared using xanthydrol[3] (I) as a protective agent by the following procedures. N^{α}-Cbzo*-N^{γ}-xanthyl-L-glutamine (II) was prepared from N^{α}-cbzo-L-glutamine (III) in glacial acetic acid containing an equimolar amount of I. Yield 80%; m. p. 182~183°C, $[\alpha]_D^{17}$ −5.7° (*c* 5.7, dimethylformamide). Found: C, 66.36; H, 5.55; N, 6.13. Calcd. for $C_{26}H_{24}O_6N_2 \cdot 1/2H_2O$: C, 66.52; H, 5.37; N, 5.97%.

When II was treated with hydrogen bromide in glacial acetic acid, L-glutamine (IV) was recovered in 55% yield. IV had the same optical activity with the glutamine which was obtained directly from the starting material III, m. p. 187°C, $[\alpha]_D^{32.5}$ +6.4° (*c* 2.8, H_2O). It is interesting that N^{γ}-xanthyl-L-glutamine (V) was not obtained from IV and I in acetic acid. The substance V was first obtained by selective hydrogenation of II in ethanol using palladium-charcoal as catalyst; m. p. 222°C (dicomp.). Found: C, 65.71; H, 5.60; N, 8.97. Calcd. for $C_{18}H_{18}O_4N_2$: C, 66.24; H, 5.56; N, 8.58%.

Synthesis of Glycyl-L-glutamine. — N^{α}-Cbzo-N^{γ}-xanthyl-L-glutamine methylester (VI) was prepared from II in dioxane by treatment with diazomethane. Recrystallization of VI from dioxane gave fine colorless needles (80~85%); m. p. 235~235.5°C. Found: C, 68.21; H, 5.58; N, 5.94. Calcd. for $C_{27}H_{26}O_6N_2$: C, 68.34; H, 5.52; N, 5.90%. The cbzo-group was removed by catalytic hydrogenation, and N^{γ}-xanthyl-L-glutamine methylester acetate (VII) was obtained as colorless needles (67%); m. p. 148~148.5°C. Fuond: C, 62.72; H, 6.07; N, 6.90. Calcd. for $C_{21}H_{24}O_6N_2$: C, 62.99; H, 6.04; N, 7.00%. Substance VII was coupled with cbzo-glycine *p*-nitrophenylester (VIII) in anhydrous chloroform[4,5], and cbzo-glycyl-N^{γ}-xanthyl-L-glutamine methylester (IX) was obtained as fine colorless needles after recrystallization from dioxane (70%); m. p. 184°C. Found: C, 65.49; H, 5.64; N, 7.89. Calcd. for $C_{29}H_{29}O_7N_3$: C, 65.52; H, 5.50; N, 7.91%. The product IX was carefully saponified in dioxane using *N*-sodium hydroxide, and cbzo-glycyl-N^{γ}-xanthyl-L-glutamine (X) was obtained. It was recrystallized from methanol-toluene (4 : 1) and water (77%): m. p. 198°C. Found: C, 65.17; H, 5.39; N, 8.04; eq. wt.: Na, 516. Calcd. for $C_{28}H_{27}O_7N_3$: C, 64.98; H, 5.26; N, 8.12%; mol. wt. 517.5. Treatment of X with hydrogen bromide, foffowed by purification by Amberlite IR-4B, gave glycyl-L-glutamine monohydrate (XI) in 70% yield; m. p. 206°C (decomp.). Found: C, 38.02; H, 7.02; N, 19.12. Calcd. for $C_7H_{13}O_4N_3 \cdot H_2O$: C, 38.00; H, 6.84; N, 19.00%. $[\alpha]_D^{15} = -1.8°$ (*c* 3.8, water). Thierfelder[6] reported; m. p. 199~200°C, $[\alpha]_D^{15}$ −2.47° (*c* 4.20, water).

Synthesis of L-Alanyl-L-glutamine. — Cbzo-L-alanyl-N^{γ}-xanthyl-L-glutamine methyl ester (XII) was prepared by coupling cbzo-L-alanine *p*-nitrophenyl ester with VII in the same manner, and was recrystallized from ethanol (90%); m. p. 208°C (decomp.). Found: C, 65.17; H, 5.69; N, 7.79. Calcd. for $C_{30}H_{31}O_7N_3$: C, 66.04; H, 5.73; N, 7.70%. L-Alanyl-L-glutamine monohydrate was obtained from XII by the similar procedure to that of XI, m. p. 214~215°C (decomp.). Found: C, 40.42; H, 7.52; N, 17.82. Calcd. for $C_8H_{15}O_4N_3 \cdot H_2O$: C, 40.84; H, 7.28; N, 17.86%. $[\alpha]_D^{14} = +11.4°$ (*c* 3.70, water).

Detailed results will be published elsewhere.

Institute for Protein Research
Osaka University
Kita-ku, Osaka

1) J. Rudinger, *Angew. Chem.*, **71**, 742 (1959).
2) M. Frankel, Y. Liwschitz and A. Zilkha, *J. Am. Chem. Soc.*, **75**, 3270 (1953).
3) R. F. Phillips et al., *J. Org. Chem.*, **8**, 1355 (1943).
* Cbzo.....carbobenzoxy.
4) R. Schwyzer and P. Sieber, *Angew. Chem.*, **68**, 518 (1956).
5) M. Bodanszky and V. du Vigneaud, *J. Am. Chem. Soc.*, **81**, 5688 (1959).
6) H. Thierfelder et al., *Z. Physiol. Chem.*, **105**, 58 (1919).

Steric Configuration of the α, β-Diaminobutyric Acid Isolated from the Antibiotic Glumamycin

By Masahiko FUJINO, Michitaka INOUE, Jisaburo UEYANAGI and Akira MIYAKE

(Recived February 20, 1961)

Inoue[1] previously isolated α, β-diaminobutyric acid from the acid hydrolysate of glumamycin, an acidic peptide antibiotic. Martin et al.[2] also reported the separation of α, β-diaminobutyric acid from Aspartocin, an antibiotic resembling glumamycin. Although both products seem to have the same configuration from their optical rotation, this has so far not been studied. Inoue has shown[3] that only one β-amino group of the two α, β-diaminobutyric acids* of glumamycin is free.

The configuration of the α-amino group has been studied by conversion of free amino group of glumamycin into a hydroxyl group and subsequent hydrolysis to α-amino-β-hydroxybutyric acid, and that of the β-amino group by oxidation of α, β-diaminobutyric acid to alanine.

Glumamycin was treated with sodium nitrite in 80% acetic acid to convert the free amino group into hydroxyl and the resulting hydroxyglumamycin was hydrolyzed with hydrochloric acid. The reaction mixture was developed on a column of Dowex 50x4 (200 ~ 400 mesh) with ammonium formate buffer (pH 3.4)[4] and the crystals obtained from the threonine fraction of the eluate were recrystallized from aqueous ethanol (Found: C, 40.06; H, 7.81; N, 11.90. Calcd. for $C_4H_9O_3N$: C, 40.33; H, 7.62; 11.76%). The product was found to be a mixture of threonine and allothreonine by paper chromatography with *n*-butalnol·acetone·ammonia·water (50: 6.25: 6.25: 37.5)[5]. However, since the β-position of α, β-diaminobutyric acid of glumamycin may undergo partial Walden inversion under the conditions, it is impossible to decide the configuration of the α-carbon atom directly from the optical rotation of the product. But DNP-L-threonine and DNP-L-allothreonine exhibit the same optical rotation, $[M]_D^{25} = +305°$ (4% sodium bicarbonate)[6]. The above product was converted into its DNP-derivative by the method of Levy[7] and then subjected to chromatography on Amberlite IRC-50 according to the method of Seki[8] to remove the DNP-OH which formed as a by-product. DNP-derivative showed an optical rotation of $[M]_D^{24} = -294° \pm 14$ (*c* 0.48, 4% sodium bicarbonate) and its yield was 92%. This fact shows that above product is a mixture of D-threonine and D-allothreonine, therefore α-carbon atom of α, β-diaminobutyric acid has the D-configuration. Further, as α, β-diaminobutyric acid obtained from the hydrolysate of hydroxy-glumamycin, and that obtained from the hydrolysate of glumamycin have the same optical rotation and physical properties, the two moles of α, β-diaminobutyric acid in glumamycin evidently have the same steric configuration.

Oxidation of α, β-diaminobutyric acid with hydrogen peroxide was conducted by the method of Dakin[9]. Namely, the compound was allowed to react with 2 mol. of 3% hydrogen peroxide at 50°C for one hour. The reaction mixture was passed through a column of Amberlite IR-120, the column was eluted with N-ammonium hydroxide, and the effluent was concentrated to give D-alanine (Found: C, 40.51; H, 7.88; N, 15.44%), $[\alpha]_D^{20} = -16$, (*c* 1, 6 N hydrochloric acid) which was confirmed by infrared spectrum and paper chromatography.

Thus, it was found that the β-carbon atom of α, β-diaminobutyric acid belongs to the D-series, and consequently α, β-diaminobutyric acid takes D-erythro-configuration.

The authors wish to express their sincere thanks to Dr. Satoru Kuwada, the Director of Research Laboratories, Dr. Sueo Tasuoka, Vice Director of Research Laboratories, Dr. Kuniyoshi Tanaka, the Head of 2nd Division of Research Laboratories for their guidance and encouragement.

Research Laboratories
Takeda Chemical Industries, Ltd.
Higashiyodogawa-ku, Osaka

1) M. Inoue et al., This Bulletin, **33**, 1014 (1960).
2) J. H. Martin and W. K. Hausmann, *J. Am. Chem. Soc.*, **60**, 2079 (1960).
3) M. Inoue, in press.
* It is already recognized that glumamycin contains two moles of α, β-diaminobutyric acid and both amino groups of one mole are not free.
4) C. H. W. Hirs, S. Moore and W. H. Stein, *J. Biol. Chem.*, **195**, 669 (1952).
5) K. N. F. Shaw and S. W. Fox, *J. Am. Chem. Soc.*, **75**, 3421 (1953).
6) K. R. Rao and H. A. Sober, ibid., **76**, 1328 (1954).
7) A. L. Levy, *Nature*, **174**, 126 (1954).
8) T. Seki, *Chemistry of Proteins* (*Tokyo*), **4**, 209 (1956).
9) H. D. Dakin, *J. Biol. Chem.*, **1**, 171 (1905); **4**, 63 (1908).

The Structure of Todomatuic Acid. Synthesis of (±)-Dihydro-desoxo-todomatuic Acid

By Masao NAKAZAKI and Sachihiko ISOE

(Received March 6, 1961)

Todomatuic acid, $C_{15}H_{24}O_3$, monocyclic unsaturated keto-acid (m. p. 58.5°C, b. p. 200~215°C/3 mmHg, $[\alpha]_D^{32.5}+85.84°$; semicarbazone, m. p. 193.2~193.7°C), was first isolated by Tuchihashi and Hanzawa[1] on hydrolysis of the high boiling fraction of an oil, obtained as a by-product when *Abies sachalinensis* Mast. (to do matu) was digested with sulfite in pulp industry.

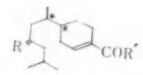

Ia R=O R'=OH
b R=H$_2$ R'=OH
c R=H$_2$ R'=OCH$_3$

The structure Ia was advanced by Momose[2], mainly by the results of oxidative degradation of Ia with potassium permanganate which gave oxalic acid and an acyclic saturated keto-dicarboxylic acid (II), $C_{13}H_{22}O_5$ (semicarbazone, decomp. p. 185~186°C). Further oxidation of II with nitric acid gave isovaleric acid and β-(α-carboxyethyl)glutaric acid. Among various possible structures which satisfy the results of the degradation, Ia was favored because Ia is compatible with the isoprene rule.

In this communication, the synthesis of (±)-dihydro-desoxo-todomatuic acid (Xb) is reported.

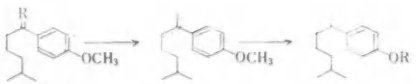

IIIa R=O IV Va R=CH$_3$
b R=OH, CH$_3$ b R=H

(4-Anisyl)-isohexyl ketone (IIIa) (b. p. 131~133°C/1 mmHg; semicarbazone, m. p. 124~125°C) obtained by Friedel-Crafts reaction of anisole with isocaproyl chloride, was converted into IIIb by Grignard reaction with methylmagnesium bromide, and then IIIb was dehydrated by boiling with acetic anhydride to the unsaturated phenol ether IV (b. p. 109~115°C/1 mmHg).

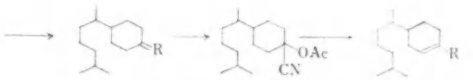

VIa R=OH, H VII VIIIa R=CN
b R=O b R=COOH

Catalytic hydrogenation of IV gave Va (b. p. 107~113°C/1 mmHg), which was hydrolyzed by boiling with hydroiodic acid in acetic acid to afford the phenol Vb (b. p. 127~128°C/1 mmHg). High pressure catalytic hydrogenation of Vb (Raney nickel, 130 atms., 30°C) yielded the alcohol VIa (b. p. 120~121°C/1 mmHg), which was oxidized with potassium dichromate in sulfuric acid to the ketone VIb (b. p. 113~114°C/1 mmHg; semicarbazone, m. p. 149~150°C). The cyanohydrin acetate VII (b. p. 145~147°C/1 mmHg) prepared from VIb with potassium cyanide and acetic anhydride, was pyrolyzed by passing through a heated Pyrex tube(600°C) packed with ceramic Raschig rings to give unsaturated cyanide VIIIa, which was then hydrolyzed to the unsaturated acid VIIIb (b. p. 163~165°C/1 mmHg).

IXa R=OH Xa R=OCH$_3$
b R=OCH$_3$ b R=OH
c R=NHC$_6$H$_5$
(or its antipode) (or its antipode)

Although two racemic forms are expected for the structure VIIIb, the infrared absorption spectrum of synthetic VIIIb was found superimposable on that of (+)-desoxo-todomatuic acid (Ib) (m. p. 59~60°C, $[\alpha]_D^{27}+94.3°$ in ethanol; anilide, m. p. 78~79°C) obtained by Wolff-Kishner reduction of Ia. Catalytic hydrogenation of the methyl ester Ic of natural Ib gave saturated methyl ester IXb in which only one asymmetric center remains.

Heating with sodium methoxide converted IXb into more stable methyl ester Xa, which was hydrolyzed to give (+)-dihydro-desoxo-todomatuic acid (Xb) (b. p. 150~153°C/1 mmHg, n_D^{18} 1.4723, $[\alpha]_D^{27}+14.1°$ in ethanol; anilide Xc, m. p. 115~116°C). Following the same procedure, racemic IXb gave (±)-dihydro-desoxo-todomatuic acid (Xb) (b. p. 152~155°C/1 mmHg, n_D^{18} 1.4723; anilide, Xc

1) R. Tuchihashi and T. Hanzawa, *J. Chem. Soc. Japan, Pure Chem. Sec.* (*Nippon Kagaku Zasshi*), **61**, 1041 (1940).
2) T. Momose, *J. Pharm. Soc. Japan* (*Yakugaku Zasshi*), **61**, 288 (1941).

m. p. 105~106°C). The infrared absorption spectra of racemic Xb, Xc and natural Xb, Xc were found superimposable in every detail.

These findings firmly establish the structure of todomatuic acid.

Department of Chemistry
Institute of Polytechnics
Osaka City University
Kita-ku, Osaka

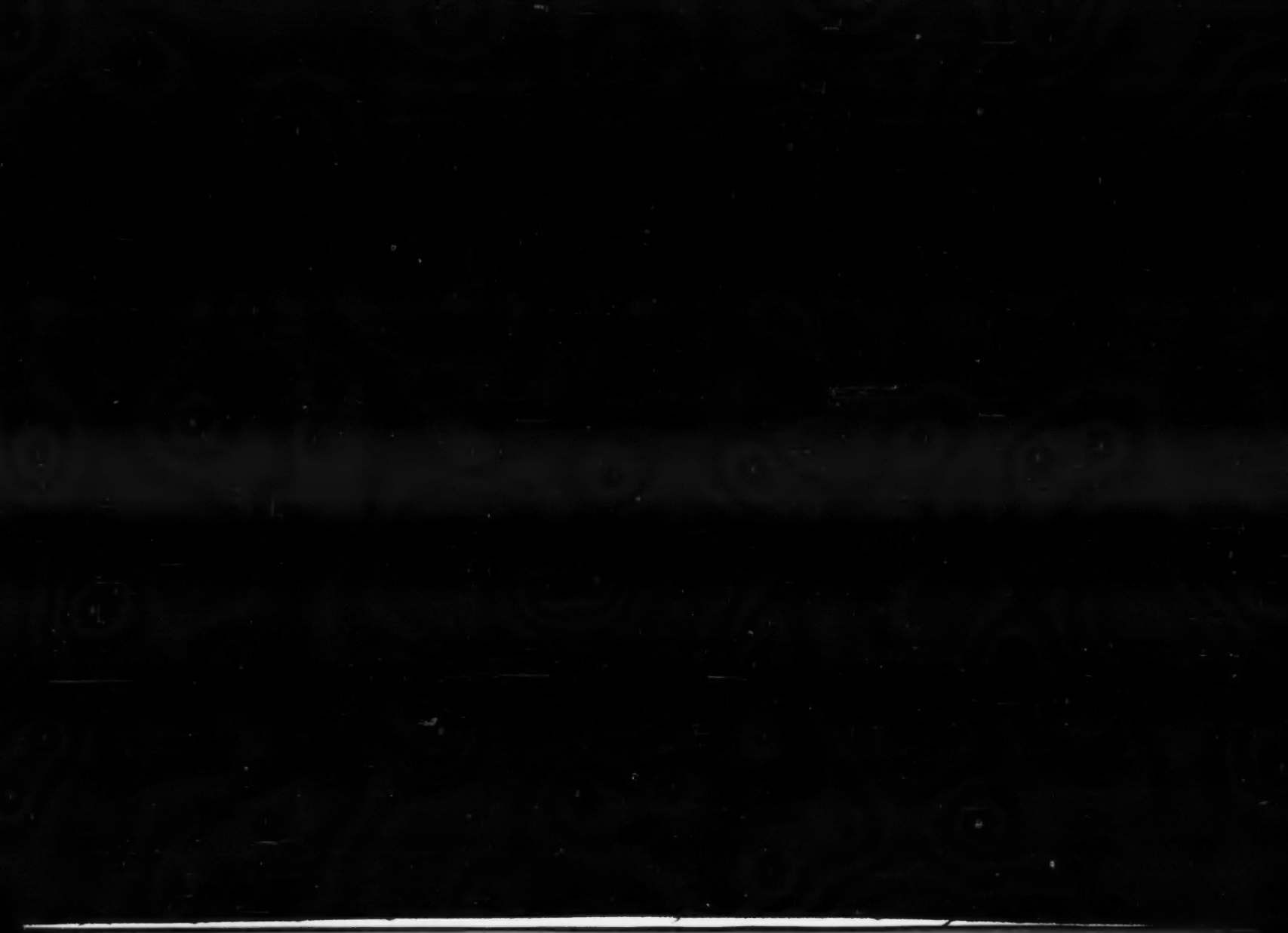

6

昭和33年12月25日　昭和36年6月8日 印刷［毎月1回
第3種郵便物認可　昭和36年6月15日 発行］15日発行

CHEMISTRY HALL LIBRARY

BULLETIN

OF THE

CHEMICAL SOCIETY OF JAPAN

STATE
UNIVERSITY
AUG 19 1961
LIBRARY

Vol. 34 No. 6 June 1961

CONTENTS

General and Physical

Nuclear Magnetic Resonance Study of the Steric Effect in Dimethylphenols . . . I. YAMAGUCHI 744
A UAO Treatment of the van der Waals Force . . . . . T. YONEZAWA, H. KATO, K. MOROKUMA and K. FUKUI 747
On the Electrical Conductivity of the Organic Thin Films: Perylene, Coronene and Violanthrene . . . . . H. INOKUCHI, H. KURODA and H. AKAMATU 749
Proton Magnetic Resonance Studies on the Thermally Dehydrated Products of Alumina Trihydrate . . . . . T. SAITO 757
Infrared Spectra of Water of Crystallization in Some Inorganic Chlorides and Sulfates. . I. GAMO 760
Infrared Absorption Spectra of Water of Crystallization in Copper Sulfate Penta- and Monohydrate Crystals . . . . . I. GAMO 764
Polymerization of Propylene with Tin Tetraalkyl-Titanium Tetrachloride Catalyst . . . . . N. ASHIKARI and M. HONDA 767
On the pd Hybridization of the Sulfur Atom in Thiothiophten. I. The Calculations of the Overlap Integrals Involving d Orbitals . . . . . K. MAEDA 785
The Effects of pH on the Flocculation of Quartz Aqueous Suspensions . . . . . T. OHYAMA, J. SHIMOHZAKA and S. USUI 790
Differential Thermal Analysis of Aluminum Soaps . . . . . S. SHIBA 804
Differential Thermal Analysis of the Systems Aluminum Soap-Hydrocarbon. . . . . S. SHIBA 809
Diffusion in Glassy Polymers. II. Effects of Polymer-penetrant Interaction; Diffusion of Ethyl Methyl Ketone in Atactic Polystyrene . . . . . H. ODANI, J. HAYASHI and M. TAMURA 817
Infrared Spectra of Acyclic Imides. III. Infrared Dichroism of Dipropionamide and *N*-Acetylpropionamide Crystals . . . . . T. UNO and K. MACHIDA 821
Theory on the Light Scattering of High Polymer Solutions Considering the Anisotropy of Segments . . . . . M. NAKAGAKI 834
Iodine-catalyzed Thermal cis-trans Isomerization of Azobenzene . . . . . S. YAMASHITA 842
n-π Absorption Spectra of Some Aliphatic Aldehydes. . . . . H. OSHIMA 846
A Molecular Orbital Treatment of Triallyl Isocyanurates and Related Allyl Esters . . . . . K. FUKUI, H. KATO, T. YONEZAWA, F. TANIMOTO and H. KITANO 851
Studies on the Chemical Equilibrium Lag during the Rapid Expansion through the Rocket Nozzle. . . . . S. TSUCHIYA 854
Infrared Spectra and the Structure of Some Metal-oxamide Complexes . . . . . Y. KURODA, M. KATO and K. SONE 877

Analytical and Inorganic

Spectrophotometric Determination of Nitrite in Nitrate and Sulfate. . . . . Y. KATSUBE, K. UESUGI and J. H. YOE 743
Spectrophotometric Determination of Uranium with Sodium 2'',6''-dichloro-4'-hydroxy-3,3'-dimethylfuchsone-5,5'-dicarboxylate . . . . . Y. KATSUBE, K. UESUGI and J. H. YOE 826
Studies on Metal Complex Species Using an Anion Exchange Resin. I. Derivation of Equations and Application to Mercury(II)-Nitrate Complex. . . . . H. WAKI 829
Solvent Extraction of Inorganic Nitrates with Diphosphonate Ester. I. Zirconium, Yttrium and Lanthanide Nitrates . . . . . H. SAISHO 859

(Continued on inside cover)

Published by the Chemical Society of Japan

THE CHEMICAL SOCIETY OF JAPAN
(NIPPON KAGAKUKAI)

Founded in 1948

Successor to the former Chemical Society of Japan founded in 1878 and to the Society of Chemical Industry, Japan founded in 1898.

BULLETIN OF THE CHEMICAL SOCIETY OF JAPAN

Editor: Tadao SHIBA, Tokyo Institute of Technology, Tokyo
Assistant Editor: Tadashi SUEHIRO, Gakushuin University, Tokyo
Editorial Board:

Yoshié BANSHO	Hidehiro GOTÔ	Keniti HIGASI
Yoshimasa HIRATA	Hiroo INOKUCHI	Tatsujiro ISHIMORI
Tadashi KAMIKUBO	Michio KOBAYASHI	Ichiro MIYAGAWA
Masazumi NAKAGAWA	Shigeru OAE	Shigeru OHASHI
Kazuo SATAKE	Syûzô SEKI	Osamu SIMAMURA
Yoshitada TOMODA	Iwao YASUMORI	Koshiro YOSHIOKA

(Continued from outside cover)

Organic and Biological

Studies on the Chemical Decomposition of Simple Sugars. X. Acetol Formation from ^{14}C-Labeled Hexoses . . . . . R. GOTO, J. HAYAMI, K. KUDO and S. OTANI 753
Neutron and γ-Irradiation of Propionamide . . . . . E. TACHIKAWA and G. TSUCHIHASHI 770
Stereochemistry and Mechanisms of Catalytic Hydrogenolysis and Hydrogenation. I. Catalytic Hydrogenolysis of Optically Active Compounds with Raney Nickel . . . . . S. MITSUI and S. IMAIZUMI 774
Dehydrogenation of Secondary Alcohols with Reduced Copper. IV. Catalytic Dehydrogenation of Isopropyl Alcohol (Part 2) . . . . . K. KAWAMOTO 795
Dehydrogenation of Secondary Alcohols with Reduced Copper. V. Catalytic Dehydrogenation of *sec*-Butyl Alcohol . . . . . K. KAWAMOTO 799
The Preparation of Diethyl Phosphate . . . . . T. MUKAIYAMA and T. FUJISAWA 812
Non-benzenoid Aromatic Heterocycles. V. An Attempted Synthesis of 4,7-Dihydro-4,7-phenanthroline Derivatives. . . . . H. KATO and M. OHTA 814
The Mannich Base of Troponoid and its Application. V. On the Mannich Base of 3-Isopropyltropolone (α-Thujaplicin). . . . . K. OGURA 839
Cyclic Acetylenes. V. Syntheses and Properties of Strained Cyclic Ethers of *o,o'*-Dihydroxydiphenyldiacetylene . . . . . F. TODA and M. NAKAGAWA 862
Cyclic Acetylenes. VI. Transannular and Proximity Effects in the Cyclic Derivatives of *o,o'*-Dihydroxydiphenyldiacetylene. . . . . F. TODA and M. NAKAGAWA 874

Applied

Fischer-Tropsch Synthesis with Tubular Reactor of 18.1 l. Catalyst Bed. I. Reactor with Constant Temperature Wall . . . . . M. KURAISHI, M. KURITA, T. HOSOYA, H. ICHINOKAWA, K. OGAWA and H. UCHIDA 780

Short Communications

Nuclear Magnetic Resonance of Tar Products. II . . . . . S. FUJIWARA and T. WAINAI 881
The Crystallinity of Polyaldehydes . . . . . H. SOBUE and H. KUBOTA 883
Syntheses of Two Kinds of Metal-free Tetra-azaporphines by the Urea-melt Method. N. FUKADA 884
Constituents of the Antibiotic, Glumamycin . . . . . M. INOUE 885
Anionoid Substitution of Bromo-3,4-benzotropolones . . . . . S. EBINE 887
The Synthesis of 3-α-Carboxyethylcyclopentanol Lactone . . . . . T. TANAKA 888
4,5-Dimethoxycanthin-6-one and 2,6-Dimethoxy-*p*-benzoquinone from *Picrasma ailanthoides* Planchon . . . . . N. INAMOTO, S. MASUDA, O. SIMAMURA and T. TSUYUKI 888
The Crystal Structure of Phenazine-5,10-dioxides . . . . Y. NAMBA, T. ODA and T. WATANABÉ 889
Synthesis of Isoxazolecarboxylic Acids from Schiff Bases and Nitroacetate. . . . . S. ZEN and S. UMEZAWA 890
Polarographic Studies of Metallic Complexes. VI. Tetracyanocobaltate(III) Complex. . . . . N. MAKI and R. TSUCHIDA 891
Catalytic Dimerization of Monoalkyl Acetylenes . . . . . N. HAGIHARA, M. TAMURA, H. YAMAZAKI and M. FUJIWARA 892
Electron Spin Resonance of Tetracene-Antimony Pentachloride . . . . . Y. MATSUNAGA 893

Spectrophotometric Determination of Nitrite in Nitrate and Sulfate

By Yukiteru KATSUBE, Katsuya UESUGI and John H. YOE

(Received November 17, 1960)

The purpose of this paper is to develop a rapid and sensitive method for the spectrophotometric determination of trace amounts of nitrite in the presence of large amounts of nitrate and sulfate. The method is based on the colored compound formed by the reaction between disodium 1-(4′-aminobenzeneazo)-2-amino-8-hydroxynaphthalene-2′, 6-disulfonate and nitrous acid. Details of this compound have been described in our previous paper[1].

For the determination of trace amounts of nitrite useing this compound, seventeen kinds of ions were found to cause the interference (As^{3+}, Fe^{3+}, $Ce^{3+,4+}$ *, $Hg^{+,2+}$, Mn^{2+}, $Sn^{2+,4+}$, Ti^{4+}, Zr^{4+}, Br^-, F^-, I^-, MnO_4^-, MoO_4^{2-}, SeO_3^{2-}**). The study of the effect of other ions in the previous paper suggested the possibility that they could be used for the determination of nitrite in nitrate and sulfate without any special procedure.

Experimental

The apparatus and reagents were the same as those used in our previous work.

Procedure.—Transfer to a 25 ml. volumetric flask 1 ml. of the sample solution adjusted so as to contain 5 to 60 p.p.m. of nitrous acid. Add 20 ml. of distilled water, and 2.5 ml. of 0.05% reagent solution. Add 0.3 ml. of 6 N hydrochloric acid and shake well. Bring up to the mark with distilled water, thoroughly mix and, after ten minutes, measure the absorbance at 625 mμ, using a reagent blank solution*** as a reference.

Results

The determination of nitrite in the presence of nitrate and sulfate was made. The results are given in Table I.

Summary

A simple procedure has been developed for the determination of trace amounts of nitrite in large amounts of nitrate and sulfate, with disodium 1-(4′-aminobenzeneazo)-2-amino-8-hydroxy-naphthalene-2′, 6-disulfonate. The method is accurate and precise.

TABLE I. DETERMINATION OF NITROUS ACID

Taken HNO_2 p. p. m.	Added NO_3^- mg./25 ml.	Added SO_4^{2-} mg./25 ml.	Absorbance* at 625 mμ	Standard deviation in absorbance unit
0.20			0.080	0.002
	0.5		0.082	0.003
	50.0		0.076	0.003
	5000.0		0.082	0.003
		0.5	0.079	0.002
		50.0	0.079	0.003
		5000.0	0.082	0.004
	500.0	500.0	0.079	0.004
0.75			0.307	0.002
	500.0	500.0	0.304	0.004

KNO_3 and K_2SO_4 were used to make up the solution.

* These values were the averages of six replicate determinations.

1) Y. Katsube and J. H. Yoe, This Bulletin, 33, 190 (1960).

* In the previous paper, the reagent was tested with 67 kinds of ions not including Ce^{4+}.

** In the previous paper, SeO_3^{2-} was mistyped as CeO_3^{2-}.

*** Use the sample solution as the reference when the sample contains Cu^{2+} or Ni^{2+}.

Himeji Technical Institute
(Y. K. & K. U.)

John Lee Pratt Trace Analysis Laboratory
University of Virginia
Charlottesville, Va., U. S. A.
(J. H. Y.)

Nuclear Magnetic Resonance Study of the Steric Effect in Dimethylphenols

By Ichiro YAMAGUCHI

(Received November 9, 1960)

In their various physicochemical properties, six isomers of dimethylphenol (xylenol) were observed to be slightly different from each other[1-5]. These differences have been ascribed mainly to the difference in the steric effect of the methyl group on the formation of an intermolecular hydrogen bond. The present author observed obvious differences among the nuclear magnetic resonance spectra of dimethylphenols. The difference could be closely correlated with the position of the methyl groups in the benzene ring relative to the hydroxyl group.

Experimental

NMR measurements were carried out at 20°C with a Varian High Resolution NMR spectrometer operated at 56.4 Mc. The dimethylphenols measured were guaranteed grade reagents. The solvents used were carbon tetrachloride and acetone. These were purified with a Podobiedniak fractional distillator. The values of the chemical shift were obtained referring to an external reference of water in a capillary, and the correction for bulk diamagnetic susceptibility was made. The solubility of dimethylphenols in carbon tetrachloride was poor except for 2,4-dimethylphenol. Therefore the measurements were made up to their saturated solutions at 20°C.

Results and Discussion

Figure 1 shows the chemical shift-concentration diagrams for dimethylphenols in carbon tetrachloride solution. The curves with the highest chemical shift are due to methyl protons, and the ones with lower chemical shift are due to benzene ring protons and hydroxyl proton (thick line). The resonance fields for the methyl protons and the ring protons decrease on dilution. This is a characteristic feature of aromatic systems and is ascribed to the effect of the ring current in the neighboring solute molecules. The detailed results and discussions for each proton group are described as follows.

Methyl Proton Resonance. The methyl protons in 3,4- and 3,5-dimethylphenols give only one resonance line. This means that the difference between the screening constants for *m*- and *p*-Me protons is so small that it can not be observed. In contrast to this, the

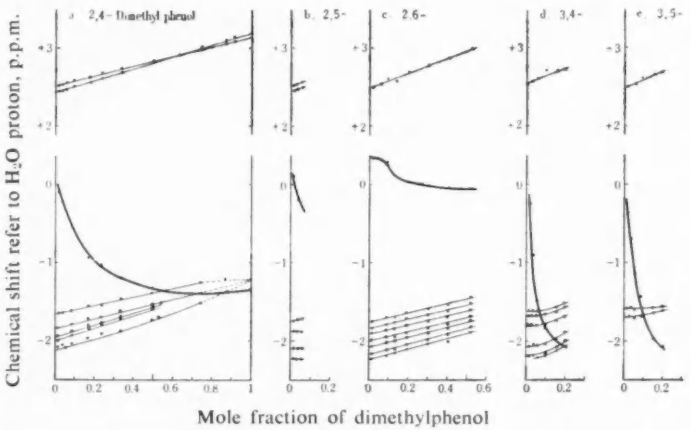

Fig. 1. Concentration dependence of chemical shift for CCl_4 solutions of dimethylphenols.

1) W. C. Sears and L. J. Kitchem, *J. Am. Chem. Soc.*, **71**, 4110 (1949).
2) A. Burawoy and J. T. Chamberlain, *J. Chem. Soc.*, **1952**, 2310.
3) M. Neuilly, *Compt. rend.*, **238**, 781 (1954).
4) W. Suetaka and M. Sanesi, *Ann. chim. (Rome)*, **46**, 1133 (1956).
5) D. Bono, *Bull. soc. chim. France*, **1956**, 1368; *Compt. rend.*, **242**, 375, 637 (1956).

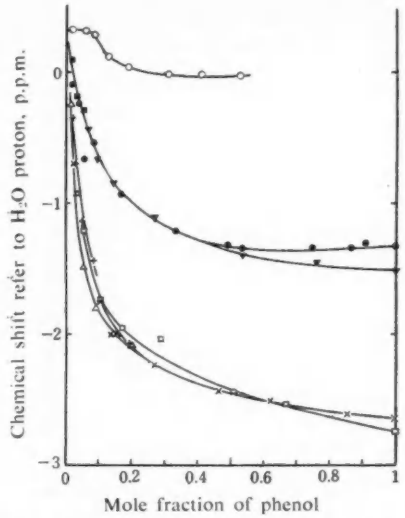

Fig. 2a. Concentration dependence of chemical shift of OH proton in various methyl phenols in CCl_4 solution.

- 2,4-Dimethylphenol
- 2,5- 〃
- 2,6- 〃
- 3,4- 〃
- 3,5- 〃
- *o*-Cresol[a)]
- *m*- 〃 [a)]
- *p*- 〃 [a)]

a) I. Yamaguchi, unpublished work.

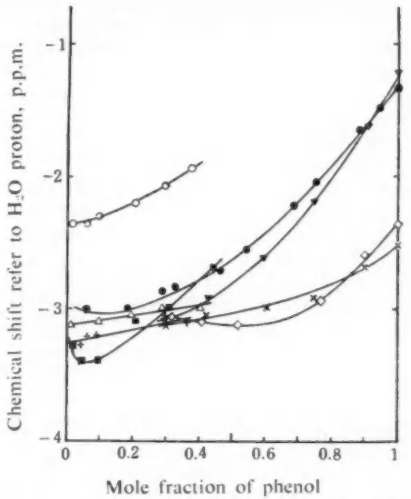

Fig. 2b. Concentration dependence of chemical shift of OH proton in various methylphenols in acetone solution.

- 2,4-Dimethylphenol
- 2,5- 〃
- 2,6- 〃
- 3,4- 〃
- 3,5- 〃
- *o*-Cresol[b)]
- *p*- 〃 [b)]
- Phenol[b)]

b) R. L. Batdort, Ph. D. Thesis, Univ. of Minnesota, 1955.

methyl protons in both 2,4- and 2,5-dimethylphenols give two resonance lines caused by the difference between the screening constants of the protons in 2(*o*)-Me group and that in 5(*m*)- or 4(*p*)-Me group. Furthermore, the two resonance curves for 2,4-dimethylphenol intersect each other at an intermediate concentration of carbon tetrachloride solution. Thus the concentration dependence of the resonance in 2(*o*)-Me protons is clearly different from that in 4(*p*)-Me protons. This suggests that the 2(*o*)-Me protons interact strongly with the OH group owing to the proximity of the two groups to each other.

Several effects are considered to induce the specific interaction between the groups. They might be the inductive and mesomeric effects of the OH group, effect of the electrostatic field[6)] originating from the bond moment of the OH group, or the effect of the dispersion force. The interaction caused by each effect should be greater with the *o*-Me protons than with the *m*- or *p*-Me protons. The magnitude of these effects would be affected by the change in the hydrogen bonding situations of the OH group. Therefore, the resonance line for the *o*-Me protons might be displaced by the change in the concentration of the solution in a way different from that for the *m*- or *p*-Me protons. However, it is unfortunately impossible to treat the resultant effect quantitatively. And at the present stage, we can not decide which curve should be assigned to *o*-Me protons.

Hydroxyl Proton Resonance.—Fig. 2 shows the concentration dependence of the chemical shift of the OH proton in dimethylphenols and cresols. Fig. 2a is of carbon tetrachloride solutions and Fig. 2b is of acetone solutions. Three types of the curves with distinctly different concentration dependence from one another are observed in the figures. The first group (a) at the highest field includes 2,6-dimethylphenol, the second (b) at the middle 2,4- and 2,5- dimethylphenols and *o*-cresol, and the third (c) at the lowest 3,4- and 3,5-dimethylphenols and *m*- and *p*-cresols. At the concetration of 1 mol. fraction (pure phenol), the values of the chemical shift are

6) A. D. Buckingham, *Can. J. Chem.*, **38**, 300 (1960).

about (a) +0.1 p.p.m., (b) −1.3 p.p.m. and (c) −2.5 p.p.m. This classification clearly correlates with the location of the methyl groups in the molecule: The phenol in (a) has two methyl groups at both the ortho positions to the OH group, and those in (b) and (c) have one and no methyl group ortho to the OH respectively. The methyl groups at the meta and para positions do not take part in this classification. In carbon tetrachloride solutions, all of the curves approach about +0.3 p.p.m. at the concentration of infinite dilution (extrapolated). Therefore, it would be reasonable to consider that in a free single molecule the effect of the *o*-Me group on the screening constant of a non-hydrogen bonded OH proton is very small.

These results that the difference in the resonance field of the OH proton among the isomers may primarily be ascribed to the steric hindrance of the *o*-Me group to form the intermolecular hydrogen bond. The values of the chemical shift for pure phenols may correlate with the extent of the steric effect of the methyl group on the hydrogen bond formation.

A flat range was observed for 2,6-dimethylphenol below the concentration of 0.05 mol. fractions. This implies the complete dissociation of the intermolecular hydrogen bond at the concentration range. This is an evidence that the two methyl groups at the 2(*o*)- and 6(*o*)-positions sterically inhibit the formation of the intermolecular hydrogen bond appreciably.

The concentration dependence of the chemical shift of the OH proton for the acetone solution is somewhat different from that for the carbon tetrachloride solution. For carbon tetrachloride solutions, the OH curve suggests a simple dissociation process of the intermolecular hydrogen bond on dilution. In contrast to this, for acetone solutions the curve shows a process to form a new hydrogen bond with acetone.

Ring Proton Resonance. The dimethylphenol molecule has only three ring protons giving a rather simple spectrum. Therefore, the assignment of each spectral line to one of the protons can be made without any strict mathematical treatment of the spectrum. Fig. 3 shows the spectra for the ring protons in dimethylphenols in carbon tetrachloride and in acetone solutions with a concentration of about 0.1 mol. fractions. The position of the resonance field for each proton is indicated with a thick line with the figure of the location in the ring referring to the OH group.

The width of the ring proton resonance spectrum decreases generally with the increasing concentration as shown in Fig. 1. From detailed examinations of these spectra, it appears that the *o*- and *p*-proton resonance lines are at a higher field than that for the *m*-proton, and the slope of the curves for *o*- and *p*-protons is gentle compared with that for *m*-proton. Thus the curves for these protons approach each other as the concentration increases. This is the cause of the decrease of the width. The different concentration dependences of *o*- and *p*-protons from that of *m*-proton may be ascribed to the change in the magnitude of the mesomeric effect of the OH group on the ring protons with the change in the hydrogen bonding situation.

The differences between the ring proton spectra for carbon tetrachloride solution and that for acetone solution are observed as shown in Fig. 3. These arose from the different situations of the molecule in different mediums; one is a nearly free, non-hydrogen bonded molecule in carbon tetrachloride solution and another a hydrogen bonded molecule with the solvent in acetone solution. A noticeably different point is the displacement of the *o*-proton resonance lines to a lower field for 2, X-dimethylphenols (X = 4 or 5) in acetone solution. It seems very probable that the displacement is caused by the formation of a hydrogen bond between the *o*-proton and the C=O group in an acetone molecule[7]: An

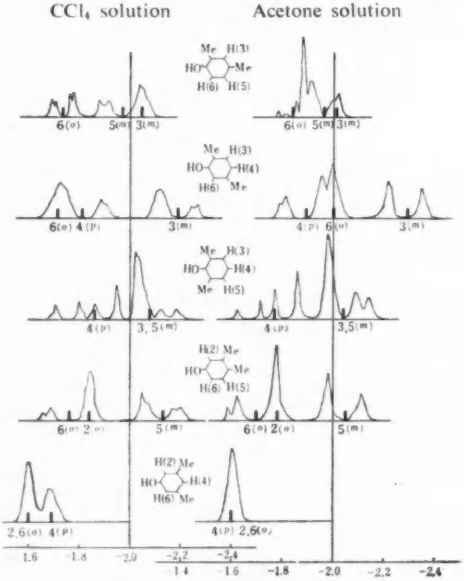

Fig. 3. Ring proton resonance spectra of dimethylphenols in CCl_4 and acetone solutions with concentration of about 0.1 mol. fraction.

7) T. Schaefer and W. G. Schneider, *J. Chem. Phys.*, 32, 1218 (1960).

acetone molecule forms a strong hydrogen bond with the OH group. Therefore this O–H bond would be orientated inevitably to the side of the *o*-proton because of the steric hindrance of the *o*-Me group, and a weak hydrogen bond would be formed between the *o*-proton and the C=O group because of the proximity of these groups. Thus the decreased electron density in *o*-proton caused by the formation of the hydrogen bond would displace the resonance field of the *o*-proton to a lower field.

In 2,6-dimethylphenol, two methyl groups would inhibit the formation of a hydrogen bond with any proton donor or acceptor. Therefore, merely a minute change is observed in the ring proton spectrum with the change is observed in the ring proton spectrum with the change in solvent and concentration. 3,X-dimethylphenols (X=4 or 5) also show minute changes in their ring proton spectra. These molecules have no *o*-Me group, and the OH group may be able to rotate freely about the C–O axis. Therefore, there is no specific steric effect on the *o*-protons. This would be a reason why the changes in solvent and concentration do not displace the *o*-proton resonance lines appreciably.

Summary

The nuclear magnetic resonance in dimethylphenols were observed. The dependences of the chemical shifts for the methyl, hydroxyl and ring protons on solvent and concentration were measured and several clear differences were observed among the spectra of the isomers. The phenols with one or two ortho methyl groups showed peculiar behaviors which may be ascribed to the interaction between the hydroxyl group and the ortho proton or ortho methyl protons. The evidience of the steric hindrance of the ortho methyl group to form an intermolecular hydrogen bond is also shown in the present measurements.

The author wishes to express his sincere thanks to Professor S. Fujiwara and Dr. A. Danno for their kind guidance and encouragement throughout the present work. His thanks are also due to Drs. N. Nakagawa, H. Shimizu and N. Hayakawa who discussed the problem and gave their valuable suggestions.

Radiation Application Division
Japan Atomic Energy
Research Institute
Tokai, Ibaragki-ken

A UAO Treatment of the van der Waals Force

By Teijiro YONEZAWA, Hiroshi KATO, Keiji MOROKUMA and Kenichi FUKUI

(Received November 17, 1960)

Dispersion forces for numerous molecules and atoms have been estimated by London's[1] and Slater-Kirkwood's[2] dispersion formula. However, the exact theoretical evaluation is nearly impossible to achieve except for the simplest molecules and atoms. Approximate formulas are usually used to estimate the magnitude of this force between them.

London's one-term approximation formula is written as:

$$\langle \Delta E \rangle_{AV} = -\frac{3}{2R^6} \frac{I_1 I_2}{I_1 + I_2} \alpha_1^0 \alpha_2^0 \qquad (1)$$

Here the subscripts refer to the two different molecules, α^0 is the polarizability, and I is taken to be equal to the ionization energies of the molecules.

In the present paper, non-empirical calculation is made on the dipole-dipole interaction term of dispersion force between two CH_4, NH_4^+ and H_2O molecules and two neon atoms by the perturbation theory. In the course of calculation, we make use of the UAO[3,4] (united atom approach or central field approximation) which was used to obtain ionization potential, dissociation energy and so on in simple molecules with nearly spherical configuration. By the UAO method, the total wave function for CH_4, NH_4^+ and H_2O which involves only three parameters is a ten-electron Slater determinant Φ with configuration $(1s)^2\ (2s)^2\ (2p)^6\ ^1S$ as same as neon atom. The one electron wave function of each molecule and atom is as follows:

1) F. London, *Trans. Faraday Soc.*, **33**, 8 (1937).
2) J. C. Slater and J. G. Kirkwood, *Phys. Rev.*, **37**, 682 (1931).
3) K. Funabashi and J. L. Magee, *J. Chem. Phys.*, **26**, 407 (1957).
4) M. J. M. Bernal, *Proc. Phys. Soc.*, **A66**, 514 (1953).

TABLE I. DISPERSION FORCE. THE VALUES OF THE COEFFICIENT OF R^{-6} TERM (IN UNITS OF 10^{-60} erg. cm^6)

	Ne	NH_4^+	CH_4		H_2O	
			1	2	1	2
α	9.7	6.71	5.01	5.18	7.1648	7.3551
β	5.86	2.17	5.01	5.18	7.1648	7.3551
γ	5.86	1.62	3.00	2.59	3.5824	2.9420
Our results	5.75	153.9	181.5	375.4	112.7	278.4
In Margenau's table[5]	7.97 7.48 4.67	(107.9)	112		47	
Estimated by second virial coefficient[6]	8.32	—	240		—	
E_{AV}*	51.4	25**	28.2		25.6	

* The values of E_{AV} adopted in this paper are the same as those in Margenau's paper[5].
** The value of ionization potential is roughly estimated from those of NH_3 and CH_4, and α^0 is 2.68×10^{-24} cm^3 estimated from atomic refractive indexes.

For CH_4 and H_2O molecules[5]

$$\varphi_{1s}=\left(\frac{\alpha^3}{\pi}\right)^{1/2}e^{-\alpha r}$$

$$\varphi_{2s}=\frac{1}{4}\left(\frac{\beta^5}{2\pi}\right)^{1/2}(2-\beta r)e^{-(\beta/2)r}$$

$$\left.\begin{matrix}\varphi_{2px}\\ \varphi_{2py}\\ \varphi_{2pz}\end{matrix}\right\}=\left(\frac{\gamma^5}{32\pi}\right)^{1/2}re^{-(\gamma/2)r}\left\{\begin{matrix}\sin\theta\cos\varphi\\ \sin\theta\sin\varphi\\ \cos\theta\end{matrix}\right.$$

For NH_4^+ ion, the radial factors are[5]

$$R_{1s}=(2\alpha)^{3/2}e^{-\alpha r}$$

$$R_{2s}=\left(\frac{12\beta^5}{\alpha^2-\alpha\beta+\beta^2}\right)^{1/2}\left(1-\frac{1}{3}(\alpha+\beta)r\right)e^{-\beta r}$$

$$R_{2p}=\left(\frac{4\gamma^5}{3}\right)^{1/2}re^{-\gamma r}$$

As to the neon atom, we use the Slater orbitals, and the effective nuclear charge in each orbital is calculated by Slater's rule.

The values of the three parameters adopted are the same as in the quoted papers, and they aer listed in Table I.

The unperturbed total wave function Φ can be written as $\Phi=\Phi_1\cdot\Phi_2$, since the exchange of electrons does not occur in the range where the intermolecular distance between molecules (or atoms) 1 and 2 is very great.

The potential due to the dipole-dipole interaction between to molecules (or atoms) is given as follows:

$$V=\frac{e^2}{R^3}\sum_{i,j}(x_{1i}x_{2j}+y_{1i}y_{2j}-2z_{1i}z_{2j}) \qquad (2)$$

where R is the distance between molecules or atoms, and x_{1i}, y_{2j} are the x and y coordinates for ith and jth electrons belonging to molecules (or atoms) 1 and 2, respectively. The z-axes are taken along the intermolecular distance R.

Taking the interaction V as a perturbation, the perturbation energy between the same molecules (or atoms) is given by

$$\Delta E=(00|V|00)+\sum_{k_1,k_2}\frac{|(00|V|k_1k_2)|^2}{2E(0)-E(k_1)-E(k_2)} \qquad (3)$$

where index 0 refers to the state function of the ground state, k referring to all possible excited states.

In the above equation, it can be shown that $(00|V|00)$ is zero in the present treatment. In the second term, if one replaces the dominator of Eq. 3 by a mean E_{AV}, the second order perturbation energy can be

$$\Delta E=\frac{1}{E_{AV}}\sum_{k_1,k_2}|(00|V|k_1k_2)|^2=\frac{(00|V^2|00)}{E_{AV}} \qquad (4)$$

E_{AV} is put equal to twice the ionization potential according to the treatment of Margenau[5].

Thus, ΔE is calculated as follows:

$$\Delta E=-\frac{24e^4}{R^6E_{AV}}\left[\frac{1}{3}(1s|r^2|1s)+\frac{1}{3}(2s|r^2|2s)+(2p_a|z^2|2p_a)+2(2p_z|z^2|2p_z)-2(1s|z|2p_a)^2-2(2s|z|2p_a)^2\right] \qquad (5)$$

where $2p_z$ refers to φ_{2px} or φ_{2py} and $2p_a$ is to φ_{2pz}, and

$$(1s|r^2|1s)=\int\varphi_{1s}^*r^2\varphi_{1s}\,d\tau$$

$$(2p_a|z^2|2p_a)=\int\varphi_{2pz}^*z^2\varphi_{2pz}\,d\tau$$

The numerical values of the coefficient of

5) H. Margenau, *Rev. Modern Phys.*, **11**, 1 (1939).

R^{-6} term in ΔE of the present molecules and atoms are listed in Table I.

As to methane and neon with uniformly charged spherical configuration, the values of the coefficient of R^{-6} term in ΔE almost agree with those calculated by London's approximate formula and also with those estimated by the second virial coefficient[6]. But, for H_2O, the value of the coefficient of R^{-6} term in ΔE is greater than the one obtained by London's formula, since the H_2O molecule belongs to C_{2v} and its UAO treatment may be inadequate.

Two kinds of calculations referring respectively to case 1 and case 2, are made, in which three different parameters are adopted for wave functions. The results indicate that the values of the coefficient of ΔE depend greatly on the values of parameters, in particular, on those of the outermost shell orbital. For example, the calculated values in H_2O in case 1 is three times as great as those in case 2. However, it may be remarked that the modification of these parameters in cases 1 and 2 causes a change of only less than 1% in the total electronic energy[3].

In regard to NH_4^+, R^{-6} term in interaction energy is of minor importance, since this molecule is an ion. However, in a rough estimation of this term by Eq. 1, the coefficient of R^{-6} term becomes 107.9. Hence, the calculated values seem to be reasonable.

The UAO procedure will also be applicable to SiH_4[7], PH_3 and other molecules which have at least a nearly spherical symmetry. This point will be investigated in future.

Our conclusion is as follows:

1) The UAO calculation of intermolecular interaction energy due to dipole-dipole is rather simple and easy, while the agreement is comparatively good.

2) Care must be taken, however, when one treats the molecule which deviates to a great extent from spherical symmetry.

3) The parameter dependence of the interaction energy is greater than that of the electronic energy of a molecule.

4) Therefore, to adopt better parameters is most important in carrying out the calculation by the UAO method. For this purpose, attention should be paid to the polarization which may take place when two molecules come near each other.

Faculty of Engineering
Kyoto University
Sakyo-ku, Kyoto

6) M. Mizushima, "Bunshiron", Kyoritu, Tokyo (1950), p. 270.
7) C. Carter, *Proc. Roy. Soc. (London)*, **A235**, 321 (1956).

On the Electrical Conductivity of the Organic Thin Films: Perylene, Coronene and Violanthrene

By Hiroo Inokuchi, Haruo Kuroda and Hideo Akamatu

(Received November 1, 1960)

In recent years, the electronic conduction in organic compounds has aroused interest and a number of reports on their related behaviors have been accumulated[1,2]. The early works in this field were of the preliminary survey type, but recent articles tend to concentrate on the physico-chemical properties of the specific compounds under more carefully controlled conditions. However, some substantial discrepancies are still found in the results observed by different investigators. Some of the discrepancies may be due to the difference in the preparation or the formation of the specimens. For instance, thin evaporated films of aromatic hydrocarbons are frequently applied to the investigation of the semi- and photoelectrical conductivity. However, relatively little attention has been given to the structure of these films.

The present paper deals with the electrical conductivity and structural survey of thin organic films prepared in vacuo upon various substrates.

Experimental

Materials.—*Coronene (I).*—This aromatic compound, including a small amount (nearly 5%) of higher condensed aromatic compounds, was provided

1) H. Akamatu and H. Inokuchi, "Proceedings of the Third Conference on Carbon", Pergamon Press, London (1959), p. 51.
2) C. G. B. Garrett, "Semiconductors", (N. B. Hannay, ed.), Reinhold, New York (1959), p. 634.

by Badische Anilin and Soda Fabrik A. G. in Germany[3]. First, the crude hydrocarbon was purified carefully by means of the recrystallization method from its benzene solution. In addition, through the repeated high vacuum sublimations, pure coronene, for which the melting point was 438°C, was separated as a beautiful yellow hydrocarbon[4].

Perylene (II) and Violanthrene (III).—These two polycyclic aromatic hydrocarbons were synthesized by Drs. T. Handa and J. Aoki. The purified hydrocarbons were obtained by evaporation in vacuo in a manner similar to that reported in the previous article[5].

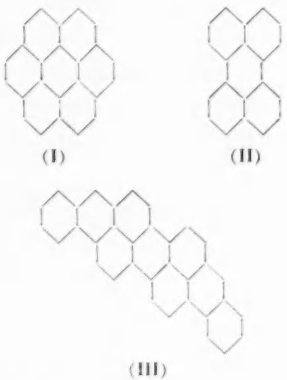

Procedures.—The following three types of conductivity cells were employed to measure the electrical resistivity of the organic compounds.

The Sandwich-type Cell.—The aromatic hydrocarbons having approximately one or two microns in thickness was deposited by vacuum evaporation on a pyrex glass plate, which had been coated in advance with aluminium film to provide one electrode. A second electrode, thereafter, was formed by evaporation of aluminum film under a high vacuum as shown in Fig. 1. The electrical resistivity of this cell was measured in an atmosphere of argon. The estimation of specific resistivity was not so accurate, because of large errors incurred in the observation of the dimensions of the specimens.

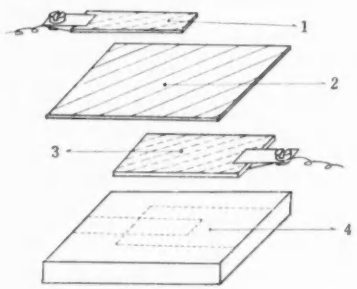

Fig. 1. The sandwich-type of cell. 1 and 3 are metal films which serve as electrodes. 2 is an organic film and 4 is a glass substrate.

The Surface-type Cell.—This type of cell was prepared by evaporation of an organic film on a pyrex glass plate which has parallel electrodes that are separated from each other by a gap of 2 mm. This cell was placed in a glass chamber as shown schematically in Fig. 2. These electrodes were

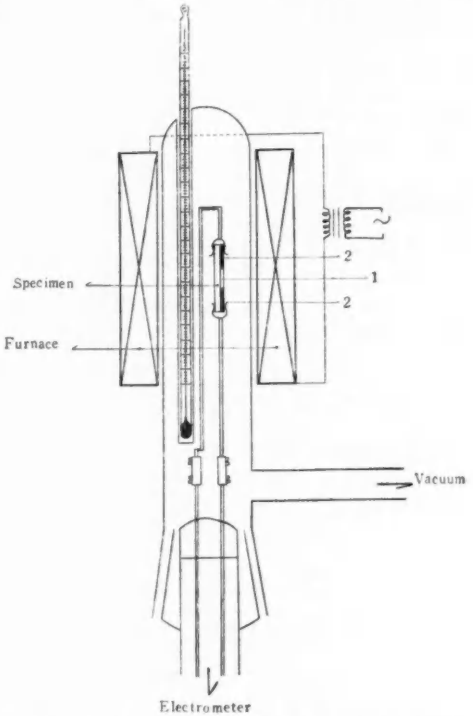

Fig. 2. The surface-type of conductivity cell placed in a glass chamber.
1, Organic thin layer
2, Terminal electrode

connected through two metal-to-glass seals to the vibration-reed electrometer. Throughout all the experiments, this chamber was maintained in a vacuum of 10^{-5} mmHg or less, to preclude an effect of air and/or of humidity on the films*.

The Bulk Specimen.—The crystalline powders were packed into a quartz cylinder, area 0.5 cm^2, between two platinum-plated brass electrodes. The specimens were compressed in the cylinder up to 116 kg./cm^2 by a lever system.

Technique.—*Electric Conduction.*—The resistances of the above specimens, at room temperature, were from 10^9 to 10^{14} Ω. The measurements of high resistance were carried out, therefore, with the

3) L. Boente, *Brennstoff-Chem.*, **36**, 210 (1955).
4) E. Clar and W. Kelley, *J. Chem. Soc.*, **1956**, 3875.
5) H. Inokuchi, *J. Org. Synth. Japan*, **13**, 486 (1955).

* From a preliminary experiment, an introduction of air into the chamber is one of the most important reasons for the instability of the conductivity of thin films and also one of the interesting aspects of their studies.

association of the vibration-reed electrometer apparatus.

X-Ray Diffraction.—The transparent organic films evaporated on several substrates—glass, potassium chloride crystal, copper plate and also the cleavage surface of graphite—were examined as to their textured structures by means of a Geiger counter X-ray diffractometer.

Electron Micrograph.—The electron micrographs were made with association of the Hitachi electron-microscope, HU-10. The structural analysis of the small individual crystals ($1\mu \times 1\mu$) in the thin organic films could be carried out easily by means of the electron microdiffraction combined with the electron micrograph. As a specimen for the above two methods, the transparent organic films on glass substrates were stripped off from the substrates and in addition the carbon-replica technique was applied on them.

Results and Discussions

Through all the experiments, the results of the electrical resistivity of various types of conductivity cells can be expressed by a semi-conductive equation[1] (Fig. 3):

$$\rho = \rho_0 \exp(\Delta\varepsilon/2kT)$$

where $\Delta\varepsilon$ is an apparent energy gap. The various forms of specimens with regard to the type of cells are thus compared with each other conveniently in terms of $\Delta\varepsilon$ and the electrical resistivity ρ at 15°C in Table I.

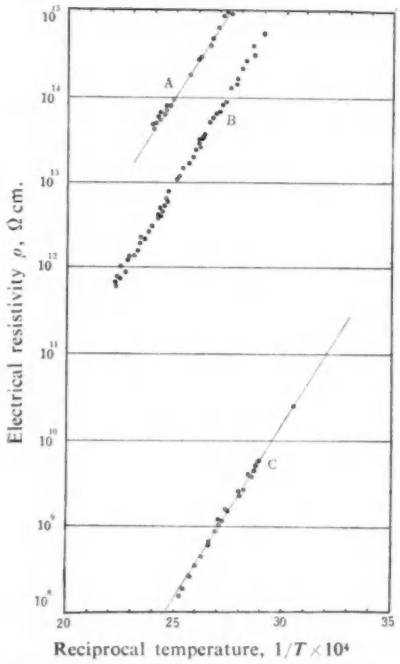

Fig. 3. The electrical resistivity versus temperature of various types of violanthrene conductivity cells.
A. Sandwich-type B. Bulk C. Surface-type

Table I. The electrical resistivity of polycyclic aromatics, observed from the various types of cell

Compound	Perylene	Coronene	Violanthrene
From bulk specimen			
ρ_{15}(Ω cm.)	4×10^{15}	1.7×10^{17}	2.1×10^{14}
$\Delta\varepsilon$(eV.)	2.0	1.7	0.85
From surface-type cell			
ρ_{15}(Ω cm.)	$\sim10^{13}$	$10^{12}\sim10^{13}$	$\sim10^{9}$
$\Delta\varepsilon$(eV.)	2.2	1.65	0.9
From sandwich-type cell			
ρ_{15}(Ω cm.)	$10^{15}\sim10^{19}$	$10^{17}\sim10^{15}$	$\sim10^{14}$
$\Delta\varepsilon$(eV.)	2.0	1.6	0.9

In this table, it is found that the electrical resistivity observed with the sandwich-type cell is in quite good agreement with that of the bulk specimen. However, a great difference is found between the resistivities of the sandwich-type cell and the surface-type one. The resistivity of the sandwich-type cell is much less than that of the surface-type by a factor of $10^4\sim10^5$. The electric field is applied along the surface of the film in the surface-type cell, while it is applied perpendicularly to the film for the sandwich-type cell. Therefore, the difference implies that there is an anisotropy of resistivity in the thin film.

It is well known that when a substance is deposited onto a substrate from solution or vapor phase to produce a thin film, a textured

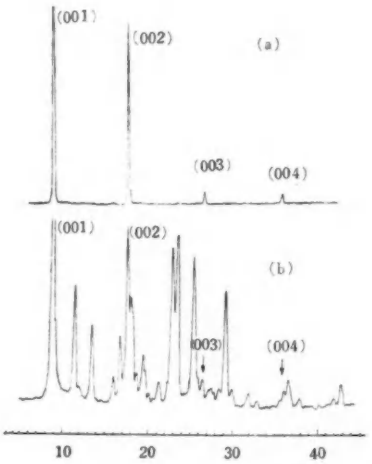

Fig. 4. The X-ray diffractometer records of (a) powder and (b) evaporated film of coronene.

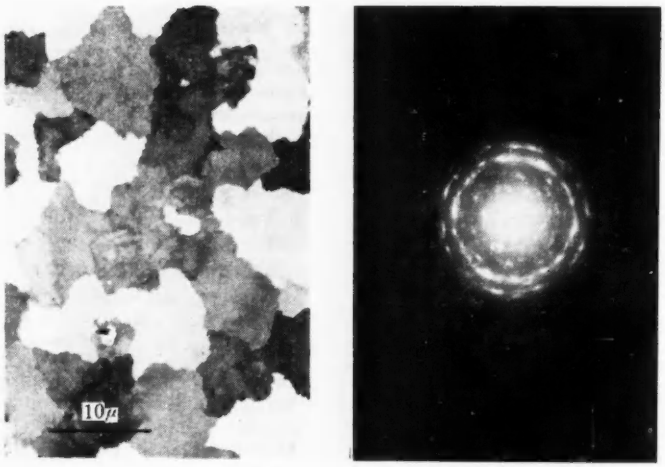

(a) (b)

Fig. 5. (a) The electron micrograph and (b) the electron microdiffraction pattern of an evaporated film of coronene.

structure in which crystallites are arranged with a preferred orientation usually occurs. This was proved for the evaporated film of the aromatic compounds by means of X-ray diffraction. When the X-ray diffraction pattern of these organic thin films was examined with the diffractometer, it was found that diffraction lines were composed only of (00*l*) reflection and other reflections were missing completely (Fig. 4). This is the evidence for the fact that the crystallites of aromatic hydrocarbons were in alignment with their a·b planes parallel with the film surface. The mode of arrangement of crystallites is quite independent on the substrate materials which were described in the above section.

The electron microscopic observation and the application of electron microdiffraction verified the foregoing conclusion: From the electron micrographs (Fig. 5), it is found that the films consist of a number of single crystals which are arranged in closed packing with each other on the substrate, and the electron microdiffraction reveals that the crystallites are in alignment with their a·b planes parallel with the film surface.

Therefore, the discrepancy in resistivity between the surface-type and the sandwich-type cells could be attributed to the substantial anisotropy of resistivity of the crystals. Thus, the resistivity along the a·b plane of crystal should be much smaller than that perpendicular to the same plane for these compounds.

This conclusion is consistent with the results observed with anthracene single crystal. Mette and Pick have reported the anisotropy of electrical resistivity in anthracene[6], that is to say, the conductivity in a·b plane was a few times higher than that in a·c plane. Compton, Schneider and Waddington observed that the photocurrent along the b-axis direction is about one hundred times higher than that in the c-axis direction and several times larger than that along the a-axis direction[7].

The a·b plane is the cleavage plane of the crystal, and the molecules are so arranged that the molecular planes are nearly perpendicular to this plane. The nearest approach of neighboring molecules is found in the a·b plane. If there could be overlapping of molecular orbitals of π-electrons between neighboring molecules, it should take place along the direction parallel to this a·b plane. On the other hand, there is no reason to expect a stronger interaction between molecules in the direction along the c-axis. Therefore, it is reasonable to find the least value of resistivity along the a·b plane.

From Table I, it is seen that the anisotropy is found in the value of resistivity but not in the value of energy gap. Hence, there is no reason to expect a difference in the number of charge carriers which are in excited state. There should, however, be a large difference in the mobility of carriers depending on the direction of drift.

6) H. Mett and H. Pick, *Z. Physik*, **134**, 566 (1953).
7) D. M. J. Compton, W. G. Schneider and T. C. Waddington, *J. Chem. Phys.*, **27**, 160 (1957).

Summary

It was found that the various types of conductivity cells of aromatic hydrocarbons possess great discrepancies of their electrical resistivity. The resistivity observed with the sandwich-type cell, perylene; $10^{15\sim16}\,\Omega$cm., coronene; $10^{17\sim18}\,\Omega$cm., and violanthrene; $10^{14}\,\Omega$cm., is in quite good agreement with that of the bulk specimen. However, a great difference was found between the resistivities of the sandwich-type and the surface-type cells, perylene; $10^{13}\,\Omega$cm., coronene; $10^{12\sim13}\,\Omega$cm., and violanthrene; $10^{9}\,\Omega$cm. This discrepancy in resistivity can be assumed to be introduced from the textured structure of the evaporated films and the substantial anisotropy of crystals; the crystals are in alignment with their a·b plane with the film surface. This orientation was found from the X-ray diffraction results, combined with the electron microscopic observation and the electron microdiffraction results.

The authors express hearty thanks to Drs. T. Handa and J. Aoki who prepared the samples of this work. The cost of research has been defrayed from the Scientific Research Encouragement Grant from the Minstry of Education, to which the authors' thanks are due.

Department of Chemistry
Faculty of Science
The University of Tokyo
Hongo, Tokyo

*Studies on the Chemical Decomposition of Simple Sugars. X. Acetol Formation from ^{14}C-Labeled Hexoses**

By Ryozo Goto, Jun'ichi Hayami, Kenichi Kudo and Sinichi Otani

(Received November 17, 1960)

As is well known, carbohydrates, especially monosaccharides, have many reactive functional groups, and these compounds show various kinds of reactions. In an aqueous solution, monosaccharides show the following fourma in types of reactions, which depend upon the pH of the reaction medium.

These are a) the "Lobry de Bruyn-Alberda Van Eckenstein reaction[1]), b) the formation of furfural derivatives[2a]) in acid medium, c) the reverse aldolization[3]) which gives rise to the formation of smaller fragments, a possible recombination reaction of these fragments which may occur, and d) an acid formation in an alkaline medium to yield lactic and saccharinic acids[4a]).

Each of these reactions has been well-examined for a long time, and detailed mechanisms for these reactions were proposed. Recently, some of them have been confirmed chemically and also radiochemically[1,2b,4b]).

Besides these reactions, there is another decomposition reaction, for example, when an aqueous solution of hexoses (pH 3~11) is heated, sugars are decomposed and some steam volatile products are formed. From the decomposition mixture Dakin[5]), Nef[6]), and Evans[7,8]) have obtained methylglyoxal phenylosazone, and they concluded that the reaction product might be methylglyoxal. However, it is easily understood that methylglyoxal phenylosazone can be derived from either acetol or lactic aldehyde as well as from methyl glyoxal. Therefore methylglyoxal cannot be (concluded to be) a sole product. But with the use of semicarbazide, it is possible to distinguish methylglyoxal from acetol.

* Presented at the 11th Annual Meeting of the Chemical Society of Japan, Tokyo, April, 1958 and the 12th Annual Meeting of the Chemical Society, Kyoto, April 1959.

1) J. C. Speck, Jr., "Advances in Carbohydrate Chem.", Vol. 13 (1958), p. 63.

2) a) F. H. Newth, ibid., Vol. 6, (1951), p. 83, and references cited therein; J. Kennerand G. N. Richards, *J. Chem. Soc.*, **1956**, 2921.
b) W. A. Bonner and M. R. Roth, *J. Am. Chem. Soc.*, **81**, 5454 (1959).

3) W. L. Evans, *Chem. Revs.*, **31**, 537 (1942).

4) a) J. C. Sowden, "Advances in Carbohydrate Chem.", Vol. 12, (1957), p. 36; R. L. Whistler and J. N. BeMiller, ibid., Vol. 13, (1958), p. 289; G. Machell and G. N. Richards, *J. Chem. Soc.*, **1960**, 1924, 1932, 1938.
b) J. C. Sowden et al., *J. Am. Chem. Soc.*, **79**, 6450 (1957); J. C. Sowden and E. K. Pohlen, ibid., **80**, 242 (1958).

5) H. J. Dakin and H. W. Duddley, *J. Biol. Chem.*, **15**, 127 (1913).

6) J. U. Nef, *Ann.*, **357**, 214 (1907); **376**, 1 (1910); **403**, 204 (1914).

7) W. L. Evans, *J. Org. Chem.*, **1**, 1 (1937) and references cited therein.

8) C. Enders et al., *Naturwiss.*, **29**, 46 (1941); *Biochem. Z.*, **312**, 349 (1942).

Nodzu[9] and Goto[10] have examined the decomposition products of glucose in a weakly acid and a weakly alkaline solution and isolated acetol semicarbazone instead of methylglyoxal bissemicarbazone. In a series of extensive experiments, they confirmed the fact that a) hexose[11a,b], methylpentose[10], and pentose[10] gave acetol accompanied by small amounts of diacetyl and of lactic aldehyde[11c] and these sugars gave substantially no methylglyoxal, b) tetrose[10] gave only diacetyl and did not produce acetol and c) triose[11d] gave methylglyoxal and diacetyl.

Recently, Sattler[12] observed the formation of acetol by the decomposition of simple sugars in a weakly alkaline aqueous solution. Prey[13], also, thoroughly examined the alkaline degradation of simple sugars and observed the formation of acetol.

As it has been reasonably accepted that hexose and pentose can yield trioses through a reverse-aldolization[3], and that trioses in turn are easily dehydrated to methylglyoxal, the supposition of the formation of methylglyoxal which was claimed by early workers would be rather natural. Therefore, the formation of acetol, instead of methylglyoxal, seemed to be a novel reaction of a sugar. But little has been known regarding the mechanism of acetol formation from simple sugars.

Nodzu et al.[11d] noticed the formation of acetol accompanied by pyruvic acid and under the supposition of their simultaneous formation, the following mechanism (Scheme 1) which included acetylformoin[14] as a direct precursor of acetol was proposed. Acetylformoin is an acyloin formed from methylglyoxal.

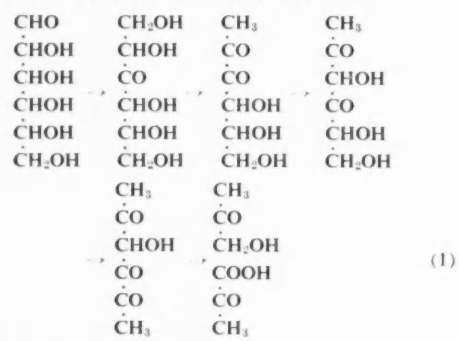

(1)

Later on, Goto inferred from Nodzu's mechanisms, that if it was applied to a pentose, it would lead to the formation of triketopentane as is shown in the following scheme:

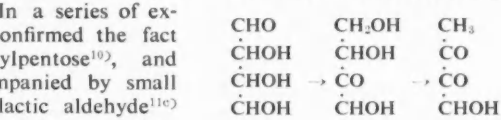

(2)

Since no acetol is derived from this triketopentane, he propounded an alternative mechanism for the formation of acetol. His mechanism for this reaction is illustrated in Scheme 3:

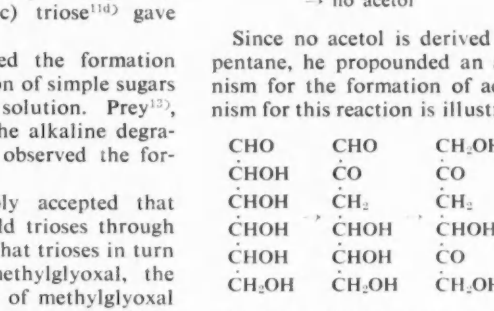

(3)

These mechanisms, however, lack any positive evidence. For the better understanding of the mechanism of acetol formation, more detailed knowledge is required. To establish the nature and to confirm the precise mechanism for the acetol formation, the authors undertook the syntheses of ^{14}C-labeled monosaccharides and examined the decomposition of these ^{14}C-labeled monosaccharides.

In the present study, glucose-1-^{14}C, glucose-3,4-^{14}C, and glucose-6-^{14}C were decomposed in a concentrated phosphate buffer to yield acetol, and the relative distribution of a label in the acetol was determined.

Experimental

Radioactive Sugars and Assay Method. — D-Glucose-1-^{14}C was prepared from D-arabinose by a cyanohydrin synthesis[15]. D-Glucose-3,4-^{14}C was prepared from rat liver glycogen injected with $NaH^{14}CO_3$, according to Wood's method[16] with minor modifications. D-Glucose-6-^{14}C was prepared from 1,2-*O*-isopropylidene-D-*xylo*-dialdopentofuranose[17]. In the course of synthesis, deionization at an ice temperature was undertaken with Amberlite type I IRCG-120, instead of ordinary IR-120, to secure a satisfactory exchange.

For an assay, except for specified ones, all sample were converted into barium carbonate by Van Slyke-Folch wet conbustion. Barium carbonate was collected on a filterpaper and counted in an infinite

9) R. Nodzu, This Bulletin, **10**, 122 (1935). (weakly acid region.)

10) R. Goto, ibid., **15**, 209 (1940); *J. Chem. Soc. Japan, Pure Chem. Sec.* (*Nippon Kwagaku Kwaisi*), **64**, 999, 1054, 1183 (1943). (weakly alkaline region.)

11) a) R. Nodzu and K. Matsui, This Bulletin, **10**, 467 (1935); b) R. Nodzu and R. Goto, ibid., **11**, 381 (1936); c) R. Goto, ibid., **15**, 103 (1940); d) R. Nodzu, et al., *Mem. Coll. Sci. Kyoto Imp. Univ.*, **A20**, 197 (1937).

12) L. Sattler and F. W. Zerban, *J. Am. Chem. Soc.*, **70**, 1975 (1948).

13) V. Prey and E. Waldman, *Monatsh.*, **83**, 55 (1952).

14) R. Nodzu and S. Kunichika, This Bulletin, **15**, 211 (1940).

15) H. S. Isbell et al., *J. Research N. B. S.*, **48**, 163 (1952).

16) H. G. Wood et al., *J. Biol. Chem.*, **159**, 475 (1945).

17) R. Schaffer and H. S. Isbell, *J. Research N. B. S.*, **56**, 191 (1956).

thickness under an end-window type G. M. counter. Probable errors of the counting were within 3% except for specified ones.

Decomposition of Labeled Sugars.—A solution of 5 g. of D-glucose in 200 ml. of concentrated potassium acid phosphate buffer (40%, pH 6.7) was heated and distilled, fresh water was added to maintain a constant volume. Two hundred and fifty mililiters of distillate was collected every 90 min., and distillation was continued until the distillate showed only a faint iodoform reaction, (total volume of distillate 5 l., 284 mg. as acetol). The amount of acetol contained in the distillate was determined by iodometric titration according to Nodzu[9] (1 ml. of 0.1 N I_2 solution corresponds to 0.73 mg. of acetol).

By the above titration, the methyl carbon of acetol was converted into iodoform. This compound was collected and assayed for activity.

Acetol Semicarbazone.—The combined distillate cited above was treated with semicarbazide hydrochloride and with sodium acetate (5 fold equivalents of acetol). The mixture was heated over a boiling water bath for 30 min., cooled and concentrated to a small volume under reduced pressure. Semicarbazone was separated and fractionally recrystallized from hot water. Successive recrystallizations gave 70 mg. of acetol semicarbazone as colorless needles, m. p. 199~200°C. The melting point showed no depression when mixed with an authentic sample.

Degradation of Acetol.—*Formaldehyde Dimedone from Acetol.*—An aqueous solution of acetol was treated with 50% excess of sodium metaperiodate in sodium bicarbonate buffer, and stood overnight at room temperature. The aqueous solution was concentrated under reduced pressure, and from the distillate, formaldehyde was precipitated as formaldehyde dimedone. It was recrystallized from an aqueous ethanol to give colorless needles, m. p. and mixed m. p. 190~191°C.

Separation and Degradation of Barium Acetate.—The residue from the periodate oxidation was treated with a carrier acetate, acidified, and was steam distilled. The iodic and periodic acid in the distillate were removed by silver carbonate[15], and formic acid was removed by oxidation with mercuric oxide*, according to Osburn's method[19]. The acetic acid was refluxed for a further 15 min. After cooling and filtration, acetic acid was distilled out with steam.

Scheme 4

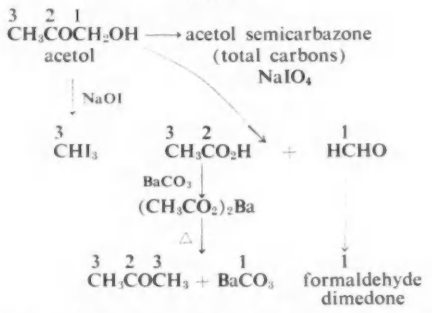

Note: Numbers correspond to the one in the present acetol.

TABLE I. RADIOASSAY DATA FOR ^{14}C-LABELED GLUCOSE (RADIOACETOL FROM GLUCOSE-1-^{14}C)

	Sample	Carbon atom(s)	Radioactivity μc./mol.
Glucose-1-^{14}C			435
Acetol	Acetol semicarbazone	all	203
	Formaldehyde dimedone	CH_2OH	0
	$BaCO_3$ from Ba acetate	CO	—*1
	Iodoform	CH_3	+*2

TABLE II. RADIOASSAY DATA FOR ^{14}C-LABELED GLUCOSE (RADIOACETOL FROM GLUCOSE-3,4-^{14}C)

	Sample	Carbon atom(s)	Radioactivity μc./mol.
Glucose-3,4-^{14}C			31.7
Acetol	Acetol semicarbazone	all	32.6
	Formaldehyde dimedone	CH_2OH	33*3
	$BaCO_3$ from Ba acetate	CO	—*1
	Iodoform	CH_3	—*4

*1 Free from radioactivity, a carrier was used.
*2 Radioactivity was present.
*3 Probable error was less than 10%.
*4 Free from radioactivity.

TABLE III. RADIOASSAY DATA FOR ^{14}C-LABELED GLUCOSE (RADIOACETOL FROM GLUCOSE-6-^{14}C)

	Sample	Carbon atom(s)	Radioactivity μc./mol.
Glucose-6-^{14}C			616
Acetol	Acetol semicarbazone	all	141
	Formaldehyde dimedone	CH_2OH	35
	—*1	CO	—*1
	Iodoform	CH_3	106*2

TABLE IV. RADIOASSAY DATA FOR ^{14}C-LABELED GLUCOSE (RADIOACETOL FROM GLUCOSE-1-^{14}C, pH 11)

	Sample	Carbon atom(s)	Radioactivity μc./mol.
Glucose-1-^{14}C			435
Acetol	Acetol semicarbazone	all	173
	Formaldehyde dimedone	CH_2OH	73
	$BaCO_3$ from Ba acetate	CO	—*3
	Iodoform	CH_3	108

*1 Not determined.
*2 Indirectly calculated.
*3 Almost free from radioactivity, a carrier was used.

* About 250 mg. of crude sodium acetate (with carrier), was dissolved in 50 ml. of water, 3 drops of sulfuric acid and 5 g. of mercuric oxide were added, and the mixture was refluxed. After 20 min., 3.5 ml. of phosphoric acid (85%) and 2 ml. of water were added, and the mixture

18) P. W. Clutterbuck and F. Reuter, *J. Chem. Soc.*, 1935, 1467.
19) O. L. Osburn et al., *Anal. Chem.*, 5, 247 (1933).

thus purified, was converted into barium salt, and recrystallized from water for an assay and a degradation. Barium acetate was degraded to acetone and barium carbonate by pyrolysis[20] in the usual way. Acetone was converted into 2, 4-dinitrophenylhydrazone and assayed directly.

The course of the degradation of acetol is summarized in Scheme 4, and radioactivity assay data are given in Tables I–IV respectively.

Results and Discussion

The contents of assay data which are shown in Tables I–IV can be summarized as follows:

1) In the case of D-glucose-1-^{14}C, radioactive acetol of about a half molar activity of the original glucose was formed. Periodate oxidation of the acetol provided formaldehyde (corresponding to carbinol carbon of the acetol), which was almost free from activity. The other carbons (methyl and carbonyl carbon) were converted, at the same time, into acetic acid. The acetic acid was degraded by the usual method of pyrolysis and afforded radioactive acetone and nonactive barium carbonate. These facts show that acetol-3-^{14}C was formed from glucose-1-^{14}C.

2) In the case of D-glucose-3, 4-^{14}C, radioactive acetol was obtained which preserved the original molar activity of the reactant glucose. The acetol was degraded to radioactive formaldehyde and nonactive acetic acid. This means that radioactivity was present at the primary carbinol carbon of the acetol. From these facts, it is quite possible that acetol-1-^{14}C is produced from D-glucose-3, 4-^{14}C.

3) D-Glucose-6-^{14}C, as was expected from the results of Tables I and II, afforded acetol, labeled mainly at the methyl carbon. But it should be noted that between the methyl and the carbinol carbon an appreciable randomization of a label is observed. This randomization was confirmed by another repeated run. But, as the label was found mainly at the methyl carbon, it might be possible to say that D-glucose-6-^{14}C produces acetol-3-^{14}C.

The patterns of the label cited above would reveal that, in the formation of acetol from glucose (hexose), C-1 and C-6 of the original glucose are converted into the methyl carbon of an acetol, while C-3 and C-4 of the original glucose are converted into the carbinol carbon of an acetol.

It is also remarkable that the acetol-1-^{14}C, which was produced from D-glucose-3, 4-^{14}C, preserves the molar radioactivity of the original glucose. This, coupled with the pattern of the label cited above, implies that, in the formation of acetol, C-1, 2, 3 and C-4, 5, 6 of the original glucose behave as a unit, and that no skeletal rearrangement in these C_3 units is involved. These facts further exclude the possibility of a random scission of the carbon-chain of a glucose in this reaction. This is because according to the mechanism of a random scission, universally labeled acetol might be produced, but it is not the case.

The randomization of a label might be attributed to the reverse-aldolization[5,21] and the recombination reaction of a hexose. This is because, as Sowden[22] pointed out, glucose-1-^{14}C and/or glucose-6-^{14}C could be converted into a hexose-1, 3, 4, 6-^{14}C through a reverse-aldolization and a recombination reaction of a hexose*. These reverse-aldolization and recombination reactions are shown to prevail in a high pH region, and in the present instance, radiactive acetol formed from glucose-1-^{14}C at pH 11 shows an appreciable randomization of a label (Table IV), where the carbinol carbon shows about 2/3 activity of the methyl carbon.

On the other hand, in a neutral or a weakly acid medium, the reverse aldolization and the recombination of a hexose have been believed not to occur[21,23]. And also, the lower half of a hexose was suspected to behave somewhat differently from the upper half of a hexose[21]. Therefore, at this stage, it is better not to attribute the randomization of a label in the case of glucose-6-^{14}C (pH 6.7, Table III) to the reverse aldolization (and recombination) of a hexose.

The pattern and the relative distribution of the label found in the present investion, would give the contribution ratio of the upper and the lower half of a hexose molecule[24]. For example Table III shows that 77% of the acetol would come from the nonactive upper half and 23% would come from the active lower half of the glucose-6-^{14}C. But, as the substantial nature of the randomization of the label remains unresolved, the validity of these figures of contribution ratio contains much ambiguity, and will require further examination.

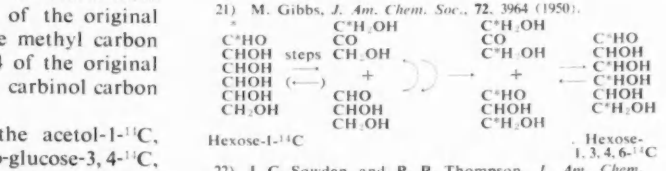

20) S. Aronoff et al., *Science*, **110**, 476 (1949).

21) M. Gibbs, *J. Am. Chem. Soc.*, **72**, 3964 (1950).

22) J. C. Sowden and R. R. Thompson, *J. Am. Chem. Soc.*, **80**, 1435 (1958).

23) V. Prey et al., *Monatsh.*, **85**, 1186 (1954).

24) A. A. Bothner-By and M. Gibbs, *J. Am. Chem. Soc.*, **72**, 4805 (1950).

25) H. G. Hers et al., ibid., **76**, 5160 (1954).

26) H. F. Bauer and C. Teed, *Can. J. Chem.*, **33**, 1824 (1955); F. Weygand and G. Billek, *Z. Naturforsch.*, **12b**, 601 (1957).

The authors wish to express their sincere thanks to Professor Teruaki Simamoto of the Pharmaceutical Institute of Kyoto University who offered much convenience and suggestions for the the use of animals for experiments.

Institute of Chemistry
Faculty of Science
Kyoto University
Sakyo-ku, Kyoto

Proton Magnetic Resonance Studies on the Thermally Dehydrated Products of Alumina Trihydrate

By Tatsuo SAITO

(Received November 19, 1960)

In the previous communications[1-2], the proton magnetic resonance absorption spectra of thermally dehydrated products have been studied to obtain information about the mechanism of the thermal decomposition of bayerite. In the present paper, the author has tried to investigate the rehydration of the thermally dehydrated product of alumina trihydrate by means of the proton magnetic resonance absorption spectra.

The rehydration of the thermal decomposition product of alumina trihydrate has recently been studied by many investigators[3-6]. The present author has examined the rehydration of the hydrous alumina dehydrated at various temperatures in high vacuum system. The rehydration was carried out under the vapor pressure of saturated water vapor at room temperature in the vacuum system.

Experimental

Starting Material.—The alumina trihydrate, bayerite, was prepared by a chemical reaction of 1 N aluminum chloride solution with a small excess of 1 N ammonium hydroxide solution at room temperature. The resulting precipitate was washed by decantation for about 10 days till it was free from chloride and was then dried at 50°C for 24 hr. This starting material was checked by X-ray diffraction study and it was found that the resulting diffraction diagram was the same as that of bayerite, as shown in Fig. 1.

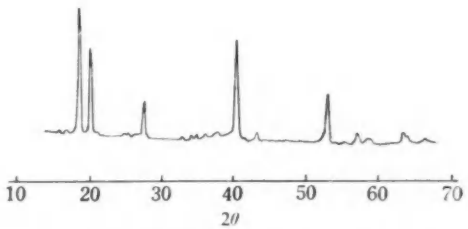

Fig. 1. X-Ray diffraction diagram of the starting material.

Apparatus and Procedure.—The NMR measurements were performed using the modulation technique described by Bloembergen, Purcell and Pound[7]. The detecting apparatus has the ordinary constitution, which is composed of an r-f oscillator, an r-f amplifier, a detector, an audio-frequency amplifier, a lock-in amplifier and a recorder. More detailed reviews of this apparatus may be found in the article by Yano[8].

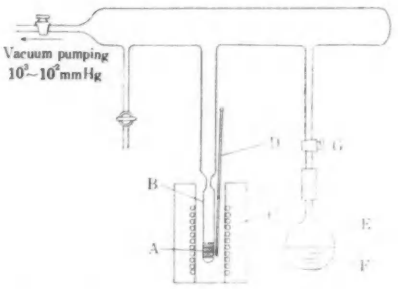

Fig. 2. Apparatus used to prepare the specimen for the NMR measurement.
A; Sample cake (dia. 8mm.)
B; Resonance sample tube
C; Electric furnace
D; Thermometer or thermocouple
E; Flask (100 cc.)
F; Distilled water in evacuated flask
G; Cock

1) T. Hagiwara and T. Saito, This Bulletin, **33**, 1463 (1960).
2) T. Saito, ibid., **33**, 1626 (1960).
3) M. K. B. Day and V. J. Hill, *Nature*, **170**, 539 (1952); *J. Phys. Chem.*, **57**, 946 (1953).
4) R. Tertian and D. Papée, *Compt. rend.*, **236**, 1565 (1953); **238**, 98 (1954); **241**, 1575 (1955).
5) B. Imelik, ibid., **233**, 1284 (1951).
6) H. Thibon and E. Calvet, ibid., **239**, 1133 (1954).
7) N. Bloembergen, E. M. Purcell and R. V. Pound, *Phys. Rev.*, **73**, 679 (1948).
8) S. Yano, *J. Phys. Soc. Japan*, **14**, 942 (1959).

Each specimen used for the NMR measurement was prepared by the device of vacuum system illustrated in Fig. 2.

For the preparation of each specimen of thermally dehydrated product in vacuo, about 2 g. of the starting material was pressed into small cakes and they were put into the resonance sample tube which was connected to the high vacuum system. Then, each resonance sample tube was evacuated and heated from outside by the electric furnace for 3 hr. and it was then sealed off. The dehydration temperature was 100, 150, 200, 250, 300, 400 and 500 °C, respectively.

For the preparation of rehydration-specimens, each sample after the treatment of the thermal dehydration in vacuo was immediately exposed at room temperature for 15 hr. to the saturated water vapor which entered through the cock (G) from the flask (E) (shown in Fig. 2).

Then, each sample tube containing this rehydrated specimen was pumped out to a high vacuum, either at room temperature during 12 hr. or at 110 °C during 6 hr. and it was then sealed off.

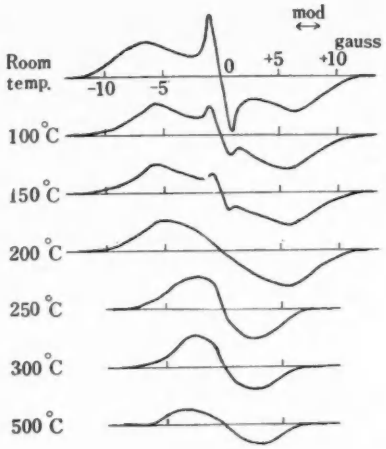

Fig. 3. Recorded derivatives of proton resonance in the thermal dehydration products in vacuo.

Results and Discussion

Thermal Dehydration in Vacuo.—The derivative curves of the proton resonance absorption taken on the thermally dehydrated products in vacuo are shown in Fig. 3. The line shapes obtained from the specimens dehydrated at 100 and 150 °C are both similar to that of the starting material, but the intensity of center peaks observed for these line shapes somewhat decreases with the rise of temperature. The line shape obtained from the specimen at 200 °C has no central component though its line width is almost equal to that obtained from the specimen at 150 °C.

This means that at the thermal dehydration till the temperature reaches 200 °C, the structure water is not released but the adsorbed water

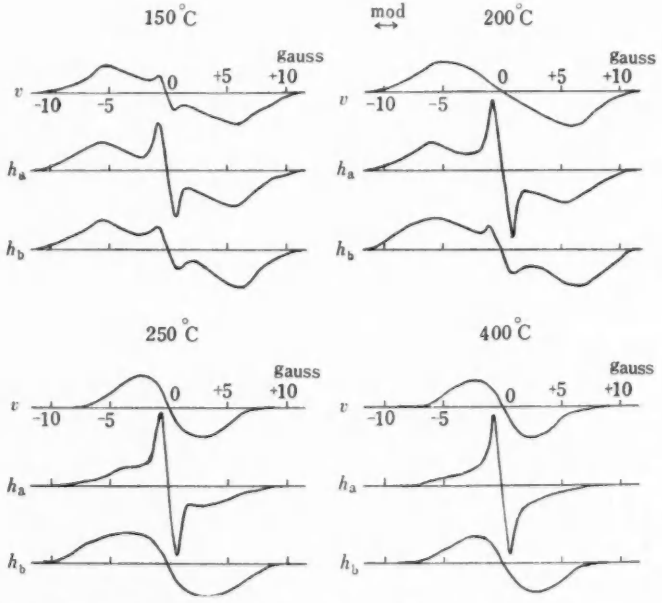

Fig. 4. Recorded derivatives of proton resonance in the thermal dehydration products in vacuo and their rehydrated samples.

vaporizes from the compound with the rise of temperature.

However, as shown in Fig. 3, the line width obtained from the specimen at 250°C suddenly becomes narrow and then the specimens at 300 and 500°C have also the same narrow width. This means that the starting material directly decomposes to the hydrous alumina at 200~250°C.

Rehydration of Thermally Dehydrated Products in Vacuo.—The NMR measurements were carried out on the specimens prepared by the rehydration of the thermally dehydrated products of bayerite in vacuo. The experimental derivative curves obtained from these measurements are shown in Fig. 4.

In Fig. 4, "v" is the recorded derivative of dehydrated product in vacuo at each temperature, and both "h_a" and "h_b" are the recorded derivatives of the rehydrated sample of the above dehydration-product. In this case, "h_a" shows the rehydrated sample having the after-treatment of a high vacuum pumping at room temperature during 12 hr. and "h_b" shows one having the after-treatment of a high vacuum pumping at 110°C during 6 hr.

As is seen in Fig. 4, the line shape of "h_a-series" has a sharp and intensive central component, but in the line shape of "h_b-series", the center peak observed for this line shape remarkably reduces in its intensity as compared with that of "h_a-series" or disappears. At 150°C, the line shape of the derivative "h_b" is the same as that of "v", but at 200°C, the line shape of the derivative "h_b" shows the difference from that of "v". This means that on the dehydration in vacuo at 200°C, the starting material partially decomposes to hydrous alumina and then this decomposed product is rehydrated by water vapor to aluminum hydroxide. At 250°C, the line width of the derivative "h_b" becomes larger than that of "v" and at 400°C, the line width of the derivative "h_b" is the same as that of "v".

The second moments calculated from these experimental derivative curves of "v-series" and "h_b-series" are shown in Table I and the variation of these values of second moments plotted as the function of the temperature are shown in Fig. 5.

As is seen in Fig. 5, the second moments of the thermal dehydration series in vacuo decrease from the value of 13~14 gauss^2 to that of 4~5 gauss^2 suddenly at 250°C and this value of 4~5 gauss^2 constantly continues till 500°C. In the variation curve of the second moments of the rehydration series—"h_b-series", the values of second moments below 200°C

TABLE I. THE VALUES OF THE SECOND MOMENTS CALCULATED FROM THE EXPERIMENTAL DERIVATIVE CURVES

Dehydration temp., °C	Thermally vacuum dehydration series, gauss^2	Rehydration series "h_b-series" gauss^2
room temp.	13.6	
100	13.4	
150	13.3	14.0
200	12.1	13.9
250	4.8±0.5	8.2±0.3
300	4.3±0.2	5.8±0.3
400	4.5	4.6±0.2
500	4.1	4.4

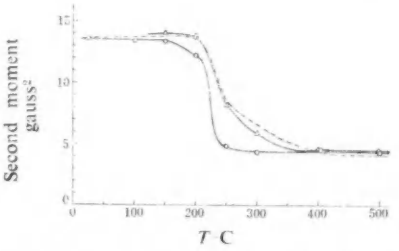

Fig. 5. Variation of the second moments with the temperature in the thermally vacuum-dehydration series and the rehydration series—"h_b-series"
○—○; Thermally vacuum-dehydration series
●—●; Rehydration series—"h_b-series"
·····; Thermal dehydration series in the air

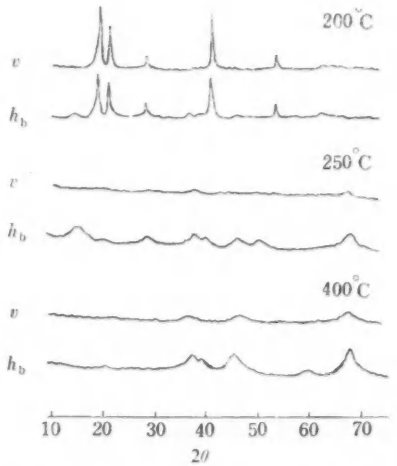

Fig. 6. X-Ray diffraction diagrams of the samples in the thermally vacuum-dehydration series and in the rehydration series—"h_b-series".
v; Thermally vacuum-dehydration series
h_b; Rehydration series—"h_b-series"

are about 13～14 gauss[2] and in the range from 200 to 400°C, the values gradually decrease with the rise of temperature. Then, in the range from 400 to 500°C, the second moments become stationary values of 4～5 gauss[2].

The above difference of the variation curve of second moments in the range from 200 to 400°C between "v-series" and "h_0-series" is interpreted as a result due to the formation of aluminum hydroxide by the rehydration of the thermally dehydrated product in vacuo.

This interpretation of the rehydration was ascertained by the X-ray diffraction study of the products. The diffraction diagrams of several specimens obtained in this study are shown in Fig. 6. From these diagrams, it is ascertained that, while the specimen of the thermal dehydration in vacuo at 250°C is crystallographically amorphous, the specimen obtained by the rehydration for the above sample shows a mixed phase of böhmite and γ-alumina.

Conclusion

1) The center peak observed for the line shape of the experimental derivative curve of proton resonance in the starting material decreases in its intensity during the thermal dehydration in vacuo at the temperature below 200°C, but it does not disappear till 150°C. The author assumes that this center peak shows the existence of the movable water which entered into the crevice of the lump of fine particles or entered into the space of the layer lattice of crystal.

2) On the thermal dehydration series in vacuo, the starting material directly decomposes to the hydrous alumina at the temperature of 200～250°C and the intermediary product, böhmite, is not found in the specimens at 250 and 300°C. This is ascertained in present NMR experiments.

3) The water which was adsorbed by the rehydration of the thermally dehydrated products in vacuo at 150°C is wholly removed by the treatment of a high vacuum pumping at 110°C.

4) In the rehydrated product of the thermally dehydrated sample in vacuo at 250°C, the adsorbed water of the product changes partially into the structure water and the formation of aluminum hydroxide occurs partially. This is ascertained by the NMR measurements.

5) In the rehydration specimen of the dehydration-product in vacuo at 400°C, the formation of aluminum hydroxide is not observed.

6) It is noteworthy that the variation curve of second moments for the rehydration series—"h_0-series" shows the same figure as the variation curve of second moments for the thermal dehydration series in the air[3].

The author wishes to express his sincere thanks to Dr. Y. Kotera of this Institute for his kind advice. The author also wishes to express his hearty thanks to Professor T. Hagiwara of Hiroshima University for his kind direction and also wishes to express his sincere thanks to Professor T. Sidei and Dr. S. Yano of Kyoto University for their continual guidance and encouragement throughout this study.

Government Chemical Industrial Research Institute, Tokyo
Shibuya-ku, Tokyo

Infrared Spectra of Water of Crystallization in Some Inorganic Chlorides and Sulfates

By Itaru GAMO

(Received September 3, 1960)

The infrared investigation of water of crystallization provides much information on its binding state in the crystal[1,2]. The frequency shifts of its characteristic bands from those of the water vapor seem to be caused mainly by the coördination of water oxygen with metal and by the hydrogen bonding with outer ions. In the present paper, the absorption bands are investigated from this standpoint.

Experimental

Preparation.—The samples were of commercial guaranteed grade. Most of them were recrystallized from water.

1) J. Lecomte, *J. Chim. Phys.*, **50**, C53 (1953).
2) J. Fujita, K. Nakamoto and M. Kobayashi, *J. Am. Chem. Soc.*, **78**, 3963 (1956).

Measurements.—The spectra were obtained by a Perkin-Elmer Infracord double beam spectrophotometer using a rock salt prism. The potassium bromide disk and the Nujol and H. C. B. mull techniques were employed.

Results and Discussion

The results are shown in Table I together with those hitherto obtained. In general our values are in good agreement with them within experimental error. As examples, absorption bands of nickel chloride hexahydrate and zinc sulfate heptahydrate are shown in Figs. 1 and 2, respectively. The error is estimated to be about 2.5 cm^{-1} in the 14 μ region, whereas it is 14 cm^{-1} and 57 cm^{-1}, respectively, in the 6 μ and the 3 μ region. As will be shown later, the 14 μ band is very sensitive to coördination and hydrogen bonding. The 6 μ and the 3 μ band are less sensitive. Furthermore the error is very small in the 14 μ band. For these two reasons attention shall be focussed on the 14 μ region in the following discussion, though they are less prominent.

The author may consider the M—OH$_2$ and the O—H···X(X = Cl or O) distance as a measure

Table I[a]. Observed wave numbers, cm^{-1}[b]

Substance	This research Region					Other researches	Lit.
	3 μ	5 μ	6 μ	14 μ	others		
$CaCl_2 \cdot 6H_2O$	3440 s	2170 w	1630 s	719 m		3432, 3417, 3387, 1663	1
						3440, 3298, 3250	2
$SrCl_2 \cdot 6H_2O$	3470 s	2130 w	1640 m	690 w		3438, 3418, 3383, 1663	1
						3611, 3436, 3391, 3221	3
						3437, 2915, 1629	4
$BaCl_2 \cdot 2H_2O$	3380 s	2060 w	1620 m	709 w		3455, 3324, 3237	5
						3456, 3376, 3345, 3285, 717	6
						3466, 3385, 3327, 3228	7
						3568, 3300, 3230	8
						3370, 1645, 1615, 700	9
$MgCl_2 \cdot 6H_2O$	3430 s	2250 w	1630 s	714 w		3387, 3227	5
						3497, 3352	10
$AlCl_3 \cdot 6H_2O$	3030 s, b	2420 m	1640 m	844 m	1950 w	3312, 3044	11
					1160 w, v. b	3272, 3057	10
						3410, 2915, 1625	4
$CoCl_2 \cdot 6H_2O$	3440 s		1620 m	781 w		3513, 3393, 3151	5
$NiCl_2 \cdot 6H_2O$	3370 s		1610 m	763 w		3513, 3424, 3163	5
						1481, 1089, 1018, 803	12
$Na_2SO_4 \cdot 10H_2O$	3550 s	2080 w	1650 m	719 m		3513, 3431, 3372, 3276	3
$MgSO_4 \cdot 7H_2O$	3290 s		1650 w	749 w		3300, 3214, 3078, 2125, 2044	5
						3393～3506, 3179～3346	10
$ZnSO_4 \cdot 7H_2O$	3230 s	2170 w	1590 w	758 w		3407, 3292～3353	10
$Al_2(SO_4)_3 \cdot 18H_2O$	3330 s	2460 w	1640 w	704 w	2940 s	2957～3528	10
$FeSO_4 \cdot 7H_2O$	3360 s		1630 m	712 w		3330, 1625, 611	9
$CoSO_4 \cdot 7H_2O$	3230 s		1620 w	755 w			
$NiSO_4 \cdot 7H_2O$	3280 s		1630 w	760 w		3279, 3208, 3091, 2078	5

a) Abbreviations: s, strong; m, medium; w, weak; b, broad; v. b, very broad
b) Observed frequencies attributable to SO_4^{2-} modes are omitted.

1) A. W. Marchand, *Compt. rend.*, **242**, 1791 (1956). R
2) G. P. Nayar, *Proc. Ind. Acad. Sci.*, **A8**, 419 (1938). R
3) E. Canals and Peyrot, *Compt. rend.* **207**, 224 (1938). R
4) P. J. Lucchesi and W. A. Glasson, *J. Am. Chem. Soc.*, **78**, 1347 (1956). IR
5) J. Lecomte, *J. Chim. Phys.*, **50**, C53 (1953). IR
6) A. Galy, *Compt. rend.*, **235**, 1504 (1952). R
7) O. Salvetti and D. Nobili, *Chem. Abstr.*, **51**, 12656b (1957). IR
8) C. Duval, *Anal. Chim. Acta*, **13**, 32 (1955). IR
9) F. A. Miller and C. H. Wilkins, *Anal. Chem.*, **24**, 1253 (1952). IR
10) O. Theimer, *Mh. Chem.*, **81**, 301 (1950). R
11) G. P. Nayar, *Proc. Ind. Acad. Sci.*, **A28**, 469 (1948). R
12) C. Duval, R. Duval and J. Lecomte, *Bull. soc. chim. France*, (V) **14**, 1048 (1947). IR

IR: observed in infrared spectra; R: observed in Raman spectra.

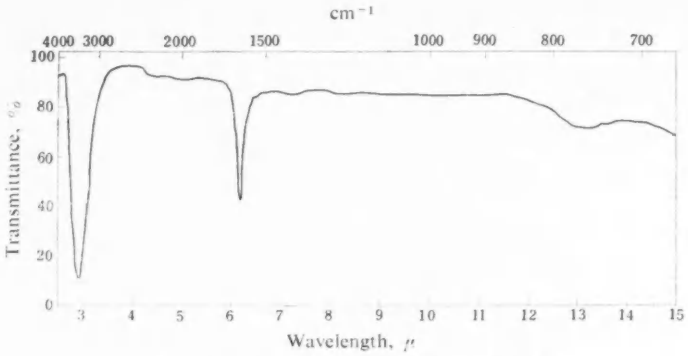

Fig. 1. Absorption bands of $NiCl_2 \cdot 6H_2O$.

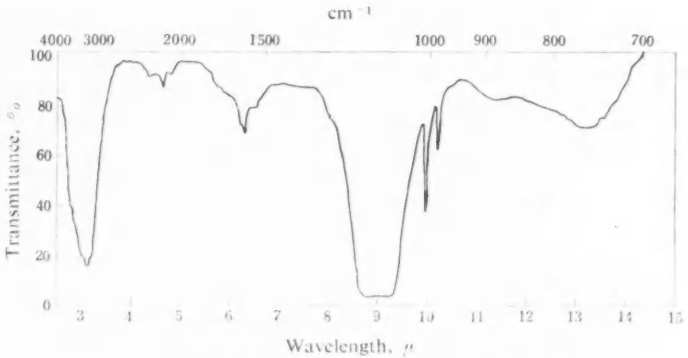

Fig. 2. Absorption bands of $ZnSO_4 \cdot 7H_2O$.

for the strength of coördination and that of hydrogen bonding respectively. The 14 μ band is attributable to either one of the wagging, twisting and rocking modes[3]. In the case of metal ammine complexes the rocking frequency of ammonia[3] seems to increase with increasing coördination and hydrogen bonding[4]. Assuming the additivity for these two effects in the case of water of crystallization also[3], and attributing tentatively our 14 μ band to the rocking mode, the wave number will decrease with increasing distance O—H···X, if the hydrogen bonding effect is predominant. Fig. 3 shows this to be inverse for strontium chloride hexahydrate and magnesium chloride hexahydrate. (The straight hydrogen bondings were assumed throughout, and in case there are more than two kinds of equivalent positions of water in one crystal, the nearest approaches were adopted for O—H···X and for M—OH$_2$ assuming that the observed band peaks correspond to them.). Therefore the coördination effect is larger in the magnesium-water bond than in that of the strontium-water. Correspondingly the former distance is considerably smaller than the latter.

The frequency of the rocking mode increases in the order, strontium chloride hexahydrate, cobaltous chloride hexahydrate and aluminum chloride hexahydrate. These three substances have a nearly equal O—H···Cl distance (3.10 Å), and the metal-water distance decreases in this order. Plotting the observed frequency against the metal-water distance, we obtain a straight line in Fig. 4. In the next place, magnesium chloride hexahydrate and nickel sulfate heptahydrate each occupies a position in the left side of this line corresponding to their metal-water distance. Also, the perpendicular distance between this point and the line is greater in the former than in the latter. This is understandable, since the weaker hydrogen bonding results in the lower frequency and O—H···Cl distances of the former and the latter are 3.21

3) S. Mizushima, I. Nakagawa and J. V. Quagliano, *J. Chem. Phys.*, **23**, 1367 (1955).
4) J. Fujita, K. Nakamoto and M. Kobayashi, *J. Am. Chem. Soc.*, **78**, 3295 (1956).

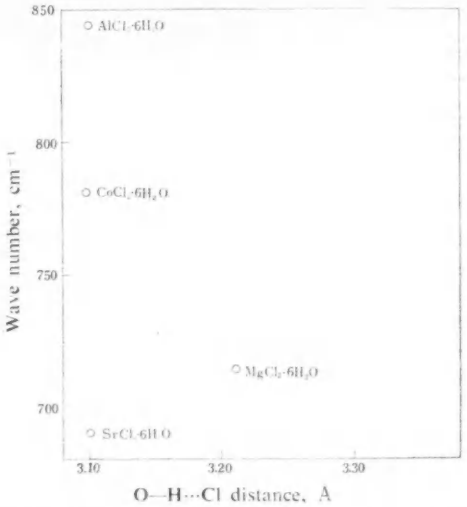

Fig. 3. Rocking frequency versus O—H···Cl distance. References for the interatomic distances :
$SrCl_2 \cdot 6H_2O$, A. T. Jensen, *Kgl. Danske. Videnskab. Selskab. Math-fys. Medd.*, **17**, No. 9 (1940).
$MgCl_2 \cdot 6H_2O$, K. R. Andress and J. Gundermann, *Z. Krist.*, **A87**, 345 (1934).
$CoCl_2 \cdot 6H_2O$, J. Mizuno, K. Ukei and T. Sugawara, *J. Phys. Soc. Japan*, **14**, 383 (1959).
$AlCl_3 \cdot 6H_2O$, K. R. Andress and C. Carpenter, *Z. Krist.*, **A87**, 446 (1934).

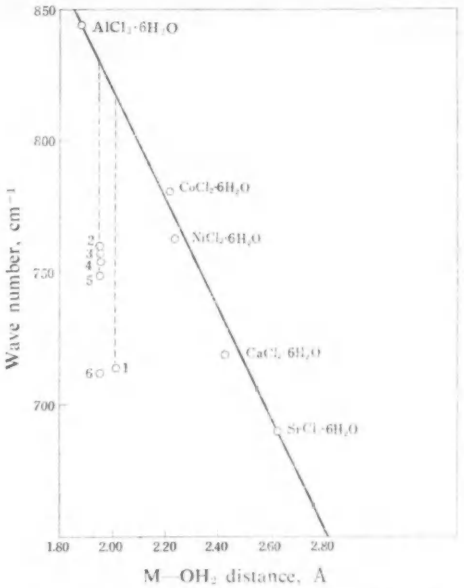

Fig. 4. Rocking frequency versus M—OH_2 distance.

1, $MgCl_2 \cdot 6H_2O$	4, $CoSO_4 \cdot 7H_2O$
2, $NiSO_4 \cdot 7H_2O$	5, $MgSO_4 \cdot 7H_2O$
3, $ZnSO_4 \cdot 7H_2O$	6, $FeSO_4 \cdot 7H_2O$

and 3.13 Å*, respectively. The structures of the other crystals are not yet completely determined. Among them, however, nickel chloride hexahydrate is completely isomorphous with cobaltous chloride hexahydrate[6]. Therefore the periodic table suggests that nickel-water bond has nearly the same distance as cobalt-water. The position of nickel chloride hexahydrate in Fig. 4 seems to be valid on this assumption.

A similar consideration leads to the determination of other points. (Zinc sulfate heptahydrate and magnesium sulfate heptahydrate are isomorphous with nickel sulfate heptahydrate[7], and calcium chloride hexahydrate with strontium chloride hexahydrate[7]. Cobaltous sulfate heptahydrate and ferrous sulfate heptahydrate are mutually isomorphous[8].)

As a whole, the coördination seems to have a considerably greater effect upon this mode than the hydrogen bonding.

These relationships are less definite for the 6 μ (bending[1]) and the 3 μ (stretching[1]) mode. A more exact measurement will permit an analogous treatment.

The 5 μ band of the chlorides seems to be attributable to the combination of the bending and the rocking mode, as in the case of 2222 cm^{-1} band in ice[1,9], although there remains a possibility of assigning it to the stretching mode strongly affected by the two effects, as Fujita et al. did for the weak band at 2270 cm^{-1} in nickel glycinate dihydrate[2]. For the sulfates, this combination band may probably be overlapped with that of the totally symmetric and the triply degenerate stretching mode of sulfate ion.

Summary

The characteristic bands of water of crystallization in various chlorides and sulfates were determined in the rock salt region. The results were classified and explained inclusively

* This 3.13 Å is obtained by subtracting the radius of oxygen atom 1.32 Å from the observed O—H···O distance[5], and adding the radius of chlorine atom 1.81 Å.

5) C. A. Beevers and C. M. Schwartz, *Z. Krist.*, **A91**, 157 (1935).

6) J. Mizuno, K. Ukei and T. Sugawara, *J. Phys. Soc. Japan*, **14**, 383 (1959).

7) A. T. Jensen, *Kgl. Danske Videnskab. Selskab. Math.-fys. Medd.*, **17**, No. 9 (1940).

8) I. Ness, *Naturwiss.*, **28**, 78 (1940).

9) J. J. Fox and A. E. Martin, *Proc. Roy. Soc.*, **A174**, 234 (1940).

by the effects of coördination and hydrogen bonding.

The author wishes to express his thanks to Professor Takehiko Shimanouchi of the University of Tokyo for his guidance throughout the course of this study.

Chemical Laboratory
Department of General Education
Faculty of Science and Engineering
Waseda University
Shinjuku-ku, Tokyo

Infrared Absorption Spectra of Water of Crystallization in Copper Sulfate Penta- and Monohydrate Crystals

By Itaru GAMO

(Received September 20, 1960)

Infrared spectra of copper sulfate penta- and monohydrate have been separately subject to several investigations[1-3]. However, there has been no comparative study of these spectra in relation to their structural difference.

In the present paper, observed spectra were examined in relation to this difference, mainly to that of the binding state of the water molecules in them.

Experimental

Preparation.— Copper sulfate pentahydrate of commercial first grade was made free from iron according to Gmelin's handbook[4]. The sample was then twice recrystallized from water. Copper sulfate monohydrate was obtained by keeping this purified pentahydrate at 110°C for 3 hr. under reduced pressure in an Abderhalden apparatus[5].

Measurements.— Spectra were obtained by means of a Perkin-Elmer Infracord spectrophotometer with a rock salt prism. The Nujol mull technique was employed throughout. The potassium bromide disk technique was unsuitable for the pentahydrate, because the prepared disk became dark brown. A similar phenomenon was observed in the case of cupric chloride dihydrate.

Results

The spectra are given in Fig. 1. In the 3 μ region one peak is observed for the pentahydrate at 3420 cm^{-1}, and two peaks for the monohydrate at 3340 and 3190 cm^{-1}. These compare with the peak of various inorganic hydrated sulfates[6] in this region, and can be assigned to O-H stretching vibrations of water. Overlapping of the symmetric and the antisymmetric mode together with their splitting is probably responsible for the broadness of these three bands. In the 5 μ region the spectrum of the pentahydrate shows a weak band at 2120 cm^{-1}, attributable to a combination of the bending and the rocking mode of water or that of the totally symmetric and the triply degenerate stretching mode of sulfate ion. Of course there is a possibility of their overlapping. In the 6 μ region a band of medium intensity is observed at 1640 cm^{-1} for the pentahydrate. At the same position a broad weak band is observed for the monohydrate, with an additional band of medium intensity at 1510 cm^{-1}. These three can be assigned to the bending modes of water, the latter two resulting from splitting.

In the 8 μ region, characteristic bands of inorganic sulfates[7] are observed for the pentahydrate at 1200 and 1170 cm^{-1} and for the monohydrate at 1200 and 1120 cm^{-1}, attributable to the triply degenerate stretching vibrations of sulfate ion. The sharp 1000 and 966 cm^{-1} bands of the former and the 1020 cm^{-1} band of the latter can be assigned to the totally symmetric stretching vibrations that have become active in infrared by some perturbations. In this connection it is to be noticed that the intensities of the former two bands are considerably greater than in the usual cases of sulfates. The 875 cm^{-1} band of

1) J. Lecomte, *Compt. rend.*, **226**, 1088 (1948); *J. chim. Phys.*, **50**, C53 (1953).
2) O. Matsumura, *Mem. Fac. Sci., Kyushu Univ., B*, **1**, 1 (1951).
3) J. Fujita, K. Nakamoto and M. Kobayashi, *J. Am. Chem. Soc.*, **78**, 3963 (1956).
4) "Gmelins Handbuch der anorganischen Chemie", part 60, Cu B1 (1958), p. 508.
5) ibid., p. 523.
6) I. Gamo, This Bulletin, **34**, 760 (1961).
7) L. J. Bellamy, "Infrared Spectra of Complex Molecules", Methuen and Co., Ltd., London (1958), p. 345.

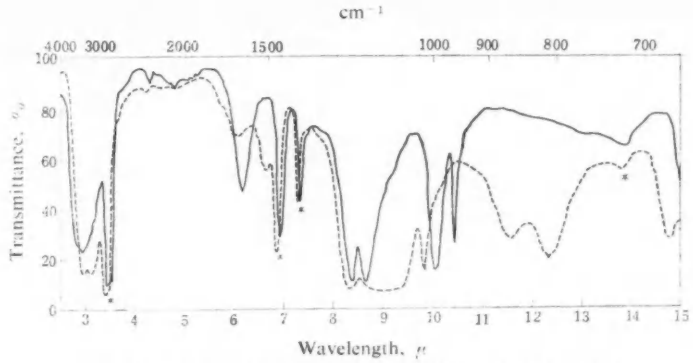

Fig. 1. Observed bands of $CuSO_4 \cdot 5H_2O$ and $CuSO_4 \cdot H_2O$.
——, $CuSO_4 \cdot 5H_2O$; – – –, $CuSO_4 \cdot H_2O$
* Nujol bonds

the pentahydrate found by Fujita et al.[3] was observed in our study only when the spectrum in this region was recorded immediately after the mull preparation. In the 12μ region of the monohydrate spectrum, strong but broad peaks are observed at 866 and 813 cm^{-1}, in rough accord with Lecomte's values[1], 850 and 796 cm^{-1}, respectively. They are tentatively assigned to the rocking modes of water. The 676 cm^{-1} band of the monohydrate are assigned to the triply degenerate bending vibration of sulfate ion.

Tables I and II summarize these results.

TABLE I. OBSERVED FREQUENCIES OF $CuSO_4 \cdot 5H_2O$

Wave number, cm^{-1}	Assignment
3420 s	ν (H_2O) stretch.
2120 w	$\nu_3 - \nu_1$ (SO_4) and/or $\nu_{II} - \nu_2$ (H_2O)
1640 m	ν_2 (H_2O) bend.
1200 s	ν_3 (SO_4) stretch.
1170 s	ν_3 (SO_4) stretch.
1000 s	ν_1 (SO_4) stretch.
966 s	ν_1 (SO_4) stretch.
875 s[a]	ν_{II} (H_2O) rock.

a. Observed by Fujita et al. (See Ref. 3.)

TABLE II. OBSERVED FREQUENCIES OF $CuSO_4 \cdot H_2O$

Wave number, cm^{-1}	Assignment
3340 s	ν (H_2O) stretch.
3190 s	ν (H_2O) stretch.
1640 w	ν_2 (H_2O) bend.
1510 w	ν_2 (H_2O) bend.
1200 s	ν_3 (SO_4) stretch.
1120 s	ν_3 (SO_4) stretch.
1020 s	ν_1 (SO_4) stretch.
866 m	ν_{II} (H_2O) rock.
813 m	ν_{II} (H_2O) rock.
676 m	ν_4 (SO_4) bend.

Discussion

According to X-ray analysis[2], four of the water molecules in copper sulfate pentahydrate crystal are closely coördinated with a copper atom by fairly covalent bonds, making a square with the copper atom at the center. The fifth occupies a hole in the structure, and hardly differs from the free water molecule.

Although the interatomic distances in copper sulfate pentahydrate crystal are determined well by the X-ray analysis, those in the monohydrate crystal are completely unknown. Nevertheless comparison of the unit cell parameters (see Table III) shows that the structure of the latter is quite different from that of the former, corresponding to a considerable rearrangement of atoms upon partial dehydration. In the following, we shall confine our discussion mainly to water bands.

Since copper sulfate pentahydrate belongs to the symmetry class C_1^1[8], we can expect theoretically many water bands, due mainly to the splitting of the bands of the free molecule. Actually, only two peaks were observed in our study that are attributable to water. The resolving power of the instrument, which becomes rapidly small with increasing wave number, seems to be partly responsible for this poor observation. Nevertheless some interesting results are obtained.

The author assume tentatively the 3420 cm^{-1} band to be due to the antisymmetric stretching vibration affected by the coördination of copper-water and by the hydrogen bonding between the water molecule and the outer oxygen atom of sulfate ion. Its deviation from the vapor

8) C. A. Beevers and H. Lipson, *Proc. Roy. Soc.*, **A146**, 570 (1934).
9) F. Hammel, *Ann. Chim.*, (11) **11**, 247 (1939).

TABLE III. COMPARISON OF UNIT CELL PARAMETERS

	Type	Symmetry	a	b	c	β	M	Lit.
$CuSO_4 \cdot 5H_2O$	$H_{4,0}$	C_1^1	6.12 Å	10.70 Å	5.97 Å	107.4°	2	8
$CuSO_4 \cdot H_2O$	—	m k l	6.80	7.90	12.6	~90	—	9

frequency (3756.5 cm^{-1}) is reasonable as compared with those of other hydrated salts. The fairly large covalent character of the copper-water bond (distance 1.98 Å), together with the strong hydrogen bond of 2.75 Å, is sufficient to explain this order of magnitude. In the next place, both the 3340 and the 3190 cm^{-1} band of the monohydrate can be reasonably assigned either to antisymmetric or to symmetric vibration. The observed doublings of the bending and the rocking vibration (see later) together with the nearly equal intensity of the two bands, seem to support this assignment strongly. The main cause of this doubling is probably a rather strong coupling of two neighboring water molecules through hydrogen bonding to the same oxygen atom of sulfate ion. The values of the two frequencies suggest that in this crystal, the binding strength between one water molecule and the neighboring sulfate ion is considerably greater than in the pentahydrate crystal. The magnitude of the change in the bending frequency of the pentahydrate is reasonable as compared with the values of other salts. In the monohydrate one of the two frequencies is reasonably higher than that in the vapor state (1595.5 cm^{-1}). The other is lower and therefore rather exceptional for this mode. Both bands are broader than in the usual cases of sulfates. This suggests stronger interaction. In these two respects, the bending modes of the water molecule in this crystal deserve to be noticed.

The shapes and the frequency values of the two rocking bands of the monohydrate are the same as usual. The great value of the splitting (53 cm^{-1}) as well as the value in the case of the bending mode (130 cm^{-1}) seems to support the above assumption of hydrogen bonding. An intensity consideration in the two modes (see Fig. 1) suggests that the two hydrogen bonds are not completely equivalent. This is understandable, since the numerical ratio of water molecules to sulfate ions in the crystal is 1 : 1, preventing the two water molecules from occupying a position equivalent to the same oxygen atom. We can roughly estimate the mean value of the two O-H···O distances by using the relation obtained in the preceding paper. The two water molecules are assumed to make covalent bonds of equal length (1.98 Å, value in the ligand water molecule of the pentahydrate) with two different copper atoms respectively. In Fig. 4 of that paper the O-H···O distance is thus estimated to be somewhat smaller than 2.61 Å using the mean value of the two rocking frequencies and the covalent bond length 1.98 Å.

The author could not observe the band peaks expected from the fifth almost free water molecule in the pentahydrate crystal. Probably they are weak and hidden in other bands.

The author shall now proceed to a brief discussion of the sulfate ion bands. For the pentahydrate, the observed two frequencies of ν_3 are higher than that in solution (1104 cm^{-1} [10]). For ν_1, however, one component is higher and the other, lower than ν_1 in solution (981 cm^{-1} [10]). According to X-ray analysis[5], the four sulfate oxygen atoms in this crystal are all making different contacts with other atoms or molecules. Probably this is responsible for these splittings. For the monohydrate, the bands are fairly broader than in the pentahydrate. It is very interesting that one component of the doublet band ν_1 (966 cm^{-1} of the pentahydrate) disappears upon the partial dehydration.

Summary

The observed spectra of water in the penta- and monohydrate crystals were interpreted by the effects of coördination copper-water and hydrogen bonding O-H···O. The whole difference in the spectra of the two crystals were explained in relation to the escape of the four ligand water molecules and the resulting rearrangement of atoms. The stretching, bending and rocking modes, which are single in the case of the pentahydrate, split into doublets in the monohydrate. This result was explained by a single assumption of strong coupling of two neighboring water molecules in the latter.

The author is indebted to Professor Takehiko Shimanouchi of the University of Tokyo for his helpful guidance.

Chemical Laboratory
Department of General Education
Faculty of Science and Engineering
Waseda University
Shinjuku-ku, Tokyo

10) K. W. F. Kohlrausch, "Ramanspektren. Hand- und Jahrbuch der chemischen Physik", 9, part 6 (1943), p. 399.

Polymerization of Propylene with Tin Tetraalkyl-Titanium Tetrachloride Catalyst

By Nobuyuki ASHIKARI and Masakazu HONDA

(Received November 19, 1960)

Many studies[1] on the catalyst for preparing polypropylene have been performed, since Natta obtained the polypropylene having high molecular weight and high stereoregularity. On the polymerization of propylene using tin tetraalkyl as a catalyst component, only a Du Pont patent[2] has been known. However, the description is so brief that the details are not explained. From our preliminary experiments of the polymerization of propylene using tin tetraalkyl in combination with titanium tetrachloride, titanium trichloride, dichlorodialkyl titanate, or tetraalkyl titanate, it was found that the effective catalyst was only the complex comprising titanium tetrachloride as a component. Moreover, when the catalyst was used as soon as the two components were mixed, the polymer produced thereby contained a greater part of low polymer. Accordingly, the polymerization in this study was performed considering the adequate times for the production of the complex.

Experimental and Results

Reaction between Tin Tetraalkyl and Titanium Tetrachloride.—The reaction between tin tetraalkyl and titanium tetrachloride does not proceed very fast, and so prolonged reaction times are required for the completion of the complex. The reaction rate depends, of course, upon the reaction temperature, the length of alkyl chain in the tin tetraalkyl, and the ratio of the catalyst components. Besides, the presence of a solvent will affect the reaction rate. However, the catalyst preparation in this study was performed without solvent, because the presence of the solvent makes the end-point of reaction obscure.

When the catalyst is prepared in a solvent without vigorous stirring, the product precipitates at the bottom of the vessel as an adhesive mass which can not be easily dispersed into the solvent. Generally, if the ratio of the two components deviates greatly from unity, both components still remain in liquid form after the reaction is over. Therefore, in this case, the end-point of reaction is not clear. On the other hand, when the ratio is about 1.0, the whole becomes solid exhibiting a comparatively apparent end-point. Therefore, the experiments for observing the times required for the production of the complex were carried out without any solvent at about equimolar composition of tin tetraalkyl and titanium tetrachloride. In Fig. 1, the effects of the alkyl radical in the tin tetraalkyl molecule and the reaction temperature upon the rate of the production of the complex are represented.

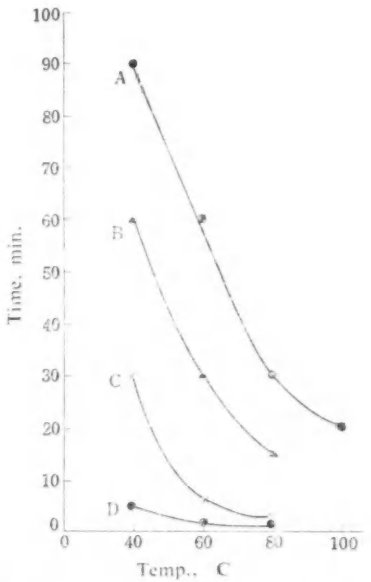

Fig. 1. Time required for the complex production.

A; *n*-Butyl C; Isopropyl
B; *n*-Propyl D; Ethyl

The vertical axis in Fig. 1 represents the times required for the solidifying of the two components which were mixed at a given temperature. The preparation of catalyst complex in the following experiments was performed referring to this condition; also analogously in the case where the ratio of the two component deviates passably from unity.

Polymerization Procedure.—In a cooled polymerization tube containing the complex which had been prepared by mixing the two components, a definite amount of monomer was introduced. The complex was shattered in a high speed shaker. In the case of polymerization in solution, the shattering of the complex was taken before the monomer

1) For example, G. Natta, I. Pasquon and E. Giachetti, *Angew. Chem.*, **69**, 213 (1957).
2) E. I. Du Pont de Nemours & Co., Brit. Pat. 777538 (June 26, 1957).

was introduced. The tube was immersed in a constant temperature bath. After the reaction proceeded for definite reaction times, the tube was cooled by dry ice-methanol, and vented. Then, the contents of the tube were treated with methanol acidified by hydrochloric acid to decompose the catalyst, washed with methanol several times, and dried under reduced pressure.

Measurement of Viscosity.—The viscosity of the polymer solution was measured using tetralin, as a solvent, which had been purified by distillation after being dried over sodium, using an improved Ubbelohde viscometer of dilution type, at 135±0.05 C. The viscometer was filled with nitrogen during the measurement.

The molecular weight of the polymer was calculated using Ciampa's equation[3] shown below.

$$[\eta] = 0.25 \times 10^{-4} M$$

Dependence of Conversion and Insoluble Part of Polymer in Boiling *n*-Hexane on the Composition of Catalyst.—The influence of the ratio of catalyst components upon the conversion and the insoluble part of polymer in boiling *n*-hexane was investigated by the polymerization using a catalyst complex of tin tetraethyl-titanium tetrachloride. In each experiment, 5 g. of monomer was polymerized with a catalyst containing 9.26×10^{-2} mol. of titanium tetrachloride and a definite amount of tin tetraethyl (which is represented in Table I), in 5 cc. of *n*-hexane at 30 C for 25 hr. The Results are shown in Table I.

TABLE I. EFFECT OF THE RATIO OF COMPONENTS IN THE COMPLEX UPON THE CONVERSION AND THE INSOLUBLE PART IN BOILING *n*-HEXANE

No.	SnR_4 $TiCl_4$	Convertion %	Insoluble part in *n*-hexane, %
1	0.54	4.01	8.61
2	0.82	2.72	11.52
3	1.09	0.71	12.21
4	1.36	2.11	15.14
5	1.64	15.75	18.32
6	1.91	8.73	17.26

$TiCl_4$; 9.26×10^{-2} mol., Monomer; 5 g. *n*-Hexane; 5 cc., Temp.; 30 C.

It is seen that a minimum for the rate of polymerization exists where the ratio of tin tetraethyl to titanium tetrachloride is about unity. This respect is discussed afterward.

Effects of Alkyl Radical in SnR_4 and the Temperature of Complex Preparation upon the Conversion and the Molecular Weight of Polymer.—In each experiment, 15 g. of monomer was polymerized with the catalyst which was prepared by mixing the two components, i.e., 2.024×10^{-2} mol. of tin tetraalkyl and 1.852×10^{-2} mol. of titanium tetrachloride, in a sealed tube at 40 C for 15 hr. Each polymer was then extracted by boiling *n*-hexane. This procedure was made to find the percentage of so-called isotactic polymer which had been defined by Natta as an isoluble part in boiling *n*-heptane. In this sence, the extraction has to be made, if possible, by *n*-heptane. However, the greater part of the polymer which would be extracted by boiling *n*-heptane is also extracted by boiling *n*-hexane, as is shown in Table III. Accordingly, the solvent, *n*-hexane was used. These results are shown in Table II.

The effect of the temperature of catalyst preparation upon the conversion is represented in Fig. 2.

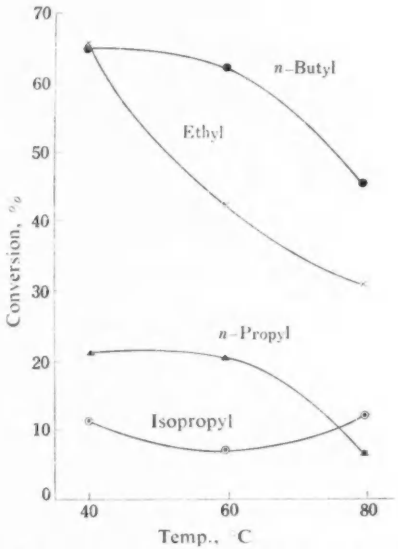

Fig. 2. Effect of the temperature of the catalyst preparation upon the conversion.

The polymerization with the catalyst prepared at lower temperature resulted in higher conversion, which gave lower molecular weight and further lower percentage of polymer insoluble in boiling *n*-hexane (except for the case of tin tetraethyl).

Extraction of the Polymer with Various Solvents.—To find the percentage of atactic and isotactic parts which are contained in the polymer prepared with the tin tetraethyl-titanium tetrachloride catalyst, 55.774 g. of the polymer was successively extracted by such series of solvents as acetone, diethyl ether, *n*-hexane, and *n*-heptane. The sample employed in this extraction was prepared by polymerizing 75 g. of monomer with the catalyst which had been prepared at 20 C by the reaction between 1.012 mol. of tin tetraethyl and 0.926 mol. of titanium tetrachloride. In this polymerization reaction (at 40 C, for about 15 hr.), 57.428 g. of the polymer was obtained (conversion; 76.6%). The viscosity of each fraction was measured by means of the aforementioned method. These results are shown in Table III.

It[4] has already been known that an organo

3) G. Ciampa, *Chim. e ind.* (*Milan*), **38**, 298 (1956).

4) N. G. Gaylord and H. F. Mark, "Linear and Stereoregular Addition Polymers" Interscience Publishers, Inc., New York (1959), p. 129.

TABLE II. POLYMERIZATIONS AT VARIOUS TEMPERATURES USING VARIOUS TIN TETRAALKYLS

R in SnR_4	Cat. preparation temp., C	Conversion %	Insoluble part (%) in boiling hexane	$[\eta] \times 10$	$M \times 10^{-3}$
Ethyl	40	65.7	18	2.4	9.7
〃	60	42.5	12	1.5	6.2
〃	80	31.6	14	1.9	5.1
n-Butyl	40	65.4	4	0.8	3.2
〃	60	62.4	3	1.0	4.1
〃	80	45.7	5	1.4	5.6
Isopropyl	40	11.5	—	0.4	1.4
〃	60	7.4	—	0.4	1.7
〃	80	12.1	—	0.3	1.1
n-Propyl	40	21.1	2.6	0.8	3.2
〃	60	20.4	4.2	1.1	4.0
〃	80	6.4	4.0	1.3	5.1

The viscosity was measured for the original polymer.
Monomer; 15 g., Temp.; 40 C, Time; 15 hr.
SnR_4; 2.024×10^{-2} mol., $TiCl_4$; 1.852×10^{-2} mol.
The polymers prepared with $Sn(i\text{-}C_3H_7)_4$-$TiCl_4$ were grease-like, and so, the extractions were not carried out.

TABLE III. EXTRACTION WITH VARIOUS SOLVENTS

Solvent	Polymer, g.	Fraction, %	$[\eta]$	$M \times 10^{-3}$	M. p., C
Acetone	2.584	4.6	—	—	
Ether	22.370	40.1	0.11	4.4	
n-Hexane	20.363	40.4	0.13	5.2	
n-Heptane	2.036	3.7	0.26	10.4	120
(Residue)	6.255	11.2	1.02	40.8	155~160

metallic compound containing the metal with smaller ionic radius, results in a higher yield of isotactic polymer. Accordingly, it is natural that the polymerization using a compound of tin as a catalyst component results in a lower yield of isotactic polymer.

Rate of Polymerization.—In order to find the rate of polymerization, the following experiment was performed. Each polymerization was carried out in a sealed tube with tin tetraethyl-titanium tetrachloride catalyst consisting of 2.024×10^{-2} mol. of the former and 1.852×10^{-2} mol. of the latter. The catalyst was shattered finely by a high speed shaker in 15 cc. of *n*-hexane before the monomer (10 g.) was introduced. The polymers were treated by means of the aforementioned method. The relation between the conversion and the reaction time is represented in Fig. 3.

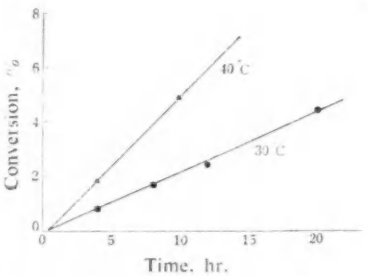

Fig. 3. Polymerization rate in *n*-hexane.

The rates at 30 and 40 C were calculated from Fig. 3 as 0.22%-conversion/hr. and 0.5%-conversion/hr., respectively. The values indicate that the polymerization of propylene with tin tetraalkyl-titanium tetrachloride catalyst proceeds very slowly in the solution system.

Infrared Spectra.—In order to compare the microstructure of the polymer prepared by the tin tetraethyl-titanium tetrachloride catalyst with that

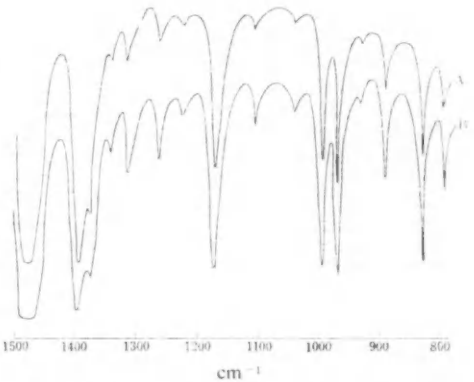

Fig. 4. Infrared spectra of in boiling heptane insoluble polymers.
A; Polymer prepared with SnR_4 $TiCl_4$
B; Moplen

of 'Moplen', the polymer prepared by aluminium-trialkyl-titanium trichloride catalyst, the infrared spectrum of the insoluble part in boiling *n*-heptane was observed. B is a spectrum of *n*-heptane insoluble part of Moplen. From the comparison of A with B, it is obvious that these polymers are strikingly similar in their microstructures.

Discussion

Generally, the Ziegler catalyst consists of Lewis acid and Lewis base. Therefore, a cationic or an anionic reaction will predominantly occur according to the catalyst composition in which Lewis acid or base is contained in excess, respectively.

The double bond of propylene, of course, is easily attacked by a cationic catalyst, owing to the effect of the methyl group. Moreover, it is also well known that, in the case of cationic polymerization, the growth of the chain easily terminates by a chain transfer. Thus, the rate of cationic polymerization is steady, but the polymer produced has usually a low molecular weight and further low stereoregularity. On the other hand, in the case of anionic polymerization, a polymer having a high molecular weight and further high stereoregularity is usually obtained, while the rate of reaction becomes smaller than that of cationic reaction.

From the facts mentioned above, it may be said that the decrease of conversion (from No. 1 to No. 3) with an increase in the amount of tin tetraethyl will mean that the cationic character is replaced gradually by the anionic character. It is also considered that, in Nos. 3—6, the effective anionic catalyst increases with the increase of the amount of tin tetraethyl.

Next we discuss the effects of temperature of catalyst preparation upon the convertion, the insoluble part in boiling *n*-hexane and stereospecificity. As is apparent from Fig. 1, the reducing power is the strongest in the case of tin tetraethyl, so that the effective anionic catalyst will be produced even at a lower temperature, in such a case. The fact that both the conversion and the stereospecificity decrease with an increase in the temperature will mean a decreasing of the active center which is in suitable valence state.

In the case of the propyl or butyl radical, the reducing power is so much weaker than that of the ethyl radical, that a temperature which is suitable for preparing the effective complex containing the latter, is unsuitable for producing the effective one containing the former. At such a lower temperature, the somewhat cationic character will still remain in the complex. When the temperature becomes higher, the cationic character will decrease, and so the conversion decreases while the stereospecificity increases, as is seen in Table II.

In regard to the effects of the length of the alkyl radical upon the conversion and the stereospecificity, no distinct relations between them were obtained.

Electrical Communication Laboratory
Nippon Telegraph and
Telephone Public Corporation
Musashino-shi, Tokyo

Neutron and γ-Irradiation of Propionamide

By Enzō TACHIKAWA and Gen-ichi TSUCHIHASHI

(Received August 12, 1960)

When molecules containing nitrogen atoms are irradiated with neutron, the nuclear transformation

$$^{14}N + n \rightarrow (^{15}N)^* \rightarrow {}^{14}C + p$$

takes place. A carbon-14 atom thus produced immediately ruptures the bond which holds it due to its tremendous recoil energy and becomes a hot atom. Therefore, an unusual reaction is expected to occur as the hot atom loses its energy by collision. As an example of neutron irradiation of nitrogenous organic compound, ammonium nitrate was first studied with a view of the production of carbon-14 activity by Ruben and Kamen[1] in 1940. Recently, several researchers have attempted the neutron irradiation of many compounds[2]. But these results were not completely accounted for either by the simple random substitution of carbon atom or, of course, by ordinary thermal reaction.

1) S. Ruben and M. D. Kamen, *Phys. Rev.*, 57, 549 (1940).
2) R. C. Extermann, "Radioisotopes in Scientific Research", Vol. II, Pergamon Press, London (1958), p. 114.

In order to examine the mechanism of hot atom reaction in detail, the present authors carried out the neutron irradiation of propionamide and found that the methylation of the amide was the main results and the authors determined the activity distributions in the products: ^{14}C-propionamide, ^{14}C-butyramide, ^{14}C-isobutyramide, ^{14}C-ethyl methyl ketone. Methyl radicals produced by γ-irradiation are less energetic than the hot atoms produced from the nuclear transformation. In order to compare the reactivity of the carbon-14 hot atoms with those of methyl radicals from carbon-carbon bond fissions by γ-ray irradiation, the γ-ray irradiation of propionamide-(carbonyl-^{14}C) was studied also in the present work and the yields of butyramide and isobutyramide were determined by the isotope dilution method.

Moreover, the reaction of propionic acid with thermal methyl radicals produced by the decomposition of acetyl peroxide was studied and the abnormality in the distribution of products in the above cases is discussed in comparison with the result of the thermal reaction.

Experimental

Neutron Irradiation.—*Irradiation of Sample.*—Propionamide was synthesized from propionic acid and ammonium carbonate by Coleman-Alvarado's method[3] and recrystallized from methanol-ether solution. The butyramide and isobutyramide used as carriers were synthesized by the same method as propionamide. Commercial ethyl methyl ketone was purified by fractionation with a Podbielniak high temperature distillation apparatus (60-plates heli-grid packing column). Fifteen grams of the propionamide were covered with a polyethylene sheet and then packed in a polyethylene capsule. The assembled mass was iraadiated in the J. R. R.-1 reactor at an approximate flux of 10^{11} neutron/cm^2/sec. for about 120 hr. After irradiation, about a month was allowed for the decay of short-lived species in the capsule. As soon as it was opened, the irradiated sample was separated into several portions for the subsequent experiments.

Separation of Products.—To separate butyramide and isobutyramide a carrier was added to the irradiated sample. In the case of propionamide, some more non-active carrier was added. The mixture was hydrolyzed by refluxing for 2 hr. with 50% hydrochloric acid and the resulting substance was purified by distillation and by a Podbielniak gas chromatography on a 1/4"×4ft. column containing fire brick celite (30~80 mesh): 50% D. C. 710 silicone plus 10% stearic acid constituted the liquid phase. The column temperature was kept at 100 C and helium was used as the carrier gas.

3) G. H. Coleman and A. M. Alvarado, "Organic Syntheses", Coll. Vol. I, (1948), p. 3.

Separation of Ethyl Methyl Ketone.—Ethyl methyl ketone was separated as 2,4-dinitrophenyl hydrazone by addition of 2,4-dinitrophenylhydrazine and this was recrystallized from ethanol several times to give a constant specific activity.

Table I. The quantities of irradiated sample and carriers

Separated sample	Irradiated sample, g.	Carrier, g.
Propionic acid	4.133	—
Butyric acid	3.465	4.809
Isobutyric acid	3.465	4.581
Ethyl methyl ketone	0.243	1.193

γ-Irradiation.—*Irradiation of Sample.*—About 5 g. of propionic acid purified with the distillation apparatus was added to sodium propionate (carbonyl-^{14}C) (0.1 mg., 0.1 mc./mg.). Propionyl chloride-(carbonyl-^{14}C) was synthesized from the mixture and benzoyl chloride by the method that is cited in the literature[4]. The distillate up to 81 C was dissolved in benzene and converted to propionamide-(carbonyl-^{14}C) with ammonia. It was recrystallized from methanol-ether several times to give a constant specific activity of 4.7×10^2 μc./mol. Three grams of the propionamide-(carbonyl-^{14}C) were irradiated by the 10000-curie ^{60}Co γ-source[5] with a dose rate of 1.2×10^5 r./hr. at room temperature. The dose rate was determined by both cerous-ceric[6] and ferric-ferrous[7] dosimeter. The absorbed dose was 2×10^5 r.

After irradiation the sample was separated into several portions for the subsequent experiments.

Separation of Products.—In this case, propionamide was added as a hold back carrier, also. Acids were separated by the same procedure as that described above. The acids were converted again to amide by benzoyl chloride and ammonia and then were recrystallized.

Table II. The quantities of irradiated sample and carriers

Separated sample	Irradiated sample, g.	Carrier g.	Hold back carrier, g.
Butyric acid	1.00	1.50	2.00
Isobutyric acid	1.00	1.50	2.00

3. Decomposition of Acetyl Peroxide in Propionic Acid-(Carboxyl-^{14}C).—*Preparation and Purity of Acetyl Peroxide.*—Acetyl peroxide was synthesized by the Gambarjan method[8] modified by Kharasch[9].

Its purity was 99.86%.

4) N. D. Cheronis, "Technique of Organic Chemistry", Vol. VI, "Micro and Semimicro Method", Interscience Publishers, Inc., New York (1954), p. 284.

5) A. Danno et al., Abstract of the 7th Hot Laboratories and Equipment Conference, Cleveland (1959), p. 349~360.

6) For example, T. Rigg, G. Stein and J. Weiss, *Proc. Roy. Soc.*, **A211**, 375 (1952).

7) G. R. A. Johnson and J. Weiss, ibid., **A240**, 189 (1952).

8) S. Gambarjan, *Ber.*, **42**, 4010 (1909).

9) M. S. Kharasch, H. C. Mckay and W. H. Urry, *J. Org. Chem.*, **10**, 394 (1945).

Propionic Acid-(Carboxyl-^{14}C).—Non-active propionic acid which was purified by the Podbielniak high temperature distillation apparatus was added to the sodium propionate-(carboxyl-^{14}C) (0.1 mc./mg.).

The mixture was purified by several distillations in the distillation apparatus. The specific activity of the purified propionic acid-(carboxyl-^{14}C) was 4.25 mc./mol.

Decomposition of Acetyl Peroxide.—Acetyl peroxide (507.8 mg.) was dissolved in 4.00 ml. of propionic acid-(carboxyl-^{14}C). The mixture was heated at 95~100°C for five hours.

Separation of Acids.—Acids were separated and purified by the same procedure as in the case of γ-irradiation.

Table III. The quantities of solution and carriers

Separated sample	Reaction mixture, ml.	Carrier ml.	Hold back carrier, ml.
Isobutyric acid	1.00	2.00	2.00
Butyric acid	1.00	2.00	2.00

Oxidation and Counting.—The purified compounds were converted to carbon dioxide by the Van Slyke-Folch oxidation method[10].

The resulting carbon dioxide was absorbed by 0.74 N sodium hydroxide solution and then precipitated as barium carbonate by the addition of barium chloride-ammonium chloride solution. The specific activity of the barium carbonate was measured at infinite thickness by a Tracerlab T. G. C-14 counter.

Result and Discussion

The obtained results about the neutron irradiation of propionamide are shown on Table IV. The approximate relative ratio of the yields of ethyl methyl ketone, butyric acid, isobutyric acid, propionic acid were 1:2:3:4. ^{14}C-Propionamide would be produced by the replacement of a carbon atom in the parent molecule with the recoiling carbon-14.

$$CH_3CH_2CONH_2 \xrightarrow{^{14}N(n,p)^{14}C} \text{recoil } ^{14}C + \text{molecular fragments} \quad (1)$$

$$\text{recoil } ^{14}C + CH_3CH_2CONH_2 \longrightarrow {}^{14}CH_3CH_2CONH_2,\ CH_3{}^{14}CH_2CONH_2,\ CH_3CH_2{}^{14}CONH_2 + \text{knockon-}^{14}C + \text{etc.} \quad (2)$$

Ethyl methyl ketone was produced by a "knockon" reaction by ^{14}C at nitrogen in the parent compound. Butyramide and isobutyramide were formed by the replacement of hydrogen in propionamide with ^{14}C-radicals, respectively.

$$(^{14}CH_3\cdot)^* \text{ or } (^{14}CH_2{:})^* + CH_3CH_2CONH_2 \longrightarrow {}^{14}\text{C-butyramide or } {}^{14}\text{C-isobutyramide} + \text{etc.} \quad (3)$$

It is known that in ordinary free radical reactions, the hydrogen attached to a secondary carbon atom is more reactive with a free radical than that attached to a primary carbon atom. If butyramide and isobutyramide were formed by the thermal reaction of free methyl or methylene radical, the yield of isobutyramide which would be produced by the substitution of the hydrogen atom attached on the secondary carbon of propionamide would be much larger than that of butyramide. However, the ratio of the yields of butyr- and isobutyramide in the present study was about 3:2 as is shown in Table IV. The value agrees with the ratio of the number of hydrogen atoms available for substitution in the propionamide to give butyr- or isobutyramide. Accordingly, another mechanism should be considered instead of the ordinary free radical mechanism. Here the present authors propose the following mechanism:

(1) ^{14}C-Propionamide is produced by a "knockon" reaction of the carbon in the compound by the carbon-14 having high kinetic energy. (Eq. 2). (2) Most of the recoil carbon-14 are cooled by collisions with atoms or molecules to some extent so that its energy would be in the order of 25~50 eV.[11] However the recoil carbon-14 is extremely active and reacts with its surroundings, and its predominant tendency will be to gain hydrogens as follows.

$$\text{recoil carbon-14} + \text{organic matrix} \longrightarrow {}^{14}CH_3\cdot,\ {}^{14}CH_2{:},\ {}^{14}CH_3{}^+,\ \text{etc.} \quad (4)$$

The energy of these radicals will be so high that, at random, substitution reaction will occur. Assuming the above mechanism, the distribution of activity in butyric and isobutyric acid would be 3:2.

γ-Irradiation. When the organic compounds are irradiated by γ-rays, the C-H, and C-C bonds are broken to yield CH_3 and other radicals. To compare the reactivity of the radicals produced by γ-irradiation with that of ^{14}C-hot atom, the ^{60}Co γ-ray irradiation of propionamide-(carbonyl-^{14}C) was performed. Methyl radical, ethyl radical, carbon monoxide and so on are formed from propionamide by γ-rays irradiation. Methyl radical attacks the propionamide to produce butyramide or isobutyramide. The ratio of the yield of butyramide- and isobutyramide was determined by the

10) D. D. Van Slyke and H. Folch, *J. Biol. Chem.*, **136**, 509 (1940).

11) A. P. Wolf, C. S. Redvanly and C. Anderson, *J. Am. Chem. Soc.*, **79**, 3717 (1959).

Table IV. The neutron irradiation of propionamide

Product	Activity, μc. 1.	2.	Average	% to the total activity	Relative ratio
Propionamide	1.40	1.30	1.35	3.3	4.2
Butyramide	0.86	0.90	0.88	2.1	2.7
Isobutyramide	0.69	0.71	0.70	1.7	2.1
Ethyl methyl ketone	0.31	0.33	0.32	0.8	1.0
Total activity	42.0	40.0	41.0		

Table V. γ-Irradiation of propionamide (carbonyl-^{14}C)

Product	Activity, $\times 10^{-1}$ μc. 1.	2.	Average, $\times 10^{-1}$ μc.	Relative ratio	G-Value
Butyramide	2.49	2.68	2.59	3.1	0.83
Isobutyramide	1.65	1.61	1.63	2.0	0.53

isotope dilution method using propionamide-(carbonyl-^{14}C.).

As it is shown in Table V, the ratio of the yield of butyric acid to that of isobutyric acid from the corresponding amides was 3 : 2. This ratio shows a good agreement with that in the case of the neutron irradiation.

These results can not be explained by thermal free radical reactions, but by the following mechanism: Propionamide decomposes to methyl and other radicals by the action of γ-rays as indicated by Eq. 5.

$$CH_3CH_2CONH_2 \xrightarrow{\gamma\text{-rays}} CH_3\cdot, \quad CH_3CH_2\cdot, \ CONH_2\cdot, \text{ etc.} \qquad (5)$$

The energy of methyl radicals will be so high that random substitutions will take place. Its energy, perhaps, is in the order of 5～10 eV.[12], so that the so-called "high energy reaction" should be considered to take place in this case and, by this mechanism, the present experimental results can be sufficiently explained.

Thermal Free Radical Reaction in Solution. In order to compare such a high energy reaction as that indicated above with thermal free radical reaction, decomposition of acetyl peroxide in propionic acid-(carboxyl-^{14}C) was carried out.

Acetyl peroxide is decomposed in solution by heat as follows.

$$(CH_3COO)_2 \xrightarrow{\text{heat}} CH_3\cdot + CO_2\cdot + CH_3COO\cdot \qquad (6)$$

Most of the methyl radicals would carry out hydrogen abstraction reaction on the analogy of the reaction of acetyl peroxide with acetic acid[13].

However some of the methyl radicals formed combine with propionic acid-(carboxyl-^{14}C) to give butyric acid-(carboxyl-^{14}C) or isobutyric acid-(carboxyl-^{14}C). The isotope dilution method was applied to the determination of the ratio of butyric and isobutyric acid. The results are summarized in Table VI and the

Table VI. The Decomposition of acetyl peroxide in propionic acid (carboxyl-^{14}C)

Product	Activity, $\times 10^{-1}$ μc.	Relative ratio
Butyric acid	2.31	1.0
Isobutyric acid	5.14	2.2

ratio of the yields of butyric and isobutyric acid is 1 : 2. The number of hydrogen atoms available for the substitution being taken into account, the result of the above ratio is that the hydrogen atom at the 2-position is three times more reactive with methyl radical compared with that at the 3-position, in the case of the substitution reaction of propionic acid. This result is quite different from those in the cases of neutron and γ-ray irradiation. The reaction of methyl radical from acetyl peroxide with propionic acid must be classified as a typical thermal free radical reaction in solution.

Summary

Two methylation reactions of propionamide by ^{14}C-hot atom, and of methyl radical from ^{60}Co γ-ray irradiation and methylation reaction of propionic acid by methyl radical from thermal decomposition of acetyl peroxide were carried out and the reactivities of these species were studied. The methyl radical produced by ^{60}Co γ-ray irradiation of propionamide gave the 3 : 2 mixture of butyr- and isobutyramide. This ratio agrees with the activity distribution of butyr- and isobutyramide in the neutron irradiation of propionamide. On the other hand the methyl radical produced by the

12) T. Watanabe, private communication.
13) A. Fry, B. M. Tolbert and M. Calvin, *Trans. Faraday. Soc.*, **49**, 1444 (1953).

thermal decomposition of acetyl peroxide in propionic acid gave 1:2 mixture of butyric and isobutyric acid. From the above results the reactions in the neutron irradiation and in the γ-ray irradiation are considered to be high energy reactions, whereas the methylation reaction of acetyl peroxide in propionic acid is considered to be a free radical reaction.

The authors wish to express sincere thanks to Professor K. Kimura and Dr. A. Danno for their kind encouragement and helpful discussions throughout the present work.

Division of Radiation Applications
Japan Atomic Energy Research Institute
Tokai, Ibaraki-ken

Stereochemistry and Mechanisms of Catalytic Hydrogenolysis and Hydrogenation. I. Catalytic Hydrogenolysis of Optically Active Compounds with Raney Nickel

By Sekio MITSUI and Shin IMAIZUMI

(Received August 15, 1960)

There have been only a few investigations on the mechanisms of catalytic hydrogenolysis taking the action of catalysis into consideration. Brenner and Keeys[1] presumed that the furyl carbonium ion was produced at an intermediate stage of the course of catalytic hydrogenolysis reaction of furfuryl alcohol, which yielded methylfuran, and this concept was supported by Lukes[2]. Pines et al.[3] presumed that the dehydroxylation reaction of alcohols at high temperature and pressure takes place via the carbonium ion. On the other hand, Mitsui et al.[4] presented papers reporting as follows: in the case of catalytic hydrogenolysis of phenyl benzyl ethers, these substances are adsorbed on the catalyst surface and the electron density between C–O bond decreases, and also the carbon of benzyl group becomes δ^+, and the hydrogen adsorbed on the catalyst surface dissociates into H^- and H^+. This hydride is presumed to attack δ^+ carbon.

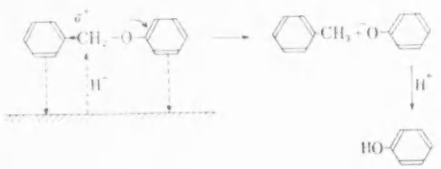

The above mentioned mechanism elucidates clearly the cases of various benzyl ether and benzylamine derivatives[5]. The question as to the mechanism by which the reaction takes place, may be clearly elucidated upon catalytic hydrogenolysis of optically active compounds with tertiary carbon. That is, if carbonium ion is formed, optically inactive compounds would be produced and if attacking reaction of hydride ion occurs, optically active compounds must be produced. Ott et al.[6], already reported that (+)-α-phenylpropionic acid was obtained when (−)-α-phenyl-α-chloropropionic acid was subjected to catalytic hydrogenolysis using palladium-charcoal as a catalyst and that (−)-α-phenylpropionic acid was obtained when (−)-α-phenyl-α-chloropropionic acid was reduced with zinc and acetic acid. Bonner[7,8] performed catalytic hydrogenolysis of several atrolactic acid derivatives I and III with excess of Raney nickel in boiling alcohol. The results were as follows: in cases of phenyl thioether (I, X = SC_6H_5) and of α-phenyl-α-benzenesulfinylpropionamide (I, X = SOC_6H_5), racemic α-phenylpropionamide (II) was produced. However, in cases of α-phenyl-α-benzenesulfonylpropionamide (I, X = $SO_2C_6H_5$) and of ethyl α-phenyl-α-benzenesulfonylpropionate (III, X = $SO_2C_6H_5$), II or

1) J. G. M. Brenner and R. K. F. Keeys, *J. Chem. Soc.*, **1947**, 1067.
2) R. M. Lukes and C. L. Wilson, *J. Am. Chem. Soc.*, **73**, 4792 (1951).
3) H. Pines, M. Shamarieger and W. S. Postl, ibid., **77**, 5999 (1955); H. Pines, J. Marechal and W. S. Postl, ibid., **77**, 6390 (1955).
4) S. Mitsui, N. Inoue and A. Kasahara, *J. Chem. Soc. Japan, Pure Chem. Sec.* (*Nippon Kagaku Zasshi*), **71**, 203 (1951); *Chem. Abstr.*, **46**, 8102 i (1952).
5) S. Mitsui and N. Kiseki, ibid., **70**, 203 (1950); *Chem. Abstr.* **45**, 6631 g (1951); S. Mitsui, A. Kasahara and N. Endo, ibid., **75**, 234 (1954); *Chem. Abstr.*, **49**, 10210 d (1955); S. Mitsui and S. Imaizumi, ibid., **75**, 974 (1954); *Chem. Abstr.*, **51**, 14608 i (1957); S. Mitsui, S. Imaizumi and J. Kusume, ibid., **75**, 1065 (1954); *Chem. Abstr.*, **51**, 14609 c (1957).
6) E. Ott and K. Krömer, *Ber.*, **68**, 1655 (1935).
7) W. A. Bonner, *J. Am. Chem. Soc.*, **74**, 1034 (1952).
8) W. A. Bonner, ibid., **74**, 5089 (1952).

ethyl α-phenylpropionate (IV), with only 10% recemization, was obtained, and it was definitely evidenced that Walden inversion accompanied this occasion. Thus he presented the mechanisms of these reactions. Developing this investigation, Bonner et al.[9,10] obtained ethyl D(+)-α-phenylpropionate (IV) with 79% of retention of configuration from ethyl D(−)-atrolactate (III, X=OH) and methyl D(+)-α-phenylpropionate with 72% of retention of configuration from methyl D(+)-α-phenyl-α-methoxypropionate, respectively. Cram et al.[11] obtained (+)-2-phenylbutane with 64% retention of optical activity from (+)-2-hydroxy-2-

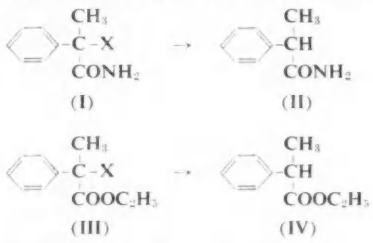

(I) (II)

(III) (IV)

phenylbutane over excess of Raney nickel by means of boiling in alcohol. Barnes et al.[12] conducted catalytic hydrogenation of L(−)-1,2-diphenyl-1,2-propanediol over copper-chromium oxide catalyst at 200°C with hydrogen at 1400 p. s. i. and obtained L(+)-1,2-diphenylpropane with 22.3% retention of optical activity (61.2% retention of configuration).

The results indicate that optically active hydrogenolyzed products are obtained exclusive of poisonous compounds such as thioether and sulfinyl compounds. This fact seems to support the present author's concept described earlier.

The author et al. have conducted many investigations on catalytic hydrogenolysis of optically active derivatives of atrolactic acid in order to elucidate more clearly the mechanism of catalytic hydrogenolysis by which the mechanism of catalytic hydrogenation may be explained. One of the present authors, Imaizumi[13], already performed catalytic hydrogenation of ethyl L(+)-atrolactate (III, X=OH), $[\alpha]_D^8 +25.30°$ (92.4% optical purity), over Raney nickel catalyst at ordinary temperature and pressure and obtained ethyl L(−)-α-phenylpropionate (IV)*, $[\alpha]_D^9 -54.82°$, which upon hydrolysis gave L(−)-α-phenylpropionic acid (V), $[\alpha]_D^7 -73.2°$ (82.2% optical purity), with 89% retention of optical activity. Upon catalytic hydrogenation of ethyl L(+)-α-phenyl-α-chloropropionate (III, X=Cl), $[\alpha]_D^{21} +2.36°$ (42.1% optical purity), over 7.7% palladium-charcoal, L(−)-IV, $[\alpha]_D^{19} -4.97°$ (L(−)-V, $[\alpha]_D^{18} -7.20°$, 7.6% optical purity), was obtained with 18% of optical activity. However, ethyl L(−)-α-phenyl-α-phenoxypropionate (III, X=OC_6H_5), $[\alpha]_D^{15} -2.10°$ (35.9% optical purity), gave D(+)-IV, $[\alpha]_D^{14} +23.3°$ (D(+)-V, $[\alpha]_D^{13} +30.5°$, 34.2% optical purity), and ethyl D(+)-α-phenyl-α-phenoxypropionate, $[\alpha]_D^{15} +1.02°$ (18.4% optical purity), gave L(−)-IV, $[\alpha]_D^{16} -11.61°$ (L(−)-V, $[\alpha]_D^{15} -16.10°$, 17.1% optical purity), with 95% and 93% retention of optical activity. It was evident that the Walden inversion accompanied this process simultaneously. An optically inactive product IV resulted from the hydrogenolysis of ethyl D(+)-α-phenyl-α-ethylmercaptopropionate (III, X=SC_2H_5), $[\alpha]_D^{20} +4.11°$, and ethyl D(−)-α-phenyl-α-phenylmercaptopropionate (III, X=SC_6H_5), $[\alpha]_D^{20} -31.3°$ [14]. Accordingly, in the case of thioethers, nearly perfect racemization is observed to occur, which is in accord with the result of Bonner's experiments.

Considering the results of catalytic hydrogenolysis of these optically active ethylatrolactate derivatives, the authors[15] proposed to classify them into the following four kinds (or six kinds) of mechanisms of catalytic hydrogenolysis, according to both chemical constitution of compounds and stereochemical constitution of compounds. Explained in detail, in the case of strong catalytic poisonous compounds like thioether (III, X=SC_2H_5, SC_6H_5), the carbon-sulfur bond cleaves to radicals because three groups, carboethoxy, phenyl and sulfur atom, of the molecules may be adsorbed and chemisorption of the sulfur atom occurs strongly, and then hydrogen is incorporated with the radicals (radical cleavage reaction I). Accordingly racemization ensues. If groups, incorporated into the asymmetric carbon atom, are not chemisorption groups such as carboethoxy or phenyl but are like alkyl groups, which do not cause chemisorption —if they cause any, it is an extremely weak one—, these groups probably act as electron releasing groups, and accordingly they cleave both to carbonium ion and to sulfide anion and then hydrogen is incorporated, ensuing on this occasion racemization too (S_N1 reaction,

9) W. A. Bonner, J. A. Zderic and G. A. Casaletto, ibid., **74**, 5086 (1952).
10) W. A. Bonner and J. A. Zderic, ibid., **78**, 3218 (1956).
11) D. J. Cram and J. Allinger, ibid., **76**, 4516 (1954).
12) R. A. Barnes and B. R. Juriano, ibid., **81**, 6462 (1959).
13) S. Imaizumi, *J. Chem. Soc. Japan, Pure Chem. Sec. (Nippon Kagaku Zasshi)*, **77**, 1511 (1956); *Chem. Abstr.*, **53**, 5179 g. (1959).
* D(−) Atrolactic acid has been correlated in two independent ways with D(+) α-phenylpropionic acid by E. L. Eliel and J. P. Freeman [*J. Am. Chem. Soc.*, **74**, 923 (1952)] and Bonner[9]. Rotations of the acid and its ethyl ester have the same sign.
14) S. Imaizumi, *J. Chem. Soc. Japan, Pure Chem. Sec. (Nippon Kagaku Zasshi)*, **78**, 1396 (1957); *Chem. Abstr.*, **54**, 1403 h (1960).
15) S. Mitsui and S. Imaizumi, ibid., **77**, 1516 (1956); *Chem. Abstr.*, **53**, 5180 e (1959).

reaction 2). However, in the case of oxygen compounds like ethyl atrolactate (III, X=OH) and its phenyl ether (III, $X=OC_6H_5$), cleavage does not occur by the adsorption on the catalyst surface because chemisorption of the oxygen atom proceeds comparatively weakly. By the chemisorption of phenyl, carboethoxy and OR groups, the asymmetric carbon atom bears a positive charge (δ^+), to which electron and proton or electrons and proton are transferred from the catalyst to produce ·OR radical or :OR anion and thereupon the reaction completes itself with the incorporation of electron and proton or proton to hold optical activity. On this occasion, if carboethoxy, phenyl and OR groups are adsorbed on the same catalyst surface, and the electron is transferred from the same catalyst surface, the reaction is the retention of configuration which we have designated as S_Ni type reaction on catalyst (reactions 3 and 4). In the case of ethyl atrolactate, since carboethoxy, phenyl and hydroxy groups can be easily adsorbed on the same surface of the catalyst without any steric hindrance, the S_Ni type reaction with retention of configuration occurs (Fig. 1). In the case of phenoxy compound (III, $X=OC_6H_5$), owing to the plane structure of the phenoxy group, when this plane is adsorbed on a catalyst surface, three groups, carboethoxy, phenyl and phenoxy, of the compound can not be so easily adsorbed on the same catalyst surface because of steric hindrance among these groups. However, when the phenoxy group is adsorbed on one catalyst surface and carboethoxy and phenyl groups are adsorbed on another catalyst surface, adsorption proceeds easily on the catalyst surfaces as there occurs no steric hindrance (Fig. 2). Then the asymmetric carbon atom is drawn near to the latter surface and the electron or electrons are transferred from the latter surface pushing out the phenoxy group to another catalyst surface and thereupon Walden inversion occurs. We have designated this reaction as S_N2 type reaction on catalyst (reactions 5 and 6).

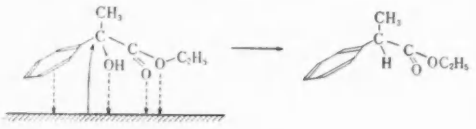

Fig. 1

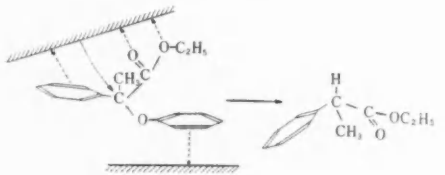

Fig. 2

In the case of ethyl α-phenyl-α-chloropropionate (III, X=Cl), palladium-charcoal was used as the catalyst and because of comparatively strong chemisorption of chlorine, radical cleavage reaction 1 occurred predominantly. Besides this reaction, S_Ni type

i) Radical cleavage reaction on catalyst

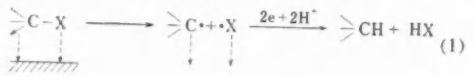

(1)

ii) S_N1 type reaction on catalyst

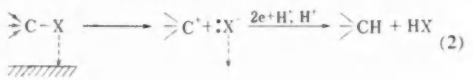

(2)

iii) S_Ni type reaction on catalyst

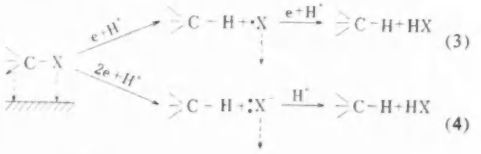

(3)

(4)

iv) S_N2 type reaction on catalyst

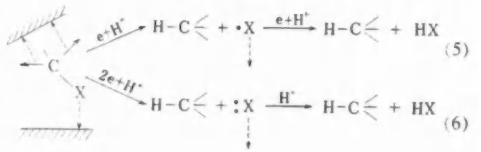

(5)

(6)

reactions 3 and 4 proceeded as well, which led us to consider that retention of optical activity seemed to be scanty.

To verify the previously presented mechanisms of catalytic hydrogenolysis, investigations on catalytic hydrogenolysis of various optically active derivatives of ethyl atrolactate over Raney nickel were conducted. First, from ethyl L(−)-α-phenyl-α-ethoxypropionate (III, $X=OC_2H_5$), $[\alpha]_D^{17}-31.93°$ (82.4% optical purity), which is presumed to undergo chemisorption in a similar manner as that of ethyl atrolactate, ethyl (−)L-α-phenylpropionate (IV), $[\alpha]_D^{18}-53.4°$ (74.1% optical purity), was obtained with retention of configurations, as was expected, and the retention of optical activity was 90%. As for methyl α-phenyl-α-methoxypropionate, Bonner et al.[10] reported as mentioned before and the present authors investigated the matter also to obtain D(+)-IV, $[\alpha]_D^{16}+53.7°$ (74.4% optical purity), from ethyl D(+)-α-phenyl-α-methoxypropionate (III,

X=OCH_3), $[\alpha]_D^{15}+47.96°$ (88.6% optical purity), with 83% retention of optical activity. Secondly, from several aryloxy compounds (III, X=OAr) which are presumed to undergo chemisorption over Raney nickel in a similar manner as that of phenoxy compound (III, X=OC_6H_5), IV with Walden inversion was obtained with more than 90% retention of optical activity.

These facts can be explained as follows: ethyl α-phenyl-α-aryloxypropionate is adsorbed on both sides of the surface of Raney nickel catalyst to react readily and react with difficulty when adsorbed on one side of the surface. In the case of ethyl α-phenyl-α-alkyloxypropionate, as there exists no steric hindrance, it is adsorbed on one side of the surface to react. Thus, the previously presented conception is verified as correct and also indicates that Raney nickel catalyst has such a surface structure that ethyl α-phenyl-α-aryloxypropionate is easily adsorbed on both sides of its surface. This fact elucidates the fact that when palladium-charcoal or palladium-alumina is used as catalyst, ethyl α-phenylpropionate produced in the catalytic hydrogenolysis of optically active ethyl α-phenyl-α-phenoxypropionate accompanies retention of configuration if palladium concentration is dilute against carrier, and Walden inversion if palladium concentration is dense. According to the structure of catalyst surface, either retention of configuration or Walden inversion occurs, the fact concerning which will be reported in the next paper.

In Table I are shown the results of investigations of catalytic hydrogenolysis of optically active ethyl atrolactate derivatives over Raney nickel, which have been carried out so far.

Ethyl α-phenylpropionate was produced with Walden inversion from acyloxy compounds (III, X=OCOR) which is prevented from being adsorbed on one side of the surface because of steric hindrance as in the case of aryloxy compounds. However, in the case of benzoyloxy compound (III, X=$OCOC_6H_5$) retention of optical activity is as small as 34%. These results lead us to presume that these phenomena occur because radical cleavage reaction and/or S_N1 type reaction and/or S_Ni type reaction partially occur with S_N2 type reaction in the case of benzoyloxy compound owing to their benzoyloxy group's strong power of adsorption. We will report about this mechanism at a later date.

The above-mentioned mechanism may clarify not only catalytic hydrogenolysis of benzyl-, aralkyl-, and allyl-compounds but also hydrogenolysis of compounds of aromatic ring, hetero-aromatic ring and unsaturated bond to which are combined halogens, OR, SR, CN etc., directly. In these cases, however, there exists Y=C-X on the same plane and it is scarcely possible for adsorption on both sides to occur. Accordingly S_N2 type reaction is not supposed to occur. If adsorption of double bond occurs, production of carbonium ion is least probable. But when this adsorption of X is strong, 2′ reaction might occur. In the case of strong adsorption of X (catalytic poisonous compounds), mainly 1′ reaction would proceed. When adsorption of X is comparatively weak and temperature is comparatively low, mainly 3′ or 4′ reaction proceeds. If temperature is high, 1′ reaction proceeds. Also the dehydroxylation reaction

TABLE I

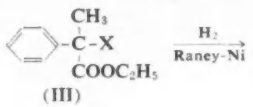

(III)

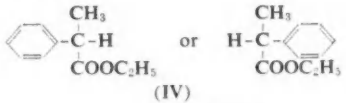

(IV)

	X	Maintained optical activity % a)		Configuration
1	O-H	89[13]	79[9,10]	rentention
2	O-CH_3	83	72[b,10]	〃
3	O-C_2H_5	90		〃
4	O-CH_2-C_6H_5	87[16]		〃
5	O-C_6H_5	95[13]		inversion
6	O-C_6H_4-CH_3(*o*)	96		〃
7	〃 (*p*)	92		〃
8	O-C_6H_4-OCH_3(*o*)	94		〃
9	〃 (*p*)	92		〃
10	O-$C_{10}H_7$(β)	91		〃
11	SO_2-C_6H_5	81[16]	90[7]	〃
12	SO_2-C_6H_4-CH_3(*p*)	75[16]		〃
13	S-C_2H_5	0[14]		racemization
14	S-C_6H_5	0[14]		〃
15	S-C_6H_4-CH_3(*p*)	0[16]		〃
16	Cl	0[c]		〃
17	O-$COCH_3$	67[16]		inversion
18	O-COC_2H_5	82[16]		〃
19	O-COC_6H_5	34[16]		〃

a) Author's %=(optical activity of IV/optical activity of III)×100=2×Bonner's %−100. Bonner's %=50+author's %/2.
b) Methyl ester.
c) In case of 7.7% palladium charcoal catalyst, which maintained optical activity of resulting IV was 18% with retention of configuration[13]. However, in case of Raney nickel catalyst, the resulting IV was almost completely racemic (cf. Experimental).

16) S. Imaizumi, ibid., **81**, 625, 631, 633 (1960).

of saturated alcohol at high temperature is presumed to be the type of 2′.

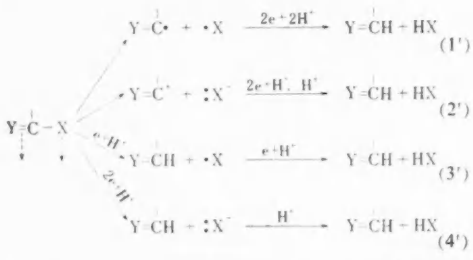

The hydrogenolysis of such bonds as $\ddot{N}$–$\ddot{N}$ and $\ddot{N}$–$\ddot{O}$ which have lone pairs is presumed to undergo exactly the same mechanism[17].

On the basis of this mechanism of catalytic hydrogenolysis, when the mechanism of catalytic hydrogenation is speculated upon, the following may be indicated. π-Electrons of unsaturated linkage transfer into d-band vacancy of the catalyst metal surface to form π-complex VI. Then, according to the kinds of catalyst and to the reaction condition, the unsaturated linkage cleaves to radicals or to carbonium ion and to anion to which $e+H^+$ or $2e+H^+$ transfers to become the half-hydrogenated state[18], VII or VIII. To this $e+H^+$ or H^+ transfers and the reaction is completed (1″, 2″ reactions). Otherwise by forming π-complex, carbon becomes δ^+, to which transfers $e+H^+$ or $2e+H^+$ from catalyst and the reaction is completed via half-hydrogenated state VII or VIII (3″ and 4″ reactions). At comparatively low temperature, the reaction is of mainly 3″ or 4″ type, and at high temperature, 1″ or 2″ type reaction may occur.

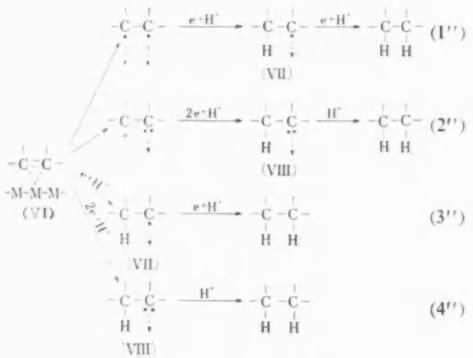

17) S. Mitsui and S. Imaizumi, ibid., **78**, 812 (1957).
18) J. Horiuchi and M. Polanyi, *Trans. Faraday Soc.*, **30**, 1164 (1934).
19) L. Smith, *J. Prakt. Chem.*, [2] **84**, 738 (1911).
20) A. McKenzie and G. W. Clough, *J. Chem. Soc.*, **97**, 2564 (1910).

Experimental

Optically Active Ethyl Atrolactate (III_1).—Atrolactic acid was resolved according to the procedure of Smith[19] and converted to the ethyl ester III_1[20]. The value for the rotation of optically pure ester III_1 is 27.38° (neat)[18].

Optically Active Ethyl α-Phenyl-α-chloropropionate (III_{16}).—This chloride was prepared from the above optically active ester III_1 and thionyl chloride by the method of McKenzie and Clough[20]. This reaction has been demonstrated to occur with the retention of configuration[20]. For the rotation of optically pure chloride III_{16}, we adopted the greatest value, $[\alpha]_D+5.6°$ (neat)[20], reported hitherto for the chloride.

Optically Active Ethyl α-Phenyl-α-aryloxypropionate (III_{6-10}).—Related phenol (0.05 mol.) was dissolved in a solution of sodium (0.05 mol.) in absolute ethanol (50 ml.). The above optically active chloride III_{16} (0.05 mol.) was added to the alcoholic solution, and the mixture was boiled under reflux for 15 hr. The reaction mixture was freed of solvent by distillation, and after being cooled poured into water. The mixture was extracted twice with ether, and the extract was washed twice with 5% sodium hydroxide solution, and twice with water. The extract was then dried over anhydrous sodium sulfate, and the solvent was distilled. The residual oil was distilled thrice at reduced pressure to give 20~40% yield of arylethers III_{6-10}. This reaction has been demonstrated to occur with inversion of configuration in other systems[21]. Considering the stereochemical results of catalytic hydrogenolysis of these arylethers, the reaction of these arylethers formation took place with almost complete retention of optical activity. Therefore, optical activities of these arylethers were taken from the optical activity of chloride III_{16}.

Ethyl D(−)-*α-Phenyl-α-(o-cresoxy)propionate* (III_6). — B. p. 145~146°C/3 mmHg, $[\alpha]_D^5-7.3°$ (*c* 5.6, absolute ethanol), 45.2% optical purity.

Found: C, 75.85; H, 7.23. Calcd. for $C_{15}H_{20}O_3$: C, 76.03; H, 7.09%.

Ethyl L(+)-*α-Phenyl-α-(p-cresoxy)propionate* (III_7). — B. p. 143~145°C/0.5 mmHg, $[\alpha]_D^5+3.5°$ (*c* 5.4, absolute ethanol), 37.5% optical purity.

Found: C, 76.16; H, 7.36. Calcd. for $C_{15}H_{20}O_3$: C, 76.03; H, 7.09%.

Ethyl L(+)-*α-Phenyl-α-(o-anisoxy)propionate* (III_8). — B. p. 158~160°C/2 mmHg, $[\alpha]_D^5+13.6°$ (*c* 4.2, absolute ethanol), 52.5% optical purity.

Found: C, 72.21; H, 6.99. Calcd. for $C_{15}H_{20}O_4$: C, 71.98; H, 6.71%.

Ethyl D(−)-*α-Phenyl-α-(p-anisoxy)propionate* (III_9). — B. p. 170~172°C/3 mmHg, $[\alpha]_D^4-8.4°$ (*c* 5.3, absolute ethanol), 45.2% optical purity.

Found: C, 71.95; H, 6.64. Calcd. for $C_{15}H_{20}O_4$: C, 71.98; H, 6.71%.

Ethyl D(+)-*α-Phenyl-α-(β-naphthoxy)propionate* (III_{10}).—B. p. 190~191°C/1 mmHg, m. p. 65~66°C, $[\alpha]_D^8+4.8°$ (*c* 7.3, absolute ethanol), 45.2% optical purity.

21) H. Hart and H. S. Eluterio, *J. Am. Chem. Soc.*, **76**, 519 (1954).

Found: C, 78.74; H, 6.56. Calcd. for $C_{21}H_{20}O_3$: C, 78.72; H, 6.29%.

Optically Active Ethyl α-Phenyl-α-alkyloxypropionate (III_{2-3}).—The following preparation is an adaptation of the methods of Freudenberg[22] and Bonner[10]. A mixture of alkyl halide (6 ml.), silver oxide (6 g.) and optically active ethyl atrolactate (6 g.) was stirred at room temperature for 5 days, whereupon it was treated with ether and filtered. The filter cake was washed thrice with ether, and the filtrate and washings were freed of solvent. The residual oil was distilled at reduced pressure, and the specific rotation of the oil was examined, and then the oil was retreated in the above manner six additional times. The specific rotation and boiling point of the six treated materials were compared with seven treated ones. The final oil was distilled at reduced pressure to give optically active alkylether III_{2-3}. It is clear that the reaction proceeds without modification of configuration.

Ethyl D(+)-*α-Phenyl-α-methoxypropionate* (III_2).—B. p. 128~129°C/14 mmHg, d_4^{15} 1.047, $[\alpha]_D^5$ −47.96° (neat). On the basis of the ethyl D(−)-atrolactate (III_1) ($[\alpha]_D^{31}$ −24.27° (neat)) used, the methyl ether appears to be 88.6% optically pure.

Found: C, 69.54; H, 7.82. Calcd. for $C_{12}H_{16}O_3$: C, 69.21; H, 7.74%.

Ethyl L(−)-*α-Phenyl-α-ethoxypropionate* (III_3).—B. p. 130~131°C/13 mmHg, d_4^{17} 1.041, $[\alpha]_D^{17}$ −31.93° (neat). On the basis of the ethyl L(+)-atrolactate (III_1) ($[\alpha]_D^{5}$ −22.56° (neat)) used, the ethyl ether appears to be 82.4% optically pure.

Found: C, 70.33; H, 8.15. Calcd. for $C_{13}H_{18}O_3$: C, 70.24; H, 8.16%.

Catalytic Hydrogenation of Optically Active Ethyl α-Phenyl-α-aryloxypropionate (III_{6-10}).—A mixture of 1.5 g. of optically active arylether III_{6-10}, 50 ml. of absolute ethanol and 1.5 g. of W-5 Raney nickel was shaken under hydrogen at ordinary temperature and pressure for 5 hr. The catalyst was filtered and rinsed with ethanol, and the solvent was distilled. The residual oil was taken up in ether, and extracted with 5% sodium hydroxide solution. The alkali-insoluble material was dried over anhydrous sodium sulfate, and the solvent was removed. The residual oil was distilled at reduced pressure to give ethyl α-phenylpropionate (IV). The specific rotation of optically pure IV is 67.5° (neat) and 72.2° (absolute ethanol)[14].

The alkaline extract was acidified with hydrochloric acid, and the resulting oil was taken up in ether, dried, and the solvent was removed by distillation and the residue was converted into a solid derivative. These results were as follows.

D(−)-III_6 (45.2% optical purity) gave L(−)-IV (b. p. 101~102°C/10 mmHg, $[\alpha]_D^7$ −31.2° (*c* 6.4, absolute ethanol), 43.2% optical purity) and *o*-cresol (its tosylate, m. p. 54~55°C[23]).

L(−)-III_7 (37.5% optical purity) gave D(+)-IV (b. p. 103~104°C/12 mmHg, $[\alpha]_D^2$ +23.3° (*c* 8.6, absolute ethanol), 34.5% optical purity) and *p*-cresol (its tosylate, m. p. 69~70°C[23]).

L(+)-III_8 (52.5% optical purity) gave D(+)-IV (b. p. 101~102°C/10 mmHg, $[\alpha]_D^5$ +34.2° (*c* 8.1, absolute ethanol), 47.4% optical purity) and guaiacol (*o*-anisoxyacetic acid, m. p. 126~127°C[24]).

D(−)-III_9 (45.2% optical purity) gave L(−)-IV (b. p. 103~104°C/12 mmHg, $[\alpha]_D^5$ −28.20° (neat), $[\alpha]_D^4$ −30.1° (*c* 7.0, absolute ethanol), 41.7% optical purity) and *p*-methoxyphenol (m. p. 52~53°C).

D(+)-III_{10} (45.2% optical purity) gave L(−)-IV (b. p. 103°C/11 mmHg, $[\alpha]_D^{13}$ −29.6° (*c* 9.1, absolute ethanol), 41.0% optical purity), 1,2,3,4-tetrahydro-β-naphthol (its phenylurethane, m. p. 98~99°C[25]) and 5,6,7,8-tetrahydro-β-naphthol (m. p. 57~59°C).

It is calculated from the above results that the percentages of retention of optical activity in the catalytic hydrogenolysis of III_{6-10} to IV on Raney nickel, accompanied by inversion of configuration, are 96, 92, 94, 92 and 91%, respectively.

Catalytic Hydrogenation of Ethyl D(+)-α-Phenyl-α-methoxypropionate (III_2).—A mixture of 1 g. of D(+)-III_2 (88.6% optical purity), 30 ml. of absolute ethanol and 10 g. of W-5 Raney nickel was shaken under hydrogen at ordinary temperature and pressure for 3 days. The catalyst was filtered and rinsed with ethanol, and then the solvent was removed. The residual oil was distilled at 110~112°C (17 mmHg) to give 0.4 g. of D(+)-IV, $[\alpha]_D^{16}$ +53.6° (*c* 6.7, absolute ethanol), 74.4% optical purity. The percentage of retention of optical activity in IV is calculated to be 83% with retention of configuration.

The above mixture was shaken for 6 days in the same condition. The usual processing yielded 0.6 g. of D(+)-IV, $[\alpha]_D^{15}$ −34.5° (*c* 7.0, absolute ethanol), 47.8% optical purity. In this case, partial racemization of the IV produced appears to take place in the prolonged reaction time.

Catalytic Hydrogenation of Ethyl L(−)-α-Phenyl-α-ethoxypropionate (III_3).—A mixture of 1 g. of L(−)-III_3 (82.4% optical purity), 30 ml. of absolute ethanol and 10 g. of W-5 Raney nickel was shaken under hydrogen at ordinary temperature and pressure for 3 days. The catalyst was filtered and rinsed with ethanol, and then the solvent was removed. The residual oil was distilled at 110~111°C (16 mmHg) to give 0.3 g. of L(−)-IV, $[\alpha]_D^{18}$ −53.4° (*c* 5.2, absolute ethanol), 74.1% optical purity. The percentage of retension of optical activity in IV is calculated to be 90% with retention of configuration.

The above mixture was shaken under hydrogen at about 70°C for 20 hr. The customary work-up gave 0.5 g. of oil, b. p. 110~120°C/17 mmHg, $[\alpha]_D^{17}$ −13.5° (*c* 5.0, absolute ethanol). The product could not be identified, but seems to be a mixture of IV and cyclohexyl derivatives of III_3 and/or IV.

Catalytic Hydrogenation of Ethyl L(+)-α-Phenyl-α-chloropropionate (III_{16}).—A mixture of 2.1 g. of L(+)-III_{16} ($[\alpha]_D^{12}$ +3.40° (neat), 60.7% optical purity), 50 ml. of absolute ethanol and 6 g. of W-5 Raney nickel was shaken under hydrogen at ordinary themperature and pressure for 2 hr. The catalyst was filtered and rinsed with ethanol and the solvent was distilled. The residual oil was taken up in ether, and extracted with 5% sodium

22) K. Freudenberg, J. Todd and R. Seidler, *Ann.*, **501**, 199 (1933).
23) F. Beverdin and P. Crépieux, *Ber.*, **35**, 1439 (1902).
24) O. Behaghel, *J. prakt. Chem.*, **114**, 296 (1926).
25) F. Straus and A. Rohrbacher, *Ber.*, **54**, 55 (1921).

carbonate solution. The alkali-insoluble material was dried over anhydrous sodium sulfate, and the solvent was removed. The residual oil was distilled at 108~110°C (14 mmHg) to give 1.2 g. of IV, $[\alpha]_D^{18}$ +0.49° (neat), 0.7% optical purity. The percentage of retention of optical activity in IV is calculated to be 1% with inversion of configuration. Therefore, in the hydrogenolysis, almost complete racemization occurred.

Department of Applied Science
Faculty of Engineering
Tohoku University, Sendai

Fischer-Tropsch Synthesis with Tubular Reactor of 18.1 l. Catalyst Bed. I. Reactor with Constant Temperature Wall

By Michio KURAISHI*, Minoru KURITA, Tadasuke HOSOYA, Hideo ICHINOKAWA, Kiyoshi OGAWA and Hiroshi UCHIDA

(Received September 13, 1960)

In our previous paper[1] dealing with the Fischer-Tropsch synthesis in a tubular reactor, a procedure for calculating temperature profiles from experimental concentration gradients of components along the reactor was proposed. The procedure was developed by making use of experimental data available with the reactor which contained a catalyst bed of 2 l., and which was held in a circulating oil bath at a constant temperature. Under the assumption that situations in the synthesis are similarly realized independently of the sizes of the reactor, the procedure promises that we may foresee performances of reactors of a larger size. Along this line of expectation, precalculations of temperature profiles are made for the synthesis with any reactor of similar construction but about ten times as large as the previous one. The applicability of the procedure may then be checked by comparing the results of precalculation with the experimental temperature profile in the synthesis with the present reactor of the larger size. Moreover, the same procedure is followed to give the temperature profiles from the experimental concentration gradients along the present reactor.

Experimental

Raw water-gas for the synthesis is produced from coke and steam by the usual procedure. Hydrogen sulfide and carbon dioxide in the gas are removed in a gas purification train consisting of a sodium carbonate solution washer, an iron oxide box, and finally a caustic soda solution washer. The gas is then compressed at about 100 kg./cm² into a high pressure gas storage of 2000 l. (B), from which the compressed gas is introduced into a synthesis unit through a vessel (C) containing active charcoal for removal of organic sulfur. As shown in Fig. 1, the synthesis unit consists of a reactor (D), two hot separators (E), two cold separators (G) with

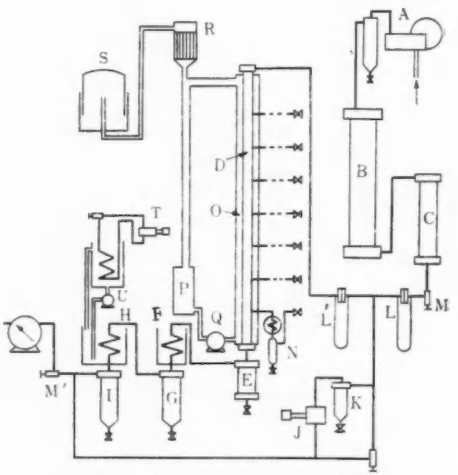

Fig. 1. Flow diagram of synthesis.

A, Gas compresser	B, Pressure reservoir
C, Desulfrizer	D, Reactor
E, Hot separator	F, Water cooler
G, Cold separator	H, Brine cooler
I, Cold separator	J, Gas circulating pump
K, Oil separator	L, L', Flow meter
M, M', Reducing valves	N, Cold separator
O, Oil bath	P, Hot oil reservoir
Q, Hot oil pump	R, Condenser
S, N_2 gas holder	T, Refrigerator
U, Brine pump	

* Present address: Japan Gas Chemical Co., Enoki-cho, Niigata.

1) M. Kuraishi, H. Ichinokawa, K. Ogawa, M. Kurita, T. Hosoya and H. Uchida, *J. Chem. Soc. Japan, Ind. Chem., Sec.* (*Kogyo Kagaku Zasshi*), **63**, 1588 (1960).

coolers (F), a low temperature separator (I) with a cooler (H), and a gas circulating pump (J) equipped with an oil separator (K), every one of which is of a design similar to, but about ten times as large as the corresponding equipment in the previous plant[1]. Having been mixed with part of the end-gas from the low temperature separator, an amount of the fresh gas is fed through a flow meter (L) into the reactor top where it flows in a downward direction through the catalyst bed. The volume of the fresh gas thus introduced is estimated from the degree of pressure decrease in the pressure gas storage and the flow rate is controlled by means of are ducing valve (M) and a flow meter (L). The volume of the fresh gas having been once estimated, one can easily calculate the flow rate of the circulating gas from carbon dioxide balance between the gases after and just before the reactor. Part of the gas after being separated at the low temperature separator is purged through a reducing valve (M'). In the above estimation, the volume of the gas thus purged is to be taken into account.

The reactor is 70 mm. in outer diameter and 50 mm. in inner diameter by 10 m. high[2], and is a simple reactor type with a constant temperature wall, being placed coaxially in a cylinder of oil (Dowtherm) bath (O). Into the bottom of the cylinder hot oil is fed at the flow rate of 2.5 m^3/hr., and flows upwards through an annular space between the cylinder wall and the reactor to the top, where the oil is allowed to flow down to a hot oil reservoir (P) which is being kept at a definite temperature. The recycling system of hot oil is always enclosed in an atmosphere of nitrogen which is supplied from a nitrogen gas holder (S) through an oil condenser (R).

The reactor contains a bed of 18.1 l. reduced catalyst (37.06 kg.). Two coaxial thermocouple wells 5 m. in length, 10 mm. in outer diameter, and 5 mm. in inner diameter, either one of which is fixed at the top or the bottom cover, go through the catalyst bed, and scanning of the temperature profile along the whole length of the reactor is made by moving the thermocouples in the wells. From seven successive ports at different heights along the catalyst bed, all of which are 1.2 m. apart from each other, a small portion of the fluid is withdrawn through a small cold separator (N) to be freed of water and oil, and the residual gaseous mixture is analyzed for the compositions. From the results of the analyses together with weighed amounts of the water, concentration gradients of the individual components along the catalyst bed are determined.

A sintered catalyst has been employed in the present synthesis. It was prepared, according to the procedure reported in our previous paper[4], from powders of a fused iron oxide catalyst containing in parts by weight 93.25 Fe_3O_4, 3 Al_2O_3, 1 CaO, 1 MgO, 1 WO_3, 0.25 CuO and 0.5 K_2O. The catalyst powders less than 100 mesh in size were pressed into tablets of 4×4 mm., which were sintered at 1000°C for one hour. Before use in the synthesis, the finished catalysts were completely reduced in a separate oven in a current of hydrogen at 500°C, and were removed from the oven to be packed into the synthesis reactor in carbon dioxide atmosphere.

Prediction of Temperature Profile

Among the synthesis experiments with the reactor of 2 l. catalyst bed (25 mm. I. D.)[1], Exp. No. 6 showed that a temperature difference of 24°C appeared between the oil bath and the center across the bed during the synthesis where by using a sintered catalyst[5] a product (oil plus wax) yield of 2.72 kg./day was obtained under the following synthesis conditions: the pressure was 25 kg./cm^2, and the space velocities based on the recycle and the fresh gases were 1975 and 763, respectively. This makes us feel uncertain whether a smooth operation of the synthesis can be made with the present reactor, since the temperature in the present synthesis may be liable to rise too high. In this connection, a preliminary calculation is made to predict the temperature rise. The precalculation is made by the aid of the procedure proposed by us[1], being combined with reasonable assumptions on the synthesis for the scaled-up reactor.

Heat transfer in a catalyst bed packed in a single tubular reactor is generally given by the following equation,

$$C_pG\frac{\partial t}{\partial x}=\frac{1}{r}\left\{\frac{\partial}{\partial r}\left(\lambda_r\cdot r\,\frac{\partial t}{\partial x}\right)+\frac{\partial}{\partial x}\left(\lambda_x\cdot r\,\frac{\partial t}{\partial x}\right)\right\}+\sum v_i q_i \qquad (1)$$

with the following boundary conditions,

$$\begin{aligned}&[t]_{x=0}=t_0\\&\left[\lambda_r\frac{\partial t}{\partial r}+Ut\right]_{r=r_1}=0\\&\left[\frac{\partial t}{\partial r}\right]_{r=r_2}=0\end{aligned} \qquad (2)$$

where C_p is the heat capacity per unit mass of fluid, G is the mass velocity, t is the temperature difference between a catalyst bed and an oil bath, x is the distance from the top of the bed, r is the distance in lateral direction, λ is the effective thermal conductivity of the catalyst bed fluid system, v is the reaction rate, q is the reaction heat, U is the overall heat transfer coefficient, r_1 and r_2 are the inner and the outer radii of the catalyst bed, respectively.

2) According to the paper by Tramm[3], a great number of the reactors of this size are placed in an oven for the Industrial synthesis.

3) H. Tramm, a paper presented at the Fifth World Petroleum Congress, Section III (1959).

4) H. Uchida and H. Ichinokawa, *J. Chem. Soc. Japan, Ind. Chem. Sec.* (*Kogyo Kagaku Zasshi*), **58**, 563 (1955).

5) The sintered catalyst used in the previous study was prepared from powders of a fused iron oxide catalyst containing in parts by weight 94 Fe_3O_4, 4 Al_2O_3, 1 CaO and 1 K_2O.

The last term in the right side of Eq. 1 concerns heat quantities of the reaction. It is usually determined according to a rate equation of the synthesis, and is a function of temperature and concentration. However, our previous work[1] pointed out that the term could be approximated to the following formula[6].

$$\sum v_i q_i = Q(\text{kcal./m}^3\text{ hr.}) = c_1 e^{-Mx} - c_2 e^{-Nx} \quad (3)$$

where Q stands for the heat evolved per hour in unit volume of the catalyst bed at a distance x from the top, and c_1, c_2, M and N are constants. Numerical values of the constants could then be determined from the distribution curve of the reaction heat given as a function of x. In this respect our previous paper[1] stated details of drawing the curve on the basis of experimental concentration gradients along the reactor.

Substitution of Eq. 3 into Eq. 1 and subsequent solution of the resulting equation result in the following formula,

$$t = t_0 \sum_1^{\infty} \frac{2U_1(a_n)U_0(a_n r/r_2)\exp(-\alpha_n^2 y)}{\left(a_n[\{1+(a_n^2/b^2)\}U_1^2(a_n) - (r_1/r_2)^2 U_0^2(a_n r_1/r_2)]\right)} + \sum_1^{\infty} \frac{2U_1(a_n)U_0(a_n r/r_2)}{\left(a_n[\{1+(a_n^2/b^2)\}U_1^2(a_n) - (r_1/r_2)^2 U_0^2(a_n r_1/r_2)]\right)} \times \left\{ \frac{[c_1(\exp(-my) - \exp(-\alpha_n^2 y))]}{[\lambda_r(a_n^2/r_2^2 - m - \lambda_x M^2/\lambda_r)]} - \frac{[c_2(\exp(-ny) - \exp(-\alpha_n^2 y))]}{[\lambda_r(a_n^2/r_2^2 - n - \lambda_x N^2/\lambda_r)]} \right\} \quad (4)$$

$$U_0(a_n r/r_2) \equiv J_0(a_n r/r_2) - cY_0(a_n r/r_2)$$

$$U_1(a_n r/r_2) \equiv J_1(a_n r/r_2) - cY_1(a_n r/r_2)$$

$$C \equiv J_1(a_n r_1/r_2) - Y_1(a_n r_1/r_2) = [a_n J_1(a_n) - bJ_0(a_n)]/[a_n Y_1(a_n) - bY_0(a_n)]$$

In Eq. 4 a_n and α_n stand for roots of equations $a_n U_1(a_n) = aU_0(a_n)$ and $A\alpha_n^4 + \alpha_n^2 - a_n^2/r_2^2 = 0$, respectively. In addition, there are following relations,

$$A \equiv \lambda_x \lambda_r / (C_p G)^2,\ b \equiv Ur^2/\lambda_r,\ y \equiv \lambda_r x / C_p G,$$

$$m \equiv MC_p G/\lambda_r \text{ and } n \equiv NC_p G/\lambda_r.$$

J_0 and J_1 are Bessel functions of first kind, zeroth and first order, respectively, and Y_0 and Y_1 are the same functions of second kind, zeroth and second order, respectively.

Let us calculate t with the present reactor by the aid of Eq. 4. Before proceeding to the calculation, it is assumed that the same synthesis conditions as these for Exp. No. 6 with the previous reactor hold again for the predicted synthesis, and that the same situations are realized in the predicted synthesis as were realized in the previous Exp. No. 6. Under these assumptions, the flow rate of the gaseous components and the yield of the product (oil plus wax) are 18.1/2 times as great as they were in Exp. No. 6. Hence the product yield attains 24.6 kg./day, and the flow rate of the gaseous components is 30 kg./hr.. Modified Reynolds number ($R_{ep} = d_p G/\mu$) takes a value of 7.22×10^2, where d_p is 4 mm. Characteristic constants, such as the specific heat (C_p), the viscosity (μ), and the thermal conductivity (k) of the fluid are determined in the following manner where compromise averages are taken between these based on the inlet and the exit gases. This results in the following values of $C_p = 0.42$ kcal./kg.°C, $\mu = 0.088$ kg./m. hr. and $k = 0.088$ kcal./m. hr.°C, respectively.

Moreover, the following values of the heat transfer constants are obtained as regards the predicted synthesis: $\lambda = 5.65$ kcal./m. hr.°C (2.61), $h = 866$ kcal./m² hr. °C (1086), and $h_L = 174$ kcal./m² hr. °C (120)[10], where h and h_L are the tube wall coefficients of heat transfer based on the inner and the outer surfaces of the reactor, respectively. Numericals in the brackets give the corresponding values for Exp. No. 6 with the previous reactor. As a consequence, a higher value of the overall heat transfer coefficient (U), which is 184 kcal./m² hr. °C as compared with 160 kcal./m²·hr. °C in Exp. No. 6, is obtained. Anyhow, the increase in the value of U is mainly due to the higher value of h_L in the predicted synthesis.

The constants in Eq. 3 have remained undetermined as yet. In interpretation of the data of Exp. No. 6, they were evaluated to be

$$Q(\text{kcal./m}^3\text{ hr.}) = 6.12 \times 10^5 e^{-0.18x} - 4.99 \times 10^5 e^{-1.01x} \quad (5)$$

The length of the reactor being denoted by L, the equation can be rewritten

$$Q(\text{kcal./m}^3\text{ hr.}) = 6.12 \times 10^5 e^{-0.82x/L} - 4.99 \times 10^5 e^{-4.60x/L} \quad (6)$$

since L for the previous reactor was 4.55 m. Eq. 6 can represent the distribution of the reaction heat independently of the dimensions of the reactor, provided that the synthesis proceeds with the same tendency as that which took place in Exp. No. 6, namely that the

6) Kodama et al.[7], Shindo[8], and Maeda[9] had already given the exprssion of $\sum v_i q_i = ce^{-kx}$.
7) S. Kodama and K. Fukui, *Kagaku Kikai*, **12**, (1948).
8) M. Shindo, *Memoir Muroran Univ. Eng.*, **1**, 51 (1950).
9) S. Maeda, *Kagaku Kikai*, **15**, 5 (1951).
10) λ and h have been evaluated by using the formula by Hatta et al.[11], while h_L has been evaluated by using the formula recommended by McAdams[12].
11) S. Hatta and S. Maeda, *Kagaku Kikai*, **13**, 79 (1949).
12) W. H. McAdams, "Heat Transmission", McGraw Hill Co. New York (1954).

heat evolving within unit volume of the catalyst bed at a value of x/L is equal to the corresponding one in Exp. No. 6. The constants for the predicted synthesis are then given by putting $L=9.6$ m. in Eq. 6, which follows

$$Q(\text{kcal./m}^3\,\text{hr.}) = 6.12\times10^{7}e^{-0.985x} - 4.99\times10^{7}e^{-0.45x} \quad (7)$$

For the sake of convenience, a graphical representation of the results is given in Fig. 2 (curve A) as a plot of q (kcal./m. hr.), which is defined by $q=Q/\pi(r_2^2-r_1^2)$, against x. According to the definition, q stands for the reaction heat evolved in an hour within the catalyst bed occupying the unit length of the reactor.

By putting the above numerical values of the constants into Eq. 4, the temperature profile either along or across the catalyst bed can be drawn, as shown in Fig. 2 (curves B and B'). The curves indicate that in the predicted synthesis with the present reactor the temperature difference between the oil bath and the center cross the catalyst bed attains only 31.5°C at the highest. Considering that the temperature difference in Exp. No. 6 was 24°C, and that the reaction heat evolving within a volume occupying the unit length of the present reactor becomes about fourtimes[13] as great as the heat with the previous reactor, the difference appears rather small.

We experienced the fact that with the previous reactor the synthesis could be carried out without serious difficulties, even when the temperature difference between the oil bath and the catalyst bed attained as high as 49°C (refer to Exp. No. 5 in our previous paper[1]). Based on the magnitude of predicted temperature rise, an operation of the synthesis with the present reactor may be expected to be probable.

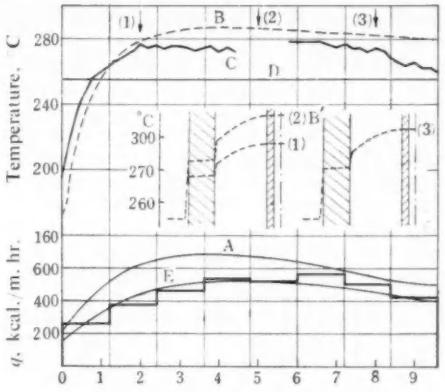

Fig. 2. Above, predicted and experimental temperature profiles. Below, distribution of q.
A, Predicted distribution of q
B, B', Predicted temperature profile (B, axial, B', radical)
C, Experimental temperature profile
D, Oil bath temperature
E, Experimental distribution of q

In the drawing of curves B', the magnitude of temperature rise from the oil bath to the outer wall-surface of the reactor (t_{w0}) and that to the inner wall-surface (t_{w1}) are given by the respective following formulae of the heat balance,

$$t_{w0}=t_{r=r_2}r_2U/r_1h_L, \quad t_{w1}=t_{r=r_2}(1-U/h)$$

where r_1 is the outer radius of the reactor.

Results and Discussion

Experimental Results. — The synthesis was made under the operating conditions as cited in Table I. The table also includes the operating conditions, product yield, and other points

Table I. Synthesis conditions, conversion, product yield, and other matters with those of predicted synthesis

	Pressure kg./cm²	Oil bath temperature °C	Space velocity, hr⁻¹ Base on fresh gas	Space velocity, hr⁻¹ Based on recycle gas	Volume contract %
Exp.	30	255	620	2070	42.2
Predicted	25	255*	763	1975	43.1
	Oil plus wax kg./day	Water kg./day	Oil plus wax per (H_2+CO) m³	Use ratio (H_2/CO)	Recycle ratio
Exp.	14.42	22.65	99.4	1.074	2.35
Predicted	24.62	19.10	130.5	0.819	1.59

* In the prediction of the temperature profile, wit as needless to consider the oil bath temperature, while for a convenient comparison of the predicted profile with the actual one curve A in Fig. 2 is drawn on the basis of the oil bath temperature of 255°C.

13) Strictly speaking, the heat is $(25^2-5^2)/(12.5^2-4^2)$ times in amount, where the numerals 5 and 4 are radii (mm.) of the thermocouple wells in the present and the previous reactors, respectively.

for the predicted synthesis. In the synthesis a much lower yield of oil plus wax[14] has been obtained with a greater amount of water than was predicted. As naturally expected from the lower yield, the actual temperature profile lies lower than the predicted profile (refer to Fig. 2). It may be noted, however, that the shape of the predicted profile is very similar to the actual profile except that the actual one is higher by 20°C at the topzone of the catalyst bed.

Calculation of Temperature Profile from Concentration Gradient.—Figure 3 shows the determined concentration gradients of reactants

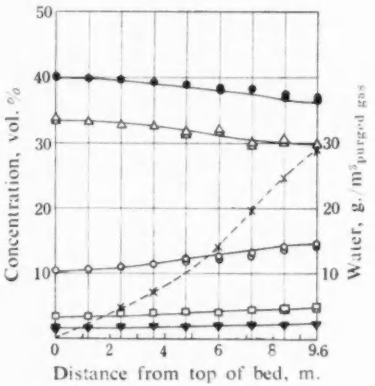

Fig. 3. Concentration gradients and amounts of water produced as a function of x.

—●— Hydrogen
--△-- Carbon monoxide
—○— Carbon dioxide
—□— Gaseous paraffin
—▼— Gaseous olefin
--×-- Water

(H_2, CO) and products (H_2O, CO_2, et al.) as a function of distance from the top along the catalyst bed. Our previous paper[1,15] reported that amounts of carbon monoxide consumed either by the hydrocarbon synthesis according to consecutive reactions of $H_2+CO\rightarrow >CHOH$ and $>CHOH+H_2\rightarrow -CH_2-+H_2O$ or by the water-gas shift[17,18] could be estimated from the concentration gradients, and the same procedure is now followed to result in Fig. 4. As soon as the carbon monoxide consumptions

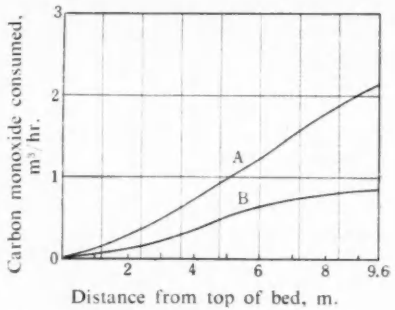

Fig. 4. Carbon monoxide consumptions.
A, By the hydrocarbon synthesis
B, By the water-gas shift reaction

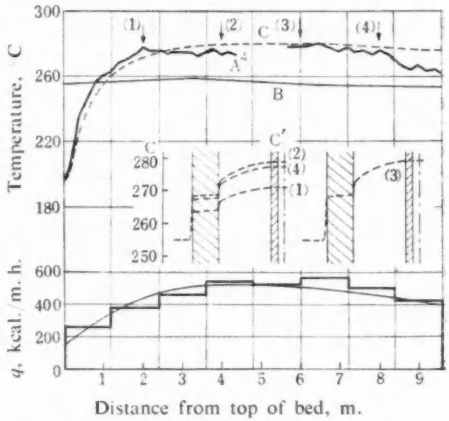

Fig. 5. Above, predicted and experimental temperature profiles. Below, distribution of q.
A, Experimental temperature profile
B, Oil bath temperature
C, C', Temperature profiles calculated from experimental concentration gradients
D, Experimental distribution of q

have been determined, magnitudes of the reaction heat can easily be calculated by taking theoretical quantities of the reaction heat into consideration. The quantities are 1.86 kcal./l. $CO_{consumed}$ and 0.41 kcal./l. $CO_{consumed}$ for the reaction heats with the hydrocarbon synthesis and the water-gas shift, respectively. The results are given in Fig. 5 as a stepwise plot (steplength, 1.2 m.) of the heat evolved per volume occupying unit length of the catalyst bed against the bed length. From the plot one can evaluate the constants in Eq. 3 to give $c_1=5.84\times10^5$, $c_2=5.05\times10^5$, $M=0.095$, and $N=0.35$. On the other hand, the other constants included in Eq. 4 have been evaluated on the basis of the actual synthesis conditions, which

14) The lower yield may have been partly owing to the poisoning of the catalyst with organic sulfur in the raw gas, since the capacity of active charcoal was insufficient to maintain the sulfur content less than 1~2 mg./m³ throughout the period of the synthesis.
15) Refer to the paper by Anderson et al.[16] also.
16) R. B. Anderson, A. Krieg et al., *Ind. Eng. Chem.*, **41**, 2189 (1949).
17) H. Koelbel and F. Engelhartdt, *Chem. Ing. Tech.*, **22**, 27 (1950).
18) R. B. Anderson et al., *Ind. Eng. Chem.*, **44**, 391 (1952).

appear to be: $C_p=0.41$ kcal./kg.°C, $\mu=0.090$ kg./m.hr., $k=0.085$ kcal./m. hr. °C, $G=1.682\times10^4$ kg./m² hr., $R_{ep}=7.48\times10^2$ ($d_p=0.004$ m.), $\lambda=5.62$ kcal./m. hr.°C, $h=836$ kcal./m² hr. °C, $h_L=174$ kcal./m² hr. °C, and $U=183$ kcal./m² hr. °C.

The problem is to draw the temperature profiles. This can be done by putting the above numerical values into Eq. 4. The results are shown in Fig. 5 as the temperature profiles along and across the catalyst bed, of which the former profile agrees well with the actually determined one. We have thus been able to obtain the temperature profile from the experimental concentration gradient with the present reactor.

However, the reactor suffered from the following limitation, that temperature in the catalyst bed was liable to fluctuate, even though the output remained less than had been expected. This may have been brought about by a slight change in either the composition or the flow rate of the feed gas, fine control of which was difficult. As it is, temperature may rise so high until the catalyst bed beomes ignited with the increasing output, unless greater amount of the reaction heat is carried away from the catalyst bed. As expected from a higher value of h than that of h_L, the heat transfer encounters more difficulty at the outer surface area than at the inner surface area of the reactor. This is shown more substantially with the radial temperature profile in Fig. 5 (refer to 3 in the figure): namely, the temperature difference within the bed remains only 6.3°C at a reactor cross section which is 6 m. apart from the top, while the difference between the center and the oil bath attains as high a point as 24.1°C. For the more satisfactory operation of the synthesis it, therefore, is desired to improve the heat transfer referred to the outer surface area by any chosen device. The result with the reactor improved along this line will be reported in the next paper.

Summary

By the aid of the calculating procedure developed by us on the basis of experimental data available in the synthesis with the reactor of 2 l. catalyst bed, prediction of the temperature profile as regards the synthesis with the reactor of 18.1 l. catalyst bed has been made. The predicted temperature profile expresses the tendencies observed in the actual synthesis with the latter reactor, though a complete agreement has not yet been obtained because of a lower output than was expected.

The calculating procedure has been applied to draw the temperature profile on the basis of the present experimental concentration gradients along the reactor. The profile thus drawn agrees well with the measured one.

The authors are particularly indebted to Messrs. M. Oba, A. Matsuda and H. Imai for their assistance in the synthesis experiment.

Governments Chemical Industrial Research Institute, Tokyo
Shibuya-ku, Tokyo

On the pd Hybridization of the Sulfur Atom in Thiothiophten. I. The Calculations of the Overlap Integrals Involving d Orbitals

By Kôgorô Maeda

(Received October 6, 1960)

The structure of a molecule named "thiothiophten" was recently clarified through the X-ray analysis study by Bezzi, Mammi and Garbuglio[1], who proposed for this compound a condensed ring system similar to that of thiophten[2] (see Fig. 1), and characterized it by no-bond resonance structure. Giacometti and Rigatti[3], following the deduction to this peculiar structure, have made simple LCAO treatment on the superimposed σ and π systems of non-localized electrons in thiothiophten, by using only p type orbitals for bonding with respect to sulfur atoms. However, since the system involving no-bond resonance structure is somewhat unlikely to occur, an alternative

1) S. Bezzi, M. Mammi and C. Garbuglio, *Nature*, **182**, 247 (1958).
2) H. C. Louguet-Higgins, *Acta. Cryst.*, 3, 76 (1950).
3) G. Giacometti and G. Rigatti, *J. Chem. Phys.*, **30**, 1633 (1959).

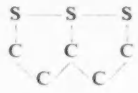

Fig. 1. Molecular structure of thiothiophten.

interpretation on the electronic structure of thiothiophten was given in the previous paper of this series[4], where the explicit participation of d orbitals on the sulfur atoms in bonding was attempted through pd hybridization. Adopting the hybridization for the central sulfur atom, the electronic structure of thiothiophten was treated according to the usual LCAO π approximation without considering the σ skeleton of the molecule. The results obtained there were appropriate in any case, although they were not necessarily the best.

In the present report, further discussions will be conducted on the pd hybridization of the central sulfur atom in thiothiophten, and the possibility of participation of the d orbital will be examined on the standpoint of overlap criterion, giving the values of the overlap integrals.

pd Hybridization.—In considering the valency state of the central sulfur atom in thiothiophten it is convenient to define its coordinates with the sulfur atom as origin so that straight bond S-S-S may go along the coordinate axis and the second axis may be perpendicular to the molecular plane. In this case, the central C–S bond lies on the remaining one, because S-S-C bond with respect to the central sulfur atom has its valency angle of 90°.

It is possible that a 3p electron of the sulfur atom is promoted to a 3d orbital and interacts with other 3p electrons through pd hybridization[5]. The pd configuration of electrons is used in the formation of σ orbitals and the linear arrangement of bonds is obtained from this electron configuration[6]. Then, as pointed out in the previous paper, it may be reasonable to consider that the central sulfur atom in the straight bond S-S-S is not in the normal electron configuration but in a valency state capable of forming a σ skeleton of the bond through the pd hybridization. The central sulfur atom is no longer in the bivalent state, but as the result of the hybridization, is in a tetra-valent state as in the case of the carbon atom. The expected valency state of the central sulfur atom would be in the electron configuration $3s^2 3p^3 3d$; two orbitals of 3p's are adopted to form a C–S σ bond with one of the sp^2 orbitals of the neighboring central carbon atom and to participate in the π electron conjugation system of thiothiophten. The remaining 3p orbital would hybridize with a 3d orbital, and would be going to make up the σ bonds of S-S-S in the linear arrangement. These configurations can account for both the right angle of S-S-C with respect to the central sulfur atom and the so-called abnormal length of the bond between two sulfur atoms[5,7,8].

Now a problem still remains, the discussion as to which of the d orbitals of the sulfur atom may hybridize with the 3p orbital to form the σ skeleton of the S-S-S bond. On the sulfur atom there are five d orbitals available for bonding. Of these, two orbitals would be ready to participate in the hybridization, namely $3d_z$ and $3d_{xy}$ orbitals (notation of Pauling and Wilson[9]), both of which have their maximum densities of electron distributions along the respective coordinate axes. In general, the bond-forming power should be a maximum along the direction with maximum electron distributions of the orbitals concerned[10]. The hybrid orbitals may be written as the linear combination of the 3p and the 3d orbitals. The approximate forms of the orbitals after the hybridization are shown in Fig. 2. Either set of the hybrid orbitals may go to form the σ bonds with 3p orbitals of neighboring sulfur atoms.

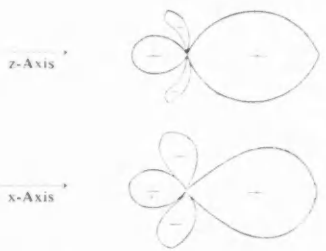

Fig. 2. Approximate forms of hybrid orbitals.

Overlap Integral.—It is, in general, impracticable to calculate accurately the energy of formation of a bond between two atoms. Instead of this, the overlap criterion may be used conveniently in discussing the bond formation[7-9]. The value of the overlap integral may give some measure of the strength of a

4) K. Maeda, This Bulletin, **33**, 1466 (1960).
5) K. Maeda, ibid., **33**, 303 (1960).
6) H. Eyring, J. Walter and G. E. Kimball, "Quantum Chemistry", John Wiley & Sons, Inc., New York (1944), p. 230.
7) D. P. Craig, A. MacColl, R. S. Nyholm, L. E. Orgel and L. E. Sutton, *J. Chem. Soc.*, **1954**, 332.
8) D. P. Craig and E. A. Magnusson, ibid., **1956**, 4895.
9) L. Pauling and E. B. Wilson, "Introduction to Quantum Mechanics", McGraw-Hill, New York (1935), p. 138.
10) C. A. Coulson, "Valence", Oxford University Press, London (1952), p. 195.

TABLE I. OVERLAP INTEGRALS: $S(3p_\sigma - 3d_{xy})$

p/t	−0.5	−0.4	−0.3	−0.2	−0.1	0.0	0.1	0.2	0.3	0.4	0.5
0	0	0	0	0	0	0	0	0	0	0	0
0.5						−0.145	−0.161	−0.163	−0.151	−0.126	−0.093
1.0	−0.028	−0.063	−0.110	−0.165	−0.220	−0.265	−0.293	−0.298	−0.276	−0.232	−0.173
1.5						−0.342	−0.377	−0.383	−0.358	−0.304	−0.229
2.0	−0.055	−0.106	−0.171	−0.242	−0.310	−0.366	−0.402	−0.410	−0.387	−0.334	−0.257
2.5						−0.341	−0.372	−0.382	−0.367	−0.324	−0.258
3.0	−0.063	−0.107	−0.154	−0.200	−0.242	−0.275	−0.301	−0.312	−0.307	−0.283	−0.236
3.5						−0.187	−0.203	−0.217	−0.224	−0.220	−0.197
4.0	−0.052	−0.071	−0.083	−0.087	−0.088	−0.091	−0.099	−0.113	−0.132	−0.147	−0.148
4.5						−0.000	−0.000	−0.015	−0.042	−0.079	−0.096
5.0	−0.029	−0.022	−0.002	0.026	0.055	0.076	0.082	0.069	0.038	−0.004	−0.046
5.5						0.134	0.145	0.135	0.101	0.053	−0.001
6.0	−0.003	0.021	0.057	0.100	0.141	0.172	0.186	0.178	0.148	0.098	0.038
6.5						0.192	0.208	0.204	0.178	0.130	0.069
7.0	0.016	0.047	0.087	0.129	0.168	0.197	0.215	0.214	0.193	0.151	0.092
7.5						0.192	0.208	0.211	0.196	0.161	0.107
8.0	0.027	0.057	0.092	0.125	0.154	0.178	0.194	0.199	0.191	0.163	0.116
8.5						0.160	0.175	0.182	0.178	0.159	0.120
9.0	0.031	0.056	0.081	0.104	0.123	0.139	0.152	0.162	0.163	0.151	0.120
9.5						0.119	0.131	0.140	0.146	0.139	0.117
10.0	0.031	0.049	0.065	0.078	0.089	0.099	0.110	0.120	0.126	0.126	0.117

bond. In practice, it was used successfully in discussing the possibility of participation of d orbital in the π conjugation system with respect to the sulfur atom in thiophene. In this paper, as in the case of thiophene, with the aid of the overlap criterion, the contribution of the d orbital to the hybridization will be examined on the central sulfur atom in thiothiophten. Comparison is made between the values of overlap integral of the 3p and the 3d orbitals with $3p_\sigma$ of the neighboring sulfur atom. A larger amount of the value about the 3d orbital will be associated by a greater extent of the contribution, to the hybridization because the integral of the hybrid orbital may be written as the sum of those of the participating orbitals. The values of the integral of $3p_z - 3d_z$ were already given by Craig et al.[7], while those of $3p_\sigma - 3d_{xy}$ have not been published yet. In this paper, therefore, the values for $3p_\sigma - 3d_{xy}$ were calculated, together with those of $B_n(\alpha)$ necessary to evaluate the overlap integral. In Tables I and II are given the results.

In calculating the integral $S(3p_\sigma - 3d_{xy})$, one must pay some attention to the orientation of the $3d_{xy}$ orbital, because the internuclear axis is usually taken as the z-axis of the coordinate system of integration. The orbital should be rotated by 90° about the y-axis. After the rotation, the angular part of the orbital, $\sin^2\vartheta\cos^2\varphi$, turns into $(\cos^2\vartheta - \sin^2\vartheta\sin^2\varphi)$. The explicit expressions for the overlap integral are as follows:

for $t \neq 0$,

$$S(3p_\sigma - 3d_{xy}) = (1/2^7 \times 3\sqrt{5})(1-t^2)^{7/2} \times p^7 \times \{-A_0(3B_5 - B_3) - A_1(3B_4 - 2B_1 - B_0) + A_2(3B_1 + B_2 + 2B_3) + A_3(3B_0 - B_2 + B_1 - 3B_3) - A_4(2B_1 + B_2 + 3B_3) - A_5(B_0 + 2B_2 - 3B_4) - A_6(B_1 - 3B_5)\}$$

for $t = 0$,

$$S(3p_\sigma - 3d_{xy}) = (1/2^6 \times 315\sqrt{5}) \times p^7 \times (-48A_1 + 256A_3 - 112A_5)$$

for $p = 0$, $\quad S(3p_\sigma - 3d_{xy}) = 0$

where the method of evaluation described by Mulliken et al. and their notations[11] were used. The values of the function $A_n(\alpha)$'s which appear in the above expressions were taken from the table given by Kotani and his collaborators[12]. Those of $B_n(\alpha)$'s were evaluated by them for a wide range of the parameter α and also by Craig et al. for the small values of α[7]. However, some of the values necessary in the calculations of Table I were not available. Therefore, in this paper, a number of $B_n(\alpha)$ were calculated and the results are shown in Table II, together with those obtained by Craig et al.[7] In calculating the values of $B_n(\alpha)$, the recursion formula for $B_n(\alpha)$,

11) R. S. Mulliken, C. A. Rieke, D. Orloff and H. Orloff, *J. Chem. Phys.*, **17**, 1248 (1949).
12) M. Kotani, A. Amemiya, E. Ishiguro and T. Kimura, "Table of Molecular Integrals", Maruzen Co., Tokyo (1955), p. 146.

TABLE II. $B_n(\alpha)=\int_{-1}^{+1}x^n e^{-\alpha x}dx$

α	$B_0(\alpha)$	$-B_1(\alpha)$	$B_2(\alpha)$	$-B_3(\alpha)$	$B_4(\alpha)$	$-B_5(\alpha)$	$B_6(\alpha)$
0	2	0	0.666667	0	0.400000	0	0.285714
0.05	2.00083	0.033342	0.667167	0.020006	0.400357	0.014290	0.286055
0.10	2.00334	0.066733	0.668668	0.040048	0.401429	0.028609	0.286824
0.15	2.00751	0.100225	0.671173	0.060161	0.403219	0.042982	0.288218
0.20	2.01336	0.133867	0.674686	0.080382	0.405729	0.057440	0.290171
0.25	2.02090	0.167711	0.679213	0.100746	0.408965	0.072009	0.292688
0.30	2.03014	0.201806	0.684763	0.121290	0.412932	0.086718	0.295776
0.35	2.04108	0.236204	0.691346	0.142051	0.417639	0.101596	0.299439
0.40	2.05376	0.270958	0.698973	0.163067	0.423095	0.116672	0.303687
0.45	2.06819	0.306119	0.707657	0.184374	0.429310	0.131975	0.308527
0.50	2.08438	0.341741	0.717416	0.206011	0.436297	0.147534	0.313969
0.55	2.10237	0.377879	0.728265	0.228016	0.444069	0.163382	0.320025
0.60	2.12218	0.414586	0.740224	0.250431	0.452640	0.179547	0.326706
0.65	2.14384	0.451920	0.753315	0.273294	0.462029	0.196063	0.334027
0.70	2.16738	0.489937	0.767562	0.296648	0.472253	0.212961	0.342003
0.75	2.19284	0.528696	0.782989	0.320534	0.483332	0.230274	0.350650
0.80	2.22026	0.568256	0.799625	0.344995	0.495288	0.248037	0.359985
0.85	2.24968	0.608679	0.817499	0.370077	0.508144	0.266285	0.370028
0.90	2.28115	0.650027	0.836643	0.395825	0.521925	0.285052	0.380800
0.95	2.31470	0.692365	0.857093	0.422286	0.536658	0.304377	0.392322
1.00	2.35040	0.735759	0.878885	0.449507	0.552373	0.324297	0.404618
1.05	2.38830	0.780277	0.902057	0.477540	0.569099	0.344852	0.477714
1.10	2.42845	0.825988	0.926653	0.506435	0.586869	0.366083	0.431636
1.20	2.51577	0.921285	0.980294	0.567025	0.625685	0.410739	0.462076
1.25	2.56307	0.971022	1.00944	0.598833	0.646806	0.434253	0.478656
1.30	2.61290	1.02226	1.04019	0.631726	0.669124	0.458620	0.496188
1.35	2.66532	1.07507	1.07263	0.665766	0.692683	0.483888	0.514708
1.40	2.72043	1.12955	1.10679	0.701106	0.717529	0.510108	0.534254
1.50	2.83904	1.24385	1.18057	0.775410	0.771280	0.565613	0.576587
1.60	2.96946	1.36592	1.26206	0.855464	0.830800	0.625579	0.623538
1.65	3.03935	1.43011	1.30589	0.897799	0.862869	0.657384	0.648864
1.70	3.11251	1.49654	1.35187	0.941778	0.896560	0.690487	0.675494
1.75	3.18904	1.56533	1.40009	0.987483	0.931941	0.724956	0.703482
1.80	3.26908	1.63659	1.45065	1.03500	0.971858	0.753143	0.758606
1.90	3.44017	1.78700	1.55912	1.13584	1.04893	0.837261	0.796188
1.95	3.53149	1.86639	1.61724	1.18935	1.09181	0.877915	0.830218
2.00	3.62686	1.94877	1.67809	1.24505	1.13675	0.920311	0.865927
2.20	4.05191	2.31086	1.95113	1.49202	1.33916	1.10910	1.02709
2.25	4.16993	2.41031	2.02743	1.56038	1.39592	1.16158	1.07238
2.30	4.29301	2.51367	2.10721	1.63165	1.45535	1.21638	1.11985
2.50	4.84016	2.96977	2.46435	1.94861	1.72239	1.46106	1.33362
2.55	4.99177	3.09546	2.56396	2.03658	1.79713	1.52923	1.39359
2.60	5.14979	3.22624	2.66807	2.12838	1.87536	1.60047	1.45641
2.70	5.48612	3.50401	2.89056	2.32417	2.04291	1.75274	1.59114
2.80	5.85137	3.80503	3.13349	2.53749	2.22638	1.91913	1.73895
2.85	6.04559	3.96492	3.26319	2.65125	2.32454	2.00804	1.81814
2.90	6.24797	4.13145	3.39870	2.77002	2.42725	2.10101	1.90106
3.00	6.67858	4.48558	3.68820	3.02358	2.64715	2.29987	2.07885
3.20	7.65368	5.28738	4.34907	3.60191	3.15130	2.75525	2.48758
3.40	8.80315	6.23362	5.13632	4.29074	3.75522	3.30040	2.97892
3.50	9.45293	6.76935	5.58473	4.68327	4.10062	3.61216	3.26065
3.60	10.15859	7.35194	6.07418	5.11195	4.47864	3.95343	3.56953
3.80	11.75758	8.67526	7.19166	6.09173	5.34523	4.73615	4.27944
4.00	13.64496	10.24288	8.52352	7.26148	6.38348	5.67476	5.13281

TABLE III. OVERLAP INTEGRALS: $S(3p_z-3d_z)$

p/t	−0.5	−0.4	−0.3	−0.2	−0.1	0.0	0.1	0.2	0.3	0.4	0.5
0	0	0	0	0	0	0	0	0	0	0	0
0.5						−0.167	−0.185	−0.188	−0.174	−0.146	−0.107
1.0	−0.033	−0.072	−0.127	−0.190	−0.254	−0.306	−0.339	−0.344	−0.319	−0.268	−0.199
1.5						−0.395	−0.435	−0.443	−0.413	−0.351	−0.265
2.0	−0.063	−0.122	−0.197	−0.279	−0.358	−0.423	−0.464	−0.473	−0.447	−0.386	−0.297
2.5						−0.393	−0.430	−0.441	−0.423	−0.375	−0.298
3.0	−0.073	−0.123	−0.178	−0.231	−0.279	−0.318	−0.347	−0.360	−0.355	−0.327	−0.272
3.5						−0.216	−0.235	−0.251	−0.259	−0.254	−0.228
4.0	−0.060	−0.082	−0.096	−0.101	−0.102	−0.105	−0.114	−0.131	−0.152	−0.170	−0.171
4.5						−0.000	−0.001	−0.017	−0.048	−0.092	−0.111
5.0	−0.033	−0.025	−0.002	0.030	0.063	0.088	0.095	0.080	0.044	−0.005	−0.053
5.5						0.155	0.167	0.156	0.117	0.061	0.001
6.0	−0.004	0.024	0.066	0.116	0.163	0.199	0.215	0.206	0.171	0.113	0.044
6.5						0.222	0.240	0.236	0.205	0.150	0.079
7.0	0.018	0.054	0.100	0.149	0.194	0.228	0.248	0.247	0.223	0.174	0.106
7.5						0.221	0.241	0.244	0.226	0.186	0.124
8.0	0.031	0.066	0.106	0.144	0.178	0.205	0.224	0.230	0.220	0.188	0.134
8.5						0.184	0.202	0.210	0.206	0.184	0.139
9.0	0.036	0.065	0.094	0.120	0.142	0.161	0.176	0.187	0.188	0.174	0.138
9.5						0.137	0.151	0.162	0.169	0.161	0.135
10.0	0.036	0.057	0.075	0.090	0.103	0.114	0.127	0.138	0.146	0·145	0.128

$$B_n(\alpha)=(1/\alpha)\{(-1)^n e^{\alpha}-e^{-\alpha}+nB_{n-1}(\alpha)\}$$

was used, and the values of e^{α} and $e^{-\alpha}$ were taken from the table published by the Computation Laboratory of NBS[13]. Some of the exponential functions were derived by using the table of hyperboric functions[14]. According to Mulliken's convention concerning the sign of t [11], the values of $S(3p_{\sigma}-3d_{xy})$ for $t<0$ were also evaluated. These are given in Table I. These values can easily be derived by replacing $B_n(\alpha)$ with $B_n(-\alpha)$ of the above expression and $B_n(-\alpha)$ is obtained from $B_n(\alpha)$ through the relation $B_n(-\alpha)=(-1)^n\times B_n(\alpha)$. These integrals are corresponding to the values obtained when $3d_{xy}$ orbital has its greater effective nuclear charge than that of $3p_x$. Further, in Table III, the overlap integrals $S(3p_z-3d_z)$ with the parameter p at intervals of 0.5 and of 1.0 are shown for $t>0$ and $t<0$ respectively. Some of the values were already given, as mentioned above, by Craig et al.[7], who evaluated the values with p at intervals of 1.0.

In order to estimate the values of overlap integrals using the above tables, it is necessary to know the effective nuclear charges of the orbitals concerning the atoms. The respective charges found in accordance with Slater's formula[15] are as follows: 5.80 and 1.00 for 3p and 3d orbitals on the central sulfur atom and 5.45 for 3p orbital on the neighboring sulfur atom. Since the bond distance S–S is 2.36 Å, the values about 3p−3d give 0.7 and 5 for t and p (see Ref. 11) respectively. From Tables I and III it is inferred that negative values of overlap integrals result from these t and p values. With this result, one might not expect any participations of the d orbitals in bonding to occur through the hybridization. This may be due to the straightforward application of Slater's rule to the estimation of the effective nuclear charges of the atoms. As already mentioned[5], since the maximum of the radial function of the d orbital with its effective nuclear charge 1 lies at 9 atomic units, the orbital may be regarded as including the full σ skeleton of thiothiophten, so that it would be impossible to avoid the influence of the neighboring atoms in the molecule. The charges of the atoms may contract the d orbital and enlarge its nuclear charge, leading to a comparable value of the overlap integral to that of 3p orbital. Then it might be expected that the participation of the d orbital in the hybridization would take place to an extent not much smaller than that of 3p orbital. It is necessary, therefore, to examine the influence of the nuclear charges of the neighboring atoms of thiothiophten upon the d orbital of the central sulfur atom. Further discussions, however, will be given in subsequent publications.

It is of interest to notice the following

13) Computation Laboratory, "Tables of the Exponential Function e^x", Natl. Bur. Standards, Washington (1951).
14) Committee for the Calculation of Mathematical Tables, "British Association Mathematical Tables", I, 30 (1951).
15) J. C. Slater, *Phys. Rev.*, **36**, 57 (1930).

points with respect to the values of overlap integral given in Tables I and III; the value $S(3p_z-3d_z)$ is greater than that of $S(3p_x-3d_{xy})$. This may predict a greater possibility of the participation of $3p_z$ orbital than that of $3d_{xy}$. In both tables, the value for $t<0$ is small, as a whole, compared with that for $t>0$. This may imply that it is not easy to form a bond between 3d with a greater effective nuclear charge and 3p with a smaller one.

The author wishes to express his sincere thanks to Dr. S. Nagakura, The University of Tokyo, for his kind advice and helpful discussions.

Electrochemical Laboratory
Tanashi, Tokyo

The Effects of pH on the Flocculation of Quartz Aqueous Suspensions

By Tadashi OHYAMA, Junzo SHIMOIZAKA and Shinnosuke USUI

(Received November 2, 1960)

Control of the state of dispersion or flocculation of mineral suspension is widely required for proper operation of many chemical engineering processes. It is well known that, especially in the case where metal ions are dissolved, the pH of the solution is closely related to the stability of suspensions. From this point of view, the effects of pH on the flocculation of quartz aqueous suspensions containing a cation, such as Ba^{2+}, Fe^{3+} or Cu^{2+}, respectively, are investigated by means of electrokinetic measurements.

Experimental

Quartz suspensions, 6% by weight, were provided for the flocculation experiments. A monocrystalline quartz was ground by a laboratory roll crusher, and it was washed with hydrochloric acid; the washing was followed by successive decantation with distilled water until no Cl^- could be detected, and the quartz powder under 150 mesh was well reground in an agate mortar after drying. Ba^{2+}, Fe^{3+} or Cu^{2+} was supplied by $BaCl_2$, $FeCl_3$ or $CuSO_4 \cdot 5H_2O$ in reagent grade, respectively. The pH of solution was adjusted with hydrochloric acid or sodium hydroxide and measured by a glass electrode pH meter. The degree of flocculation was evaluated by measuring the transparency of suspensions, a Hitachi EPO-B photoelectric photometer was available for transparency measurements. The ζ potential of quartz in the solution containing Fe^{3+} or Cu^{2+} was measured by a microscopic electrophoresis cell, considering the fact that, for the system in which insoluble hydroxide is formed, the condition of streaming potentential method made on relatively coarse particles may differ from that of flocculation experiment carried out on the suspensions containing fine particles. For the solution of Ba^{2+}, on the other hand, the streaming potential method was adopted.

The quartz in the streaming potential measurements is the 48/65 mesh fraction, and the apparaturs is the same as that used by Gaudin and Fuerstenau[1].

The Effects of pH on the Flocculation of Quartz Suspensions Containing Ba^{2+}. — Fig. 1 shows transparency-time curves under various pH of the suspension containing Ba^{2+} of 1 mmol./l. in concentration. The abscissa is the elapsed time after shaking the suspension, the ordinate being

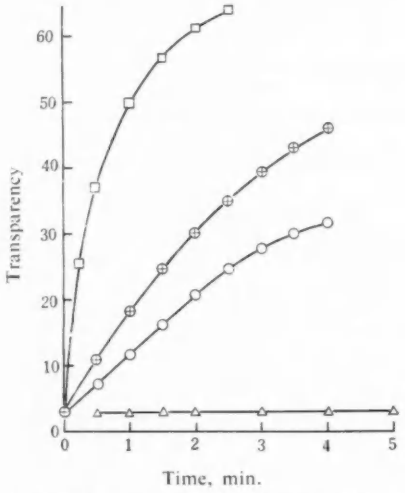

Fig. 1. Transparency-time curves of quartz suspension under various pH at the concentration of $BaCl_2$ 1.0 mmol./l.
△ pH=3.0, 6.8, 8.8
○ pH=10.8
⊕ pH=11.0
□ pH=12 or more

1) A. M. Gaudin and D. W. Fuerstenau, *Min. Eng.*, **7**, 66 (1955).

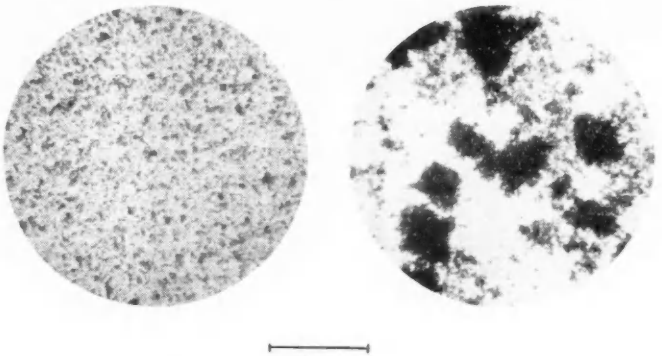

(a) $BaCl_2$ 10 mmol./l., pH 5.0 (b) $BaCl_2$ 10 mmol./l., pH 11.5

Fig. 2. Photomicrographs of flocs.

the degree of flocculation. From this figure it can be seen that the degree of flocculation becomes stronger with increasing pH in alkaline solutions. The flocculation in high pH is characterized by the formation of gel-like flocs. When the concentration of Ba^{2+} is increased to more than 3 mmol./l., which is the flocculation value of Ba^{2+} for the quartz suspension adopted at pH 7, the flocculation of the suspension is also observed in the acidic side. The flocculation in acidic solution, however, is relatively weak and no gel-like floc formation is observed. Fig. 2 shows the photomicrographs of flocs formed at the concentration of Ba^{2+} 10 mmol./l.; Figs. 2a and 2b show flocs at pH 5.0 and pH 11.5, respectively. The flocculation of the quartz suspension disappears with decrease of the Ba^{2+} concentration even in the solution of high pH, and the critical Ba^{2+} concentration for flocculation is found to be 0.6 mmol./l. at pH 11.0. The critical Ba^{2+} concentration decreases with increasing pH of the solution. When the pH is lowered to that of the acidic side the critical Ba^{2+} concentration is also decreased, and at pH about 2 flocculation occurs without the addition of Ba^{2+}.

The Effects of pH on the Flocculation of Suspensions Containing Fe^{3+} or Cu^{2+}. — In the suspensions containing Fe^{3+}, no visible flocculation takes place in the range of low pH even though the Fe^{3+} concentration reaches 0.4 mmol./l. However, the addition of sodium hydroxide to the above suspension produces a violent flocculation at about neutral pH. This flocculation is weakened, however, by the increase of pH and dissappears at the pH region higher than 10. Fig. 3 gives the relation between the transparency at 5 min. after shaking the suspension and pH of the solution containing Fe^{3+} of 0.4 mmol./l. in concentration. For the suspension containing Cu^{2+}, 4 mmol./l., a remarkable flocculation takes place in the pH range of 6~12. This is also illustrated in Fig. 3. It is always observed in the above experiments that the upper solution appearing after sedimentation of flocs is colorless and transparent, and the sediment with

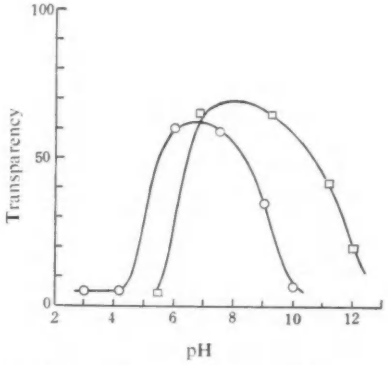

Fig. 3. Transparency at 5 min. after preparation of suspensions containing Fe^{3+} or Cu^{2+} as a function of pH.

○ Fe^{3+} 0.4 mmol./l.
□ Cu^{2+} 4.0 mmol./l.

color of the hydroxide of the respective ion is formed, such as light brown for Fe^{3+} and light blue for Cu^{2+}. The deflocculation of the suspensions occurs when the pH exceeds 10 for Fe^{3+} and 12 for Cu^{2+}. On the other hand, in the suspension containing Ba^{2+} the violent flocculation still takes place even in the pH region higher than 12.

These observations seem to indicate that the pH range in which the violent flocculation occurs is related to the solubility of the hydroxide of the ion involved; the larger the solubility of the hydroxide, the higher pH range where the flocculation is maintained is expected.

ζ Potential.—ζ Potential of quartz in the solutions of various concentrations of Ba^{2+}, i.e. 0.1, 0.2 and 1.0 mmol./l., as a function of pH is given in Fig. 4. The ζ potential at pH 11 in the presence of Ba^{2+} of 0.6 mmol./l., the critical concentration for the flocculation, is also plotted in the same figure. Fig. 5 represents the ζ poten-

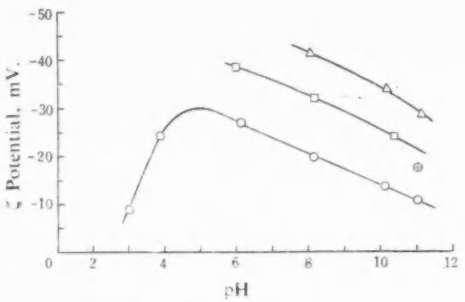

Fig. 4. Influence of pH on ζ potential of quartz in $BaCl_2$ solutions.

△ $BaCl_2$ 0.1 mmol./l.
□ $BaCl_2$ 0.2 mmol./l.
⊖ $BaCl_2$ 0.6 mmol./l.
○ $BaCl_2$ 1.0 mmol./l.

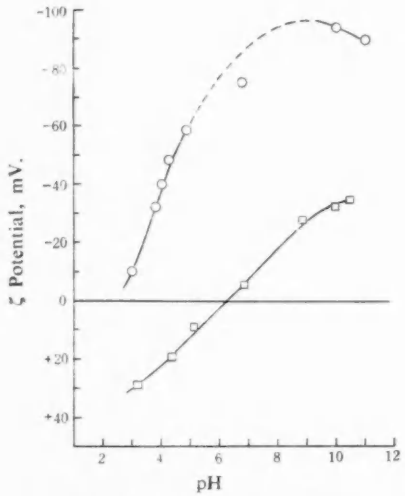

Fig. 5. ζ Potential of quartz in the absence or presence of Fe^{3+} as a function of pH.

○ Absence of Fe^{3+}
□ Fe^{3+} 0.4 mmol./l.

tial of quartz in the solutions containing only hydrochloric acid or sodium hydroxide and Fe^{3+}, 0.4 mmol./l., as a function of pH. From these figures it can be seen that the ζ potential decreases with increasing pH in alkaline solution at the respective Ba^{2+} concentration, on the other hand, its value is considered to be determined mainly by H^+ in acidic solution. Gaudin and Fuerstenau[1] have shown that, in the streaming potential study made on 48/65 mesh quartz, the reliable values of the ζ potential were obtainable in the solution over 10^{-4} in ionic strength, below which it was necessary to consider the effect of surface conductivity. In the present investigation, the effect of surface conductivity was not appreciated, so that in Fig. 5 the region of lower ionic strength was expressed by a dotted line; if the correction is made, higher negative potential values would be expected. In the absence of Fe^{3+}, the isoelectric point of quartz seems to be in the neighbourhood of pH 2.5. On the other hand, the isoelectric point shifts to higher value of pH, i.e. about pH 6, in the presence of Fe^{3+}.

Discussion

The stability of lyophobic colloids or suspensions depends upon the energy of interaction between two approaching particles. According to Verwey and Overbeek[2] the energy is composed of electrical repulsion and long range van der Waals attraction. For a given suspension the attraction is assumed to be constant while the repulsion changes with the electrolyte content of the system. These concepts will lead us to the prediction that the violent flocculation of the quartz suspension containing Ba^{2+} in alkaline solution is due to the decrease of electrical repulsion. Verwey and Overbeek have calculated the repulsive potential of interaction between two flat double layers in the solution containing a species of binary electrolyte, and Eq. 1 has been obtained as the repulsive potential per unit area if the interaction is not so strong;

$$\left.\begin{aligned} V_R &= (64nkT/\kappa)\gamma^2 \exp(-2\kappa d) \\ \kappa &= (8\pi ne^2v^2/\varepsilon kT)^{1/2} \\ \gamma &= \{\exp(z/2)-1\}/\{\exp(z/2)+1\} \\ z &= ve\phi_0/kT \end{aligned}\right\} \quad (1)$$

where n is the number of ions per cm^3 far from the surface, k the Boltzmann constant, T the absolute temperature, e the elementary charge, v the valency of counter ion, ε the dielectric constant, ϕ_0 the surface potential and d the half-distance of separation.

Eq. 1, however, cannot be applied to the system in which more than two species of counter ions of different valency is involved. It is difficult to obtain a general formula representing the repulsive potential energy, but the repulsive potential can be expressed as Eq. 2[3] if ζ potential is not so high;*

$$\left.\begin{aligned} V_R &= (\varepsilon/2\pi)\kappa\zeta^2 \exp(-2\kappa d) \\ \kappa &= (4\pi e^2 \Sigma n_i v_i^2/\varepsilon kT)^{1/2} \end{aligned}\right\} \quad (2)$$

Thus, the repulsive potential is directly related to κ and ζ. As indicated in Fig. 1, a remarkable flocculation takes place at pH 11 (NaOH,

2) E. J. W. Verwey and J. Th. G. Overbeek, "Theory of the Stability of Lyophobic Colloids", Elsevier, Amsterdam, (1948).

3) S. Usui, *J. Mining and Metallurgical Inst. Japan, (Nippon Kogio Kaishi)*, **75**, 1025 (1959).

* On the system containing a binary electrolyte, it is calculated that Eq. 2 gives the value of 1.0~1.1 times the one evaluated from Eq. 1 in the range of $Z(=ve\zeta/kT$ for Eq. 2) 0~1.5.

1 mmol./l.), while no flocculation appears at pH 3 (HCl, 1 mmol./l.) despite of the same concentration of Ba^{2+}, i.e. 1 mmol./l. The values of κ at pH 11 and pH 3 may be almost equal since it is evaluated by analogy with the experimental results by Gaudin and Chang[4] that the decrease of Ba^{2+} concentration in bulk solution resulting from the adsorption of Ba^{2+} is of the order of 10%, which corresponds to the decrease of κ of about 3% under the adopted condition. As illustrated in Fig. 4, the ζ potential of quartz in the solution containing Ba^{2+} of 1 mmol./l. is -11 mV. at pH 11 and -9 mV. at pH 3; the value of ζ at the former where the remarkable flocculation is exhibited is somewhat higher than that at the latter where no visible flocculation is observed. From the inspection of κ and ζ, it is difficult to explain the singular flocculation in alkaline solution in terms of the decrease of repulsion in alkaline solution. These considerations will lead to the conclusion that such a flocculation in alkaline solution is not due to the decrease of the repulsion but to the incease of attraction.

The attractive potential energy should be known in addition to the repulsive potential energy in order to obtain the total potential energy of interaction between approaching particles. London-van der Waals attractive potential for two approaching flat plates has been expressed as Eq. 3[5], when d is small compared with the thickness of the plates;

$$V_A = -A/48\pi d^2 \tag{3}$$

where A is called "Hamaker constant". It is necessary to determine the value of A in calculating V_A according to Eq. 3. However, since the proper evaluation of A has not yet been established, the examination by which A is determined empirically has been undertaken by using Eq. 4,

$$C_{floc.} = 3.1\times10^{-21} z^4/A^2 v^6 \text{ mmol./l.} \quad \text{at } 25^\circ\text{C} \qquad z = v e\zeta/kT \tag{4}$$

which is derived as a flocculation value from Eqs. 2 and 3 on the basis of the Verwey-Overbeek theory. Thus, A was determined to be 3.4×10^{-13}*, where the empirical value of $C_{floc.}$ of Ba^{2+} and ζ potential were 3 mmol./l. and -20 mV. respectively. In Fig. 6, the total potential energy curves at pH 11 under various

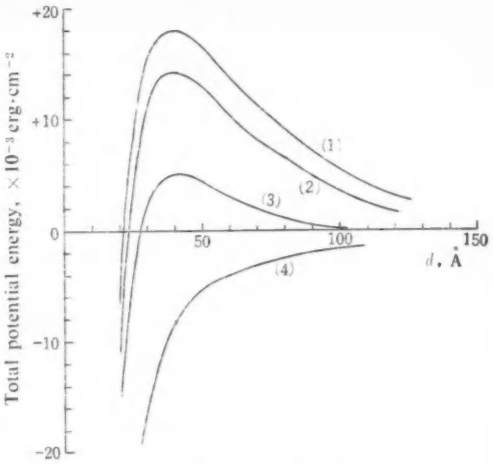

Fig. 6. Total potential energy between approaching quartz particles in solutions containing Ba^{2+} at pH 11.0 as a function of half-distance of separation.
(1) Ba^{2+} 0.1 mmol./l.
(2) Ba^{2+} 0.2 mmol./l.
(3) Ba^{2+} 0.6 mmol./l.
(4) Ba^{2+} 1.0 mmol./l.

concentrations of Ba^{2+}, i.e. 0.1, 0.2, 0.6 and 1.0 mmol./l., are illustrated as a function of half-distance of approaching particles. It can be seen from this figure that there is a potential barrier of about 5×10^{-3} erg./cm^2 at Ba^{2+} concentration of 0.6 mmol./l. which is the flocculation value at pH 11. The barrier corresponds to $7500\,kT$ per particle if a stably suspended quartz perticle is assumed to be a cube of 1 μ edge length, or to 75 kT if 0.1 μ edge length is assumed*; This will be an insurmountable obstacle to flocculation.

Now, the discrepancy between the flocculation experiment and the potential energy consideration may well be explained by assuming a certain attractive force by which the potential barrier is lowered. Mattson[7] has suggested that the strong flocculation of quartz particles in alkaline solution is due to the formation of particle-paricle linkage action through polyvalent cation, see Fig. 7. These linkage actions may well be supported by the consideration of energy described above. At first sight, it seems possible to explain the remarkable flocculasion of the suspention containing Fe^{3+} in the range of neutral pH in terms of the

4) A. M. Gaudin and C. S. Chang, *Min. Eng.*, **4**, 193 (1952).
5) E. J. W. Verwey and J. Th. G. Overbeek, "Theory of the Stability of Lyophobic Colloids", Elsevier, Amsterdam, (1948), p. 101.
* A is taken as $1\sim2\times10^{-12}$ by Verwey and Overbeek, and $<5\times10^{-14}$ by Derjaguin[6].
6) B. V. Derjaguin, *Discussions Faraday Soc.*, **18**, 36 (1954).

* A sphere of 1.0 μ in diameter and of specific gravity 2.7 falling in water under the influence of gravity aquires a kinetic energy of only 6×10^{-21} erg or of 1.5×10^{-7} in unit of kT.
7) S. E. Mattson, *Kolloidchem. Beihefte*, **14**, 227 (1922).

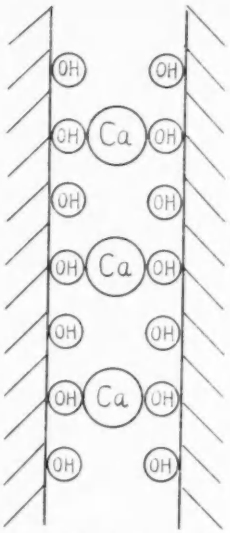

Fig. 7. Schematic illustration of linkage action of Ca^{2+}.

lowering of ζ potential (see Figs. 3 and 5); the value of ζ lies in zero or in its vicinity at about neutral pH. However, there is no visible flocculation of quartz particles in a solution containing Fe^{3+} 0.14 mmol./l. at pH 3.5 despite the fact that the ζ potential is zero. In the case of the suspension containing Cu^{2+}, it is understood by the inspection of ζ potential data that the repulsive potential between particles in the pH range of 9~11, wherein a violent flocculation takes place, is higher than that at pH 5.2 wherein no visible flocculation is observed.

Thus, the flocculation depending upon the pH of the solution containing Fe^{3+} or Cu^{2+}, as well as the case where Ba^{2+} is contained, can not be interpreted only in terms of the decrease of repulsion caused by the decrease of ζ potential. An uncertainty still remains whether these flocculation characteristics are due to the bridging action by metal ion and OH^- as in the case of Ba^{2+} and OH^- or to the so-called "heteroflocculation"[8], between metal hydroxide and quartz perticles. The flocculation mechanism of macromolecular flocculants for suspensions has been interpreted by the concept of molecular bridging action caused by its fibrous structure[9]. It is now worthwhile to point out that, in the case where a simple metallic ion is involved, not only London-van der Waals attractive force but also a certain attractive force by which a special linkage action is brought about must be taken into account.

Summary

The effects of pH on the flocculation of quartz aqueous suspensions containing Ba^{2+}, Fe^{3+} or Cu^{2+}, respectively, were investigated by means of electrokinetic measurements. The violent flocculation takes place in the characteristic range of pH with respective cation involved. The calculation of the potential energy between approaching quartz particles indicates that the violent flocculation is readily explained, not by the decrease of electrical repulsion, but by the consideration of an attractive force other than van der Waals attraction.

Department of Mining
Faculty of Engineering
Tohoku University
Sakurakoji, Sendai

8) B. V. Derjaguin, *Discussions Faraday Soc.*, **18**, 85 (1954).
9) R. A. Ruehrwein and D. W. Ward, *Soil Sci.*, **73**, 485 (1952).

Dehydrogenation of Secondary Alcohols with Reduced Copper. IV[1]. *Catalytic Dehydrogenation of Isopropyl Alcohol (Part 2)**

By Kazuaki KAWAMOTO**

(Received October 24, 1960)

As has already been pointed out in the preceding paper[1], the activity and the selectivity of various copper catalysts depend not only upon the reaction temperature at which the catalysts are employed, but also on the precipitants in the preparation of the copper catalysts. For instance, the catalyst prepared with potassium bicarbonate shows the greatest activity for dehydrogenating isopropyl alcohol to acetone with no side reaction, while the copper catalyst prepared with sodium hydroxide under the same condition shows the smallest dehydrogenating activity, producing condensation products.

Earlier, Audibert and Raineau[2] reported that a highly active catalyst for the decomposition of methanol was obtained by adding a solution of alkali hydroxide to a boiling solution of copper nitrate, and reducing the black precipitate with hydrogen, and that the catalyst prepared from the oxide precipitated with ammonia from a cold copper nitrate solution was totally inactive for the same reaction. On the other hand, Frolich et al.[3] prepared copper catalysts from the precipitates obtained by adding ammonia to a solution of copper nitrate at various temperatures (0, 10, 22, 55, 85 and 100°C), and found that the greatest activity for the decomposition of methanol was achieved with the precipitate at 22°C. Thus there is non-conformity in the results obtained by various workers.

The present author found that dehydrogenation of isopropyl alcohol at 220~250°C with the copper catalysts prepared with alkali hydroxide gives oily products (isobutyl methyl ketone and diisobutyl ketone) in addition to acetone, and that the copper catalyst prepared with potassium hydroxide gives a smaller yield of the oily products than that prepared with sodium hydroxide under the same condition[1]. The present investigation was undertaken to confirm this unexpected behavior of the copper catalyst prepared with sodium hydroxide, and to study the effect of the precipitation temperature on the amounts of acetone and the oily products to find a preparation procedure of the most suitable copper catalyst for the production of acetone, precipitation being carried out at 5, 22, 55 and 90°C[4].

It was presumed in the preceding paper that the formation of isobutyl methyl ketone is due to the condensation of the isopropyl alcohol and acetone produced. In order to confirm this formation process, and to determine whether a large quantity of the oily products could be formed from a mixture of isopropyl alcohol and acetone, various mixtures of the alcohol and acetone were passed over the copper catalyst prepared with sodium hydroxide at 22°C.

Experimental

Purification of Isopropyl Alcohol and Acetone. —Isopropyl alcohol and acetone were purified as in the preceding paper. Isopropyl alcohol: b. p. 82~82.5°C, n_D^{25} 1.3753, d_4^{25} 0.7811. Acetone: b. p. 56.2~56.3°C, n_D^{25} 1.3564, d_4^{25} 0.7844.

TABLE I. PREPARATION OF PRECIPITATES

Catalyst	Temperature of precipitation °C	Time of drying hr.	Color
Cu VI	5	24	dark gray
Cu VII	22	20	dark gray
Cu VIII	55	20	black

TABLE II. PREPARATION OF PRECIPITATES

Catalyst	Precipitant and amount g.	Distilled water ml.	Time of drying hr.	Color
Cu IX	K_2CO_3, 25	500	10	green
Cu X	$KHCO_3$, 40	400	10	green
Cu XI	$Ba(OH)_2$, 57	1000	20	dark gray

TABLE III. PREPARATION OF PRECIPITATES

Catalyst	Precipitant and amount g.	Distilled water ml.	Time of drying hr.	Color
Cu XII	NaOH, 15	300	20	dark gray
Cu XIII	K_2CO_3, 25	500	10	green
Cu XIV	$KHCO_3$, 40	400	10	green

1) Part III. This Bulletin, **34**, 161 (1961).

* Presented at the Chugoku Shikoku Local Meeting of the Chemical Society of Japan, Kochi, November, 1959.

** Present address: Institute of Commodities, Faculty of Economics, Kagawa University, Takamatsu.

2) E. Audibert and A. Raineau, *Ind. Eng. Chem.*, **20**, 1105 (1928).

3) P. K. Frolich, M. R. Fenske and D. Quiggle, *J. Am. Chem. Soc.*, **51**, 61 (1929).

4) The case of 90°C was described in the preceding paper[1].

Preparation of Catalysts.—Cupric nitrate hexahydrate was prepared from electrolytic copper and nitric acid, and was purified by recrystallization. The catalysts were prepared as shown in Tables I, II and III. Precipitates for catalysts Cu VI~Cu VIII (Table I) were prepared as follows: A solution of 30 g. of cupric nitrate hexahydrate in 900 ml. of distilled water was heated or cooled to the temperature chosen for precipitation. A sodium hydroxide solution, prepared from 15 g. of sodium hydroxide and 300 ml. of distilled water, was brought to the same temperature and added rapidly to the copper nitrate solution with stirring. After the mixture was stirred at the same temperature for 30 min., the precipitate was washed well by decantation with distilled water at the same temperature, collected on a glass filter, dried in an electric oven at 105°C for the time given in the table, powdered in an agate mortar, and stored in a stoppered bottle. Precipitates for Cu IX~Cu XI (Table II) were prepared by the same method as for Cu VII except for the precipitants and the volume of distilled water to dissolve them. Precipitates for Cu XII~Cu XIV (Table III) were prepared by the following method: Thirty grams of cupric nitrate hexahydrate was dissolved in 600 ml. of distilled water, and 300 ml. of ethyl alcohol was then added. To the solution kept at 22°C a solution of the precipitant dissolved in distilled water as shown in Table III was added, and the precipitate was treated similarly.

Apparatus and Procedure.—The apparatus was exactly the same as that described in the preceding paper. A definite amount (10 g.) of the precipitate was placed in the reaction tube and reduced by passing hydrogen (750~900 ml./hr.) at a temperature below 185°C. The resulting catalyst was then heated to the operating temperature. Experiments were usually performed at 185, 220, 250, 305 and 325°C under the ordinary pressure, and isopropyl alcohol and the various mixtures of isopropyl alcohol and acetone were passed through the tube, respectively, at a constant rate of flow. The liquid product was collected by the method similar to that described in the preceding paper. The volume of the noncondensable gas evolved by the reaction was measured at intervals of 15~30 min., and the change in catalytic activity was denoted by the volume. All values given in the present research are averages of three to four measurements under a constant operating condition.

Analysis of the Products.—The reaction mixture was treated with water to remove the acetone and unchanged isopropyl alcohol. The content of acetone in the aqueous solution was determined by the hydroxylamine method. The oily products obtained in some of the experiments were dried with anhydrous sodium sulfate and fractionally distilled, and the constituents of the cuts were identified by boiling points, densities, refractive indices, 2,4-dinitrophenylhydrazones and semicarbazones. The oily products were found to consist mainly of isobutyl methyl ketone and diisobutyl ketone.

Results

Influences of the Temperature of Precipitation and That of Reaction on the Dehydrogenating Activity of Reduced Copper.—The influences of the temperature of precipitation and that of reaction on the activity of copper catalysts are shown in Table IV. The amounts of reaction products given in Tables IV~VII are reproducible within 1%. Experiments were carried out under controlled conditions in order to eliminate so far as possible effects[5] other than that of the temperature of precipitation or reaction. Table IV indicates that the dehydrogenating activity to give acetone and the condensing activity to give isobutyl methyl ketone and diisobutyl ketone depend on the temperatures of precipitation and of the reaction. As the catalytic activity for the dehydrogenation of isopropyl alcohol varied irregularly with the precipitation temperature, it is impossible to find any simple relation between them. The highest dehydrogenation activity is obtained with the catalyst (Cu VIII) precipitated at 55°C. On the other hand, the yield of the oily products is the highest with the catalyst (Cu VII) precipitated at 22°C. As the dehydrogenating activity of reduced copper varies with the precipitation temperature, it is necessary to fix the precipitation temperature to get the constant activity.

In Fig. 1, the yield of acetone with various specimens of reduced copper is plotted against the reaction temperature. The yield of acetone

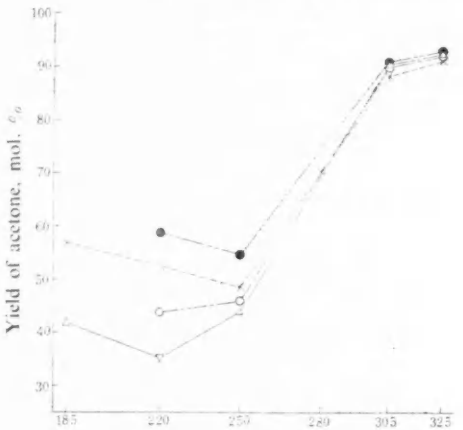

Fig. 1. The effect of temperature on the dehydrogenation of isopropyl alcohol with various copper catalysts.
○ Cu VI, △ Cu VII, ● Cu VIII, × Cu I (described in the preceding paper).

5) Those from the reducing condition of precipitates with hydrogen and the velocity of passing the substance over reduced copper.

Table IV. Influences of the temperature of precipitation and that of reaction on the dehydrogenating activity of copper catalysts

Catalyst	Temp. °C	Isopropyl alcohol g.	Velocity g./hr.	Acetone g.	Oily products g.	Gases collected l.	Percentage of conversion %
Cu VI	220	39.38	11.53	16.66	11.58	8.85	60.2
	250	39.28	13.46	17.42	12.31	9.42	64.3
	305	39.36	11.52	34.31	0	13.69	93.2
	325	39.31	11.79	35.12	0	14.08	96.0
Cu VII	185	38.96	11.69	15.72	5.47	7.35	50.5
	220	38.93	11.39	13.24	15.29	8.19	56.4
	250	38.83	11.65	16.48	13.40	9.11	62.9
	280	39.19	11.47	32.22	0.67	13.01	89.0
	305	39.02	11.15	34.21	0	13.78	94.7
	325	38.95	11.40	34.94	0	14.04	96.6
Cu VIII	220	38.70	12.55	21.98	4.14	9.79	67.8
	250	39.21	11.48	20.72	9.69	10.28	70.3
	305	38.72	12.56	34.14	0	13.60	94.2
	325	38.90	11.67	35.04	0	13.95	96.2

Table V. Influence of precipitants on the dehydrogenating activity of reduced copper

Catalyst	Temp. °C	Isopropyl alcohol g.	Velocity g./hr.	Acetone g.	Oily products g.	Gases collected l.	Percentage of conversion %
Cu IX	185	39.36	10.99	19.86	0	7.90	53.8
	220	39.24	11.48	27.67	0	10.99	75.1
	250	39.24	11.48	32.36	0	12.80	87.5
	280	39.32	11.51	34.24	0	13.55	92.4
	305	39.36	11.81	35.54	0	14.05	95.7
	325	39.34	11.80	36.00	0	14.11	96.2
Cu X	185	39.21	11.20	19.80	0	7.88	53.9
	220	39.26	11.49	27.43	0	10.85	74.1
	250	39.30	10.97	31.41	0	12.38	84.5
	305	39.24	11.21	35.17	0	13.77	94.1
	325	39.40	11.53	35.96	0	14.19	96.6
Cu XI	220	38.77	13.29	16.35	12.59	9.00	62.2
	250	38.68	11.16	15.72	13.58	8.90	61.7

increases rapidly with the rising reaction temperature, becoming almost quantitative at 325°C, but is reduced by the formation of considerable amounts of the oily products at lower temperatures.

Influence of Precipitants on the Dehydrogenating Activity of Reduced Copper. — Comparison of Tables IV and V shows that Cu IX and Cu X, obtained by using potassium carbonate and potassium bicarbonate respectively as precipitants, gave the highest yield of acetone at the highest temperature as far as the experiments were performed. These copper catalysts act only to dehydrogenate isopropyl alcohol to acetone at all temperatures, while the catalysts prepared with sodium hydroxide act similarly at the higher temperatures but act on isopropyl alcohol at the lower temperatures not only to dehydrogenate it to acetone but also to produce isobutyl methyl ketone and diisobutyl ketone. The catalyst prepared with barium hydroxide behaves at the lower temperatures similarly to those prepared with sodium hydroxide.

The precipitate prepared with potassium carbonate at 90°C was dark brown, and the catalyst prepared from it gave isobutyl methyl ketone and diisobutyl ketone together with acetone[1].

Use of Isopropyl Alcohol and Acetone as Starting Materials. — Investigation was made as to whether or not the amount of the oily products is changed by adding acetone to isopropyl alcohol in the charge. The results summarized in Table IV show that acetone mixed beforehand does not essentially participate in the production of isobutyl methyl ketone and diisobutyl ketone.

Influence of the Addition of Ethyl Alcohol to Copper Nitrate Solution. — Investigation was made as to whether or not the dehydrogenating activity of reduced copper could be

TABLE VI. THE EFFECT OF THE RATIOS OF ISOPROPYL ALCOHOL TO ACETONE ON THE YIELD OF OILY PRODUCTS

Acetone g.	Isopropyl alcohol g.	Temp. °C	Velocity g./hr.	Acetone in reaction product g.	Oily products g.	Gases collected l.	Percentage of conversion %
38.82	0	220	12.59	37.54	0	0.17	—
38.98	0	250	12.64	37.72	0	0.17	—
31.93	7.71	220	12.52	34.26	—	1.63	56.6
19.50	19.70	220	12.71	25.44	5.06	3.87	52.7
7.68	31.45	220	11.45	21.04	8.08	7.04	60.0
0	38.93	220	11.39	13.24	15.29	8.19	56.4
0	38.83	250	11.65	16.48	13.40	9.11	62.9

TABLE VII. INFLUENCE OF THE ADDITION OF ETHYL ALCOHOL TO COPPER NITRATE SOLUTION

Catalyst	Temp. °C	Isopropyl alcohol g.	Velocity g./hr.	Acetone g.	Oily products g.	Gases collected l.	Percentage of conversion %
Cu XII	220	39.07	10.90	13.91	15.10	8.38	57.5
	250	38.95	11.68	16.73	13.42	9.20	63.3
	305	39.06	11.72	34.89	0	13.83	94.9
	325	39.03	11.71	35.57	0	14.08	96.7
Cu XIII	220	39.30	10.97	25.92	0	10.21	69.6
	250	39.33	10.98	31.37	0	12.35	84.2
	305	39.33	11.80	35.76	0	13.96	95.1
	325	39.19	10.94	36.35	0	14.23	97.3
Cu XIV	220	38.97	12.64	16.28	0	6.56	45.1
	250	39.05	12.33	26.57	0	10.39	71.3
	305	39.08	11.44	33.70	0	13.35	91.6
	325	39.06	11.43	35.59	0	14.03	96.3

increased by the addition of ethyl alcohol in the preparation of the precipitate. The results are shown in Table VII. Comparison of Table VII with Table IV (Cu VII) and with Table V (Cu IX and Cu X) shows that the catalytic activity of reduced copper is not significantly affected by the addition of ethyl alcohol except that the catalyst (Cu XIV), prepared with potassium bicarbonate and used at the lower temperatures, is less active.

Catalysts. — Frolich et al.[3] reported that the gels precipitated at 85°C or higher temperatures consist essentially of copper oxide and only a small amount of copper hydroxide, and that lowering of the temperature of precipitation increases the amount of copper hydroxide. Further, it was found by Milligan[6] that the pure blue gel is hydrous cupric hydroxide and the black gel is hydrous cupric oxide. As shown in Table I, the precipitates obtained at various temperatures differ from each other in color. Thus the precipitates prepared at 5 and 22°C are blue, and these precipitates change gradually to dark gray in color. On the other hand, the precipitates prepared at 55 and 90°C are black. The precipitates resulting from lower precipitation temperatures are much more hydrated and bulky than those obtained at higher precipitation temperatures.

Orito and Kawachi[7] found that the activity of the mixed Cu-Cr basic carbonate catalyst for the liquid-phase hydrogenation of acetone is high when it is calcined previously at about 350°C and reduced before use in a stream of hydrogen. However, it seems that the copper prepared by direct reduction of basic copper carbonate possesses a higher dehydrogenation activity than that resulting from copper oxide.

Discussion

Cause of Condensation. — It was reported[8] that the copper catalyst, containing an alkaline oxide such as zinc oxide or magnesium oxide and composed of oxides having dehydrogenating and dehydrating properties, converts isopropyl

6) W. O. Milligan, *J. Phys. & Colloid Chem.*, **55**, 497 (1951).

7) Y. Orito and S. Kawachi, *J. Chem. Soc. Japan, Ind. Chem. Sec.* (*Kogyo Kagaku Zasshi*), **60**, 703 (1957).

8) V. N. Ipatieff and V. Haensel, *J. Org. Chem.*, **7**, 189 (1942); L. L. Gershbein, H. Pines and V. N. Ipatieff, *J. Am. Chem. Soc.*, **69**, 2888 (1947); F. W. Major and F. E. Salt, Brit. Pat. 656405 (1951); *Chem. Abstr.*, **46**, 8147 (1952); S. Kudo, *J. Chem. Soc. Japan, Ind. Chem. Sec.* (*Kogyo Kagaku Zasshi*), **58**, 785 (1955). T. Kanamori, ibid., **61**, 1576 (1958).

alcohol to isobutyl methyl ketone and diisobutyl ketone along with others. As described in the preceding paper, similar condensation products were obtained by employing copper catalysts prepared with alkali hydroxides as precipitants. Such a condensation has not yet been reported to occur with a copper catalyst alone.

The present author first assumed that this condensation was caused by traces of alkali in the catalyst, but the copper catalyst prepared with an excess of potassium bicarbonate did not cause this condensation. Takayasu[9] determined the amounts of the residual oxide in various specimens of reduced copper, and observed that hydrogen might be incapable of reducing copper oxide completely into metallic copper. Further, he showed that the precipitates prepared by adding aqueous sodium hydroxide to aqueous copper nitrate at 100°C and at 30°C consist of $5CuO \cdot H_2O$ and $3CuO \cdot H_2O$, respectively. Audibert and Raineau[2] found that the precipitate prepared by adding an alkali hydroxide to a boiling solution of copper nitrate consists of $4CuO \cdot H_2O$. Ipatieff and Haensel[8] reported that an infinitesimal amount of water is required to start the condensation reaction. Considered from these items of information in the literature, the formation of the higher ketones in the present research seems also to be attributed to the effect either of traces of water or of a lower oxide of copper in the catalysts.

9) M. Takayasu, *J. Chem. Soc. Japan (Nippon Kwagaku Kwaisi)*, **64**, 675 (1943), **65**, 46 (1944).

Summary

The present work is to determine whether the yields of acetone and of the oily products (isobutyl methyl ketone and diisobutyl ketone) to be obtained from isopropyl alcohol by the catalytic action of reduced copper are affected by the precipitation temperature in the preparation of the catalysts, and to find a catalyst efficient for the production of oily products. Isopropyl alcohol was changed to acetone in 91~95% yield with no side reaction, by being passed over various copper catalysts at 325°C. The maximum yield of the oily products was obtained with the catalyst prepared with sodium hydroxide as a precipitant and at 22°C as the precipitation temperature, and at the reaction temperature of 220°C, amounting to 39.28% based on isopropyl alcohol used.

The author wishes to express his hearty thanks to Professor Tamon Matsuura for his kind guidance throughout this work.

Department of Chemistry
Faculty of Science
Hiroshima University
Hiroshima

Dehydrogenation of Secondary Alcohols with Reduced Copper. V[1]*. Catalytic Dehydrogenation of sec-Butyl Alcohol**

By Kazuaki KAWAMOTO

(Received November 18, 1960)

The preparation of copper catalysts, and the production of acetone and oily products (isobutyl methyl ketone and diisobutyl ketone) from isopropyl alcohol were described in detail in the previous papers[1,2], and it has been found that two distinct types of copper catalysts are obtained according to the precipitants. One type catalyses the decomposition of isopropyl alcohol to acetone and hydrogen. The other type catalyses the conversion of isopropyl alcohol into isobutyl methyl ketone and diisobutyl ketone together with acetone and hydrogen. That is to say, the copper catalysts prepared by reducing precipitates obtained by adding a solution of potassium bicarbonate or potassium carbonate to a solution of copper nitrate at 22°C gave the highest yield of acetone when used at the highest reaction temperature (325°C). On the other hand, the copper catalyst prepared by the reduction of the precipitate obtained from sodium hydroxide and copper nitrate at 22°C showed the greatest activity for the condensation of isopropyl alcohol. The

1) K. Kawamoto, This Bulletin, **34**, 795 (1961).

* The major part of this research was presented at the 13th Annual Meeting of the Chemical Society of Japan, Tokyo, April, 1960.

2) K. Kawamoto, This Bulletin, **34**, 161 (1961).

TABLE I. INFLUENCE OF PRECIPITANTS AND THE REACTION TEMPERATURE ON THE DEHYDROGENATION OF *sec*-BUTYL ALCOHOL

Expt. No.	Precipitant	Temp. C	*sec*-Butyl alcohol g.	Velocity g/hr.	Reaction product					Ketone in aq. soln. g.	Gas collected l.	Yield of ketone* mol. %	Percentage of conversion** %
					Yield g.	n_D^{25}	d_4^{25}	Ketone g.	Unchanged alcohol, g.				
1	NaOH	185	40.03	9.61	38.58	1.3862	0.8077	19.99	16.29	0.37	6.60	52.3	54.5
2	K_2CO_3	185	40.22	10.49	39.24	1.3840	0.8061	23.77	13.60	0.58	7.86	62.2	64.6
3	NaOH	220	40.08	10.02	38.76	1.3862	0.8105	26.15	7.67	0.52	8.61	68.4	71.0
4	K_2CO_3	220	40.03	11.72	38.59	1.3807	0.8057	28.90	8.22	0.82	9.45	76.3	78.1
5	NaOH	250	39.99	10.00	38.58	1.3802	0.8100	31.49	4.38	0.83	10.32	83.1	85.3
6	K_2CO_3	250	39.45	10.76	38.86	1.3793	0.8073	32.13	5.21	0.92	10.58	86.1	88.7
7	NaOH	280	40.07	10.23	38.41	1.3781	0.8077	33.40	3.44	0.91	10.95	88.0	90.3
8	K_2CO_3	280	40.22	10.06	38.38	1.3775	0.8060	34.68	2.70	0.98	11.33	91.2	93.2
9	NaOH	305	40.03	11.44	38.20	1.3777	0.8076	34.82	1.60	1.06	11.41	92.1	94.2
10	K_2CO_3	305	40.26	11.24	38.29	1.3774	0.8044	36.13	0.94	1.03	11.77	94.9	96.7
11	NaOH	325	40.06	10.23	38.40	1.3775	0.8081	35.42	1.43	1.10	11.63	93.7	96.0
12	K_2CO_3	325	40.22	10.63	38.46	1.3779	0.8081	36.20	0.55	1.17	11.86	95.5	97.5

* This value was an average of three determinations under the constant operating condition, but the fluctuation in the yield of ethyl methyl ketone obtained by the repeated experiments was less than 1%.

** The percentage of the volume of the gaseous product to the theoretical calculated on the assumption that original *sec*-butyl alcohol were transformed completely either into the ketone and hydrogen or into butylenes and water.

TABLE II. THE PROPERTIES OF DISTILLED FRACTIONS OF EXPERIMENT No. 3

Fraction	B. p. C	Yield %	n_D^{25}	d_4^{25}	Ketone %	Unchanged alcohol %
1	72.5~80	40.31	1.3788	0.8221	81.14	8.52
2	80~85	19.58	1.3799	0.8050	77.99	19.71
3	85~90	14.14	1.3818	0.7990	66.82	32.16
4	90~100	10.11	1.3897	0.8007	25.77	73.01
5	100~155	1.51	1.4016	0.8060	—	—
6	155~158	12.53	1.4129	0.8162	—	—
7	residue	0.34	1.4194	—	—	—

TABLE III. THE PROPERTIES OF DISTILLED FRACTIONS OF EXPERIMENT No. 4

Fraction	B. p. C	Yield %	n_D^{25}	d_4^{25}	Ketone %	Unchanged alcohol %
1	71.5~80	36.45	1.3782	0.8170	86.84	6.09
2	80~85	41.15	1.3782	0.8016	83.45	16.09
3	85~90	7.29	1.3814	0.7999	69.12	30.78
4	90~98	11.45	1.3907	0.8022	19.32	79.12
5	residue	1.68	1.4032	—	—	—

Table IV. The properties of distilled fractions of Experiment No. 11

Fraction	B. p. °C	Yield %	n_D^{25}	d_4^{25}	Ketone %	Unchanged alcohol %
1	71.5~80	66.84	1.3770	0.8136	93.07	1.48
2	80 ~81	29.36	1.3770	0.8006	94.71	4.50
3	residue	1.17	1.3852	—	—	—

Table V. The properties of distilled fractions of Experiment No. 12

Fraction	B. p. °C	Yield %	n_D^{25}	d_4^{25}	Ketone %	Unchanged alcohol %
1	71.5~80	67.00	1.3772	0.8100	94.12	0.66
2	80 ~80.8	28.50	1.3772	0.8000	96.32	3.06
3	residue	1.24	1.4085	—	—	—

highest yield of the condensation products was obtained with the catalyst at the reaction temperature of 220°C.

The present paper describes the results of similar experiments with *sec*-butyl alcohol and the two types of catalysts. In the present research, one type was prepared with potassium carbonate, and the other type with sodium hydroxide. The vapor phase dehydrogenation of *sec*-butyl alcohol was carried out with these two types of catalysts at several temperatures between 185 and 325°C.

Up to the present, there have been a large number of patents and a few reports about the vapor phase dehydrogenation of *sec*-butyl alcohol to ethyl methyl ketone, and the majority deal with the use of copper mixed with other metals. Dunbar and Arnold[3] found that in the presence of a copper-chromium-oxide catalyst, the dehydrogenation of *sec*-butyl alcohol at 300~325°C furnishes 68% of ethyl methyl ketone.

Experimental

Purification of *sec*-Butyl Alcohol.—Commercial extra pure *sec*-butyl alcohol was purified by being dried with quick lime, followed by fractional distillation. B. p. 98.7~99.2°C, n_D^{25} 1.3950, d_4^{25} 0.8029.

Preparation of Catalysts.—The two specimens of copper catalysts used in the present research are identical with Cu VII and Cu IX which were described in the preceding paper[1].

Apparatus and Procedure.—The apparatus for the dehydrogenation was exactly the same as that previously described[2]. The precipitate (10 g.) to be reduced was placed in the reaction tube. After the tube was filled with hydrogen, the furnace was heated to the reduction temperature below 185°C. Hydrogen was passed through the tube at the rate of 750~900 ml. per hour, and *sec*-butyl alcohol was passed under the ordinary pressure over the catalyst heated to 185, 220, 250, 280, 305 and 325°C, respectively. The vapor coming out from the reaction tube was condensed by passing it through a condenser cooled with ice water and the gas escaping from the condenser was scrubbed with ice-cooled distilled water (50 ml.) to remove the ethyl methyl ketone and the unchanged alcohol from the hydrogen stream. The volume of the non-condensable gas was measured at intervals of 15~30 min. At the end of a run, the weight of liquid products and of that absorbed by the distilled water were measured.

Analysis of the Products.—The relative content of ethyl methyl ketone and unchanged *sec*-butyl alcohol in the liquid product was determined by the hydroxylamine method[4] and the acetic anhydride-pyridine method[5], respectively. The product in the aqueous solution was recognized to be ethyl methyl ketone by the preparation of its 2,4-dinitrophenylhydrazone (m. p. 118°C) and semicarbazone (m. p. 144°C), and further its content was determined by the hydroxylamine method. The reliability of these analytical methods was checked by titrating the known samples of ethyl methyl ketone and *sec*-butyl alcohol, respectively. The result was found to be correct within experimental errors. The liquid product was dried with anhydrous sodium sulfate in every case, and then fractionally distilled through an electrically heated Widmer column. As examples, the properties of distilled fractions of Experiments No. 3, 4, 11 and 12 in Table I are shown in Tables II, III, IV and V.

Fractions 1, 2 and 3 in Table II correspond in physical constants to ethyl methyl ketone. The 2,4-dinitrophenylhydrazone and semicarbazone melted at 118 and 144°C, respectively, both alone and in admixture with the corresponding derivatives of authentic ethyl methyl ketone. From Fraction 4 a phenylurethan was obtained, which was identified as that of *sec*-butyl alcohol by mixing with an authentic specimen. Fraction 6 gave a crystalline

3) R. E. Dunbar and M. R. Arnold, *J. Org. Chem.*, **10**, 501 (1945).

4) M. Katsuno, *J. Soc. Chem. Ind., Japan* (*Kōgyō Kagaku Zassi*), **46**, 112 (1943).

5) C. L. Ogg, W. L. Porter and C. O. Willits, *Ind. Eng. Chem. Anal. Ed.*, **17**, 394 (1945).

semicarbazone melting at 95~96°C which was identified with the semicarbazone of 5-methyl-3-heptanone[6]. Judging from the physical constants of this fraction, the semicarbazone and the formation of isobutyl methyl ketone from isopropyl alcohol as described previously, it seems that Fraction 6 (b. p. 155~158°C) consists mainly of 5-methyl-3-heptanone. The formation of unsaturated and hydroxy ketones such as 5-methyl-4-hepten-3-one and 5-methyl-5-hydroxy-3-heptanone was not detected in the reaction product. As shown in Table III, no fraction corresponding in the boiling point to 5-methyl-3-heptanone was found in the reaction product obtained by employing the copper catalyst prepared with potassium carbonate.

Results and Discussion

The results are summarized in Table I. In the range of 185 to 325°C *sec*-butyl alcohol does not decompose in the absence of catalysts. Consequently the changes observed in the present research do not involve the simple pyrolysis of *sec*-butyl alcohol. The yield of ethyl methyl ketone and the percentage of conversion recorded in Table I do not necessarily represent the maximum values. The difference between the yield of ethyl methyl ketone and the percentage of conversion was a few per cent. Therefore, the dehydration of *sec*-butyl alcohol to butylenes seems to occur little at temperatures below 325°C, and the yield of total ethyl methyl ketone agrees closely with the value calculated from the amount of the escaping gas in each experiment.

Influence of the Reaction Temperature on the Dehydrogenating Activity of Reduced Copper. — In Fig. 1 the yield of ethyl methyl ketone is plotted against the reaction temperature. As seen from Tables I—V and Fig. 1, the rates of the dehydrogenation of *sec*-butyl alcohol to ethyl methyl ketone and that of the conversion of *sec*-butyl alcohol to 5-methyl-3-heptanone depend upon the reaction temperature. The reaction products obtained at the higher temperatures contained more ethyl methyl ketone than those obtained at the lower temperatures, and the conversion of *sec*-butyl alcohol to ethyl methyl ketone was very high at the highest reaction temperature (325°C) so that unchanged *sec*-butyl alcohol was scarcely found in the reaction products. The higher ketone was not obtained at all or only a little was obtained except in Experiment No. 3, where 5-methyl-3-heptanone was produced along with ethyl methyl ketone.

6) 5-Methyl-3-heptanone was prepared according to Powell and Secoy's method: Ethyl methyl ketone was first condensed in the presence of powdered barium oxide, and the 5-methyl-4-hepten-3-one thus formed was reduced selectively over platinum catalyst to give 5-methyl-3-heptanone, and its semicarbazone melted at 95~96°C. S. G. Powell and C. H. Secoy, *J. Am. Chem. Soc.*, **53**, 765 (1931).

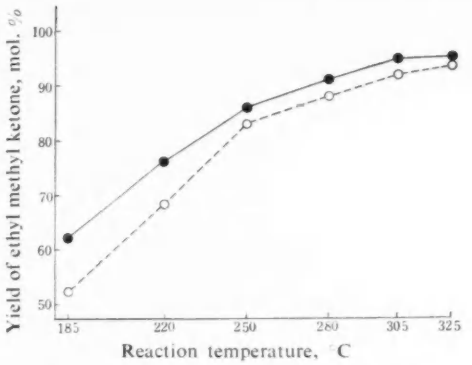

Fig. 1. The effect of temperature on the dehydrogenation of *sec*-butyl alcohol with two types of copper catalysts.
●: Catalyst prepared with potassium carbonate.
○: Catalyst prepared with sodium hydroxide.

The volume of the evolved gas, mainly consisting of hydrogen, is plotted against the reaction time in Figs. 2 and 3, which show that the activity of the catalysts holds over the period of the operation. Further, a parallelism exists between the amount of gas evolved and the temperature.

Two Types of Reduced Copper. — As in the case of isopropyl alcohol, the copper catalyst prepared with potassium carbonate promotes dehydrogenation alone, but that prepared with sodium hydroxide catalyses not only dehydrogenation but also condensation reactions.

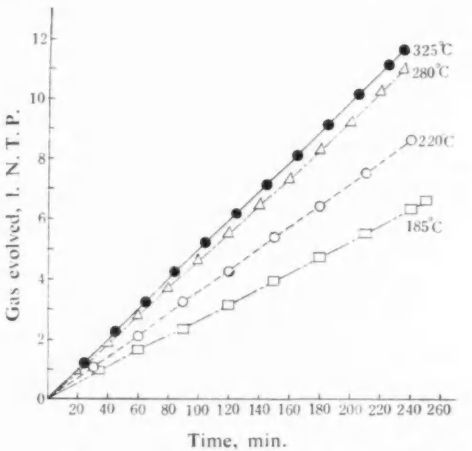

Fig. 2. Relation between volume of gas evolved and time of reaction at various temperatures (Precipitant in the preparation of catalyst; NaOH).

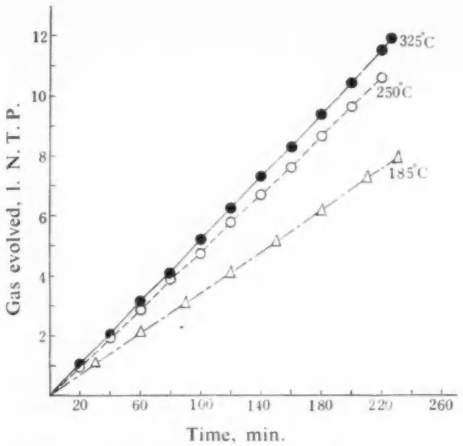

Fig. 3. Relation between volume of gas evolved and time of reaction at various temperatures (Precipitant in the preparation of catalyst; K_2CO_3).

The Activity of Dehydrogenating Various Secondary Alcohols to the Corresponding Ketones. — The copper catalyst prepared by reduction of the precipitate obtained by adding an excess of a dilute sodium hydroxide solution to an aqueous solution of cupric nitrate changed isoborneol[7] to camphor (yield 96%) at 220°C, *l*-menthol[7] to menthones (*d*-isomenthone and *l*-menthone) (yield 74%) and a small amount of thymol under similar conditions, and cyclohexanol[8] to cyclohexanone (yield 63%) and a trace of phenol. In the case of isopropyl alcohol[1], the yield of acetone amounted to about 93% at 325°C, while at 220°C the yield of acetone decreased to 35% with the formation of the condensation products, isobutyl methyl ketone and diisobutyl ketone. *sec*-Butyl alcohol behaved similarly, giving a condensation product (5-methyl-3-heptanone) along with ethyl methyl ketone at 220°C but the latter alone did so at higher temperatures with greater ease than isopropyl alcohol.

Thus the copper catalyst is suitable for dehydrogenating secondary alcohols to the corresponding ketones, but the dehydrogenating and the condensing abilities of the copper catalyst vary with the species of alcohols, and it seemed that the alcohols which possess a methyl group adjacent to the hydroxylated carbon atom give rise to the condensation reaction.

7) T. Matsuura and K. Kawamoto, *J. Chem. Soc. Japan, Pure Chem. Sec.* (*Nippon Kagaku Zasshi*), **80**, 94 (1959).
8) K. Kawamoto, ibid., **80**, 681 (1959).

5-Methyl-3-heptanone. — Up to the present, 5-methyl-3-heptanone has been prepared by the following methods: (1)[6,9] *sec*-Butyl alcohol is first dehydrogenated to ethyl methyl ketone, and the latter is condensed in the presence of alkali or calcium carbide to give 5-methyl-4-hepten-3-one and then the unsaturated ketone thus formed is hydrogenated to 5-methyl-3-heptanone. (2)[10] It is prepared by treating *sec*-butyl alcohol with ethyl methyl ketone in the vapor phase under pressure in the presence of a mixed catalyst with dehydrogenating and dehydrating properties. A new synthetic process for 5-methyl-3-heptanone, consisting in passing *sec*-butyl alcohol over reduced copper under the atmospheric pressure at 220°C, is now proposed.

Summary

It was confirmed that ethyl methyl ketone and 5-methyl-3-heptanone are produced from *sec*-butyl alcohol with reduced copper alone. Two distinct types of reduced copper were prepared by precipitation with sodium hydroxide and with potassium carbonate. They differ somewhat in their ability to promote dehydrogenation of *sec*-butyl alcohol and differ greatly in their power to bring about condensation. The copper catalyst prepared with potassium carbonate acts to dehydrogenate *sec*-butyl alcohol at all the temperatures examined (185 ~325°C), giving ethyl methyl ketone, but the catalyst prepared with sodium hydroxide acts to dehydrogenate and to condense simultaneously at a certain temperature (220°C), giving 5-methyl-3-heptanone along with ethyl methyl ketone, and this affords a new synthetic method for 5-methyl-3-heptanone. *sec*-Butyl alcohol was converted into ethyl methyl ketone in 94~96% yield with no side reaction by passing it over these catalysts at 325°C.

The author wishes to express his hearty thanks to Professor Tamon Matsuura of Hiroshima University for his kind guidance and valuable suggestions throughout this work, and also to Mr. T. Hiraki for his able assistance of this work.

Institute of Commodities
Faculty of Economics
Kagawa University, Takamatsu

9) V. I. Esafov, V. M. Gulyakov, V. V. Kargopol'tseva, A. P. Kulakova, G. V. Razmyslov and N. D. Toporov, *Chem. Abstr.*, **35**, 3958 (1941); C. Weizmann, Brit. Pat. 573724 (1945); *Chem. Abstr.*, **43**, 4287 (1949); R. Ya. Levina and N. P. Shusherina, ibid., **44**, 9336 (1950); A. N. Pudovik, R. D. Sabirova and T. A. Tener, ibid., **49**, 8790 (1955).
10) J. W. Mecorney and Geo. W. Gaertner, Jr., U. S. Pat. 2725400 (1955); *Chem. Abstr.*, **50**, 10762 (1956); N. V. de Bataafsche Petroleum Maatschappij, Dutch Pat. 83028 (1956); *Chem. Abstr.*, **52**, 2890 (1958).

Differential Thermal Analysis of Aluminum Soaps

By Sukekuni SHIBA

(Received November 19, 1960)

It has been known that the metal soaps show complex thermal behaviors due to their polymorphism when they are heated. Lawrence[1] pointed out the temperature at which the soaps become plastic, before they reach the melting points, and the soaps show swelling and gellation in hydrocarbon media. The application of the differential thermal analysis, which has been used in metallography and in the study of clay minerals, to these phenomena, was attempted first by Vold[2], and the phase state of the metal soaps and soap-hydrocarbon systems were investigated successfully. Later, many authors reported the differential thermal analysis of metal soaps and the experimental apparatus applicable to such substances[3-5].

The thermal behaviors of aluminum soaps have not yet been fully clarified, and conflicting data were reported due to their relatively low heat of transition and the difficulty of obtaining pure soaps[6]. It is generally believed from various experiments, that the aluminum soaps, prepared by the usual metathetic process from aqueous solution of alkali soaps and aluminum salt, consist mainly of aluminum hydroxydisoaps, $Al(OH)A_2$, and they are the only definite compounds as aluminum soaps[7-9]. Recently, it was found that the aluminum trisoaps can be obtaind through interaction of aluminum trialkoxide or trialkyl aluminum with fatty acids in anhydrous organic media, and they are decomposed to disoaps in the presence of water[10-12].

The present investigation was carried out to examine the thermal behaviors of aluminum soaps by differential thermal analysis, and to obtain some information on the structure of aluminum soaps from thermal data.

Experimental

Preparation of Soaps. — The aluminum soaps used in this work were prepared from purified fatty acids by an aqueous metathetic process. The fatty acids which were solid at room temperatures (stearic-lauric) were purified by repeated recrystallization from 80 vol. % ethanol. Capric and caprylic acids were purified by distillation under reduced pressure. The purity of the acids was examined by melting points and neutralization equivalent through titration, as is shown in Table I.

TABLE I. PHYSICAL CONSTANTS OF FATTY ACIDS

Fatty acid	M. p., °C		Neut. equiv.	
	Found	Lit.[13]	Found	Calcd.
Stearic	69.5	69.6	282	284.5
Palmitic	62.2	62.9	258	256.4
Myristic	54.5	54.4	229	228.4
Lauric	43.3	44.0	201	200.3
Capric	30.1	31.3	173	172.3
Caprylic	14.3	16.3	144	144.2

Fatty acid was treated with an excess of sodium hydroxide solution and distilled water to yield an approximately 5% solution of sodium soap. The mixture was heated to dissolve the soap and the solution was kept completely transparent at 70~80°C for soaps from stearate to laurate, at 50°C for caprate and caprylate. A hot solution of aluminum sulfate was added slowly while being stirred vigorously, until a slight excess was present and the precipitation was complete. The precipitated aluminum soap was filtered off and washed with distilled water, until the filtrate was free from sulfate when tested with barium chloride solution under slightly acidic medium. The soap was then dried to constant weight at 110°C, and stored in a desiccator over phosphorus pentoxide. Dried soaps were analyzed for aluminum by ignition to oxide.

The reaction between sodium soap and aluminum salt solution in the presence of excess of sodium hydroxide is expressed generally by,

$$2n\mathrm{NaA} + \mathrm{Al_2(SO_4)_3} + 2(3-n)\mathrm{NaOH} \rightarrow 2\mathrm{Al(OH)_{3-n}A_n} + 3\mathrm{Na_2SO_4} \quad (1)$$

$$n = 0 \sim 3 \quad (2)$$

1) A. S. C. Lawrence, *Trans. Faraday Soc.*, **34**, 660 (1938).
2) R. D. Vold, *J. Phys. Chem.*, **49**, 315 (1945).
3) C. J. Penter, S. T. Abrams and F. H. Stross, *Anal. Chem.*, **23**, 1459 (1951).
4) D. Evans, J. F. Hutton and J. B. Matthews, *J. Applied Chem.*, **2**, 252 (1952).
5) D. B. Cox and J. F. McGlynn, *Anal. Chem.*, **29**, 960 (1957).
6) G. S. Hattiangdi, M. J. Vold and R. D. Vold, *Ind. Eng. Chem.*, **41**, 2320 (1949).
7) V. R. Gray and A. E. Alexander, *J. Phys. Colloid Chem.*, **53**, 23 (1949).
8) W. W. Harple, S. E. Wiberley and W. H. Bauer, *Anal. Chem.*, **24**, 635 (1952).
9) W. H. Bauer, J. Fisher, F. A. Scott and S. E. Wiberley, *J. Phys. Chem.*, **59**, 30 (1955).
10) J. Glazer, T. S. McRoberts and J. H. Schulman, *J. Chem. Soc.*, **1950**, 2082.
11) A. Gilmour, A. A. Jobling and S. M. Nelson, ibid., **1956**, 1972.
12) A. E. Leger, R. L. Haines, C. E. Hubley, J. C. Hyde and H. Sheffer, *Can. J. Chem.*, **35**, 799 (1957).
13) A. W. Ralston, "Fatty Acids and their Derivatives", John Wiley and Sons Inc., New York (1948), p. 23.

where, A is the acid radical, and it is assumed that the soaps containing continuously 0~3 mol. of fatty acids per 1 mol. of aluminum are obtainable. It is possible by this relation to control the composition of the aluminum soap changing the excess of the sodium hydroxide in the aqueous medium. The composition of the soaps is shown in Table II.

TABLE II. COMPOSITION OF ALUMINUM SOAPS

Al soap	No. of C atoms in acid	Excess of NaOH %	Al wt.% analyzed	Mol. acid per mol. Al
Stearate-3.22	18	−25	2.91	3.22
〃-2.29	〃	0	3.92	2.29
〃-2.12	〃	10	4.25	2.12
〃-1.89	〃	25	4.68	1.89
〃-1.71	〃	40	5.10	1.71
〃-0.95	〃	100	8.23	0.95
Palmitate	16	45	5.80	1.62
Myristate	14	〃	5.96	1.77
Laurate	12	〃	6.38	1.87
Caprate	10	〃	7.36	1.87
Caprylate	8	〃	9.17	1.72

Apparatus. — An apparatus adequate to analyze the soaps or soap-oil systems, which are liable to be oxidized below their melting points, was constructed. The apparatus is able to control and record the temperatures automatically, in the temperature range up to 300°C, with a small amount of sample.

The apparatus consists of four basic parts; the sample and reference cells, electric furnace, temperature control mechanism, and recorder. The sample cells used are similar to those of Vold[14]. They are made of 18-8 stainless steel, machined to a wall thickness less than 0.4 mm., and have a sample capacity of 2 cc. The cells are closed by screw caps; a protection tube for the thermocouple is fitted in the center of the cap. The furnace is heated by a two-element heater, and the cells are set through a teflon collar and sleeve in a hole of a copper block which is placed in the center of the furnace.

The temperature of the block is detected by a chromel-alumel thermocouple, and is regulated by a potentiometer type controller. The controller detects the difference in the electromotive force of the couple and the settled potential which varies linearly with time, and regulates the temperature. The rate of heating or cooling is adjusted by changing the gear ratio of the controller. For the detection of the differential temperature of the sample and the reference cells, a chromel-alumel thermocouple was used, because of its sensitivity, stability, and linearity of the emf against temperature. The thermoelements were insulated with glass fiber tubing and impregnated with silicone varnish. The potential difference obtained from two cells is amplified by a chopper type DC amplifier, and recorded on a strip chart multipoint electronic recorder with the temperature of the reference cell. By a proper selection of the rang of amplifier and recorder, it is possible to record the temperature difference of ±0.3~±25°C on the full scale of the recorder.

Analysis of Thermogram. — The thermogram is analyzed for temperature and latent heat of transition. When the thermal transition does not occur, the temperature difference between the sample and the reference cells, y, is expressed by a curve which approaches y_∞ at time infinity; i. e.,

$$y = y_\infty + (y_0 - y_\infty)\exp(-a(t - t_0)) \tag{3}$$

$$y_\infty = (C_s/\alpha_s - C_r/\alpha_r)\frac{dT_r}{dt} \tag{4}$$

$$a = \alpha_s/C_s \tag{5}$$

where, T is the temperature; C, the heat capacity, α, a constant including the coefficient of the overall heat transfer to the cell and dimensions of the thermal path as a whole: the subscripts s and r mean that the quantities refer to sample cell and to the reference cell. The interaction of the two cells are neglected. The temperature difference between the center (T_c) and wall (T_f) of the cell is expressed approximately by,

$$T_f - T_s = \frac{C_s}{\alpha_s} \cdot \frac{dT_s}{dt} \tag{6}$$

The actual temperature, at which the sample near the wall of the cell begins to undergo transition, is determined by the breaking point of the thermogram corrected by this relation.

When a transition of the sample is observed, enthalpy change of the sample cell, ΔH, is expressed as follows;

$$\Delta H = \alpha_s \int_{t_1}^{t_2} (y - y')\, dt = \alpha_s A \tag{7}$$

where t_1 and t_2 are the optional time before and after the transition, y' is the temperature difference when the transition does not occur, and A is the area of the peak of the thermogram.

The apparatus was calibrated with stearic acid (m.p. 69.3°C, heat of melting, 47.6 cal./g.) and benzoic acid (m. p. 122°C, heat of melting, 33.9 cal./g.). It was shown that the determination of the transition temperature could be made accurately by adopting the temperature at the apex of the peak in the thermogram, after being corrected to the temperature difference between the sample and reference cells. A conversion factor, 0.370 cal. per unit area of the peak (in deg. min.), was obtained from both acids, when 0.5~1.0 g. of the sample was used.

Procedure.—The soap was weighed in the sample cell, and alumina or Nujol as a reference material was also filled in the reference cell. The cells were placed in the furnace, and heating and cooling at a constant rate were repeated. Experimental conditions were;

Temperature,	up to 300°C
Rate of heating,	0.5~1.2 deg./min.
Weight of the specimen,	0.5~1.0 g.

14) M. J. Vold, *Anal. Chem.*, **21**, 683 (1949).

15) S. Shiba, *Railway Technical Research Report*, No. 162 (1960).

Details of the apparatus, analysis, and procedure were described in the previous paper[15].

Results and Discussion

Thermogram of Aluminum Stearate. — For most of the aluminum soaps, transition points are observed between room temperature and their melting points. Typical examples of the heating and cooling thermograms of an aluminum stearate are shown in Figs. 1 and 2.

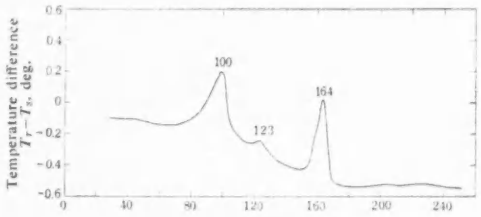

Fig. 1. Heating thermogram of aluminum stearate. (Ste−1.71).

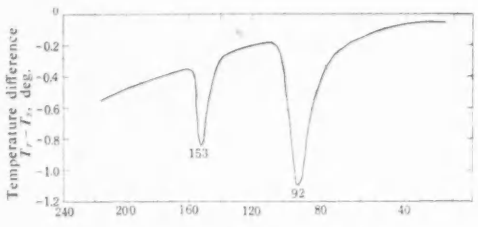

Fig. 2. Cooling thermogram of aluminum stearate. (Ste−1.71).

Three distinct peaks of transition are found in the heating thermogram, and two peaks are found in the cooling thermogram. Numbers in the thermograms show the temperature of the sample cell at the apex of the peaks. The cooling thermograms show a lower transition temperature and less repeatability due to the super-cooling of the soaps.

When heating and cooling are repeated for one specimen, the thermal behaviors are repeatable in general. However, the initial heating sometimes gives a little different thermogram from that obtained by the following runs; e. g., two indistinct peaks are observed in the initial run instead of one peak near 100°C in the following runs. These facts were reported by Vold[16], and they may be ascribed partly to the condition of the specimen packed in the cell before it is melted. In fact, the aluminum soap powders, when once melted, give a transparent glue-like mass, and show different bulk physical properties. No appreciable chemical changes of the specimen during the thermal analysis, oxidation, dehydration etc., were ascertained by the infrared absorptions before and after the analysis. In this report, discussions are held on the definite transitions which are obtained repeatably, and the small peaks which are obscure as found occasionally near 82°C are neglected.

Aluminum Stearates of Different Compositions. —The transition temperatures and heats of transition of aluminum stearates are summarized

TABLE III. TRANSITION TEMPERATURES AND HEATS OF TRANSITION OF ALUMINUM STEARATES

Sample	Heating		Cooling	
	Tr. temp. °C	Heat of tr. cal./g.	Tr. temp. °C	Heat of tr. cal./g.
Ste-3.22	69	16.0	58	14.2
	104	7.0	79	7.0
Ste-2.29	65	8.0	59	2.4
	104	8.1	87	6.8
Ste-2.12	66	3.0	85	7.4
	99	5.8	134	0.9
	150	0.9		
Ste-1.89	101	7.8	88	9.2
	157	3.2	137	2.1
Ste-1.71	99	5.8	89	10.6
	119	0.4	144	2.5
	162	2.1		
Ste-0.95	97	2.8	95	7.8
	124	0.8	145	1.1
	162	1.3		

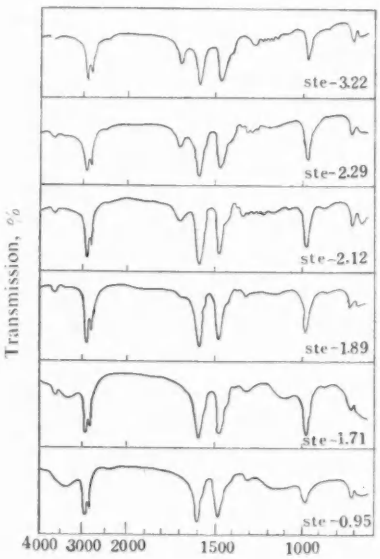

Fig. 3. Infrared spectra of aluminum stearates.

16) M. J. Vold, G. S. Hattiangdi and R. D. Vold, *Ind. Eng. Chem.*, **41**, 2539 (1949).

in Table III. Infrared absorption spectra of the same soaps, obtained by the potassium bromide disk method using a double beam spectrometer (Perkin-Elmer IR-21), are also shown in Fig. 3.

The thermograms of these soaps are somewhat different from those of examples shown in Figs. 1 and 2. The soaps containing more than 2 mol. of fatty acid per mole of aluminum, exhibit transitions near 70°C which are not found in Fig. 1. This transition point corresponds to the melting point of stearic acid. The heat of transition of this peak increases with an excess of the fatty acid over 2 mol. per aluminum. The infrared absorption at 1720 cm^{-1}, which is due to the presence of the carbonyl group, shows the same tendency. These facts confirm the fact that these soaps contain free fatty acids, and that the peaks are due to the melting of the acids. The results also indicate that the preparation of aluminum trisoaps by metathetic processes is impossible. Even though trisoaps exist, they will be decomposed to hydroxydisoaps and fatty acids by the effect of water. The soaps containing more than 2 mol. of fatty acids per aluminum, show weak transition peaks or lack of them at higher temperatures. This is attributed to the co-existence of fatty acids which melt at lower temperatures. When the fatty acids in the soap are extracted off by heptane, the transition at 160°C is found for the residual soap.

The soaps containing less than 2 mol. of acid per aluminum show no additional peaks, and they show less heat of transition, probably due to the presence of aluminum hydroxide in the soap. Infrared absorptions at 3720 cm^{-1} which are assigned to free OH stretching, are found for most of the soaps; while in the soap Ste-0.95, a broad absorption is found near 3400 cm^{-1} corresponding to bonded OH, and both absorptions are found for Ste-1.71. The infrared data retain the possibility of the existence of dihydroxymonosoaps as a discrete compound; however, the thermal data offer no positive evidence for the existence of the monosoaps.

The heat of transition obtained, show rather disjoined results, presumably because of the difference in heat transfer between specimen and cell, and in the specimen. Total heat of transition per mole of Ste-1.89 is about 6.4 kcal./mol., considerably less than that of alkali soaps (e. g., NaSte, 14.6 kcal./mol.).

Aluminum Soaps from Various Fatty Acids.—Transition temperatures and heats of transition of various aluminum soaps are summarized in Table IV. The structure and composition of these soaps are essentially the same,

Table IV. Transition temperatures and heats of transition of aluminum soaps from various fatty acids

Sample	Heating		Cooling	
	Tr. temp. °C	Heat of tr. cal./g.	Tr. temp. °C	Heat of tr. cal./g.
Palmitate	90	4.0	80	4.5
	128	1.0	152	2.0
	170	2.1		
Myristate	92	3.0	84	2.1
	136	1.4	156	2.7
	179	2.5		
Laurate	86	1.4	78	1.2
	149	1.2	152	3.0
	185	3.2		
Caprate	196	4.8	160	4.2
Capylate	216	6.4	176	4.1

and no free fatty acids are incorporated in the soaps, as are ascertained by the infrared spectra.

The thermograms of palmitate, myristate, and laurate show three distinct transition points similar to stearate; whereas, caprate and caprylate show only one transition point corresponding to the highest one of the soaps from higher fatty acids. The transition heat of the lowest transition decreases with the decrease in number of carbon atoms in the fatty acid, and disappears for caprate and caprylate. On the other hand, the heat of the highest transition increases with the decrease in number of carbon atoms, resulting in a similar total heat of transition per gram. The lack of these characteristic transitions of the aluminum soaps in the lower soaps, is consistent with the change of may other properties of the soaps with the change in the length of the constituent fatty acids; e. g., the thickening and gelling

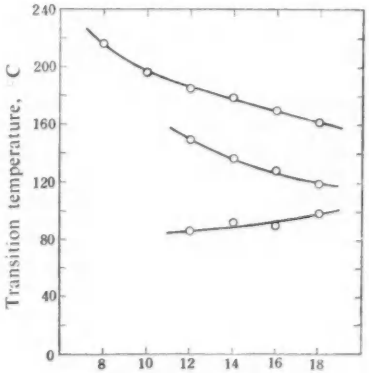

Fig. 4. Transition temperatures of aluminum soaps.

properties of aluminum soaps in organic media[17], etc.

Changes in corresponding transition temperatures with the carbon number of the fatty acids are shown in Fig. 4. Each transition temperature changes regularly, and it seems that the temperatures approach constant values as the chain length increases.

Assignment of Transition Points. — It is an inherent characteristic of the differential thermal analysis that it enables some thermal change in the specimen to be caught, but gives no information on the nature of the transition. Some other data are necessary for this purpose.

The additional peaks which are obtained for the soaps containing more than 2 mol. of fatty acids in a soap molecule, are assigned to the fatty acid, and the disappearance of the higher transitions is also due to the presence of the fatty acid, as shown previously.

An observation was made on the visual change of the soaps under a hot stage microscope. The apparent melting points are summarized in Table V. It is apparent that these melting points correspond to the highest transition points, excluding some exceptions; i. e., the highest transition is due to melting.

TABLE V. APPARENT MELTING POINTS AND THE HIGHEST TRANSITION TEMPERATURES OF ALUMINUM SOAPS

Sample	M.p., °C	Tr. temp., °C
Ste-3.22	111	104
Ste-2.29	122	104
Ste-2.12	133	150
Ste-1.89	157	157
Ste-1.71	163	162
Ste-0.95	—	162
Palmitate	171	170
Myristate	183	178
Laurate	188	185
Caprate	196	196
Caprylate	209	216

Many disagreements have been reported on the melting points of aluminum soaps. Licata reported the melting point of aluminum monostearate as 158~163°C; Lawrence, as 280°C for stearate[1,18]. The disagreement comes probably from the difference in the composition of the samples and in the experimental techniques used. Recently, Wagner reported the softening points of industrial aluminum soaps; 109~118°C for tristearate, 121~133°C for distearate, and 165~170°C for monostearate[19]. It is interesting that these points correspond nearly to the three major transition points, or to the melting point of Ste-3.22, Ste-2.12 and Ste-1.71 in this experiment; however, in his report, one of the three transition points might be observed as melting points due to the impurities contained in the soaps.

The soap at room temperature is in crystalline phase, as found by X-ray diffraction measurement, although the crystallinity of the soap is not so good. The transition below their melting temperature, will be ascribed to some change in crystal structure of the soaps, and the soap passes into a plastic phase with less degree of crystallinity, presumably owing to the disordering of the lateral arrangement. It will be possible to consider that the degree of the loss in the crystallinity by a transition is proportional to the heat of the transition. In this consideration, the stearate shows the most plastic phase at temperatures between the lower and higher transition points. A less degree of crystallinity is found for the soap cooled from the liquid state, in X-ray diffraction measurement, which supports the fact that phase change in the initial heating is irreversible.

Mechanism of Formation of Aluminum Soaps. —The mechanism of soap formation in the aqueous metathetic process is examined. Alexander stated that the precipitate, formed by addition of aluminum salt solution into alkali soap solution, is fatty acid adsorbed on the precipitated aluminum hydroxide, and that the soaps are formed in the drying process. In fact, the fatty acids which are heated at 160°C with aluminum hydroxide give infrared absorption at 980 cm^{-1}, which shows the formation of the aluminum soap polymer skeleton, Al–O–Al. Similarly, the soaps containing more than 2 mol. of acid per aluminum and dried by heating to 110°C, show more intense absorption at 980 cm^{-1} and less absorption at 1720 cm^{-1} than the same soap dried in vacuum at room temperature; these facts suggest that the formation of the soap proceeds by heating, from the fatty acids and aluminum hydroxide in the precipitate. However, the soaps containing less than 2 mol. of acid per aluminum dried by the two methods, give quite identical spectra, which shows that in these conditions, the soaps are formed when precipitated from aqueous solutions.

Summary

Differential thermal analysis of two series of aluminum soaps—aluminum stearates of different compositions, and aluminum soaps from various parent fatty acids—are carried out, and

17) S. Shiba, This Bulletin, 34, 198 (1961).
18) F. J. Licata, "Metallic Soaps", Metasap Chemical Co., Harrison, New Jersey (1940).
19) E. S. Pattison (Editor), "Industrial Fatty Acids and their Applications", Reinhold Publishing Corp., New York (1959), p. 104.

transition temperatures and the heats of transition are obtained. Each transition point is assigned to a certain change in the structure of the soap or to the soap composition. The structure of the the soaps and the mechanism of soap formation are also discussed, based on the differential thermal analysis and infrared data.

The author wishes to express his sincere thanks to Professor H. Akamatu and Dr. H. Takahashi, both of the University of Tokyo, for their interest and kind discussions throughout this investigation; thanks are also due to Dr. M. Kawano, of the Railway Technical Research Institute, for the infrared measurements.

Railway Technical Research Institute
Kunitachi, Tokyo

Differential Thermal Analysis of the Systems Aluminum Soap-Hydrocarbon

By Sukekuni SHIBA

(Received November 19, 1960)

Studies on the metal soap-hydrocarbon systems have been carried out in order to obtain basic knowledge on the industrial applications of the metal soaps, especially for the manufacture of lubricating greases. Visual observation and optical methods have been used to establish the relation of the phase state on temperature and composition. Recently, differential thermal analysis offered a powerful means for obtaining such diagrams precisely.

Disagreements in the results have been observed due to the complex behaviors of the systems and the differences in the experimental techniques used: Doscher and Vold[1], and also, Stross and Abrams[2] reported quite different types of phase diagrams on the system sodium stearate-cetane; Vold[3] and Cox[4], on the system lithium stearate in cetane and in mineral oils.

Phase behaviors of the aluminum soaps were discussed in the preceding paper with the aid of differential thermal analysis[5]. In this paper, the thermal behaviors of aluminum soap-hydrocarbon systems are studied by the same method to obtain the phase behaviors of the systems and to have some information on the structure of the systems and the aluminum soaps themselves.

Experimental

The aluminum soaps used in this study were prepared by an aqueous metathetic process. Details of the preparation were described in the preceding paper[5]. Nujol, a liquid paraffin of commercial grade, was used as a model of the mineral oils. The purity of the Nujol was checked by infrared absorption measurement, which proved that it is a paraffin-rich hydrocarbon, and showed the absence of aromatic components or impurities. The physical properties were, $d_4^{25}=0.8429$, $n_D^{25}=1.467$, $\eta_{25}=0.217$ poise.

The apparatus and procedure were also described previously.

Results and Discussion

The System Aluminum Stearate-Nujol. The transition temperatures and heats of transition, obtained from the heating and cooling thermograms on the aluminum stearate-Nujol, are summarized in Table I. The aluminum soaps have three transition points in general. They are named for convenience the transitions I, II and III, from low to high temperatures. Thermograms for repeated heating and cooling show that the phase changes are practically reversible. In the initial heating, however, slightly different transition temperatures and appearance of peaks, for instance, that of the soap itself, are obtained incidentally, and they are not found in the following runs. This may be due to the difference in heat transfer in the specimens and incomplete mixing of the soaps in oil.

An equilibrium phase diagram for the

1) T. M. Doscher and R. D. Vold, *J. Colloid Sci.*, **1**, 299 (1946).
2) F. H. Stross and S. T. Abrams, *J. Am. Chem. Soc.*, **73**, 2825 (1951).
3) M. J. Vold and R. D. Vold, *J. Colloid Sci.*, **5**, 1 (1950).
4) D. B. Cox, *J. Phys. Chem.*, **62**, 1254 (1958).
5) S. Shiba, This Bulletin, **34**, 2611 (1961).

TABLE I. TRANSITION TEMPERATURES AND HEATS OF TRANSITION OF THE SYSTEM ALUMINUM STEARATE-NUJOL

Soap conc. wt. %	Heating		Cooling	
	Tr. temp. °C	Heat of tr. cal./g.	Tr. temp. °C	Heat of tr. cal./g.
100	99	5.8	89	10.6
	119	0.4	144	2.5
	162	2.1		
90	94	5.0	85	12.8
	114	1.1	140	1.9
	159	0.7		
70	96	14.4	81	12.4
	109		95	
50	101	11.8	87	14.7
30	99	13.4	80	14.1
10	98	12.6	71	15.4
5	100	13.3	71	11.5

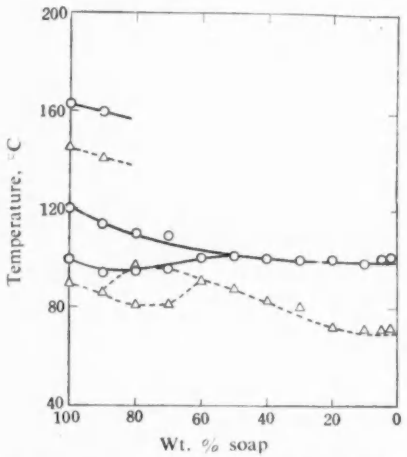

Fig. 1. Phase diagram of the system aluminum stearate-Nujal.

system, obtained from the transition temperatures, is shown in Fig. 1. The full lines represent the phase transitions on heating, and the dotted lines, on cooling. The transition temperatures when they are heated, undergo changes by the addition of Nujol. The heat of transition at high temperatures decreases conspicuously, and the transition III disappears when more than 10 wt.% of Nujol is contained. The transition II coincides with the transition I, when more than 30 wt.% is contained. In the system containing more than 30 wt.% of Nujol, the soap dissolves in Nujol at the transition I, and shows no transition above this temperature. Concerning the transition I, when a small amount of Nujol is added, the peak is broadened, showing sometimes 2 or 3 apexes. In this diagram, the most intense apexes are adopted as the transition temperatures. By further addition of Nujol, the peak of the transition I becomes sharp again, and the temperature reaches a constant value.

The phase diagram obtained by cooling shows only two transition temperatures which are lower than the temperatures obtained by heating, and in this case, both a change in transition temperatures and disappearance of the transition points are observed.

The disappearance of the transition points, which was also found in the case of the contaminant free fatty acids in the soaps[5], shows an entirely different behavior of aluminum soaps compared with other metal soaps. Most of the systems, metal soaps-hydrocarbon, undergo phase transitions on heating, which are either related to the transitions on heating, which are either related to the transitions of the oil-free soaps or are more complicated; and the transition temperatures are reduced in general by the addition of hydrocarbon[6].

The phase diagram is obtained concerning one vehicle, Nujol; however, essentially the same or at least similar results are expected for other hydrocarbons, e.g., petroleum oils, as were found for lithium soaps in various petroleum oils[1].

Systems of Aluminum Palmitate and Laurate-Nujol.—The phase diagrams for the systems of aluminum palmitate-Nujol and aluminum laurate-Nujol are shown in Figs. 2 and 3. Aluminum palmitate shows similar results to stearate: although slightly different transition temperatures are obtained. Aluminum laurate shows different behaviors. The transition

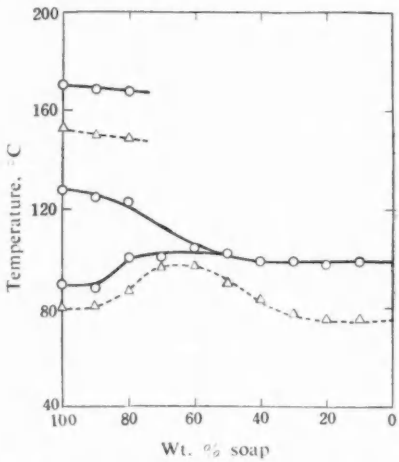

Fig. 2. Phase diagram of the system aluminum palmitate-Nujol.

6) M. J. Vold, G. S. Hattiangdi and R. D. Vold, *Ind. Eng. Chem.*, **41**, 2539 (1949).

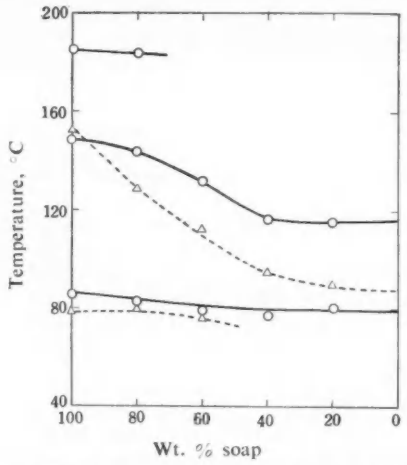

Fig. 3. Phase diagram of the system aluminum laurate-Nujol.

temperature varies definitely with the concentration of the soap, in both heating and cooling thermograms. The transition II shows marked absorption of heat, as the Nujol is added; on the contrary, the heat of the transition III decreases and disappears at the concentration of Nujol above 20 wt. %; and the heat of transition I remains unchanged. For instance, the heats of transitions I, II and III, of the system containing 40% of Nujol are 1.2, 6.3 and 0 cal./g., whereas the soap itself shows 1.4, 1.2 and 3.2 cal./g., respectively. In the system containing more than 20% of Nujol, the soap dissolves in hydrocarbon at temperatures above the transition II.

The phase transition of the system aluminum laurate-Nujol on cooling, shows tendencies similar to the transition on heating. In this case, the lower transition disappears and only the higher transition remains in dilute systems.

Colloidal Structures of the Aluminum Soaps in Hydrocarbon.—The aluminum soaps, which are composed mainly of aluminum hydroxy disoaps, and a small amount of contaminant aluminum hydroxide, free fatty acid, and a trace of water, make the stable skeletons of Al-O-Al with adjacent soap molecules through the hydroxyl group, which shows the polymeric nature of the soaps. These skeletons form fibrous soap polymer, and are maintained even when the soaps are dispersed in hydrocarbon media, and result in the extraordinarily strong gelling or thickening properties.

The dispersed systems, aluminum soap gels in hydrocarbon, are essentially a dispersion of aluminum soap particles combined weakly with secondary bonding, as found from X-ray diffraction, electron microscope techniques, and rheological measurements[7-9]. The results of differential thermal analysis, which show that the systems are thermally reversible, suggest that the structure of the soap particles at room temperatures, dispersed by heating in hydrocarbon media, are almost identical with the original solid phase of the soaps; i. e., the isotropic solution becomes a jelly by cooling, and the soap micelles in the jelly convert rapidly to soap crystallites.

At higher temperatures above their transition points, the soap crystallites are dissolved in the hydrocarbon media, and the system becomes a transparent viscous solution. It is supposed that the soaps retain their polymeric nature even in the solutions, because of their typical visco-elastic properties.

In the practical applications of the aluminum soaps, the soaps are used generally at concentrations of a few per cent. In such cases, the phase behavior is very simple as is expected from the phase diagrams as shown in Figs. 1—3, and the transition points correspond to the temperatures at which the systems become transparent viscous solution on heating, and turbid gel on cooling. The phase changes of the dilute systems obtained in this experiment are consistent with the results from the sudden change in dynamic rheological properties with temperature[10].

Summary

The phase behaviors of the system aluminum stearate, palmitate, and laurate-Nujol are studied by differential thermal analysis. Phase diagrams are obtained, and it is found for stearate and palmitate that soaps dissolve in hydrocarbon at the lower transition points of the soaps, and that the higher transition points disappear by addition of hydrocarbon. Differences in phase behaviors are found between laurate and other soaps. Some discussions are made on the colloidal structures of the dispersed systems aluminum soaps-hydrocarbon.

The author wishes to express his sincere thanks to Professor H. Akamatu and Dr. H. Takahashi, both of the University of Tokyo, for their interest and kind discussions throughout this work.

Railway Technical Research Institute
Kunitachi, Tokyo

7) S. S. Marsden, Jr., K. J. Mysels and G. H. Smith, *J. Colloid Sci.*, **2**, 265 (1947).
8) D. Evans and J. B. Matthews, ibid., **9**, 60 (1954).
9) W. H. Bauer, N. Weber and S. E. Wiberley, *J. Phys. Chem.*, **62**, 106 (1958).
10) S. Shiba, This Bulletin, **34**, 194 (1961).

The Preparation of Diethyl Phosphate

By Teruaki MUKAIYAMA and Tamotsu FUJISAWA

(Received November 7, 1960)

Intramolecular dehydration reactions of primary nitroparaffins[1,2], aldoximes[3,4] and hydroxamic acids[5] into nitrile oxides, nitriles and isocyanates, respectively, by means of organic reagents have been described in preceding papers. It was shown in them[4] that benzaldoxime is dehydrated by means of esters of phosphoric acid and it was demonstrated that the dehydration proceeds through an intermediate, diethyl benzaldimino phosphate (I), formed by the bond fission of pyrophosphate linkage by an attack of benzaldoxime.

$$(EtO)_2\overset{\uparrow}{P}(=O)\text{-}O\text{-}\overset{\uparrow}{P}(=O)(EtO)_2 + HO\text{-}N{=}CHC_6H_5 \rightarrow [(EtO)_2\overset{\uparrow}{P}(=O)\text{-}O\text{-}N{=}CHC_6H_5] + (EtO)_2\overset{\uparrow}{P}(=O)OH$$

(I)

$$(EtO)_2\overset{\uparrow}{P}(=O)OH + C_6H_5CN \leftarrow$$

This type of reaction was extended to the preparation of diethyl phosphate from diethyl chlorophosphonate by means of compounds containing a hydroxyl group which are readily dehydrated to give unsaturated compounds, such as benzaldoxime and *tert*-butyl alcohol.

The reaction of benzaldoxime with diethyl chlorophosphonate initially yields diethyl benzaldimino phosphate (I), which in turn decomposes to give diethyl phosphate and benzonitrile in good yields.

$$(EtO)_2\overset{\uparrow}{P}(=O)\text{-}Cl + HO\text{-}N{=}CHC_6H_5 \rightarrow [(EtO)_2\overset{\uparrow}{P}(=O)\text{-}O\text{-}N{=}CHC_6H_5] + HCl$$

(I)

$$(EtO)_2\overset{\uparrow}{P}(=O)OH + C_6H_5CN \leftarrow$$

When diethyl chlorophosphonate and benzaldoxime are allowed to react in dry benzene at room temperature, a violent reaction takes place and a large amount of benzaldoxime hydrochloride, which retards the formation of I, precipitates. Since the hydrochloride decomposes into benzaldoxime and hydrogen chloride on gentle heating, the reaction is best effected when two reactants are mixed at one time and heated at about 70°C.

On the other hand, the reaction of *tert*-butyl alcohol with diethyl chlorophosphonate does not take place at room temperature, but it is effected well by refluxing them in carbon tetrachloride for 3 hr. Isobutylene, hydrogen chloride and *tert*-butyl chloride formed by the addition of hydrogen chloride to isobutylene are obtained along with diethyl phosphate.

$$(EtO)_2\overset{\uparrow}{P}(=O)\text{-}Cl + HO\text{-}C(CH_3)_3 \rightarrow [(EtO)_2\overset{\uparrow}{P}(=O)\text{-}O\text{-}C(CH_3)_3] + HCl$$

$$(EtO)_2\overset{\uparrow}{P}(=O)OH + CH_2{=}C(CH_3)_2 \leftarrow$$

$$CH_2{=}C(CH_3)_2 + HCl \longrightarrow (CH_3)_3C\text{-}Cl$$

As described in the experimental part, *tert*-butyl alcohol is dehydrated in a nearly quantitative yield; however, the yield of diethyl phosphate is comparatively low. This may be attributed to a useless dehydration of *tert*-butyl alcohol catalyzed by the phosphate formed. The use of 2 mol. of *tert*-butyl alcohol did not lead to a good result though the yields of isobutylene and *tert*-butyl chloride were increased.

These methods for the preparation of diethyl phosphate from diethyl chlorophosphonate are a simpler procedure than that reported by Toy[6] which involves 2 steps of hydrolysis.

Moreover, an attempt to prepare diethyl chlorophosphonate in a better yield by the reaction of phosphorus oxychloride with 2 mol. of ethyl alcohol gave a successful result. Several methods[7-10] are reported in the literature for this reaction; however, the yield is less than 25% even when a basic medium

1) T. Mukaiyama and T. Hoshino, *J. Am. Chem. Soc.*, **82**, 5339 (1960).
2) T. Mukaiyama and T. Hata, This Bulletin, **33**, 1382 (1960).
3) T. Mukaiyama and T. Hata, ibid., **33**, 1712 (1960).
4) T. Mukaiyama and T. Hata, ibid., **34**, 99 (1961).
5) T. Mukaiyama and H. Nohira, *J. Org. Chem.*, **26**, 782 (1961).
6) A. D. F. Toy, *J. Am. Chem. Soc.*, **70**, 3882 (1948).
7) P. Nylén, Dissertation, Uppsala, 1930.
8) J. Walczynska, *Roczniki Chem.*, **6**, 110 (1926).
9) H. Wichelhaus, *Ann. Suppl.*, **6**, 257 (1868).
10) T. W. Mastin, G. R. Norman and E. A. Weilmuenster, *J. Am. Chem. Soc.*, **67**, 1662 (1945).

such as pyridine is used. In the present experiment, in order to avoid unnecessary heating, the reaction was carried out in petroleum ether under 0°C over a period of 4.5 hr. After the completion of the reaction, the solvent was removed at room temperature under reduced pressure and distilled. By this method, a 76% yield of diethyl chlorophosphonate was obtained.

As shown in Table II, the yield of diethyl chlorophosphonate became higher when the amount of reactants was smaller, and also it can be noted that the elevation of reaction temperature over 0°C resulted in a decrease of the yield.

Experimental

Diethyl Phosphate.—*By Means of Benzaldoxime.*—To 17.2 g. (1/10 mol.) of diethyl chlorophosphonate dissolved in 10 ml. of carbon tetrachloride was added at one time with vigorous stirring a solution of 12.1 g. (1/10 mol.) of benzaldoxime in 10 ml. of carbon tetrachloride. Then the reaction mixture was refluxed on a water bath for an hour. After the evolution of hydrogen chloride, the carbon tetrachloride was removed and 9 g. (87% yield) of benzonitrile (b. p. 78°C/16 mmHg) and 11 g. (71% yield) of diethyl phosphate (b. p. 112~127°C/0.02 mmHg) were obtained.

If a solution of the aldoxime was added more slowly at room temperature, a white precipitate melting at about 80°C was obtained. This substance generated hydrogen chloride on heating and gave benzaldoxime by means of distillation. Besides that, from the filtrate were obtained benzonitrile and diethyl phosphate in 51% and 35% yields, respectively.

By Means of tert-Butyl Alcohol.—A mixture of 17.2 g. (1/10 mol.) of diethyl chlorophosphonate and 7.5 g. (1/10 mol.) of *tert*-butyl alcohol dissolved in 10 ml. of carbon tetrachloride was refluxed on a water bath for 3 hr. During this period, isobutylene and hydrogen chloride were generated from the mixture. Distillation gave *tert*-butyl chloride and diethyl phosphate. The yields and boiling points are listed in Table I.

Table I

Product	Yield		B. p.
Isobutylene	1.5 l.	67%	
tert-Butyl chloride	3.5 g.	38%	49~50°C/760 mmHg
Diethyl phosphate	7.5 g.	48%	111~114°C/0.005 mmHg

Diethyl Chlorophosphonate.—The preparation of diethyl chlorophosphonate from phosphorus oxychloride was tried under several conditions as listed in Table II. In the case of 1 mol. of phosphorus oxychloride, the best procedure was found to be as follows: To 153.5 g. (1 mol.) of phosphorus oxychloride dissolved in 80 ml. of petroleum ether cooled by an ice-salt bath was added with vigorous stirring a solution of 105 g. (2.28 mol.) of 99% ethyl alcohol in 50 ml. of petroleum ether at a rate such that the addition was completed in about 3.5 hr. The stirring was continued for an hour after all the solution of ethyl alcohol had been added. During this period, the temperature was maintained under 0°C and then the stirring was further continued without the ice-salt bath until the mixture was warmed to room temperature. After the hydrogen chloride dissolved in the reaction mixture and the petroleum ether were removed under reduced pressure at room temperature, diethyl chlorophosphonate was obtained by distillation, b. p. 72°C/6 mmHg, yield 130 g. (76%).

Table II

Solvent	Rate of addition hr.	Reacn. time hr.	Moles of $POCl_3$	Yield %	Reacn. temp. °C
CCl_4	1	1.5	0.2	80	0
CCl_4	1	1.5	0.2	43	room temp.
PE	1	2	0.2	85	0
PE	3.5	5	1	76	0
CCl_4	2	4.5	1.65	50	0

PE=petroleum ether

Department of Chemistry
Tokyo Institute of Technology
Meguro-ku, Tokyo

Non-benzenoid Aromatic Heterocycles. V[1]. An Attempted Synthesis of 4,7-Dihydro-4,7-phenanthroline Derivatives*

By Hiroshi KATO and Masaki OHTA

(Received November 15, 1960)

Heptalene (I) was first proposed by Baker[2] in 1945 as a possible aromatic, wholly conjugated compound. Many synthetic trials of its derivatives have since been carried out[3], and yet their synthesis has not been successful with only one exception of condensed heptalene derivative II[4], while this compound should rather be regarded as an azulene derivative. The results of a few theoretical treatments[5] on this compound I also do not coincide with one another in the stability of this hydrocarbon.

In connection with this problem, the authors attempted the synthesis of 4,7-dihydro-4,7-phenanthroline derivatives III. These compounds are planar without undue strain and are wholly conjugated, and they have seven π-electrons in each hetero-ring. In this respect, these compounds are similar in their electronic structure to the supposed hydrocarbon heptalene (I).

As a possible route to III, the hydrogenation of 4,7-phenanthroline dimethiodide (IV) was first attempted. The reduction of 4,7-phenanthroline 4,7-dimethiodide was reported by Karrer et al.[6] They used sodium hyposulfite and obtained a red substance, to which the formula V was suggested. The present authors attempted the reduction of IV by catalytic hydrogenation or by zinc powder. In neither case was the expected III (R, R''=Me, R', R'''=H) obtained, but instead an intense red solution, presumably the same substance as reported by Karrer, was formed.

Next, the dehydrogenation of tetrahydro-4,7-phenanthroline was attempted. It has been found[7] with quinoline that the methiodide reacts with Grignard reagents to form 1,2-dihydroquinoline derivative, and the present authors expected a reaction of the same type in 4,7-phenathroline dimethiodide. 4,7-Phenanthroline 4,7-dimethiodide reacted with methylmagnesium iodide as expected, to give the desired 3,4,7,8-tetrahydro-3,4,7,8-tetramethyl-4,7-phenanthroline (VI). It is markedly unstable to air and quickly combines with oxygen on being kept in air and an intensely green substance was formed. When VI was treated with chloranil, a dark precipitate (presumably an addition complex) was rapidly formed, and even after four hours' reflux in xylene, no tetrachlorohydroquinone was formed, which showed that no dehydrogenation had occurred in tetrahydrophenanthroline (VI). When VI was treated with concentrated sulfuric acid, the starting material was recovered accompanied by an intensely green substance.

Finally, an addition of organometallic compounds to 4,7-phenanthroline (VII) was attempted. It has been reported that phenazines give *N,N'*-disubstituted *N,N'*-dihydrophenazines by the action of Grignard reagents or organolithium compounds, followed by alkyl halides[8]. Hence, if the structure III is sufficiently stable, the organometallic compounds should add to VII to form 4,7-disubstituted 4,7-dihydro-4,7-phenanthrolines (III). Although phenanthroline was recovered unchanged by the action of phenylmagnesium bromide, when it was treated with phenyllithium followed by methyl iodide, a yellow compound of a formula $C_{19}H_{16}N_2$ with strong green fluorescence (VIII) was obtained. Evidently, the addition of phenyllithium took place, but structures VIIIa and VIIIb would be possible to this substance because the addition of phenyllithium to 1,2-position of pyridines and quinolines has been reported[9]. The yellow color of this substance suggests that it is not the expected 4,7-dihydro-4,7-phenanthroline derivatives. Further, the hydrochloride and the picrate of VIII are red, while Karrer et al.[6] reported that *N*-methyl-1,2,3,4-tetrahydro-4,7-phenanthroline hydrochloride also is red. This fact also throws doubt on the supposed structure VIIIa. The

* Presented at the Meeeting of the Chemical Society of Japan, Tokyo, October, 1960.

1) Part IV. H. Kato and M. Ohta, This Bulletin, **34**, 357 (1961).

2) W. Baker, *J. Chem. Soc.*, **1945**, 258.

3) Cf. for example, W. Baker and J. F. W. McOmie, "Non-benzenoid Aromatic Compounds", in "Progress in Organic Chemistry", Vol. 3, Butterworths Scientific Publications, London (1955), p. 44.

4) K. Hafner and J. Schneider, *Ann.*, **624**, 37 (1959).

5) R. B. Brown, *Trans. Faraday Soc.*, **45**, 296 (1949); **46**, 146 (1950); D. P. Craig, *J. Chem. Soc.*, **1951**, 3175, etc.

6) P. Karrer, A. Pletscher and W. Manz, *Helv. Chim. Acta*, **30**, 1146 (1947).

7) W. Bradly and F. Jeffrey, *J. Chem. Soc.*, **1954**, 2770.

8) H. Gilman and Dietrich, *J. Am. Chem. Soc.*, **79**, 6178 (1957).

9) K. Ziegler and H. Zeiser, *Ber.*, **63**, 1847 (1930); *Ann.*, **485**, 174 (1931).

structure of VIII was proved to be VIIIb by treating 4,7-phenanthroline monomethiodide (IX) with phenylmagnesium bromide to give the indentical product with VIII.

In connection with this reaction, the reaction of phenyllithium to 4,7-phenanthroline was studied in more detail. When two or more molar equivalents of phenyllithium was used, no disubstituted tetrahydrophenanthroline derivative was formed, and the dihydro-derivative VIIIb was the sole product. When the addition product of phenyllithium was hydrolyzed with water, 3-phenyl-4,7-phenanthroline (X) was formed, probably via the dihydro compound.

From these facts, one may reasonably assume that the compound of the type III, although planar and wholly conjugated, are not stable and of which no aromaticity can be expected.

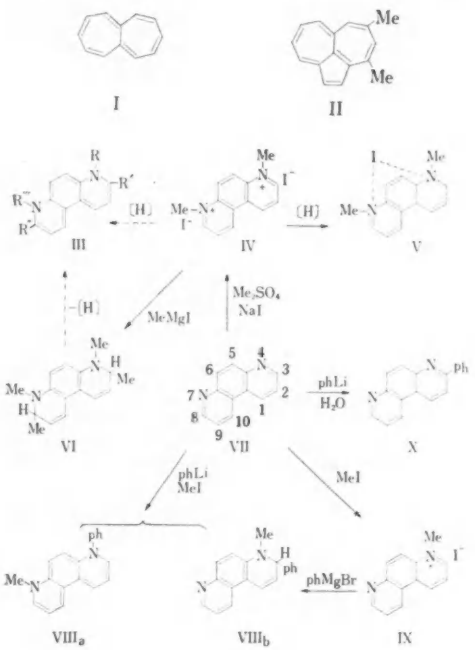

Experimental

4,7-Phenanthroline (VII).—a) To a mixture of 6-aminoquinoline (12 g.), orthoarsenic acid (13 g.) and glycerol (36 g.), there was added dropwise concentrated sulfuric acid (32 g.) with stirring and heating at 130~140°C. The mixture was heated and stirred for four hours and then poured into a solution of potassium hydroxide in ice-water. The black resinous residue and the aqueous layer were extracted continuously for fifteen hours with benzene, and the benzene extract was treated with a large quantity of charcoal. On evaporation of benzene, practically pure 4,7-phenanthroline was obtained (11 g.), m. p. 170~173°C[10]. This substance was used directly for the following reactions.

b) To a mixture of *p*-phenylenediamine (60 g.), orthoarsenic acid (150 g.) and glycerol (300 g.), there was added dropwise concentrated sulfuric acid (150 g.), with stirring and heating at 130~140°C. The mixture was heated and stirred for six hours; then the mixture was diluted with ice-water and neutralized with ammonia. The black resinous product was extracted several times with hot benzene, and the benzene extract was treated with charcoal. On evaporation of benzene, crude 4,7-phenanthroline (48 g.) was obtained, m. p. 165~169°C. Recrystallization from benzene afforded pale yellow needles, m. p. 173°C.

4,7-Phenanthroline Monomethiodide (IX).—A benzene solution of 4,7-phenanthroline (2 g.) and methyl iodide was gently refluxed for thirty minutes; then methyl iodide was added further and reflux was continued for another half an hour. The yellow crystals which separated out (3 g.) were collected and recrystallized from water to give bright yellow needles (2 g.), m. p. 270°C[12].

4,7-Phenanthroline Dimethiodide (IV).—A mixture of 4,7-phenanthroline (20 g.) and dimethyl sulfate (40 g.) was heated at 160°C for two hours and then diluted with water, and sodium iodide (50 g.) was added. The brown precipitate which separated out was collected and recrystallized from water to give pale brown plates (18 g.), m.p. 264°C[13].

Reduction of 4,7-Phenanthroline Dimethiodide.—To a solution of 4,7-phenanthroline dimethiodide (2.3 g.) in water (50 ml.), there was added zinc powder (0.7 g.) in small portions with stirring and warming. The solution quickly turned to an intense wine-red color. The colored substance could not be extracted with ether, benzene, chloroform, etc.

When this reaction was carried out in cold water, or in aqueous or absolute ethanol, the same result was observed. When 4,7-phenanthroline dimethiodide was hydrogenated with Pd-C (5%) or Pd-$CaCO_3$ (2%) in water, ethanol or acetone, the same coloration took place accompanied by the starting material.

3,4,7,8-Tetrahydro-3,4,7,8-tetramethyl-4,7-phenanthroline (VI).—To an ether solution (25 ml.) of methylmagnesium iodide (prepared from 1 g. of magnesium and 5.7 g. of methyl iodide), there was added portionwise fine powdered 4,7-phenanthroline dimethiodide (2.3 g.) with stirring and under an atmosphere of nitrogen. Stirring was continued for an additional two hours after the addition was complete, while heat was evolved slightly and the dimethiodide gradually dissolved. The solution was decomposed with aqueous ammonium chloride and extracted with ether. The ether extract was dried over potassium carbonate, the ether was evaporated under nitrogen and the residue was washed with methanol and ether to give a dark

10) Reported m. p.[11] 173°C.
11) I. Heilbron, "Dictionary of Organic Compounds", Vol. IV, Oxford University Press, New York (1953), p. 87.
12) Reported m. p.[11] 268~269°C.
13) Reported m. p.[11] 265°C.

yellow powder (0.7 g.), m. p. 113~117°C. Recrystallization from ether afforded yellow prisms (0.2 g.), m. p. 147°C. This compound is very sensitive to air and rapidly turns intense green on standing.

Found: C, 79.80; H, 8.68; N, 11.76. Calcd. for $C_{16}H_{20}N_2$ (VI): C, 79.95; H, 8.39; N, 11.66%.

Air Oxidation of VI.—A current of air was bubbled into an ethanolic solution of VI (0.1 g.) for two days. The resultant intensely green substance (0.07 g.) was purified by chromatography (alumina-benzene) to give a dark green amorphous powder. This compound does not show a definite m. p. but melts at about 230°C.

Found: C, 65.68; H, 6.92%.

When it was allowed to stand in air for a long time, it became practically insoluble in most solvents.

Attempted Dehydrogenation of VI with Chloranil.—Chloranil (0.2 g.) and VI (0.2 g.) were refluxed for four hours in xylene (10 ml.). A black precipitate was rapidly formed. This precipitate (0.4 g.) was scarcely soluble in most organic solvents and is positive to Beilstein's halogen test. On treatment of the filtrate with aqueous potassium hydroxide, no tetrachlorohydroquinone was obtained.

Treatment of VI with Concentrated Sulfuric Acid.—A solution of VI (0.2 g.) in concentrated sulfuric acid (10 ml.) was warmed at 60~70°C for an hour and was kept standing overnight at room temperature. The starting material was recovered unchanged accompanied by a small amount of green insoluble substance.

3,4-Dihydro-4-methyl-3-phenyl-4,7-phenanthroline (VIIIb).—a) An ether solution (20 ml.) of phenyllithium (prepared from 3.14 g. of bromobenzene and 0.3 g. of lithium) was added dropwise under an atmosphere of nitrogen into a tetrahydrofuran solution (30 ml.) of 4,7-phenanthroline (3 g.) with cooling and stirring. The solution turned wine-red. After half an hour, a tetrahydrofuran solution (10 ml.) of methyl iodide (3 g.) was added to the solution with cooling and stirring. The solution turned greenish yellow after the addition was complete. After two hours, the solution was decomposed by addition of an aqueous solution of ammonium chloride and the resultant solution was extracted with ether followed by chloroform and each extract was dried over calcium chloride.

The ether extract was concentrated to give a yellow residue (2.8 g.). Recrystallization from acetone afforded yellow fine needles with strong green fluorescence, m. p. 155°C.

Found: C, 83.50; H, 6.08; N, 10.53. Calcd. for $C_{19}H_{16}N_2$ (VIIIb): C, 83.79; H, 5.92; N, 10.27%.

The same compound was obtained when two or more molar equivalents of phenyllithium were reacted with 4,7-phenanthroline.

This compound turns red-colored on addition of hydrochloric acid.

Picrate: red needles (from aqueous dimethylformamide), m. p. 173°C.

Found: N, 13.85. Calcd. for $C_{25}H_{19}N_5O_7$: N, 13.97%.

The chloroform extract in the above experiment was concentrated and the residue (0.5 g.) was recrystallized from benzene to give white needles, m. p. 171~172°C, undepressed on admixture with an authentic specimen of 4,7-phenanthroline.

When 4,7-phenanthroline was treated with phenylmagnesium bromide followed by methyl iodide, the starting material was recovered.

b) To an ether solution (30 ml.) of phenylmagnesium bromide (prepared from 3.2 g. of bromobenzene and 0.5 g. of magnesium), there was added fine powdered 4,7-phenanthroline monomethiodide with stirring. After an hour, this solution was poured into aqueous ammonium chloride, extracted with ether and benzene and the extract was dried over calcium chloride. The solvent was removed and the residue (1.2 g., m. p. 152~154°C) was recrystallized from acetone to give yellow fine needles with strong green fluorescence, m. p. 155°C. Picrate, red needles, m. p. 173°C. Neither melting point was depressed on admixture with the specimens prepared by procedure a).

3-Phenyl-4,7-phenanthroline (X).—An ether solution (40 ml.) of phenyllithium (prepared from 6.3 g. of bromobenzene and 0.6 g. of lithium) was added dropwise under an atmosphere of nitrogen into a tetrahydrofuran solution (30 ml.) of 4,7-phenanthroline (3 g.) with stirring and cooling. After thirty minutes, the reaction mixture was decomposed by addition of aqueous ammonium chloride and extracted with ether, the ether extract was dried over calcium chloride, and the solvent was removed. Recrystallization of the residue from acetone afforded yellow fine needles with green fluorescence (1 g.), m. p. 187°C[14].

Found: C, 83.85; H, 4.92; N, 10.81; Mol. wt. (Rast) 260. Calcd. for $C_{15}H_{12}N_2$ (X): C, 84.35; H, 4.72; N, 10.85%; Mol. wt. 255.

The authors are indebted to Dr. Asaji Kondo for performing the microanalyses.

Laboratory of Organic Chemistry
Tokyo Institute of Technology
Meguro-ku, Tokyo

14) Reported m. p.[15] 183°C.
15) C. Willgerodt and S. Jabolinsky, *Ber.*, 33, 2918 (1900).

Diffusion in Glassy Polymers. II. Effects of Polymer-penetrant Interaction; Diffusion of Ethyl Methyl Ketone in Atactic Polystyrene

By Hisashi ODANI, Jun HAYASHI and Mikio TAMURA

(Received November 21, 1960)

Sorption processes of organic vapors in glassy polymers exhibit a variety of anomalous or "non-Fickian" features[1]. In the hope of obtaining information about how the polymer-penetrant interaction affects these feature, we have measured in the present work the rates of absorption of ethyl methyl ketone by atactic polystyrene, using both the integral and differential absorption techniques and have compared the data obtained with those reported previously for the system benzene-atactic polystyrene[1,2]. Ethyl methyl ketone and benzene have about the same molecular volumes, but their solvent powers for polystyrene are different; ethyl methyl ketone is less soluble in polystyrene than benzene is. Thus it is expected that the comparison of the present data with the previous ones for benzene will provide us with some useful information pertaining to the purpose mentioned above.

Experimental

The atactic polystyrene (A-PS) used was the same as that described previously[1]. Its viscosity-average molecular weight was 2.2×10^5. Films 2.40×10^{-3} cm. thick were used. Ethyl methyl ketone was purified by fractional distillation after drying over anhydrous potassium carbonate. Both integral and differential sorptions were studied under a variety of conditions at 25°C. This temperature is well below the glass transition temperature of the polymer[3].

Results and Discussion

Absorption Isotherms.—Absorption isotherm data for this system at 25°C are given in Fig. 1. Here the ordinate represents the mass of absorbed penetrant in grams per gram of dry polymer and the abscissa the relative pressure of ambient vapor. The data from integral absorption experiments and those from differential ones fall satisfactorily on a single curve. The corresponding data for the system A-PS-benzene at the same temperature are included in the figure for comparison. We see that the solubility of ethyl methyl ketone in A-PS is lower than that of benzene over the entire range of vapor pressure investigated.

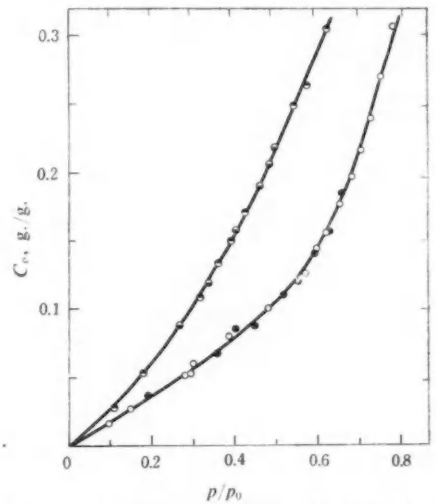

Fig. 1. Absorption isotherms of A-PS-ethyl methyl ketone and A-PS-benzene at 25°C.

	Integral absorption	Differential absorption
A-PS-ethyl methyl ketone	○	●
A-PS-benzene	◓	◒

Successive Differential Absorptions.—The data of successive differential absorptions for the A-PS-ethyl methyl ketone system at 25°C are given in Fig. 2. The increments of ethyl methyl ketone concentration in successive steps were kept approximately constant, about 0.01 g. of penetrant per gram of dry polymer, which is almost the same as those used in the previous experiments for benzene at the same temperature. The successive differential absorption curves shown in Fig. 2 change their type with the initial concentration according to the following scheme;

sigmoid type → pseudo-Fickian type
→ two-stage type → pseudo-Fickian type
→ Fickian type.

1) A. Kishimoto, H. Fujita, H. Odani, M. Kurata and M. Tamura, *J. Phys. Chem.*, **64**, 594 (1960).
2) H. Odani, S. Kida, M. Kurata and M. Tamura, This Bulletin, **34**, 571 (1961).
3) H. Mark and A. V. Tobolsky, "Physical Chemistry of High Polymeric Systems", Interscience Pub. Inc., New York (1950), p. 347.

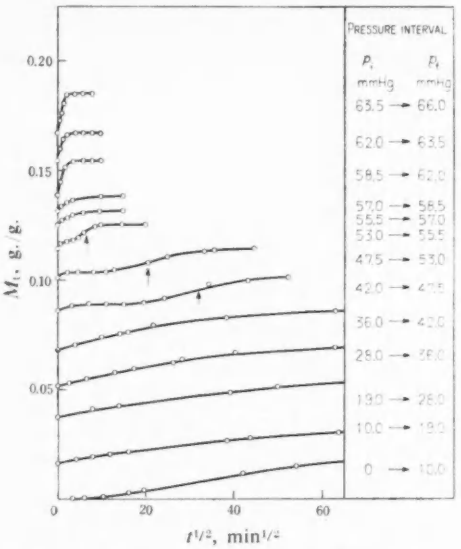

Fig. 2. Successive differential absorptions. Initial and final pressures, p_i and p_f, of each step are given in the right columns.

Though the general character of the family of curves for the present system is similar to that obtained for the benzene system[1], we may point out some significant and interesting differences between the two systems.

First, in the region of fairly low initial concentrations, only the first step is sigmoid and the second step already exhibits the pseudo-Fickian character. On the other hand, for benzene the shift from the sigmoid type to the pseudo-Fickian type began at a much higher concentration than for the present system. This relation is also the case with the initial concentration at which the transition from the pseudo-Fickian type to the two-stage type occurs. Secondly, the ninth and the tenth steps in Fig. 2 exhibit the typical pseudo-Fickian character, differing from the data for benzene where the transition from two-stage to the normal Fickian process occurred without the intervention of any pseudo-Fickian process.

It was demonstrated in the previous paper[1] that the successive differential absorption curves changed their type from pseudo-Fickian to Fickian when the penetrant concentration passed the point at which the polymer-penetrant mixture underwent glass transition at the temperature of the experiment. From the data shown in Fig. 2 and also from other differential absorption data obtained with concentration intervals of nearly the same magnitude, we may estimate such a critical concentration for the present system to be 0.139 g. ethyl methyl ketone per gram of dry A-PS. This value is lower than that for benzene at the same temperature. In that case the critical concentration of benzene was 0.191 g./g. As noted above, the solubility of ethyl methyl ketone in A-PS is lower than that of benzene, and the molar volumes of the two penetrants do not differ appreciably from each other. It appears, therefore, that for a given polymer at a given temperature a penetrant of poorer solubility gives a lower critical concentration if comparison is made for penetrants of about the same molar volumes. This implies that a penetrant molecule of less solvent-ability for the polymer will cause a greater decrease in the activation energy required for the segmental motion of polymer chains. In this connection it is of interest to note that Jenckel and Heusch[4] demonstrated that with solvents of about the same molar volumes the weaker the thermodynamic interaction with the polymer molecule the lower was the solvent concentration at which the mixture underwent the glass transition at a given temperature.

Concentration Dependence of the Second-stage Mechanism. — As mentioned in the previous paper[1], it is generally accepted that the second stage portion of a two-stage absorption is governed by the rate at which the network of polymer chains changes configuration under swelling pressure, while the first stage involves the ordinary diffusion mechanism. In accordance with the treatment presented in the previous investigation[1], we have chosen the quantity t_* to characterize the position of the second stage portion on the time axis, where t_* is the time corresponding to the inflection point on the second stage of the two-stage curve. In general, the value of t_* for the given initial concentration, C_i, increases with the decrease of the pressure interval Δp of each experiment and converges to the limit characteristic of the given C_i. This is also true in the case of the present system.

The values of t_* determined from the data of Fig. 2 and from other differential absorption data with about the same magnitude of Δp are plotted semi-logarithmically against C_i in Fig. 3*. For the sake of comparison, the corresponding data for other systems reported in the previous paper[1] are included in the figure. It is seen that the data for the present system are approximately linear and that the slope of this line is as steep as those for the other amorphous polymer-organic vapor systems indicated. It is of special interest that the plot for the A-PS-ethyl methyl ketone system is nearly

4) E. Jenckel and R. Heusch, *Kolloid-Z.*, **130**, 89 (1953).

* The magnitudes of Δp used in these differential absorption experiments are sufficiently small to give the values of t_* characteristic of a given C_i. This will be seen later in Fig. 6.

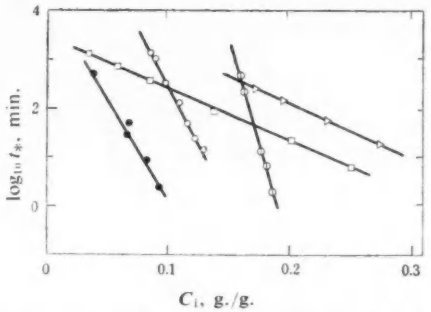

Fig. 3. Logarithmic correlation plots of t_* and initial concentration C_i for some polymer-vapor systems. t_* is the time corresponding to the inflection point of the second stage of the two-stage process:
○ A–PS-ethyl methyl ketone at 25°C;
◑ A–PS-benzene at 25°C;
● Polymethyl methacrylate-methyl acetate at 30°C;
□ Cellulose acetate-methyl acetate at 20°C;
△ Cellulose nitrate-acetone at 25°C.

parallel with that for the A–PS-benzene system at the same temperature. This suggests that for a given polymer the slope of $\log t_*$ vs. C_i plot is approximately independent of penetrant species. As noted above, it is generally conceived that the rate-determining factor for the second stage absorption process is the rate of relaxation of the polymer chains. Thus it appears reasonable that the second stage absorption process primarily reflects the characteristic relaxation-motion of the network chains of a given polymer, irrespective of any difference in penetrant species. This may explain the independence of the slope of $\log t_*$ vs. C_i plot upon penetrant species. The position of the $\log t_*$ vs. C_i plot for methyl ethyl ketone is in the region of values of C_i lower than that for benzene. This is the reflection of the fact that the value of C_i at which absorption curves change their shape from pseudo-Fickian to two-stage type is lower for the former system than for the latter.

Integral Absorptions. — We have studied integral absorptions by choosing the initial concentrations in the regions corresponding to the four types of differential absorption, i.e., sigmoid type, pseudo-Fickian type, two-stage type and Fickian type.

Fig. 4 gives data of integral absorptions from zero concentration, and this initial concentration corresponds to a differential absorption of sigmoid type. The integral absorption processes are sigmoid for all pressure intervals studied and the initial rate of desorption is greater than that of the corresponding absorption. The absorption curves show a pronounced dependence on the final concentration, C_f.

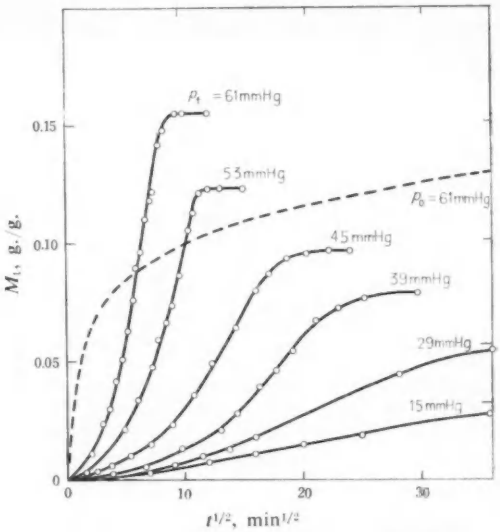

Fig. 4. Integral absorption and desorption curves from and to zero concentration. p_f is the final pressure of a particular run. Solid line, absorption; Dashed line, desorption.

In accordance with the treatment of the A–PS-benzene system[2], we chose the value of $1/(t/l^2)_{1/2}$ as a measure of the absorption rate of each curve, where l is the thickness of the film, t is time and $(t/l^2)_{1/2}$ is the value of t/l^2

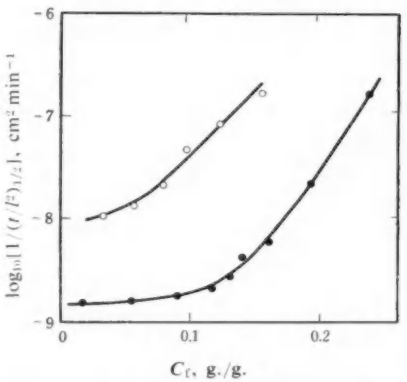

Fig. 5. Logarithmic correlation plots of $1/(t/l^2)_{1/2}$ and final equilibrium concentration C_f for A–PS-ethyl methyl ketone and for A–PS-benzene at 25°C. $(t/l^2)_{1/2}$ is the value of t/l^2 when the amount of vapor in polymer reaches one half of the final equilibrium value; l is the thickness of film and t is time. ○, A–PS-ethyl methyl ketone. ●, A–PS-benzene.

when the amount of vapor in the film reaches one half of the final equilibrium value. The values of $1/(t/l^2)_{1/2}$ determined from Fig. 4 are plotted semi-logarithmically against C_f in Fig. 5, where the corresponding data for benzene system are also included for the sake of comparison. We see that the values of $1/(t/l^2)_{1/2}$ for ethyl methyl ketone increase with increasing C_f and, though the slope of the curve is quite similar to that for benzene they are always higher than those for benzene when compared at fixed values of C_f. This fact implies that the rate of diffusion of ethyl methyl ketone into A-PS is faster than that for benzene in the region of C_f studied.

Integral absorptions from an initial concentration corresponding to a differential absorption of pseudo-Fickian type were investigated at C_i 0.055 g./g. Although the results are not given here, the shape of absorption curves for small values of Δp was of pseudo-Fickian type, and with further increase in Δp the absorption curves changed to the sigmoid type and this feature persisted up to the largest of the Δp investigated. The values of $1/(t/l^2)_{1/2}$ increased with the difference between the initial and final concentrations, $\Delta C(=C_f-C_i)$, and the dependence of $1/(t/l^2)_{1/2}$ upon ΔC was about the same as that obtained for the series of absorption curves from $C_i=0$.

Fig. 6 shows integral absorption curves from $C_i=0.100$ g./g. This C_i was in the region where differential absorption curves exhibited two-stage behavior. It is seen that for small Δp the curves are similar in shape and the values of t_* are practically the same. With further increase in Δp the inflection point on the second stage portion shifts markedly to the short time region. The two-stage behavior is still apparent at $p_f=62$ mmHg, but the absorption curve for $p_f=80$ mmHg exhibits a sigmoid character. For this C_i the absorption rates changed more mildly with ΔC than in the regions of C_i corresponding to differential absorptions of sigmoid and pseudo-Fickian types.

Integral absorptions and desorptions from an initial concentration corresponding to a differential absorption of Fickian type were studied at the critical concentration at which the A-PS-ethyl methyl ketone mixture undergoes the glass transition at the temperature of the experiment. The features of the curves obtained were those of the true Fickian diffussion in which the diffusion coefficient increases with increasing concentration. However, the results from experiments with films of various thicknesses revealed a thickness anomaly as in the case of the corresponding experiments with the A-PS-benzene system[2]. A detailed study of the sorption behavior in this region of C_i is now in progress in this laboratory and will be reported in near future. The dependence of $1/(t/l^2)_{1/2}$ on ΔC in this region of C_i was much milder than those in the regions of lower C_i corresponding to non-Fickian differential absorptions.

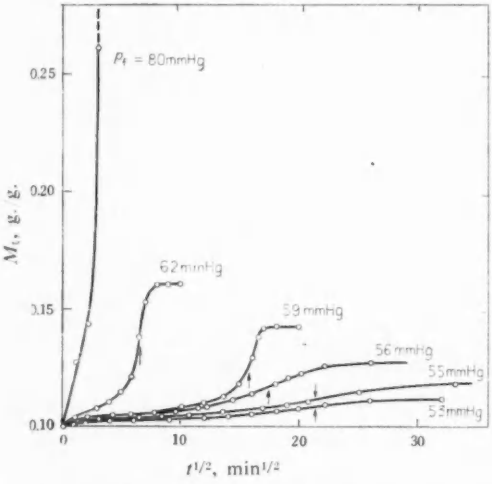

Fig. 6. Absorptions from a fixed non-zero initial concentration to different final pressures. p_f is the final pressure of a particular run. Initial pressure $p_i=47.5$ mmHg. The arrows indicate the positions of the inflection points of the second stage curves.

Summary

The successive differential absorptions for the A-PS-ethyl methyl ketone system change with the initial concentration according to the same scheme as that presented previously as typical systems of amorphous polymer-organic vapor; that is,

sigmoid type → pseudo-Fickian type
→ two-stage type → pseudo-Fickian type
→ Fickian type

The last transition, from pseudo-Fickian to Fickian types, for ethyl methyl ketone occurs at lower concentration than that for benzene. The second stage portion of the two-stage process shifts rapidly to the short time regions as the initial concentration of each step increases. The rate of this shift depends upon initial concentration in nearly the same manner as in the A-PS-benzene system. The general features of integral absorptions for the present system are very similar to those for benzene system, irrespective of the difference in the penetrant-polymer interaction between the two systems. The dependence of absorption rate

upon ΔC is also similar in general character to that for benzene system.

We wish to thank Professors H. Fujita, M. Kurata and Dr. A. Kishimoto of this University for their helpful advice during the course of this invesigation. The study reported in this paper was partly supported by the Ministry of Education, to which grateful acknowledgement is made.

Department of Industrial Chemistry
Faculty of Engineering
Kyoto University
Sakyo-ku, Kyoto

Infrared Spectra of Acyclic Imides. III. Infrared Dichroism of Dipropionamide and N-Acetylpropionamide Crystals

By Toyozo Uno and Katsunosuke Machida

(Received November 10, 1960)

In order to obtain information on the molecular structure of acyclic imides in the form B, infrared dichroic measurement has been made for dipropionamide and *N*-acetylpropionamide. These compounds were chosen as examples of the simplest acyclic imides being stable in the form B. Their oriented crystals were easily prepared on sodium chloride plates. Further evidences for the trans-trans planar structure[1] could be given to these molecules from the dichroic properties of the imide characteristic bands and some other bands. With the aid of these evidences, the splitting of the N–H stretching bands which is one of the important features in the infrared spectra of the form B, will be discussed in terms of the Fermi resonance.

Results and Discussion

Configurations of Imide Group and Molecular Symmetries.—Since the dichroic property of an infrared absorption band, if the molecule in question has any symmetry at all, depends on the symmetry of the vibrational mode from which the band arises, the interpretation of infrared dichroism should be closely related to molecular symmetry. In this connection, a brief survey of the relationship of molecular symmetry to the configurations of the –CONHCO– group will be presented here. In the trans-trans or the cis-cis configuration of this group, both the C–O bonds take an equivalent position with respect to the N–H bond. Consequently, as long as we are concerned with an isolated molecule, symmetrically substituted acyclic imides in the trans-trans configuration, as well as cyclic imides with polymethylene chains can be regarded to have the molecular symmetry C_{2v}. However, for actual molecules in the crystalline state, this is not always true exactly. For instance, although succinimide clearly takes the cis-cis configuration, those two C=O bonds in this molecule are not equivalent to each other regarding their nature in the crystalline state. The X-ray diffraction study[2] has shown that only one C=O bond for each molecule is involved in hydrogen bond, the other C=O bond not being so. Thus, just as in the case of diacetamide in the form A[3], every two molecules of succinimide form a ring dimer in the crystalline state. Furthermore, the five-membered ring of this molecule forms an oblique pentagon in which no two-fold axis exists. Speaking thus more strictly, the molecular symmetry of succinimide is not C_{2v} but C_s, in which only the plane of symmetry coinciding with the molecular plane remains. A similar situation may be seen for symmetrically substituted acyclic imides in the trans-trans configuration since they can exactly have the symmetry C_{2v} only if those two C–O bonds in the –CONHCO– group are equivalent to each other in their nature as well as in their configuration. Although we have shown that the infrared spectra of acyclic imides in the form B are reasonably interpreted in terms of the symmetry C_{2v}[1], it is not yet determined whether they exactly have the symmetry C_{2v} or whether the deviations from C_{2v} are too small to affect their infrared spectra. Under these situations,

1) T. Uno and K. Machida, This Bulletin, **34**, 545, 551 (1961).
2) R. Mason, *Acta Cryst.*, **9**, 405 (1956).
3) T. Watanabé and K. Osaki, unpulished.

the results of infrared dichroic measurements in the present study will be discussed on the basis of the approximation in which symmetrically substituted acyclic imides in the trans-trans configuration are regarded to have the symmetry C_{2v}. Discussions will also be made on the nature of the hydrogen bond in the form B which is closely related to whether those two C=O bonds in the –CONHCO– group are equivalent or not.

As shown in Figs. 1 and 2, dipropionamide

TABLE I. INFRARED DICHROISM OF DIPROPIONAMIDE

Frequency, cm^{-1}	Intensity*1 //	Intensity*1 ⊥	Assignments (species)
3500	w	—	1736×2 (A_1)
3280	vs	—	N–H stretch. (A_1)
3200	vs	—	1690+1504 (A_1)
3005	sh	—	1504×2 (A_1)
2992	s	s	C–H stretch.
2948	—	sh	
2923*2	—	m	
2875	—	w	
2693	w	—	1504+1180 (A_1)
1860	vw	—	?
1736	vs	vw	sym. imide I (A_1)
1690	sh	w	antisym. imide I (B_1)
1504	—	vs	imide II (B_1)
1459	m	m	CH_3 asym. def. (//: A_1, ⊥: B_1 and B_2)
1420	s	w	CH_2 bend. (//: A_1, ⊥: B_1)
1384	m	sh	CH_3 sym. def. (//: A_1, ⊥: B_1)
1367	—	s	CH_2 wag., imide II and imide III (B_1)
1263	w	w	//: C–N–C sym. stretch., CH_2 wag. (A_1); ⊥: CH_2 twist. (B_2)
1180	w	vs	imide III (B_1)
1080	—	w	C–C stretch. (//: A_1, ⊥: B_1)
1075	m	—	
1009	—	w	
994	m	—	CH_3 rock. (//: A_1, ⊥: B_1 or B_2)
955	w	w	
843	—	w	CH_2 rock. (⊥: B_2)
806	—	w	
732	—	w	imide V (B_2)

*1 vs: very strong, s: strong, m: medium, w: weak, vw: very weak, sh: shoulder.
*2 Probably due to the CH_2 out-of-phase stretch. (B_2) mode.

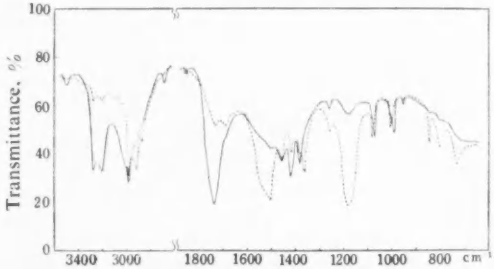

Fig. 1. Infrared dichroism of dipropionamide ($CH_3CH_2CONHCOCH_2CH_3$)
solid line: //, broken line: ⊥

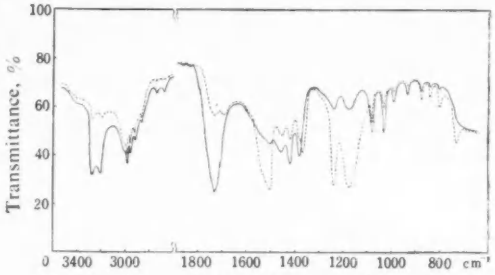

Fig. 2. Infrared dichroism of *N*-acetylpropionamide ($CH_3CH_2CONHCOCH_3$)
solid line: //, broken line: ⊥

TABLE II. INFRARED DICHROISM OF *N*-ACETYLPROPIONAMIDE

Frequency, cm^{-1}	Intensity //	Intensity ⊥	Assignments (species)
3280	vs	w	N–H stretch. (A')
3200	vs	w	1690+1504 (A')
3000	sh	sh	1504×2 (A')
2978	m	m	C–H stretch.
2960	m	m	
2920	w	w	
2875	w	w	
2750	w	—	1504+1240 (A')
2690	w	—	1504+1180 (A')
1734	vs	w	sym. imide I (A')
1690	—	w	antisym. imide I (A')
1504	vw	vs	imide II (A')
1458	m	w	CH_3 (β) asym. def. (A' or A'')
1419	m	w	CH_3 (α) asym. def. (A' or A''), CH_2 bend. (A')
1380	m	sh	CH_3 (α or β) sym. def. (A')
1370	—	s	CH_2 wag., imide II and imide III (A')
1240	w	vs	imide III (A')
1180	w	vs	imide III (A')
1081	m	w	C–C stretch. (A'); CH_3 rock. (A' or A''); CH_2 rock. (A'')
1035	m	w	
994	w	vw	
938	w	vw	
879	w	w	
845	vw	w	
808	vw	w	
733	—	w	imide V (A'')

and *N*-acetylpropionamide show marked infrared dichroism. Tables I and II show the dichroic properties of the absorption bands of these acyclic imides together with the assignments given to these bands. The symbols // and ⊥ are used for the polarized light with the electric vector parallel and perpendicular, respectively, to the elongation direction of the crystal. Since the molecular symmetry of dipropionamide (C_{2v}) and that of *N*-acetylpropionamide (C_s) are different from each other with respect to their alkyl groups, discussions will be made separately for these two compounds.

Dipropionamide.—As shown in Table I, the dichroic properties of the characteristic bands of dipropionamide in the sodium chloride region, previously assigned on the basis of the trans-trans configuration of the –CONHCO– group, are closely related to the symmetry species of these bands. That is to say, the bands belonging to A_1 species show parallel dichroism while the bands belonging to B_1 or B_2 species show perpendicular dichroism. In order to explain these facts, the following structure may be proposed for the crystal preparations. In this structure, the two-fold axis of each molecule is parallel to the elongation direction of crystal while there are molecules whose molecular planes are not perpendicular to the incident light. The latter situation may be realized by the uniaxial orientation of the crystallites even in a case where the unit cell consists only from molecules whose molecular planes are parallel to one another. It will now be shown that the consistency between the dichroic properties of individual characteristic bands and the proposed structure is quite sufficient. The marked parallel dichroism of the bands at 3280 and 3200 cm^{-1}, whose origin will be discussed later, may be taken as indicating that the direction of the N–H bond involved in hydrogen bond (i.e. the direction of the two-fold axis) is parallel to the elongation direction of the crystal. The strong band at 1736 cm^{-1} also shows marked parallel dichroism supporting the assignment to the C=O symmetric stretching mode (A_1) as well as the trans-trans configuration of the –CONHCO– group, in which all the N–H and the C=O bonds are nearly parallel to one another. The weak band at 1690 cm^{-1}, which has been assigned to the C=O antisymmetric stretching mode (B_1), seems to show perpendicular dichroism although this is not so obvious owing to the broadness of the adjacent strong band at 1736 cm^{-1}. On the other hand, the marked perpendicular dichroism of the imide II (1504 cm^{-1}) and the imide III (1180 cm^{-1}) band is consistent with the assignment to B_1 fundamentals whose vibrational transition moments are perpendicular to the plane of symmetry bisecting the angle C–N–C. The imide V band at 732 cm^{-1}, to which the N–H out-of-plane deformation vibration mainly contributes, shows perpendicular dichroism. If all the molecular planes in the crystal are perpendicular to the incident radiation, the band due to an out-of-plane vibration will not be observed, regardless of polarization. The proposed structure, however, may afford reasonable elucidation to the dichroic property of this band. The weak band at 1263 cm^{-1} shows no dichroism. This fact may be taken as indicating that the band showing parallel dichroism resulting from the C–N–C symmetric stretching vibration (A_1) is overlapped by a band due to B_1 or B_2 vibration. This is probable since the B_2 CH_2 twisting band may occur in this region.

Further evidences for the proposed structure are obtained from the dichroic properties of the bands due to the vibrations of the C–H bonds. In the region where the C–H stretching bands occur, no band shows appreciable dichroism except for the band at 2923 cm^{-1}, which shows perpendicular dichroism and may be assigned to the CH_2 out-of-phase stretching mode. If the C_{2v} trans-trans configuration is assumed for dipropionamide, each of the C–H stretching vibrations will belong to the following symmetry species shown in parentheses: the CH_2 symmetric (A_1, B_1), the CH_3 asymmetric (A_1, B_1, A_2, B_2), the CH_2 in-phase (A_1, B_1) and the CH_2 out-of-phase (A_2, B_2). Thus, the dichroic properties of the C–H stretching bands are consistent with the proposed structure. A similar situation is seen for the C–H deformation bands at 1459, 1420 and 1384 cm^{-1}, each of which occurs for the polarized light with the electric vector along the elongation direction of the crystal as well as for the light polarized perpendicular to this direction. However, the dichroic ratio $I_{//}/I_{\perp}$ of the band at 1420 cm^{-1}, which is due to the CH_2 bending vibrations, is appreciably greater than unity, indicating that the magnitude of the vibrational transition moment of the A_1 mode is greater than that of the B_1 mode. This fact is consistent with the proposed structure where a molecule of dipropionamide has two equivalent CH_2 groups. With respect to the bending vibration of the CH_2 group at either side of the N–H bond, the component of the vibrational transition moment parallel to the N–H bond (the two-fold axis) is greater than the perpendicular component. Thus, the interaction between this vibration and the same vibration of the other CH_2 group results in a greater change of dipole moment for the

in-phase (A_1) vibration than for the out-of-phase (B_1) vibration. The band at 1367 cm^{-1}, which disappears on deuteration, shows marked perpendicular dichroism. Possible vibrations which contribute to this band may be the B_1 CH_2 wagging, the N–H in-plane deformation, and the C–N–C antisymmetric stretching mode. Thus, we may notice that the coupling between the imide characteristic vibrations (the imide II and the imide III mode) and the C–H deformation vibrations takes place to some extent.

Generally speaking, for the bands which exhibit distinguished dichroism in the region 1800 to 900 cm^{-1}, there is a simple relation between the dichroic property and the behavior on deuteration. In other words, the bands showing perpendicular dichroism (1504, 1367, 1180, 1080 and 1009 cm^{-1}) shift, while the bands showing parallel dichroism (1736, 1075 and 994 cm^{-1}) do not shift on deuteration. This fact means that two propionyl groups in a molecule take an equivalent configuration with respect to the central N–H bond. There are three cases which satisfy this condition, namely, the symmetry C_2 with the two-fold axis coinciding with the N–H bond, the symmetry C_s with the plane of symmetry bisecting the angle C–N–C, and the symmetry C_{2v} with both of these symmetry elements. However, the first two are not likely since an appreciable angle between two C=O bonds in the –CONHCO– group is inconsistent with the weakness of the C=O antisymmetric stretching band at 1690 cm^{-1}.

As discussed in the previous section, the study only on the infrared spectra seems to be insufficient to estimate the deviation from the exact equivalence of these two C=O bonds. Furthermore, since the imide hydrogen atom is clearly involved in the hydrogen bond, the exact equivalence of the proton acceptors can not be attained without the presence of the so-called bifurcated hydrogen bond, whose existence, however, has been reported for few molecules[4]. Although more detailed investigations such as the X-ray diffraction study must be carried out to decide the exact feature of this hydrogen bond, it is here pointed out that molecular structures where both the bonded and the free C=O bond exist can hardly elucidate the experimental results up to the present study; for instance, the occurrence of only one strong C=O stretching band with comparatively high frequency (1736 cm^{-1}) and its parallel dichroism. The bands in the 3 μ region observed for these acyclic imides are very sharp in contrast with other cases where the bonded N–H stretching bands are very broad. Furthermore, the imide II band, which is partly due to the N–H in-plane deformation mode, is remarkably broad. It is suggested that these features may be closely related to the nature of hydrogen bonds in these acyclic imides in the form B.

***N*-Acetylpropionamide.** — The dichroic properties of the imide characteristic bands of *N*-acetylpropionamide are quite similar to those of the corresponding bands of dipropionamide. It is noticed here that both of the two imide III bands (1240 and 1180 cm^{-1}) of *N*-acetylpropionamide show the same perpendicular dichroism. Although this molecule has no two-fold axis, the vibrational transition moments of these bands are considered to be almost perpendicular to the N–H bond owing to the large amplitude of the N–H in-plane deformation vibration contributing to the vibrational modes of these bands. The weak antisymmetric imide I band, which has not been resolved from the strong symmetric imide I band at 1734 cm^{-1} in the spectrum of non-oriented sample, appears at 1690 cm^{-1} with the light with electric vector perpendicular to the elongation direction of the crystal. On the other hand, the clear-cut relation between the behavior on deuteration and the dichroic property which is seen for all the bands showing remarkable dichroism in the region 1800 to 900 cm^{-1} of dipropionamide, does not hold well for the bands in the region 1100 to 900 cm^{-1} of *N*-acetylpropionamide. That is to say, all the bands showing parallel dichroism (1081, 1035, 994 and 938 cm^{-1}), which may be due to the vibrations of alkyl groups, shift or split on deuteration. These results are consistent with the trans-trans configuration of the –CONHCO– group since *N*-acetylpropionamide in this configuration can be regarded to have the symmetry C_{2v} only in the approximation where the difference between the CH_3 and the CH_3CH_2 groups is neglected.

Fermi Resonance in the 3 μ Region.—On the basis of the planar trans-trans configuration, the origin of the splitting of the N–H stretching bands of these acyclic imides in the form B will now be discussed. From the spectral features of the *N*-deuterated species in the region 2500 to 2300 cm^{-1}, where no more than one strong band appears, it is obvious that the situation giving rise to this splitting must be what vanishes on deuteration. From this point of view, the band near 3280 cm^{-1} is assigned to the N–H stretching mode and the band near 3200 cm^{-1} to a combination band of some lower fundamentals enhanced by Fermi resonance with the N–H stretching mode. Other possible reasons for the splitting of the band

4) For instance, see R. Marsh, *Acta Cryst.*, **11**, 662 (1958).

Table III. The combination frequencies of the *N*-deuterated species of saturated acyclic imides near 2300 cm^{-1}

Compound	Frequency cm^{-1}	Intensity	Imide II′ frequency cm^{-1}	Imide III′ frequency cm^{-1}
Diacetamide-*d*	2295	w	1348	951
N-Acetylpropionamide-*d*	2300	w	1329	961
Dipropionamide-*d*	2283	m	1304	986
N-Propionyl-*n*-butyramide-*d*	2290	w	1307	987
Di-*n*-butyramide-*d*	2300	w	1332	985
Di-*n*-butyramide-*d*	2283	w	1314	985

in the 3 μ region, such as the intermolecular interaction in the unit cell, or the presence of two species of hydrogen bonds, must hold equally well for the undeuterated and the *N*-deuterated species to give rise to the splitting of the N–D stretching band of the latter. It is also difficult to explain the same parallel dichroism of these two bands near 3280 and 3200 cm^{-1} from these reasons. On the other hand, regarding whether appropriate fundamentals giving rise to an overtone or a combination tone in the regions in question exist or not, the situation for the undeuterated species is obviously different from that for the *N*-deuterated species. As the fundamentals which combine to give rise to the band near 3200 cm^{-1}, the antisymmetric imide I band (near 1700 cm^{-1}) and the imide II band (near 1500 cm^{-1}) are the most reasonable ones. In the C_{2v} approximation for the planar trans-trans configuration, these two bands belong to the B_1 species. Thus, it may be expected that the N–H stretching vibration (A_1) is involved in Fermi resonance with the combination tone of these two frequencies to give rise to two bands showing parallel dichroism in the 3 μ region just as has been observed. The constant frequencies of these lower fundamentals (near 1700 and 1500 cm^{-1}) throughout all of these acyclic imides result in a practically identical feature of the bands near 3280 and 3200 cm^{-1}. Similar Fermi resonance has already been reported for both the trans and the cis configuration of monosubstituted amides[5,6]. For the *N*-deuterated species of these acyclic imides in the form B, one or two weak bands sometimes appear near 2300 cm^{-1}. In contrast with the band near 3200 cm^{-1} for the undeuterated species, appreciable differences in frequencies and intensities of these weak bands are observed among the *N*-deuterated species of these acyclic imides. These bands may be assigned to the combination tones of the imide II′ and the imide III′ bands which also belong to the B_1 species. The imide II′ and the imide III′ frequencies of the *N*-deuterated species of these acyclic imides in the form B are appreciably different from one another and give rise to their combination bands in a somewhat different manner regarding both the frequencies and the intensities. These combination frequencies are shown in Table III, where good correspondences of these frequencies to the sums of the imide II′ and the imide III′ frequencies are observed.

5) R. M. Badger and A. D. E. Pullin, *J. Chem. Phys.*, **22**, 1142 (1954); M. Beer, H. B. Kessler and G. B. B. M. Sutherland, ibid., **29**, 1097 (1958).
6) T. Miyazawa, *J. Mol. Spectroscopy*, **4**, 168 (1960).

Conclusion

By the examination of infrared dichroism of dipropionamide and *N*-acetylpropionamide, not only the assignments previously given to the characteristic and the C–H deformation bands have been confirmed, but further information concerning some other bands has also been obtained on the basis of the trans-trans configuration of the –CONHCO– group. Although some of the assignments proposed in the present study may be tentative, it seems significant that nearly all the infrared active vibrations in the sodium chloride region for the structure in question could have been attributed to the bands observed in this region.

The origin of the splitting of the N–H stretching band has been made clear in terms of Fermi resonance from the dichroic properties and the behavior on deuteration of these bands although there remains an interesting problem in regard to the nature of the hydrogen bond in which the N–H and the C=O bonds may be involved.

Experimental

Materials.—Oriented crystallites of *N*-acetylpropionamide and those of dipropionamide from molten liquid were prepared on sodium chloride plates with the application of temperature gradient. Their infrared spectra were confirmed to be identical with those of the crystals from petroleum ether in the paste method.

Dichroic Measurement.—The Hitachi EPI-2 infrared spectrophotometer with the sodium chloride prism, the IM-2P infrared microilluminator and the silver chloride transmission polarizer were used.

The measurements were carried out in the region 4000 to 650 cm^{-1}. The 1 m. gas cell was inserted in the path of the reference beam. The application of the radiations polarized parallel and perpendicular to the elongation direction of the crystal was attained with the rotation of the polarizer by 90°. The 100% line was adjusted by the attenuator for each radiation. Other conditions were similar to those described in the preceding papers[1].

The authors express their thanks to Dr. T. Miyazawa of Osaka University and to Dr. K. Nakamura of the Research Laboratory, Dainihon & Co. Ltd., for their frequent kind advice. Thanks are also due to Dr. H. Tadokoro of Osaka University and to Mr. K. Tatsuka of Osaka Custom House for infrared dichroic measurements.

Faculty of Pharmacy
Kyoto University
Sakyo-ku, Kyoto

Spectrophotometric Determination of Uranium with Sodium 2'',6''-dichloro-4'-hydroxy-3,3'-dimethylfuchsone-5,5'-dicarboxylate

By Yukiteru KATSUBE, Katsuya UESUGI and John H. YOE

(Received November 24, 1960)

For the colorimetric determination of uranium, various organic reagents have been used: sodium salicylate[1], tannic acid[2], thioglycollic acid[3], oxine[4-6], chromotropic acid[7-9], dimethyldithiocarbamate[10], dibenzoylmethane[11-15], morin[16], acetylacetone[17], thorin[18], neothorin[19] and arsenazo[20-21].

In this paper, a new method is described for the colorimetric determination of small amounts of uranium. It is based on the colored complex formation between uranyl ions and sodium 2'', 6''-dichloro-4'-hydroxy-3,3'-dimethylfuchsone-5, 5'-dicarboxylate. This compound has recently been used for the determination of beryllium, iron and copper and observations suggested a possibility that it could also be used for uranium[22].

1) H. Muller, *Chemiker Ztg.*, **43**, 739 (1919).
2) P. N. Das Gupta, *Analyst*, **55**, 154 (1930).
3) W. H. Davenport and P. F. Thomason, *Anal. Chem.*, **21**, 1093 (1949).
4) A. A. Smales and H. N. Wilson, *U. S. Atomic Energy Comm. Report*, BR-150, Feb. 22 (1943).
5) E. F. Orelemann, ibid., CD-2228, Feb. 26 (1945).
6) C. L. Rulfs, A. K. De, J. Lakritz and P. L. Elving, *Anal. Chem.*, **27**, 1802 (1955).
7) W. B. Mason and N. H. Furman, *U. S. Atomic Energy Comm. Report*, A-1057, Sec. 2E, Sept. 30 (1944).
8) E. Ware, ibid., MDDC-1432, Aug. 20 (1945).
9) A. K. Mukerjee, *J. Indian Chem. Soc.*, **35**, 113 (1958).
10) R. J. Lacoste, M. H. Earing and S. E. Wiberly, *Anal. Chem.*, **23**, 871 (1951).
11) J. H. Yoe, F. Will and R. A. Black, *Anal. Chem.*, **25**, 1200 (1953).
12) R. Pribil and M. Jelinek, *Chem. listy*, **47**, 512 (1953).
13) P. Blanquet, *Anal. Chim. Acta*, **16**, 44 (1957).
14) C. A. Francois, *Anal. Chem.*, **30**, 50 (1958).
15) C. A. Horton and J. C. White, *Anal. Chem.*, **30**, 1779 (1958).
16) M. T. Beck and E. Hantos, *Acta. Chim. Acad. Sci. Hung.*, **8**, 233 (1955).

Experimental

The spectrophotometer and photoelectric photometer were the same as those used in our previous work[22].

Ion Exchange Resin.—Tube, 10 mm. in diameter, with a high-porosity glass filter disk fused to the lower end was used. The resin was a quaternary ammonium anion exchange type, a modification of Amberlite IRA-410. Before use, the resin was converted into the sulfate form by treating it with 10% sulfuric acid. The treated resin was washed with distilled water until the effluent solution was neutral. The resin was added to the tube with distilled water to give a column height of 15 cm.

Uranium Standard Solution.—A standard stock solution of uranium was prepared by dissolving uranyl nitrate in distilled water. The solution contained 100 γ of uranyl ions per milliliter.

Reagent Solution.—A 0.2% reagent solution was prepared by dissolving sodium 2'', 6''-dichloro-4'-hydroxy-3, 3'-dimethylfuchsone-5, 5'-dicarboxylate in 99% ethanol.

***p*-Nitrophenol Indicator.**—A 0.4% solution was prepared by dissolving *p*-nitrophenol in distilled water.

All other chemicals were of analytical reagent grade.

17) A. Kirshen and H. Freiser, *Anal. Chem.*, **29**, 288 (1957).
18) J. K. Foreman, C. J. Riley and T. D. Smith, *Analyst*, **82**, 89 (1957).
19) S. Shibata and T. Matsumae, This Bulletin, **31**, 377 (1958).
20) J. S. Fritz and M. J. Richard, *Anal. Chim. Acta.*, **20**, 164 (1955).
21) H. P. Holcomb and J. H. Yoe, *Anal. Chem.* **32**, 616 (1960).
22) Y. Katsube, K. Uesugi and J. H. Yoe, This Bulletin, **34**, 72 (1961).

Separation of Interfering Ions.—Uranium was separated from other ions according to Fisher's procedure[23].

Procedure for Determination of Uranium.—Pipet 23 ml. of a slightly acidified sample solution, which has been adjusted so as to contain 1 to 10 γ uranium per milliliter, and one drop of *p*-nitrophenol indicator solution to a 25 ml. volumetric flask. Add 0.05 N sodium hydroxide solution dropwise until the indicator just turns yellow, then discharge yellow color by careful addition of 0.05 N hydrochloric acid dropwise. The resultant solution should be adjusted to pH 5.2±0.4. Add one milliliter of the reagent solution, shake well, make up to the mark with distilled water and mix thoroughly. Measure the absorbance at 610 mμ, after ten minutes, using distilled water as reference. Determine the weight or the concentration of uranium in the sample from a calibration curve prepared by the same procedure used for the sample.

Results and Discussion

Absorption Spectra.—Color reactions between many ions and sodium 2'',6''-dichloro-4'-hydroxy-3, 3'-dimethylfuchsone-5, 5'-dicarboxylate were recorded in our previous paper[22]. Uranyl ions react with the compound to give a blue complex in dilute acid solution. Absorption spectra of the compound in a solution and of its uranyl complex are shown in Fig. 1.

The maximum absorption of the uranyl complex solution occurs at 610 mμ. The reagent solution has little or no absorption at this wavelength. A large excess of the reagent must be avoided because its solution has a slight absorption at 610 mμ when the concentration is greater than about 80 p.p.m. It is not necessary, however, to use the same concentration of the reagent for standards and unknowns, when the concentration of unreacted reagent is in range of 80 to 40 p.p.m.

Molar Ratio.—The colored complex in solution was found to have a molar ratio of 2 to 1, reagent to uranyl ions. The mole ratio method[24] and the continuous variation method[25-26] were used to establish the molar ratio. The continuous variation method was applied by mixing X ml. of 3.7×10^{-3} M reagent solution and $(1.00-X)$ ml. of uranyl solution of 3.7×10^{-3} M and diluting to 25 ml. after adjusting to pH 5.2. The results are shown in Figs. 2 and 3.

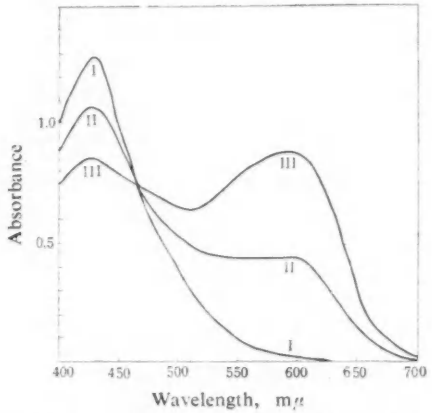

Fig. 1. Absorption spectra of the reagent solution and of its uranyl complex. pH 5.2.
I : Reagent 80 p.p.m.
II : Reagent (80 p.p.m.)+U(4.0γ/ml.)
III: Reagent (80 p.p.m.)+U(8.0γ/ml.)

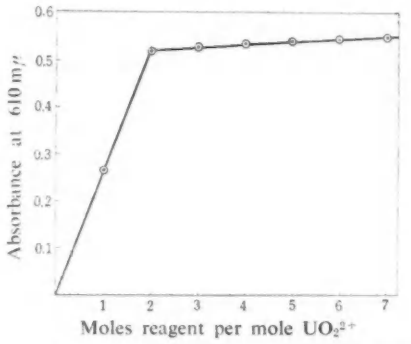

Fig. 2. Mole ratio method showing a ratio of 2 to 1, reagent to UO_2^{2+}, in the colored complex. pH 5.2.

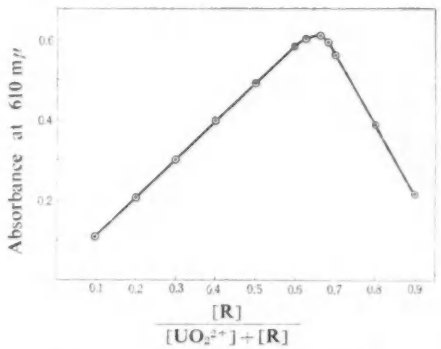

Fig. 3. Continuous variation method showing a ratio of 2 to 1, reagent to UO_2^{2+}, in the colored complex. pH 5.2.

23) S. Fisher, U. S. Atomic Energy Comm., Document RMO-2530 (1954).

24) J. H. Yoe and A. L. Jones, *Ind. Eng. Chem., Anal. Ed.*, **16**, 111 (1944).
25) P. Job, *Ann. chim.*, (10), **9**, 113 (1928).
26) W. C. Vosburgh and G. R. Cooper, *J. Am. Chem. Soc.*, **63**, 437 (1941).

Effect of pH.—The effect of pH on the color reaction was examined by measuring the absorbance of a colored solution, at 610 mμ, containing 3.52 p.p.m. of uranium and 80 p.p.m. of the reagent, the pH being adjusted by adding dilute hydrochloric acid or dilute sodium hydroxide solution. The uranyl complex has a maximum intensity in the pH range 4.8 to 5.8 as shown in Fig. 4.

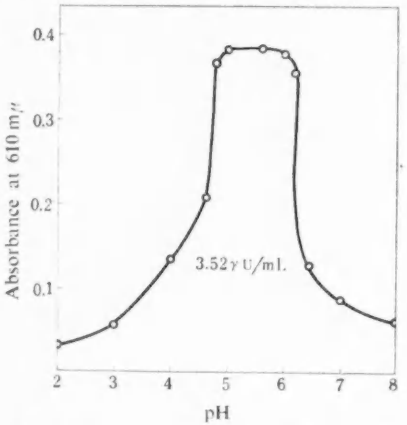

Fig. 4. Effect of pH on the uranyl complex.

A pH of 5.2±0.4 should be used when making absorbance measurements of the complex.

Several buffer solutions were tried: borax-succinic acid, acetate-acetic acid, phthalate, and phosphate buffers were unsatisfactory. All lowered the color intensity of the complex. Dilute hydrochloric acid and sodium hydroxide solution were satisfactory for pH adjustment with *p*-nitrophenol as indicator.

Rate of Color Formation.—Within the optimum pH range (5.2±0.4), the color intensity reaches a maximum in ten minutes and remains unchanged for about an hour. It is necessary, therefore, to allow the colored solution to stand at least ten minutes and then to measure the absorbance within an hour.

Effect of Temperature.—There is no variation in the absorbance of the colored complex over a temperature range 15 to 30°C.

Interfering Ions.—The reagent was tested on a spot plate[22]. Twelve ions were found to interfere: Al^{3+}, Be^{2+}, Cu^{2+}, Fe^{2+}, Fe^{3+}, Ga^{3+}, Gd^{3+}, Nd^{3+}, Ni^{2+}, Pr^{3+}, Sc^{2+} and Y^{3+}. The effect of some common ions on the determination of uranium is shown in Table I. The limiting concentration was taken to be one that causes a deviation of more than 0.01 unit in the absorbance of a solution containing 5.28 γ uranium per milliliter.

TABLE I. EFFECT OF DIVERSE IONS

Ion	Added as	Limiting concentration, γ ions per milliliter
Al^{3+}	sulfate	0.02
Be^{2+}	chloride	0.02
Ca^{2+}	chloride	>1500
Cu^{2+}	sulfate	1
Cr^{3+}	sulfate	150
Fe^{2+}	Mohr's salt	2
Fe^{3+}	iron alum	0.8
Ni^{2+}	nitrate	80
Mg^{2+}	chloride	>1500
Zn^{2+}	chloride	>1000

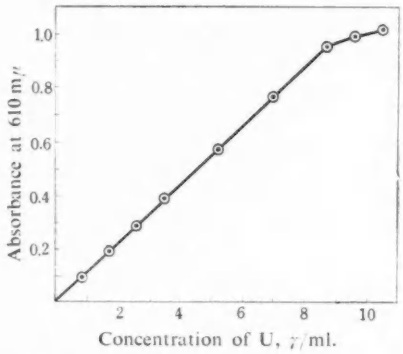

Fig. 5. Beer's law curve. pH 5.2.

TABLE II. DETERMINATION OF URANIUM

Solution analyzed		Added γ/50 ml.	Found U* γ	Error %
1	Al^{3+}	200		
	Be^{2+}	50		
	Fe^{2+}	200		
	Fe^{3+}	200		
	U	132.0	130.0	−0.2
2	Al^{3+}	1000		
	Be^{2+}	200		
	Fe^{3+}	500		
	U	176.0	169.6	−3.6
3	Al^{3+}	1000		
	Be^{2+}	500		
	Cu^{2+}	1000		
	Cr^{3+}	1000		
	Fe^{2+}	1000		
	Ni^{2+}	1000		
	U	44.0	45.8	−4.1

* These values are the averages of 5 replicate determinations.

Several methods were tried to eliminate interfering ions. The method proposed by Fisher[23] was adopted. It makes use of an anion exchange resin as mentioned in this paper. Ferric ions are reduced to ferrous

ions with sulfurous acid before passing the sample solution through the resin column.

Beer's Law.—Beer's law is obeyed up to about 8.8 γ of uranium per milliliter (See Fig. 5).

Determination of Uranium in Synthetic Solutions Containing Other Ions.—The determination of uranium in the presence of certain other ions was made. The results are given in Table II.

Summary

A procedure has been developed for the spectrophotometric determination of small amounts of uranium with sodium 2'',6''-dichloro-4'-hydroxy-3,3'-dimethylfuchsone-5,5'-dicarboxylate. Beer's law is obeyed up to about 9 γ of uranium per milliliter. The accuracy and precision are satisfactory. Interference of foreign ions is eliminated by using an anion exchange resin.

Himeji Technical Institute
Idei-600, Himeji
(Y. K & K. U.)

John Lee Pratt Trace Analysis Laboratory
University of Virginia
Charlottevill Va.
U. S. A.
(J. H. Y.)

Studies on Metal Complex Species Using an Anion Exchange Resin. I. Derivation of Equations and Application to Mercury(II)-Nitrate Complex

By Hirohiko WAKI

(Received October 10, 1960)

An equation and a method for determining the composition of metal complex species using an anion exchange resin have been developed by Kraus et al.[1,2] These are mostly applicable[3] in the case where a stable negatively-charged complex ion of a metallic element is formed even in a dilute solution and adsorbed in the same form as that in the solution when it is in contact with the resin. On the other hand, it is also often observed that a metallic element may be significantly adsorbed on an anion exchange resin even from a solution in which the presence of any complex anion seems hardly to be considered. In this case it is likely enough that a metal ion or a low complex ion of the metallic element enters the resin phase and then converts itself there into a complex anion or a higher complex ion respectively, because the resin phase may be regarded as a kind of extremely concentrated solution of electrolytes. Accordingly, the complex formation in such a case should rather depend directly on the concentration of an anion as a ligand and on the ionic strength in the resin phase. In this paper an equation for determining the composition of metal complex species, including the cases mentioned above, will be derived by introducing the complex formation equilibrium in the resin phase and applied to mercury-nitrate complex taken up by anion exchange resin.

1) K. A. Kraus and G. E. Moore, *J. Am. Chem. Soc.*, 73, 9 (1951).
2) K. A. Kraus and F. Nelson, "Anion Exchange Studies of the Fission Products" in "Peaceful Uses of Atomic Energy", Proceedings of the International Conference in Geneva, Vol. 7, p. 113 (1955) (United Nations).
3) S. Misumi and T. Taketatsu, This Bulletin, 32, 876 (1959).

Derivation of Equations

Since the ion exchange can be theoretically treated as a Donnan equilibrium, the following relationship holds between the ion concentrations in the resin phase [ ] and in the external solution ( ) in the equilibrium state:

$$[M^{a+}]\,[X^{b-}]^{a/b}\gamma_{[M]}^{a,b}\gamma_{[X]}^{a,b} = (M^{a+})\,(X^{b-})^{a/b}\gamma_{(M)}^{a,b}\gamma_{(X)}^{a,b} \qquad (1)$$

where M^{a+} and X^{b-} represent a metal ion and an anion respectively, and γ stands for the activity coefficient of the ion given as subscript. When a complex ion $MX_m^{(bm-a)-}$ is formed in the external solution, the formation constant is defined by

$$K_m = \frac{(MX_m^{(bm-a)-})}{(M^{a+})\,(X^{b-})^m} \cdot \frac{\gamma_{(MX_m^{(bm-a)-})}}{\gamma_{(M)}\gamma_{(X)}^m} \qquad (2)$$

Since the resin phase may be regarded as a concentrated aqueous solution of electrolytes, the formation constant may also be defined by

$$K_n = \frac{[MX_n^{(bn-a)-}]}{[M^{a+}][X^{b-}]^n} \cdot \frac{\gamma_{[MX_n^{(bn-a)-}]}}{\gamma_{[M]}\gamma_{[X]}^n} \quad (3)$$

for a complex ion $MX_n^{(bn-a)-}$ in the resin phase, in analogy to Eq. 2. For the purpose of the determination of the complex form, the formation equilibria in both phases should be taken into account.

The distribution coefficient may be defined at

$$D = \sum[M]/\sum(M) \quad (4)$$

where $\sum[M]$ and $\sum[M]$ are the total stoichiometric concentrations of the metallic element in the resin and the solution phase (irrespective of species). If it is assumed for simplicity that the greater part of the metallic element in the resin exists in the form $MX_n^{(bn-a)-}$ and in the solution in the form $MX_m^{(bm-a)-}$ (generally n is not equal to m), the coefficient may be written as

$$D \doteqdot \frac{[MX_n^{(bn-a)-}]}{(MX_m^{(bm-a)-})} \quad (5)$$

From Eqs. 1, 2, 3 and 5 the following equation is derived:

$$D = \frac{[X^{b-}]^{n-a/b}}{(X^{b-})^{m-a/b}} \cdot \frac{K_n}{K_m} \cdot \frac{\gamma_{(MX_m^{(bm-a)-})}\gamma_{[X]}^{n-a/b}}{\gamma_{[MX_n^{(bn-a)-}]}\gamma_{(X)}^{m-a/b}} \quad (6)$$

or

$$\log D = (n - \frac{a}{b})\log[X^{b-}] - (m - \frac{a}{b})\log(X^{b-}) + K + G \quad (7)$$

where

$$K = \log\{K_n/K_m\}$$

$$G = \log\frac{\gamma_{(MX_m^{(bm-a)-})}\gamma_{[X]}^{n-a/b}}{\gamma_{[MX_n^{(bn-a)-}]}\gamma_{(X)}^{m-a/b}}$$

And

$$\frac{d\{\log D + (m - a/b)\log(X^{b-})\}}{d\log[X^{b-}]} = n - \frac{a}{b} \quad (8)$$

$$\frac{d\{\log D - (n - a/b)\log[X^{b-}]\}}{d\log(X^{b-})} = -(m - \frac{a}{b}) \quad (9)$$

when K and G are constant. When m is known and D, (X^{b-}) and $[X^{b-}]$ are measurable, n can be determined graphically, and m is also obtained when n is known. Even if both are unknown, one of them can be determined in a case where either (X^{b-}) or (X^{b-}) can be kept constant.

Although it is practically impossible to set a condition in which the activity coefficient term is strictly constant, this condition may be realized roughly when a small quantity of the metallic element is used and the ionic strengths in the two phases are each kept constant by the addition of an indifferent anion, and therefore the complex form may be determined through measurements in the range where the greater part of the anion given is X^{b-}.

In the case of the mercury(II)-nitrate complex in the presence of sodium nitrate and perchlorate, where Hg^{2+} is taken as M^{a+}, NO_3^- as X^{b-} and ClO_4^- as an additional anion, Eq. 7 may become as follows:

$$\log D = (n-2)\log[NO_3^-] - (m-2)\log(NO_3^-) + K + G \quad (10)$$

Assuming that a mercuric ion does not form any metal-nitrate complex species in a moderately concentrated aqueous solution of nitrates, the following equations may be applicable,

$$\log D - 2\log(NO_3^-) = (n-2)\log[NO_3^-] + K + G \quad (11)$$

and

$$\frac{d\{\log D - 2\log(NO_3^-)\}}{d\log[NO_3^-]} = n - 2 \quad (12)$$

where K and G are constant. From the slope of the curve $\log D - 2\log(NO_3^-)$ vs. $\log[NO_3^-]$, n can be determined. When n is not in the vicinity of an integer, the coexistence of two complexes may be presumed.

Experimental

Sodium nitrate solution and sodium perchlorate solution were prepared from the guaranteed and the first class reagent, respectively. Mercuric nitrate solution was prepared by dissolving the guaranteed reagent $Hg(NO_3)_2 \cdot 1/2 \sim 1\ H_2O$ in diluted nitric acid. These solutions were added to the resin so that the mixture of solutions had a volume of 10 ml., and contained 0.1 mmol. of mercury, 0.5 mmol. of nitric acid and a series of $NaNO_3 + NaClO_4$ of various mixing ratios, providing that its total concentration was constant at individual series.

An anion exchanger Dowex 1-X8 of nitrate form was swollen in water and then filtered under suction, followed by the removal of the attached water by pressing between filter papers. Two or three grams of this resin was at once put in a stoppered small glass vessel. At the same time another 0.5 g. of this resin was converted into

chloride form in a small column and its exchange capacity was determined by the elution of the chloride ion with a sodium nitrate solution and by Mohr's titration of the effluent. The resin set in this way have a relatively constant exchange capacity and does not suffer an appreciable change in volume when it comes in contact with nitrate solution.

The batch experiment was carried out at total concentrations of the solution of 0.5, 1, 2, 3 and 5 M, and each series consisted of 4—6 batches of various nitrate concentrations. The resin and the solution were equilibrated at room temperature by being allowed to stand for an hour with frequent shaking.

After the supernatant liquid was directly taken for the dilute solution or the resin was separated from the solution by filtering with a glass filter under suction without further washing for the concentrated solution, the mercury in the solution was titrated as follows: mercury in 5 ml. of the supernatant or the filtrate was titrated with 0.0100 M EDTA solution after 1 ml. of 0.05 M Mg-EDTA, 1 ml. of NH_4OH-NH_4Cl buffer (pH=10) and a few drops of Eriochrome Black T indicator were added. The amount of mercury in the resin was estimated by subtraction of that in the solution from the total amount. The distribution coefficient was calculated as

$$D=\frac{\left(\begin{array}{c}\text{millimole of Hg adsorbed per}\\ \text{milliequivalent of the resin}\end{array}\right)}{\left(\begin{array}{c}\text{millimole of Hg per milliliter}\\ \text{of the solution}\end{array}\right)}$$

On the other hand, the nitrate in the resin was determined spectrophotometrically as follows: the resin separated from the solution in the way described above was wrapped in a filter paper and pressed to remove the solution attached to the surface. About 1 g. of this resin was transferred into a short column, and then the nitrate ions were desorbed by 25 ml. of 2 M perchloric acid. The effluent was diluted to 50 ml. and its absorbance was measured at 300 mμ using the Shimadzu spectrophotometer QB-50. As shown by the calibration curve in Fig. 1, it may be recognized that the absorption of nitrate ion in the region $\sim 10^{-1}$ M in the presence of 1 M perchloric acid obeys Beer's law. The presence of mercuric, sodium and perchlorate ions has no effect. The exchange capacity of resin in the column was determined in the same way as was done before, for the purpose of estimating the total amount of nitrate in the resin. The amount of nitrate in the solution was estimated by subtraction. The nitrate concentration in the resin phase was represented as millimole of the ion per milliequivalent of the resin as in the calculation of D, because the quantity of an ion adsorbed per apparent weight of the resin is not suitable for a representation of concentration in a mixed solution system, since the density of resin varies with the nitrate-perchlorate exchange.

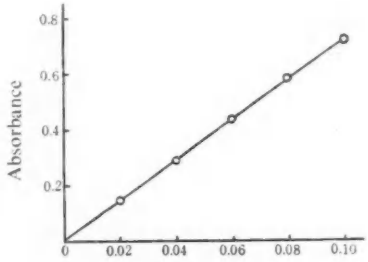

Fig. 1. The calibration curve of nitrate ion in the 1 M perchloric acid by spectrophotometric measurement at 300 mμ.

Results and Discussion

Data of the measurement and the calculation are tabulated in Table I. $[NO_3]^*$ from spectrophotometric measurement means the total nitrate concentration in the resin phase i. e., the sum of concentrations of the free nitrate ion and the nitrate ion bound to the mercuric ion. Accordingly, the free nitrate ion concentration is represented by

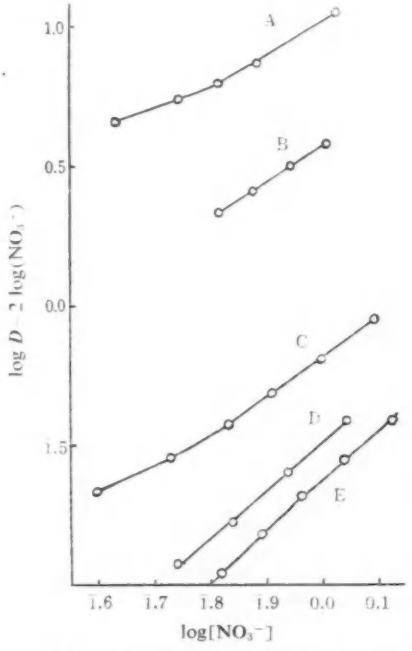

Fig. 2. Determination of n at various total concentrations of the external solution in the nitrate-rich range. The rightest point in each curve is one in the absence of perchlorate.
Total external concentration: A: 0.5 M, B: 1 M, C: 2 M, D: 3 M and E: 5 M.

$$[NO_3^-] = [NO_3]^* - n[Hg]$$

assuming that almost all mercury in the resin exists as $Hg(NO_3)_n^{(n-2)-}$. Since n is still unknown, $[NO_3^-]$ is practically estimated by

$$[NO_3^-] = [NO_3]^* - n^*[Hg]$$

where n^* represents an approximate value of n, which may be obtained by $\log D - 2\log(NO_3^-)$ vs. $\log[NO_3]^*$ plot. A little deviation of n^* from n may hardly affect $[NO_3^-]$ and therefore the value of n.

In Fig. 2, $\log D - 2\log(NO_3^-)$ is plotted

TABLE I

A. 0.5 M series

Resin: 4.68 meq.
Solution: 10 ml.

Batch No.	1	2	3	4	5
$NaNO_3$ given, mmol.	1.80	2.40	3.00	3.60	4.80
$NaClO_4$ 〃, 〃	3.00	2.40	1.80	1.20	0.00
HNO_3 〃, 〃	0.50	0.50	0.50	0.50	0.50
$Hg(NO_3)_2$ 〃, 〃	0.105	0.105	0.105	0.105	0.105
(Hg), mmol./ml.	0.00678	0.00632	0.00584	0.00538	0.00448
[Hg], mmol./meq.	0.00795	0.00893	0.00996	0.01094	0.01286
D, ml./meq.	1.17	1.41	1.71	2.04	2.87
$[NO_3]^*$, mmol./meq.	0.452	0.582	0.686	0.804	1.107
(NO_3^-), mmol./ml.	0.507	0.507	0.518	0.523	0.500
$\log D - 2\log(NO_3^-)$	0.659	0.740	0.803	0.872	1.060
n^*[Hg], mmol./meq. ($n^*=3.2$)	0.026	0.029	0.032	0.036	0.041
$[NO_3^-]$, mmol./meq.	0.426	0.553	0.654	0.767	1.065
$\log[NO_3^-]$	$\bar{1}.629$	$\bar{1}.743$	$\bar{1}.815$	$\bar{1}.885$	0.027

B. 1 M series

Resin: 4.72 meq.
Solution: 10 ml.

Batch No.	1	2	3	4
$NaNO_3$ given	7.60	8.40	9.20	10.00
$NaClO_4$ 〃	2.40	1.60	0.80	0.00
HNO_3 〃	0.50	0.50	0.50	0.50
$Hg(NO_3)_2$ 〃	0.105	0.105	0.105	0.105
(Hg)	0.00544	0.00484	0.00418	0.00370
[Hg]	0.01072	0.01199	0.01338	0.01440
D	1.97	2.48	3.20	3.89
$[NO_3]^*$	0.687	0.794	0.922	1.068
(NO_3^-)	0.954	0.983	1.003	1.014
$\log D - 2\log(NO_3^-)$	0.336	0.409	0.502	0.578
n^*[Hg] ($n^*=3.3$)	0.035	0.039	0.043	0.047
$[NO_3^-]$	0.652	0.755	0.879	1.021
$\log[NO_3^-]$	$\bar{1}.814$	$\bar{1}.878$	$\bar{1}.944$	0.009

C. 2 M series

Resin: 6.90 meq.
Solution: 10 ml.

Batch No.	1	2	3	4	5	6
$NaNO_3$ given	14.0	15.2	16.4	17.6	18.8	20.0
$NaClO_4$ 〃	6.0	4.8	3.6	2.4	1.2	0.0
HNO_3 〃	0.50	0.50	0.50	0.50	0.50	0.50
$Hg(NO_3)_2$ 〃	0.102	0.102	0.102	0.102	0.102	0.102
(Hg)	0.00670	0.00598	0.00524	0.00450	0.00384	0.00320
[Hg]	0.00507	0.00612	0.00719	0.00826	0.00922	0.01014
D	0.76	1.02	1.37	1.84	2.40	3.17
$[NO_3]^*$	0.414	0.555	0.706	0.841	1.030	1.287
(NO_3^-)	1.88	1.90	1.91	1.94	1.93	1.87
$\log D - 2\log(NO_3^-)$	$\bar{1}.333$	$\bar{1}.454$	$\bar{1}.574$	$\bar{1}.688$	$\bar{1}.810$	$\bar{1}.957$
n^*[Hg] ($n^*=3.5$)	0.018	0.021	0.025	0.029	0.032	0.035
$[NO_3^-]$	0.396	0.534	0.681	0.812	0.998	1.252
$\log[NO_3^-]$	$\bar{1}.598$	$\bar{1}.728$	$\bar{1}.833$	$\bar{1}.910$	$\bar{1}.999$	0.097

TABLE I (Continued)

D. 3 M series — Resin: 4.96 meq. Solution: 10 ml.

Batch No.	1	2	3	4
$NaNO_3$ given	26.4	27.6	28.8	30.0
$NaClO_4$ 〃	3.6	2.4	1.2	0.0
HNO_3 〃	0.50	0.50	0.50	0.50
$Hg(NO_3)_2$ 〃	0.104	0.104	0.104	0.104
(Hg)	0.00688	0.00596	0.00484	0.00380
[Hg]	0.00701	0.00887	0.01112	0.01322
D	1.02	1.49	2.30	3.48
$[NO_3]$*	0.579	0.728	0.912	1.156
(NO_3^-)	2.92	2.97	3.00	3.00
$\log D - 2\log(NO_3^-)$	$\bar{1}$.073	$\bar{1}$.227	$\bar{1}$.407	1.588
n*[Hg] (n*=3.8)	0.027	0.034	0.042	0.051
$[NO_3^-]$	0.552	0.694	0.869	1.105
$\log[NO_3^-]$	$\bar{1}$.742	$\bar{1}$.841	$\bar{1}$.939	0.043

E. 5 M series — Resin: 4.84 meq. Solution: 10 ml.

Batch No.	1	2	3	4	5
$NaNO_3$ given	45.2	46.4	47.6	48.8	50.0
$NaClO_4$ 〃	4.8	3.6	2.4	1.2	0.0
HNO_3 〃	0.50	0.50	0.50	0.50	0.50
$Hg(NO_3)_2$ 〃	0.103	0.103	0.103	0.103	0.103
(Hg)	0.00470	0.00382	0.00304	0.00242	0.00190
[Hg]	0.01161	0.01342	0.01504	0.01632	0.01740
D	2.47	3.51	4.94	6.74	9.16
$[NO_3]$*	0.706	0.829	0.981	1.155	1.429
(NO_3^-)	4.73	4.79	4.84	4.87	4.86
$\log D - 2\log(NO_3^-)$	$\bar{1}$.043	$\bar{1}$.185	$\bar{1}$.326	$\bar{1}$.454	1.588
n*[Hg] (n*=3.8)	0.045	0.052	0.058	0.063	0.079
$[NO_3^-]$	0.661	0.777	0.923	1.092	1.350
$\log[NO_3^-]$	$\bar{1}$.820	$\bar{1}$.890	$\bar{1}$.965	0.038	0.130

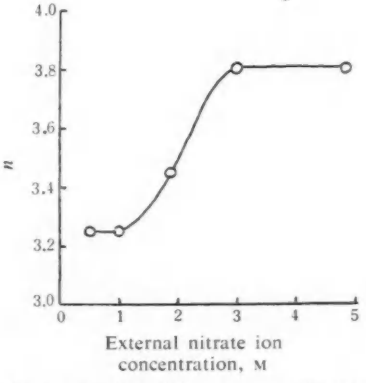

Fig. 3. n-Value of the mercury (II)-nitrate complex adsorbed from sodium nitrate solution of various concentrations.

against $\log[NO_3^-]$. Each curve is approximately linear in the range where nitrate is rich compared with perchlorate in the resin. The gradient increases with the external total concentration from 1 M to 3 M, and scarcely varies in a region less than 1 M and from 3 to 5 M.

In Fig. 3, n obtained from the slope is plotted against the concentration of the external solution.

From this curve, it will be recognized that mercury is taken up from a sodium nitrate solution as $Hg(NO_3)_3^-$ in the region from 0.5 to 1 M of the external concentration, as $Hg(NO_3)_4^{2-}$ in the region from 3 to 5 M, and as a mixture of $Hg(NO_3)_2^-$ and $Hg(NO_3)_4^{2-}$ in the region from 1 to 3 M. One might presume that some portions are adsorbed as $Hg(NO_3)_3^-$ in the region from 3 to 5 M solution, since n=3.8. However, this possibility may be weakened by considering the fact that n does not rise with an increase of the external nitrate concentration in this region. Furthermore, it may be reasonable to consider that the complex contains no hydrogen ion because the concentration of nitric acid is low.

Although it was assumed that mercury exists only as Hg^{2+} in the solution phase, it may

also be possible that a lower complex, such as $Hg(NO_3)^+$ or $Hg(NO_3)_3^-$, exists there when the nitrate concentration is as high as 3 or 5 M. When the presence of these species is assumed in the solution phase, *n*-value may somewhat deviate from that in the case when the presence of Hg^{2+} only is assumed, through the change of *m* in Eq. 10. However, these deviations are so small at 3 and 5 M, as estimated from data in Table I, that this uncertainty may hardly affect the conclusion as a whole. The reason why *n* at the plateau does not take an integer is not clear enough at present.

A number of sources of error are considered. First, failure in realizing the condition where the activity coefficient term is constant for lack of knowledge on activity in a resin and a concentrated solution, must be mentioned. The ideal condition could not be established even by keeping the external ionic strength constant. Besides, there are experimental errors; namely, poor reproducibility of dryness of the resin on weighing, the change in volume on mixing of the resin and the solution, and imperfect removal of the attached solution from the resin. In spite of these difficulties, the present method appears to give some conclusion on a metal complex form.

Though the changes of pH and temperature may have some appreciable effect, they were not studied in this work.

Summary

1) The equations for determining the composition of a metal complex using an anion exchange resin have been derived by considering the complex formation equilibria in both the resin phase and the solution phase.

2) The method based on these equations was successfully applied to the investigation of mercury(II)-nitrate complex at various external nitrate concentrations by means of the sodium nitrate-sodium perchlorate mixed solution.

3) Mercury(II) adsorbed from a sodium nitrate solution exists in the form of $Hg(NO_3)_3^-$ at the external nitrate concentration of 0.5~1 M, $Hg(NO_3)_4^{2-}$ at 3~5 M and a mixture of $Hg(NO_3)_3^-$ and $Hg(NO_3)_4^{2-}$ at the middle of these concentrations, though no anionic complex appears to be present in an ordinary nitrate solution.

The author wishes to express his sincere thanks to Professor J. Yoshimura of Kyushu University for his suggestions and encouragement.

Department of Chemistry
Faculty of Science
Kyushu University
Hakozaki, Fukuoka

---

*Theory on the Light Scattering of High Polymer Solutions Considering the Anisotropy of Segments**

By Masayuki NAKAGAKI

(Received November 21, 1960)

To discuss the physico-chemical properties of high polymer solutions, the so-called pearl necklace model is often used. In the theory of light scattering, too, the segments are usually assumed to be small spheres which scatter light according to Rayleigh's theory, and the interference between scatterd light from these Rayleigh spheres is considered[1,2]. In some cases, however, the segments of high polymer are not spherical but optically anisotropic.

In the present paper, the angular distribution of the intensity of light scattered by the high polymer solution is calculated theoretically, taking the anisotropy of the segments into account, and the theory is applied for the analysis of the Zimm plot.

Theoretical

Scattering at Infinite Dilution.—In the studies of light scattering of high polymer solutions, the Zimm plot method is often used. Curves on the Zimm plot are usually formulated by the following equation for the polymers of spherical segments and for infinite dilution ($c \to 0$):

* Presented at the 9th Annual Meeting of the Society of Polymer Science, Osaka, May, 1960.

1) B. H. Zimm, R. S. Stein and P. Doty, *Polymer Bull.*, **1**, 90 (1945).

2) P. Debye, *J. Phys. & Colloid Chem.*, **51**, 18 (1947).

$$Kc/R_u(\theta) = 1/MP_1(\theta) \quad (1)$$

where K is the well-known constant, c is the concentration, M is the molecular weight, and $P_1(\theta)$ is the intramolecular (intersegmental) interference factor given by[1,2]

$$P_1(\theta) = (2/\sigma^2)[\exp(-\sigma) - (1-\sigma)] \quad (2)$$

In this equation,

$$\sigma = (8\pi^2/3)(\overline{R^2}/\lambda^2)\sin^2(\theta/2) \quad (3)$$

where $\overline{R^2}$ is the mean square end-to-end distance, λ is the wavelength of light in the medium, and θ is the scattering angle. The wavelength in the medium λ is related to the the wavelength in vacuum λ_0 by the equation,

$$\lambda = \lambda_0/\mu_1 \quad (4)$$

where μ_1 is the refractive index of the medium.

The quantity $R_u(\theta)$ is defined by

$$R_u(\theta) = \frac{J_u(\theta)/I_0}{1+\cos^2\theta} \quad (5)$$

where $J_u(\theta)$ is the intensity of scattered light per unit solid angle at the scattering angle θ when unpolarized incident light is used, and I_0 is the intensity of incident light (per unit area). The factor $(1+\cos^2\theta)$ in Eq. 5 expresses the angular dependency of the scattered light from a Rayleigh sphere or a spherical segment, and because of this factor, the quantity $R_u(\theta)$ is called reduced scattering intensity. It is, however, obvious that the angular dependency of scattered intensity can not be reduced by the factor $(1+\cos^2\theta)$ if the segments are not spherical. In the latter case, another factor $P_u(\theta)$ must be introduced, and Eq. 1 must be rewritten to

$$Kc/R_u(\theta) = 1/M^*P_1(\theta)P_u(\theta) \quad (6)$$

where M^* is the apparent molecular weight of the high polymer, and

$$P_u(\theta) = \frac{2}{1+\cos^2\theta} \cdot \frac{\langle i_u(\theta)\rangle}{\langle i_u(0)\rangle} \quad (7)$$

The quantity $\langle i_u(\theta)\rangle$ is defined by the equation:

$$J_u'(\theta)/I_0 = (\lambda^2/4\pi^2)\langle i_u(\theta)\rangle \quad (8)$$

where $J_u'(\theta)$ is the intensity of light scattered by one segment.

Scattering from an Anisotropic Segment.—A segment or a particle may have two kinds of optical anisotropy: the one is "intrinsic" anisotropy and the other is "form" anisotropy. The intrinsic anisotropy occurs when the dispersed phase (that is the material composing the particle) itself has optical anisotropy because of, e.g., the orientation of valence bonds in the phase. In this case, the "excess" polarizability[3] of the dispersed phase can be expressed by an ellipsoid (a tensor in a more mathematical terminology) or a spheroid. For the sake of simplicity, a spheroid of the excess polarizability with principal axes $(\alpha_a, \alpha_b, \alpha_b)$ will be considered here. Then, the optical anisotropy is expressed by the ratio p_α,

$$p_\alpha = (\alpha_b/\alpha_a) \quad (9)$$

The form anisotropy, on the other hand, is the optical anisotropy due to the anisometry. In other words it is due to the anisotropic shape of the particle made of isotropic phase. If the shape of the particle is assumed to be a spheroid (it may of course be an ellipsoid in more general cases) and its semi-axes are (a, b, b), the anisometry is expressed by the axial ratio:

$$p = a/b \quad (10)$$

If the particle is sufficiently small compared to the wavelength of light, it may be assumed that one dipole is induced in a particle and the oscillation of the dipole radiates the scattered light. In this case, too, a spheroid of excess polarizability can be considered for each spheroidal particle, although the axial ratio of the polarizability spheroid p_α is not necessarily equal to the axial ratio p of the particle. Therefore, it can be expected that both kinds of anisotropy give the same type of expression for the angular dependency of the scattered light intensity.

The intensity of scattered light can easily be calculated for a particle having a spheroid of excess polarizability $(\alpha_a, \alpha_b, \alpha_b)$ by assuming that the electric vector of the scattered light is parallel and proportional to the induced dipole, the proportionality constant being set at k. On the other hand, the intensity of scattered light by an anisometric particle has already been calculated by Rayleigh[4] and Gans[5], if the particle is sufficiently small compared to the wavelength of light. These two theories give equations of the same form as expected above:

$$\left.\begin{aligned} i_{//\to//} &= \left[A\cos\theta + B\left(\sin^2\Theta\cos^2\varphi\cos\theta + \frac{1}{2}\sin 2\Theta\cos\varphi\sin\theta\right)\right]^2 \\ i_{//\to\perp} &= \left[\frac{1}{2}B\sin^2\Theta\sin 2\varphi\right]^2 \\ i_{\perp\to//} &= \left[\frac{1}{2}B(\sin^2\Theta\sin 2\varphi\cos\theta + \sin 2\Theta\sin\varphi\sin\theta)\right]^2 \\ i_{\perp\to\perp} &= [A + B\sin^2\Theta\sin^2\varphi]^2 \end{aligned}\right\} \quad (11)$$

3) It is the difference between the polarizabilities of particle and medium as already used, for example, by A. Peterlin, W. Heller and M. Nakagaki [*J. Chem. Phys.*, **28**, 470 (1958)].

4) L. Rayleigh, *Phil. Mag.*, **44**, 28 (1897).

5) R. Gans, *Ann. Phys.*, (4), **37**, 881 (1912), **62**, 331 (1920).

where θ is the scattering angle and (Θ, φ) are the spherical coordinates of the direction of the symmetry axis of the spheroid (α_a-axis or a-axis). The suffixes $i_{//\to\perp}$ and so forth mean that the incident light is oscillating parallel to the observation plane and the component of scattered light oscillating prependicularly to the observation plane is observed and so forth. The constants A and B are, in the case where the spheroid of excess polarizability is considered

$$\left.\begin{aligned} A &= k\alpha_b \\ B &= k(\alpha_a - \alpha_b) \end{aligned}\right\} \quad (12)$$

and in the case of anisometric particle

$$\left.\begin{aligned} A &= p^2\alpha^3(m^2-1)/[3+(m^2-1)(3/4\pi)P'] \\ B &= p^2\alpha^3(m^2-1)/[3+(m^2-1)(3/4\pi)P] - A \end{aligned}\right\} \quad (13)$$

Here

$$\alpha = 2\pi a/\lambda \quad (14)$$

and

$$m = \mu_2/\mu_1 \quad (15)$$

where μ_2 and μ_1 are refractive indices of the particle and the medium, respectively. As shown by Gans[3]

$$P + 2P' = 4\pi \quad (16)$$

For a prolate spheroid ($p \leqslant 1$),

$$P = 4\pi[(1-e^2)/e^2] \times \{(1/2e)\ln[(1+e)/(1-e)] - 1\} \quad (17)$$

where e is the eccentricity given by

$$e = \sqrt{1-p^2} \quad (18)$$

and for an oblate spheroid ($p \geqslant 1$),

$$P = (4\pi/\varepsilon^2)[1-(\sqrt{1-\varepsilon^2}/\varepsilon^2)\sin^{-1}\varepsilon] \quad (19)$$

where ε is the eccentricity given by

$$\varepsilon = \sqrt{1-1/p^2} \quad (20)$$

Optical Anisotropy of Anisometrical Segments. —As already stated, a spheroid of excess polarizability can be considered for each spheroidal particle (segment in the present paper) if the size of the spheroid is small compared to the wavelength of light used, but the axial ratio of these spheroids, p_α and p, are not necessarily equal. Now, on the basis of Eq. 12,

$$p_\alpha = 1/(B/A+1) \quad (21)$$

and according to Eq. 13,

$$p_\alpha = [1+(m^2-1)(P/4\pi)]/[1+(m^2-1)(P'/4\pi)] \quad (22)$$

For spherical particles ($p=1$), the relation $P=P'=4\pi/3$ is obtained from Eq. 17 and also from Eq. 19, which gives

$$p_\alpha = 1 \qquad \text{for } p=1 \quad (23)$$

In this case, and only in this case, $p_\alpha = p$. On the other hand, if the particle is an infinitesimally thin rod ($p=0$), the relations $P=0$ and $P'=2\pi$ are obtained from Eqs. 16 and 17, which give

$$p_\alpha = 2/(m^2+1) \qquad \text{for } p=0 \quad (24)$$

while if the particle is an infinitesimally thin disk ($p=\infty$), the relations $P=4\pi$ and $P'=0$ are obtained from Eqs. 16 and 19, which give

$$p_\alpha = m^2 \qquad \text{for } p=\infty \quad (25)$$

Referring to these extreme cases, it can be concluded that the value of p and p_α are not equal for anisometric particles. Moreover, the value of p_α must be in the range,

$$2/(m^2+1) < p_\alpha < m^2 \quad (26)$$

for anisometrical particles and, if the value of p_α is out of this range, particles must have the intrinsic anisotropy.

Scattering from Randomly Oriented Segments. —If the orientation of segments in a flexible high polymer molecule is assumed to be completely random, the value of $\langle i \rangle$ can be calculated by averaging Eq. 11 over all ranges of Θ and φ. The results are:

$$\left.\begin{aligned} \langle i_{//\to//}\rangle &= (1/15)B^2 + [A^2 + (2/3)AB + (2/15)B^2]\cos^2\theta \\ \langle i_{//\to\perp}\rangle &= \langle i_{\perp\to//}\rangle = (1/15)B^2 \\ \langle i_{\perp\to\perp}\rangle &= A^2 + (2/3)AB + (1/5)B^2 \end{aligned}\right\} \quad (27)$$

Therefore, the quantity $\langle i_u(\theta)\rangle$ for unpolarized light:

$$\langle i_u(\theta)\rangle = (1/2)\langle i_{//\to//} + i_{//\to\perp} + i_{\perp\to//} + i_{\perp\to\perp}\rangle \quad (28)$$

can be expressed as follows:

$$\langle i_u(\theta)\rangle = (1/2)\{[A^2 + (2/3)AB + (2/5)B^2 + [A^2 + (2/3)AB + (2/15)B^2]\cos^2\theta\} \quad (28a)$$

This gives the following value of $P_u(\theta)$ of Eq. 7.

$$\left.\begin{aligned} P_u(\theta) &= 1 + Q_u(1-\cos^2\theta)/(1+\cos^2\theta) \\ Q_u &= (2/15)(B/A)^2/[1+(2/3)(B/A) + (4/15)(B/A)^2] \end{aligned}\right\} \quad (29)$$

The value of $P_u(\theta)$ reduces to unity for spherical segments, because $B=0$ and $Q_u=0$ if $p=1$.

In an actual high polymer molecule, the mutual orientation of segments in a molecule might not be completely random, and this might require us to recalculate $P_2(\theta)$ of Eq. 6, but it is not easy to know the mutual orientation of segments in a polymer molecule. However, one may, at first, average the intensity of light scattered from each segment over all

possible orientations of the segment, and then consider the interference of these scattered beams, because the segments are originally defined as dynamically independent units. In this method of approximation, one can use Eq. 6 together with Eq. 29 for $P_u(\theta)$ and Eq. 2 for $P_1(\theta)$. Of course, the extension of the high polymer chain might be different according to whether the segments are isotropic or anisotropic. This affects the value of $P_1(\theta)$. This effect, however, had already been taken care of by $\overline{R^2}$ in Eq. 3.

Apparent Molecular Weight.—In the case of $\theta=0$, Eq. 6 reduces to

$$Kc/R_u(0)=1/M^* \tag{30}$$

but the apparent molecular weight M^* thus obtained does not coincide with the true molecular weight M except when the segments are spherical.

Debye's theory[6] of light scattering based upon the fluctuation theory is originally derived for the turbidity τ, but not for the reduced scattering intensity $R_u(\theta)$. Therefore,

$$Hc/\tau=1/M \tag{31}$$

is always correct for infinitely dilute solutions irrespective of whether the particles (segments in the present paper) are spherical or not, but Eq. 30 is not always correct because the relation used in order to convert τ to $R_u(\theta)$:

$$R_u(\theta)/\tau=3/16\pi \qquad \text{for } p=1 \tag{32}$$

is correct only for spherical particles. Therefore, the relation

$$K=(3/16\pi)H \tag{33}$$

must not be used for anisometric particles to obtain the correct values of the molecular weight, or, if the Eq. 33 is still used for anisometric particles, the apparent molecular weight M^* thus obtained must be reduced to the true molecular weight M, by using a correction factor to be obtained from the true relationship between $R_u(\theta)$ and τ.

The reduced scattering intensity $R_u(\theta)$ is given by

$$R_u(\theta)=(\lambda^2N/4\pi^2)\,[\langle i_u(\theta)\rangle/(1+\cos^2\theta)]\,P_1(\theta) \tag{34}$$

where N is the number of segments per unit volume, while the turbidity τ is given by

$$\tau=(\lambda^2N/2\pi)\int_0^\pi \langle i_u(\theta)\rangle \sin\theta\, d\theta \tag{35}$$

By using Eq. 28a,

$$\tau=(2\lambda^2N/3\pi)\,[A^2+(2/3)AB+(1/3)B^2] \tag{35a}$$

is obtained. Then referring to Eq. 29 and to the equation:

$$R_u(\theta)/\tau=(3/16\pi)P_1(\theta)P_u(\theta)M^*/M \tag{36}$$

the relation:

$$M/M^*=1+(1/15)(B/A)^2/[1+(2/3)(B/A)+(4/15)(B/A)^2] \tag{37}$$

is obtained, keeping the relation between K and H as it is in Eq. 33.

Comparison with Experimental Data

Serious anomalies in the Zimm plots have been found by Ehrlich and Doty[7] for aqueous solutions of copolymers of methacrylic acid and 2-dimethylaminoethyl methacrylate. Their data for isoionic P-7 (a fractionated sample) in 0.10 M sodium chloride and in distilled water are read off from their figures and plotted in Figs. 1 and 2 for the values extrapolated

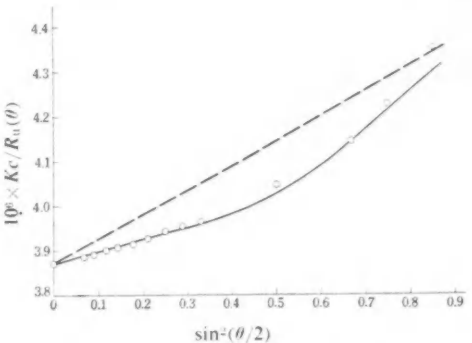

Fig. 1. Isoionic P-7 in 0.10 M sodium chloride.

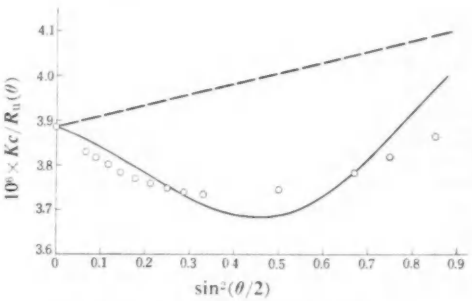

Fig. 2. Isoionic P-7 in distilled water.

to the infinite dilution. They also stated in their paper that the molecular weight of the sample P-7 obtained from light scattering measurement by the dissymmetry method was 270000 and that the square root of the mean

6) P. Debye, *J. Appl. Phys.*, **15**, 338 (1944).

7) G. Ehrlich and P. Doty, *J. Am. Chem. Soc.*, **76**, 3764 (1954).

square end-to-end distance $\sqrt{R^2}$ obtained from viscosity data on the basis of the Flory-Fox theory with the correction for polydispersity was 410 Å in 0.10 M sodium chloride and 270 Å in distilled water. The wavelength used was $\lambda_0=4360$ Å in vacuum, so that $\lambda=3254$ Å in water since $\mu_1=1.33986$ at 25°C. By using these values in Eqs. 2 and 3, the value of $P_1(\theta)$ can be calculated. If the segments are assumed to be spherical and $P_u(\theta)=1$, the value of $Kc/R_u(\theta)$ can be calculated from Eq. 6 by using the experimental values of $Kc/R_u(0)$, which is equal to $1/M^*$. The results of calculations are shown in Figs. 1 and 2 with broken lines. Experimental values shown by open circles are definitely lower than broken lines especially at about $\sin^2(\theta/2)=0.5$ or $\theta=90°$. If these discrepancies are due to the anisotropy of segments, the deviation of $P_u(\theta)$ from unity must be expressed by Eq. 29. Using the values of Q_u determined to obtain the best fit with the experimental plots and cited in Table I, solid curves in Figs. 1 and 2 are obtained.

TABLE I. CONSTANTS FOR ISOIONIC P-7

	In 0.10 M NaCl (Fig. 1)	In water (Fig. 2)
Q_u	0.0291	0.0870
B/A	0.565	1.190
p_a	0.639	0.457
ρ_2	3.26	5.93
M^*	258000	257000
M/M^*	1.0146	1.0448
M	262000	269000

In the case of 0.10 M sodium chloride as the solvent (Fig. 1), the initial slope of the Zimm plot is smaller than that of the broken curve, although its sign is still positive. In the case of distilled water as the solvent (Fig. 2), the initial slope is negative. The anomalous negative slope could not be expected from any theory presented so far. On the basis of the present aspect, however, the anomalous negative value can be explained by the great value of Q_u, the value being about three times greater for Fig. 2 than for Fig. 1. The value of B/A calculated from Eq. 29 is about twice as great for Fig. 2 as for Fig. 1. However, the axial ratio p_a of the spheroid of polarizability to give the anisotropy of segments is only 30% smaller for Fig. 2 than for Fig. 1. This demonstrates that only the small difference in the anisotropy of segments results in any very great difference in the initial slope of the Zimm plot.

The value of p_a for either case is smaller than unity. This means that the spheroid of the excess polarizability is prolate in both cases. To discuss whether this anisotropy is due to intrinsic anisotropy or anisometry, the value of the relative refractive index m must be known. On the basis of the mixture rule,

$$d\mu_{12}/dc=(m-1)\mu_1/\rho_2 \qquad (38)$$

By using $d\mu_{12}/dc=0.188$ as reported by the original authors, the value of m is obtained if the value of the density of the polymer ρ_2 is known. If the value of ρ_2 is 1.4, the value of m is 1.20. These values seem to be reasonable. Then, according to Eq. 26,

$$0.82<p_a<1.44 \qquad \text{for } m=1.20 \quad (39)$$

if the anisotropy is due to the anisometry. Since the values cited in Table I are smaller than the limiting value, the anisotropy in these cases must be intrinsic. Putting it the other way around, the value of ρ_2, which is necessary to explain the anisotropy as the form anisotropy, may be estimated according to Eq. 24 for infinitesimally thin rods. The values of ρ_2 must be greater than 3~6 as shown in Table I, which is too great for polymers. Therefore, the anisotropy seems to be intrinsic.

On the molecular weight of the polymer, the value of the apparent molecular weight M^* obtained from the value of $Kc/R_u(0)$ and cited in Table I is a little too small compared to the value $M=270000$ reported by the original authors. The correction factor M/M^* given by Eq. 37 is calculated and cited in Table I. The molecular weight corrected by this factor (M in Table I) is closer to 270000 than M^* is.

Thus the essential feature of the anomalous θ dependency of the Zimm plot of isoionic P-7 could be explained by assuming that the segments are anisotropic. However, the agreement between the experimental plots and the theoretical curves in Figs. 1 and 2 is not perfect yet. For the discrepancy, several reasons may be pointed out: Some errors might have been made in the double extrapolation in the Zimm-plot to obtain the value of $Kc/R_u(0)$; the estimation of $\overline{R}^2$ used to calculate $P_1(\theta)$ might not be correct; the effect of the molecular weight distribution was neglected; the mutual orientation of segments in a polymer chain is not completely random, but this effect was neglected. Some of these points, especially the last one, will be discussed in a later paper.

Proposal for the Direct Measurement of Q_u

If the value of Q_u can be measured directly, it will give a good criterion to see whether the phenomenon is actually due to the anisotropy of segments or not. This will be done by measuring the scattering ratio, S, that is

the ratio of scattered intensities from parallelly and perpendicularly polarized incident beams.

$$S(\theta)=J_{//}(\theta)/J_{\perp}(\theta)=\langle i_{//}(\theta)\rangle/\langle i_{\perp}(\theta)\rangle \quad (40)$$

According to the relations:

$$\begin{aligned}\langle i_{//}\rangle &= \langle i_{//\to//}+i_{//\to\perp}\rangle = (2/15)B^2 \\ &\quad + [A^2+(2/3)AB+(2/15)B^2]\cos^2\theta \\ \langle i_{\perp}\rangle &= \langle i_{\perp\to//}+i_{\perp\to\perp}\rangle = A^2 \\ &\quad + (2/3)AB+(4/15)B^2\end{aligned} \quad (41)$$

the value of $S(\theta)$ theoretically obtained is

$$S(\theta)=Q_u+(1-Q_u)\cos^2\theta \quad (42)$$

At $\theta=90°$,

$$S(90)=Q_u \quad (43)$$

Therefore, the scattering ratio at 90° is the value of Q_u.

Summary

The anomaly of the angular dependency of the reduced scattering intensity in the Zimm plot for infinitely dilute solution was discussed for the solutions of high polymer molecules having anisotropical segments, and the theoretical relationship between $Kc/R_u(\theta)$ and θ was derived. The equation had the same form for both intrinsic anisotropy and form anisotropy. In the latter case, the axial ratio of the spheroid of excess polarizability was concluded to be not equal to the axial ratio of the segment. Moreover, the correction factor for the molecular weight was derived.

Applying these theoretical equations to the experimental data by Ehrlich and Doty on the solution of copolymer of methacrylic acid and 2-dimethylaminoethyl methacrylate, it was shown that the anomalies of the Zimm plot could be explained by assuming that the segments have intrinsic anisotropy.

It was also suggested that the scattering ratio is a good criterion to see whether the anomaly is actually due to the anisotropy of segments or not.

Faculty of Pharmacy
Kyoto University
Sakyo-ku, Kyoto

The Mannich Base of Troponoid and its Application. V. On the Mannich Base of 3-Isopropyltropolone (α-Thujaplicin)

By Kyozo OGURA

(Received December 2, 1960)

Seto and the present author applied the Mannich reaction to 3, 7-dibromotropolone and prepared various 5-substituted derivatives of tropolone[1-3]. In order to make further extension of the Mannich reaction to tropolones, examinations were made on the Mannich reaction of 3-isopropyltropolone. The present paper describes the syntheses of a few Mannich bases of 3-isopropyltropolone and some of their properties.

Treatment of 3-isopropyltropolone (I) with folmaldehyde solution and morpholine, in the presence of acetic acid, affords 3-isopropyl-5, 7-dimorpholinomethyltropolone (II) as colorless crystals,, m. p. 76°C. The use of piperidine in place of morpholine gives 3-isopropyl-5, 7-dipiperidinomethyltropolone (III) as yellow crystals, m. p. 79.5°C. The morpholinomethyl group in II and the piperidinomethyl group in III are easily substituted by cationoid reagents. Reaction of II and III with *p*-tolyldiazonium salt respectively gives 3-isopropyl-5-tolylazo-7-morpholinomethyl- (IV), m. p. 134°C, and 3-isopropyl-5-tolylazo-7-piperidinomethyltropolone (V), m. p. 192°C. Both II and III give the known 3-isopropyl-5, 7-dibromotropolone[4] (VI) by the action of two molar equivalents of bromine. Treatment of II with excess of piperidine and formaldehyde solution gives III. In this case, no reaction occurs if formaldehyde is not used so that the above reaction is not a simple amine exchange but the substitution of the morpholinomethyl group with piperidinomethyl group.

Addition of one molar equivalent of bromine to II and III affords the respective monobromo compounds of m. p. 93°C and of m. p. 137°C.

1) S. Seto and K. Ogura, This Bulletin, 32, 493 (1959).
2) S. Seto and K. Ogura, ibid., 32, 1118 (1959).
3) S. Seto and K. Ogura, ibid., 33, 1084 (1960).

These were identified from experimental facts described below as 3-isopropyl-5-morpholinomethyl-7-bromotropolone (VII) and 3-isopropyl-5-piperidinomethyl-7-bromotropolone (VIII). Addition of formaldehyde solution and morpholine to 3-isopropyl-7-bromotropolone[4] affords the same monobromo compounds as that derived from II. However, this fact alone is not sufficient to conclude that the structure of this substance is represented by VII since the bromine in the 7-position might have undergone rearrangement to 5-position during the Mannich reaction of 3-isopropyl-7-bromotropolone*1.

The reaction of VII and VIII with *p*-tolyldiazonium salt results in the formation of 3-isopropyl-5-tolylazo-7-bromotropolone (IX), m. p. 145°C from both compounds and IX is also obtained by the application of bromine to IV, V or 3-isopropyl-5-tolylazotropolone[4] (X). Hydrogenolysis of VII and VIII over palladium-carbon catalyst results in absorption of one molar equivalent of hydrogen and a monomorpholinomethyl- (m. p. 78°C) and a monopiperidinomethyl derivative (m. p. 113°C) are obtained respectively. Since these substances form 3-isopropyl-5-tolylazotropolone (X) by the reaction with *p*-tolyldiazonium salt, these are known to be 3-isopropyl-5-morpholinomethyl- (XI) and 3-isopropyl-5-piperidinomethyltropolone (XII). These facts prove that the above-mentioned monobromo compounds are VII and VIII.

Recrystallization of VII from methanol produces yellow granular crystals (VIIa) of m. p. 93°C which, upon further recrystallization from petroleum ether, change into colorless rods (VIIb), m. p. 64°C. The mixed melting point of these substances gives an intermediate value and when VIIb is left in air, it gradually acquires a yellowish tint and changes into VIIa. From elemental analytical values and comparison of infrared absorption spectra in the solid state, the former VIIa was found to have one mole of water of crystallization and to take the zwitter-ion structure. The infrared spectrum of VIIa lacked the absorption band due to the OH stretching vibration of tropolone and exhibited an intense absorption of N^+H stretching mode at 2530 cm^{-1}. There were absorption bands at 3470 and 3400 cm^{-1} due to crystal water. On the other hand, the infrared spectrum of VIIb lacked the absorption corresponding to N^+H stretching mode but exhibited a strong absorption band of OH stretching mode at 3180 cm^{-1}. Similarly, examination of the infrared spectra showed that the yellow crystalline III, VIII and XII took the zwitter-ion structure and that the colorless crystalline II and XI did not take such a structure.

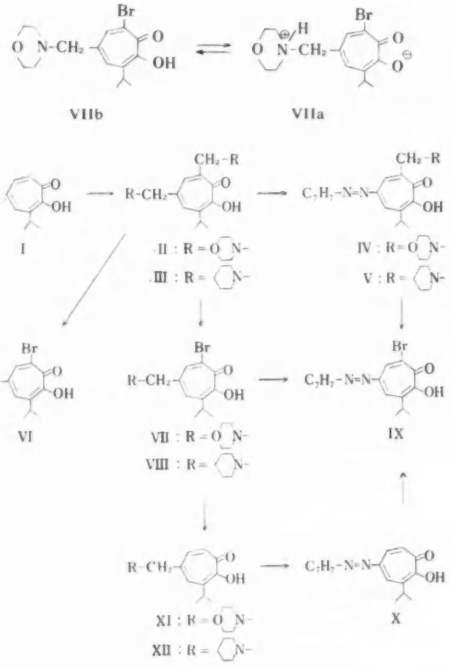

Experimental*2

3-Isopropyl-5,7-dimorpholinomethyltropolone (II). — A mixture of 1 g. of 3-isopropyltropolone, 4 ml. of 37% formalin, 4 ml. of morpholine and 0.8 ml. of acetic acid was stirred mechanically at 60°C for 1 hr., 10 ml. of water was added, and wall of the vessel was scratched with a glass rod while being cooled with ice, by which crystals gradually precipitated. After allowing the mixture to stand overnight in an ice chamber, the crystals were collected by filtration, washed with water, and recrystallized from methanol to colorless needles (II), m. p. 74~76°C. Yield, 1.8 g.

Found: C, 66.22; H, 7.74; N, 7.83. Calcd. for $C_{20}H_{30}O_4N_2$: C, 66.27; H, 8.34; N, 7.73%.

UV λ_{max}^{MeOH} mμ (log ε): 246 (4.47), 326 (3.92), 370 (3.74).

3-Isopropyl-5,7-dipiperidinomethyltropolone (III). — A mixture of 0.6 g. of 3-isopropyltropolone, 2 ml. of 37% formalin, 2 ml. of piperidine, and 0.4 ml. of acetic acid was stirred mechanically at 60°C for 1 hr., 5 ml. of water was added, and wall of the vessel was scratched with a glass rod while being cooled in ice, by which yellow crystals gradually

4) T. Nozoe, Y. Kitahara and T. Ikemi, *Proc. Japan Acad.*, **27**, 193 (1951).

*1 S. Seto and T. Sato found that application of the Mannich reaction to 4-isopropyl-7-bromotropolone afforded 3-bromo-4-isopropyl-7-morpholinomethyltropolone.

*2 All melting points are uncorrected. The microanalyses were carried out by Mr. S. Oyama and Miss Y. Endo of this Institute, to whom the author is indebted.

precipitated out. After standing in an ice chamber overnight, the crystals were collected by filtration, washed with water, and recrystallized from methanol. M. p. 78~79.5°C. Yield, 0.9 g.

Found: C, 73.41; H, 9.22; N, 7.43. Calcd. for $C_{22}H_{34}O_2N_2$: C, 73.70; H, 9.56; N, 7.81%.

UV λ_{max}^{MeOH} mμ (log ε): 250 (4.36), 346 (3.88), 400 (3.58).

IR ν N^+–H 2220 and 2480 cm^{-1} (broad) (KBr disk).

3-Isopropyl-5-tolylazo-7-morpholinomethyltropolone (IV). — To a solution of 180 mg. of II in 1 ml. of pyridine, a diazonium salt prepared from *p*-toluidine, 40 mg. of sodium nitrite, and 0.2 ml. of concentrated hydrochloric acid was added under cooling with ice by which a red precipitate separated out immediately. The precipitate was collected and recrystallized from methanol to reddish orange crystals (IV), m. p. 133~134°C. Yield, 150 mg.

Found: C, 69.03; H, 7.02; N, 10.87. Calcd. for $C_{22}H_{27}O_3N_3$: C, 69.27; H, 7.13; N, 11.02%.

UV λ_{max}^{MeOH} mμ (log ε): 237 (4.26), 290 (4.07), 400 (4.36), 460 (4.08).

3-Isopropyl-5-tolylazo-7-piperidinomethyltropolone (V). — A diazonium salt, prepared from 30 mg. of *p*-toluidine, 20 mg. of sodium nitrite, and 0.1 ml. of concentrated hydrochloric acid, was added to pyridine solution (ca. 1 ml.) of 100 mg. of III and a red precipitate formed immediately. V was obtained as orange crystals of m. p. 191~192°C by the same procedure as for IV. Yield, 50 mg.

Found: C, 72.68; H, 7.48; N, 11.18. Calcd. for $C_{23}H_{29}O_2N_3$: C, 72.79; H, 7.70; N, 11.07%.

UV λ_{max}^{MeOH} mμ (log ε): 237 (4.05), 252 (4.16), 296 (4.04), 412 (4.35), 462 (4.37).

Reaction of II with Bromine. — A solution of 280 mg. of bromine in 0.5 ml. of methanol was added dropwise into a solution of II dissolved in 0.5 ml. of methanol, while being stirred under ice cooling. After completion of the addition, the solvent was evaporated under a reduced pressure and colorless needles, m. p. 75~77°C, precipitated out. This substance showed no depression of melting point on admixture with an authentic sample of 3-isopropyl-5, 7-dibromotropolone[4] and its analytical values and ultraviolet absorption spectra showed satisfactory agreement.

Reaction of II with Formaldehyde and Piperidine. — A mixture of 100 mg. of II, 0.5 ml. of 37% formalin, 0.5 ml. of piperidine, and 0.1 ml. of acetic acid was stirred mechanically at 70°C for 4 h., 1 ml. of water was added, and the wall of the vessel was scratched with a glass rod under ice-cooling by which III was obtained as yellow crystals.

3-Isopropyl-5-morpholinomethyl-7-bromotropolone (VII). — A solution of 1.76 g. of bromine dissolved in 12 ml. of methanol was added dropwise into 4 g. of II suspended in 30 ml. of methanol, while being stirred under ice cooling. The reaction mixture gradually aquired yellow tint as bromine was added. After completion of the addition, the solvent was evaporated to dryness under a reduced pressure and left a mixture of colorless crystals, m. p. 208~209°C (decomp.), and a yellow viscous residue. The crystals were the hydrobromide of VII.

Addition of hydrochloric acid to this residual mixture resulted in solidification of the viscous residue to colorless crystals, which were collected by filtration. Addition of 15 ml. of 2 N sodium acetate solution to these crystals, changed them to a yellow viscous substance which, when heated for ca. 10 min. at 60°C, formed a yellow solid. The precipitate so formed was collected, washed with water, and recrystallized from methanol to yellow granular crystals (VIIa), m. p. 91~93°C. Yield, 3.3 g.

Recrystallization of VIIa from petroleum ether produced colorless rods (VIIb), m. p. 64~65°C.

Found (for VIIa): C, 49.10; H, 5.65; N, 3.55. Calcd. for $C_{15}H_{20}O_3NBr \cdot H_2O$: C, 50.00; H, 6.11; N, 3.89%.

Found (for VIIb): C, 52.77; H, 5.79; N, 4.47. Calcd. for $C_{15}H_{20}O_3NBr$: C, 52.63; H, 5.85; N, 4.09%.

UV λ_{max}^{MeOH} mμ (log ε): 259 (4.44), 338 (3.78), 380 (3.67).

IR (VIIa): 3470 and 3400 cm^{-1} (water of crystallization), 2660 (sh.), 2530, and 2370 cm^{-1} (sh.) (ν N^+–H).

IR (VIIb): 3200 cm^{-1} (ν O–H).

3-Isopropyl-5-piperidinomethyl-7-bromotropolone (VIII). — A solution of 1.4 g. of bromine, dissolved in 12 ml. of methanol, was added dropwise into a suspension of 3.1 g. of III in 60 ml. of methanol, while being stirred under ice cooling, and the solvent was evaporated under a reduced pressure after completion of the addition. About 15 ml. of water was added to the residue and the yellow solid that formed was recrystallized from methanol. M. p. 135~137°C (decomp.). Yield, 2.6 g.

Found: C, 56.14; H, 6.41; N, 4.17. Calcd. for $C_{16}H_{22}O_2NBr$: C, 56.46; H, 6.46; N, 4.10%.

UV λ_{max}^{MeOH} mμ (log ε): 260 (4.47), 340 (3.91), 390 (3.59).

IR 2540 cm^{-1} (broad) (ν N^+–H)

3-Isopropyl-5-tolylazo-7-bromotropolone (IX). — a) To a solution of 100 mg. of VII or VIII dissolved in ca. 0.2 ml. of pyridine, diazonium salt solution prepared from 40 mg. of *p*-toluidine, 30 mg. of sodium nitrite, and 0.1 ml. of concentrated hydrochloric acid was added while being stirred under ice cooling and red crystals precipitated out immediately. The crystals were collected and recrystallized from methanol to orange crystals (IX), m. p. 142~145°C. Yield, 120 mg.

b) To a suspension of 50 mg. of IV or V in ca. 0.2 ml. of methanol, a solution of 20 mg. of bromine dissolved in 0.5 ml. of methanol was added with stirring and the crystals that formed were collected by filtration. Recrystallization from methanol gave a product, m. p. 143~145°C which showed no depression of the melting point on admixture with the product obtained by the method (a). Yield, 30 mg.

c) A solution of 20 mg. of bromine dissolved in ca. 0.5 ml. of methanol was added to 40 mg. of 3-isopropyl-5-tolylazotropolone suspended in ca. 0.2 ml. of methanol and the crystals formed were collected by filtration. Recrystallization from methanol afforded a product which showed no depression in the melting point on admixture with

the products obtained by the methods (a) and (b). Yield, 50 mg.

Found: C, 56.58; H, 4.23; N, 7.85. Calcd. for $C_{17}H_{17}O_2N_2Br$: C, 56.52; H, 4.74; N, 7.85%.

UV λ_{max}^{MeOH} mμ (log ε): 256 (4.20), 299 (4.15), 415 (4.38), 477 (4.39).

3-Isopropyl-5-morpholinomethyltropolone (XI).— A solution of 1 g. of VII dissolved in ca. 20 ml. of ethanol and added with 220 mg. of sodium hydroxide and 200 mg. of palladium-carbon was shaken in a hydrogen stream. Absorption of hydrogen stopped after an equivalent mole was absorbed. The solvent was evaporated under a reduced pressure and addition of hydrochloric acid to the residue to neutralization precipitated crystals. The crystals were collected and recrystallized from petroleum ether to colorless prisms (XI), m. p. 77~78°C. Yield, 500 mg.

Found: C, 68.17; H, 7.64; N, 5.14. Calcd. for $C_{15}H_{21}O_3N$: C, 68.41; H, 8.04; N, 5.32%.

UV λ_{max}^{MeOH} mμ (log ε): 242 (4.41), 326 (3.92).

Treatment of XI with 3 N hydrochloric acid afforded colorless crystals, m. p. 124~129°C, the hydrochloride of XI.

Found: C, 56.23; H, 7.05; N, 4.08. Calcd. for $C_{15}H_{22}O_3NCl \cdot H_2O$: C, 56.69; H, 7.61; N, 4.41%.

3-Isopropyl-5-piperidinomethyltropolone (XII).— A suspension of 0.9 g. of VIII in 20 ml. of ethanol with 0.3 g. of potassium hydroxide and 0.1 g. of palladium-carbon added was shaken in a hydrogen stream. After absorption of an equivalent mole of hydrogen the solvent was evaporated under a reduced pressure and addition of hydrochloric acid to the yellow viscous residue to neutralization precipitated slight yellow crystals. The crystals were collected and recrystallized from methanol or benzene. M. p. 110~113°C. Yield, 0.6 g.

Found: C, 72.91; H, 8.78; N, 5.11. Calcd. for $C_{16}H_{23}O_2N$: C, 73.53; H, 8.87; N, 5.36%.

UV λ_{max}^{MeOH} mμ (log ε): 242 (4.41), 326 (3.89).

IR ν N^+–H, 2500 cm^{-1} (broad) (KBr disk).

Reaction of XI with *p*-Tolyldiazonium Salt.— To a solution of 160 mg. of XI dissolved in ca. 0.2 ml. of pyridine, a diazonium salt prepared from 30 mg. of *p*-toluidine, 20 mg. of sodium nitrite, and ca. 0.1 ml. of concentrated hydrochloric acid was added while being stirred under ice cooling, by which orange crystals separated out. The crystals were collected and recrystallized from methanol to orange prisms, m. p. 129~130°C, undepressed on admixture with an authentic sample of 3-isopropyl-5-tolylazotropolone.

Summary

The Mannich reaction was applied to 3-isopropyltropolone and 3-isopropyl-5, 7-dimorpholinomethyl, and 3-isopropyl-5, 7-dipiperidinomethyltropolone were obtained. These substituents were easily substituted by diazonium salt or bromine. Some of the Mannich bases obtained were found to retain the zwitterion structure in the solid state.

The author expresses his deep gratitude to Professor Shuichi Seto for his kind guidance. He is indebted to Mr. S. Aono for infrared spectral measurements and to Mr. F. Sato for ultraviolet spectral measurements. A part of the expense for the present research was defrayed by Sankyo Co., Ltd., to whom the author wishes to express his sincere gratitude.

The Chemical Research Institute of Non-Aqueous Solutions, Tohoku University, Katahira-cho, Sendai

---

Iodine-catalyzed Thermal cis-trans Isomerization of Azobenzene

By Shigeru YAMASHITA

(Received November 2, 1960)

Since Hartley[1] showed the existence of cis-form azobenzene, cis-trans conversion of azobenzene has been studied thermally or photochemically by Le Fevre[2], Zimmerman[3] and also by Birnbaum and Style[4]. However, all of these studies were carried out in the absence of any catalyst. In the present work, the effect of iodine catalyst on the thermal cis → trans conversion of azobenzene has been studied kinetically in *n*-hexane solution. Since azobenzene forms a molecular complex with iodine, the equilibrium constant for its formation and its bearing on the isomerization reaction have also been studied.

1) G. S. Hartley, *J. Chem. Soc.*, **1938**, 633.
2) R. J. W. Le Fevre and J. Northcott, ibid., **1953**, 867.
3) G. Zimmerman et al., *J. Am. Chem. Soc.*, **80**, 3528 (1958).
4) P. P. Birnbaum and D. W. G. Style, *Trans. Faraday Soc.*, **50**, 1191 (1954).

Experimental

Materials.—*cis-Azobenzene.*—The method of preparation presented by Hartley[1] was followed.

trans-Azobenzene.—The commercial reagent was used after repeated recrystallization. The absorption curves of these two isomers of azobenzene were in good agreement with those in the literature[1,3].

Iodine and n-Hexane.—The purification of these compounds has already been described in the previous paper[5].

Procedure.—The equilibrium of complex formation between azobenzene and iodine in *n*-hexane was studied spectrophotometerically in a manner similar to that described previously for the iodine-stilbene complex[5].

The rate of iodine-catalyzed cis → trans conversion of azobenzene was determined also spectrophotometrically by the same procedure as that described for the case of iondine-catalyzed cis → trans conversion of stilbene[6]. Since *cis*-azobenzene was found to isomerize far more easily than stilbene, the measurement of reaction rate was carried out at a lower temperature range than in the case of stilbene. The *cis*- and *trans*-azobenzene concentrations were determined spectrophotometrically in a manner similar to that described by Zimmerman[3] in his photoequilibrium study of azobenzene.

Results and Discussion

The Molecular Complex formed between Azobenzene and Iodine.—As seen in Fig. 1, the visible absorption band maximum of free iodine at 520 mμ shifts to one at a shorter wavelength of 435 mμ when combined with *cis*-azobenzene to form a complex, and at the same time a new strong absorption band maximum appears at 305 mμ. This is probably a charge-transfer band. A rather large molar extinction coefficient of 6.7×10^3 found for the latter peak (Table I) supports such an interpretation.

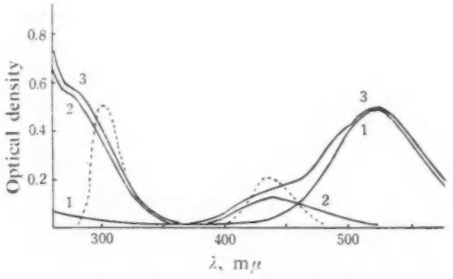

Fig. 1. Optical density increment in the mixture of *cis*-azobenzene and iodine in *n*-hexane solution. Temperature, 25°C. Curve 1: $(I_2)=5.0\times10^{-4}$(mol./l.). Curve 2: $(C)=1.0\times10^{-4}$(mol./l.), C denoting *cis*-azobenzene. Curve 3: $(C)=1.0\times10^{-4}$(mol./l.); $(I_2)=5.0\times10^{-4}$(mol./l.). Dotted line indicates the optical density increment due to the molecular complex, CI_2 (in 10 times enlarged scale of ordinate).

TABLE I. EQUILIBRIUM CONSTANTS OF *cis*-AZOBENZENE-IODINE COMPLEX AND RELATING QUANTITIES. CHARGE-TRANSFER BAND; $\lambda_{max}=305$ mμ, $\varepsilon_{max}=6.7\times10^3$. BLUE SHIFT OF IODINE ABSORPTION; $\lambda_{max}=435$ mμ

Temperature, °C	K_C, l./mol.
25.0	97
20.0	121
15.0	150
10.0	192

The equilibrium constant for the complex formation was obtained by the Benesi-Hildebrand type relations[7] represented as follows[8]:

$$1/(\varepsilon_A-\varepsilon_F)=1/(\varepsilon_C-\varepsilon_F)\,(1/K_C)\,(1/C_A)+1/(\varepsilon_C-\varepsilon_F) \quad (1)$$

Here, ε_F and ε_C are, respectively, the molar extinction coefficients for free *cis*-azobenzene and the complex in the mixture, and $\varepsilon_A=d/((Az)\cdot l)$, where d is the measured optical density of the solution containing the complex, (Az) is the total concentration of *cis*-azobenzene (free and complexed) and l is the path length of the absorption cell (1 cm.). The term C_A is actually the concentration of iodine left free in the mixture but can be equated to its total concentration when the concentration of the complex is considerably smaller than that of free iodine as it is in the present case.

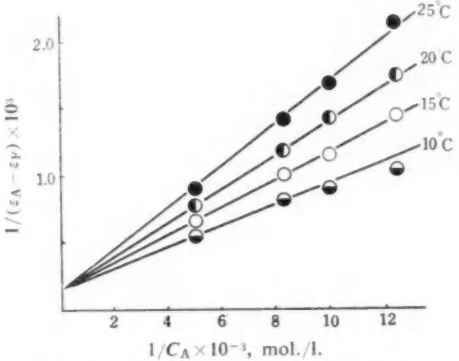

Fig. 2. $1/(\varepsilon_A-\varepsilon_F)\sim1/C_A$ diagram for the *cis*-azobenzene-iodine system in *n*-hexane.

5) S. Yamashita, This Bulletin, **32**, 1212 (1959).
6) S. Yamashita, ibid., **34**, 487 (1961).
7) a) H. A. Benesi and J. H. Hildebrand, *J. Am. Chem. Soc.*, **71**, 2703 (1949); b) L. J. Andrews and R. M. Keefer, ibid., **77**, 4202 (1955).
8) M. Chowdhury and S. Basu, *J. Chem. Phys.*, **32**, 1450 (1960).

Eq. 1 was applied to the change-transfer absorption maximum at 305 mμ, absorption of free iodine at this wavelength being taken into account[9]. The results are shown in Fig. 2. The equilibrium constants of complex formation obtained from these plots are listed in Table I. From the Arrhenius plot of these values of K_C, the heat of complex formation $-\Delta H$ was found to be 7.5±0.2 kcal./mol. This value of $-\Delta H$ and the absorption maximum of the complexed iodine, 435 mμ, satisfy the empirical relation found by Ham[9] between the heat of complex formation and the magnitude of blue shift in the absorption band of iodine caused by complex formation (Fig. 3). In the case of *trans*-azobenzene-iodine system, no appreciable spectral change was observed.

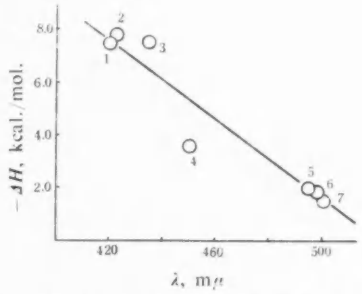

Fig. 3. Correlation between heat of formation of complex and blue shift of iodine. 1, *cis*-stilbene[5]; 2, pyridine; 3, *cis*-azobenzene; 4, dioxane; 5, xylene; 6, toluene; 7, benzene

Isomerization Reaction.—As in the previous study[6] of the iodine-catalyzed thermal cis → trans conversion of stilbene, only the initial rates of isomerization were determined. Since *cis*-azobenzene is more labile than *cis*-stilbene, reaction rate measurements could be carried out at lower temperatures than with stilbene.

In Figs. 4 and 5 the dependence of the rate of isomerization on the concentration of *cis*-azobenzene and of iodine are shown respectively. These results conform to the rate expression

$$-\mathrm{d(C)}/\mathrm{d}t = k\,(\mathrm{C})\,(\mathrm{I_2}) + k'(\mathrm{C}) \qquad (2)$$

where (C) and (I_2) are the concentration of *cis*-azobenzene and iodine, respectively. The second term in Eq. 2 represents the spontaneous isomerization of *cis*-azobenzene which can not be neglected as is evidently seen in Fig. 5[10].

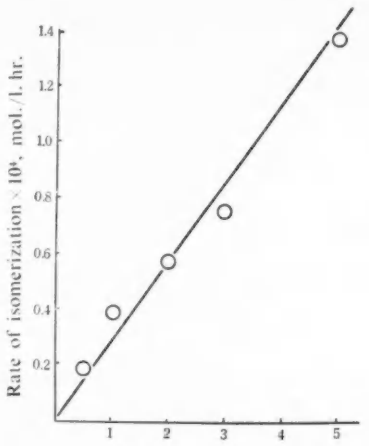

Fig. 4. Dependence of the reaction rate on the concentration of *cis*-azobenzene. Concentration of iodine, 5×10^{-4} mol./l.; temperature, 30°C.

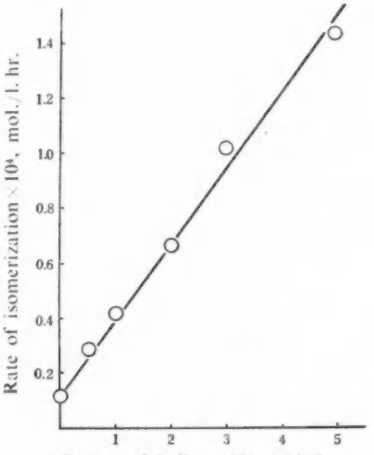

Fig. 5. Dependence of the rate on the concentration of iodine. Concentration of *cis*-azobenzene, 5×10^{-4} mol./l.; temperature, 30°C.

In Table II the values of the rate constants k and k' at varied temperatures are shown and the Arrhenius constants obtained from these values of k's are listed in Table III. Both the A-factor and activation energy for the spontaneous isomerization are in fairly good agreement with those previously reported[2]. These results suggest that the spontaneous isomerization of *cis*-azobenzene probably takes place via the "singlet mechanism" of Magee, Shand and

9) J. Ham, *J. Am. Chem. Soc.*, **76**, 3875 (1954); see also T. Kubota, *J. Chem. Soc. Japan (Nippon Kagaku Zasshi)*, **78**, 196 (1957); J. H. Hildebrand et al., *J. Chem. Phys.* **33**, 621 (1960).

10) That the spontaneous isomerization of *cis*-azobenzene is of first order has previously been shown by Hartley and Le Fevre[1,2].

Table II. Values of the rate constants k and k'

Temperature °C	$k \times 10^{-2}$ cc. mol^{-1} sec^{-1}	$k' \times 10^{6}$ sec^{-1}
30	1.84	3.75
40	2.50	11.3
50	3.50	31.4

Table III. Arrhenius constants of the rate constants k and k'

Rate constant	A-factor	Activation energy
k	6.44×10^{6} cc. mol^{-1} sec^{-1}	6.3 kcal./mol.
k'	5.20×10^{9} sec^{-1}	21.0 kcal./mol.

Eyring[11], though the activation energy is considerably lower than those for some reactions quoted by them as examples for the singlet mechanism.

A simple way to explain the conversion catalyzed by iodine might be to assume a collisional catalysis by iodine molecules which enables *cis*-azobenzene to isomerize through a "triplet mechanism" similar to that proposed by Harman and Eyring[12]. The activation energy of 6.3 kcal./mol., however, seems too small to make such a simple collisional mechanism acceptable. An alternative explanation, which seems much more probable, is given by the isomerization of the molecular complex, the existence of which was shown above:

$$C + I_2 \rightleftarrows CI_2 \qquad \text{(fast)}$$

$$CI_2 \rightarrow TI_2 \quad \text{or} \quad T + I_2 \qquad \text{(slow)}$$

where C and T represent *cis*- and *trans*-azobenzene, respectively.

According to this interpretation, the rate of iodine-catalyzed isomerization is given by

$$-d(C)/dt = k''(CI_2)$$

where

$$k'' = 2.10 \times 10^{13} \exp(-13.8 \text{ kcal. mol}^{-1}/RT) \quad (\text{sec}^{-1})$$

Here the activation energy of 13.8 kcal./mol. results from the sum of 6.3 kcal./mol. and the heat of formation of the molecular complex, 7.5 kcal./mol.

Further study seems necessary before it can be clarified whether this lowering of activation energy is accompanied by the change in mechanism from that of "singlet" to that of "triplet".

11) J. L. Magee, W. Shand and H. Eyring, *J. Am. Chem. Soc.*, **63**, 677 (1941).
12) R. A. Harman and H. Eyring, *J. Chem. Phys.*, **10**, 557 (1942).

Summary

The equilibrium of 1:1 molecular complex formation between *cis*-azobenzene and iodine in *n*-hexane has been studied spectrophotometrically in the temperature range 10~25°C. The heat of formation of the complex has been found to be $-\Delta H = 7.5$ kcal./mol. The rate of iodine-catalyzed isomerization of *cis*-azobenzene determined spectrophotometrically in *n*-hexane solution has been found to be proportional to the concentration of *cis*-azobenzene as well as to that of iodine, with an activation energy of 6.3 kcal./mol. over the temperature range 30~50°C. The most probable interpretation of the rate measurements is that the complex of *cis*-azobenzene with iodine isomerizes with an activation energy of 13.8 kcal./mol. under the experimental conditions of the present work.

The present author is particularly indebted to Professor O. Toyama of the College of Engineering and to Dr. T. Hayakawa for their discussions and encouragement during this investigation. The author wishes to thank Mr. J. Mukunoki for his assistance.

Department of Chemistry
College of General Education
The University of Osaka Prefecture
Sakai, Osaka

n-π^* Absorption Spectra of Some Aliphatic Aldehydes

By Hiroko OSHIMA

(Received October 3, 1960)

Whenever a carbonyl group is in a molecule, a weak absorption appears in a relatively long-wave region. With saturated aldehydes, this absorption appears near 2900 Å and possesses a low intensity which is about the same for all these molecules. The unfailing appearance of this absorption in molecules having a carbonyl group shows that it is due to the CO group and the constancy of its intensity in all these molecules suggests that the corresponding transitions can be given by a common interpretation. The interpretation was first made by Mulliken[1] and McMurry[2]. They say that an electron was thought to be excited from a non-bonding orbital localized on the O atom into an anti-bonding orbital. Such a transition involving the excitation of a non-bonding electron to an anti-bonding π orbital was designated an *n*-π^* transition by Kasha[3].

In this paper the effects of substituents and of solvents on the 0-0 band frequency of the *n*-π^* absorption spectra of some aliphatic aldehydes, together with their *f*-values, are investigated.

Experimental

A Hitachi automatic recording spectrophotometer EPS-2 was used for the measurement of the spectra. A 10 cm. cell was used for vapor, and a 1 cm. cell for solution. The temperature effect was investigated using a 2 cm. cell designed by Ito[4]. The optical density at various concentrations was measured and Beer's law was found to hold for all cases. For the infrared region a Hitachi double-beam recording infrared spectrophotometer EPI-2 was used.

Propionaldehyde, *n*-butyraldehyde and isobutyraldehyde were supplied by Tokyo Kasei Co. Samples were distilled just before the absorption measurement. *n*-Hexane was vigorously shaken with concentrated sulfuric acid, fuming sulfuric acid and nitric acid, then shaken with water, concentrated aqueous solutions of sodium hydroxide and potassium permanganate, dried over calcium chloride, refluxed over phosphorus pentoxide, distilled, passed through a column of freshly activated silica gel and finally distillled. Ethyl alcohol was shaken with ordinary silica gel, refluxed over sodium hydroxide, then finally distilled. Purifications of other solvents were essentially the same as those described in literature*.

Results and Discussion

Position of the *n*-π^* Absorption.—The *n*-π^* absorption spectra of aliphatic aldehydes generally appear near 2900 Å. The frequencies of absorption maxima for propionaldehyde, *n*-butyraldehyde and isobutyraldehyde are given in Table I together with values taken from literature for other aliphatic aldehydes. The maxima of the *n*-π^* absorption of corresponding carboxylic acids are cited in Table II from literature.

TABLE I. ν_{max} OF *n*-π^* ABSORPTION OF SOME ALDEHYDES IN *n*-HEXANE SOLUTION AND IN VAPOR STATE

Molecule	ν_{max}, cm^{-1}	
	n-hexane	vapor
Formaldehyde	34010[5]	
Acetaldehyde	34500[6]	34591[7]
Propionaldehyde	34119	34143
n-Butyraldehyde	33980	34003
Isobutyraldehyde	33865	33888

TABLE II. ν_{max} OF *n*-π^* ABSORPTION OF SOME CARBOXYLIC ACIDS IN LIQUID STATE

Molecule	ν_{max}, cm^{-1} liquid[8]
Formic acid	48410
Acetic acid	49003
n-Butyric acid	48764
Palmitic aic	47831

Baba and Nagakura[9] observed for carboxylic acids and ketones that the smaller the ionization potential of the substituent adjacent to the C=O group is, the greater the *n*-π^* band shifts toward the blue, interpreting the trend in the following way on the basis of the electron migration idea. In the ground state,

1) R. S. Mulliken, *J. Chem. Phys.*, **3**, 564 (1935).
2) H. L. McMurry, ibid., **9**, 231, 241 (1941).
3) M. Kasha, *Discussions Faraday Soc.*, No. **9**, 14 (1950).
4) M. Ito, *J. Mol. Spectroscopy*, **4**, 106 (1960).

* A. Weissberger, E. S. Proskauer, J. A. Riddick and E. E. Toops, Jr., "Organic Solvents", Interscience Publishers, Inc., New York (1955).
5) V. Henri and S. A. Schou, *Z. Physik.*, **49**, 774 (1928).
6) W. Herold, *Z. physik. Chem.*, **B18**, 265 (1932).
7) P. A. Leighton and F. E. Blacet, *J. Am. Chem. Soc.*, **55**, 1766 (1933).
8) H. Ley and B. Arends, *Z. physik. Chem.*, **B17**, 177 (1932).
9) H. Baba and S. Nagakura, *J. Chem. Soc. Japan, Pure Chem. Sec.* (*Nippon Kagaku Zasshi*), **72**, 72, 74, 277, 341 (1951).

electron migration from the substituent to the excited π^* orbitals of the C=O group occurs easily, but in the n-π^* excited state, this electron migration becomes difficult since the non-bonding electron then occupies the part of the π^* orbitals. As a result the stabilization energy gained by the molecule due to this electron migration is greater for the ground state than for the n-π^* excited state. So a substituent causes a blue shift for the n-π^* absorption of the unsubstituted compound. Moreover the smaller the ionization potential of the substituent adjacent to the C=O group is, the more easily the electron migration occurs. In other words, the smaller the ionization potential of the substituent is, the larger is the blue shift. The above general view was testified for the case of some aldehydes. No ionization potential data of methyl, ethyl, n-propyl and isopropyl radicals were available, but their order could be estimated from the values for paraffines given in Table III. From

Table III. Ionization potential of paraffines

Molecule	Ionization potential, eV.[10]
Methane	13.04
Ethane	11.76
Propane	11.21
n-Butane	10.80

these data it can be assumed that the ionization potential decreases in the order of methyl, ethyl, n-propyl and isopropyl radicals. From Baba and Nagakura's theory it is then expected that the n-π^* absorption band of aldehydes would show increasing blue shifts in the order of formaldehyde, acetaldehyde, propionaldehyde, n-butyraldehyde and isobutyraldehyde. However, the actual observation is that while the absorption maxima of acetaldehyde and propionaldehyde lie on the blue side of the formaldehyde maximum, n-butylardehyde and isobytyraldehyde lie on its red side. The situation is about the same as that of the corresponding carboxylic acids, where, acetic and n-butyric acids show blue shifts with respect to formic acid, but palmitic acid shows a red shift of about 580 cm^{-1}. From these observations it seems to be difficult to interpret the effect of the substituent on the absorption frequency solely by the magnitude of ionization potential and to consider only the phenomenon of blue shift as characteristic of the n-π^* transition. In addition to the blue shift caused by the ionizing tendency of the substituent, there seem to be other factors which may counteract the effect causing the blue shift. For such factors hyperconjugation, greater complexity of the molecule and hence steric effects of the alkyl radical may be considered and the general theoretical view of the spectral shift[9] due to the introduction of a substituent must be supplemented by the consideration of these additional factors.

Positions of the 0-0 Band. — Absorption spectra were measured at various temperatures

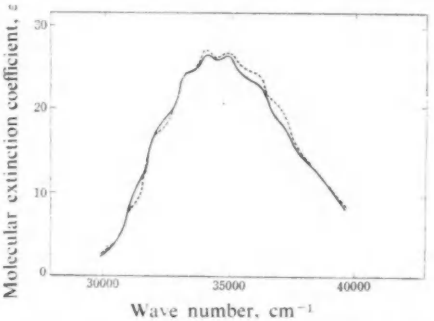

Fig. 1. Effect of temperature on the n-π^* absorption spectrum of propionaldehyde.
——, 9 °C; ----, −78 °C

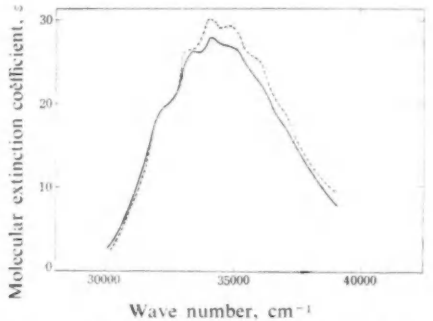

Fig. 2. Effect of temperature on the n-π^* absorption spectrum of n-butyraldehyde.
——, 9 °C; ----, 78 °C

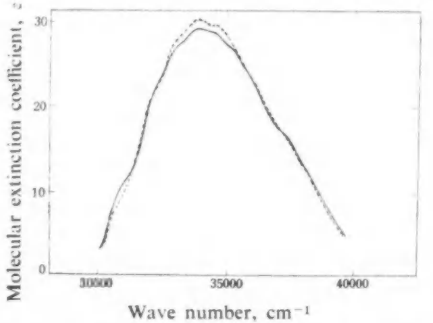

Fig. 3. Effect of temperature on the n-π^* absorption spectrum of isobutyraldehyde.
——, 9 °C; ----, −78 °C

10) R. E. Honig, *J. Chem. Phys.*, **16**, 105 (1948).

to facilitate the location of the 0-0 band. The n-π^* absorption spectra of aldehydes in n-hexane solution at 9 and -78°C are shown in Figs. 1, 2 and 3.

Absorptions on the longer wave side of the 0-0 band arise from vibrational levels in the ground state and it is expected that the absorption intensity on the red side of the 0-0 band will increase and that on the shorter wave side it will decrease with increasing temperature. If we plot the absorption curves for various temperatures, an intersection point will be obtained near the position of the 0-0 band[13]. The positions of the 0-0 bands determined in this way are given in Table IV. As shown in

TABLE IV. POSITION OF 0-0 BAND AND f-VALUE OF n-π^* ABSORPTION OF SOME ALDEHYDES

Molecule	0-0 Band, cm^{-1}	f-Value (29400~43200 cm^{-1})
Propionaldehyde	32250	5.56×10^{-4}
n-Butyraldehyde	32100	5.82×10^{-4}
Isobutyraldehyde	32000	5.58×10^{-4}

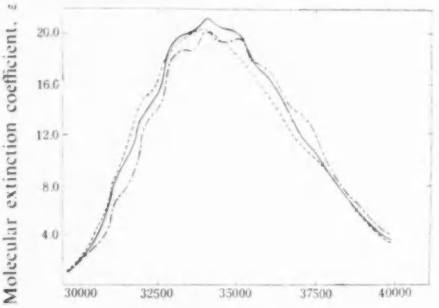

Fig. 4. n-π^* Absorption spectra of propionaldehyde (-·-·-), n-butyraldehyde (——) and isobutyraldehyde (- - - -).

Fig. 4 the n-π^* absorption spectra of propionaldehyde, n-butyraldehyde and isobutyraldehyde show the progressions of about 940 cm^{-1} interval and ν_{max}'s appear at the respective 0-2 band. The fact that the 0-0 band is weak and the 0-2 band is strong means that the minima of potential curves for the ground and excited states do not lie on top of each other but the minimum of the excited state is shifted so as to correspond to a greater equilibrium C-O distance, or that the force constant of the C-O stretching vibration decreases in the exited state.

Oscillator Strength.—As the n and π^* orbitals are both formed of the 2p orbitals of different symmetry an n-π^* transition between them is forbidden by local symmetry ("U-A" transition)[11], giving a weak absorption with the f-value of the order of 10^{-4}. f-Values calculated for aldehydes are given in Table IV. They are all of the order of 10^{-4}.

Solvent Effect.—Next we shall discuss the solvent effect on the n-π^* absorption spectra of aldehydes investigated on the basis of a theoretical equation proposed by McRae[15]. We employ McRae's equation in a simplified form after Ito et al.[16] as applied for ketone spectra,

$$\Delta\nu = \text{dispersion term} + B\frac{n_D^2-1}{2n_D^2+1} + C\left[\frac{D-1}{D+2} - \frac{n_D^2-1}{n_D^2+2}\right]$$

$$B = \frac{1}{hc}\,\frac{(M^u_{oo})^2-(M^u_{ii})^2}{a^3}$$

$$C = \frac{2}{hc}\,\frac{M^u_{oo}\{(M^u_{oo})-(M^u_{ii})\}}{a^3} \qquad (1)$$

TABLE V. PROPERTIES OF VARIOUS SOLVENTS

Solvent	Refractive index n_D	Dielectric constant D	$\frac{n_D^2-1}{2n_D^2+1}$	$\frac{D-1}{D+1}$
n-Hexane	1.375	1.89	0.186	
Carbon tetrachloride	1.460	2.238	0.215	
Benzene	1.501	2.284	0.227	
Toluene	1.498		0.226	
Dioxane	1.422	2.209	0.202	
Ethyl ether	1.356	4.335		0.526
Methyl acetate	1.362	6.68		0.654
Acetonitrile	1.344	37.5		0.924
Chloroform	1.449	4.806		0.559
Ethyl alcohol	1.361	24.3		0.809
Isobutyl-alcohol	1.398	17.7		

TABLE VI. ν_{max} OF n-π^* ABSORPTION OF SOME ALDEHYDES IN VARIOUS SOLVENTS

Solvent	ν_{max}, cm^{-1}		
	Propion-aldehyde	Isobutyr-aldehyde	n-Butyr-aldehyde
(Vapor)	34140	33980	34000
n-Hexane	34120	33870	33980
Carbon tetra-chloride	34150	33910	34050
Benzene	34330	34040	34150
Toluene	34340	33970	34150
Dioxane	34470	34070	34240
Ethyl ether	34310	33910	34170
Methyl acetate	34470	34040	34270
Acetonitrile	34760	34330	34450
Chloroform	34630	34120	34300
Ethyl alcohol	35050	34260	34470
Isobutyl alcohol	35080		34470

13) S. Broderson and A. Langseth, *Danske Mat. Fys. Medd.*, **26**, No. 3 (1951).

14) J. R. Platt, *J. Chem. Phys.*, **18**, 1168 (1950).

15) E. G. McRae, *J. Phys. Chem.*, **61**, 562 (1957).

16) M. Ito, K. Inuzuka and S. Imanishi, *J. Am. Chem. Soc.*, **82**, 1317 (1960).

For the meaning of the symbols appearing in Eq. 1 the paper by Ito et al. is referred to.

Properties of various solvents used are given in Table V and ν_{max} in Table VI.

Solvent Effect of Non-polar Solvents, *n*-Hexane, Carbon Tetrachloride, Benzene, Toluene and Dioxane.—A vibrational fine structure was fairly well observed in the *n*-hexane solution, but in other solvents the stfucture is partially blurred and in dioxane hardly observable at all. This is probably due to the slightly polar nature (0.4 D) of dioxane.

The frequency shift of the solution in non-polar solvents is given as the sum of contributions represented by the first and the second terms of Eq. 1. The contribution from the first term usually gives a red shift, while the contribution from the second term depends on the dipole-polarization force. As the dipole moment of the C=O group in aldehydes decreases during the n-π^* transition, the stabilization by this force is greater in the ground than in the excited state, so that the effect of this force gives a blue shift. If the effect due to the first term is very small compared with that of the second term, a linear relation between ν_{max} and $(n_D^2-1)/(2n_D^2+1)$ should be obtained. However, from the plots of ν_{max} against $(n_D^2-1)/(2n_D^2+1)$ shown in Fig. 5, the

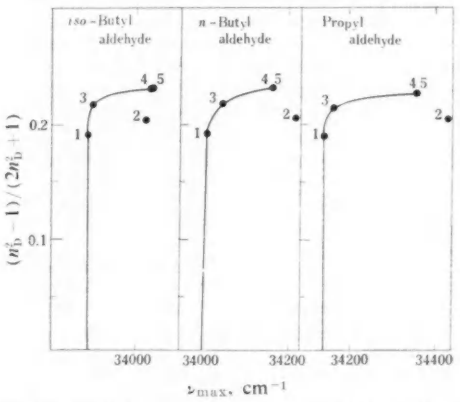

Fig. 5. Relations between ν_{max} and $(n_D^2-1)/(2n_D^2-1.)$
1, *n*-Hexane 2, dioxane 3, carbon tetrachloride 4, toluene 5, benzene.

linear relation is not observed. It is felt that the contribution from the dipole-polarization effect is greater than the dispersion effect for π-electron containing solvents such as benzene and toluene. For other solvents fairly large red shifts presumably caused by the dispersion effect are observed. The unusually large blue shift in the case of dioxane may be due to the dipole moment of the molecule as mentioned above.

Solvent Effect of Non-Hydrogen Bonding Polar Solvents, Ethyl Ether, Methyl Acetate and Acetonitrile.—The stabilization energy due to the dipole-dipole force between the solute and solvent molecules becomes smaller after the n-π^* transition. In consequence of the Franck-Condon principle, excited solute molecules will be momentarily surrounded by solvent molecules with sizes and orientations appropriate to their ground state, and as the result of this the excited state energy will become higher, leading to a blue shift. For the case of polar solvents the contribution from the third term in Eq. 1 will be the greatest and the shift depends on D. We assume here that for any of the three polar solvents 1, 2 and 3 the refractive index as well as the dispersion effect of each of them is nearly equal. Then Eqs. 2 and 3 follow from Eq. 1,

$$\nu_1-\nu_2=C\left[\frac{D_1-1}{D_1+2}-\frac{D_2-1}{D_2+2}\right] \quad (2)$$

$$\nu_1-\nu_3=C\left[\frac{D_1-1}{D_1+2}-\frac{D_3-1}{D_3+2}\right] \quad (3)$$

The plots of $\Delta\nu(\nu_{max}-\nu_{max,\,vapor})$ against $(D-1)/(D+2)$ are shown in Fig. 6. A linear

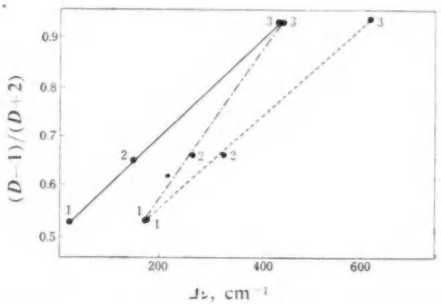

Fig. 6. Relations between frequency difference of n-π^* bands of propionaldehyde (----) *n*-butyraldehyde (-·-·-) and isobutyraldehyde (——) and $(D-1)/(D+2)$ of various solvents.
Solvent: 1, ethyl ether 2, methyl acetate 3, acetonitrile.

relationship is seen for propionaldehydehyde, *n*-butyraldehyde and isobutyraldehyde. From the slopes of the straight lines the values of C in Eq. 1 are obtained. If we know the magnitude of the quantity of a, $M^u_{oo}(M^u_{oo}-M^u_{II})$ can be calculated, and if moreover the values of M^u_{oo} are known, M^u_{II} can be obtained. Diple moment value for the ground state taken from literature and that of the excited state calculated following the above are given in Table VII. If we consider two

TABLE VII. DIPOLE MOMENT AND CONTRIBUTION OF THE C^+-O^- STRUCTURE OF SOME ALDEHYDES CALCULATED FOR $a=3$ Å IN EQUATION 1

Molecule	Dipole moment D		Contribution of the C^+-O^- structure, %	
	Ground state	Excited state	Ground state	Excited state
Propionaldehyde	2.54	1.33	43.3	22.9
n-Butyraldehyde	2.57	1.82	43.8	31.1
Isobutyraldehyde	2.58	1.48	43.9	25.2

resonating structures C=O and C^+-O^- the wave function is given by

$$\Psi = a\psi(C{=}O) + b\psi(C^+{-}O^-)$$

and the dipole moment D can be calculated as

$$D = a^2D'(C{=}O) + b^2D'(C^+{-}O^-)$$

where we take the moments of C=O and C^+-O^- as 0 and er, respectively, r being the C–O distance. The calculated results are given in Table VII, showing that the contribution from the structure C^+-O^- is small in the excited state. From this it, is obvious that the electronic configuration of the C=O group is modified greatly in consequence of the n-π^* transition.

Effect of Solvents Forming Hydrogen Bonds with Solute Molecules, Chloroform, Ethyl Alcohol and Isobutyl Alcohol. — Frequency shifts are great and ν_{max}'s appear at longer wavelengths than the respective 0-2 band. The reason for these shifts may be attributed to the hydrogen bond formation. As the non-bonding electron localized on the O atom can form hydrogen bonds with solvent molecules the stabilization energy in the ground state will be great. On the other hand, in the excited state one electron is removed from the n-orbital and the remaining one electron is not sufficient to form a strong hydrogen bond. Therefore the stabilization energy will be small. In this case a large blue shift will be expected. New bands arise at shorter wavelengths than that of the 0-2 band. The hydrogen bond formation is confirmed by infrared absorption spectra of aldehydes in carbon tetrachloride, ethyl alcohol and isobutyl alcohol solutions. The new bands are distinguished from the C=O stretching vibration bands and are clearly attributable to the hydrogen bond formation.

Summary

The n-π^* absorption spectra of propionaldehyde, n-butyraldehyde and isobutyraldehyde were measured in various solvents and the effects of substituents and solvents on the n-π^* absorption spectra were investigated. For the former effect red shifts instead of blue shifts reported as the characteristic of n-π^* transitions were observed. The latter effect was studied using McRae's equation. Hydrogen bonding between solute and solvent molecules is also considered.

The author wishes to express her hearty thanks to Professor S. Imanishi, Drs. Y. Kanda and M. Ito for their guidance and valuable discussions throughout this investigation. She is also indebted to Messrs. H. Tsukioka and S. Aziki for providing purified solvents.

Department of Chemistry
Faculty of Science
Kyushu University
Hakozaki, Fukuoka

A Molecular Orbital Treatment of Triallyl Isocyanurates and Related Allyl Esters

By Kenichi FUKUI, Hiroshi KATO, Teijiro YONEZAWA, Fumio TANIMOTO and Hisao KITANO

(Received November 29, 1960)

Triallyl cyanurate is known to be synthesized by the Schotten-Baumann reaction of allyl alcohol with cyanuric chloride[1,2]. Poly(triallyl cyanurate)[2] and triallyl cyanurate copolymer[2,3] with unsaturated polyester or other vinyl monomers have an excellent acid, alkali and heat-resistance. On the other hand, triallyl isocyanurate was prepared by the reaction of allyl chloride with potassium cyanate in acetonitrile[4] as the solvent under superatomospheric pressure, but it was not obtained in the pure crystalline form. Accordingly its melting point had not been known until triallyl isocyanurate was efficiently synthesized in our laboratory by a new method. It was carefully purified to polymerization[5]. Triallyl isocyanurate[5] which boils at 146°C/6 mmHg and melts at 23~25°C, polymerizes alone or copolymerizes with a number of vinyl monomers. The polymerization is catalyzed by peroxide to form a hard clear polymer[5].

As a preliminary consideration in connection with the experiments stated above, we are going to investigate theoretically their chemical reactivity, stability and other physical properties of some isocyanurates by the simple LCAO treatment.

The theoretically predicted properties have been found to agree well with those of the compounds which were synthesized, polymerized and treated with some reagents in our laboratory[6]. In the early stage of investigation of cyanurates and isocyanurates, Hantzsch and Bauer[7] reported the formation of mixed esters having alkyl groups on both the N and the O atom in one and the same triazine ring, and some additional, indirect evidences[8] were obtained which stood for the existence of *O,O,N*-ester (Drittel-pseudo-Cyanursäure-ester and *O,N,N*-ester (Zweidrittel-pseudo-Cyanursäure-ester). However subsequent attempts by Slotta and Tschesche[9] to prepare the mixed esters by methods diffenent from the above resulted in failure to lead them to the "Principle of Symmetry".

π-Electron Distribution in Cyanate Group.—Metal cyanates are hydrolyzed by water to liberate the active cyanate anion[10]. The isocyanate group of organic isocyanates is characterized by the polymerization or self-condensation and the condensation with various reagents containing active hydrogen atom[11]. Hence, in the first stage of LCAO molecular orbital investigation on the physical properties of isocyanurates, we calculate the π-electron distribution of NCO anion which is considered as a structural component of isocyanurates. The calculated values of total π-electron density, net charge and frontier electron density in each atom of NCO anion are listed in Table I.

Table I. The electron density in $(NCO)^-$ anion

	N	C	O
Total π-electron density	1.7204	0.6507	1.6290
Net charge	−0.7204	+0.3493	−0.6290
Frontier electron density	1.4627	0.0315	0.5048

Table II. The values of frontier electron density and one term approximation of superdelocalizability of the active methylene and the γ-carbon in allyl group in four esters

Ester	$f_{=H_2}$	$S'_{=H_2}$	$f_{=CH_2}$	$S'_{=CH_2}$
N,N,N-	0.0794	0.1145	0.1049	0.1513
N,N,O-	0.1581	0.2692	0.1089	0.1855
N,O,O-	0.1393	0.2306	0.1053	0.1743
O,O,O-	0.0847	0.1398	0.0646	0.1066

1) J. R. Dudley, J. T. Thurston, F. C. Schaefer, D. Holm-Hansen, C. J. Hull and P. Adams, *J. Am. Chem. Soc.*, **73**, 2986 (1951).
2) H. M. Day and D. G. Patterson, *Modern Plastics*, **29**, July, 116 (1951).
3) P. M. Elliott, ibid., **29**, July, 113 (1951); H. W. Starkweather, Jr., A. Adicoff and F. R. Eirich, *Ind. Eng. Chem.*, **47**, 302 (1955); W. Cummings and M. Botwick, ibid., **47**, 1317 (1955).
4) D. W. Kaiser, U. S. Pat. 2536849 (1951).
5) K. Fukui and H. Kitano, Japanese Pat. 7835 (1960).
6) K. Fukui, H. Kitano and F. Tanimoto, unpublished work (1958).
7) A. Hantzsch and H. Bauer, *Ber.*, **38**, 1005 (1905).
8) A. Hantzch, *Z. anorg. Chem.*, **209**, 213 (1932).
9) K. Slotta and R. Tschesche, *Ber.*, **60**, 301 (1927).
10) O. Masson and I. Masson, *Z. physik. Chem.*, **70**, 290 (1910).
11) R. G. Arnold, J. A. Nelson and J. J. Verbanc, *Chem. Revs.*, **57**, 47 (1957).

TABLE III. THE VALUES OF TOTAL π-ELECTRONIC ENERGIES AND CONJUGATION ENERGIES OF FOUR ESTERS

Ester	ε	ΔE_π
N, N, N-	$24\alpha + 44.5572\beta$	$1.5293\ (-\beta)$
N, N, O-	$24\alpha + 42.3475\beta$	$1.5451\ (-\beta)$
N, O, O-	$24\alpha + 40.1390\beta$	$1.5620\ (-\beta)$
O, O, O-	$24\alpha + 37.9162\beta$	$1.5647\ (-\beta)$

TABLE IV. THE VALUES OF PARAMETERS USED IN OUR CALCULATION

Coulomb integrals	Resonance integrals
$\alpha_{=H_2} = \alpha - 0.5\beta$	
$\alpha_N = \alpha + \beta$	$\beta_{C=H_2} = 2\beta$
$\alpha_{=O} = \alpha + 2\beta$	$\beta_{C=O} = \sqrt{2}\beta$
$\alpha_{-O-} = \alpha + \beta$	$\beta_{C-O-} = \beta$
$\alpha_{O^-} = \alpha + 1.5\beta$	$\beta_{N-C} = \beta$

The results show that a polarization occurs through the transfer of an electron from the carbon atom to the nitrogen and the oxygen atoms in NCO anion. It is calculated that the nitrogen atom is the reaction position in its nucleophilic attack, referring to the values of reactivity indexes, in particular to the magnitude of the frontier electron density of this anion as a nucleophilic reagent. The values of parameters used in the calculation throughout the present paper are listed in Table IV.

The Stability of the Isocyanuric Ring. — To investigate the stability of the isocyanuric ring, we calculated the conjugation energy (ΔE_π) and the resonance energy (E_R) of isocyanuric acid triester. The results obtained are compared with values of benzene.

Conjugation Energy.—The conjugation energy (ΔE_π) is defined as follows:

$$\Delta E_\pi = 3\varepsilon_M - \varepsilon_P$$

where ε_P is the total π electron energy of an isocyanurate, and ε_M is that of the isocyanate. Since the group R is not a conjugative one, it is left out of account in the calculation. An isocyanurate ring consists of three isocyanate molecules as follows:

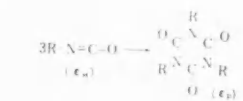

Then the conjugation energy, ΔE_π, defined above becomes $1.4888\ (-\beta)$, while with regard to benzene,

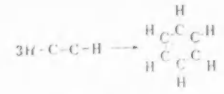

we obtain $\Delta E_\pi = 2(-\beta)$.

Resonance Energy.—The resonance energy E_R is defined

$$E_R = \varepsilon_L - \varepsilon_P$$

where ε_L is the total π electronic energy of an extreme structure in which each two π electrons are localized in each bond.

Therefore, on an isocyanurate, the resonance energy is defined as

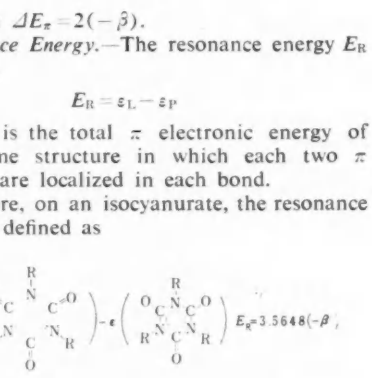

In a similar way, we calculate the resonance energy of benzene by the following equation.

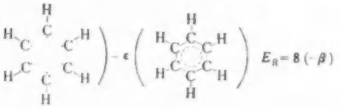

Thus we know that the conjugation energy of an isocyanurate molecule is equal to ca. 75% of that of benzene, the resonance energy of the former being 44% of benzene.

These results will account for the remarkable heat stability of the isocyanuric ring[12].

The Stability and Reactivity of Triallyl Cyanurate and Isocyanurate. — Four structural isomers of triallyl ester are indicated as *O, O, O-*, *O, O, N-*, *O, N, N-* and *N, N, N*-esters. In these are included the isomeric esters of Hantzsch and Bauer[7]. Their structure and the electrophilic frontier electron densities (f_r) are indicated in Fig. 1. We calculate further the one term approximation of superdelocalizability (S'_r)[13], the total π-elecronic energy (ε), the conjugation energy (ΔE_π)*, and the energy of the highest occupied orbital (ε_f).

The calculated results enable us to derive the following conclusions.

Reactivity of Double Bond in Polymerization and Radical Reactivity.—The values of electrophilic frontier electron density (f_r) and one term approximation of superdelocalizability (S'_r) of the methylene radical in allyl group

12) P. Lemoult, *Ann. chim. phys.*, (7) **16**, 338 (1848); A. Hofmann, *Ber.*, **3**, 264 (1879).

* In the present calculation, ally! group is taken into consideration.

13) K. Fukui, T. Yonezawa and C. Nagata, *J. Chem. Phys.*, **27**, 1247 (1957).

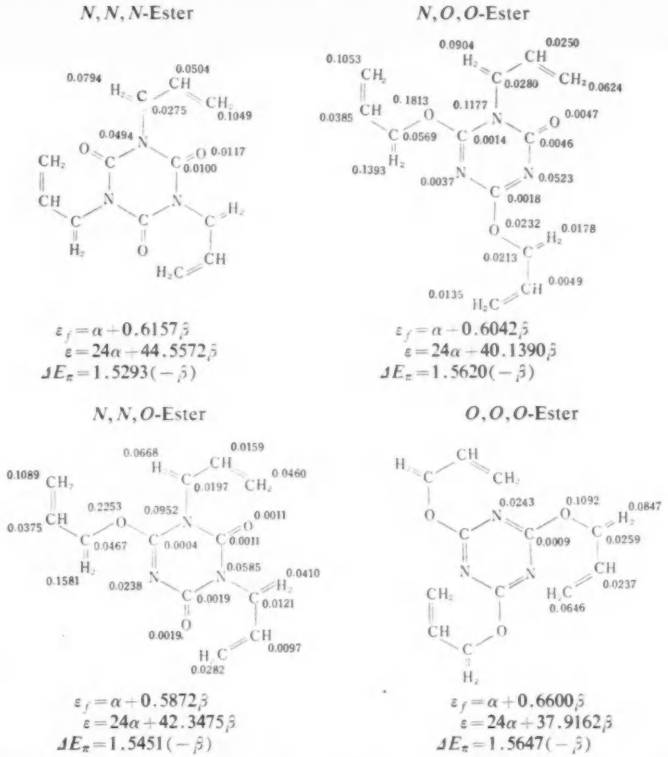
N, N, N-Ester
N, O, O-Ester
$\varepsilon_f = \alpha + 0.6157\beta$
$\varepsilon = 24\alpha + 44.5572\beta$
$\Delta E_\pi = 1.5293(-\beta)$
$\varepsilon_f = \alpha + 0.6042\beta$
$\varepsilon = 24\alpha + 40.1390\beta$
$\Delta E_\pi = 1.5620(-\beta)$
N, N, O-Ester
O, O, O-Ester
$\varepsilon_f = \alpha + 0.5872\beta$
$\varepsilon = 24\alpha + 42.3475\beta$
$\Delta E_\pi = 1.5451(-\beta)$
$\varepsilon_f = \alpha + 0.6600\beta$
$\varepsilon = 24\alpha + 37.9162\beta$
$\Delta E_\pi = 1.5647(-\beta)$

Fig. 1. Frontier electron densities, frontier orbital energy, total π-electronic energy and conjugation energy of four triallyl esters.

and the γ-carbon atom in allyl group of the isomeric esters are listed in Table II, in which are indicated the maximum values among three allyl groups of each monomer. It is found in the table that the reactivity of the methylene radical in allyl group decreases in the order *N, N, O-*; *N, O, O-* > *O, O, O-* > *N, N, N*-ester. It is worthy of note that the methylene radical in asymmetric esters should be more reactive than those in symmetric esters.

Pure triallyl isocyanurate was easily polymerized in the presence of benzoyl peroxide to give clear resin. The activation energies of the radical polymerization were observed 20.6 kcal./mol. for the *N, N, N*-ester and 43.2 kcal./mol. for the *O, O, O*-ester[6]. Further, the order of electrophilic reactivity of double bond in isomeric esters is shown to be *N, N, O-*; *N, N, N-*; *N, O, O-* ≫ *O, O, O*-ester. This result is important, because it gives us a certain of information on the reactivities of these esters in cationic polymerization.

Reaction and Heat-stability of Triallyl-cyanurate and Isocyanurate.—The values of total π-electronic energy (ε) and conjugation energy (ΔE_π) of the isomeric esters are listed in Table III. As far as π-electronic energies in these esters are concerned, the values of ΔE_π seem to indicate that the ease of hydrolysis and transesterification of allyl groups decreases in the order *O, O, O-* > *N, O, O-* > *N, N, O-* > *N, N, N*-ester, if we consider the fact that a change in activation energy parallels closely to a change of ΔE_π. Furthermore, referring to the values of ε, esters formed may have a tendency to isomerize to the *N, N, N*-ester and through this isomerization these esters beome stabilized.

In our experiments[6], however, the *N, N, N*-ester could not be prepared from the *O, O, O*-ester by thermal isomerization, because the *O, O, O*-ester decomposes and polymerizes during distillation at atmospheric pressure. On the other hand, the *N, N, N*-ester could be distilled at 289°C/760m mHg in nitrogen current. Further, the infrared spectroscopic results[6,14] for the polymer of the *O, O, O*-ester showed

14) B. H. Clampitt, D. German and J. R. Galli, *J. Polymer Sci.*, **27**, 515 (1958).

that a sort of *N, N, N*-ester structure had been formed by an isomerization during the polymerization process.

On the other hand, the weight loss on 1 hr. exposure to 300°C of the resin which was prepared by polymerization initiated by benzoyl peroxide was below 5% for the *N, N, N*-ester polymer and above 7% for the *O, O, O*-ester polymer[6]. These results indicate that the two polymers stated above are not completely identical and the *N, N, N*-ester polymer possesses a better heat stable property and a larger resistance for air oxidation than *O, O, O*-ester polymer.

Faculty of Engineeering
Kyoto University
Sakyo-ku, Kyoto

Studies on the Chemical Equilibrium Lag during the Rapid Expansion through the Rocket Nozzle

By Soji TSUCHIYA

(Received on December 2, 1960)

The expansion process causes chemical reactions in the gas flowing through a rocket nozzle, since unstable molecules and atoms involved in the combustion product reassociate in the course of the temperature drop due to the expansion. However, when the gas expands through a nozzle in very short duration as in the case of a rocket engine, the rates of chemical reactions cannot maintain the chemical equilibrium of the system, and a relaxational phenomenon occurs: in other words, the composition of the gas reaches the chemical non-equilibrium state by way of the expansion process. The observation of such a relaxational process will give information concerning the fast chemical reaction kinetics at high temperature, and also give the descriptions of hypersonic flow with chemical reactions, since great energy changes due to chemical reactions affect the velocity of flowing gas or other parameters.

These problems occur in hypersonic flows or shock waves. First, Penner pointed out this problem in the case of a rocket engine[1], and Wegener determined the rate constant of $N_2O_4 \rightleftarrows 2NO_2$ using the hypersonic nozzle flow[2], but few experimental results have been available in a nozzle flow of a rocket engine.

The present author has constructed the automatic recording pyrometer having a short response time to observe the temperature of the nozzle exhaust gas of the JP4-nitric acid rocket, and has considered the chemical equilibrium during the rapid expansion through the *de Laval* nozzle.

Pyrometer*

In the case of the pyrometry of hypersonic gas flows, optical methods are more suitable than the methods using a thermocouple or pneumatic probe to avoid a inserting material's aerodynamic heating. The automatic recording pyrometer constructed here is a modified type of the Na D line reversal method and is similar to Heidmann or Millar's technique[3], which has been improved in regard to the accuracy of measurement in this apparatus.

The Na D line reversal method is based on the fact that the flame temperature and the brightness temperature of the source lamp are the same, when the flame containing sodium atoms has neither emission nor absorption of Na D line in reference to the background spectrum of the source lamp. In the present method, the intensity of absorption or emission of the gas was measured when the source lamp had a fixed brightness temperature, and the difference between the temperature of the gas and the source lamp was determined. The accuracy obtained in the pyrometer was ± 10°K at 2000°K of the flame temperature, when the difference between the flame temperature and the brightness temperature of the lamp was 100°K. The temperature range observable by the pyrometer was from about 1500 to 3300°K.

1) D. Altman and S. S. Penner, *J. Chem. Phys.*, **17**, 56 (1949); S. S. Penner, ibid., **19**, 877 (1951).
2) P. P. Wegener, ibid., **28**, 724 (1958); *Phys. Fluid*, **2**, 264 (1959).

* Presented at the 13th Annual Meeting of the Chemical Society of Japan, Tokyo, April, 1960.
3) M. F. Heidmann and R. J. Priem, *J. Am. Rocket Soc.*, **23**, 248 (1953); G. H. Millar, J. G. Winans, O. A. Uyehara and P. S. Myers, *J. Opt. Soc. Am.*, **43**, 609 (1953).

and the response time was 0.1 sec. More detailed descriptions on the pyrometer will be given in the other paper[4].

Results

The rocket test equipment was described in the other paper[5]. The temperature measurement of the exhaust gas was performed using the following propellant:

Oxidant: White fumic nitric acid with 0.3 wt.% of sodium nitrate

Fuel: JP4 70 vol.%; *n*-Butyl vinyl ether 30 vol.%

The above propellant reacted in the combustion chamber at 20 atm., and the gas produced in the chamber expanded to atmospheric pressure through the nozzle.

The exhaust gas emitted Na D line by the contamination of sodium nitrate in the oxidant, and this contamination scarcely affected the rocket performance or the flame temperature. The results are shown in Table I.

Table I. Experimental results

Exp. No.	14	19	21	
Chamber pressure	20.2	20.0	21.4	atm.
Thrust	101	100	100	kg.
Oxidant flow rate	406	405	404	g./sec.
Fuel flow rate	81	80	82	g./sec.
O/F*	5.0	5.1	4.9	
Specific impulse	207	206	206	sec.
Exhaust temperature	1870	1830	1829	°K

* Oxidant to Fuel wt. ratio

The pyrometry by the Na D line reversal method should be applied in the case of a non-luminous flame, and the exhaust gas of a rocket engine using a hydrocarbon fuel contains carbon particles, which may cause the observed reversal temperature to be different from the real temperature of the gas. The effective emissivity due to carbon particles involved in the gas was measured without contamination of sodium nitrate by the monochromator used here and was about 0.01~0.02, which was much less than the emissivity due to sodium atoms (=0.1~0.2). Therefore, the observed exhaust temperature has nearly the same value as the real exhaust temperature.

Discussion

Calculation of Theoretical Temperatures.—First, the temperature T_c and the composition of the gas in the combustion chamber are calculated by the assumption that the chemical equilibrium is attained in the combustion chamber at pressure P_c, and that the following enthalpy relation is held:

$$\sum_i (N_i^c/\bar{M}_c)\{H^0(T_c)-H_0^0+H_f\}_i = l\{H^0(298.16)-H_0^0+H_f\}_{\text{fuel}} + m\{H^0(298.16)-H_0^0+H_f\}_{\text{oxid}} - \Delta q_c \quad (1)$$

where N_i^c is the mole fraction of component i of the product, and $\bar{M}_c$ is the mean molecular weight of the gas in the combustion chamber, and $\{H^0(T)-H_0^0+H_f\}_i$ is the total enthalpy of component i per mole[6], and l and m are the mole number of fuel and oxidant resoectively per unit mass of propellant, and Δq_c is heat loss in the combustion chamber per unit mass of the gas. Δq_c is assumed to be the same as Zucrow's experimental value[7]. The chemical equilibria considered here are the following seven equations:

$$\begin{aligned} &H_2O \rightleftarrows OH + 1/2\,H_2 \\ &H_2O \rightleftarrows H_2 + 1/2\,O_2 \\ &CO_2 \rightleftarrows CO + 1/2\,O_2 \\ &1/2\,O_2 \rightleftarrows O \\ &1/2\,H_2 \rightleftarrows H \\ &NO \rightleftarrows 1/2\,N_2 + 1/2\,O_2 \\ &1/2\,N_2 \rightleftarrows N \end{aligned} \quad (2)$$

The calculation is carried out by the trial and error method using Huff et al.'s thermodynamic tables[8].

The expansion process through the rocket nozzle is assumed to be adiabatic, and the flow of the expanding gas is considered as a one-dimentional flow ignoring the diffusion or friction. Since the entropy of the gas per unit mass is constant during the expansion;

$$(1/\bar{M}_c)\sum_i\{N_i^c S_i(T_c) - R\ln N_i^c P_c\} = (1/\bar{M}_e)\sum_i\{N_i^e S_i(T_e) - R\ln N_i^e P_e\} \quad (3)$$

where the suffixes c and e show the quantities of the gas in the combustion chamber and exhaust jet, respectively, and S_i is entropy per mole of i component of the gas. By this entropy relation, the temperature of the exhaust gas T_e can be calculated in the cases of both the frozen and shifting chemical equilibria during the nozzle expansion. In the former

4) S. Tsuchiya, *Aero. Res. Inst. Univ. Tokyo. Report*, No. 366 (1961).

5) K. Kuratani, G. Onoue and S. Tsuchiya, *Collected Pap. Aero. Res. Inst. Univ. Tokyo*, (*Kōkū Kenkyūjo Shūhō*), 2, 11 (1960).

6) Heats of formation used here are the following: H_f(JP4) = −0.419 kcal./g., H_f(*n*-Butyl vinyl ether) = −48 kcal./mol., estimated by Pauling's method, H_f(Nitric acid) = −41.10 kcal./mol., at 298.16°K.

7) M. J. Zucrow and C. M. Beighley, *J. Am. Rocket Soc.*, 22, 323 (1952).

8) V. N. Huff, S. Gordon and V. E. Morell, *NACA Rep.*, 1037 (1951).

case, the exhaust temperature T_e^{frozen} is calculated by the condition $N_i^e = N_i^c$, that is, the mole fractions of components of the gas are constant during the nozzle flow. In the latter case, however, the mole fractions vary according to the chemical equilibria in Eq. 2, which are shifting as the temperature of the gas is lowered during the expansion process; therefore $N_i^e \neq N_i^c$. The exhaust temperature T_e^{equil} has generally a higher value than T_e^{frozen} because the heat of reactions due to the shifting of the chemical equilibria is partly given to the expanded gas.

Since the nozzle expansion process is not strictly adiabatic, the entropy change Δs produced by heat loss at the nozzle should be considered;

$$\Delta s = \int dq_n / T \fallingdotseq q_n / T_t \tag{4}$$

where q_n is heat loss at the nozzle per unit mass of the flowing gas, and T_t is the temperature of the gas at the throat of the nozzle. This approximation is based on the fact that the heat loss at the nozzle occurs mostly in the throat, and the value used here is Zucrow's data[7].

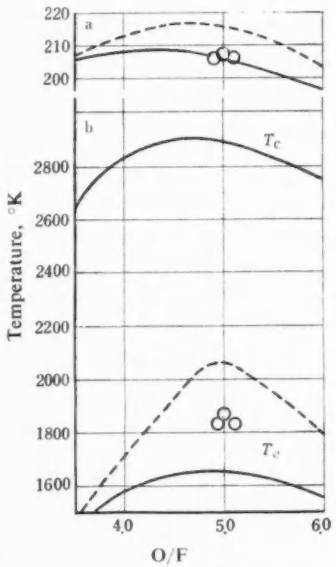

Fig. 1. Specific impulse (a) and temperature in the chamber and the exhaust (b), with correction due to heat loss in the chamber 0.05 kcal./cm²·sec., and in the nozzle 0.084 kcal./cm²·sec.;

○ : experimental value,
—— and ----: with chemical equilibria frozen and shifting, respectively.

The velocity of the exhaust gas or specific impulse I_{sp} is obtained from the enthalpy decrease of the gas due to the expansion.

$$(1/2)v_e^2 = (1/\bar{M}_c)\sum_i N_i^c\{H^0(T_c) - H_0^0 + H_f\}_i - (1/\bar{M}_e)\sum_i N_i^e\{H^0(T_e) - H_0^0 + H_f\}_i \tag{5}$$

$$I_{sp} = v_e/g \tag{6}$$

The results of calculations are given in Fig. 1 by the method above mentioned, and the equilibrium compositions of the gas in the chamber and exhaust are also given in Table II.

TABLE II. EQUILIBRIUM MOLE FRACTIONS (O/F=5.0)

	in chamber T_c=2890°K P_c=20 atm.	in exhaust T_e=2070°K P_e=1 atm.
CO_2	0.23546	0.30655
CO	0.06743	0.01062
H_2O	0.43881	0.48706
H_2	0.01750	0.00338
O_2	0.03096	0.00492
NO	0.00772	0.00072
N_2	0.17260	0.18441
OH	0.02296	0.00211
H	0.00328	0.00015
N	0.00008	0.00000
O	0.00320	0.00009

Relaxation of Chemical Equilibrium.—By comparison of the observed exhaust temperatures T_e^{obs} with the calculated values, T_e^{obs} is lower than T_e^{equil} and higher than T_e^{frozen}. This fact shows that the chemical equilibria may be neither shifting nor frozen during the actual expansion through the nozzle, and that the relaxation of the chemical equilibrium occurs during the expansion process. Since the velocity of the gas reaches 1×10^5 cm./sec. at the nozzle throat and the length of the divergent part of the nozzle used here is 7 cm., the time for the gas to pass the nozzle is of the order of 10^{-5} sec. It is considered, therefore, that the rates of the chemical reactions can not maintain the equilibrium in this short time. To analyze the situations of the chemical equilibrium during the expansion, it must be necessary that the hypersonic flow through the *de Laval* nozzle be treated taking the chemical reactions into account besides the flow descriptions[9]. This treatment is very difficult in the

9) The relaxational phenomenon on the internal energy states as well as the chemical equilibria must be considered here, but the relaxation time of internal energy may be much smaller than that of the chemical reaction, and the internal energy states scarcely deviate from equilibrium in the nozzle flow discussed here.

present nozzle flow, since the chemical reactions Eq. 2, which should occur during the expansion, are very complicated. Therefore, the approximate analysis is adopted here.

Approximate Treatment of Chemically Relaxed Flow.—Here, $-(dt/dT)$ is considered as the parameter showing whether the composition of the expanding gas has chemical equilibrium or non-equilibrium; $-(dt/dT)$ equals a time to change the temperature of the gas 1°K, and when $-(dt/dT)$ has a smaller value, the chemical equilibrium tends to be relaxed[1]. To derive the value of $-(dt/dT)$, the temperature, pressure and velocity of the expanding gas are calculated in relation to the coordinate taken in the direction of the nozzle axis. The calculation is based on the following fundamental equations:

$$\begin{aligned} &(d\rho/\rho)+(dv/v)+(dA/A)=0 && \text{conservation of mass}\\ &vdv+dh=0 && \text{conservation of energy}\\ &ds=0 && \text{isentropic relation}\\ &P=(R/\bar{M})\rho T && \text{equation of state} \end{aligned} \qquad (7)$$

where ρ is the density of the gas, v velocity of the gas, A area of the nozzle section, h enthalpy per unit mass of the gas. In the case of chemical equilibrium flow, the equations of chemical equilibria must be added to the above fundamental equations. The results are shown in Fig. 2, where the section of the *de Laval* nozzle used in this experiment is also shown. From the calculated temperature and velocity profile through the nozzle, $-(dt/dT)$ can be easily derived, and relations of $-(dt/dT)$ and the temperature of the gas are given in Fig. 3 in the cases of both frozen and equilibrium flow. At the divergent part of the nozzle, the order of $-(dt/dT)$ is 10^{-3} sec./deg., and is of much greater value near the combustion chamber. It is, therefore, probable that the nozzle flow of the gas may have chemical equilibrium near the throat of the nozzle and the relaxational phenomenon may occur after the gas passes the throat.

Then, the chemically relaxed flow of the gas can be treated by the following approximation: the combustion product in the chamber at pressure P_c expands to a pressure P^* and a

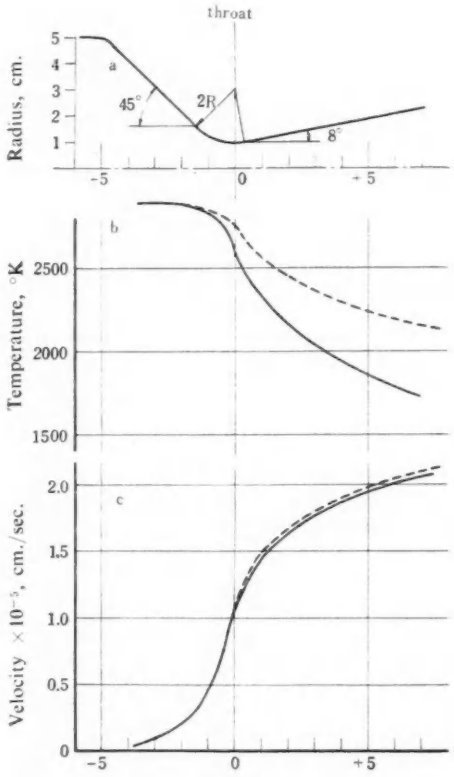

Fig. 2. Section of the nozzle parallel to the nozzle axis (a), and temperature (b) and velocity (c) profiles during the expansion process at O/F=5.0, without correction due to heat loss in the nozzle;
—— and ----: with chemical equilibria frozen and shifting, respectively.

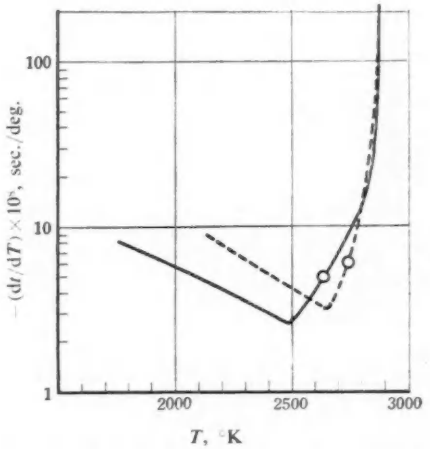

Fig. 3. Calculated curve of $-(dt/dT)$ during expansion through the nozzle in relation to the temperature of the gas at O/F=5.0, without correction due to heat loss in the nozzle;
○ : value of $-(dt/dT)$ at the throat,
—— and ----: with chemical equilibria frozen and shifting, respectively.

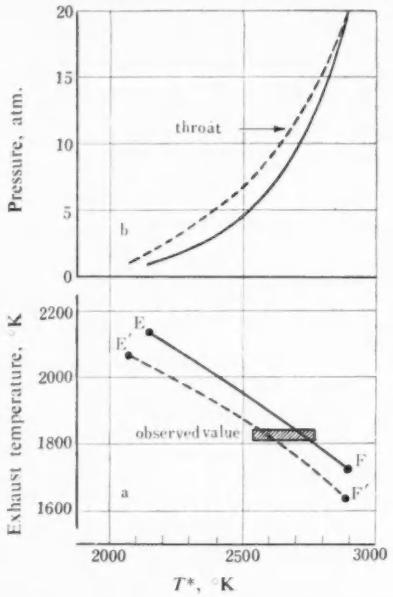

Fig. 4. Calculated exhaust temperature by 'suddenly frozen' approximation (a) and pressure of the gas (b) against T^* at O/F = 5.0;
—— and ----: without and with correction due to heat loss in the nozzle, respectively. Points F and E in curve (a) correspond to the exhaust temperatures with chemical equilibria frozen and shifting, respectively.

temperature T^* with the chemical equilibria shifting, and from a pressure P^* to the exhaust pressure P_e with the chemical equilibria frozen. This approximation means:

$$\text{at } T>T^* \text{ and } P>P^*, \quad -(dt/dT)=\infty,$$
$$\text{at } T<T^* \text{ and } P<P^*, \quad -(dt/dT)=0,$$

in other words, the expansion through the nozzle proceeds from P_c to P^* at infinitely low speed and from P^* to P_e at infinitely high speed. Recently, the author has treated the expansion process of hydrogen gas with recombining reaction of hydrogen atoms more strictly, and ascertained that the above approximation gives nearly the right illustration of the flow through the *de Laval* nozzle[10]. The foundation of this approximation is that the relaxational process ends in a very short time after the composition of the gas deviates from an equilibrium state, and that the chemical equilibria of the system are instantly frozen. In general, the relaxation of the chemical equilibrium increases the entropy of the system[11]. However, this entropy increase may be small owing to the shortness of the relaxational process, and the isentropic condition may be assumed. The same situations about the flow of diatomic gases through the *de Laval* nozzle have been considered also by Bray and by Hall and Russo[12].

The calculated results by this 'suddenly frozen' approximation are shown in Fig. 4. The pressure P^* and the temperature T^* at which the relaxation of chemical equilibrium occurs in the present nozzle flow, can be determined by a comparison of the observed exhaust temperature T_e^{obs} and the exhaust temperature T_e^{sf} calculated by the 'suddenly frozen' approximation. T_e^{obs} agrees T_e^{sf} at $T^* \fallingdotseq 2600$°K and $P^* \fallingdotseq 10$ atm. This means that the chemical equilibrium may be relaxed near about 2600°K and 10 atm. during the expansion. The position, where the temperature and pressure of the gas reach the obtained T^* and P^*, is slightly outside the throat of the nozzle. The $-(dt/dT)$ at this position is about 5×10^{-8} sec./deg., and the relaxation is estimated to occur at $-(dt/dT)^* = 3\sim8\times10^{-8}$ sec./deg.

The obtained limiting value of $-(dt/dT)$ for keeping the chemical equilibrium of the system can be related to the chemical reaction rate, but the kinetic mechanism is too complicated to analyze the present expansion through the nozzle, in which the recombination of atoms and the oxidation of carbon monoxide or hydrogen may be the main reactions, as Table II shows. Altman and Carter say that $-(dt/dT)$ ranges from about 7 to 3×10^{-7} sec./deg. at a divergent part of a nozzle in a rocket having a large thrust like the V-2, since $-(dt/dT)$ is approximately proportional to a square root of thrust. Considering the atomic recombining reaction rate, they estimate that the expansion through such a nozzle proceeds with the chemical equilibria shifting[13]. This estimation is consistent with the present experiment.

If a more simple system is treated, the rapid expansion through the *de Laval* nozzle can be used as a new technique for the measurement of fast reaction rate at high temperature.

Summary

The pyrometer fitted for the temperature measurement of exhaust gas of the rocket, was constructed, and the exhaust temperature of

10) S. Tsuchiya, to be published.

11) W. W. Wood and J. G. Kirkwood, *J. Applied Phys.*, **28**, 395 (1957).
12) K. N. C. Bray, *J. Fluid Mech.*, **6**, 1 (1959); J. G. Hall and A. L. Russo, *Cornell Aero. Lab. AFOSR TN* 59-1090 (1959).
13) D. Altman and J. M. Carter, "Combustion Process", Ed. by B. Lewis, R. N. Pease and H. S. Taylor, Princeton Univ. Press, Princeton (1956), p. 51.

the JP4-nitric acid rocket having 100 kg. of thrust, was observed. From the obtained exhaust temperature, it has been ascertained that the expansion of the gas through the present nozzle proceeds with chemical equilibria neither shifting nor frozen, and that relaxation occurs. From the approximate analysis of chemically relaxed flow, the relaxational process is assumed to occur at $-(dt/dT)^* = 3 \sim 8 \times 10^{-8}$ sec./deg., $T^* \fallingdotseq 2600$°K and $P^* \fallingdotseq 10$ atm.

The author wishes to express his sincere thanks to Assistant Professor K. Kuratani for his kind encouragement throughout this work. His thanks are also expressed to Mr. G. Onoue for his help in constructing the apparatus.

Aeronautical Research Institute
The University of Tokyo
Meguro-ku, Tokyo

Solvent Extraction of Inorganic Nitrates with Diphosphonate Ester. I. Zirconium, Yttrium and Lanthanide Nitrates

By Hideo Saisho

(Received December 8, 1960)

Various extracting agents have been investigated on the solvent extraction of many elements. Much attention has been paid to such extracting agents as organophosphorus compounds (tri-*n*-butyl phosphate and others) and β-diketones (thenoyltrifluoroacetone and others).

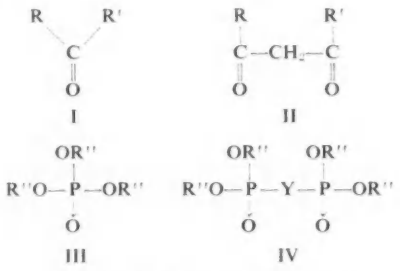

Fig. 1. The structural formulae of ketone (I), β-diketone (II), tri-*n*-alkyl phosphate (III) and diphosphonate ester (IV).

The extractability of various metal ions with β-diketone (Fig. 1-II) is much higher than that with ketone (Fig. 1-I), though both ketone and β-diketone are used for the solvent extraction. From the similarity of structural formulae as shown in Fig. 1, it is expected that diphosphonate ester (Fig. 1-IV) may show better extractability than tri-*n*-alkyl phosphate (Fig. 1-III). Thus, in the present paper tetra-*n*-butyl ethylenediphosphonate* (TBEDP), $(BuO)_2P(O)(CH_2)_2(O)P(BuO)_2$, was chosen, and the extractability of zirconium, yttrium and several lanthanide elements (cerium, promethium, europium and lutetium) was studied on the system between TBEDP-kerosene and various nitric acid concentrations.

Although Kennedy et al.[1] reported the solvent extraction of uranium with diphosphonate esters, the extracting behavior was not studied in detail. Since then, no investigations on the diphosphonate esters extraction of some elements other than uranium have been reported.

Experimental

Solvent.—TBEDP purchased from the Tama Chem. Co., Tokyo, Japan, was used without any further purification. TBEDP was diluted with kerosene to 0.1 or 0.2 M according to the experimental requirements. Kerosene used here had flash point above 60°C and was not specially purified. Nitric acid solutions were prepared by diluting concentrated nitric acid, special grade. The acidity range of the solution covered from 0.01 to 13 M. The acidity was determined volumetrically, whenever necessary.

Determination of Distribution Ratios.—The distribution ratio of a given nuclide, defined as the concentration of the nuclide in the organic phase divided by that in the aqueous phase, was determined radiochemically.

Five millilitres of nitric acid solution containing the radioactive tracer and the equal volume of TBEDP diluted with kerosene were placed together in a 30 ml. glass-stoppered cylinder, and shaken vigorously in a thermostat kept at 25±0.5°C. Shaking was continued for 30 min. Preliminary

* Tetra-*n*-butyl ethylenediphosphonate is abbreviated as TBEDP.

1) T. V. Healy and J. Kennedy, *J. Inorg. & Nucl. Chem.*, **10**, 128 (1959).

tests showed that the equilibrium was attained in less than 10 min. Then, the two phases were separated by the use of a separating funnel.

Aliquots from organic or aqueous phases were taken into small stainless steel dishes and carefully dried under an infrared lamp.

Radioactivity of Y-91, Ce-144, Pm-147, Eu-152-154 and Lu-177 was measured with a G.-M. counter having a window of 3.10 mg./cm² thick. As it took at least about four hours to evaporate aliquots to dryness, Ce-144 and its daughter, Pr-144 reached the radioactive equilibrium completely when the activities were counted. Amounts of Zr-95 were measured at the Zr-95 (0.754 and 0.722 MeV.) photopeaks by an Argonne Type 256 Channel Pulse Height Analyzer with a 3" diameter ×3" NaI(Tl) crystal.

Radioisotopes Used.—The radioisotopes used in this experiment were Zr-95, Y-91, Ce-144, Pm-147, Eu-152-154 and Lu-177. These tracers were imported from Oak Ridge National Laboratory, U.S.A. or Radiochemical Centre, U. K.

Ce-144 and Eu-152-154 received as nitrates were used without further treatments. However, Y-91, Pm-147 and Lu-177 were converted into nitrates by a cation exchange technique**, because they were imported as chlorides. The cerium tracer was always kept in the trivalent state.

Zr-95 tracer[2] was freed from Nb-95 as follows: Zr-95 was first extracted into a 0.5 M TTA (thenoyltrifluoroacetone)-xylene solution from 2 M nitric acid solution containing Zr-Nb-95. The Zr-95 tracer was stripped into 8 M nitric acid solution from the organic phase diluted with xylene by a factor of 10 or more. The solution was used immediately after the separation.

Results and Discussion

Effect of Nitric Acid Concentration.— The results obtained are plotted in Figs. 2-4, where other authors' results[3-6] for each element in the extraction with TBP (tri-*n*-butyl phosphate) from nitric acid are added for comparison.

Fig. 2 shows the variation of distribution ratio, K_d, of zirconium in the range of nitric acid concentration from 0.01 to 13 M, keeping the TBEDP concentration 0.1 M. As Fig. 2 shows, the acid-dependence curves for TBP and TBEDP have a similar tendency concerning the fact that the distribution ratios increase with increasing acidity in both cases.

Fig. 3 also shows the variation of K_d of yttrium and lutetium in the same acidity range

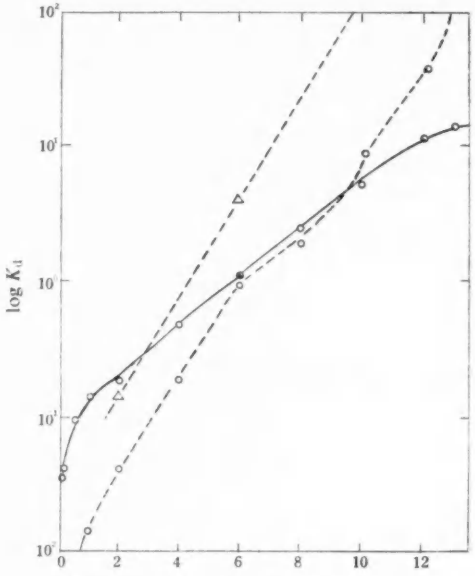

Fig. 2. The K_d values of zirconium.
—○—: 0.1 M TBEDP in kerosene
---○---: McKay et al.[3], 19% TBP in kerosene
--△--: Peppard et al.[4], 100% TBP

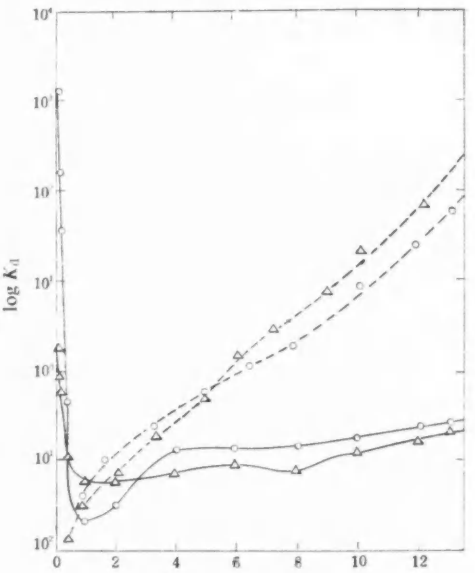

Fig. 3. The K_d values of yttrium and lutetium.
——: 0.2 M TBEDP in kerosene
----: McKay et al.[5,6], 100% TBP
○ : Yttrium △ : Lutetium

** The radioactive tracer was adsorbed on the resin Dowex 50-X8, H form column and then eluted with nitric acid solution.

2) F. L. Moore, *Anal. Chem.*, **28**, 997 (1956).
3) K. Alcock, F. C. Bedford, W. H. Hardwich and H. A. C. McKay, *J. Inorg. & Nucl. Chem.*, **4**, 100 (1957).
4) K. F. Peppard, G. W. Mason and J. L. Maier, ibid., **3**, 215 (1956).
5) D. Scargill, K. Alcock, J. M. Fletcher, E. Hesford and H. A. C. McKay, ibid., **4**, 304 (1957).
6) E. Hesford, E. E. Jackson and H. A. C. McKay, ibid., **9**, 279 (1959).

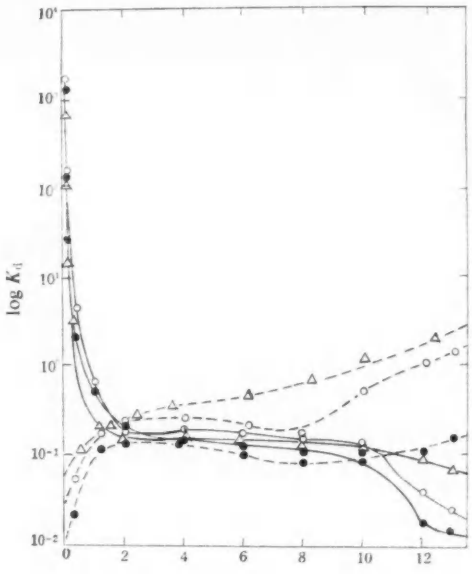

Fig. 4. The K_d values of cerium, promethium and europium.
——: 0.2 M TBEDP in kerosene
----: McKay et al.[5,6], 100% TBP
●: Cerium ○: Promethium
△: Europium

as in the case of zirconium, keeping the TBEDP concentration 0.2 M. As shown in Fig. 3, there is a remarkable difference between TBP and TBEDP in the very low acidity range below about 0.5 M nitric acid. In TBEDP extraction the K_d values are very high at 0.01 M nitric acid and decrease sharply with increasing acidity up to about 1 M nitric acid. In the higher acidity range the K_d values by TBEDP tend to increase gradually, while those by TBP increase rapidly. Similarity in the extraction of yttrium and lutetium with TBEDP appears to be in accordance with the fact that they belong to the yttrium group.

Fig. 4 indicates the results for cerium, promethium and europium under the same experimental conditions as the case for yttrium and lutetium. In the low acidity region the extracting behavior of cerium, promethium and europium is very similar to that of yttrium and lutetium; the K_d values of these three elements decrease sharply with increasing acidity. On the contrary in the higher acidity the K_d values have decreasing tendency, though those by TBP increase in this region. It is interesting for the author that the sequence of the K_d values by TBEDP in the region agrees with that by TBP.

From the above-mentioned facts, it may be said that this extracting agent is very excellent for the extraction of trivalent elements such as lanthanide elements especially in the low acidity region. The difference between K_d values for a lanthanide element and zirconium is so great in the low acidity region that a lanthanide element may be separated from zirconium very easily.

Effect of Nitrate Concentration on Extraction of Zirconium.—The results obtained with 0.1 M TBEDP concentration are given in Table I. This table shows that the distribution ratios

Table I. Effect of nitrate concentration on extraction of zirconium (0.1 M TBEDP in kerosene)

Molarity					Distribution
HNO_3	NH_4NO_3	$Ca(NO_3)_2$	$Al(NO_3)_3$	Total NO_3	ratio
4	—	—	—	4	0.50
8	—	—	—	8	2.85
4	4	—	—	8	1.43
4	—	2	—	8	2.81
4	—	—	1.33	8	3.45
10	—	—	—	10	5.40
4	6	—	—	10	1.93
4	—	3	—	10	3.49
4	—	—	2	10	6.53
12	—	—	—	12	10.75
4	8	—	—	12	3.45
4	—	4	—	12	8.09
4	—	—	2.66	12	11.10

can increase when other nitrates are added to nitric acid. This fact suggests that the extraction of zirconium by TBEDP depends on nitrate ion concentration to some extent. The results also indicate that zirconium is extracted much more readily from nitric acid solution containing aluminum nitrate, than from pure nitric acid solution of the same total nitrate ion concentration.

The author wishes to express his sincere thanks to Dr. Hiroshi Ohinouye, Director of the Laboratory of Mitsubishi Atomic Power Industries, Inc., and Mr. Kazumu Sugimoto, Chief of Chemistry Section of the Laboratory for their support and permission to present this work.

Thanks are also due to Professor Nobufusa Saito and Assistant Professor Yuji Yokoyama of the University of Tokyo for their suggestions and guidance, and Mr. Ryoichi Uehara for his effort in the synthesis of tetra-*n*-butyl ethylenediphosphonate.

Engineering & Research Laboratory
Mitsubishi Atomic Power Industries, Inc.
Ohmiya, Saitama

Cyclic Acetylenes. V. Syntheses and Properties of Strained Cyclic Ethers of o, o'-Dihydroxydiphenyldiacetylene

By Fumio TODA and Masazumi NAKAGAWA

(Received December 9, 1960)

In the previous paper of this series[1], the present authors reported the syntheses and the ultraviolet spectroscopic properties of a series of diacetylenic macrolides (I, $n=3$, 4, 5 and 7). In the course of the synthesis of the compound I, it was found that the ester linkages are

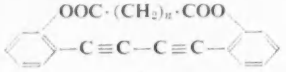

I

cleft when the number of methylene groups is 2 or 3 yielding 2, 2'-dibenzofuranyl and other related compound, and the cleavage of the ester linkage was attributed to the large ring strain involved in I. The present paper deals with the syntheses of a series of analogous cyclic diacetylenes in which the ester linkage is replaced by the ether linkage to avoid the cleavage reaction in the course of the ring closure. The synthesis was carried out according to the following series of reactions.

The diketone III which was obtained by the reaction of polymethylene dihalide ($n=4$, 5 and 6) with sodium salt of *o*-hydroxyacetophenone (II) was treated with phosphorus pentachloride to yield the chloro-derivative. The chloro-derivative was dehydrochlorinated with sodamide in liquid ammonia to yield the terminal diacetylene IV, ($n=4$, 5 and 6).

The terminal diacetylene IV, ($n=1$, 2, 3 and 4) was also prepared by the reaction of sodium *o*-ethynylphenoxide (V) with polymethylene dihalide ($n=1$, 2, 3 and 4). The terminal diacetylene IV thus obtained was submitted to the oxidative coupling reaction according to Eglinton's procedure[2]. The yields of the cyclic diacetylenes VI$_b$, VI$_c$, VI$_d$ and VI$_e$ formed by the intramolecular oxidative coupling were found to be 3, 40, 40 and 40%, respectively. In the case of $n=2$, the cyclic diacetylene could not be isolated from the reaction mixture. This is probably attributable to the high strain which may arise from the ring formation. The cyclic tetraacetylenes VII$_a$, VII$_b$, VII$_c$ and VII$_e$ which are the products of the bimolecular

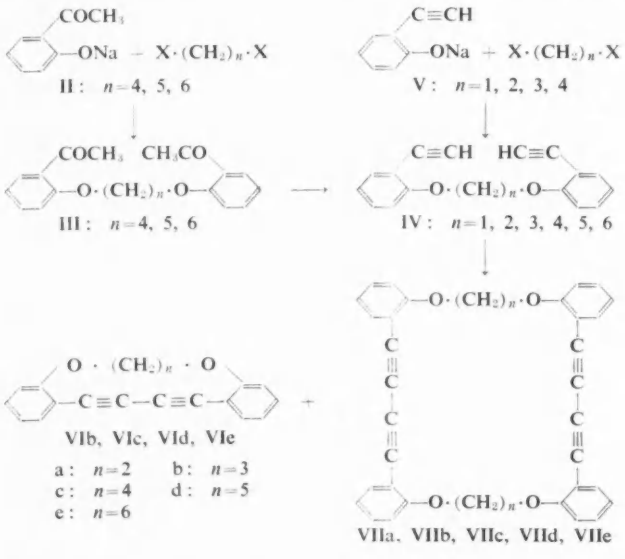

II: $n=4$, 5, 6

V: $n=1$, 2, 3, 4

III: $n=4$, 5, 6

IV: $n=1$, 2, 3, 4, 5, 6

VIb, VIc, VId, VIe

a: $n=2$ b: $n=3$
c: $n=4$ d: $n=5$
e: $n=6$

VIIa, VIIb, VIIc, VIId, VIIe

1) F. Toda and M. Nakagawa, This Bulletin, **33**, 223 (1960).

2) G. Eglinton and A. R. Galbraith, *Chem. & Ind.*, **1956**, 737; *J. Chem. Soc.*, **1959**, 889.

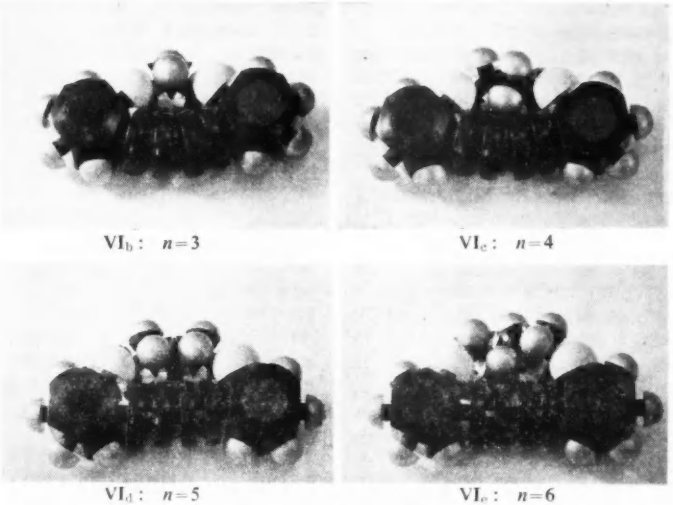

VI_b: $n=3$ VI_c: $n=4$

VI_d: $n=5$ VI_e: $n=6$

Fig. 1. The molecular models of VI (Courtauld model).

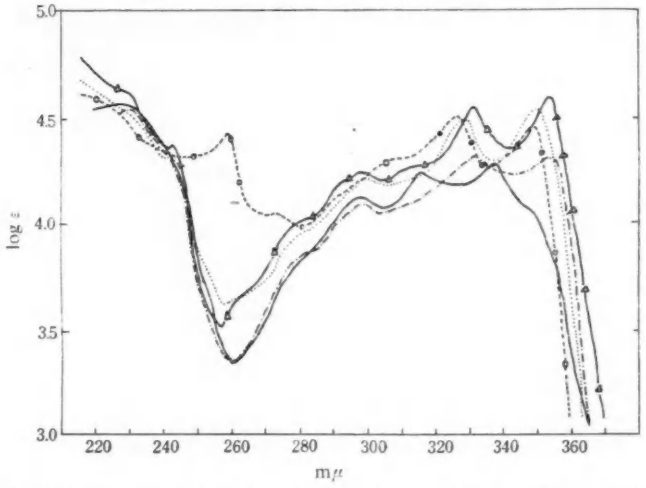

Fig. 2. The ultraviolet spectra of the cyclic diacetylenes (VI) and $VIII_a$.

——: VI_b in 99.5% ethanol
—△—△: VI_d in 95% ethanol
--□--□: $VIII_a$ in 95% ethanol
—·—·—: VI_c in 95% ethanol
·····: VI_e in 95% ethanol

coupling reaction were isolated from the reaction mixture in the yield of 2.5, 1, 2, trace and 10%, respectively. The formation of a cyclic dimer is an interesting contrast to the fact that the oxidative coupling of di-*o*-ethynylphenyl polymethylene dioate gave only the monomeric cycle I and the formation of the dimeric tetraacetylene was not observed[1].

The structures of VI and VII were determined by the analytical data, molecular weight determination and ultraviolet and infrared spectroscopic evidences. VI is a fairly stable compound, except in the case of VI_b which is found to be unstable to heat. The molecular weight of VI_b could not be determined by the Rast method due to its thermal instability; therefore the molecular weight was estimated by the X-ray method*.

* The determination of molecular weight by the X-ray method was kindly performed by Dr. Y. Tomiie of the Laboratory of Physical Chemistry of this Department to whom the authors express their sincere gratitude.

TABLE I

Compound	Solvent	Absorption					
VI_b	E	231 (300)	298 (111)	316 (144)	337 (159)		
VI_c	E*	230 (345)	299 (122)	331 (201)	353 (199)		
VI_d	E*	243 (218)	299 (161)	331 (317)	353 (365)		
VI_e	E*	242 (203)	299 (158)	328.5 (297)	349 (336)		
VII_a	D	260 (285)	**272** (112)	310 (186)	324 (240)		344 (174)
VII_b	D	259.5 (100)	**276** (76)	310 (135)	324 (232)		351 (216)
VII_c	D	261 (350)	**275** (105)	310 (185)	321 (196)		349 (115)
VII_d	D	260 (148)	276 (97)	313 (197)	331 (324)		353 (331)
VII_e	D	261 (269)	274 (100)	313 (188)	329 (257)		351.5 (212)
$VIII_a$	E*	259.5 (265)	274.5 (111)	**309** (203)	326 (321)		349 (286)
$VIII_a$	E	259 (260)	273 (107)	**310** (199)	326 (327)		348 (293)
$VIII_b$	E	259.5 (282)	274 (108)	**310** (194)	326 (297)		349 (253)
IX_a	D		**280** (91)	299 (199)	320 (333)		343 (390)
IX_a	E	**230** (377)	**280** (98)	298 (205)	319 (338)		341 (392)
IX_b	E	**230** (395)	**280** (100)	298 (182)	322.5 (241)		341 (248)
XII	E	**230** (399)	**280** (93)	298 (172)	319 (226)		341 (247)
XIII	D	261 (222)	**275** (104)	309 (184)	328 (251)		350 (202)
XV	D	261 (287)	**275** (130)	310 (212)	328 (323)		351 (285)
XV	E	260 (289)	273 (110)	310 (215)	326 (346)		348 (300)
XVII	E	232 (288)	**278** (75)	296 (168)	317 (269)		338.5 (291)
XVIII	E	258 (204)	273 (76)	307 (168)	323.5 (278)		346 (239)
XIX	E*	260 (213)	275 (85)	305 (168)	323 (270)		345 (236)
DDD	E	258 (262)	273 (100)	291 (127)	326 (300)		348.5 (277)
DDD	NaOH aq.	218 (616)	**261** (228)	278 (97)	296 (99)	317 (110)	359 (226)

The figures indicate the λ_{max} in mμ.
The figures in parentheses are $\varepsilon_{max} \times 10^{-2}$.
The bold figures indicate shoulders.
E, E* and D denote 99.5% ethanol, 95% ethanol and dioxane, respectively.
DDD means *o*, *o'*-dihydroxydiphenyldiacetylene.

It is to be noted that VI_c and VII_c exist in dimorphic forms and the melting points of the former substance were found to be 96 and 112°C, and those of the latter were 184~185°C (stable form) and 207~208°C. The analytical data and the measurement of solvent of crystallization revealed that VII_b contains 2 mol. of benzene.

An examination of the scale model of VI reveals that the polymethylene bridge in VI_d is slightly short and that of VI_e is slightly long to hold the molecule in a uniplanar, strain free conformation, but the ring strain involved in VI_d and VI_e seems to be very small and these molecules may have an almost planar and rigid structure. On the other hand, the diacetylenic linkage in VI_c is forced to bend owing to the length of its bridging chain, the

degree of bending of the diacetylenic bond being much larger in VI_b in accordance with the shorter methylene bridge as illustrated in Fig. 1. *o,o'*-Dimethoxydiphenyldiacetylene ($VIII_a$) and *o,o'*-diethoxydiphenyldiacetylene ($VIII_b$) were prepared and the ultraviolet spectra of these open chain analogues were compared with those of VI. As indicated in Fig. 2 and Table I, the location of the absorption maxima in the spectra of VI_d and VI_e at the long wavelength region were found to be almost identical with those of the open chain models $VIII_a$ and $VIII_b$. But the absorption intensities (ε_{max}) of VI_d and VI_e are found to be larger than those of $VIII_a$ and $VIII_b$ indicating the rigid and planar structure of these cyclic diacetylenes. The sequence of

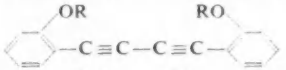

VIIIa : R = CH_3 VIIIb : R = C_2H_5

decrease of the ε_{max}-values are found to be $VI_e > VI_d > VI_c > VI_b$. This sequence of the ε_{max} indicates that the planarity of the molecule increases the transition probability and the increase in the bending of diacetylenic linkage causes the decrease of the probability. It is remarkable that the λ_{max} of VI_b shifted about 12 mμ to shorter wavelength as compared with VI_d, VI_e and the open chain models. It has been already known in numerous examples, especially in substituted biphenyls[4] or substituted acetophenones[5], that relatively weak steric hindrance in the excited state of these molecules diminishes the transition probability resulting in the decrease of absorption intensity, and the presence of a strong steric hindrance in the excited state causes a hypsochromic shift of the absorption maxima as the result of the increased transition energy. As the two phenyl groups in the molecule of VI_b are held in a coplanar position owing to the short methylene bridge, the hypsochromic shift and the hyperchromic effect observed in VI_b may be attributed to the bending of the diacetylenic linkage. This may be the first example in which the bending of acetylenic linkage results in a hypsochromic shift of the characteristic K-band. The methylene chain in VI is held closely parallel with the diacetylenic unit and the ultraviolet spectra of these cycles show a sharp and intense λ_{min} at ca. 260 mμ making a sharp contrast with those of VIII and VII in which a λ_{max} exists at the same wavelength. This absorption minimum was also observed in the spectra of I ($n=3$ and 4). As pointed out in the previous paper[1], the disappearance of λ_{max} at this position may be ascribed to the presence of a proximity effect of the methylene group to the acetylenic linkage (Figs. 3 and 4, Table I). Also the appearance of a new λ_{max} in the spectra of VI near 230~240 mμ is the same trend as observed in I. These results are also confirmed with X_a, X_b, XIII and XV, which will be discussed in the following section.

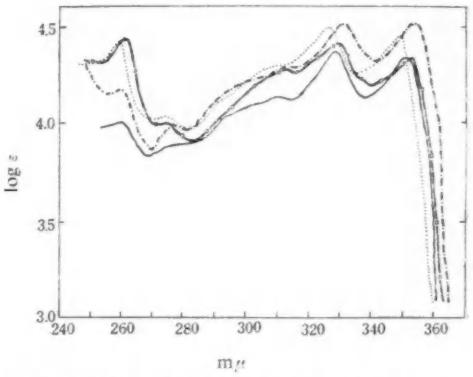

Fig. 3. The ultraviolet spectra of the cyclic dimers (VII) and $VIII_b$.
——— : VII_b in dioxane
- - - - - : VII_d in dioxane
—○—○— : VII_e in dioxane
····· : $VIII_a$ in 95% ethanol
The curve of VII was drawn using the reduced ε values corresponding to a diyne-unit.

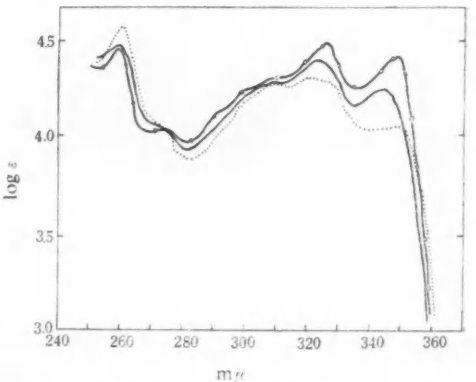

Fig. 4. The ultraviolet spectra of the cyclic dimers (VII) and $VIII_b$.
····· : VII_c in dioxane
——— : VII_a in dioxane
—○—○— : $VIII_b$ in 99.5% ethanol
The curve of VII was drawn using the reduced ε values corresponding to a diyne-unit.

4) E. A. Braude and E. A. Evans; *J. Chem. Soc.*, **1954**, 607; M. T. O. Shaughnessy and W. H. Rodebush, *J. Am. Chem. Soc.*, **62**, 2906 (1940).
5) E. A. Braude, F. Sondheimer and W. F. Forbes, *Nature*, **173**, 117 (1954).

The ultraviolet spectra of VII_b, VII_d and VII_e do not depart from those of the open chain analogues as illustrated in Fig. 3 (cf. Table I). On the other hand, abnormal absorption spectra were observed in the case of VII_a and VII_c (Fig. 4 and Table I). An examination of the scale models of these cyclic dimers reveals that the molecule bearing a short methylene bridge of an even number of carbon atoms can not take uniplanar structure, and the abovementioned anomalous ultraviolet spectra of VII_a and VII_c may be attributed to the non-planar geometry of these molecules.

The reaction of sodium *o*-ethynylphenoxide (V) with *cis*- or *trans*-1, 4-dichloro-2-butene yielded the terminal diacetylene, IX_a and IX_b, respectively. The oxidative coupling of IX by means of cupric acetate in pyridine[2] resulted in the cyclic diacetylenes, X_a and X_b in a 33 and 30% yield, respectively. These diacetylenic cycles were found to be unstable to heat. It was observed that X_a (m. p. 154°C (decomp.)) is completely decomposed when heated to a temperature of 145°C for 30 min. The structure of X_a and X_b were inferred from its analytical data and its ultraviolet and infrared spectroscopic evidences. The molecular weight of X_a and X_b could not be determined by Rast's method on account of its thermal instability, therefore the molecular weight of the decahydroderivatives XI were determined by Rast's method in camphor. Also the structure of XI was confirmed by the identity with the reduction product of VI_c. Inspection of the scale models of X_a and X_b indicates that the molecules involve large ring strain due to the bending of the diacetylenic linkage as shown in Fig. 5. The ultraviolet spectra of X_a and X_b showed a shift to shorter wavelength about 8 mμ as illustrated in Fig. 6 (Table I). This fact may be ascribed to the increase of the transition energy on account of the strong ring strain. Interestingly, enough, the ultraviolet spectrum of X_b has broad absorption peaks as compared with those of X_a (Fig. 6). The scale models of X_a and X_b indicate that the ethylenic bond in the former is held apart from the diacetylenic unit in the cycle; on the other hand, the double bond in the bridging chain in the latter molecule is held closely to

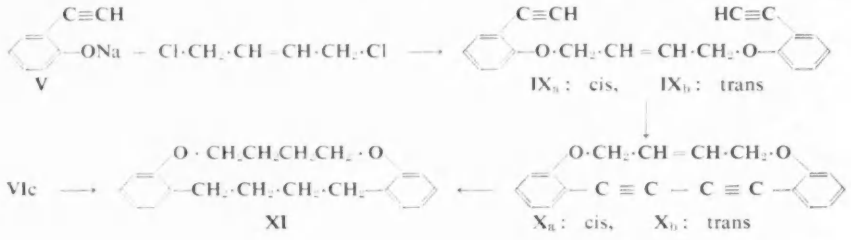

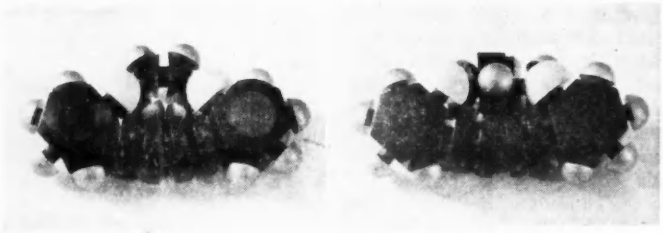

X_a X_b

XII

Fig. 5. The molecular models of X and XII (Courtauld).

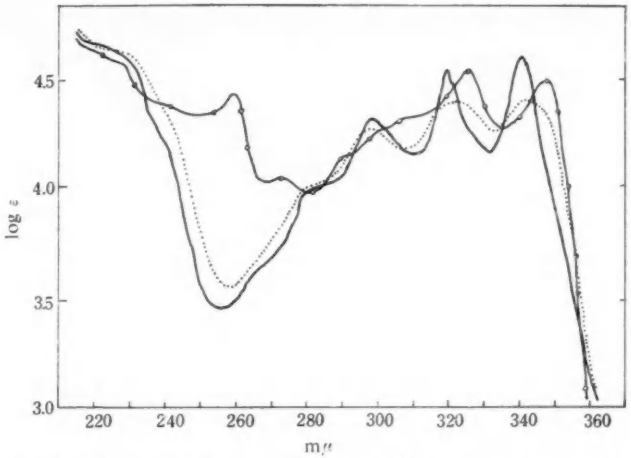

Fig. 6. The ultraviolet spectra of X and $VIII_a$ (in 99.5% ethanol).
———: X_a ·····: X_b —·—: $VIII_a$

the diacetylenic linkage (Fig. 5). Therefore the above-mentioned anomalousness of the absorption peaks of X_b seem to be associated with a transannular interaction between the π-electrons of the double bond in the bridging chain and those of the diacetylenic unit. Another example of the same type of transannular phenomenon will be discussed in the following paper[6].

The oxidative coupling of the terminal diacetylene obtained by the reaction of *o*-xylylene dibromide with V afforded the cyclic diacetylene XII and the cyclic dimer XIII in a yield of 8 and 3%, respectively. XII was found to be a heat sensitive substance, and the molecular weight was determined with the reduction product, XIV. The ultraviolet spectrum of XII does not depart from that of X_a indicating that the ring strain in XII is almost equal to that of X_a. Also the similarity of the ultraviolet spectra of XII and X_a exclude the possibility of the presence of a transannular interaction between the phenylene group in the bridging chain and the diyne unit. In the most probable geometry of the molecule of XII which was inferred from the inspection of the scale model; the *o*-phenylene group seems to hold too far apart from the diacetylenic linkage for interstitial effects to operate (Figs. 5 and 7). The fact that the cyclic dimer XIII crystallized with two moles of benzene is the same as in the case of VII_b. The configuration of XIII seem to be almost strain free, since the ultraviolet absorption spectrum of XIII is similar to those of VIII and XV as recorded in Fig. 8 and Table I.

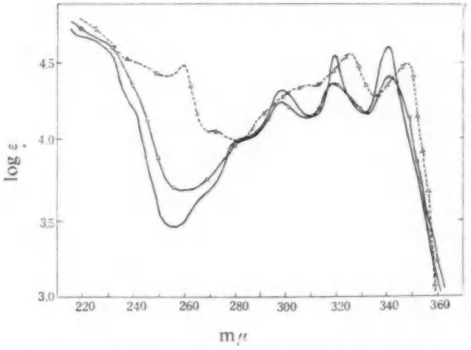

Fig. 7. The ultraviolet spectra of X_a, XII and XV (in 99.5% ethanol).
———: X_a —·—: XII ···△···△: XV

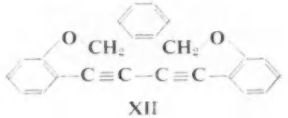

XII

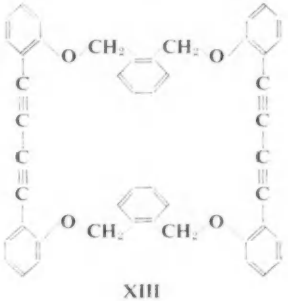

XIII

6) F. Toda and M. Nakagawa, This Bulletin, 32, 514 (1959).

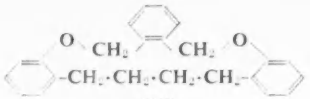

XIV

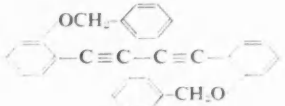

XV

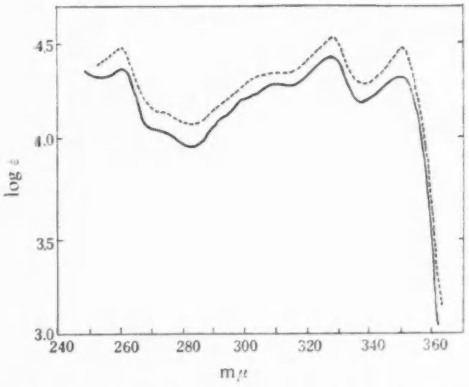

Fig. 8. The ultraviolet spectra of the cyclic tetraacetylene (XIII) and the open chain analogue (XV) (in dioxane).
——: XIII ·····: XV
The curve of XIII was drawn using the reduced ε values corresponding to a diyne-unit.

The diethynyl compound XVI which was prepared by the reaction of 1,4-dichloro-2-butyne and V was oxidized according to the procedure of Eglinton. The cyclic triacetylene XVII was obtained in a yield of 3.5% as heat sensitive crystals together with a large amount of sparingly soluble amorphous solid with high melting point. The monomeric structure of XVII was inferred from the ultraviolet and infrared spectroscopic evidences. It was observed that the ultraviolet absorption maxima in the spectrum of XVII shifts to shorter wavelength (ca. 8 mμ) as compared with those of the open chain analogue (XVIII). (Fig. 9 and Table I). Substitution of a hydrogen atom in the methyl group of

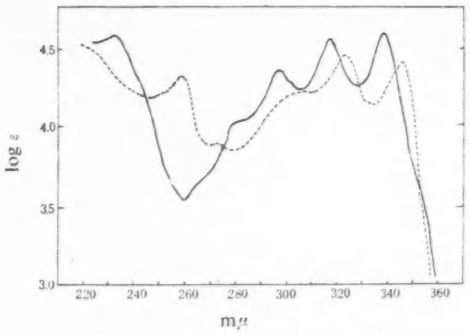

Fig. 9. The ultraviolet spectra of the cyclic triacetylene (XVII) and the open chain analogue (XVIII) (in 99.5% ethanol).
——: XVII ------: XVIII

the phenoxy ether by an electron attracting group such as ethynyl or carboxymethyl group result in a slight hypsochromic shift of the ultraviolet spectra as illustrated in Fig. 10, therefore XVIII was chosen as a linear model of XVII. Conversly the ultraviolet spectrum of *o*,*o*'-dihydroxydiphenyldiacetylene in an

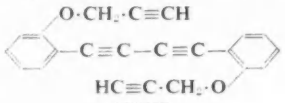

XVIII

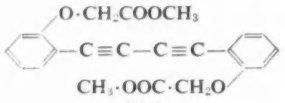

XIX

aqueous alkali showed a red-shift with a change in the absorption curve as compared with that of in a neutral solution (Fig. 11). The ultraviolet spectroscopic behavior of the derivatives of *o*,*o*'-dihydroxydiphenyldiacetylene indicates that the availability of electrons on the oxygen atoms in the conjugated position to the chromophor system of *o*,*o*'-dihydroxydiphenyldiacetylene is responsible for the abovementioned blue- or red-shift of the spectrum. The heat sensitivity and the hypsochromic shift of the spectrum of XVII may be associated with the deformation of diacetylenic linkage due to the large ring strain.

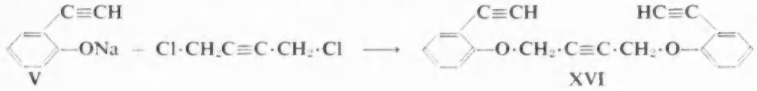

V XVI

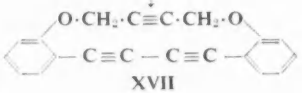

XVII

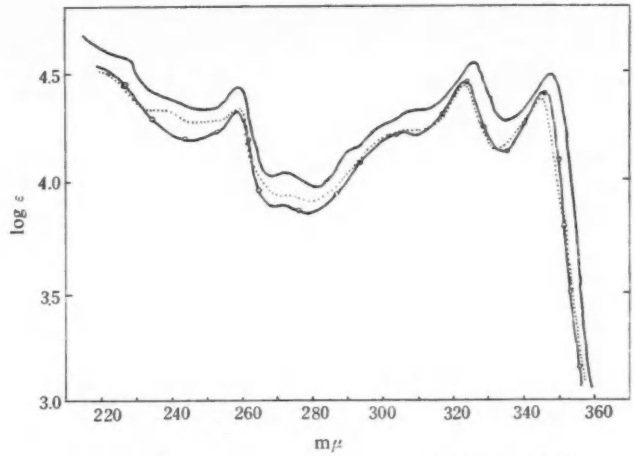

Fig. 10. The ultraviolet spectra of XVIII, XIX and $VIII_a$.
——: $VIII_a$ in 99.5% ethanol —○—○: XVIII in 99.5% ethanol
·····: XIX in 95% ethanol

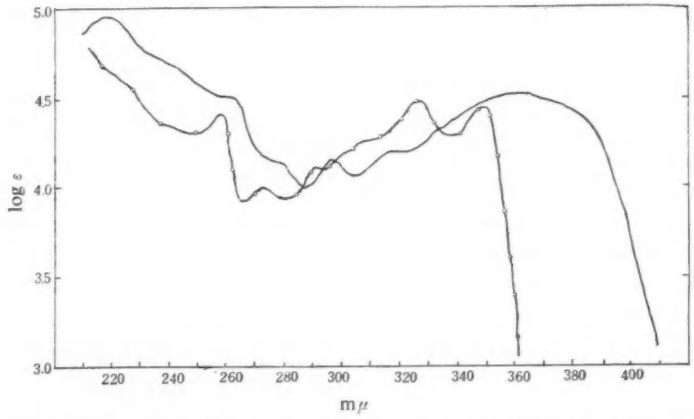

Fig. 11. The ultraviolet spectra of *o,o'*-dihydroxydiphenyldiacetylene in a neutral and an alkaline solution.
—○—○: in 99.5% ethanol ——: in an aqueous sodium hydroxide

It was revealed from the above-mentioned observations that the bending of the diyne in the diphenyldiacetylene system in which the two phenyl groups are held in a uniplanar or in a near uniplanar position exerts a minor effect on the ultraviolet spectrum. It was well-known that the twist of single bond in a conjugate system such as *o,o'*-disubstituted acetophenones[4] or 2,2'-disubstituted biphenyls[5] results in a remarkable change in their ultraviolet spectra. An insulation of conjugation at the position of the twisted single bond was assumed from the change of the ultraviolet spectra of *o,o'*-disubstituted acetophenones and 2,2'-disubstituted biphenyls bearing substituents with large steric requirement. The maximal shift among the abovementioned strained cyclic diacetylenes was found to be 12 mμ. The

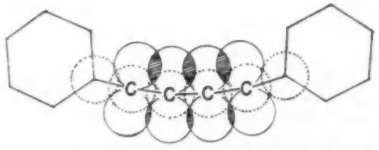

Fig. 12. A schematic illustration of p-orbital overlapping in a bent diphenyldiacetylene system.

minor effect on the bending of the diyne unit on the spectrum is quite understandable if we consider the shape of p-orbitals of conjugated acetylenic linkage. As schematically illustrated in Fig. 12, the bending of the diacetylenic linkage causes only a minor change in the overlapping of its p-orbitals. This may be the cause of the slight hypsochromic shift of the strained diacetylenic cycles.

As reported in the previous paper[1], the smallest macrolide I, ($n=3$) was a very photosensitive substance, and the sensitivity was attributed to the bending of the diacetylenic linkage. But the highly strained ether analogues such as VI_b, X_a, X_b, XII and XVII were found to be fairly stable to light, but sensitive to heat. These findings indicate that the photosensitivity of I ($n=3$) may possibly be attributable to a photochemical reaction of the carbonyl function with the acetylenic bond which is held in the proximity of the ester linkage or the creavage of the strained ester linkage by the photoexcitation on the molecule. To confirm this point, it appeared desirable to examine the photosensitivity of another cyclic diacetylene containing carbonyl function in the bridging chain. The present authors have attempted the synthesis of a keto-ether derivative of *o*, *o'*-dihydroxydiphenyldiacetylene. The high dilution Dieckmann condensation of carbomethoxymethyl ether of *o*,*o'*-dihydroxydiphenyldiacetylene (XIX)[1] to yield a cyclic ketocarboxylate resulted in the formation of a brown red resinous material, and the expected ketoester could not be isolated.

Experimental**

1, 5-Bis-(*o*-acetylphenoxy)-pentane (III, $n=5$).—*o*-Hydroxyacetophenone (10.9 g., 0.08 mol.) was added to an ethanolic solution of sodium ethoxide (sodium, 2.0 g. and absolute ethanol, 25 ml.), and the solvent was removed under reduced pressure. The sodium phenoxide thus obtained II was mixed with 1,5-diiodopentane (13.6 g., 0.042 mol.) and the mixture was heated to 160~170°C for 4 hr. The cooled reaction mixture was filtered and the solid was washed with ethanol, hot water and ethanol, successively. The dried material was recrystallized from benzene or ethanol yielding III ($n=5$), colorless needles, m. p. 104~105°C. 5.5 g. (40%).

Found: C, 74.14; H, 7.16. Calcd. for $C_{21}H_{24}O_4$: C, 74.09; H, 7.11%.

IR max., 1665 (C=O), 1245 (=C-O-) cm^{-1}.

1, 6-Bis-(*o*-acetylphenoxy)-hexane (III, $n=6$).—The reaction of 1,6-diiodohexane and II according to the method similar to that described above resulted in III ($n=6$), colorless plates or needles, m. p. 121°C in a yield of 42%.

Found: C, 74.80; H, 7.47. Calcd. for $C_{22}H_{26}O_4$: C, 74.55; H, 7.39%.

IR max., 1667 (C=O), 1250 (=C-O-) cm^{-1}.

1, 4-Bis-(*o*-acetylphenoxy)-butane (III, $n=4$).—The reaction of II with 1,4-diiodobutane was carried out according to the above-mentioned procedure yielding III ($n=4$), colorless needles, m. p. 147°C in a yield of 34%.

Found: C, 73.18; H, 6.88. Calcd. for $C_{20}H_{22}O_4$: C, 73.60; H, 6.79%.

IR max., 1665 (C=O), 1242, 1231 (=C-O-) cm^{-1}.

Syntheses of IV ($n=4$, 5 and 6) from III.—The mixture of phosphorus pentachloride (12.0 g., 0.058 mol.), $III_{n=6}$ (9.0 g., 0.025 mol.) and phosphorus oxychloride (15 ml.) was heated to 80~85°C for 45 min. The phosphorus oxychloride was removed under reduced pressure. The crude chloride thus obtained was dissolved in anhydrous ether (50 ml.). The ethereal solution was added into the solution of sodamide in liquid ammonia (prepared from sodium, 5 g., 0.23 mol. and ammonia, 200 ml.) during a period of 20 min. under mechanical stirring. Stirring was continued for a further 1.5 hr., and the ammonia was allowed to evaporate. The residual solid was mixed with water (200 ml.) and extracted with ether (350 ml.). The extract was washed with water and dried over magnesium sulfate. The solvent was distilled, resulting in a crystalline solid. The solid was recrystallized repeatedly from ethanol using active charcoal to yield $IV_{n=6}$, colorless needles, m. p. 89~90°C, 3.8 g. (47%).

Found: C, 82.49; H, 7.22. Calcd. for $C_{22}H_{22}O_2$: C, 82.98; H, 6.96%.

IR max., 3270 (-C≡CH), 1245 (=C-O-) cm^{-1}.

The reaction of $III_{n=5}$ with phosphorus pentachloride followed by dehydrochlorination yielded $IV_{n=5}$, colorless needles, m. p. 91.5~92°C, (38%).

Found: C, 82.65; H, 6.85. Calcd. for $C_{21}H_{20}O_2$: C, 82.86; H, 6.62%.

IR max., 3280 (-C≡CH), 2110 (-C≡C-), 1252 (=C-O-) cm^{-1}.

Similar treatment of $III_{n=4}$ afforded $IV_{n=4}$, colorless prisms, m. p. 82°C, (40%).

Found: C, 82.43; H, 6.24. Calcd. for $C_{20}H_{18}O_2$: C, 82.73; H, 6.25%.

IR max., 3250 (-C≡C-), 1250 (=C-O-) cm^{-1}.

Syntheses of IV ($n=1$, 2, 3 and 4) from V.—*o*-Hydroxyphenylacetylene (2.3 g., 0.02 mol.) was added to a solution of sodium ethoxide in ethanol (sodium, 9.5 g. and absolute ethanol, 5 ml.). The solvent was removed under reduced pressure at room temperature to yield V. A solution of 1,4-diiodobutane (3.1 g., 0.01 mol.) in dimethylformamide (20 ml.) was added to V, and the mixture was refluxed for 2.5 hr. The cooled reaction mixture was poured into ice-water (200 ml.). The crude crystals deposited were filtered, then washed with water and ethanol, successively. The crude $IV_{n=4}$ thus obtained was recrystallized from ethanol using active charcoal to give pure $IV_{n=4}$, colorless prisms, m. p. 82°C, 1.7 g. (59%), undepressed on admixture with $IV_{n=4}$ which was derived from $III_{n=4}$.

The reaction of *o*-hydroxyphenylacetylene (1.5 g.)

** No melting points were corrected. Infrared spectra were measured by the Nujol mull method and molecular weights were obtained by the Rast method (in camphor). Otherwise some special indication was given.

with 1,3-dibromopropane according to the above-mentioned procedure yielded crude $IV_{n=3}$ as a viscous oil, (1.7 g.), IR max., 3400 (-C≡CH), 2160 (-C≡C-), 1260 (≡C-O-) cm^{-1}. The crude oil was used without further purification for the oxidative coupling.

A similar reaction of *o*-hydroxyphenylacetylene (1.5 g.) with ethylene dibromide gave $IV_{n=2}$, colorless prisms, m. p. 150°C, 250 mg., (15%).

Found: C, 82.27; H, 5.29. Calcd. for $C_{18}H_{14}O_2$: C, 82.42; H, 5.38%.

IR max., 3280 (-C≡CH), 2130 (-C≡C-), 1252 (≡C-O-) cm^{-1}.

Similarily the reaction of *o*-hydroxyphenylacetylene (1.5 g.) with dibromomethane yielded $IV_{n=1}$, viscous oil, (1.9 g.), IR max., 3370 (-C≡CH), 2160 (-C≡C-) and 1230 (≡C-O-) cm^{-1}.

Oxidative Coupling of $IV_{n=6}$. — The mixture of cupric acetate monohydrate (15 g.), pyridine (150 g.) and $IV_{n=6}$ (1.5 g.) was stirred for 4 hr. at 55~60°C. The solvent was distilled under reduced pressure at a temperature below 40°C. Water was added to the residue, and extracted with ether (300 ml.). The extract was washed with an aqueous solution of cupric acetate and water, successively. The ether solution was dried over anhydrous magnesium sulfate. The residue obtained by evaporating the solvent was dissolved in benzene (20 ml.) and treated with active charcoal. The crude crystals obtained by concentrating benzene were fractionally recrystallized from ethyl acetate. The crystals from the more soluble portions were recrystallized from aqueous acetic acid to yield pure VI_c, colorless needles, m. p. 130°C, 0.6 g. (40%).

Found: C, 83.43; H, 6.59. Mol. wt., 322. Calcd. for $C_{22}H_{20}O_2$: C, 83.51; H, 6.37%. Mol. wt., 316.

IR max., 2150 (-C≡C-), 1272, 1243 (≡C-O-) cm^{-1}.

The crystals obtained from the less soluble portions were recrystallized from ethyl acetate yielding VII_c, colorless needles, m. p. 207~208°C, 0.15 g. (10%). The melting point of this substance changed to 184~185°C on standing at room temperature for several days.

Found: C, 83.13; H, 6.49. Mol. wt., 630. Calcd. for $C_{44}H_{40}O_4$: C, 83.51; H, 6.37%. Mol. wt., 632.

IR max., 2137 (-C≡C-), 1250 (≡C-O-) cm^{-1}.

Oxidative Coupling of $IV_{n=5}$.—$IV_{n=5}$ (1.0 g.) was added to the mixture of pyridine (150 g.) and cupric acetate monohydrate (10 g.), and the mixture was stirred for 3 hr. at 55°C. The crude crystals obtained by the treatment of the reaction mixture were recrystallized repeatedly from aqueous acetone yielding needles mixed with a small amount of crystalline grains. The crystalline mixture was digested with ethyl acetate to dissolve the needles. The insoluble crystalline grains were filtered and the filtrate was concentrated to dryness. Repeated recrystallization of the residual solid from aqueous acetone yielded pure VI_d, colorless needles, m. p. 132~132.5°C, 0.4 g. (40%).

Found: C, 83.27; H, 5.93. Mol. wt., 312. Calcd. for $C_{21}H_{19}O_2$: C, 83.42; H, 6.00%. Mol. wt., 302.

IR max., 2200 (-C≡C-), 1250 (≡C-O-) cm^{-1}.

The elementary analysis of the crystalline grains (m. p. 180~181°C) could not be performed owing to its small amount, but the molecular weight determination (Found: 514) indicates that the grains should be the cyclic dimer (VII_d, $C_{42}H_{36}O_4$: Mol. wt., 604) of $IV_{n=5}$. IR max., 2200, 2137 (-C≡C-), 1250 (≡C-O-) cm^{-1}.

Oxidative Coupling of $IV_{n=4}$. — A solution of $IV_{n=4}$ (1.0 g.) and cupric acetate monohydrate (10.0 g.) in pyridine (100 g.) was stirred for 4 hr. at 50°C. The crude crystals isolated from the reaction mixture were digested with hot ethanol. The insoluble material was filtered, and the filtrate was cooled to deposite crystals. The crystals, on recrystallization from ethanol, gave pure VI_c, colorless needles or plates, m. p. 96 or 112°C, 0.4 g. (40%). It was observed that VI_c melts at 112°C when the temperature of a heating bath is gradually raised from room temperature. But VI_c melts at 96°C when the bath was heated previously to 80°C. The solid obtained by cooling the molten crystals melts at 112°C by the ordinary method of measurement, but it melts also at 96°C in a preheated bath.

Found: C, 83.01; H, 5.42. Mol. wt., 271. Calcd. for $C_{20}H_{16}O_2$: C, 83.31; H, 5.59%. Mol. wt., 288.

IR max., 2210 (-C≡C-), 1240 (≡C-O-) cm^{-1}.

The above-mentioned insoluble solid was recrystallized from ethyl acetate yielding VII_c, colorless needles, m. p. 237~238°C, 20 mg. (2%).

Found: C, 82.52; H, 5.45. Mol. wt., 533. Calcd. for $C_{40}H_{32}O_4$: C, 83.31; H, 5.59%. Mol. wt., 576.

IR max., 2210, 2150 (-C≡C-), 1240 (≡C-O-) cm^{-1}.

Hydrogenation of VI_c.—VI_c (100 mg.) in benzene (15 ml.) was reduced over 5% palladium-on-charcoal (20 mg.). After removal of the solvent in a vacuum, the residue was recrystallized from aqueous ethanol yielding XI, colorless plates, m. p. 63.5°C, 100 mg.

Found: C, 80.48; H, 8.09. Mol. wt., 303. Calcd. for $C_{20}H_{24}O_2$: C, 81.04; H, 8.16%. Mol. wt., 296.

XI showed no depression of the mixed melting point on admixture with the hydrogenation products of X_a and X_b. Also the infrared spectra of these saturated macrocycles are found to be identical over the entire region of wavelength.

Oxidative Coupling of $IV_{n=3}$. — Treatment of $IV_{n=3}$ (1.7 g.) with Eglinton's reagent (cupric acetate monohydrate, 10 g. and pyridine, 100 g.) at 47°C for 4 hr. gave crude crystals. The crude material was digested with hot ethanol (30 ml.) to remove the insoluble material. The crystals obtained by diluting the ethanolic solution with water was recrystallized repeatedly from aqueous ethanol to give pure VI_b, colorless needles, m. p. 115°C, (decomp.), 50 mg. (3%).

Found: C, 83.31; H, 5.34. Calcd. for $C_{19}H_{14}O_2$: C, 83.20; H, 5.15%.

IR max., 2210 (-C≡C-), 1227 (≡C-O-) cm^{-1}.

The monomeric nature of VI_b was deduced from the X-ray crystallographic data (space group, C_{2h}^6 – C^2/c, dimension of unit cell, a=22.22 Å, b=13.04 Å, c=11.20 Å, Z=8).

The abovementioned ethanol insoluble material was dissolved in benzene and treated with active charcoal. The crystals deposited from the benzene solution were recrystallized from benzene resulting in VII_b, colorless needles, m. p. 228~229°C (decomp.), 20 mg. (1%). It was observed that the transparent crystals on the hot stage of a Kofler

block became turbid at about 100°C. This phenomenon could be ascribed to the loss of the solvent of crystallization (benzene).

Found: C, 85.13; H, 5.76, benzene of crystallization, 22.47%. Calcd. for $C_{38}H_{28}O_4 \cdot 2C_6H_6$: C, 85.20; H, 5.72, benzene of crystallization, 22.03%.

The analytical data of the solvent-free material was found to be as follows:

Found: C, 83.83; H, 5.11. Mol. wt., 534. Calcd. for $C_{38}H_{28}O_4$: C, 83.20; H, 5.15%. Mol. wt., 548.

IR max., 2160 (-C≡C-), 1250 (=C-O-) cm^{-1}.

Oxidative Coupling of $IV_{n=2}$.—A mixture of $IV_{n=2}$ (200 mg.), cupric acetate monohydrate (3.0 g.) and pyridine (30 g.) was kept for 4.5 hr. at 40°C under mechanical stirring. The reaction mixture was treated according to the usual manner. The crude crystals thus obtained were recrystallized from ethyl acetate or ethyl acetate-methanol yielding VII_n, colorless needles, m. p. 250~252°C (decomp.), 5 mg. (2.5%), Mol. wt., 505. Calcd. for $C_{36}H_{24}O_4$: Mol. wt., 520. IR max., 1245 (=C-O-) cm^{-1}.

***o,o'*-Dimethoxydiphenyldiacetylene ($VIII_n$).**—*o,o'*-Dihydroxydiphenyldiacetylene (1.0 g., 0.043 mol.) was dissolved in an ethanolic solution of sodium ethoxide (sodium, 0.23 g. and absolute ethanol, 30 ml.). Methyl iodide (14.2 g., 0.1 mol.) was added to the solution. The mixture changed to neutral after heating at 50~60°C for 0.5 hr. and at 95°C for 1 hr. The crystals obtained by cooling the reaction mixture were filtered, then washed with water and ethanol, successively. The crude material was recrystallized from ethanol giving $VIII_n$, colorless prisms, m. p. 138°C, 1.0 g. (90%).

Found: C, 82.13; H, 5.57. Calcd. for $C_{15}H_{14}O_2$: C, 82.42; H, 5.38%.

IR max., 2146 (-C≡C-), 1246 (=C-O-) cm^{-1}. (measured by KBr-disk method).

***o,o'*-Diethoxydiphenyldiacetylene ($VIII_b$).**—A mixture of *o,o'*-dihydroxydiphenyldiacetylene (1.0 g., 0.0043 mol.), sodium ethoxide in ethanol (sodium, 0.46 g. and absolute ethanol, 20 ml.) and ethyl bromide (10 g., 0.1 mol.) was heated to 55~60°C for 30 min. and to 95°C for 2 hr. The neutral reaction mixture was filtered to remove the inorganic salt. Water was added to the filtrate and extracted with ether (50 ml.). The extract was washed with aqueous potassium hydroxide and water, successively, and dried over anhydrous magnesium sulfate. The oily material obtained by evaporating the solvent changed gradually to a crystalline mass. $VIII_a$ was obtained as colorless needles, m. p. 72°C, 1.1 g. (91%) on the recrystallization of the mass from ethanol.

Found: C, 82.59; H, 6.27. Calcd. for $C_{20}H_{18}O_2$: C, 82.73; H, 6.25%.

IR max., 2180 (-C≡C-), 1250 (=C-O-) cm^{-1}.

Synthesis of IX_b.—*o*-Hydroxyphenylacetylene (2.1 g., 0.018 mol.) was dissolved in a solution of sodium ethoxide in ethanol (sodium, 0.4 g. and absolute ethanol, 5 ml.). After removal of the alcohol in a vacuum at room temperature, the residue was mixed with *trans*-1,4-dichloro-2-butene (1.2 g., 0.009 mol.), a catalytic amount of potassium iodide and dimethylformamide (20 ml.) and the mixture was refluxed for 1 hr. The neutral reaction mixture was poured into ice-water. The crystals deposited were filtered, then washed with water and ethanol, successively. The crude crystals were recrystallized from ethanol yielding IX_b, colorless leaflets, m. p. 118~119°C, 1.5 g. (60%).

Found: C, 82.72; H, 5.66. Calcd. for $C_{20}H_{16}O_2$: C, 83.31; H, 5.59%.

IR max., 3255 (-C≡CH), 2105 (-C≡C-), 1240 (=C-O-), 975 (*trans*-ethylene) cm^{-1}.

Synthesis of IX_a.—The reaction of *cis*-1,4-dichloro-2-butene (1.2 g., 0.009 mol.) with *o*-hydroxyphenylacetylene (2.1 g., 0.018 mol.) according to the same procedure as that described above yielded IX_a, red oil, 2.3 g. (85%).

IR max., 3400 (-C≡CH), 2160 (-C≡C-), 1250 (=C-O-) cm^{-1}.

The crude IX_a was employed without further purification to the subsequent reaction.

Oxidative Coupling of IX_a.—IX_a (2.3 g.) was oxidized with cupric acetate monohydrate (15 g.) in pyridine (110 g.). After stirring for 4 hr. at 50~52°C, the solvent was removed under reduced pressure at a temperature below 30°C. The residue was extracted with ether (250 ml.), washed with aqueous cupric acetate and water, successively, and dried over anhydrous sodium sulfate. The crude crystals from the ether extract, on repeated recrystallization from benzene, gave X_a, colorless prisms, m. p. 154°C (decomp.), 0.7 g. (33%). Complete decomposition was observed when the crystals were heated to 140°C for 30 min.

Found: C, 83.73; H, 4.94. Calcd. for $C_{20}H_{14}O_2$: C, 83.90; H, 4.93%.

IR max., 2230, 2165 (-C≡C-), 1257, 1215 (=C-O-), 742, 720 (*cis*-ethylene) cm^{-1}.

The monomeric nature of X_a was inferred from the molecular weight of the reduction product XI.

Hydrogenation of X_a.—X_a (200 mg.) in benzene (20 ml.) was hydrogenated over 5% palladium-on-charcoal (20 mg.). The reduction product was recrystallized from aqueous ethanol yielding XI, colorless plates, m. p. 63.5°C, 200 mg. (96%). This substance showed no depression of the melting point on admixture with the reduction product of VI_a and X_b. Also the infrared spectra of these reduction products were found to be identical over the entire region of wavelength.

Oxidative Coupling of IX_b.—A solution of IX_b (1.3 g.) and cupric acetate monohydrate (15 g.) in pyridine (120 g.) was heated to 50°C for 3 hr. Treatment of the reaction mixture according to the usual method afforded crude crystals. The crude material was repeatedly recrystallized from ethyl acetate containing a small amount of ethanol yielding X_b, colorless plates, m. p. 130°C (decomp.), 0.4 g. (30%).

Found: C, 83.80; H, 5.02. Calcd. for $C_{20}H_{14}O_2$: C, 83.90; H, 4.93%.

IR max., 2205 (-C≡C-), 1237 (=C-O-), 960 (*trans*-ethylene) cm^{-1}.

Hydrogenation of X_b.—Hydrogenation of X_b in benzene over 5% palladium-on-charcoal gave XI, colorless plates, m. p. 63.5°C in a yield of 96%.

Syntheses of XII and XIII.—*o*-Hydroxyphenylacetylene (2.4 g., 0.02 mol.) was dissolved in a solution of sodium methoxide in methanol (sodium, 0.5 g. and absolute methanol, 7 ml.). After removal of the solvent under reduced pressure at room

temperature, the residue was mixed with *o*-xylylene dibromide (2.7 g., 0.01 mol.), a trace of potassium iodide and dimethylformamide (20 ml.), and the mixture was refluxed for 1.5 hr. The cooled neutral reaction mixture was poured into ice-water, and extracted with ether. The ether layer was washed with water and dried over magnesium sulfate. The viscous oil (3.5 g., IR max., 3360 (-C≡CH), 2160 (-C≡C-), 1250 (≡C-O) cm^{-1}) from the ether layer, was mixed with a solution of cupric acetate monohydrate (15 g.) in pyridine (150 g.). The mixture was stirred for 4 hr. at 50 °C. Isolation with ether as before yielded crude crystals. The crude substance was washed with a small amount of cold benzene and digested with hot ethanol. The insoluble material was removed by filtration. The crystals from the filtrate were recrystallized from ethanol to yield XII, colorless needles, m. p. 148.5 °C, (decomp.), 250 mg. (8%).

Found: C, 85.37; H, 4.83. Calcd. for $C_{24}H_{16}O_2$: C, 85.69; H, 4.79%.

IR max., 2220 (-C≡C-), 1222, 1208 (≡C-O-), 1375 (δ CH) cm^{-1}. (measured by KBr-disk method).

It is to be noted that the infrared spectrum of XII lacks the absorption peak arising from the stretching of methyl group.

Owing to the thermal instability, the molecular weight of XII was inferred from that of the reduction product XIV.

The abovementioned insoluble solid was recrystallized from benzene yielding XIII, colorless plates, m. p. 230~231 °C, 100 mg. (3%). It was observed that the transparent crystals turn to opaque at about 100 °C. This phenomenon is attributable to the loss of benzene of crystallization. The amount of benzene of crystallization was found to be 19.06%. (Calcd. for $C_{48}H_{32}O_4 \cdot 2C_6H_6$: 18.84%).

Found: C, 85.29; H, 4.82. Mol. wt., 667. Calcd. for $C_{48}H_{32}O_4$: C, 85.69; H, 4.79%. Mol. wt., 672.

IR max., 1240 (≡C-O-) cm^{-1}.

Hydrogenation of XII.—XII (130 mg.) in benzene (15 ml.) was reduced over 5% palladium-on-charcoal (20 mg.). After removal of the catalyst, the solvent was distilled and the residual solid was recrystallized from ethyl acetate-ethanol resulting in XIV, colorless needles, m. p. 180 °C, 125 mg.

Found: C, 83.55; H, 7.06. Mol. wt., 346. Calcd. for $C_{24}H_{24}O_2$: C, 83.69; H, 7.02. Mol. wt., 344.

IR max., 2930, 2865 (ν CH), 1383 (δ CH), 1230 (≡C-O-) cm^{-1} (KBr-disk).

***o,o'*-Dibenzyloxydiphenyldiacetylene (XV).**—*o,o'*-Dihydroxydiphenyldiacetylene (1.0 g., 0.0086 mol.) and a trace of potassium iodide were added to a solution of sodium ethoxide in ethanol (sodium, 0.2 g., and absolute ethanol, 20 ml.). After refluxing for 1 hr., the reaction mixture was cooled. The crystals deposited were filtered, then washed with water and ethanol, successively. The crude material was recrystallized from benzene or ethyl acetate to give XV, colorless needles, m. p. 152~152.5 °C, 0.9 g. (53%).

Found: C, 86.91; H, 5.23. Calcd. for $C_{30}H_{22}O_2$: C, 86.93; H, 5.35%.

Synthesis of XVI.—*o*-Hydroxyphenylacetylene (1.5 g., 0.013 mol.) was dissolved in a solution of sodium ethoxide in ethanol (sodium, 0.3 g. and absolute ethanol, 5 ml.). After the removal of the ethanol at room temperature in a vacuum, the residue was mixed with 1,4-dichloro-2-butyne (0.8 g., 0.0065 mol.), dimethylformamide (13 ml.) and a catalytic amount of potassium iodide, and refluxed for 1.5 hr. The cooled reaction mixture was poured into ice-water and extracted with ether (100 ml.). The extract was washed with aqueous potassium hydroxide and water, successively, and dried over sodium sulfate. The crude crystals obtained by evaporating the ethereal solution were purified by repeated recrystallization from aqueous ethanol resulting in XVI, colorless needles, m. p. 75 °C, 0.5 g. (35%).

Found: C, 83.48; H, 5.01. Calcd. for $C_{20}H_{14}O_2$: C, 83.90; H, 4.93%.

IR max., 3370 (-C≡CH), 1240 (≡C-O-) cm^{-1}.

Oxidative Coupling of XVI.—The mixture of XVI (420 mg.), cupric acetate monohydrate (4.5 g.) and pyridine (45 g.) was stirred at 40 °C for 4 hr. and then at 50 °C for 1 hr. The solvent was removed under reduced pressure at a temperature below 35 °C. The residue thus obtained was extracted with ether (100 ml.). An amorphous solid with high melting point suspended in ethereal solution was removed by filtration (300 mg.). No investigation on the nature of the amorphous solid was carried out. The ethereal solution was treated according to the usual procedure yielding crude XVI. This was recrystallized from benzene-light petroleum (b. p. 60~70 °C) to give pure XVI, colorless needles, m. p. 167 °C (decomp.), 15 mg. (3.5%).

Found: C, 84.48; H, 4.06. Calcd. for $C_{20}H_{12}O_2$: C, 84.49; H, 4.25%.

IR max., 2230 (-C≡C-), 1267 (≡C-O-) cm^{-1}.

XVI was found to be a heat sensitive substance. The crystals of XVI changed to pink, then to red when heated to 120 °C and melted at 167 °C, forming a reddish brown liquid.

Synthesis of XVIII.—*o,o'*-Dihydroxydiphenyldiacetylene (1.1 g., 0.047 mol.) was dissolved in a solution of sodium ethoxide in ethanol (sodium, 0.2 g. and absolute ethanol, 20 ml.). Propargyl bromide (1.1 g., 0.094 mol.) and a small amount of potassium iodide were added to the ethanolic solution and refluxed for 1.5 hr. The crude crystals obtained by chilling the reaction mixture were washed with ethanol, hot water and ethanol, successively. The crude substance thus obtained was recrystallized from benzene-light petroleum (b. p. 60~70 °C). It was observed that the crystals were contaminated with a small amount of 2,2'-dibenzofuranyl[6]. The last mentioned substance was removed by digesting the crude crystals with benzene. The crystals remained were recrystallized from benzene resulting in XVIII, colorless needles, m. p. 151~152 °C (decomp.), 200 mg., (14%).

Found: C, 84.89; H, 4.64. Calcd. for $C_{22}H_{14}O_2$: C, 85.14; H, 4.55%.

IR max., 3270 (-C≡CH), 2160, 2130 (-C≡C-), 1225 (≡C-O-) cm^{-1}.

The attempt of the intramolecular oxidative coupling of XVIII resulted in the formation of a resinous material.

The authors are grateful to Professor Yasuhide Yukawa for his valuable discussions.

They are also indebted to Mr. M. Okumiya for the microanalyses. A part of the expenses of this research was defrayed from the Grant-in-Aid of the Ministry of Education, to which the authors thanks are also due.

Department of Chemistry
Faculty of Science
Osaka University
Nakanoshima, Osaka

Cyclic Acetylenes. VI. Transannular and Proximity Effects in the Cyclic Derivatives of o,o'-Dihydroxydiphenyldiacetylene

By Fumio TODA and Masazumi NAKAGAWA

(Received December 9, 1960)

It was pointed out in Part II[1] of this series that the cyclic terephthalate of *o,o'*-dihydroxydiphenyldiacetylene (I) may be a suitable substance for the study of the transannular effect between the benzene ring of the bridging chain and the diacetylenic function. But the

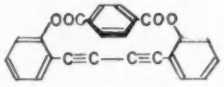

I

attempts to prepare I by the intramolecular oxidative coupling of 2-ethynylphenyl terephthalate gave unsatisfactory results. It was observed that the ester linkage is easily cleft during the course of oxidative coupling giving benzofurane derivatives. Therefore the authors have carried out the synthesis of an analogous substance of I in which the ester linkage is replaced by ether linkage.

Sodium *o*-ethynylphenoxide (II) was treated with *p*-xylylene dibromide to yield the terminal diacetylene III. Oxidative coupling of III, according to Eglinton's procedure[2], gave the cyclic diacetylene IV in 25% yield. The monomeric nature of IV was inferred from the molecular weight of the octahydroderivative V, since IV itself was found to have a poor solubility in camphor.

As illustrated in Fig. 1, the scale model of IV indicates that the molecule is almost strain

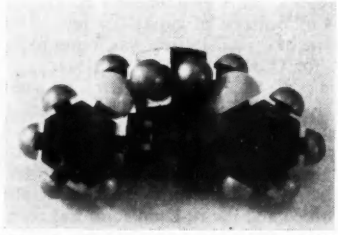

Fig. 1. The molecular model of IV (Courtauld model).

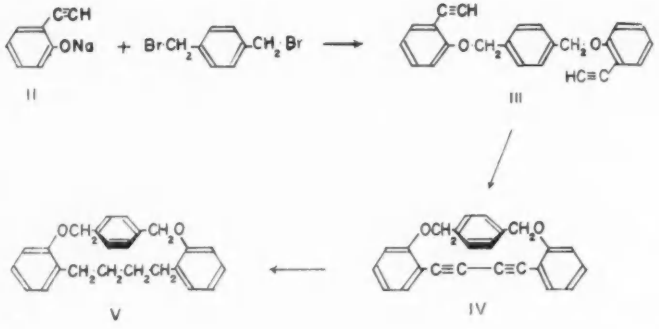

II III IV V

1) F. Toda and M. Nakagawa, This Bulletin, 33, 230 (1960).

2) G. Eglinton and A. R. Galbraith, *Chem. & Ind.*, **1956**, 737; *J. Chem. Soc.*, **1959**, 889.

free and the benzene nucleus in the bridging chain is held closely parallel to the diacetylenic linkage. A part of the infrared spectra of III, IV and V are recorded in Fig. 2. The absorption bands arising from the out-of-plane deformation of the adjecent two hydrogen atoms

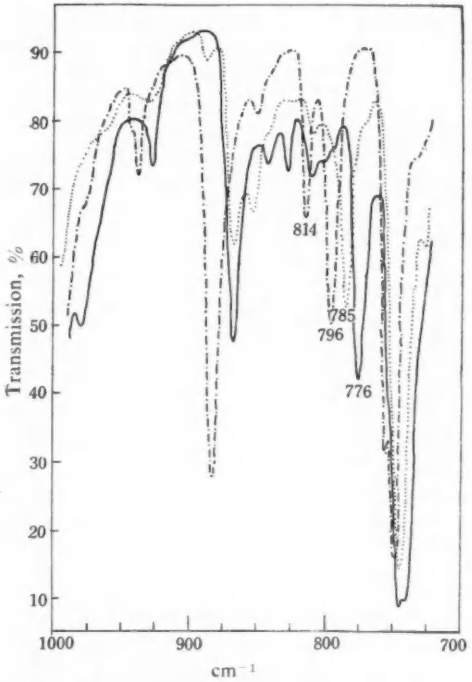

Fig. 2. The infrared spectra of III, IV and V.
----: III ——: IV ·····: V

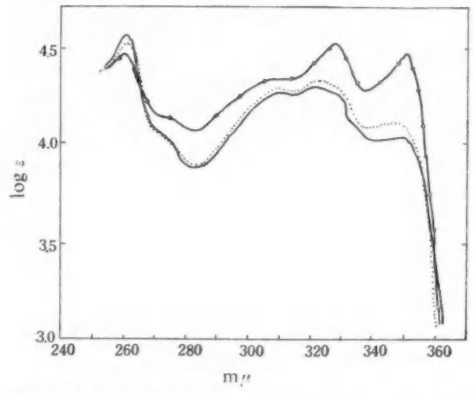

Fig. 3. The ultraviolet spectra of the cyclic diacetylene (IV), the cyclic tetraacetylene (IX) and the open chain analogue (VI) (in dioxane).
·····: IV ——: IX ----: VI

in the *p*-disubstituted benzene nucleus appeared at 814 cm^{-1} and 796 cm^{-1} in the case of III, whereas the corresponding absorption band shifted to 776 cm^{-1} and 785 cm^{-1} in IV and V, respectively. The infrared spectroscopic anomalousness of IV and V can be explained on the basis of a non-bonded interaction of hydrogen atoms in the benzene nucleus of the bridging chain with the diacetylenic linkage or with the $-(CH_2)_4-$ chain which is held in a proximate position to the hydrogen atoms. As indicated in Fig. 3 and Table I, the ultraviolet spectrum

TABLE I

Compound	Absorption				
IV	261 (322)	**275** (105)	310 (189)	322 (208)	346 (127)
VI	261 (287)	**275** (130)	310 (212)	328 (323)	351 (285)
IX	261 (350)	**275** (105)	310 (185)	321 (196)	349 (115)

All spectra were measured in dioxane.
The figures indicate the λ_{max} in mμ.
The figures in parentheses are $\varepsilon_{max} \times 10^{-2}$.
The bold figures indicate shoulders.

of IV also shows an anomalous feature. Loss of the sharpness and the marked decrease of the absorption intensities of the peaks at the longer wavelength region were observed in the spectrum of IV as compared with that of the open chain analogue, *o*, *o'*-dibenzyloxydiphenyldiacetylene (VI)[3].

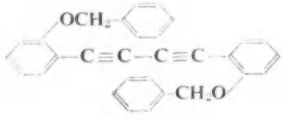

VI

It is to be noted that the ultraviolet spectrum of VII[3] also showed broad absorption peaks. On the other hand, the *ortho*-isomer of IV (VIII)[3] has a well defined, fine structure in

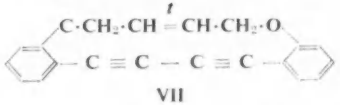

VII

the ultraviolet spectrum, in spite of the shifts in the absorption peaks. As already discussed in the preceding paper, the *trans*-ethylenic

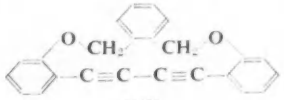

VIII

3) F. Toda and M. Nakagawa, This Bulletin, 34, 862 (1961).

bond in VII is held closely to the diacetylenic function; on the contrary, the *o*-xylylene group in VIII is fixed fairly far apart from the diacetylenic linkage. Therefore the anomalousness in the ultraviolet spectra of IV and VII is probably associated with a transannular interaction of π-electrons in the bridging chain with those of the diyne function.

As already pointed out in the previous papers[3,4], the strained cyclic derivatives of *o*, *o'*-dihydroxydiphenyldiacetylene have a sharp and intense λ_{min} at ca. 260 mμ in their ultraviolet spectra, and the presence of this λ_{min} was attributed to a proximity effect of *o*, *o'*-bridging chain to the diacetylenic linkage. The ultraviolet spectrum of IV lacks the λ_{min}, but has a λ_{max} at the same wavelength. An examination of the scale model of IV reveals that the methylene groups in the benzyl position of the bridging chain are fixed fairly far apart from the diacetylenic function owing to the presence of the rigid benzene nucleus. As the result of the above-mentioned spatial position of the methylene groups, there might be no proximity effect to operate in IV, in spite of the fact that the cycle has a short bridging chain.

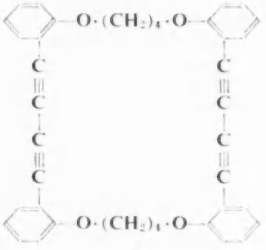

IX

The ultraviolet spectrum of the cyclic tetraacetylene IX which was reported in the preceding paper[3] was found to be quite similar to that of IV (Fig. 3). The spectroscopic similarity suggests the possibility that the molecule of IX can assume the geometry of a puckered ring in which two of the four benzene rings are faced to the diacetylenic functions making it possible for some transannular effect to operate (Fig. 4).

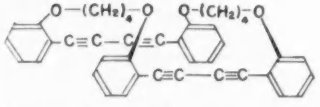

Fig. 4. A puckered structure of IX.

4) F. Toda and M. Nakagawa, 33, 223 (1960).

Experimental*

Synthesis of 1, 4-Bis-(*o*-ethynylphenoxymethyl)-benzene (III).—*o*-Hydroxyphenylacetylene (3.54 g., 0.03 mol.) was dissolved in a solution of sodium ethoxide in ethanol (sodium, 0.69 g., 0.03 mol. and absolute ethanol, 10 ml.) and the solvent was removed in vacuo. The sodium phenoxide thus obtained was mixed with *p*-xylylene dibromide (3.96 g., 0.015 mol.), a catalytic amount of potassium iodide and dimethylformamide (25 ml.). After being refluxed for 2.5 hr., the mixture was cooled and poured into ice-water. The solid deposited was filtered and then washed with water and ethanol. The dried material was repeatedly recrystallized from ethanol giving III, colorless prisms or needles, m. p. 93~94 C, 3.90 g. (78%).

Found: C, 84.91; H, 5.40. Calcd. for $C_{24}H_{18}O_2$: C, 85.18; H, 5.36%.

IR max., 3280 (-C≡CH), 2940, 2880 (ν CH), 2110 (-C≡C-), 1470, 1386 (δ CH), 1242 (=C-O-), 814, 796 (*p*-disubst. benzene), 740 (*o*-disubst. benzene) cm^{-1}.

Oxidative Coupling of III.—The mixture of III (1.5 g.), cupric acetate monohydrate (15 g.) and pyridine (150 g.) was stirred for 4 hr. at 50 C. The reaction mixture was cooled and the crystals deposited were filtered and then washed with water and ethanol. The filtrate was concentrated under reduced pressure yielding crystals. The crystals were washed with water and ethanol, and combined with the first crop. Repeated recrystallization of the combined material from benzene afforded cyclic diacetylene IV, colorless needles, m. p. 274~275 C (decomp.), 370 mg. (25%).

Found: C, 85.34; H, 4.99, Mol. wt., 354. Calcd. for $C_{24}H_{16}O_2$: C, 85.69; H, 4.79%, Mol. wt., 336.

IR max., 2920, 2870 (ν CH), 2220, 2150 (-C≡C-), 1380 (δ CH), 1245, 1220 (=C-O-), 776 (*p*-disubst. benzene), 746 (*o*-disubst. benzene) cm^{-1}.

Hydrogenation of IV.—IV (210 mg.) was hydrogenated in benzene (100 ml.) over 5% palladium-on-charcoal (20 mg.). After removal of the catalyst, the solvent was distilled, resulting in crystals. On recrystallization from ethyl acetate-ethanol or benzene-petroleum ether (b. p. 60~70 C) the crystals afforded V in quantitative yield, colorless needles, m. p. 195~197 C.

Found: C, 83.67; H, 6.83, Mol. wt., 381. Calcd. for $C_{24}H_{24}O_2$: C, 83.69; H, 7.02%, Mol. wt., 344.

IR max., 2930, 2860 (ν CH), 1380 (δ CH), 1230 (=C-O-), 785 (*p*-disubst. benzene), 745 (*o*-disubst. benzene) cm^{-1}.

The authors are grateful to the Ministry of Education for the Grant-in-Aid for fundamental scientific research.

Department of Chemistry
Faculty of Science
Osaka University
Nakanoshima, Osaka

* All melting points were not corrected. The infrared spectra were measured by KBr-disk method. The microanalyses were performed by Mr. M. Okumiya of the microanalytical laboratory of this Department.

Infrared Spectra and the Structure of Some Metal-oxamide Complexes

By Yoko KURODA, Michinobu KATO* and Kôzô SONE**

(Received December 4, 1960)

Many kinds of proteins, polypeptides and biuret-like compounds react with Cu^{2+} ions in basic solutions, forming chelate complexes with characteristic red or violet colors ("biuret reaction")[1-4]. Oxamide is known to be the simplest one among molecules that exhibit this reaction, and the composition of the red product can be formulated as $A_2[Cu(C_2H_2N_2O_2)_2]$, where A represents a univalent ion (e.g. alkali metal ion). It is also known that Ni^{2+} ions form a yellow complex of analogous composition[5,6].

Although the formula of these complexes and the reported diamagnetism of the nickel complex[7] afford some evidence in favor of the presumption that these complexes are tetra-coordinated chelates, their structure has not yet been established definitely***. The reason is as follows: An oxamide molecule contains two nitrogen and two oxygen atoms capable of forming coordinate bonds with a metal, while the constitution of a tetra-coordinated complex with a bivalent central ion does not permit all these atoms to be involved in metal-ligand linkages. This situation makes a number of structures conceivable, e.g.,

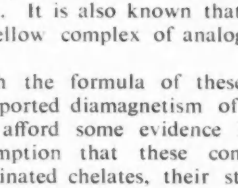

(I)

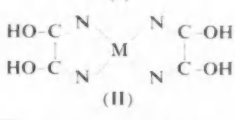

(II)

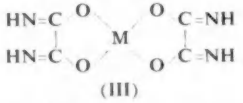

(III)

etc., among which the formula I seems to be more probable than the others, because of the analogy of the color and general mode of formation of these complexes with those of biuret complexes of the corresponding metals[1-4].

In connection with this problem, it can be expected that infrared spectroscopy will provide a powerful means for the determination of the kind of donor atoms in these complexes, and the elucidation of their geometric structure. In this paper, the infrared absorption spectra of $K_2[Ni(C_2H_2N_2O_2)_2]$ and $K_2[Cu(C_2H_2N_2O_2)_2]$ are reported and discussed from this point of view.

Experimental Procedure and Results

Materials. — Potassium bis(oxamido)niccolate(II) and potassium bis(oxamido)cuprate(II) were prepared by the method of Hofmann and Ehrhardt[6], and dried over potassium hydroxide.

Found: Ni, 18.1; N, 16.8. Calcd. for $K_2[Ni(C_2H_2N_2O_2)_2]$: Ni, 19.0; N, 18.1%.

Found: Cu, 18.5; N, 17.4. Calcd. for $K_2[Cu(C_2H_2N_2O_2)_2]$: Cu, 20.2; N, 17.9%.

A specimen of oxamide, $C_2H_4N_2O_2$, was obtained from L. Light & Co. Ltd.

Measurements. — The infrared spectra were recorded by means of a Hilger H-800 spectrophotometer. The absorption measurements were made at room temperature using pressed potassium bromide disk technique in the wave number range from 700 to 4000 cm^{-1} with a rock-salt prism. A fluorite prism was also used for a range above 1200 cm^{-1}, but no additional information was obtained. The results were checked using Nujol mulls. The spectra obtained are shown in Fig. 1, and the observed frequencies of the absorption bands are listed in Table I. The present data on oxamide are in good agreement with those reported by Miyazawa[8] and by Scott and Wagner[9].

Discussion

A close resemblance exists between the absorption patterns of the metal complexes, indicating that they have a similar structure. On

* Chemical Laboratory, Aichi Prefectural University for Women, Mizuho-ku, Nagoya.
** Chemical Laboratory, Aichi Gakugei University, Higashi-ku, Nagoya.

1) G. Wiedemann, *Ann.*, **68**, 323 (1848).
2) M. M. Rising, J. S. Hicks and G. A. Moerke, *J. Biol. Chem.*, **89**, 1 (1930).
3) M. Kato, *Z. anorg. u. allgem. Chem.*, **300**, 84 (1959).
4) K. Sone and M. Kato, Proc. Symposium on the Chemistry of Co-ordination Compounds, Agra (India), Part III, 16 (1960).
5) H. Schiff, *Ann.*, **299**, 236 (1898).
6) K. A. Hofmann and U. Ehrhardt, *Ber.*, **46**, 1457 (1913).
7) L. Cambi and E. Tremolada, *Gazz. chim. ital.*, **65**, 322 (1935).
*** The recent X-ray studies by Freeman et al. (H. C. Freeman, J. E. W. L. Smith and J. C. Taylor, *Nature*, **184**, 707 (1959).) on the structure of bis(biureto)cuprate(II) is of interest in connection with this study.

8) T. Miyazawa, *J. Chem. Soc. Japan, Pure Chem. Sec. (Nippon Kagaku Zasshi)*, **75**, 86 (1954).
9) T. A. Scott, Jr. and E. L. Wagner, *J. Chem. Phys.*, **30**, 465 (1959).

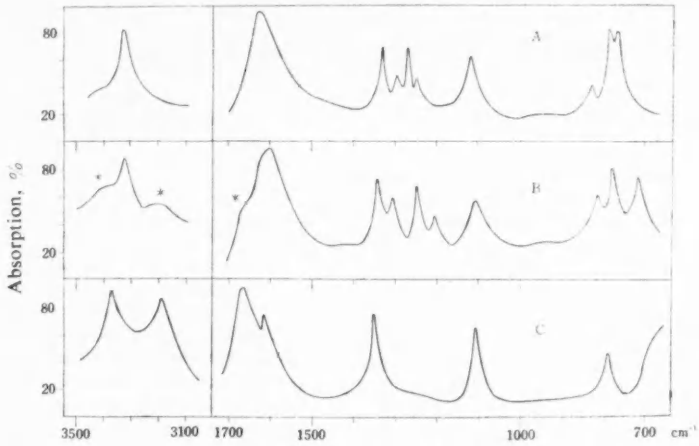

Fig. 1. The infrared spectra of (A): potassium bis(oxamido)niccolate(II), (B): potassium bis-(oxamido)cuprate(II), and (C): pure oxamide. The peaks marked with an asterisk seem to be due to the contamination of oxamide[2] produced by the decomposition of the easily hydrolyzable copper complex, because their positions coincided with those of the strong absorption bands of oxamide and their intensity increased considerably after the complex was exposed to atmospheric moisture.

TABLE I. OBSERVED INFRARED ABSORPTION FREQUENCIES IN cm^{-1}

$K_2[Ni(C_2H_2N_2O_2)_2]$	$K_2[Cu(C_2H_2N_2O_2)_2]$	Assignment
3320 (s)	3313 (s)	ν_{N-H}
1628 (vs)	1600 (vs)	$\nu_{C=O}$
1325 (m)	1343 (m)	ν_{C-N}
1285 (w)	1305 (w)	
1268 (m)	1253 (m)	
1250 (w)	1215 (w)	
1124 (m)	1120 (m)	ρ_{N-H}
831 (w)	815 (w)	ν_{C-C}
786 (s)	788 (s)	ω_{N-H}
765 (s)	722 (s)	$\rho_{C=O}$

Absorption intensities are shown by letters in parentheses, i.e., vs: very strong, s: strong, m: medium, w: weak.

Vibrational types are expressed by greek letters, i.e., ν: stretching, ρ: in-plane deformation, ω: out-of-plane deformation.

the other hand, the feature of these spectra is much different from that of an oxamide molecule. It has revealed that heavy atoms in an oxamide molecule are arranged in a trans (C_{2h}) form in solid state[8,9]. However, it is unbelievable that an oxamide molecule having the trans form can act as a bidental ligand, provided that the coordination takes place through one kind of donor atoms. A more complicated spectral feature of the metal complexes probably reflects a less symmetrical structure of the ligand. The complication of the spectra should partly be caused by vibrational couplings between two ligands through coordination linkages. This effect is expected to be more appreciable for the vibrational modes of groups directly attached to the metal than for those of end groups.

In the first place, a remarkable difference between the spectra of an oxamide molecule and those of the metal complexes was found in the region from 3100 to 3400 cm^{-1}. The former show two strong bands arising from the N-H stretching vibrations of primary amide groups, O=C-NH_2, while the latter show only one peak. This fact means that the primary amide structure is absent in these metal complexes. Another evidence in favor of the absence of an NH_2 group in metal complexes is provided by a spectral feature in the wave number range near 1600 cm^{-1}. For an oxamide molecule, the NH_2 bending frequency was found at 1610 cm^{-1}, whereas the corresponding band is absent in the spectra of the metal complexes. The values of 3320 cm^{-1} for the nickel complex and of 3313 cm^{-1} for the copper complex are reasonable for the N-H stretching frequencies of secondary amides in solid state[10], although there still remains a possibility of assigning them to the frequency of hydrogen-bonded OH groups. This ambiguity of assignment for these frequencies can be removed by examining the C=O stretching

10) L. J. Bellamy, "The Infrared Spectra of Complex Molecules", 2nd Ed., Methuen, London (1958), p. 205.

band. If the metal complexes take a structure having OH groups, such as II, an intense absorption at about 1600 cm^{-1} characteristic of C=O bonds should be replaced by a C=N stretching band which is generally less intense than a C=O band. But this was not the case. In this region, both of the metal complexes show a band of nearly the same intensity as the C=O stretching band of an oxamide molecule. Therefore, the band at about 3320 cm^{-1} of the metal complexes was assigned unequivocally to the N–H stretching vibration.

Also the characteristic C=O band above 1600 cm^{-1} is expected to disappear from the spectra of metal complexes, if the ligands were coordinated to the metal through oxygen atoms (structure III), since it can be reasonably presumed that the formation of metal-oxygen bonds will cause a shift in the C=O stretching band to a much lower frequency owing to the decreasing double bond character of the C=O group. Moreover the CO bonds incorporated in a five-membered chelate ring will have no longer the character of end groupswhich display a simple absorption band, so that the appearance of the absorptions is expected to be greatly complicated because of coupling with other skeletal vibrations. Therefore, the presence of a simple C=O band in the spectra of metal complexes may be taken as sufficient evidence for the fact that these complexes have metal-nitrogen bonds rather than metal-oxygen bonds.

The value of 1628 cm^{-1} for the nickel complex and that of 1600 cm^{-1} for the copper complex are slightly lower than the value of 1660 cm^{-1} for the C=O frequency of an oxamide molecule, indicating the decreased double bond character of the C=O bonds in the coordinated ligands. This effect is certainly due to the increased ionic character of such ligands, because the metal-nitrogen bonds are expected to have only a partial covalent character. It is of interest to note that the infrared spectra of the oxalate complexes of bivalent metals, $[M^{II}(C_2O_4)_2]^{2-}$, bear a close resemblance to this case[11]. The carboxylate frequencies of these complexes are intermediate between those of the oxalates of alkali metals and those of dimethyl oxalate, suggesting a partial covalent character of their metal-oxygen bonds. The fact that the observed frequency of the C=O stretching vibration of the nickel complex is higher than that of the copper complex indicates that the metal-nitrogen bonds of the former have a greater covalent character than those of the latter.

The spectral changes caused by the formation of the metal complexes are most apparent in the wave number range from 1350 to 1200 cm^{-1}. An oxamide molecule has a strong absorption band at 1355 cm^{-1} arising from the C–N stretching vibration, while the metal complexes exhibit four peaks, two of which are of medium intensity and others are weak. It can be expected that the C–N stretching frequencies of the metal complexes will also appear in this region, since the double bond character of these bonds should not be affected so much on substitution of the hydrogen atoms of the NH_2 groups with a metal atom. However, the absorption feature will be complicated by vibrational coupling through the metal-nitrogen linkages. The spectral pattern in this region must therefore depend on the geometric structures of these complexes.

Conceivable models for these complexes are as follows. (1) A planar structure in which four metal-nitrogen bonds as well as all the heavy atoms of the two ligands lie on a plane (D_{2h}). (2) Structures in which the coordination type is planar and each ligand takes a non-planar form, owing to a rotation about a C–C single bond from the cis configuration. Depending on the relative orientation of two ligands, two forms are conceivable, one of which has a center of symmetry (C_{2h}) while the other has not (D_2). (3) One form of tetrahedral chelation of two planar ligands (D_{2d}). (4) Two forms of tetrahedral chelation of two non-planar ligand (D_2 and C_2).

Selection rules operating on these models are summarized in Table II. These rules should hold rather strictly in the skeletal vibrations such as C–C and C–N vibration, while the end groups are presumed to be free from these. Actually, no splitting was observed for the N–H and C=O stretching bands of the metal complexes.

For the C–N stretching vibration, D_{2h} and C_{2h} models have two infrared active modes and two inactive ones. A D_{2d} model has two active modes, one of which is degenerate, and an inactive one. A D_2 model has three active ones and an inactive one. With a model having C_2 symmetry, all four modes are active. The four bands observed in this wave number region readily permit one to exclude the D_{2d} and D_2 models. However, it is difficult for other models (D_{2h}, C_{2h} and C_2) to decide which is the closest one to the actual structure, because these selection rules are valid only for a free molecule and the removal of prohibition can be expected to some extent in the solid state, for which intermolecular or interlattice effects should not be ignored. Therefore, there is a possibility of assigning these two weak bands to the inactive modes of the D_{2h} or C_{2h} model.

11) M. J. Schmelz, T. Miyazawa, S. Mizushima, T. J. Lane and J. V. Qaugliano, *Spectrochim. Acta*, **9**, 51 (1957).

TABLE II. CLASSIFICATION OF VIBRATIONAL TYPES FOR CONCEIVABLE MODELS OF $[M^{II}(C_2H_2N_2O_2)_2]^{2-}$

	D_{2h}	C_{2h}	D_{2d}	D_2	C_2
ν_{N-H}, $\nu_{C=O}$, ν_{C-N}, ρ_{N-H}, $\rho_{C=O}$	$A_{1g}(R)$	$A_g(R)$	$A_1(R)$	$A_1(R)$	2A(R, I)
	$B_{1u}(I)$	$A_u(I)$	$B_2(R, I)$	$B_1(R, I)$	
	$B_{2g}(R)$	$B_g(R)$	$E(R, I)$	$B_2(R, I)$	2B(R, I)
	$B_{3u}(I)$	$B_u(I)$		$B_3(R, I)$	
ν_{C-C}	$A_{1g}(R)$	$A_g(R)$	$A_1(R)$	$A_1(R)$	2A(R, I)
	$B_{1u}(I)$	$B_u(I)$	$B_2(R, I)$	$B_1(R, I)$	
ω_{N-H}	$A_{1u}(ia)$	$A_u(I)$	$B_1(R)$	$A_1(R)$	2A(R, I)
	$B_{1g}(R)$	$A_g(R)$	$A_2(ia)$	$B_1(R, I)$	
	$B_{2u}(I)$	$B_u(I)$	$E(R, I)$	$B_2(R, I)$	2B(R, I)
	$B_{3g}(R)$	$B_g(R)$		$B_3(R, I)$	

The meaning of letters in parentheses are as follows; R: Raman active, I: Infrared active, ia: inactive in both.

On the other hand, it has been revealed from a magnetic study[7] that the nickel complex is diamagnetic and hence tetrahedrally chelated structures are unlikely. Furthermore, it is possible that the π electron systems of the four amide groups give rise to some extent of conjugation effects through the d_π orbitals of the central metal, and if such effects are taken into account, the planar form (D_{2h}) seems to be the most probable among the possible models. The whole spectra of these complexes are satisfactorily interpreted in terms of the structure I with a D_{2h} symmetry, although there is an alternative possibility that the symmetry may be of C_{2h}.

Bands of the nickel complex at 831 cm^{-1} and of the copper complex at 815 cm^{-1} have no counterpart in the spectra of oxamide, but the frequencies are very close to a Raman frequency 800 cm^{-1} ascribed to the C-C stretching vibration of oxamide[8]. The position and the weak intensity of these bands give a good evidence for assigning them to the C-C stretching mode.

Other frequencies expected to appear in the rock-salt region are the in-plane N-H deformation, the out-of-plane N-H deformation and the in-plane C=O deformation. According to general knowledge, the first has the highest frequency among them. Therefore, a band of the nickel complex at 1124 cm^{-1} and a band of the copper complex at 1120 cm^{-1} were assigned to this vibration. Two other bands of the nickel complex at 786 and 765 cm^{-1} as well as those of copper complex at 788 and 722 cm^{-1} were tentatively assigned to the out-of-plane N-H deformation and the in-plane C=O deformation, respectively. These assignments seem to be adequate, because in *N*-monosubstituted amides, it was found that the frequency of the former vibration is higher and its intensity is larger than those of the latter[12]; for example, the former is assigned to 778 cm^{-1} and the latter to 765 cm^{-1} in the case of *N*, *N'*-dimethyloxamide, which was examined by studying the deuteration effect[13].

These assignments are also listed in Table I.

Summary

The infrared absorption spectra of potassium bis(oxamido)niccolate(II) and potassium bis-(oxamido)cuprate(II) were recorded in the wave number region from 700 to 4000 cm^{-1} and compared with those of pure oxamide. These spectra revealed that metal-nitrogen bonds are formed in these complexes. The observed frequencies were interpreted in terms of a planar structure having the symmetry D_{2h}.

The authors wish to express their appreciation to Professor Masaji Kubo of Nagoya University for helpful discussions.

Chemistry Department
Nagoya University
Chikusa, Nagoya

12) T. Miyazawa, *J. Chem. Soc. Japan, Pure Chem. Sec.* (*Nippon Kagaku Zasshi*), **77**, 526 (1956).
13) T. Miyazawa, ibid., **76**, 1018 (1955).

SHORT COMMUNICATIONS

*Nuclear Magnetic Resonance of Tar Products. II**

By Shizuo FUJIWARA and Tohru WAINAI

(Received December 14, 1960)

Tar products consist of chemically similar components of high boiling points, which are very difficult to be distinguished from each other. As the means of analyses of these products, measurements of infrared spectra are usually made, but, other methods seem necessary to be explored. Nuclear Magnetic Resonance (NMR) technique has the advantage that we can analyze the functional groups in any liquid samples under nondestructive condition. Thus, Williams[1] made NMR measurements for saturated aromatic and olefinic components in distilled fractions of petroleum, Richards[2] for the aromatic compounds in various kinds of coals, and Schoolery[3] tried to determine the hydrogen contents of naphthalene derivatives.

The present authors performed the analysis of α- and β-methyl-naphthalenes and reported elsewhere*. This paper will present the preliminary results of NMR measurements for distilled fractions of tar products.

Samples.—Samples used in this experiments are shown in Table I, which were collected from the plant of Yokohama Factory of Tokyo Gas Co., Ltd. at the working condition.

NMR Measurements.—Measurements of the NMR absorption spectra were caried out at 27 Mc./sec., and 40 Mc./sec. by the apparatus constructed by one of the authors (S. F.) and by the Japan Electron Optics Laboratory Co., Ltd., respectively. The concentration of sample is 50% (wt.) in carbon tetrachloride which contains a small amount of cyclohexane as the internal reference. Sample was spun rapidly during measurements.

Results.—The characteristic features of NMR spectra at 27 Mc./sec. were complicated and found to be insufficient for the analyses of functional groups. Even so, we could easily identify the paraffinic, alpha-alkyl and aromatic protons in the spectra. As the preliminary investigations, the results of measurements at 40 Mc./sec. seem satisfactory, which are shown in Fig. 1. Light oil has four absorptions in the aromatic region as well as the absorptions of aromatic hydroxyls of phenol and cresol at 6.3 and 8.6 P./10 M. (benzene 0), respectively. The absorption at 39.1 P./10 M. results from pyridine or picoline. The absorption in paraffinic region is stronger in light oil than in carbolic oil. The absorption of light oil in alpha-alkyl region overlaps those of methyl hydrogens of toluene and xylene. Four absorption bands at 2.4~7.5 P./10 M. observed in carbolic oil were assigned to hydroxyl groups of phenol and of cresol. Carbolic oil is also characterized by three strong absorptions at naphthalene region and a weak one at alpha-methyl region, which is weaker than that in light oil. According to the results of Fig. 1, we can see that naphthalene oil and top oil of the second tower are close to each other in the compositions. Heavy oil showed a broad absorption at aromatic region and other spectra at 37.1, 39.9 P./10 M. which are attributed to β-alkyl hydrogen.

We also examined the fractions obtained by rectifying distillation. The fractions of the

TABLE I

No.	Sample	B.p., C	S.g.	Tar acid %	Naphthalene %
1	Light oil	85~190	0.919	14	—
2	Carbolic oil	180~200	1.025	46	16.8
3	Naphthalene oil	200~250		9	58.0
4	Heavy oil	225~295	1.079	6	2.5
5	Top oil (2nd tower)	195~270		9	29.6

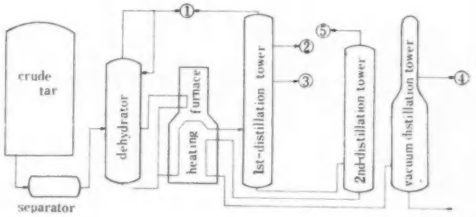

1) R. B. Williams, A. S. T. M. Special Technical Publication, No. 224, p. 168 (1958).
2) R. E. Richards and R. W. Yorke, *J. Chem. Soc.*, **1960**, 2489.
3) J. N. Schoolery, Lectured at the Chemical Society of Japan, Tokyo, Oct. 1960.
* Report I: *Anal. Chem.*, in press.

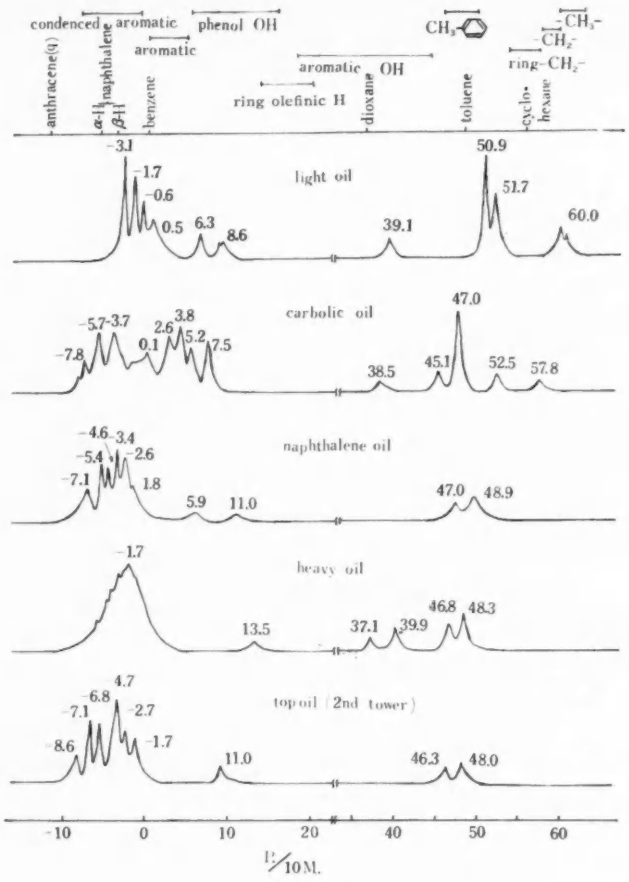

Fig. 1

factory distills which were rectified through the rectifying column were measured by NMR. According to the results of these measurements (not shown here) as well as those shown above, we conclude that the NMR method is quite useful for the analysis of tar products, and useful to figure out the efficiencies of the fractionation processes.

The authors are grateful to Mr. M. Takeuchi of the Japan Electron Optics Laboratory Co., Ltd. for measurement of the spectra at 40 Mc./sec. and to the Tokyo Gas Co., Ltd. for the supply of samples.

Department of Chemistry
Faculty of Science
The University of Tokyo
Hongo, Tokyo
(S. F.)

Department of Industrial Chemistry
Faculty of Science and Engineering
Nihon University
Surugadai, Tokyo
(T. W.)

The Crystallinity of Polyaldehydes

By Hiroshi SOBUE and Hideo KUBOTA

(Received February 27, 1961)

Recently a few reports[1-3] on the stereospecific polymerization of aliphatic aldehydes were published, but the properties of these polymers remain hardly known[2]. As the crystalline property of the polymer is very interesting from practical point of view, we have examined the crystalline properties of some aldehyde polymers, i. e. the polymers of propionaldehyde, *n*-butyraldehyde, isobutyraldehyde, *n*-capraldehyde, *n*-enauthaldehyde. The polymerization was carried out in hydrocarbon solvent such as heptane or toluene, with triethylaluminum as catalyst, at the temperature −80 or −40°C. In usual procedure we used 20 ml. of solvent, 0.0014 mol. of catalyst and 10 ml. of monomer.

All of the polymers obtained are crystalline. The X-ray diffraction patterns of powders of these polymers treated under various conditions are shown in Figs. 1—5. When treated with boiling chloroform or benzene for several hours, all of these polymers give sharper X-ray diagram than the untreated. As shown in Figs. 1, 3, 4 and 5, the samples swelled in some organic solvents were also examined by X-ray diffractometer. The untreated polymers of *n*-butyraldehyde depolymerize in certain condition to give gel-substances, whose patterns are shown in Fig. 2. Generally, the polymer which was kept at higher temperature than 170°C, partially depolymerized to give more diffused patterns.

Assuming the amorphous parts are given by dotted lines in each diagram, (the pattern of amorphous parts will be discussed in detail later,) we calculated the crystallinity of the polymers by integral intensity; as following

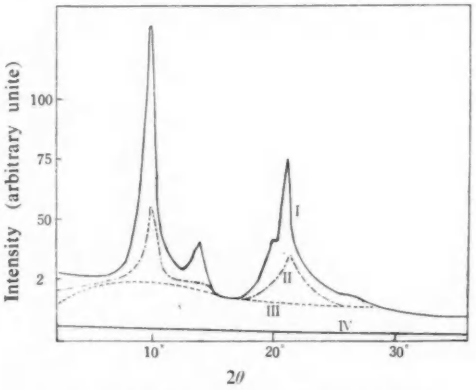

Fig. 1. The X-ray diffraction patterns of poly-propionaldehydes.
- I Sample treated with boiling chloroform for 8 hr. (polymerization at −78°C).
- II Sample swelled in chloroform. Amorphous part assumed.
- III Amorphous parts assumed.
- IV Pattern by air.

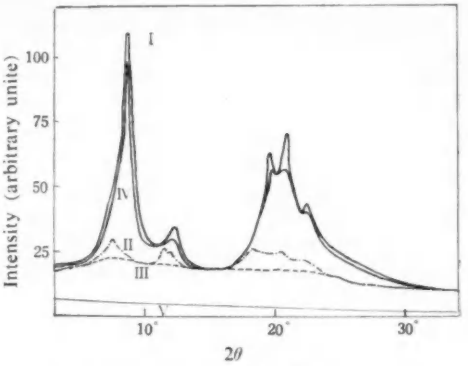

Fig. 2. The X-ray diffraction patterns of poly-*n*-butyraldehydes.
- I Sample treated with boiling chloroform for 6 hr. (polymerization at −80°C).
- II Sample partially depolymerized (gel-form).
- III Amorphous parts assumed.
- IV Untreated sample (polymerization at −40°C).
- V Pattern by air.

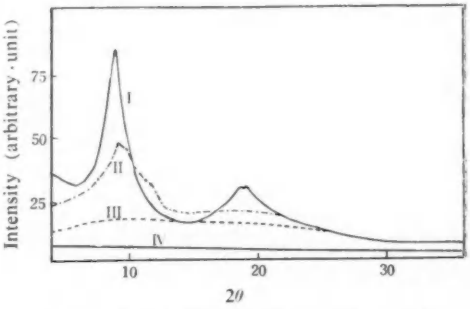

Fig. 3. The X-ray diffraction patterns of poly-isobutyraldehydes.
- I Sample treated with boiling chloroform for 6 hr. (polymerization at −78°C).
- II Sample swelled in chloroform.
- III Amorphous parts assumed.
- IV Pattern by air.

1) G. Natta et al., *Makromol. Chem.*, **37**, 156 (1960).
2) J. Furukawa et al., ibid., **37**, 149 (1960).
3) O. Vogl, *J. polymer Sci.* **46**, 261 (1960).

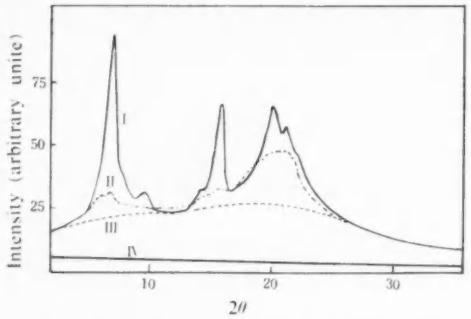

Fig. 4. The X-ray diffraction patterns of poly-*n*-caproaldehyde.
I Sample treated with boiling benzene for 6 hr. (polymerization at −78 C).
II Sample swelled in benzene.
III Amorphous parts assumed.
IV Pattern by air.

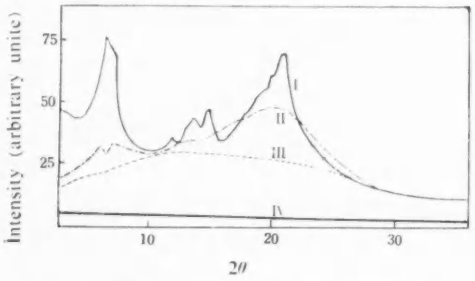

Fig. 5. The X-ray diffraction patterns of poly-*n*-enauthaldehydes.
I Sample treated with benzene.
II Sample swelled in benzene-chloroform.
III Amorphous parts assumed.
IV Pattern by air.

about 40% for poly-propion-, 45% for poly-butyr-, 49% for poly-isobutyr-, 37% for poly-*n*-capro-, 32% for poly-*n*-enauth-aldehyde. These polymers are crystalline even in untreated state and can not be dissolved in usual organic solvents, but are capable to be made a film by calendering at higher temperature than 100 C. The essential difference between the polymers obtained at −80 and −40 C, and the difference between the polymers prepared in heptane and toluene could not be found in the case of poly-*n*-butyraldehyde. At higher temperature than −35 C, the polymers could not be obtained. The kinetics of the polymerization will be reported later.

Department of Applied Chemistry
Faculty of Engineering
The University of Tokyo
Hongo, Tokyo

*Syntheses of Two Kinds of Metal-free Tetra-azaporphines by the Urea-melt Method**

By Naomi FUKADA

(Received November 15, 1960)

In previous papers, it was shown that various metallo-derivatives (metal chelates) of ammonium phthalocyaninetetra-(4)-sulfonate[1] and of tetra-2, 3-pyridinoporphyrazine[1] were synthesized by the so-called urea-melt method in good yields and that the metal-free macrocycles of these metallo-derivatives, namely the parent substances, were prepared from the derivative of magnesium[2], of manganese[1], or of zinc[1]. In the present paper, it is reported that the metal-free macrocycles were obtained directly by the urea process.

No blue product was obtained from the mixtures of triammonium 4-sulfophthalate (10 g.) and urea (50～75 g.), or of quinolinic acid (10 g.) and urea (50～75 g.) by heating to 230 C. However, boric acid (0.5～1.5 g.) and ammonium molybdate (1.0～2.5 g.) were added to them as catalysts and heated together at 170～250 C for 0.5～1.5 hr., ammonium phthalocyaninetetra-(4)-sulfonate or tetra-2, 3-pyridinoporphyrazine was synthesized in fairly well yields (8～18%). It was further found that the metal-free macrocycles were prepared in high yields (26～42%), when a powdered metal (1.0～2.5 g.), such as chromium, molybdenum, or manganese, was used with boric acid and ammonium molybdate and that while in the absence of both boric acid and ammonium molybdate only very small amounts of the macrocycles were formed. When molybdenum was used, no metal chelate of the macrocycle was mixed, but when chromium or manganese was used, a small amount of the metal chelate was mingled. In the case of ammonium phthalocyaninetetra-(4)-sulfonate, a mixture of the metal-free macrocycle and the chromium chelate (about 9 : 1) was obtained. The chromium chelate was removed by extracting with a mixture of water, methanol and acetone (4 : 5 : 1). In the case of tetra-2, 3-pyridinoporphyrazine, a mixture of the free base and the

* Presented partly at the 10th Symposium on Coordination Compounds held by the Chemical Society of Japan, Sendai, September, 1960, and at the Takada Local Meeting of the Chemical Society of Japan, Takada, October, 1960.

1) N. Fukada, *J. Chem. Soc. Japan, Pure Chem. Sec.* (*Nippon Kagaku Zasshi*), **75**, 378, 380, 586, 1141 (1954); **76**, 1378 (1955); **77**, 1421 (1956); **78**, 1378 (1957); **79**, 396, 980 (1958).
2) R. P. Linstead et al., *J. Chem. Soc.*, **1937**, 911.

chromium chelate (about 2 : 1), or of the free base and the manganese chelate (about 4 : 1) was obtained. The manganese chelate was converted into the free base by the action of 98% sulfuric acid. On the contrary, the chromium chelate, as its coordinated chromium could not be eliminated by dissolving in strong mineral acids, was separated from the free base by treating with aqueous solution (50~75%) of benzenesulfonic acid because of the greater solubility of the free base.

The purification of crude ammonium phthalocyaninetetra-(4)-sulfonate was carried out as follows. The reaction mixture was powdered and extracted with water. The extract was evaporated to dryness. The residue was again extracted with water and the extract evaporated to dryness. This treatment was repeated about 10 times. The residue was thoroughly washed with 70% ethanol and added into an ammoniac saturated solution of ammonium carbonate and the solution was warmed. The macrocycle was salted out to give ammonium sulfonate. The crude ammonium salt was thoroughly washed with 70% ethanol and then boiled in 95% ethanol. Its chemical formula was $(C_8H_3N_2 \cdot SO_3NH_4)_4H_2$ (Found: S, 14.0; N, 18.3; NH_3, 7.2%).

The tetraammonium sulfonate was converted into the corresponding tetrasulfonic acid by treating with 6 N or more concentrated hydrochloric acid. The blue crystalline product formed was collected by filtration, washed with 6 N hydrochloric acid and dissolved in a small amount of ethanol. The ethanol solution was evaporated to dryness. The sulfonic acid was recrystallized from 8 N hydrochloric acid to give long thready crystals. The chemical formula of the acid was $(C_8H_3N_2SO_3H)_4H_2$ (Found: S, 15.1; N, 13.0%). The tetrasulfonic acid in solid form had an intense purple reflex and was hygroscopic. The tetrasulfonic acid was found to be identical with the one reported previously[1].

The purification of crude tetra-2, 3-pyridinoporphyrazine was carried out as follows. The reaction mixture was powdered, mixed with a large amount of 1 N hydrochloric acid, allowed to stand overnight at room temperature and filtered off. The residue was boiled with water, heated several times with 0.2 N hydrochloric acid at 80~90°C for 0.5 hr. and heated further several times with 0.1 N sodium hydroxide solution at 80~90°C for 0.5 hr., each time filtered off, and washed with dilute hydrochloric acid and with water. The bluish-black residue was dried at 100°C. The dried solid was dissolved in a small quantity of 98% sulfuric acid and the solution after being filtered was poured into a large excess of water. The blue crystalline product thereby deposited was collected, washed with hot dilute aqueous sodium hydroxide and with hot water, and dried at 100°C. The dried solid was powdered, heated under reflux (Soxhlet) with 95% ethanol, acetone and ether, successively, and filtered off. The purified product was dried at 185°C for 1 hr. Its chemical formula was $(C_8H_3N_2)_4H_2$ (Found: N, 31.5%). The metal-free macrocyclic pigment was found to be identical with the one reported previously by Linstead et al.[2] from its coincidence in physical and chemical properties as well as in elementary composition.

Department of Chemistry
Faculty of Science
Niigata University
Niigata

Constituents of the Antibiotic, Glumamycin

By Michitaka INOUE

(Received February 20, 1961)

In the previous paper[1] it was reported that glumamycin, an acidic peptide antibiotic, consists of six amino acids and an unsaturated fatty acid.

Subsequently another acidic amino acid was detected by paper chromatography in the acidic amino acid portion of the glumamycin hydrolyzate; this acidic portion was submitted to partition column chromatography and colorless needle-like crystals, m. p. 254~256°C, $[\alpha]_D^{20} = +13°$ (c 1, 5 N HCl) were obtained (Found: C, 40.54; H, 6.18; N, 9.27; C-CH_3, 10.33. Calcd. for $C_5H_9NO_4$: C, 40.82; H, 6.12; N, 9.52; C-CH_3, 10.20%). The infrared spectrum of this compound was in good agreement with that* of α(L), β-methylaspartic acid (β-Me-L-Asp), separated by Baker et al.[2]

Also in the previous paper[1] the basic amino acid component of glumamycin was presumed to be α, β-diaminobutyric acid (α, β-Dab). In the present work, the basic amino acid was converted with one mole of sodium nitrite

1) M. Inoue et al., This Bulletin, 33, 1014 (1960).

* The author wishes to express his thanks to Dr. N. Bohonos and Dr. J. H. Martin, Lederle Laboratories Division American Cyanamid Co., for their kind information on infrared spectrum of β-Me-L-Asp.

2) H. A. Baker et al., *Arch. Biochem. Biophys.*, **78**, 468 (1958).

into α-hydroxy-β-aminobutyric acid monohydrate, m. p. 223°C (Found: C, 35.08; H, 7.98; N, 9.81; H_2O, 13.98%), and oxidation of the amino acid with periodic acid gave acetaldehyde. Thus, the structure of the basic amio acid was established to be α, β-diamino-*n*-butyric acid.

For further confirmation of this structure, an attempt** was made to synthesize α, β-diamino-*n*-butyric acid from ethyl α, β-dibromobutyrate via the azide compound II by the method used for the synthesis of β-alanine by Horner et al.[3] Hydrolysis with hydrobromic acid of the phosphin imine compound, obtained by the reaction between II and triphenyl phosphin, produced α, β-Dab, m. p. 178°C (decomp.) (IIIa), and reduction of II under high pressure yielded IIIa and hydrochloride of its isomer (IIIb), m. p. 199~201°C (decomp.). Benzoylation of IIIa by Schotten-Baumann's method gave IV, m. p. 216~218°C (Found: C, 66.14; H, 5.41; N, 8.73%). The ethyl α, β-dibenzoylaminobutyrate (V) from IV and from glumamycin exhibited the same infrared spectrum in chloroform.

The DNP-glumamycin obtained by Sanger's[4] method was hydrolyzed with 6 N hydrochloric acid and the hydrolyzate was extracted with ether, but no DNP-amino acid was found in the ether-soluble portion. Therefore the free amino group of glumamycin was assumed to be the α- or β-amino group of the α, β-Dab of glumamycin. The water soluble portion of the hydrolyzate was spotted on paper in the *n*-butanol, acetic acid, water (4 : 1 : 5) system, and gave a spot at R_f 0.68. On the other hand, in this system the β-mono-DNP-α, β-diaminobutyric acid had a R_f of 0.68 and α-mono-DNP-α, β-diaminobutyric acid had a R_f of 0.75. These two DNP-derivatives were prepared by partial dinitrophenylation of α, β-Dab from glumamycin hydrolyzate. Therefore the fact that a DNP-amino acid with R_f 0.68 was obtained from the DNP-glumamycin hydrolyzate shows that, in glumamycin, the β-amino group of α, β-Dab was dinitrophenylated. Consequently the β-amino group of the α, β-Dab is free, and the α-amino group takes part in the peptide linkage in glumamycin.

The amino acid components of glumamycin were determined quantitatively. Four moles of Asp, 2 mol. of Gly, 1 mol. of Pro, and 1 mol. of Val were detected by the method of Moore and Stein[5], but in this method, β-Me-L-Asp had the same elution curve with that of Asp, pipecolic acid gave an anomalous ninhydrin coloration, and α, β-Dab was not eluted respectively. For the determination of these three abnormal amino acids, the method of Levy[6] which comprises subjecting DNP-amino acids to paper chromatography was used. To obtain the analytical values, the determination was conducted after ascertaining that the dinitrophenylation rate and elution rate of each amino acid can be measured with an error within ±4%. Even with two dimensional paper chromatography (the first solvent; *n*-butanol saturated with 2 N aqueous ammonia, the second solvent; 1.5 M phosphate buffer)[7], Asp could not be separated from β-Me-L-Asp, but the analytical values of 4 mol. of Asp (including β-Me-L-Asp), 2 mol. of Gly, 1 mol. each of Pro, Val, and 2 mol. of α, β-Dab were in good agreement with the results by the method of Moore, Stein.

In the previous paper[1] the molecular weight of glumamycin was supposed to be about 1800 from its titration value, and about 1500 from the yield of unsaturated fatty acid. However, the molecular weight is calculated to be about 1300 from the result of the above amino acid determination; therefore about 1300 seems to represent the correct minimum molecular weight*** of glumamycin.

Aspartocin[8] in an antibiotic closely resembling glumamycin, but it is clearly different from the latter in the behavior in paper chromatography.

Research Laboratories
Takeda Chemical Industries, Ltd.
Higashiyodogawa-ku, Osaka

** Synthesis of α, β-Dab was carried out by Neuberg (*Biochem. Z.*, **1**, 282 (1906)), but since it could not be isolated in crystalline form, it was converted to the phenylisocyanate and picrate. Recently, Martin[8] attempted the synthesis but did not report the results in detail.

3) L. Horner and A. Gross, *Ann.*, **591**, 117 (1955).
4) F. Sanger, *Biochem. J.*, **39**, 507 (1945); **45**, 563 (1949).
5) S. Moore and W. H. Stein, *J. Biol. Chem.*, **192**, 663 (1951); **176**, 367 (1948).
6) A. L. Levy, ibid., **213**, 187 (1955); **213**, 487 (1955); *Nature*, **174**, 126 (1954).
7) K. Satake et al., Kagaku no Ryoiki Supplementum, **34**, 77 (1959).
*** The molecular weight of glumamycin is calculated to be 1350 from the adsorbance of DNP-glumamycin (M. Fujino, M. Inoue and A. Miyake; unpublished).
8) J. H. Martin et al., *J. Am. Chem. Soc.*, **60**, 2079 (1960).

*Anionoid Substitution of Bromo-3, 4-benzotropolones**

By Seizi EBINE

(Received April 15, 1961)

It was recently reported that 3, 4- and 4, 5-benzotropolones failed to react with thionyl chloride[1]. The present author has studied on anionoid substitution of bromo-3, 4-benzotropolones in detail and the results are summarized herein.

7-Bromo-3, 4-benzotropolone (I) reacts with thionyl chloride to yield an adduct, m. p. 147°C (Found: C, 35.77; H, 1.80. Calcd. for $C_{11}H_7O_2Br \cdot SOCl_2$: C, 35.69; H, 1.91%), which, on recrystallization from ethanol, gives 5, 7-dichloro-3, 4-benzotropolone, m. p. 137°C (Found: C, 54.97; H, 2.40. Calcd. for $C_{11}H_6O_2Cl_2$: C, 54.80; H, 2.51%). 5, 7-Dibromo-3, 4-benzotropolone (II) with thionyl chloride affords the same dichlorobenzotropolone. The methyl ethers of I and II react with dilute hydrochloric acid in methanol at reflux temperature to give 7-chloro-3, 4-benzotropolone methyl ether, m. p. 97°C (Found: C, 65.30; H, 4.06. Calcd. for $C_{12}H_9O_2Cl$: C, 65.31; H, 4.11%) and 5, 7-dichloro-3, 4-benzotropolone methyl ether, m. p. 106°C (Found: C, 56.46; H, 3.11. Calcd. for $C_{12}H_8O_2Cl_2$: C, 56.49; H, 3.16%), respectively. The methyl ether of I, on treatment with dilute alkali in methanol at room temperature, affords 6-hydroxy-7-methoxy-2, 3-benzotropone, m. p. 115~116°C (Found: C, 71.56; H, 5.06. Calcd. for $C_{12}H_{10}O_3$: C, 71.28; H, 4.99%). In these reactions, the hydroxyl groups of bromobenzotropolones and the methoxyl groups of their methyl ethers remained unaffected, whereas the bromine atoms at 5- and 7-positions of these compounds were replaced with ease.

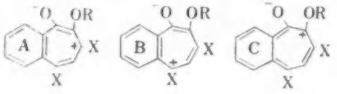

These behaviors of bromobenzotropolones and their methyl ethers are different from those of monocyclic bromotropolones and their methyl ethers; bromotropolones react with thionyl chloride to yield chlorotropones[2] and their methyl ethers, on treatment with dilute alkali are hydrolyzed or further rearranged into aromatic compounds, bromines remaining unreplaced[3]. Such a difference in behavior may be ascribed to the resonance structures of bromobenzotropolones and their methyl ethers. The contribution of the formulas A and B are great but that of the formula C is to a limited extent because its benzene ring is not aromatic but quinonoid, hence the bromines at 5- and 7-positions are highly susceptible to but the 1-hydroxyl and 1-methoxyl groups are almost inert towards the anionoid substitution.

II is reduced with hydriodic acid at 100°C to 5-bromo-3, 4-benzotropolone, m. p. 140°C (Found: C, 52.86; H, 2.67. Calcd. for $C_{11}H_7O_2Br$: C, 52.61; H, 2.81%). The methyl ether of II reacts with hydriodic acid in methanol under reflux to afford 5-bromo-7-iodo-3, 4-benzotropolone methyl ether, m. p. 130~131°C (Found: C, 36.69; H, 2.07. Calcd. for $C_{12}H_8O_2BrI$: C, 36.86; H, 2.06%) and rearranges with dilute alkali in methanol under reflux into 1-hydroxy-4-bromo-2-naphthoic acid, m. p. and mixed m. p. 237°C (decomp.). Coupling of II with diazotized *p*-toluidine produces 2-(*p*-tolylazo)-4-bromo-1-naphthol, m. p. and mixed m. p. 183~184°C. In these reactions, the bromine at 5-position of II or its methyl ether remained unreplaced, presumably because the action of iodide, hydroxide and diazonium ions on the 5-position is sterically hindered due to being the *peri* position of the condensed benzene ring. This fact seems to be another characteristic of bromobenzotropolones.

Department of Chemistry
Saitama University
Urawa, Saitama-ken

* Presented at the 14th Annual Meeting of the Chemical Society of Japan, Tokyo, April, 1961.

1) W. E. Parham, D. A. Bolon and E. E. Schweizer, *J. Am. Chem. Soc.*, **83**, 603 (1961).

2) W. von E. Doering and L. H. Knox, ibid., **74**, 5683 (1952); B. J. Abadir, J. W. Cook, J. D. Loudon and D. K. V. Steel, *J. Chem. Soc.*, **1952**, 2350.

3) T. Nozoe, Y. Kitahara and S. Masamune, *Proc. Japan Acad.*, **27**, 649 (1951).

*The Synthesis of 3-α-Carboxyethylcyclopentanol Lactone**

By Tsuguo TANAKA

(Received April 15, 1961)

The synthesis of *cis*- and *trans*-lactones of 2-α-carboxyethylcyclopentanol was previously reported[1].

Now, *cis*-3-α-carboxyethylcyclopentanol lactone was obtained as one of the reaction products of *cis*-2-α-carboxyethylcyclopentanol lactone with potassium cyanide. The formation of this lactone indicates a possibility of a new rearrangement[2] reaction.

cis-2-α-Carboxyethylcyclopentanol lactone (I) was heated with potassium cyanide[3] in a sealed tube at 250~260°C for 24 hr., and the products were isolated and fractionally distilled. These were lactone $C_8H_{12}O_2$ (II) [b. p. 85~86°C/3.5 mmHg; λ_{max}^{EtOH} 211 mμ, ν_{max} 5.83 μ[4] (C=O), 8.24 μ (C–O); Found: C, 68.05; H, 8.80. Calcd. for $C_8H_{12}O_2$: C, 68.54; H, 8.63%] and a cyanoacid $C_9H_{13}O_2N$ (III) [b. p. 126~127°C/0.6 mmHg; λ_{max}^{EtOH} 212.5 mμ, ν_{max} 5.84 μ (C=O), 4.42 μ (C≡N); Found: C, 64.12; H, 8.22; N, 6.99. Calcd. for $C_9H_{13}O_2N$: C, 64.65; H, 7.84; N, 8.38%].

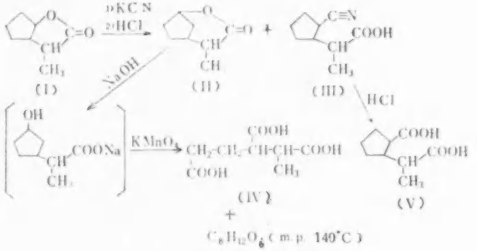

The lactone (II) was hydrolyzed with 10% aqueous sodium hydroxide solution and the sodium salt solution of hydroxyacid was oxidized with potassium permanganate.

Tricarboxylic acids $C_8H_{12}O_6$ (IV) (m. p. 180 °C.; Found: C, 47.05; H, 6.28. Calcd. for $C_8H_{12}O_6$: C, 47.06; H, 5.92%), which was identified as α-methyl-β-carboxyadipic acid[5] both by mixed melting point and infrared spectra, and $C_8H_{12}O_6$ (m. p. 140°C.; Found: C, 47.26; H, 6.21. Calcd. for $C_8H_{12}O_6$: C, 47.06; H, 5.92%), which was not identified[6], were obtained as the oxidation products.

The formation of α-methyl-β-carboxyadipic acid suggested the structure (II) of *cis*-3-α-carboxyethylcyclopentanol lactone.

Hydrolysis of cyanoacid (III) with hydrochloric acid yielded a dicarboxylic acid $C_9H_{14}O_4$ (V) (m. p. 130°C; Found: C, 57.77; H, 7.62. Calcd. for $C_9H_{14}O_4$: C, 58.05; H, 7.58%) in agreement with the structure III of cyanoacid.

The conversion from *cis*-2-α-carboxyethylcyclopentanol lactone into *cis*-3-α-carboxyethylcyclopentanol lactone, would involve intermediates such as anion of III, and carbonium ions VI and VII.

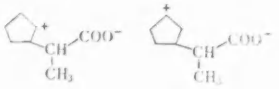

Department of Chemistry
Faculty of Liberal Arts
Saga University
Honjo, Saga-shi

* Presented at the 13th Annual Meeting of the Chemical Society of Japan, Tokyo, April, 1960.

1) T. Tanaka, This Bulletin, **32**, 1320 (1959).

2) C. C. Price and W. Kaplan, *J. Am. Chem. Soc.*, **66**, 477 (1944).

3) G. Komppa, *Ber.*, **41**, 4472 (1908); M. A. Haller, *Compt. rend.*, **112**, 446 (1896).

4) R. N. Jones, P. Humphries and K. Dobriner *J. Am. Chem. Soc.*, **72**, 956 (1950); G. Stork and R. Breslow, ibid., **75**, 3291 (1953); A. Lardon, O. Schindler and T. Reichstein, *Helv. Chim. Acta*, **40**, 666 (1957).

5) W. N. Haworth and W. H. Perkin, *J. Chem. Soc.*, **93**, 581 (1908).

6) This acid showed melting point depression by mixed melting with authentic β-(α-carboxyethyl)-glutaric acid reported by Z. H. Skraup, *Monatsh.*, **21**, 907 (1900).

4, 5-Dimethoxycanthin-6-one and 2, 6-Dimethoxy-p-benzoquinone from Picrasma ailanthoides Planchon

By Naoki INAMOTO, Shozo MASUDA, Osamu SIMAMURA and Takahiko TSUYUKI

(Received May 23, 1961)

We report the isolation of 4, 5-dimethoxycanthin-6-one, a new derivative of canthine (6H-indolo[3, 2, 1-*de*] [1, 5]-naphthyridine), and 2, 6-dimethoxy-*p*-benzoquinone from wood of *Picrasma ailanthoides* Planchon.

Methanolic extract of the wood was diluted with water, the precipitated tarry matter filtered off, the filtrate extracted with benzene, and the benzene removed. The resulting residue, chromatographed on alumina in benzene and repeatedly crystallized from methanol, gave a

compound crystallizing in pale yellow needles (ca. 0.01% based on the dried material), m. p. 147.3~147.5°C, with a formula $C_{11}H_6N_2O\cdot(OCH_3)_2$ (Found: C, 68.59; H, 4.41; N, 10.05; OCH_3, 22.38; Mol. wt. (Rast), 301. Calcd. for: C, 68.56; H, 4.32; N, 10.00; OCH_3, 22.14%; Mol. wt., 280). It was insoluble in aqueous sodium hydroxide and gave a bright-yellow solution with concentrated sulfuric acid. A methanolic solution showed a violet fluorescence, and, on addition of mineral acid, this turned into an intensely green one. The ultraviolet absorption spectrum in ethanol had characteristic peaks at 225 ($\log\varepsilon=4.38$), 247 (4.33), 267 (4.09), 290 (4.05), 299 (4.04), 340 (3.98), 355 (4.15) and 370 mμ (4.08), $\log\varepsilon$ being given in parentheses. The infrared spectrum measured in Nujol indicated the presence of an amide group (1658 cm^{-1}) and a 1,2-disubstituted benzene ring, but the absence of a nitrogen-hydrogen bond. Oxidation of this substance with potassium permanganate in acetone at 20°C gave a non-acidic compound, m. p. 164~165°C (Found: C, 69.13; H, 4.67; N, 12.29. Calcd. for $C_{13}H_{10}N_2O_2$: C, 69.01; H, 4.46; N, 12.38%) which was readily identified with methyl β-carboline-1-carboxylate by mixed melting point determination with an authentic specimen and comparison of the infrared spectra. These findings establish the structure of the new compound as 4,5-dimethoxycanthin-6-one.

Hot aqueous extract of the wood was treated with lead acetate followed by activated charcoal, the charcoal extracted with chloroform and the chloroform removed. The residue was dissolved in hot aqueous methanol and the solution, on cooling, deposited 2,6-dimethoxy-*p*-benzoquinone (0.005%). It seems of interest that this compound is also found in *Simaruba amara*, *Khaya senegalensis*, *Picrasma crenata*[1] and *Adonis vernalis*[2].

Department of Chemistry
Faculty of Science
The University of Tokyo
Hongo, Tokyo

1) J. Polonsky and E. Lederer, *Bull. soc. chim. France*, 1157 (1959).
2) W. Karrer, *Helv. Chim. Acta*, **13**, 1424 (1930).

The Crystal Structure of Phenazine-5, 10-dioxides

By Yoshiyuki NAMBA, Tsutomu ODA and Tokunosuké WATANABÉ

(Received May 4, 1961)

The authors have carried out an investigation of the crystal structure of phenazine-5, 10-dioxide in order to amplify the knowledge of the dative bond, N→O. In the course of the present investigation, the crystal structure of phenazine-*N*-oxide has been published[1].

Phenazine-5, 10-dioxide was prepared by oxidizing phenazine-*N*-oxide. It crystallizes out in needle-like crystals, deep red in color. They decompose at about 190°C. Oscillation and Weissenberg photographs taken with copper K_α radiation, showed that the crystal is monoclinic with the unit cell having the dimensions:

$$a=7.83,\quad b=3.95,\quad c=15.50\,\text{Å},\quad \beta=104°48'$$

and the space group $P2_1/c$. From the observed density, the unit cell was found to contain two molecules, implying that the molecules must be placed at special positions having centers of symmetry. The intensities of reflections, (*h0l*) and (0*kl*), obtained by the multiple-film technique were measured by the visual method, using standard scales, and no correction was made for absorption.

Since the dimension of the b-axis is short (3.95 Å), it was expected that there is no overlap of atoms in the projection to the b-plane. The optical transform methods[2] were employed to determine the orientation of the molecule in the unit cell, as well as to determine the signs of the structure factors of strong reflections[3]. The *h0l* Fourier projection was refined in the usual way and the electron density map, $\rho(xz)$, is shown in Fig. 1. To determine the *z*-coordinates of atoms, we employed usual trial and error methods taking into account the plane structure of this molecule, followed by the least square methods. The atomic arrangement projected along the b and a axes are given in Figs. 2 and 3, respectively. This arrangement of molecules is quite similar to that reported for anthraquinone[4], whose unit cell dimensions are also similar to those of phenazine-5,10-dioxide. The configuration of this molecule is found to be

1) R. Curti et al., *Acta Cryst.*, **14**, 133 (1961).
2) C. A. Taylor, et al., ibid., **4**, 261 (1951).
3) C. A. Taylor and H. Lipson, *Nature*, **167**, 809 (1951); T. Watanabé and M. Otsuka, *Acta Cryst.*, **10**, 377 (1957).
4) S. N. Sen, *Indian J. Phys.*, **22**, 347 (1948).

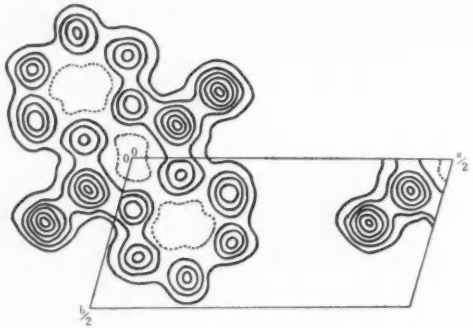

Fig. 1. Electron density map projected on the b plane.

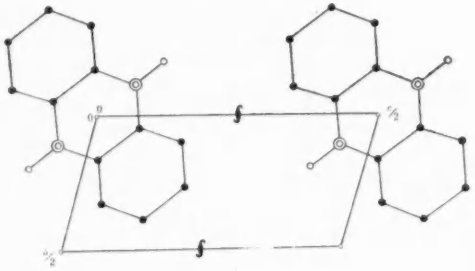

Fig. 2. Projection of the structure, on the b plane.
○ Oxygen, ◌ Nitrogen, ● Carbon.

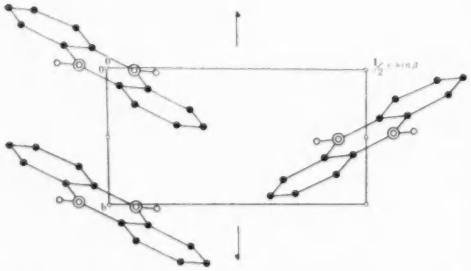

Fig. 3. The view of the structure along the a-axis.

almost planer with reasonable interatomic distances. In phenazine-*N*-oxide, a statistical arrangement of the oxygen atoms has been reported[1]. It is interesting to note that the average structure of phenazine-*N*-oxide is similar to the present structure.

The authors wish to thank Professor E. Matsumura and Mr. H. Takeda for their kind helps for the preparation of this crystal. Part of the cost of this study has been defrayed by a Grant of the Ministry of Education, to which the authors' thanks are due.

Laboratory of Physical Chemistry
Osaka University of Liberal Arts and Education
Tennoji, Osaka
(Y. N. & T. O.)

Department of Physics
Osaka University, Osaka
(T. W.)

Synthesis of Isoxazolecarboxylic Acids from Schiff Bases and Nitroacetate[1]

By Shonosuke ZEN and Sumio UMEZAWA

(Received May 9, 1961)

The authors wish to report a new and general method for the synthesis of 4-substituted isoxazole-3, 5-dicarboxylic acids. We have previously reported[2] that dibutylamides of 4-substituted isoxazole-3,5-dicarboxylic acids were obtained when α, β-unsaturated α-nitroesters were treated with *n*-butylamine in an anhydrous solvent, and assumed that the reaction proceeds through a key intermediate IV which is formed by the addition of nitroacetate to α, β-unsaturated α-nitroester. Subsequently, the authors could isolate benzylidene-*n*-butylamine (a Schiff base) from the mother liquor of 4-phenyl-3, 5-bis(*n*-butylcarbamoyl)isoxazole which is obtained from ethyl α-nitrocinnamate by refluxing with *n*-butylamine in absolute ethanol. Therefore, it is suggested that the initial reaction may involve the addition of butylamine to α, β-unsaturated α-nitroester I and the adduct II generates nitroacetate III, which adds to α, β-unsaturated system of I in the presence of a basic catalyst (*n*-butylamine) by the mechanism of the Michael reaction to give the key intermediate IV, as outlined in the following scheme:

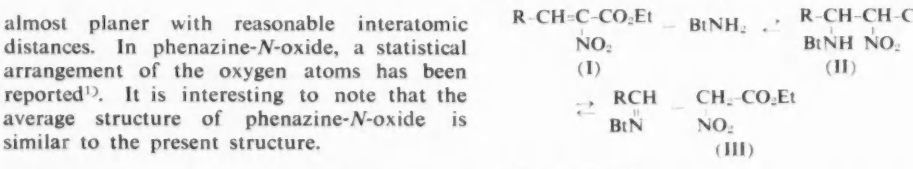

1) Presented in part at the Division of Organic Chemistry of the 14th Annual Meeting of the Chemical Society of Japan, Tokyo, April, 1961.
2) S. Umezawa and S. Zen, This Bulletin, 33, 1016 (1960).

$$\mathrm{I} + \mathrm{III} \longrightarrow \mathrm{EtO_2C{-}\underset{\displaystyle NO_2}{\underset{|}{CH}}{-}\underset{\displaystyle R}{\underset{|}{CH}}{-}CO_2Et}$$

(IV)

As regards the sequel of the path from IV to bis(*n*-butylcarbamoyl) derivatives of isoxazole, the authors had already mentioned in a previous paper[2].

If the above mechanism is valid, one should be able to obtain the derivatives of isoxazole-3, 5-dicarboxylic acid by the reaction of Schiff bases with nitroacetate in the presence of basic catalysts. The expectation has now been realized. When an excess of *n*-butylamine was added to a mixture of Schiff base (1 mol.) and ethyl nitroacetate (2 mol.) in absolute ethanol, an exothermic reaction occurred. After refluxing for several hours, the mixture was concentrated to give a crystalline solid of bis(*n*-butylcarbamoyl) derivative of isoxazole.

The following compounds were prepared by the general procedure: 4-methyl-3, 5-bis(*n*-butylcarbamoyl)isoxazole*; 4-(*n*-propyl)-3, 5-bis(*n*-butylcarbamoyl)isoxazole (V), m. p. 112.5 ~115.5°C; 4-phenyl-3, 5-bis(*n*-butylcarbamoyl)-isoxazole*, 4-(*p*-nitrophenyl)-3, 5-bis(*n*-butylcarbamoyl)isoxazole (VI), m. p. 133~135°C; 4-(*m*-nitrophenyl)-3, 5-bis(*n*-butylcarbamoyl)-isoxazole (VII), m. p. 168~169°C; 4-(*p*-chlorophenyl)-3, 5-bis(*n*-butylcarbamoyl) isoxazole (VIII), m. p. 126~127°C; 4-(2, 4-dichlorophenyl)-3, 5-bis(*n*-butylcarbamoyl) isoxazole (IX), m. p. 139~140.5°C; 4-(*p*-acetamidophenyl)-3,5-bis(*n*-butylcarbamoyl)isoxazole (X), m. p. 159~160°C; 4-(*p*-dimethylaminophenyl)-3,5-bis(*n*-butylcarbamoyl)isoxazole (XI), m. p. 117~118.5°C.

These derivatives were hydrolyzed with 10% sodium hydroxide in 50% aqueous ethanol at about 60°C to give 4-substituted isoxazole-3, 5-dicarboxylic acids. V, VI, VIII and IX were converted, respectively, to 4-(*n*-propyl)isoxazole-3,5-dicarboxylic acid, m. p. 176~177°C (decomp.), 4-(*p*-nitrophenyl)isoxazole-3, 5-dicarboxylic acid, m. p. 172~174°C (decomp.), 4-(*p*-chlorophenyl)isoxazole-3, 5-dicarboxylic acid, m. p. 187~187.5°C (decomp.), and 4-(2, 4-dichlorophenyl)isoxazole-3, 5-dicarboxylic acid, m. p. 183~186°C (decomp.). The product from X was led to methyl 4-(*p*-aminophenyl)isoxazole-3,5-dicarboxylate, m. p. 163~166°C.

The authors are indebted to Mr. S. Nakada for microanalyses.

Department of Applied Chemistry
Faculty of Engineering
Keio University, Tokyo

* Compounds marked with an asterisk were already prepared by another procedure and reported. S. Umezawa, S. Zen, loc. cit.

Polarographic Studies of Metallic Complexes. VI[1]*. Tetracyanocobaltate(III) Complex*[2]

By Nobufumi MAKI and Ryutaro TSUCHIDA

(Received May 2, 1961)

In the earlier papers[3,4] it was reported that the pentacyanocobaltate(III) complexes are all reduced in one or two steps to cobalt(I) complexes at the dropping mercury electrode (DME)[5].

A similar polarographic behaviour was found in the case of tetracyanocobaltate(III) complex, $Na_5[Co(CN)_4(SO_3)_2]$[6].

Namely, disulphono-tetracyanocobaltate(III) ion[7] gave a well-defined wave of one step at the DME in 0.5 F sodium sulphite supporting electrolyte (Fig. 1). The current is controlled only by diffusion. The diffusion current and the concentration of the depolarizer are linearly related in the concentration range from 5×10^{-4} to 10^{-2} F.

The wave, corresponding to an acceptance of two electrons, represents the reduction to a univalent cobalt complex, whose formula is presumed analogously in the cases of cyanocobalt(I) complexes[4,8,9] to be the same as that of the oxidized form. Hence, the process of the electrode reaction is considered as follows:

$$[Co^{III}(CN)_4(SO_3)_2]^{5-} + 2e^- \longrightarrow [Co^{I}(CN)_4(SO_3)_2]^{7-}$$

The above electrode process belongs to the quasi-reversible reaction polarographically. For further detail on this point, an oscillographic-polarographic study will be reported later.

The mechanism of the electron transfer and the change of the electronic configuration for the above reaction are explained by the atomic orbital method[10] as follows.

1) Part V of this series; N. Maki, Y. Shimura and R. Tsuchida, This Bulletin, **32**, 833 (1959).
2) Presented at the Symposium on Polarography, Kyoto, October, 1959.
3) N. Maki, J. Fujita and R. Tsuchida, *Nature*, **183**, 458 (1959).
4) N. Maki, ibid., **185**, 682 (1960).
5) D. N. Hume and I. M. Kolthoff, *J. Am. Chem. Soc.*, **71**, 867 (1949).
6) P. R. Rây and S. C. Chackrabarty, *Z. anorg. u. allgem. Chem.*, **211**, 173 (1933).
7) The "sulphono-group", which is SO_3^{2-} radical bound to the central metal ion by the sulphur atom, is distinguished from the "sulphito-group", OSO_2^{2-} bound by the oxygen.
8) N. Maki, *Nature*, **188**, 227 (1960).
9) W. P. Griffith and G. Wilkinson, *J. Chem. Soc.*, **1959**, 2757.
10) A. A. Vlček, *Collection Czechoslov. Chem. Communs.*, **20**, 894 (1955).

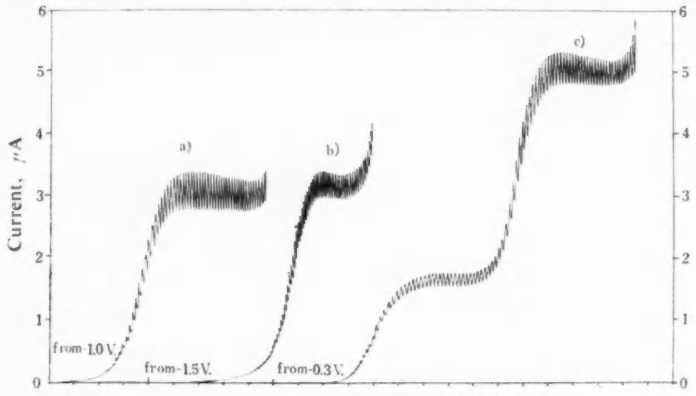

Fig. 1. Polarograms of sulphono- and sulphito-cobalt(III) complexes obtained at the concentration of 0.001 F complex ion in sodium sulphite supporting electrolyte (25°C). Each the height of the waves is seen to be proportional to the electron numbers of reduction process.

a) $Na_3[Co(CN)_4(SO_3)_2]$
Supporting salt: 0.5 F Na_2SO_3
Sensitivity: 0.04 μA/mm., Damping: 100, from −1.0 V. vs. S. C. E.
$E_{1/2} = -1.36$ V.

b) $K_4[Co(CN)_5SO_3]\cdot 2H_2O$
Supporting salt 1F Na_2SO_3
Sensitivity: 0.04 μA/mm., Damping: 200, from −1.5 V. vs. S. C. E.
$E_{1/2} = -1.54$

c) $[Co(NH_3)_5SO_3]Cl$
Supporting salt: 1F Na_2SO_3
Sensitivity: 0.04 μA/mm, Damping: 100, from −0.30 V. vs. S. C. E.
$E_{1/2}$ (1st wave) $= -0.74$ V., $E_{1/2}$ (2nd wave) $= -1.30$ V.
Voltage unit: vs. the saturated calomel electrode (S. C. E.), 100 mV./absc.

The acceptance of the electrons occurs in two stages.

$$d^5d^6d^2[D^2SP^3] \xrightarrow{e} d^5d^6d^2[D^2SP^3]d^1$$

$$d^5d^6d^2[D^2SP^3]d^1 \xrightarrow{e} d^5d^6d^2d^1[DSP^2][PD]$$

$$d^5d^6d^2d^1[DSP^2][PD] \xrightarrow{e} d^5d^6d^2d^2[DSP^2][PD]$$

First, the electron is accepted into the 4d peripheral orbitals temporarily, where it is held loosely, since the 3d atomic orbitals of Co(III) are fully occupied. After that the consecutive change of the electronic configuration and the placement of the electron in the stable 3d orbitals occur gradually. Thus, the electronic configuration of cobalt(I) complex is considered to consist of a coplanar structure through $3d4s4p^2$ hybrid orbital and a linear structure through 4p4d hybrid orbital separately, so the resulting cobalt(I) ion, $[Co^I(CN)_4\cdot(SO_3)_2]^{7-}$, may probably have a trans-configuration rather than that of cis-one.

Department of Chemistry
Osaka University
Kita-ku Osaka

Catalytic Dimerization of Monoalkyl Acetylenes

By Nobue HAGIHARA, Masuhiko TAMURA, Hiroshi YAMAZAKI and Magosaburo FUJIWARA

(Received May 4, 1961)

It has been described by some investigators[1] that acetylene and substituted acetylenes were polymerized with Ziegler type catalysts forming linear high molecular weight polymer or benzene derivatives.

We observed that with a catalyst obtained in the reaction of chromium tetra-*tert*-butoxide[2] with diethylzinc, monoalkyl acetylenes could be dimerized to the compound I in a good yield.

$$RC{\equiv}C\ CR{-}CH_2 \qquad (1)$$

1) G. Natta, P. Pino and G. Mazzanti, Belg. Pat. 546151 (1956); W. R. Smith, Brit. Pat. 820510 (1958); B. Franzus, P. J. Canterino and R. A. Wickliffe, *J. Am. Chem. Soc.*, **81**, 1514 (1959).

2) N. Hagihara and H. Yamazaki, ibid., **81**, 3160 (1959); *J. Chem. Soc. Japan, Pure Chem. Sec.* (*Nippon Kagaku Zasshi*), **81**, 821 (1960).

On the other hand, the reaction of monoalkyl acetylenes resulted only in the polymerization to trialkyl benzenes with a catalyst obtained from the reaction of chromium tetra-*tert*-butoxide with triethylaluminum.

n-Propylacetylene dimerizes to 2,4-di-*n*-propyl-1-buten-3-yne (II) in almost quantitative yield at 30°C for 10 hr. at $Et_2Zn/(tert\text{-}BuO)_4Cr$ ratio of 3. II is colorless liquid and boils at 88~89°C (40 mmHg) (n_D^{20}=1.455, Found: C, 87.80; H, 11.76. Calcd. for $C_{10}H_{16}$: C, 88.16; H, 11.84%). Fifteen moles of dimer per mole chromium compound were obtained.

The structure of the dimer was estimated as I by molecular weight determination and the presence of infrared absorption corresponding $-C\equiv C-$ and $>C=CH_2$ at 2230 and 890 cm^{-1}. Identity was established by comparison of the infrared spectrum with that of authentic sample (b. p. 87~88°C (40 mmHg), n_D^{20}=1.457, Found: C, 87.77; H, 11.97. Calcd. for $C_{10}H_{16}$: C, 88.16; H, 11.84%) which was prepared from 4-nonyen-6-one ($C_3H_7C\equiv C\text{-}COC_3H_7$) and methylene triphenyl phosphorane ($Ph_3P{=}CH_2$) according to the Wittig reaction.

Optimum ratio of diethylzinc to chromium tetra-*tert*-butoxide was 3 to 1. Although rate of the reaction is fast at high temperature, the formation of tri-*n*-propyl-benzene and high polymer is often considerable in this case.

This type of dimerization is not limited to *n*-propyl-acetylene. *n*-Butylacetylene was dimerized to 2,4-di-*n*-butyl-1-buten-3-yne (b. p. 64.5~65.0°C (5 mmHg), n_D^{20}=1.459, Found: C, 87.38; H, 12.31. Calcd. for $C_{12}H_{20}$: C, 87.73; H, 12.27%) and *tert*-butylacetylene to 2,4-di-*tert*-butyl-1-buten-3-yne (b. p. 92~93°C (90 mmHg), n_D^{20}=1.438, Found: C, 87.45; H, 11.90. Calcd. for $C_{12}H_{20}$: C, 87.73; H, 12.27%).

It is interesting that the catalytic dimerization of monoalkyl acetylenes with the catalyst in the present work gives exclusively I without the formation of 1,4-dialkylbutenyne ($RC\equiv C\text{-}CH{=}CHR$).

Osaka University
The Institute of Scientific and Industrial Research
Sakai, Osaka

Electron Spin Resonance of Tetracene-Antimony Pentachloride

By Yoshio MATSUNAGA*

(Received April 7, 1961)

It has been known that aromatic hydrocarbons give deeply colored unstable molecular compounds with antimony pentachloride[1]. Brass and his coworkers have reported the isolation of some compounds consisting of two molecules of hydrocarbon and one of antimony pentachloride[2,3]. Recently Weissman and his coworkers have observed the ESR of some of these molecular compounds both in the solid and in the dissolved states. They have suggested that singly charged hydrocarbon positive ions, which are formed by oxidation with antimony pentachloride, are responsible for, at least, part of the observed paramagnetism[4]. Hoijtink and Weijland have also pointed out the fact that the electronic absorption spectrum of perylene with antimony pentachloride in chloroform is closely similar to that of perylene monopositive ion produced in concentrated sulfuric acid[5]. Here we wish to report our preliminary ESR experiments on the products given by the reaction of antimony pentachloride with tetracene and also some other aromatic hydrocarbons.

Small amount of powdered hydrocarbon was put into a sample tube for the ESR measurements, then a dried chloroform solution of antimony pentachloride was added. After the solvent and excess of the reagent were quickly removed by evacuation, the ESR of the product in vacuum was recorded at room temperature and at a frequency of 9 kMc./sec. The rapid decrease of intensity of ESR was observed in many cases. The line width was given by the distance between the points of maximum slope. All of *g*-values were found to be near 2.004.

A sharp resonance absorption peak was detected from the products prepared with the following hydrocarbons; 1,2-benzanthracene, width 2.0 gauss, perylene 1.2, 1,12-benzperylene 0.6, mesonaphthodianthrence 1.5, bianthryl 1.2, pyranthrene 1.6, and violanthrene 1.7. In

* Present address: Cyanamid European Research Institute, Cologny, Geneva, Switzerland.

1) S. Hilpert and L. Wolf, *Ber.*, **46**, 2215 (1913).
2) K. Brass and E. Tengler, ibid., **64**, 1650 (1931).
3) K. Brass and K. Fanta, ibid., **69**, 1 (1936).
4) S. I. Weissman, E. de Boer and J. J. Conradi, *J. Chem. Phys.*, **26**, 963 (1957).
5) G. J. Hoijtink and W. P. Weijland, *Rec. trav. chim.*, **76**, 836 (1957).

the other case the spectrum was found to consist of two or three absorption peaks. The product from anthracene gives two peaks. The widths of the two may be in the range from 3.5 to 5.5 gauss. Three peaks were observed from the mixture of chrysene and antimony pentachloride. The peak in the highest magnetic field has a width of 0.9 gauss, the central one about 2.5 gauss, and the last 2.5 gauss. The separation between the first and the last is about 5.5 gauss. The estimation of these widths can not be accurate because of overlapping of the peaks. It is not yet clear whether the appearance of two or three peaks in the present cases is due to the coexistence of two or three kinds of paramagnetic species or due to the anisotropy of *g*-value in one species. However, the formation of two kinds of compounds could be definitely shown in the case of tetracene.

The spectrum obtained from the mixture of tetracene and antimony pentachloride consists of one sharp peak with a *g*-value of 2.0045 and one broad one with a *g*-value of 2.0056.

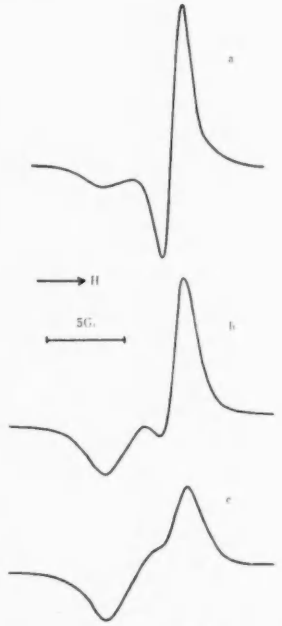

Fig. 1. Derivatives of ESR from tetracene and antimony pentachloride. a; tetracene with excess of antimony pentachloride, b and c; after removal of some amount of the reagent.

Their intensities were found to depend on the ratio of antimony pentachloride to the hydrocarbon. As shown in Fig. 1a, a sharp peak appeared in the presence of an excess of antimony pentachloride. On the removal of some amount of the reagent this peak with a width of 1.1 gauss decreases its intensity and the broad peak with a width of 5.3 gauss becomes stronger as seen in Figs. 1b and c. The reverse change could be observed on addition of antimony pentachloride. We observed also that the intensities of two peaks with *g*-values of 2.0039 and 2.0048 respectively from the mixture of triphenylene and antimony pentachloride depend similarly on the condition of preparation.

One of the two peaks, probably the broad one, appeared on addition of antimony pentachloride to tetracene may arise from the fairly stable molecular compound $2C_{18}H_{12}\cdot SbCl_5$ described by Brass and Fanta[3]. It is apparent that the species, which gives the peak with a *g*-value of 2.0045, is formed by the further addition of the complex-forming agent to the species which gives the broad peak with a *g*-value of 2.0056. The shift of *g*-value found here seems to be consistent with Wahler and Thon's observation that the magnitude of *g*-value of diarylnitrogen oxide in solution shows a marked decrease by the addition of *m*-dinitro- or *s*-trinitrobenzene[6]. The *g*-value of hydrocarbon monopositive ions in sulfuric acid has been reported to be 2.0028[7] and that of perylene perchlorate 2.0025[8]. It is unlikely that the *g*-value of paramagnetic tetracene ion becomes as high as 2.0056 by the interaction with antimony compound. Therefore, the species observed here may be not the salts of tetracene monopositive ion but the molecular compounds between the hydrocarbon and antimony pentachloride as reported by Brass[2,3]. The paramagnetic molecular compounds where the ground-state is supposed to be chiefly of non-bonding have been found in the case of aromatic hydrocarbons with halogens[9,10].

Department of Chemistry
Faculty of Science
The University of Tokyo
Hongo, Tokyo

6) B. E. Wahler and H. G. Thon, *Arch. Sci. (Geneva)*, **11**, 165 (1958).
7) A. Carrington, F. Dravnieks and M. C. R. Symons, *J. Chem. Soc.*, **1959**, 947.
8) Y. Matsunaga, This Bulletin, to be published.
9) Y. Matsunaga, ibid., **28**, 475 (1955).
10) Y. Matsunaga, *J. Chem. Phys.*, **30**, 855 (1959).